The influence of the cytotoxic necrotizing factor toxin of *Yersinia pseudotuberculosis* on pathogenesis

Von der Fakultät für Lebenswissenschaften

der Technischen Universität Carolo-Wilhelmina zu Braunschweig

zur Erlangung des Grades

einer Doktorin der Naturwissenschaften

(Dr. rer. nat.)

genehmigte

D i s s e r t a t i o n

von Wiebke Alexandra Heine
aus Braunschweig

1. Referentin: Prof. Dr. Petra Dersch
2. Referent: Prof. Dr. Michael Steinert
eingereicht am: 15.03.2017
mündliche Prüfung (Disputation) am: 19.06.2017

Druckjahr 2017

Vorveröffentlichungen der Dissertation

Teilergebnisse aus dieser Arbeit wurden mit Genehmigung der Fakultät für Lebenswissenschaften, vertreten durch die Mentorin der Arbeit, in folgenden Beiträgen vorab veröffentlicht:

Tagungsbeiträge

Heine, W., Schweer J., Beckstette, M., Heise, U., Pisano, F., Nuss, A. M., Dersch, P.: Towards the impact of the cytotoxic necrotizing factor toxin on *Yersinia pseudotuberculosis* pathogenesis. (Vortrag) 5. Nationales *Yersinia* Meeting, Münster (2016).

Heine, W., Schweer J., Pisano, F., Dersch, P.: The molecular function of the CNF_Y toxin of *Yersinia pseudotuberculosis* and its role during pathogenesis. (Vortrag) Symposium der Fachgruppe Mikrobielle Pathogenität 2014, Bad Urach (2014).

Contents

Abbreviations

°C	Degree Celsius
A	Absorbance
ACK	Ammonium-Chloride-Potassium
Ail	Attachment invasion locus
AIM2	Absent in melanoma II
ALR	AIM2-like receptors
Amp	Ampicillin
APS	Ammonium persulfate
ASC	Apoptosis-associated speck-like protein containing CARD
ATP	Adenosine triphosphate
BCA	Bicinchoninic acid
BHI	Brain-heart infusion
bp	Base pairs
BSA	Bovine serum albumin
C3	Complement factor-3 or exoenzyme of *Clostridium* spp.
ca.	Circa
CagA	Cytotoxin-associated gene A
CCD	Charge-coupled device
CD	Cluster of differentiation
cDNA	Complementary DNA
CFU	Colony forming units
CLR	C-type lectin receptor
CNF	Cytotoxic necrotizing factor
CO_2	Carbon dioxide
CRP	C-reactive protein
Ct	Cycle threshold
CTL	Cytotoxic T lymphocytes
Da	Dalton
DAMP	Damage-associated molecular pattern
DAPI	49,6-diamidino-2-phenylindole
DC	Dendritic cell
DIC	Differential interference contrast
dist.	Distilled
DNA	Deoxyribonucleic acid
dpi	Days post infection
dsDNA	Double-stranded DNA
e.g.	*Exampli gratia*
EDTA	Ethylenediaminetetraacetic acid
ELISA	Enzyme-linked immunosorbent assay
ERCC	External RNA controls consortium
et al.	*Et alii*
F-actin	Filamentous actin
FACS	Fluorescence activated cell sorting
FAE	Follicle-associated epithelium

FELASA	Federation of Laboratory Animal Science Associations
FITC	Fluorescein Isothiocyanate
FMO	Fluorescence minus one
g	Gram
G-actin	Globular actin
GALT	Gut-associated lymphoid tissue
GAP	GTPase-activating protein
GBP	Guanylate-binding proteins
GDI	Guanine nucleotide dissociation inhibitor
GDP	Guanosine diphosphate
GEF	Guanine nucleotide exchange factor
GGEP	Global gene-expression profile
GHE	Global health estimates
GO	Gene ontology
GTP	Guanosine triphosphate
GV-SOLAS	“Gesellschaft für Versuchstierkunde”/ Society of Laboratory Animal Science
h	Hour(s)
H&E	Hematoxylin-eosin
HF	High fidelity
HIV	Human immunodeficiency virus
HLA	Human leukocyte antigen
HPI	High pathogenicity island
HZI	Helmholtz Center for Infection Research
IBC	Intracellular bacterial community
ICSBP	IFN consensus-sequence binding protein
i.e.	*Id est*
IEC	Intestinal epithelial cell
IFN	Interferon
IgA	Immunoglobin A
IL	Interleukin
InvA	Invasin A
k	Kilo
Kan	Kanamycin
KEGG	Kyoto Encyclopedia of genes and genomes
l	Liter
LB	Luria Bertani
LP	Lamina propria
LPS	Lipopolysaccharide
M	Molar
m	Milli or meter
M cell	Microfold cell
MAPK	Mitogen-activated protein kinase
MHCI/II	Major histocompatibility complex class I/II
min	Minute(s)
MLN	Mesenteric lymph nodes
n	Nano
NCBI	National Center for Biotechnology Information
NEB	New England Biolabs

NFκB	Nuclear factor ‘kappa-light-chain-enhancer’ of activated B cells
NK cell	Natural killer cell
NLR	NOD-and leucine-rich repeat-containing receptor
nm	Nanometer
NOD	Nucleotide-binding and oligomerization domain
OD	Optical density
OMV	Outer membrane vesicle
OTU	Operational taxonomic units
PAGE	Polyacrylamide gel electrophoresis
PAMP	Pathogen-associated molecular pattern
PBS	Phosphate buffered saline
PCR	Polymerase chain reaction
PFA	Paraformaldehyde
PIPES	Piperazine-N,N’-bis(2-ethanesulfonic acid)
PLA_2	Phospholipase A2
PMN	Polymorphonuclear cells neutrophil
PMSF	Phenylmethylsulfonylfluorid
PP(s)	Peyer’s patch(es)
PRR	Pattern recognition receptor
pYV	Plasmid of *Yersinia* virulence
qRT-PCR	Quantitative real-time PCR
R	Resistance
Rho	Ras-homologous
RIG I	Retinoic acid-inducible gene I
RIN	RNA integrity number
RLR	RIG I-like receptor
RNA	Ribonucleic acid
ROS	Reactive oxygen species
rpm	Revolutions per minute
rRNA	Ribosomal RNA
RT	Room temperature
s	Second(s)
SA	Streptavidin
SAA	Serum amyloid A
SD	Standard deviation
SDS	Sodiumdodecylsulfate
SEM	Standard error of the mean
SLR	Sequestosome I-like receptor
SOC	Super optimal broth
SPI-1/2	*Salmonella* pathogenicity island-1/2
spp.	*Species pluralis*
TAE	Tris-acetate-EDTA
TBE	Tris-borate-EDTA
TBFI/II	Transformation buffer I/II
TE	Tris-EDTA buffer
TEMED	Tetramethylethylenediamine
T_H cell	Helper T cell
TLR	Toll-like receptor

TNF	Tumor necrosis factor
Treg	Regulatory T cell
TTS(S)	Type three secretion (system)
U	Units
UniProt	Universal Protein Resource
UPEC	Uropathogenic *E. coli*
UTI	Urinary tract infection
UV	Ultra violet
V	Volt
VacA	Vacuolating cytotoxin A
vs.	Versus
v/v	Volume per volume
w/v	Weight per volume
WHO	World Health Organization
YadA	*Yersinia* adhesin A
Ybt	Yersiniabactin
Yop	*Yersinia* outer protein
Ysc	Yop secretion
µ	Micro

Figures

Tables

1 Introduction

In the world, about 1.7 billion cases of diarrheal illness are reported every year. According to the global health estimates (GHE) for 2000-2015, diarrheal diseases are the eighth leading cause of death of the global population with 1.4 million deaths in 2015. Alarmingly, diarrheal disease in children under five years is actually the second leading cause of death worldwide (World Health Organization (WHO), Fact sheet No. 330, April 2013; WHO, GHE 2000-2015). In Germany, the main bacterial agents of diarrheal illness are *Campylobacter* (70,190 cases in 2015), *Salmonella* (13,823 cases in 2015) and *Yersinia* (2,752 cases in 2015) ("Infektionsepidemiologisches Jahrbuch meldepflichtiger Krankheiten für 2015", Robert-Koch-Institut). However, there are no global estimates or epidemiological studies that report about the prevalence of persistent bacterial infections or the amount of complications that accompany/follow bacterial infections. Although some persistent bacterial infections and their health risks have long been known, the mechanisms and factors that are required for bacterial persistence are just beginning to be understood. Even the full comprehension of the complex host-pathogen interactions during acute infections is not complete. These topics are of interest, as chronic infections increase health care expenses. Thus, there is a consequent need for exploration of new treatment possibilities to decrease the burden of chronic infections for the society and human health. In order to identify new treatment targets and strategies, the mechanisms, which cause chronic disease, have to be elucidated. This study investigates the influence and role of a *Yersinia* encoded toxin on pathogenesis and host-pathogen interactions during acute and persistent infection.

1.1 Mammalian host defense strategies against bacterial infection

In order to defend the organism against bacterial infection, mammals have evolved a complex defense machinery to prevent, recognize and clear infection. This is enabled by the maintenance and defense traits of barriers (1.1.1), cell autonomous immunity programs (1.1.2), secretion of protective factors facilitating phagocytosis (*e.g.* complement, opsonins) (1.1.3), and specific immune cells that are responsible for pathogen elimination (1.1.4).

1.1.1 Immune defenses at the intestinal barrier

The gastrointestinal tract constitutes the largest surface in mammals and is colonized by a commensal microbiota that gives a home to 10^{13} to 10^{14} microorganisms supporting the digestive process (Ley *et al*., 2006; Hill and Artis, 2010). The intestine's main function is to absorb nutrients from the digestive tract to guarantee energy and essential component supply. Beyond that, the intestinal tract has to defend and prevent microbial encroachment by commensal or pathogenic bacteria. On top, the organism must retain tolerance to food antigens and the microbiota, yet preserving the capacity to mount effective immune defense and inflammation upon intestinal infection.

Nutrient and essential component absorption is mainly facilitated through enterocytes, which make up the majority of all intestinal epithelial cells (IECs). However, enterocytes also create a dense physiological barrier. To this purpose, they affiliate to a selective, impermeable lining. This barrier is assembled by the formation of junctional complexes that consist of tight junctions and adherens junctions (Turner, 2009; Goto and Kiyono, 2012). Moreover, enterocytes express alkaline phosphatases that support detoxification of microbiota-derived

lipopolysaccharides (LPS) (Bates *et al*., 2007). Another IEC type is the goblet cell that secretes highly glycosylated mucins into the intestinal lumen in order to create a contact barrier (mucus) between the epithelium and the commensals (Bergstrom *et al*., 2010). The glycosylation of mucins also generates adhesive attachment sites that are able to capture bacteria (Sansonetti, 2004; Barr *et al*., 2013). In addition, the mucus contains immunoglobin A (IgA) and bactericidal molecules. The mucosal IgA captures antigens and microbes, thus inhibiting their encroachment to the epithelium, a mechanism termed immune exclusion (Brandtzaeg, 2009). The antimicrobial molecules are produced and secreted by IECs, called paneth cells, consequently mediating killing of the mucus-trapped bacteria. Among the antimicrobial effectors are α-defensins, C-type lectins, lysozymes, phospholipase A2 (PLA_2), and angiogenin 4 (Mukherjee *et al*., 2008). Especially, the bacteriolytic C-type lectin RegIIIγ is important for prevention of microbial invasion, since it creates a 50 µm thick bacteria-free area above the epithelial cell layer (Vaishnava *et al*., 2011; Mukherjee *et al*., 2014).
The intact microbiota is also considered as a protective organ that usually expels other bacteria from manifestation. Hence, the normal microbiota outcompetes the invader by vying for colonization niches and nutrients (O'Hara and Shanahan, 2006).
Immune responses and tolerance to harmless antigens are conferred by a special part of the intestinal epithelium, referred to as follicle-associated epithelium (FAE), that overlays the gut-associated lymphoid tissue (GALT), denoted as Peyer's patches (PPs) (Miller *et al*., 2007). Embedded into the FAE are microfold (M) cells, which sample antigens from the lumen and transfer them to the PP (Kraehenbuhl and Neutra, 2000). Controversially, this function makes the organism vulnerable to infection since many pathogens evolved mechanisms to exploit M cells as primary entry sites, *e.g. Salmonella* (Jepson and Clark, 2001). Inside the PP, antigen presentation by dendritic cells (DCs) stimulates B cells to mature into mucosal IgA-producing B cells (Wershil and Furuta, 2008). In addition, DC-mediated transport of antigens into the draining mesenteric lymph nodes (MLNs) triggers development of systemic antigen tolerance (Pabst *et al*., 2007).
Upon infection, intestinal epithelial cells are also able to initiate inflammation and contribute to pathogen killing (Eckmann and Kagnoff, 2005; Ramanan and Cadwell, 2016). These defense mechanisms are described in section 1.1.2.

1.1.2 Cell-autonomous immunity

Eukaryotic cells are a source of nutrients for pathogens. Therefore, evolution drove the development of intrinsic cellular immune defense mechanisms, referred as cell-autonomous immunity, which protect both individual immune and non-immune cells against the microbial invaders. Cellular compartmentalization and pattern recognition receptors (PRRs) that sense cellular integrity and microbial components are central elements of cellular self-defense. These sensors recognize damage-associated molecular patterns (DAMPs; *e.g.* mitochondrial DNA, glycans) after breakdown of cellular compartments or pathogen-associated molecular patterns (PAMPs; *e.g.* LPS, flagellin) (Figure 1.1). Furthermore, the PRRs are categorized into **T**oll-**L**ike **R**eceptors (TLRs), **R**etinoic acid-**I**nducible **G**ene I (RIG I)-**L**ike **R**eceptors (RLR), **C**-type **L**ectin **R**eceptors (CLRs), Nucleotide-binding and Oligomerization Domain (**N**OD)- and **L**eucine-rich repeat-containing **R**eceptors (NLRs), Absent In Melanoma II (**A**IM2)-**L**ike **R**eceptors (ALRs) and **S**equestosome I-**L**ike **R**eceptors (SLRs) (Barton and Kagan, 2009; Ronald and Beutler, 2010; Hansen *et al*., 2011; Mostowy and Shenoy, 2015; Yu and Gao,

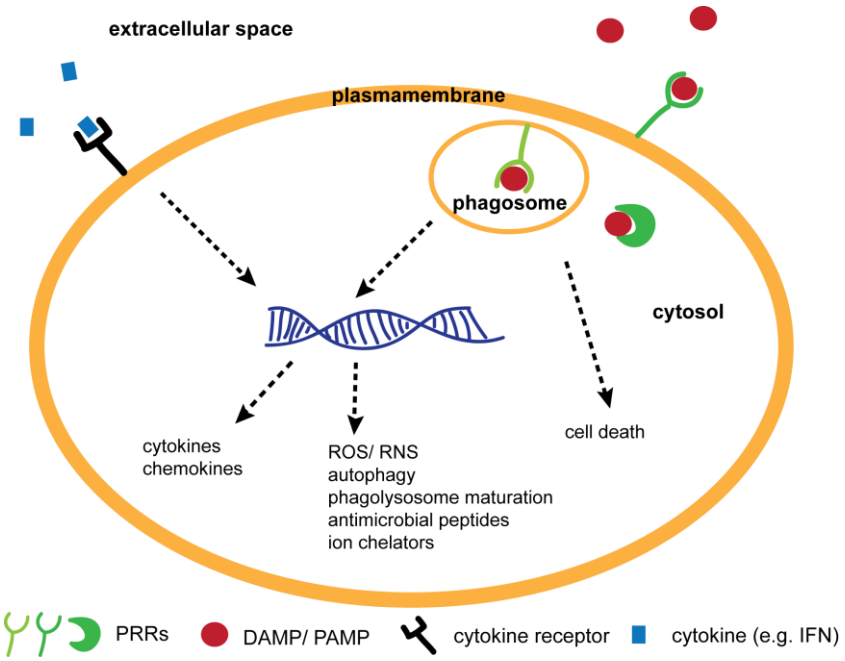

Figure 1.1 Mechanisms of cell autonomous immunity.

The eukaryotic immune and non-immune cells are able to sense DAMPs and PAMPs by the expression of special PRRs in the extracellular space, the cytosol and inside compartments, *e.g.* phagosome. Moreover, these cells are able to respond to the exposure to cytokines. After sensing of cytokines or DAMPs/ PAMPs, downstream cascades are triggered that induce cellular death pathways, the production and/or maturation of cytokines and chemokines or the activation of various bacteriostatic and/ or bactericidal defense paths.

2015). In particular, activation of TLR, RLR and ALR initiates signal transduction cascades, for instance via mitogen-activated protein kinases (MAPK), which result in the induction of transcription factors. Those trigger the expression of cellular defense genes such as pro-inflammatory cytokines (Bonizzi and Karin, 2004; Arthur and Ley, 2013). However, the immune signaling cascades can also induce apoptosis or necroptosis (programmed necrosis). Apoptosis is an immunologically silent cell death program, which facilitates the clearance of infected cells by phagocytosis, whereas necroptosis promotes membrane permeabilization, cellular swelling and finally plasma membrane rupture, thereby releasing cellular contents (Oberst, 2016; Vanden Berghe *et al.*, 2016). Besides removal of infected cells, the role of necroptosis in driving inflammation by the release of DAMPs is less clear. There are many hypotheses discussed that suggest necroptosis rather as an intrinsic adjuvant or terminator of inflammatory programs (Kiraz *et al.*, 2016; Oberst, 2016). Moreover, NLRs and ALRs recognize microbial infection through the detection of *e.g.* microbial DNA, flagellin or bacterial proteins in the host cell cytosol. Subsequently, multi-protein-platforms called inflammasomes, containing NLR/ALR, apoptosis-associated speck-like protein containing CARD (ASC) and pro-caspase-1 are assembled, leading to the proteolytic activation of pro-caspase-1. Active caspase-1 processes the pro-inflammatory cytokines interleukin (IL)-1β/-18 and triggers pro-inflammatory lytic cell death, known as pyroptosis. Besides potent induction of inflammation through the release of ATP or IL-1α, pyroptosis also supports intracellular pathogen elimination (Aachoui *et al.*, 2013; Broz and Monack, 2011). Since pathogens have evolved multiple mechanisms to subvert different types of cell death, the variety of cell death mechanisms highlights the importance for the host to eliminate infected cells (Figure 1.1) (Ashida *et al.*, 2011). In turn, production and secretion of cytokines and chemokines alerts the host immune system, fostering the activation and recruitment of immune cells to the site of infection. In addition, secreted cytokines, such as interferons (IFN), prompt further cell-

autonomous host defenses by induction of IFN-stimulated effector genes. Among those are the oxidative and nitrosative defense, phagosome maturation and autophagy (Figure 1.1) (MacMicking, 2012). Furthermore, eukaryotic cells create hostile intracellular environments by the limitation of deoxynucleotide triphosphates, amino acids, essential ions such as $Zn^{2+}$and Mn^{2+}, through the production and delivery of antimicrobial peptides, and via acidification of phagosomes (Figure 1.1) (Randow *et al*., 2013).
Those mechanisms are essential for sterilizing immunity in both immune and non-immune cells promoting microbial clearance or at least growth and dissemination control.

1.1.3 First defense lines of innate immunity

As described before, the recognition of microbial infection via PRRs not only activates cell-autonomous immunity, but also triggers secretion of pro-inflammatory cytokines. Among these are tumor necrosis factor α (TNFα), IL-1 and IL-6 that are potent inducers of acute phase response in the liver and other tissues. After the induction of the acute phase response, a set of acute phase proteins are produced and secreted, in order to enhance systemic resistance to bacterial infection (Heinrich *et al*., 1990; Alcorn *et al*., 1992; Baumann and Gauldie, 1994; Kopf *et al*., 1994; Urieli-Shoval *et al*., 2000). The major acute phase proteins are C-reactive protein (CRP) and serum amyloid A (SAA), though other proteins additionally contribute to the acute phase response, *e.g.* complement factor-3 (C3), the iron chelator haptoglobin or LPS-binding protein (Gruys *et al*., 2005). During the acute phase response, the major acute phase reactant CRP opsonizes the microbial invader concomitantly activating the complement system and phagocytosis (described below) (Black *et al*., 2004). In mice, SAA is produced as three different isoforms that fulfill diverse functions (Butler and Whitehead, 1996; Chiba *et al*., 2009). SAAs opsonize bacteria, bind retinol to restrict bacterial loads, attract phagocytes and modulate immune responses (Badolato *et al*., 1994; Patel *et al*., 1998; Furlaneto and Campa, 2000; Shah *et al*., 2006; De Santo *et al*., 2010; Derebe *et al*., 2014; Sun *et al*., 2015). Hence, the acute phase response participates in pathogen growth control and mediation of proper immune responses upon infection.
The complement system is one of the oldest first lines of innate immune defense (Zhu *et al*., 2004). Upon bacterial infection, the complement system is activated through three alternate pathways: the classical, the alternative and the lectin pathway. Two of these pathways require the initial detection of the pathogen surface by antibodies (classical pathway) or PRRs (lectin pathway) (Figure 1.2). However, the activation of complement through the alternative pathway depends on self-amplification loops via spontaneous hydrolysis of C3 or C3-binding to LPS (Figure 1.2) (Joiner *et al*., 1986; Janeway *et al*., 2001). Sequential proteolytic cascades then lead to opsonization of the pathogen with complement, resulting in phagocytosis, formation of a lytic membrane attack complex and production of pro-inflammatory mediators (anaphylatoxins) (Figure 1.2) (Dunkelberger and Song, 2010). The interaction of opsonized pathogens and phagocytes induces not only clearance of immune complexes, but also advances secretion of pro-inflammatory cytokines (IL-1), antigen presentation to B cells and their activation (Papamichail *et al*., 1975; O'Neil *et al*., 1988; Bacle *et al*., 1990; Carter and Fearon, 1992; Fang *et al*., 1998; Krych-Goldberg and Atkinson, 2001; Helmy *et al*., 2006). Hence, complement serves also as an adjuvant for development of adaptive immunity (Dempsey *et al*., 1996). Furthermore, complement by-products stimulate cytokine production, degranulation, oxidative burst and recruitment of innate immune cells (*e.g.* neutrophils and macrophages) (Figure 1.2) (Hugli and Muller-Eberhard, 1978; Haas and van Strijp, 2007).

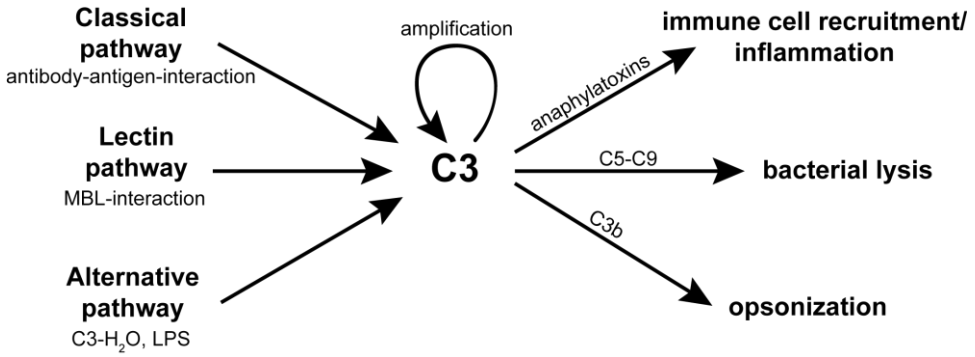

Figure 1.2 The complement system.
The recognition of bacterial pathogens leads to the activation of the complement system cascade via the classical, lectin or alternative pathway. The decomposition of C3 leads to self-amplification of the cascade. Sequential proteolysis leads to opsonization of certain pathogens and cells, the formation of the lytic membrane attack complex and immune cell recruitment/ inflammation.

Another important system of early immune defense is the coagulation cascade. As upon activation of the complement system, coagulation activation by the extrinsic pathway (tissue factor-mediated) or intrinsic pathway (contact-mediated activation at the bacterial surface) leads to a proteolytic cascade that leads to the formation of a fibrin clot (van der Poll and Herwald, 2014). This fibrin clot is able to trap pathogens prohibiting further bacterial dissemination (Loof *et al*., 2011). In addition, the whole coagulation cascade is linked to antimicrobial activities and the induction of inflammatory responses. The tissue factor regulators and the generation/release of antimicrobial peptides were associated with bactericidal actions during active coagulation (Nordahl *et al*., 2005; Frick *et al*., 2006; Papareddy *et al*., 2010). Moreover, the tissue factor and other coagulation factors were shown to trigger production of pro-inflammatory cytokines and chemokines such as IL-6, IL-8, IFNγ and MCP-1 (Chu, 2005; Monteiro *et al*., 2006; Shrivastava *et al*., 2007; Srinivasan and Bogdanov, 2012; Åberg and Siegbahn, 2013). Besides its roles during inflammation, coagulation also facilitates wound closure, tissue healing and regeneration (Versteeg *et al*., 2013). Therefore, coagulation provides a powerful innate immune mechanism during early host immunity to control bacterial dissemination, kill invading pathogens and restore tissue homeostasis.

1.1.4 Cellular defense effectors in immunity

Mammalians home a complex diversity of immune cells in their organism, which is constantly expanded by new cellular sub-populations and maturation states with specialized functions. Moreover, cellular immune defense is a multifaceted orchestra that is able to react to incoming stimuli and interact with other immune cells. In the classical view, leukocytes are divided into innate and adaptive immune cells (Dranoff, 2004). However, these distinct borders are constantly blurring. This section will concentrate on the most important basic functions of innate and adaptive immune cells.
Next to the initial recognition of bacterial infection (1.1.2), innate immune cells are rapidly recruited to the site of infection. Among them are polymorphonuclear phagocytes (PMNs), macrophages, DCs and monocytes. PMNs, also known as neutrophils, are the first recruited leukocytes before others arrive (Witko-Sarsat *et al*., 2000). After encountering the pathogenic agent, neutrophils execute potent microbial killing programs. To this purpose, neutrophils phagocytose the pathogen into the phagosome, where they are killed by the production of reactive oxygen species (ROS), and via fusion with intracellular stored granules, which contain

antimicrobial/digestive proteins (Leto and Geiszt, 2006; Borregaard *et al*., 2007; Nordenfelt and Tapper, 2011). Moreover, neutrophils de-granulate their intracellular vesicle contents and extrude nuclear DNA into the extracellular space, both inhibiting bacterial growth in the surrounding environment (Brinkmann *et al*., 2004; Soehnlein, 2009). However, PMNs are short living cells that enter apoptosis after several days, thereby commencing the resolution of inflammation and their removal by macrophages (El Kebir and Filep, 2010; Mantovani *et al*., 2011).

Since macrophages harbor diverse functionalities, they are central parts of innate immunity (Gordon and Taylor, 2005). In general, there are two main functional phenotypes of macrophages, *i.e.* classically activated (M1) and alternatively activated (M2) macrophages (Gordon and Martinez, 2010). M1 macrophages differentiate upon LPS and IFNγ exposure and proceed to pro-inflammatory (*e.g.* TNFα secretion) and antimicrobial actions. In contrast, stimulation with IL-4 and IL-13 drives M2 macrophage polarization. Those cells are participating in tissue repair, immune-regulatory and anti-inflammatory processes, for example IL-10 secretion (Locati *et al*., 2013; Striz *et al*., 2014; Juhas *et al*., 2015). The capability of phagocytosis plays not only an important role in pathogen killing, but also in the resolution of inflammation by removing dead cells and cell debris (Biswas *et al*., 2012). Macrophages process the collected pathogen-derived antigens and present them via major histocompatibility class II complexes (MHCII) to T cells (Kaye, 1995). Hence, macrophages collaborate with different arms of immunity, *i.e.* inflammation modulation, infection resolution, and adaptive immunity.

DCs are primarily known for their professional antigen presentation abilities to T cells. Via the expression of PRRs, DCs sense pathogens and tissue damage subsequently triggering phagocytosis (Merad *et al*., 2013). After antigen processing, DCs present the antigens to T cells (Dudziak *et al*., 2007; Villadangos and Schnorrer, 2007; Segura and Villadangos, 2009; Joffre *et al*., 2012). Importantly, DCs are not only able to present antigens to $CD4^+$ T cells (T_H cells) via MHCII, but also cross-present MHCI bound antigens to $CD8^+$ T cells (cytotoxic T cells, CTLs). Therefore, DCs are unique antigen presenting cells that are able to prime T_H cell and CTL responses (Banchereau and Steinmann, 1998; den Haan *et al*., 2000; Idoyaga *et al*., 2008). Yet, DCs also contribute to the development of central and peripheral tolerance through the induction of regulatory T cells (Tregs) (Proietto *et al*., 2008; McLachlan *et al*., 2009; Vitali *et al*., 2012).

The mounting of specific adaptive immunity is important to clear the infection and develop immunological memory. In general, naïve T cells become activated when they recognize their equivalent antigen and receive co-stimulatory signals. Thereafter, those cells undergo a clonal expansion and differentiate to effector T cells, for instance CTLs, T_H1, T_H2, and T_H17 (Figure 1.3) (Murphy, 2012). Effector CTLs are cytotoxic and antigen-specifically lyse target cells by degranulation of vesicles containing perforin, and granzymes A and B (Figure 1.3) (Gerritsen and Pandit, 2016). On the other hand, T_H cells are subdivided into different subsets depending on their cytokine profiles thereby performing different functions during adaptive immune responses (Figure 1.3) (Raphael *et al*., 2015; Golubovskaya and Wu, 2016). T_H1 cells mainly produce IFNγ, thus enhancing bacterial killing by phagocytes (Berger, 2000). In contrast, T_H2 cells are immune modulatory, promoting immunoglobin class switches in B cells, M2 macrophage polarization and suppress T_H1 differentiation (Vitetta *et al*., 1985; Swain *et al*., 1990; Chen *et al*., 2012). Moreover, T_H17 cells are highly inflammatory effector cells, which induce the recruitment of neutrophils, production of antimicrobial peptides and tissue repair (Ouyang *et al*., 2008). On the contrary, immune responses are dampened by

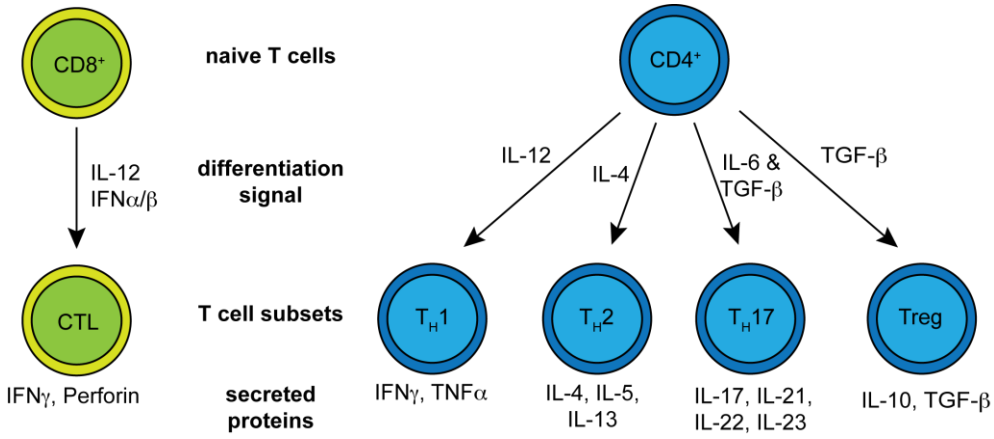

Figure 1.3 T cell differentiation.

Interaction of a naïve T cell with an antigen-presenting cell triggers effector T cell differentiation. The differentiation of activated T cells involves signaling by different cytokines, which drive the expression of transcription factors. These initiate T cell subset commitment and secretion of a certain cytokines profile. The picture is adapted from Jetten, 2007[1] and Pennock *et al*., 2013[2].

Tregs. Thus, Tregs inhibit the activation, expansion and function of various immune cell types, for example cytokine production and cytotoxic activities (Miyara and Sakaguchi, 2007).
The other branch of adaptive immunity is B cells. Those produce protective antibodies specific for an antigen. As upon T cell activation, B cells become activated by the exposure to an antigen. This is followed by somatic hyper-mutation leading to the development of high-affinity antibodies. Those antibodies opsonize pathogens, tagging them for phagocytosis (Zhang *et al*., 2016b).

1.2 The enteropathogenic *Yersinia*

The genus *Yersinia* belongs to the phylum of γ-Proteobacteria in the family of *Enterobacteriaceae* (Bottone, 1997). Generally, yersiniae are Gram-negative, non-spore forming rod-shaped coccobacilli that grow as facultative anaerobes. As they are psychrotolerant, they are capable of growing at temperatures between 4 °C and 43 °C with an optimal growth behavior at 25-29 °C (Bercovier and Mollaret, 1984; Kapatral and Minnich 1995).
In 1894, the bacteriologist Alexandre Yersin first isolated the causative agent of plague (*Pasteurella pestis*), which was later re-named in memory of its discoverer, *Yersinia pestis* (van Loghem 1944; Hawgood, 2008). Up to date, the *Yersinia* genus encompasses 15 non-human-pathogenic and three recognized human-pathogenic species (spp.): the causative agent of bubonic and pneumonic plague, *Y. pestis*, and the two enteropathogens, *Y. enterocolitica* and *Y. pseudotuberculosis* (Lehmann and Neumann 1896; van Loghem 1944; Smith and Thal 1965; Ewing *et al.* 1978; Bercovier *et al.* 1981; Brenner *et al.* 1981; Ursing *et al.* 1981; Bercovier *et al.* 1984; Aleksic *et al.* 1987; Wauters *et al.* 1988; Cover and Aber, 1989; Pfeiffer 1889; Sprague and Neubauer 2005; Sprague *et al.* 2008; Hurst *et al.* 2011; Merhej *et al.* 2008; Murros-Kontiainen *et al.* 2011a,b; Savin *et al.* 2014). These pathogenic *Yersinia* spp. share the ability to transmit via zoonotic infections but differ between their transmission and infection route. Whereas the enteropathogenic *Yersinia* spp. are transmitted via the fecal-oral route,

[1] Jetten (2007) is licensed under the Creative Commons Non-Commercial Attribution license.
[2] Permitted for use/adaptation in a doctoral thesis/dissertation by the American Physiological Society [T cell responses: naïve to memory and everything in between, Pennock *et al*., copyright ©2013].

Y. pestis exhibits a complex lifestyle and is transmitted to humans by fleas, inhalation of infectious aerosols or more rarely, via infected animals (Perry and Fetherston, 1997; Galindo *et al*., 2011) However, they still share a common tropism for lymphatic tissues and the ability to subvert host innate immune responses (Cornelis *et al*., 1998). *In silico* phylogenetic analyses revealed that the enteropathogenic *Yersinia* spp. experienced a parallel and independent evolution. Thereby, they presumably separately acquired the major *Yersinia* pathogenic factor, the virulence plasmid pYV (Reuter *et al*., 2014). Moreover, genomic and ancient DNA analysis of *Y. pestis* genomes revealed that the most virulent *Yersinia* spp., *Y. pestis*, emerged from the less pathogenic, environmental-stress adaptable *Y. pseudotuberculosis* about 35,000 to 79,000 years ago. Surprisingly, *Y. pseudotuberculosis* and *Y. pestis* still share a sequence identity of 97 % (Achtman *et al*., 1999; Rasmussen *et al*., 2015). However, about 13 % of the *Y. pseudotuberculosis* genes are either inactivated (*e.g. yadA*, O antigen cluster) or absent (*e.g. lpxL*) in *Y. pestis*. Furthermore, *Y. pestis* has acquired two additional virulence plasmids pPCP1 and pMT1 that encode important factors for vector-borne transmission and establishment of bubonic and pneumonic plague. This acquisition and decay of genes drove the evolution towards a highly virulent human pathogen with extreme adaptation capacity to its vector and hosts (Zhou and Yang, 2009; Hinnebusch *et al*., 2016).

Usually, infection with *Y. pseudotuberculosis* and *Y. enterocolitica* takes place by the ingestion of contaminated food products. Yet, both *Yersinia* spp. were isolated from environmental sources such as soil and water but were also found in animal reservoirs (*e.g.* bats, wild boars, rodents and goats) (Langford, 1972; Fukushima *et al*., 1995; Sulakvelidze *et al*., 1996; Mühldorfer *et al*., 2010; Giannitti *et al*., 2014; von Altrock *et al*., 2015). In the past years, several outbreaks and reports of *Yersinia* infections were documented in association with contaminated pork products, milk and vegetables (Nuorti *et al*., 2004; Rahman *et al*., 2011; Longenberger *et al*., 2014; Vasala *et al*., 2014; Pärn *et al*., 2015).

Infections with enteropathogenic *Yersinia*, referred to as yersiniosis, usually cause self-limiting invasive disease accompanied by an acute inflammatory response comprising of afflictions such as gastro-enterocolitis, acute mesenteric lymphadenitis, terminal ileitis and pseudoappendicitis. Furthermore, acute disease symptoms resemble most enteric bacterial infections including fever, abdominal pain and watery to bloody diarrhea (Dube, 2009). Incidence of yersiniosis is age-linked. It occurs frequently in infants and young children in case of *Y. enterocolitica*, whereas *Y. pseudotuberculosis* cases are more commonly documented in adolescents and young adults (Smego *et al*., 1999). In rare cases, yersiniosis or transfusion of *Yersinia*-contaminated blood might manifest systemically in healthy individuals or patients with either pre-existing disorders or immunodeficiency, resulting in high fatality rates (Bottone, 1997).

Occasionally, individuals develop autoimmune disorders and severe sequelae after an acute intestinal *Yersinia* infection. Besides Kawasaki disease, inflammatory bowel disease and Grave's disease, reactive arthritis and erythema nodosom are the most common ones (Hannu *et al*., 2003; Jalava *et al*., 2006 Hargreaves *et al*., 2013; Leu *et al*., 2013; Horinouchi, *et al*., 2015). Reactive arthritis frequently occurs after acute enteric infections in individuals that are positive for human leukocyte antigen (HLA) type B27 (Stavropoulos *et al*., 2015). Yet, the pathogenesis of reactive arthritis is not well understood. Upon reactive arthritis, bacterial components (microbial DNA or proteins) are detectable in synovial fluids of patients suggesting the transport of bacteria/bacterial components from the primary infection site to the joint (Granfors *et al*., 1989). This might initiate the infiltration of *Yersinia*-specific $CD4^+$ and $CD8^+$ T cells into the synovial fluids of reactive arthritis patients (Ugrinovic *et al*., 1997; Mertz *et al*., 1998). Moreover, imbalances of T_H1/T_H2 responses in the synovial fluids of patients

with reactive arthritis were documented; including decreased pro-inflammatory cytokine production (*i.e.* TNFα and IFNγ) with elevated anti-inflammatory cytokine release (*i.e.* IL-10) by $CD4^+$ T cells (Simon *et al*. 1994; Yin *et al*., 1997; Smeets *et al*., 1998; Braun *et al*., 1999; Mertz *et al*., 2000). The imbalance of cytokine production was proposed to either control the hypersensitive immune response against the bacterium or contribute to bacterial persistence and prolonged arthritis. Indeed, more studies hint towards a contribution of IL-10 to sustained reactive arthritis and delayed bacterial clearance (Sieper, 2004).
In rodent animal models, most characteristics of human yersiniosis are mimicked, including enteritis and the development of reactive arthritis (Heesemann *et al*., 1993a). Hence, the natural rodent pathogen *Y. pseudotuberculosis*, which is able to cause enteric disease in humans, represents an ideal model organism to study pathogenicity and virulence mechanisms.

1.2.1 Virulence factors of enteropathogenic *Yersinia* spp.

Virulence factors are crucial for pathogens to promote and maintain infection in a susceptible host. Furthermore, pathogens require them to gain the competence to develop a certain pathogenic mechanism, referred to as bacterial pathogenesis. Common microbial pathogenic mechanisms include (1) attachment and invasion, (2) evasion of/resistance to host immunity, (3) nutrient acquisition and growth, and (4) transmission to the environment or a new host (Groisman, 2001). Additionally, host specificity and host species barrier crossing depends on the pathogens virulence factor repertoire (Bäumler and Fang, 2013).
The enteropathogenic yersiniae possess a large collection of chromosomally and virulence plasmid encoded virulence factors to colonize different hosts and develop pathogenicity (Gemski *et al*., 1980; Portnoy and Falkow 1981; Brubaker, 1991). Although the virulence plasmid is crucial for the invasiveness of *Yersinia*, additional chromosomal factors are required to cause full pathogenicity (Zink *et al*., 1980; Heesemann and Laufs, 1983; Heesemann *et al*., 1984; Green *et al*., 2016). Since expression of virulence factors constitutes a metabolic burden for the pathogen, virulence factors of *Yersinia* are tightly regulated and respond mostly to temperature (Brubaker, 1983; Straley *et al*., 1993; Ramamurthi and Schneewind, 2002; Erhardt and Dersch, 2015).
Early after the ingestion of contaminated nutrition, *Yersinia* has to tolerate the acidic gastric environment ranging from pH 1.0 to 2.5 (Evans *et al*., 1988). To this purpose, enteropathogenic yersiniae harbor a chromosomally encoded urease operon, which leads to the neutralization of protons, diminishing acidity (De Koning-Ward and Robins-Browne, 1995; Hu *et al*., 2009).
To cross the intestinal barrier and to effectively deliver their main virulence factors into the host cells, *Yersinia* expresses several adhesins either on their chromosome (*e.g. ail*, *inv* and *psa*) or virulence plasmid (*yadA*). In the initial infection phase, invasin (InvA) is essential for initial tissue invasion in the intestine (Isberg *et al*., 1987; Clark *et al*., 1998; Hamburger *et al*., 1999). At later stages of infection, *Yersinia* adhesion A (YadA) is the major adhesin performing diverse functions. Thus, YadA mediates close contact to a broad range of host cells facilitating effector protein translocation into the host cell via binding to extracellular

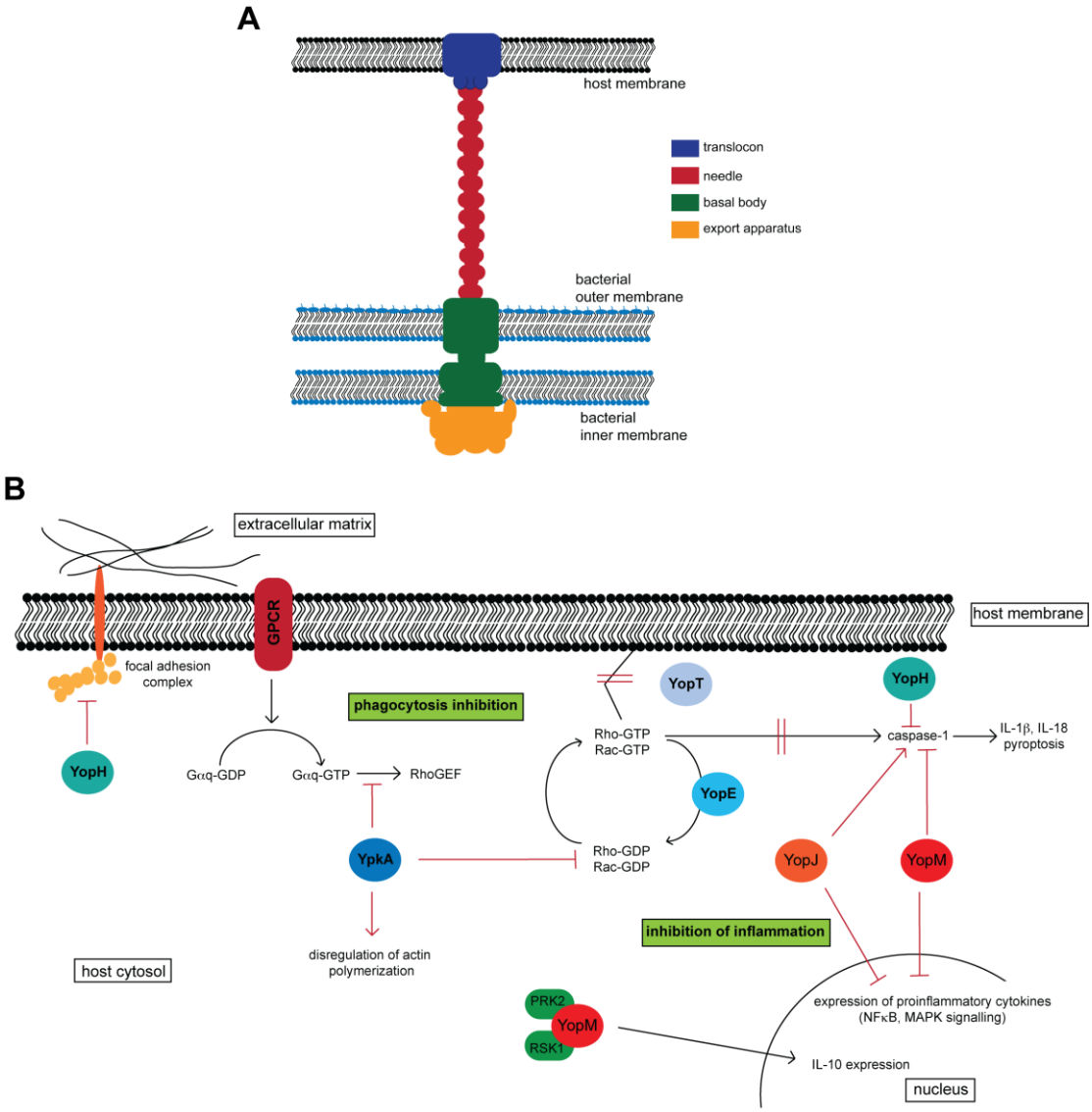

Figure 1.4 *Yersinia* type three secretion.

The TTSS is a molecular nanomachine, which, upon host cell contact, spans from the bacterial cytosol into the host cell membrane, translocating effector proteins (Yops) into the host cytosol. (A) The TTSS consists of an export apparatus conferring secretion competence (yellow), a membrane spanning basal body anchoring the secretion system into the bacterial membranes (green), a needle structure (red), and the translocon that forms a pore in the host membrane (blue). (B) The Yop effectors disrupt the host immune response by inhibition of phagocytosis and pro-inflammatory gene expression. YpkA is primary involved in inhibition of phagocytosis by deregulating actin polymerization and small Rho GTPase activities. Likewise, phagocytosis is also blocked by YopE, which deactivates small Rho-GTPases, YopT that delocalizes small Rho-GTPases from the plasma membrane, and YopH that interrupts focal adhesion complexes. The deactivation of the small Rho-GTPases interrupts caspase-1 activation and the production of pro-inflammatory reactions by the inflammasome. Moreover, YopH and YopM block inflammasome activation. Controversially, YopJ activates caspase-1 and promotes inflammation, though it blocks NFkB and MAPK signaling preventing the expression of pro-inflammatory cytokines. In line with its anti-inflammatory function, YopM also blocks transcription of pro-inflammatory cytokines and induces anti-inflammatory cytokine production (*e.g.* IL-10). G protein-coupled receptor (GPCR). The figure is adapted from Pha and Navarro, 2016.[3]

[3] Pha and Navarro (2016) is licensed under the Creative Commons Attribution Non Commercial (CC BY-NC 4.0) license. http://creativecommons.org/licenses/by-nc/4.0/

matrix components (*e.g.* collagen, fibronectin, laminin) or αV integrins (Tertti *et al*., 1992; Flügel *et al*., 1994; Visser *et al*., 1995; Tahir and Skurnik, 2001; Keller *et al*., 2015). Moreover, YadA was shown to induce hemagglutination, promote epithelial cell invasion, serum resistance, and cause bacterial auto-aggregation to phagocytosis-resistant microcolonies (Skurnik *et al*., 1984; Balligand *et al*., 1985; Hoiczyk *et al*., 2000; Eitel and Dersch, 2002; Biedzka-Sarek *et al*., 2008a; Biedzka-Sarek *et al*., 2008b; Kirjavainen *et al*., 2008). As *Yersinia* expresses several adhesins, their functions are also redundant: the chromosome encoded adhesin Ail (attachment invasion locus) and the PsaA fimbriae mediate the adherence of the bacterium to host cells, but are also contributing to agglutination of erythrocytes, serum resistance and binding of human immunoglobin (Bichowsky-Slomnicki and Ben-Efrain, 1963; Pierson and Falkow, 1993; Yang *et al*., 1996; Zav'yalov *et al*., 1996; Yamashita *et al*., 2011). This redundancy might facilitate adherence to a broad spectrum of host cells and manage crossing of host species barriers. Subsequent to invasion into the host tissue, bacteria are confronted with the host innate immune system functioning to combat the invaded pathogen. In order to evade the host immune response, pathogens employ a virulence mechanism known as Type III secretion (TTS), which allows the bacteria to directly inject effector proteins into the host cell cytosol (He *et al*., 2004a). In *Yersinia*, this TTS system (TTSS) is encoded on the virulence plasmid consisting of a collection of effector proteins, termed *Yersinia* outer proteins (Yops), and the Yop secretion (Ysc) apparatus (Cornelis, 2002). The Ysc machinery is composed of a cytosolic export apparatus, a membrane-spanning multi-protein complex called the basal body, an extracellular needle-like structure consisting of polymerized protein and the translocon at the needle tip that inserts into the host membrane (Figure 1.4A) (Izoré *et al*., 2011). Upon host cell contact, this machinery is able to translocate six different Yop effectors, namely YopH, YopE, YopT, YpkA, YopJ and YopM into the host cell cytosol to manipulate host cell functions and signaling (Figure 1.4) (Cornelis *et al*., 1998). The Yop effector proteins display diverse functions that primarily target Rho GTPases (YpkA, YopE, YopT) and ultimately lead to inhibition of phagocytosis (YopH, YpkA, YopE, YopT) (Viboud and Bliska, 2005). However, Yops also serve to inhibit/activate caspase-1 (YopM, YopE, YopJ), suppress pro-inflammatory cytokine/chemokine production (YopE, YopH, YopJ, YopM), inhibit production of ROS (YopH), activate apoptosis (YopJ, YopM), inhibit cellular immune signaling pathways (YopH, YopT) or induce anti-inflammatory cytokine production (YopM) (Figure 1.4B) (Pha and Navarro, 2016).

As the host limits the availability of essential ions (*e.g.* iron, magnesium), pathogenic bacteria have evolved iron up-take systems to ensure bacterial fitness and physiology (Carniel, 2001; Abu Kwaik and Bumann, 2013). Thus, enteropathogenic yersiniae acquired the iron siderophore yersiniabactin (Ybt). The Ybt-biosynthesis genes and its uptake system are both encoded on a high-pathogenicity island, of which the presence is linked to the level of *Yersinia* virulence (Carniel *et al*., 1987; Heesemann, 1987; Heesemann *et al*., 1993b; Fetherston *et al*., 1999).

Intriguingly, two sequenced strains of *Y. pseudotuberculosis* express the cytotoxic necrotizing factor (CNF) toxin, which was identified as a novel virulence factor of *Y. pseudotuberculosis* and will be discussed in more detail in section 1.3 (Lockman *et al*., 2002; Schweer *et al*., 2013).

1.2.2 Pathogenesis of enteric *Yersinia* infections

Upon the ingestion of contaminated food or water, *Yersinia* passes through the stomach and reaches the gut compartment. In the intestine, primary infection takes place in the terminal ileum and proximal colon (Figure 1.5) (Robins-Browne *et al*., 1985; Skurnik and Poikonen, 1986). There, yersiniae express invasin (1.2.1) and bind with high affinity to β1-integrins at the apical site of M cells (1.1.1) (Pepe, *et al*., 1994; Marra and Isberg, 1997; Clark *et al*., 1998; Schulte *et al*., 2000b). Invasin-binding further promotes β1-integrin clustering, which drives the formation of a phagocytic cup around *Yersinia* and its subsequent closure (zipper mechanism) (Cossart and Sansonetti, 2004). Moreover, yersiniae are able to re-invade the epithelial cell lining via basolaterally-expressed β1-integrins (Coconnier *et al*., 1994). Inside the M cell, the bacteria are transcytosed to the basolateral site and enter the underlying PP.

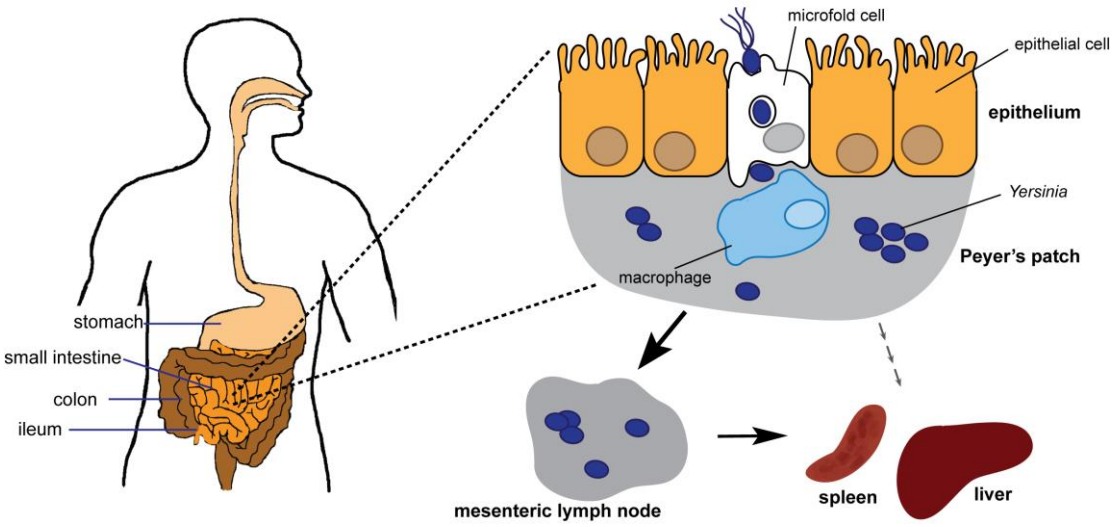

Figure 1.5 Infection route of enteropathogenic *Yersinia* spp.
After ingestion of contaminated nutrition, yersiniae pass through the stomach and reach the small intestine. In the ileum, they cross through the epithelial layer by exploiting M cells (microfold cells) that overlay the PP. After initial replication inside the PP, *Yersinia* is able to disseminate to the draining MLNs. Occasionally, highly virulent bacteria enter the blood stream and disseminate to systemic organs (*e.g.* liver and spleen). However, yersiniae are also able to directly disseminate from the gut to systemic organs. The picture is adapted from Azizi *et al*., 2010[4] and Sansonetti, 2002[5].

The PPs home a large population of innate and especially adaptive immune cells, encompassing B- and T-lymphocytes, DCs and macrophages (Wershil and Furuta, 2008). Hence, yersiniae are instantly encountering innate immunity by resident and infiltrating phagocytes (Galindo *et al*., 2011). In order to defend against the phagocytic attack, *Yersinia* utilizes its TTSS to prevent phagocytosis and pro-inflammatory cytokine production (1.2.1; Lian *et al*., 1987). Thus, yersiniae are primarily extracellular pathogens that generate extracellular microcolonies within abscesses that seem to resist phagocytosis (Simonet *et al*., 1990). Upon disease progression, *Yersinia* can disseminate to the draining MLNs. Some highly virulent *Y. pseudotuberculosis* and *Y. enterocolitica* strains even enter the blood stream and disseminate to systemic organs, *i.e.* liver and spleen (Figure 1.5) (Carter, 1975; Lian *et al*,

[4] Azizi *et al.* (2010) is licensed under the Creative Commons Attribution (CC BY 4.0) license. https://creativecommons.org/licenses/by/4.0/

[5] Adapted by permission from BMJ Publishing Group Ltd. [Host-pathogen interactions: the seduction of molecular cross talk, Sansonetti, 50, suppl 3: III2-8, copyright ©2002].

1987; Autenrieth and Firsching, 1996). However, a recent study revealed that yersiniae also directly disseminate from the small intestine to the MLNs and systemic organs by association to mononuclear phagocytes, *i.e.* CX_3CR1^+ monocyte-derived cells and $CD103^+$ DCs (Figure 1.5) (Drechsler-Hake *et al*., 2016).

1.2.3 Immune responses during *Yersinia* infection

After traversal of the epithelium, yersiniae are challenged by extracellular immune elements that recognize the invader and initiate immune reactions. To prevent eradication, *Yersinia* spp. express a variety of virulence factors to antagonize host immunity (1.2.1). During invasion of *Yersinia* into the sub-epithelial tissue, the bacteria elicit the infiltration of PMNs, which attack the pathogen and are important for initial pathogen reduction (Hanski *et al*., 1989; Conlan, 1997; Nuss *et al*., 2017). This attraction of phagocytic cells is mediated through binding of invasin to the β1-integrins at the basolateral site of intestinal epithelial cells, eventually leading to the expression of pro-inflammatory cytokines and chemokines, such as IL-8 (KC in mice), MCP-1, IL-1, GM-CSF and IL-18 (Schulte and Autenrieth, 1998; Kampik *et al*., 2000; Schulte *et al*., 2000a; Thinwa *et al*., 2014). However, yersiniae utilize their TTSS to counteract initiated cell autonomous immunity, pro-inflammatory cytokine production, as well as phagocytosis, and to induce apoptosis of naïve macrophages. Altogether, the activity of the TTSS prevents inflammation during initial colonization (1.2.1; Denecker *et al*., 2001; Grabenstein *et al*., 2004; Bergsbaken and Cookson, 2009; Moreau *et al*., 2010; Zhang *et al*., 2011). This manipulation of phagocytic and antigen presenting cells also affects the development of acquired immunity by down-regulation of MHCII (Schoppet *et al*., 2000). However, the host immune system is still able to recognize *Yersinia*-derived PAMPs such as LPS, the TTSS and Yop effectors by diverse PRR (*e.g.* TLR), triggering immune cell activation and the production of pro-inflammatory mediators (Chung and Bliska, 2016). Upon progressing *Yersinia* infection, host cell death programs switch in activated macrophages from apoptosis to caspase-1-dependent pyroptosis (1.1.2), mediating amplification of inflammatory signaling (Bergsbaken and Cookson, 2007; Bergsbaken *et al*., 2009; Philip *et al*., 2014; Weng *et al*., 2014). Moreover, it was shown that acute *Y. pseudotuberculosis* infection triggers a strong neutrophil driven inflammatory immune response, acute-phase response induction, and the expression of coagultination cascade proteins as well as metal ion scavengers in the PP of the host (Nuss *et al*., 2017). Previous studies also demonstrated that pro-inflammatory cytokines such as IL-18, IL-12, TNFα and IFNγ or IFN consensus-sequence binding protein (ICSBP) confer protection against *Yersinia* colonization and that the development of T cell immunity limits *Yersinia* infection (Autenrieth *et al*., 1992; Autenrieth *et al*. 1994; Bohn and Autenrieth, 1996; Bohn *et al*., 1998; Hein *et al*., 2000). In particular T_H1 and CTLs are controlling *Yersinia* infection, *e.g.* through production of cytokines that assist phagocyte-mediated bacterial killing or by targeting and killing infected cells (Autenrieth *et al*., 1992; Autenrieth *et al*., 1993; Bohn and Autenrieth, 1996; Bergmann *et al*., 2009; Zhang *et al*., 2015; Shen *et al*., 2016). Recently, a transcriptome analysis of *Y. pseudotuberculosis*-infected PPs detected enriched expression of T_H1 and T_H17 cytokines, suggesting that acute *Yersinia* infection elicits a mixed T_H1/T_H17 immune response to control the infection (Nuss *et al*., 2017).

1.3 Bacterial interference with the eukaryotic actin cytoskeleton

The actin cytoskeleton is an integral part of eukaryotic cell function critical for proper cellular functions and life, thereby participating in a variety of eukaryotic cell processes that involve migration, cellular shape, adhesion, phagocytosis and polarity (Freeman and Grinstein, 2014; Callan-Jones and Voituriez, 2016). Consequently, bacteria have evolved mechanisms to manipulate actin functions in order to invade the host and evade immunity.

1.3.1 The actin cytoskeleton and its regulation

The actin cytoskeleton consists of filamentous (F)-actin formed by two chains of non-covalent polymerized globular (G)-actin that twist around each other (Dominguez and Holmes, 2011). Actin reorganizes constantly and cycles between G- and F-actin states. During the assembly of F-actin, G-actin slowly forms pivotal trimeric nuclei that are elongated through G-actin association to either end, resulting in the growth of the filament. The steady-state phase structure of F-actin is also dynamic, since G-actin associates and dissociates to equal extends at both ends of the filament. Moreover, F-actin possesses a kinetic polarity defined by distinct assembly and dissociation rates at the ends of the filament: At the (+)-end G-actin associates faster than at the (-)-end (Hild *et al*., 2010). Furthermore, diverse proteins participate in the regulation of F-actin nucleation, elongation, crosslinking and bundling (Lee and Dominguez, 2010). One important class of actin cytoskeleton regulators is the small Ras-homologous (Rho) guanosine triphosphatases (GTPases) that are involved in numerous actin cytoskeleton dynamics (Heasman and Ridley, 2008). The small Rho GTPases are approximately 21-25 kDa, monomeric GTP-binding proteins that belong to the Ras superfamily and are classified into six subfamilies: Rho, Cdc42, Rac, Rnb, RhoBTB and RhoF (Wennerberg and Der, 2004; Wennerberg *et al*., 2005; Murali and Rajalingam, 2014). As other GTPases, Rho GTPases cycle between two conformational states: a GTP-bound active conformation and a GDP-bound inactive conformation (Figure 1.6A) (Bourne *et al*., 1991).

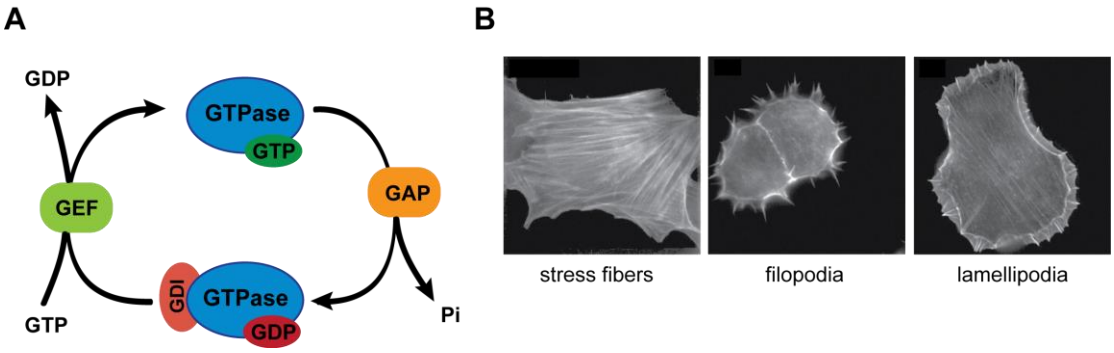

Figure 1.6 Cycling of small Rho GTPases and their influence on actin cytoskeleton morphology.
F-actin polymerization is controlled by small Rho GTPases. (A) The small GTPases cycle between a active (GTP-bound) and a inactive (GDP-bound) state. The activities are tightly controlled by GAPs, GEFs and GDIs. GEFs exchange GDP to GTP, whereas GAPs antagonize GTPase activity by assisting GTP hydrolysis and, therefore, lead to their inactivation. GDIs sequester GTPases in the cytosol stabilizing their inactivity. (B) The activation of the small Rho GTPases RhoA, Rac1 and Cdc42 drives formation of different F-actin structures. RhoA activation preferentially induces stress fibers, Cdc42 mainly participates in the formation of filopodia and Rac1 drives lamellipodia growth. The microscopy pictures were derived from Bulgin *et al*., 2010[6].

[6] Permitted for use in a doctoral thesis/dissertation by the American Society for Microbiology [Bacterial guanine nucleotide exchange factors SopE-like and WxxxE effectors, Bulgin *et al*., copyright ©2010].

In the active state, the small Rho GTPases are able to interact with proteins to target actin reorganization (Etienne-Manneville and Hall, 2002). As important key regulators of the actin cytoskeleton, three additional classes of proteins called guanine nucleotide exchange factors (GEFs), GTPase-activating proteins (GAPs) and guanine nucleotide dissociation inhibitors (GDIs) control Rho GTPase cycling between active and inactive conformation (Figure 1.6A). The GEFs release GDP from the small Rho GTPases and further GTP-loading in response to extracellular signals (Buchsbaum, 2007). Since small Rho GTPases harbor weak GTPase activity, GAPs mediate GTP hydrolysis to antagonize small Rho GTPase activation (Tcherkezian and Lamarche-Vane, 2007). Additionally, GDIs sequester small Rho GTPases in the cytosol maintaining their inactivity (Zegers and Friedl, 2013). The best-studied Rho GTPases are RhoA, Rac1 and Cdc42, which are important regulators of cellular migration and polarization. Upon activation, RhoA mainly participates in the formation of stress fibers; Rac1 drives lamellipodia growth and Cdc42 the development of filopodia (Figure 1.6B) (Nobes and Hall, 1995). Stress fibers are formed by large bundles of F-actin that are anchored at least at one end by a focal adhesion complex and extend through most of the cell body (Figure 1.6B). They participate mostly in cell migration and cellular tension (Pellegrin and Mellor, 2007; Burridge and Wittchen, 2013; Burridge and Guilluy, 2016). The lamellipodia are plane protrusions of the plasma membrane formed by short, branched F-actin filaments (Figure 1.6B). They are the main drivers of directed cell migration (Akhshi *et al*., 2014; Alblazi and Siar, 2015). The third cellular structures, called filopodia, are fine protrusions of the cell surface formed by bundled, linear-polymerized F-actin (Figure 1.6B). Along these F-actin bundles numerous proteins are transported to the tip of the filopodium. The filopodia participate in the sensing of environmental cues, cell migration, cell-to-cell adhesion, and dendritic spine formation (Jacquemet *et al*., 2015; Mattila and Lappalainen, 2008).

1.3.2 Manipulation of small Rho-GTPases – bacterial virulence strategies

The eukaryotic actin cytoskeleton is involved in universal cell functions, thereby also contributing to immunity. It participates in processes such as the maintenance of epithelial/endothelial barriers, immune cell migration, phagocytosis, immunological synapse formation and immune signaling (Bokoch, 2005; Mostowy and Shenoy, 2015). Therefore, it is an ideal target for pathogens to evade immunity, facilitate dissemination, and establish infection. The pathogenic bacteria have evolved a large repertoire of virulence factors that manipulate actin cytoskeleton dynamics (Popoff, 2014). These virulence factors are either secreted into the environment (toxins) or directly injected into host cells (effectors), *e.g.* via TTSS. Toxins are known to diffuse into the surrounding tissue causing tissue destruction, which fosters bacterial growth and dissemination, whereas injected effectors rather function to evade immune defenses (Boquet and Lemichez, 2003). Most actin manipulating bacterial toxins/ effectors target small Rho GTPases (Lemichez and Aktories, 2013). Some virulence factors such as SopE of *Salmonella enterica* serovar Typhimurium and the WxxxE effector family mimic GEFs (*e.g.* Map from *Escherichia coli*, IpgB1/2 from *Shigella flexineri* and SifA/B from *S.* Typhimurium) or inhibit GAP binding (*e.g.* DrrA from *Legionella pneumophila*), resulting in GTPase activation (Hardt *et al*., 1998; Ohya *et al*., 2005; Alto *et al*., 2006; Huang *et al*., 2008; Ohlson *et al*., 2008; Schoebel *et al*., 2009; Klink *et al*., 2010). There are also GAP-like bacterial virulence factors, *i.e.* YopE (*Y. pseudotuberculosis*), ExoS/T (*Pseudomonas aeruginosa*) or AexT (*Aeromonas salmonicida*) that inactivate the small GTPases (Goehring *et al*., 1999; Krall *et al*., 2000; von Pawel-Rammingen *et al*., 2000; Fehr *et al*., 2007; Mohammadi and Isberg, 2009). Bacterial virulence factors are also able to covalently

modify small Rho GTPases leading either to their inactivation or activation. Accordingly, Rho GTPases are activated through ADP-ribosylation by Ctx (*Vibrio cholera*) or deamidation by Pmt (*Pasteurella multocida*), while they are inactivated via ADP-ribosylation by C3 from *Clostridium botulinum*, glycosylation by TcsL from *Clostridium sordellii* or adenylation by VopS from *Vibrio paraheamolyticus* (Cassel *et al*., 1978; Aktories *et al*., 1987; Rubin *et al*., 1988; Just *et al*., 1996; Popoff *et al*., 1996; Orth *et al*., 2009; Yarbrough *et al*., 2009). The activation or inactivation of Rho GTPases influences different cellular functions. TcdA/B of *Clostridium difficile* enhances epithelial barrier permeability by disruption of tight and adherens junctions (Hecht *et al*., 1988; Nusrat *et al*., 2001). CyaA (*Bacillus pertussis*) and edema toxin (*Bacillus anthracis*) increase the endothelial cell permeability, resulting in edema formation and bacterial dissemination from the intestinal tract (Maddugoda *et al*., 2011; Gonzalez-Rodriguez *et al*., 2012). Moreover, invasive bacteria manipulate the Rho GTPases to enter cells, *e.g.* SopE from *Salmonella* mediates membrane ruffling in epithelial cells for subsequent uptake (Patel and Galán, 2005). Some pathogens evolved effectors to block phagocytosis by innate immune cells to prevent killing, for instance ExoT from *P. aeruginosa* is crucial to counteract Rac-mediated phagocytosis (Barbieri and Sun, 2004).
Yersinia also encodes for several Rho-GTPase activity modifying effectors, *i.e.* YopT, YopE and YpkA (1.2.1). In addition, two *Y. pseudotuberculosis* serogroup O:3 strains also produce the CNF toxin that modifies small Rho GTPases (1.3.3).

1.3.3 The cytotoxic necrotizing factor toxin - CNF

The first CNF toxin was discovered in *E. coli* isolated from stool samples of acute enteric infections (CNF1, Caprioli *et al*., 1983). However, CNF-positive *E. coli* are more prevalent in extraintestinal infections, especially in bladder infections (Johnson, 1991; de Rycke *et al*., 1999). To date, four CNF isoforms (CNF1-3 from *E. coli*; CNF_Y from *Y. pseudotuberculosis*) have been identified, of which CNF1 is the best studied (Oswald *et al*., 1989; Lockman *et al*., 2002; Orden *et al*., 2007). In *Y. pseudotuberculosis*, two sequenced and characterized strains from serotype O:3, *i.e.* YPIII and IP2666, encode the functional protein. Other *Y. pseudotuberculosis* strains and *Y. pestis* were found to encode truncated forms of the CNF toxin (Lockman *et al*., 2002).
All CNFs covalently modify small Rho GTPases at glutamine-61/63 by deamidation to glutamate (Schmidt *et al*., 1997; Flatau *et al*., 1997; Lerm *et al*., 1999). Due to the constitutive activation, intoxication with CNF induces several F-actin rearrangements in eukaryotic cells including cell flattening, inhibition of cytokinesis resulting in multinucleated cells, membrane ruffling, stress fiber and filopodia formation (Fiorentini *et al*., 1988; Fiorentini *et al*., 1997; Knust *et al*., 2009). Additionally, epithelial cells develop atypical phagocytic behavior and internalize bacteria (Falzano *et al*., 1993).
All CNFs are single chain AB-toxins of identical length (1014 amino acids) and are predicted to have a modular structure: they consist of an N-terminal binding domain, a central translocation domain and a C-terminal catalytic domain (Lemichez *et al*., 1997; Falnes and Sandvig, 2000; Pei *et al*., 2001). Binding studies revealed that CNF1 requires interaction with the laminin receptor and the Lutheran (Lu) adhesion glycoprotein/basal cell adhesion molecule (BCAM) (Lu/BCAM) receptor for toxin action (Kim *et al*., 2005; Piteau *et al*., 2014). Moreover, it was demonstrated that CNF1 and CNF_Y toxins interact with heperansulfate proteoglycan (HSPG). Although HSPG was crucial for CNF_Y cellular access, CNF1 displayed delayed cell entry, proposing HSPG as part of a receptor complex for CNF1 (Figure 1.7;

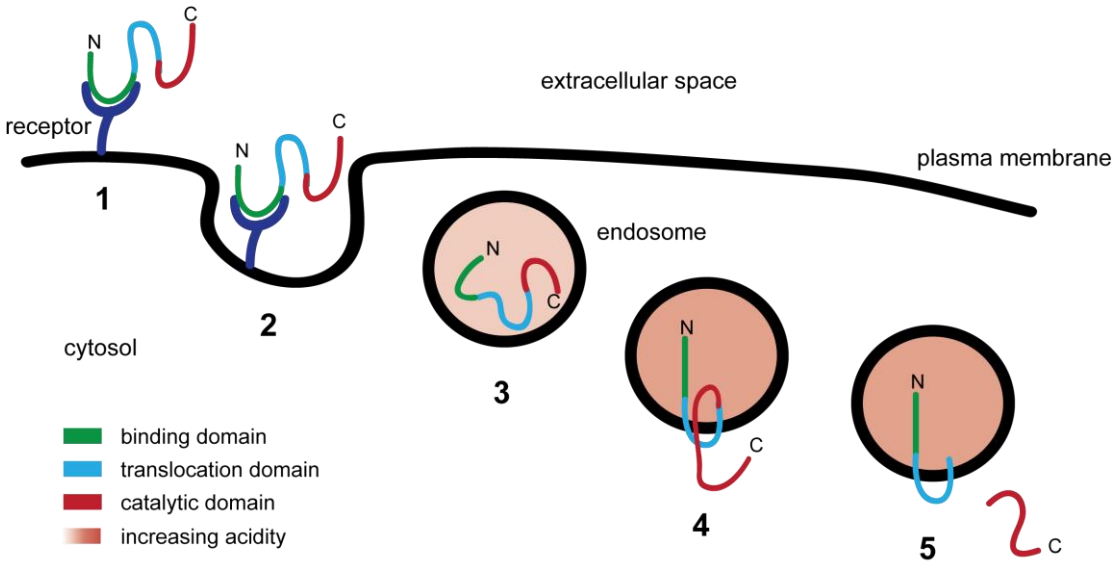

Figure 1.7 Eukaryotic uptake mechanism of CNF.
After receptor binding of the putative N-terminal binding domain of CNF (1), CNF is internalized by receptor-mediated endocytosis (2). Subsequently, the endosomal compartment gets acidified and the central translocation domain inserts into the endosomal membrane exposing the predicted C-terminal catalytic domain of CNF into the cytosol (3 & 4). The putative catalytic domain is released into the cytosol through cleavage by endosomal-located serine proteases (5). The picture is adapted from Knust and Schmidt, 2010[7].

step 1) (Blumenthal *et al*., 2007). After receptor binding, CNFs are taken up by receptor-mediated endocytosis. In the acidified endosome, the central translocation domain inserts into the endosomal membrane transferring the C-terminal catalytic domain into the cytosol. This acidification step is crucial for cytosolic access of the CNF toxin (Figure 1.7; step 2-4) (Contamin *et al*., 2000; Pei *et al*., 2001; Blumenthal *et al*., 2007). For full biological activity, the C-terminal domain of CNF(1) is released into the cytosol by serine protease-dependent unspecific proteolytic cleavage in the endosome (Figure 1.7; step 5) (Knust *et al*., 2009). Since CNF lacks classical secretion signals, the secretion mechanism of CNF from bacteria into the environment is quite understudied. For *E. coli* it was found that CNF1 is secreted into the environment by outer membrane vesicles (OMVs) (Davis, 2006; Kouokam *et al*., 2006). Two other studies showed that ferredoxin contributes to the translocation across the bacterial inner membrane and YgfZ to the secretion into the OMVs (Yu and Kim, 2010; Yu and Kim, 2012). However, the full secretion mechanism remains unknown. Whether CNF_Y secretion from *Y. pseudotuberculosis* is also conducted by OMVs remains unclear, as OMV production was only demonstrated for *Y. pestis* yet (Eddy *et al*., 2014).
In the past decade, the knowledge about the action of CNF in pathogenesis was expanded. Nevertheless, the impact of CNF1 from *E. coli* on immune cells, signaling and pathogenesis is much better understood than for *Y. pseudotuberculosis* CNF_Y. Several studies showed that the production of CNF1 increases inflammation in different infection models (Rippere-Lampe *et al*., 2001a; Rippere-Lampe *et al*., 2001b; Smith *et al*., 2015). A study by Schweer and colleagues on *in vivo* effects of CNF_Y revealed that CNF_Y also increased inflammation and tissue damage (Schweer *et al*., 2013). Moreover, production of CNF assisted bacterial colonization abilities during urinary tract and intestinal infections, respectively (Rippere-Lampe *et al*., 2001b; Schweer *et al*., 2013). CNF_Y was also shown to increase the translocation

[7] Knust and Schmidt (2010) is licensed under the Creative Commons Attribution (CC BY 3.0) license. https://creativecommons.org/licenses/by/3.0/

of Yop effectors *in vitro* and *in vivo*, which is crucial for *Y. pseudotuberculosis* YPIII virulence and pathogenesis (Schweer *et al*., 2013; Wolters *et al*., 2013). Further work on CNF1 suggested, that it might participate in colon cancer development and contributes to *E. coli*-caused meningitis by facilitating blood-brain barrier traversal (Khan *et al*., 2002; Wang and Kim, 2013; Raisch *et al*., 2014). In several publications, CNF1 and CNF_Y were also shown to promote destabilization of epithelial and endothelial barriers via activation of Rho-GTPases. However, contradicting results were obtained using different cell lines and incubation periods (Hopkins *et al*., 2003; Baumer *et al*., 2008; Schlegel *et al*., 2011). In addition, CNF1 was reported to affect immune cell functions of natural killer (NK) cells, DCs and neutrophils. In NK cells and DCs, characteristic immune functions were enhanced, whereas neutrophils were modulated in their actions (Hofman *et al*., 2000; Malorni *et al*., 2003; Davis *et al*., 2005; Shurin *et al*., 2005; Davis *et al*., 2006). In addition, the host is able to sense activation of small Rho GTPases and consequently induces pro-inflammatory responses (Müller *et al*., 2010; Keestra *et al*., 2013). For instance CNF1 was reported to trigger pro-inflammatory cytokine production and induce defense mechanisms (Falzano *et al*., 2003; Boyer *et al*., 2011; Reipschläger *et al*., 2012; Diabate *et al*., 2015).

1.4 Persisting bacterial infections - reservoirs and risks for disease

Individuals experience numerous bacterial and viral infections during their lifetime. Most of the time, acute infections are self-limited by the intervention of innate and adaptive immunity leading to pathogen clearance and restoration of tissue homeostasis. Nevertheless, resolution of acute infections requires initial disruption of tissue homeostasis. This might provoke long-lasting consequences by promoting immune dysfunction and altered tissue homeostasis. There is evidence that acute bacterial infections might initiate inflammatory diseases such as rheumatic heart disease, multiple sclerosis, Alzheimer's disease and type II diabetes (Wucherpfennig, 2001; Karin *et al*., 2006; Medzhitov, 2010; Miklossy and McGeer, 2016). Moreover, some pathogens are able to establish prolonged infections. The most prominent historical case of persistent bacterial infection was Mary Mallon, called "Typhoid Mary", who was an asymptomatic carrier of *S. enterica* serovar Typhi. During her lifetime, she caused several outbreaks and deaths by transmitting *S.* Typhi via the fecal-oral route (Marineli *et al*., 2013). Up to date, there are several known examples of human persistent bacterial infections including *Mycobacterium tuberculosis*, *S.* Typhi, *Brucella* spp., uropathogenic *E. coli* (UPEC), *Chlamydia* spp. or *Helicobacter pylori* (Monack *et al*., 2004b). Most persistent infections are asymptomatic but imply potential risks for the host leading to reactivation/recurrent infections (*M. tuberculosis*; UPEC) or severe diseases such as gastric cancer (*H. pylori*), mucosa-associated lymphoid tissue lymphomas (*Campylobacter jejuni*) or gall bladder cancer (*S.* Typhi) (Shukla *et al*., 2000; Peek and Blaser, 2002; Stewart *et al*., 2003; Guidoboni *et al*., 2006; Scott *et al*., 2015). Additionally, treatment of persistent bacterial infections is quite challenging since it requires prolonged administration of antimicrobials. Treatment of latent *M. tuberculosis* infection requires at least six month of antibiotic treatment, whereas latent syphilis demands a tremendous antibiotic treatment over 24 month (Brown and Frank, 2003; Munro *et al*., 2007). These extensive treatment periods are thought to be due to the protected bacterial habitat in the host and/or changed bacterial metabolic states that allow antibiotic tolerance without genotypic resistance. This protection is achieved by intracellular localization (*e.g.* UPEC, *S.* Typhi), formation of metabolically altered small colony variants (*P. aeruginosa*, *Staphylococcus aureus*), initiation of bacterial stringent responses due to

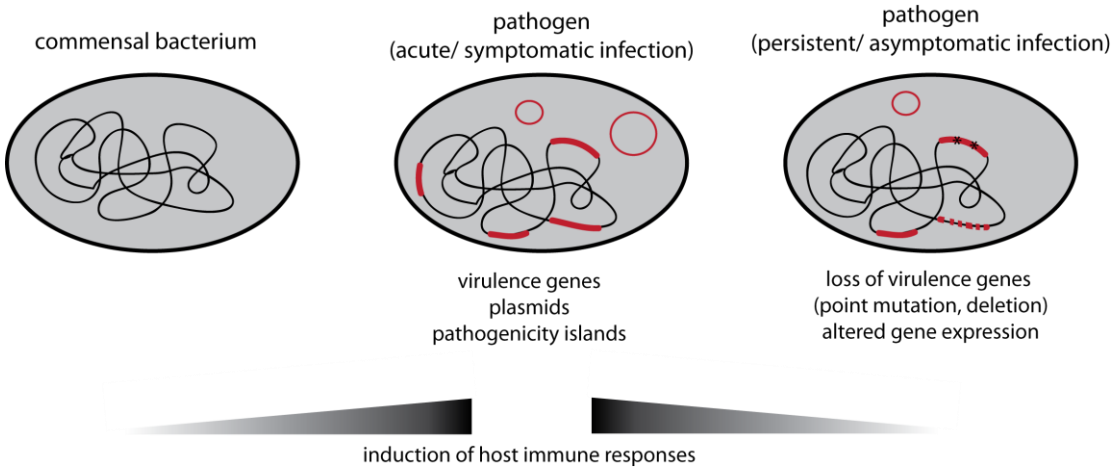

Figure 1.8 Genotypic determinants that distinguish commensals, and pathogens causing symptomatic or asymptomatic infections.

Commensal bacteria co-exist with their human host without causing any harm. They are usually not invasive and hardly induce host immune responses. Pathogens causing symptomatic disease harbor several virulence factors that are encoded on virulence plasmids, on the genome or on pathogenic islands. Acute infections with these pathogens cause a strong induction of host innate and adaptive immune responses. However, loss of virulence genes, genomic diversity and altered gene expression drives the emergence of less virulent pathogens that are adapted to asymptomatically persist in their host and provoke scarce host immunity. The picture is modified from Dobrindt *et al*., 2010[8].

environmental stresses (*M. tuberculosis*), or formation of biofilms (*P. aeruginosa*) (Schmidt-Grant and Hung, 2013; Cohen *et al*., 2013). Besides the health risks for the host, asymptomatic carriers are a public concern since they are reservoirs for spreading disease in a population, as in the case of "Typhoid Mary" (Young *et al*., 2008). Thus, commensal bacteria of the normal microbial community should be distinguished from pathogens that elicit persistent infections. A commensal bacterium harbors limited abilities to invade host tissues and does not harm its host compared to a pathogen that causes acute or persistent infection. In comparison to pathogens causing acute disease, bacteria that are able to persist asymptomatically were proven to exhibit altered gene expression and loss of virulence genes. This process, called micro-evolution, represents an adaptation mechanism to establish persistency and avoid induction of host immunity (Figure 1.8) (Oh *et al*., 2006; Dobrindt *et al*., 2010). However, some members of an individual's microbial community can also acquire context-dependent pathogenicity, by attainment of new virulence factors, outgrowth in immune-compromised patients (pathobionts), populating new niches, or shifts in the relative abundances in the microbial community (dysbiosis). These asymptomatical "context-dependent" pathogens only cause disease in a certain situation and are not considered as a persistent bacterial infection (Buttó *et al*., 2015; Nathan, 2015).

Currently, scientists hypothesize that an individual's immunity allows bacterial persistence through a complex balance between protective immune responses and pathologic consequences (Figure 1.9). In other words, the infected host will dim the immune response when it becomes more destructive than persistence of the pathogen. This is a vicious cycle, as down-regulation of protective immunity will decrease pathology but enhance pathogen persistence. Moreover, low virulence and bacterial persistence factors might potentiate pathogen persistence and

[8] Reprinted from Nosocomial Infections, Volume 300, Dobrindt *et al*., Bacterial genome plasticity and its impact on adaptation during persistent infection, pages 363-366, copyright ©2010, with permission from Elsevier. Minimal adaptations were made.

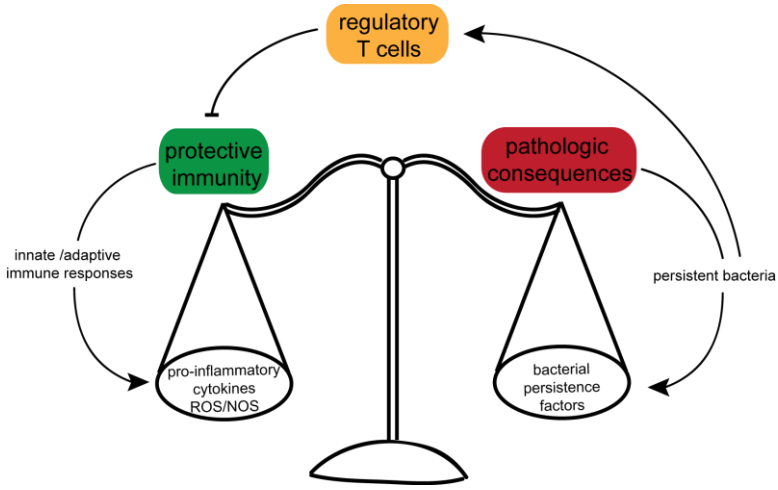

Figure 1.9 Balance of protective immunity and pathologic consequences during bacterial persistence.

Hypothetically, bacterial persistence is mediated by a complex balance between protective immune responses and pathological consequences. If protective immunity induces more damage than the pathogen itself, immune responses are limited through immune response modulation, for instance by regulatory T cells. Furthermore, persistent pathogens encode persistence factors that might cause limited inflammation and tissue disruption that restrict pathological consequences, facilitating bacterial survival and persistence. Persistent bacteria might also directly or indirectly affect regulatory T cells to their benefit. The figure is adapted from Monack *et al*., 2004b[9].

survival by means of low immunity induction and limited tissue injury (Figure 1.9). In this setting, regulatory T cells are of reasonable importance, since they are involved in limiting collateral tissue damage. They are either activated in consequence of host immune responses to restore tissue homeostasis and/or via (in-)direct stimulation by pathogens promoting prolonged infection. (Figure 1.9) (Monack *et al*., 2004b; Belkaid, 2007).

1.4.1 Persistence of *Salmonella*, *Helicobacter* and UPEC

As previously mentioned, there are a couple of recognized persistent bacterial infections in humans (1.4). In the following section, three examples will be discussed in more detail, *i.e. S. enterica*, *H. pylori* and UPEC.

S. enterica persistence

S. Typhi and *S.* Typhimurium infections in humans are leading to illnesses ranging from gastroenteritis to systemic infection (Monack *et al*., 2004b). In humans, systemic (typhoid fever) and persistent *Salmonella* infection mostly originates from infections with *S.* Typhi (Parry *et al*., 2002). In contrast, *S.* Typhimurium causes predominantly gastrointestinal disease in humans. However, murine *S.* Typhimurium infections resemble human infections with *S.* Typhi. Therefore, murine *S.* Typhimurium infections are employed to study *Salmonella* persistent infections (Monack *et al*., 2004a).

Salmonella infects individuals via the gastrointestinal tract by ingestion of contaminated food products. From there, they are able to disseminate to the underlying and deeper tissues employing multiple mechanisms (Kohbata *et al*, 1986; Jones *et al*., 1994; Vazquez-Torres *et al*., 1999). After an acute *Salmonella* infection, about 1-6 % of typhoid fever patients are persistently infected with *Salmonella* inside the gall bladder or bone marrow (Levine *et al*., 1982; Sinnott and Teall, 1987; Wain *et al*., 2001). Through the excretion of *Salmonella* containing bile from the gall bladder, bacteria are transferred into the gastrointestinal tract and

[9] Adapted by permission from Macmillan Publishers Ltd: Nature Reviews Microbiology, Monack *et al*., 2004b, copyright ©2004.

urine. Some people are egesting large amounts of *Salmonella*, which possibly lasts for one year or even the whole lifetime without the development of recurrent disease. These so-called super-shedders, such as "Typhoid Mary", frequently transfer *Salmonella* to other people (Vogelsang and Boe, 1948; Lawley *et al*., 2008). Knowledge about persistence mechanisms in humans is limited, but IL-22/IFNγ production and effective immune response mounting are crucial for reservoir clearance and prevention of prolonged *Salmonella* infection (Mastroeni and Ménager, 2003; Thompson *et al*., 2009; Dougan *et al*., 2011). Moreover, *S*. Typhi is able to generate biofilms on the surface of gallstones, potentially facilitating persistence and transmission (Crawford *et al*., 2008; Crawford *et al*., 2010).

In the murine persistent *Salmonella* infection model, *S*. Typhimurium persists inside macrophages. Therefore, survival and replication ability inside macrophages may support the establishment of persistence (Helaine *et al*., 2010). One study on *S*. Typhimurium persistence demonstrated that the TTSS effector SseI facilitates systemic long-term infection by altering phagocyte migration, thereby impairing the development of adaptive immunity. Yet, *S*. Typhi does not encode SseI (McLaughlin *et al*., 2009). Regulatory T cells have also been implicated in controlling the onset of persistent *Salmonella* infection in the mouse model. In one particular study, regulatory T cell activities were shown to reduce effector T cell responses during the first phase of persistent infection allowing the increase of bacterial loads (Johanns *et al*., 2010).

H. pylori persistence

H. pylori is the best-studied human pathogen that effectively manifests persistent infection in about 50 % of the world's population (Calvet *et al*., 2013). It is orally transmitted during the early childhood and thereafter able to persist for decades in the gastric mucosa. About 80 to 90 % of infected people with chronic gastritis never develop symptomatic disease but the infection comprises a major risk to acquire more severe diseases such as gastric cancer, mucosa-associated lymphoid tissue lymphoma or ischemic heart disease (Hunt, 1996; Amieva and El-Omar, 2008; Franceschi *et al*., 2013).

Initial colonization of *H. pylori* in the stomach is facilitated by a bacterial urease that confers acid resistance (Mobley *et al*., 1995; Weeks *et al*., 2000). After that, *H. pylori* chemotaxis permits directional movement through the mucus to the gastric epithelium (Ottemann *et al*., 2002; Croxen *et al*., 2006). At the epithelial lining, *H. pylori* persist either free-swimming in the mucus or directly adherent at the epithelium (Hessey *et al*., 1990; Ilver *et al*., 1998; Mahdavi *et al*., 2002). The cytotoxin-associated gene A (CagA) and vacuolating cytotoxin A (VacA) are important epithelial colonizing factors, supporting growth in microcolonies and iron acquisition (Tan *et al*., 2009; Tan *et al*., 2011). Besides the colonization strategies, *H. pylori* employs several immune evasion strategies to circumvent the activation of host immune responses and to establish persistence. To this purpose, *H. pylori* modifies its surface antigens, *e.g.* LPS or flagellin, to avoid PAMP recognition (Gewirtz *et al*., 2004; Moran, 2007). The activation of the inflammasome by recognition of *H. pylori* drives also the induction of Tregs that limit effector T cell activation and consequently enhances prolonged infection (Tomita *et al*., 2001; Hitzler *et al*., 2012; Oertli *et al*., 2012). T_H1 and T_H17 differentiated effector cells are essential to control *H. pylori* infection (Akhiani *et al*., 2002; Sayi *et al*., 2009; Velin *et al*., 2009). Hence, *H. pylori* evolved mechanisms to block T cell proliferation and to enhance Treg differentiation via programming of tolerogenic DCs (Gebert *et al*., 2003; Sundrud *et al*., 2004; Gerhard *et al*., 2005; Schmees *et al*., 2007; Kao *et al*., 2010; Zhang *et al*., 2010; Oertli *et al*., 2012).

UPEC persistence

About every third woman will experience a urinary tract infection (UTI) during her lifetime. Therefore, bacterial urinary tract infections are amongst the most prevalent infectious diseases with high recurrence risks (Foxman, 2003; Mehnert-Kay, 2005). The most collective source of cystitis is UPEC infection (Ronald, 2002). In order to establish an infection, UPEC has to ascent the urethra against the stream and adhere with its mannose-binding type I pili (FimH) to the urothelium to resist eradication via urination (Bahrani-Mougeot *et al*., 2002; Thomas *et al*., 2002). These pili also mediate invasion of the bacteria into superficial umbrella cells within the urothelium by the zippering mechanism (Martinez *et al*., 2000; Martinez and Hultgren, 2002). Inside the urothelial cells, UPEC persists inside secretory lysosome-like vesicles that can only be exocytosed via a TLR-4-dependent mechanism (Mulvey *et al*., 2001; Song *et al*., 2009). However, UPEC is able to disrupt the secretory lysosome-like compartments and replicates inside the cytosol creating bacterial biofilm-like aggregates, termed intracellular bacterial communities (IBCs). Due to the cellular turnover at barrier surfaces, maturating, smaller cells replace mature umbrella cells. These maturing cells are not supporting the formation of large IBCs, possibly restricting the infection extent (Anderson *et al*., 2003; Justice *et al*., 2004). Still, UPEC is able to exit the urothelium into the urine, facilitating bacterial spread and dissemination to other urothelial cells. The formation of IBC-like quiescent intracellular reservoirs at later infection stages supports the development of persistent UPEC infection (Justice *et al*., 2004; Scott *et al*., 2015).

TLR-4 and TLR-5 signaling pathways were shown to protect against acute UPEC infection (Andersen-Nissen *et al*., 2007; Song *et al*., 2007). Controversially, defective TLR-4 signaling and immunodeficiency were found to decrease the development of chronic cystitis. In line with this, Hannan and colleagues demonstrated that severe inflammation supports acquisition of chronic cystitis in women (Hawn *et al*., 2009; Hannan *et al*., 2010; Hannan *et al*., 2012). As in other bacterial infections, T cells were found to be associated with UPEC clearance (Hopkins *et al*., 1993; Jones-Carson *et al*., 1999). However, this research area needs to be further extended.

1.4.2 *Yersinia* persistence

Y. enterocolitica and *Y. pseudotuberculosis* are known to elicit acute and self-limiting gastrointestinal diseases in immunocompetent individuals (1.2). However, *Yersinia* persistence or incomplete elimination is frequently discussed to be interrelated with the development of reactive arthritis (Granfors *et al*., 1998; Cargnelutti and Di Genaro, 2013). Case reports of persistent *Yersinia* infections that resulted in inflammatory complications and reactivation of disease are supporting this hypothesis (Gaston *et al*., 1999; Watson *et al*., 2013). An interesting study by Hoogkamp-Korstanje and co-workers showed persistent *Yersinia* infections in human tissue biopsies from the intestine (*i.e.* the colon) and lymph nodes. These persistent *Yersinia* infections were also linked to recurrent and chronic inflammatory diseases (*i.e.* chronic ileitis, arthritis, lymphadenopathy, hepatosplenomegaly and hepatitis) (Hoogkamp-Korstanje *et al*., 1988). Furthermore, enteropathogenic yersiniae have also been isolated from pig and rodent reservoirs implicating their ability to persist in these animals (Mair *et al*., 1979; Fredriksson-Ahomaa *et al*., 2006; Backhans *et al*., 2011). This is reinforced by a study demonstrating *Yersinia* persistence in three rat strains after intra-venous challenge (Curfs *et al*., 1995). More recently, Fahlgren and colleagues demonstrated that yersiniae are able to persist in the cecum of mice after oral challenge with sub-lethal infection doses of *Y. pseudotuberculosis* YPIII for

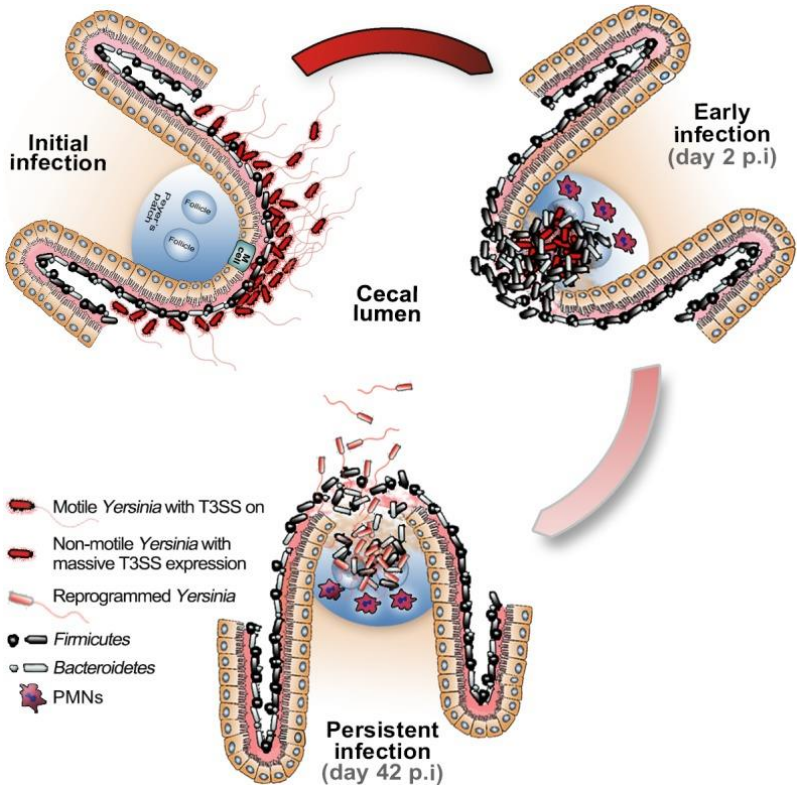

Figure 1.10 Model of *Yersinia* persistency development via transcriptional reprogramming.
To facilitate initial infection *Yersinia* is flagellated and expresses virulence genes (*e.g.* adhesins and the TTSS). During acute infection (2 dpi), bacteria become non-flagellated and strongly express the TTSS to defend against resident and attracted phagocytes, for instance PMNs. During persistent phase (42 dpi), *Y. pseudotuberculosis* becomes re-flagellated, down-regulates virulence gene expression and induces stress responses gene expression. The figure is derived from Avican *et al*., 2015[10]. p.i. post infection.

up to 115 days post infection (dpi) (Fahlgren *et al*., 2014). In the cecum of the FVB/N mice, *Y. pseudotuberculosis* primarily colonized the lymphoid tissue and resided in bacterial microcolonies or as single cells inside inflamed neutrophil containing tissue lesions (Fahlgren *et al*., 2014). Moreover, the persistently colonized mice continuously shed the *Yersinia* into the environment (Fahlgren *et al*., 2014). In a follow-up study by the same group, it was shown that persistent yersiniae are able to reprogram their gene expression profile from acute to persistent infection. Upon acute infection, *Y. pseudotuberculosis* expressed important virulence genes and regulators, such as *yopM, yopJ, ail* and *lcrF*, whereas these were down-regulated during persistence (Figure 1.10). Moreover, genes involved in environmental stress adaption and motility, such as *arcA, fliC, napA, frdA, rfaH, sodB, wrbA, hdeB, cspC* and *uspA*, were induced in the persistent state compared to acute infection (Figure 1.10) (Avican *et al*., 2015). The *Y. pseudotuberculosis* transcriptional reprogramming from acute to persistent infection stage also caused the up-regulation of *crp*, *csrA*, and *rovA* (Figure 1.10) (Avican *et al.*, 2015). The increased expression of theses regulators was also interconnected with the up-regulation of their respective regulons during *Yersinia* persistence (Avican *et al*., 2015).
The reduction of virulence and adaptation to environmental stresses by adjusting the gene expression profile is a known mechanism of persistent bacteria (1.4). Still, nothing is known about host factors and mechanisms that contribute to the development of persistent *Yersinia* infections.

[10] Avican *et al*. (2015) is licensed under the Creative Commons Attribution 4.0 (CC BY 4.0) license. https://creativecommons.org/licenses/by/4.0/

1.5 Aim of the study

Yersinia persistence after acute gastro-intestinal infection in humans has long been suggested to trigger secondary disease (Hoogkamp-Korstanje *et al*., 1988; Granfors *et al*., 1998; Gaston *et al*., 1999). However, a suitable murine infection model to study the mechanisms of *Yersinia* pathogenesis during persistent infections was not available until recently (Fahlgren *et al*., 2014). The establishment of such a model enabled the identification of Yop effectors necessary to establish persistent *Yersinia* infection (Fahlgren *et al*., 2014). Interestingly, down-regulation of TTSS expression seems important for persistent *Yersinia* infection (Avican *et al*., 2015), but in-depth knowledge about the host-pathogen interactions and the influence of further virulence factors during the switch from acute to persistent *Yersinia* infection is currently lacking. Previous work of Schweer and co-workers proposed that modulation of the Yop effector delivery by CNF_Y might dictate the competence to long-term colonize the gut of BALB/c mice (Schweer *et al*., 2013).

Given these premises, this study aims at dissecting the complex CNF_Y-dependent host-pathogen relationship during acute and chronic *Yersinia* infection. To address this, the influence of CNF_Y on the ability to persist and the course of persistent infection in BALB/c mice are investigated. In order to characterize CNF_Y-dependent pathogenic mechanisms during acute and persistent infection, tissue architecture, bacterial colonization patterns and cytokine production are examined. Moreover, the consequences of CNF_Y-dependent inflammation on the microbial community composition are analyzed. In order to obtain knowledge of the molecular mechanisms of the host-pathogen interactions, the main target of this study is to identify CNF_Y-dependent host and pathogenic factors that affect development of CNF_Y-dependent persistence. To this purpose, the host transcriptome during acute and persistent infection and the expression of important *Yersinia* virulence and persistence genes are profiled. As little is known about the effect of decreased Yop translocation on Yop-targeted immune signaling pathways during acute *in vivo* infection, the impact of CNF_Y on the inflammasome network during oral infection of C57BL/6N mice is investigated. At first, CNF_Y-dependent virulence, organ colonization, tissue architecture, immune and cytokine responses in C57BL/6N mice are explored. Thereafter, the impact of the inflammasome and downstream cytokine signals on organ colonization and dissemination are elucidated.

2 Material and methods

2.1 Material

2.1.1 Equipment and material

Equipment and materials were purchased from the following manufacturers: Amersham, BD Biosciences, BD Falcon, Beckmann Coulter, Biolegend, BioRad, BioChrom, Biometra, Brand, Braun, CytoOne, Eppendorf, GE Healthcare, Greiner bio-one, Heidolph, Heraeus, Infors, Kinematika, Millipore, Microflex Corporation, PeqLab, QIAGEN, Roth, Sarstedt, Sartorius, Schott, Scientific Industries, Sorvall, Starlab, TEMCA, Thermo Fisher Scientific, TPP, VWR International, WLD-TEC, WU Mainz and Zeiss if not mentioned otherwise.

2.1.2 Buffers and solutions

Chemicals used for the buffers and solutions were obtained from the following companies: Ambion, Applichem, BD Biosciences, Biolegend, Bioline, eBioscience, Fermentas, Fisher Scientific, Fluka, GIBCO, Hartmann Analytic, Invitrogen, Illumina, Merck, Metabion, New England Biolabs (NEB), Oxoid, PeqLab, Promega, QIAGEN, Roche, Roth, Sigma Aldrich, T.H. Geyer, VWR, and Zeiss.
The composition of the used buffers and solutions is shown in Table 2.1.

Table 2.1 Composition of buffers and solutions

Buffer/solution	Composition
ACK buffer	150 mM NH_4Cl, 10 mM $KHCO_3$, 1 mM EDTA, pH 7.4
2x Buffer A	200 mM NaCl, 200 mM Tris, 20 mM EDTA, pH 8
2x Buffer A with SDS	500 µl 2x buffer A, 200 µl 20 % SDS (w/v)
NP-40 buffer	150 mM NaCl, 50 mM Tris-HCl (pH 8.0), 1 % NP-40
10x PBS	80 g/l NaCl, 2 g/l KCl, 6.1 g/l Na_2HPO_4, 2 g/l KH_2PO_4, pH 7.3
PBS/BSA	0.2 % (w/v) BSA in 1x PBS
PMSF	100 mM in isopropyl alcohol
RNA loading buffer	9.5 ml formamide, 360 µl 0.5 M EDTA (pH 8.0), 10 µl 20 % SDS, xylen cyanol and bromphenol blue
10x TBE	900 mM Tris-HCl, 900 mM boric acid, 25 mM EDTA, pH 8.0
TE	10 mM Tris-HCl, 1 mM EDTA, pH 7.5
50x TAE	2 M Tris, 100 mM EDTA, pH 8.0
Solution D	4 M guanidinium thiocyanate, 25 mM sodium citrate, 0.5 % N-laurosylsarcosine (w/v), 0.1 M β-mercaptoethanol
TFBI	20 mM KAc, 10 mM $CaCl_2$, 50 mM $MnCl_2$, 100 mM $RbCl_2$, 15 % glycerol, pH 5.8
TFBII	10 mM PIPES, 75 mM $CaCl_2$, 10 mM RbCl, 15 % glycerol, pH 6.5

2.1.3 Media and antibiotics

All media were prepared with distilled water (dist. water). Media employed for this study and their compositions are listed in Table 2.2.

Table 2.2 Media composition

Medium	Composition
BHI (brain-heart infusion) broth	37 g/l BHI
LB (Luria Bertani) broth	5 g/l NaCl, 5 g/l yeast extract, 10 g/l tryptone
LB solid medium	LB broth, 18 g/l agar
SOC (super optimal broth) medium	20 g/l tryptone, 5 g/l yeast extract, 0.5 g/l NaCl, 2.5 mM KCl, 10 mM $MgCl_2$, 10 mM $MgSO_4$, 0.2 % glucose
Yersinia selective medium	*Yersinia* selective agar base with *Yersinia* selective supplement (Oxoid)

To specifically select for resistant bacteria, antibiotics were added to the media (Table 2.3).

Table 2.3 Final concentrations of antibiotics

Antibiotic	Final concentration
Carbenicillin	100 µg/ml
Irgasan	0.5 µg/ml
Kanamycin	50 µg/ml

2.1.4 Enzymes, antibodies and commercial kits

Enzymes used in this study were applied with their respective buffers provided by the manufacturer and are listed in Table 2.4.

Table 2.4 Enzymes

Enzyme	Reference source
DNA-Polymerases	
Mango*Taq*™ DNA polymerase	Bioline
Phusion® High-Fidelity DNA Polymerase	NEB
Digesting enzymes	
*Avr*II	NEB
*Not*I-HF	NEB
*Sac*I	NEB
TURBO™ DNase	Ambion
*Xho*I	NEB

Enzyme	Reference source
Others	
Antarctic Phosphatase	NEB
T4 DNA Ligase	NEB

Antibodies, their respective clones and the reference source are given in Table 2.5. The dilution for the antibody staining was titrated before the experiments as described in 2.6.2.

Table 2.5 Antibodies for flow cytometry

Antibody	Working concentration*	Reference source
CD16/CD32 (Fc_γ III/II Receptor)	1:100	BD Biosciences
CD3 v450 rat anti-mouse	1:100	BD Biosciences
CD19 FITC anti-mouse	1:200	BioLegend
NKp46 APC anti-mouse (CD335)	1:400	BioLegend
CD11b eFluor® 450 human, mouse (M1/70)	1:800	eBioscience
CD11c APC-eFluor® 780 anti-mouse (N418)	1:1000	eBioscience
Ly6G PE-Cy™7 rat-mouse	1:500	BD Biosciences
Ly6C, Lymphocyte antigen 6 complex, locus C	1:1000	BioLegend
F4/80 PE mouse (BM8)	1:100	eBioscience
Streptavidin-Fluorescein Isothiocyanate (SA-FITC)	1:500	BD Biosciences
CD3e Biotin hamster anti-mouse	1:100	BD Biosciences
CD19 Biotin anti-mouse	1:100	eBioscience
NKp46 Biotin anti-mouse	1:100	BioLegend
LIVE/DEAD® Fixable Blue Dead Cell Stain Kit	1:500	Invitrogen

* dependent on the batch

The used commercial kits and the supplying company are mentioned in Table 2.6.

Table 2.6 Kits

Kit	Reference source
Agilent RNA 6000 Nano kit	Agilent Technologies
Agilent RNA 6000 Pico kit	Agilent Technologies
Pierce™ BCA Protein Assay Kit	Thermo Fisher Scientific
ERCC RNA spike-in control mixes	Ambion
IL-1α ELISA MAX™ Deluxe	Biolegend
IL-1β ELISA MAX™ Deluxe	Biolegend
IL-12p70 ELISA MAX™ Deluxe	BioLegend

Kit	Reference source
LEGENDplex™ Mouse T_H Cytokine Panel (13-plex)	BioLegend
LEGENDplex™ Mouse Cytokine Panel 2 (13-plex)	BioLegend
ProcartaPlex® Mouse Cytokine & Chemokine Panel 1A (36-plex)	eBioscience
QIAprep® Spin Miniprep kit	QIAGEN
QIAquick® Gel Extraction kit	QIAGEN
QIAquick® PCR purification kit	QIAGEN
ScriptSeq™ complete kit (Human/Mouse/Rat)	Illumina
SensiFast™ SYBR® No-ROX One-Step kit	Bioline
SV total RNA Isolation System kit	Promega
T-PER™ Tissue Protein Extraction Reagent	Thermo Scientific

2.1.5 Oligonucleotides and plasmids

Oligonucleotides (Table 2.7) were purchased from Metabion, considering the manufacturer's advices for purification, synthesis scale and quality control. Primers were shipped at 100 µM in dist. water. Restriction enzyme recognition sites are bold and underlined.

Table 2.7 Oligonucleotides

Name	Sequence (5' → 3')	Description
PCR		
II348	CGG**CTGCAG**GTTTAAGGAGGAATAACCATGAC	Sense primer for *yopD*, creates *Pst*I site
II349	CGG**GCGGCCGC**CTAACCAAGGTCATCAATGG	Antisense primer for *yopD*, creates *Not*I site
II360	CGG**CTGCAG**GCGACAGGAGACTCGATG	Sense primer for *lcrQ*, creates *Pst*I site
II361	CGG**GCGGCCGC**CAGTAGATATATATTATCTCAGC	Antisense primer for *lcrQ*, creates *Not*I site
III784	GCGGCG**GCATGC**GCAAGGCGTTCAGGGAGC	Antisense primer for *rovA*, creates *Sph*I site
III947	GCG**GTCGAC**GGCGTGCTAACGACAATGAC	Sense primer for *rovA*, creates *Sal*I site
III981	TGAACGGCAGGTATATGTG	Sequencing primer for pAKH3
III982	CACTTAACGGCTGACATGG	Sequencing primer for pAKH3
IV281	GGCCC**GGATCC**TGATCTGGTGTTCAGTGAATCA	Sense primer for *yadA*, creates *BamH*I site
IV282	CCGGG**GCGGCCGC**TTACCACTCGATATTAAATGATGCG	Antisense primer for *yadA*, creates *Not*I site
VI392	GCGC**GAGCTC**TCATCTCGCACAACCAAGTTATA	Sense primer upstream fragment for integration into the *Y. pseudotuberculosis* genome; creates *Sac*I site

Name	Sequence (5' → 3')	Description
VI393	TTCATTTTCTAACTTCCGCT**CTCGAGGCGGCCGC**ATGTCATAAAAGGTAAATGGCATAATGG	Sense primer downstream fragment for integration into the *Y. pseudotuberculosis* genome; creates *Not*I and *Xho*I sites
VI394	CCATTTACCTTTTATGACAT**GCGGCCGCCTCGAG**AGCGGAAGTTAGAAAATGAAATTGA	Antisense primer upstream fragment for integration into the *Y. pseudotuberculosis* genome; creates *Xho*I and *Not*I sites
VI395	GCGC**GAGCTC**TCTTTATTTTAACTTACTTGGCATAACTGG	Antisense primer downstream fragment for integration into the *Y. pseudotuberculosis* genome; creates *Sac*I site
VI504	GCCGAACCACAGTTATGGAGG	Sequencing primer for chromosomal integration of $P_{LtetO-1}$::*mRuby2*
VI505	AGACACTGTAAGTCTCCTGTGATAGG	Sequencing primer for chromosomal integration of $P_{LtetO-1}$::*mRuby2*
VI545	GCCC**CTCGAG**TCCCTATCAGTGATAGAGATTGACA	Sense primer for $P_{LtetO-1}$; creates *Xho*I site
VI548	GCCC**GCGGCCGC**TCATTTATACAGTTCATCCATGCCG	Antisense primer for *mRuby2*, creates *Not*I site
VI556	TTTTTTTTCCTCCTTATTTTGTCGACGC	Reverse primer for $P_{LtetO-1}$
VI557	AAAATAAGGAGGAAAAAAAAATGGTGAGCAAAGGTGAAGAGT	Sense primer for *mRuby2*
Yersinia qRT-PCR		
III44	GAGACAACTCCACACCCAAAC	Sense primer for *lcrF* (pYV0076)
III45	GCAAAAGCAGTAATTCCTCAATAC	Antisense primer for *lcrF* (pYV0076)
III186	TGTAGTCGGGGACGTTATCG	Sense primer for *gyrA* (YPK_2846)
III187	CCCATCCACCAGCATATAGC	Antisense primer for *gyrA* (YPK_2846)
III393	CCGACGTAAAGCCGCGATAC	Sense primer for *sopB* (pYV0031)
III394	CCTCGTTCATAAGCACTCGTC	Antisense primer for *sopB* (pYV0031)
III788	GCTGAAACCGTTGGAACTGAC	Sense primer for *rovA* (YPK_1876)
III789	CTTCGCACGACGATCATTT	Antisense primer for *rovA* (YPK_1876)
IV549	CACCACACGAACTGGCCG	Sense primer for *wrbA* (YPK_2363)
IV550	CACGAGTCTGCGAGACATC	Antisense primer for *wrbA* (YPK_2363)
IV555	TTTCCACCGCGGCAACTACC	Sense primer for *hdeB* (YPK_1140)
IV556	CTTTCTGGGGCCTTCTTAC	Antisense primer for *hdeB* (YPK_1140)
IV961	GGTTATGAGATATTGTCACGCC	Sense primer *cnfY* (YPK_2615)

Name	Sequence (5' → 3')	Description
IV962	CGTTCCTCTCATTAGAATTACCG	Antisense primer for *cnfY* (YPK_2615)
IV966	GCCTTTCCATGACCTGCCCC	Antisense primer for *ail* (YPK_1268)
IV967	CTGATTGACGTTAATCTCGGCG	Sense primer for *uspA* (YPK_0120)
IV968	CTCCAGAAATCCTGATGATGACC	Antisense primer for *uspA* (YPK_0120)
V4	TGATTGGCGATGAGGTTACGG	Sense primer for *csrA* (YPK_3372)
V5	TTCTGCTTGGATGCGCTGGT	Antisense primer for *csrA* (YPK_3372)
V56	TGCGGCTGGCACTAAAGACA	Sense primer for *yadA* (pYV0013)
V57	TTTGGCCGCATCCAAAACAT	Antisense primer for *yadA* (pYV0013)
V588	CGTGAAAGGCTCCGTTGCGG	Sense primer for *crp* (YPK_0248)
V589	GTAAGAAATTTCAGCCACTTCAC	Antisense primer for *crp* (YPK_0248)
VI863	GGTGGCTCAAACGCTCAAGA	Sense primer for *yscF* (pYV0082)
VI864	GTAAGTCAGCAAGTAGCGCCG	Antisense primer for *yscF* (pYV0082)
VI865	CCGGGGGTTCGAGGAATCTG	Sense primer for *ail* (YPK_1268)
VI866	GCCCGCATTGGTAATCCAGG	Sense primer for *yopJ* (pYV0098)
VI867	CCCCCATGTTAATTATGAAGCGGG	Antisense primer for *yopJ* (pYV0098)
VI868	CCTGACTCAGGCTGCACGTA	Sense primer for *fliC* (YPK_2381)
VI869	CGCAGGCTGATTTCATCCTGA	Antisense primer for *fliC* (YPK_2381)
VI870	GCGGCATCGAAACCAATCCG	Sense primer for *frdA* (YPK_3813)
VI871	GTAAAGCGGCTTGTTCACCGG	Antisense primer for *frdA* (YPK_3813)
VI872	CGCTGAGTTTGACCCGGAAA	Sense primer for *rfaH* (YPK_3937)
VI873	CAGCAATGACGGTTGCTGGG	Antisense primer for *rfaH* (YPK_3937)
VI874	CGGCCCAAGTTTGGAACCAT	Sense primer for *sodB* (YPK_1863)
VI875	GGCAGCATCAGTAAATTGCGCT	Antisense primer for *sodB* (YPK_1863)
VI893	CTGCCAGGCAAAAATGGCTTG	Sense primer for *arcA* (YPK_3606)
VI894	CAGGTTACGGGCACGGATG	Antisense primer for *arcA* (YPK_3606)
VI895	GGTTTCCATCTGGCGGGTGA	Sense primer for *fnr* (YPK_1944)
VI896	GCGCAGATTGGGCATTTTACCG	Antisense primer for *fnr* (YPK_1944
VI897	CGACCGCGGTCGGTATGTTC	Sense primer for *napA* (YPK_1387)
VI898	ACCGAGGACGCCATACAATGG	Antisense primer for *napA* (YPK_1387)
VI899	GCTTCGGTTTCATCACTCCAGC	Sense primer for *cspC* (YPK_2474)

Name	Sequence (5' → 3')	Description
VI900	GGCCTTCAGCCAAGGTTTTGAAG	Antisense primer for *cspC* (YPK_2474)
VI901	CCGTCCTGGTACCGATGATGG	Sense primer for *if-3* (YPK_1821)
VI902	CATTTCACGCCCACGGAACC	Antisense primer for *if-3* (YPK_1821)

The plasmids used in this work are listed in Table 2.8. The construction of the plasmids pWH9 and pWH14 is described in 2.3.10.

Table 2.8 Plasmids

Plasmid	Description	Reference and source
pAKH3	pGP704$_{bla}$, *sacB*$^{+}$, Amp^{R}	Heroven *et al*., 2012
pFS43	pFS42, P$_{LtetO-1}$::*mCherry*, Kan^{R}	Franziska Schuster, PhD thesis
pWH9	pAKH3, -1063bp YPK_3294 to -67bp YPK_3295	This study
pWH14	pWH9, P$_{LtetO-1}$::*mRuby2*	This study

2.1.6 Bacterial strains and isolates

Bacterial strains employed in this study are mentioned in Table 2.9. The construction of *Y. pseudotuberculosis* strains YP339 and YP340 is described in 2.3.11.

Table 2.9 Bacterial strains

Strain	Description	Reference
E. coli		
DH10β	F^{-} *endA*1 *recA*1 *galE*15 *galK*16 *nupG rpsL* Δ*lacX*74 Φ80*lacZ*ΔM15 *araD*139Δ(*ara, leu*)7697 *mcrA* Δ(*mrr-hsdRMS-mcrBC*)λ^{-}	Grant *et al*., 1990
S17-1λpir	*recA1 thi pro hsdR*$^{-}$ RP4-2Tc::Mu Km::Tn7 λpir	Simon *et al*., 1983
Y. pseudotuberculosis		
YPIII	pIB1, wild type	Bölin *et al*., 1982
YP147	YPIII, pIB1, Δ*cnfY*, Kan^{R}	Schweer *et al*., 2013
YP339	YPIII, pIB1, P$_{LtetO-1}$::*mRuby2* (integrated between YPK_3294 and YPK_3295; genome position 3606960-3607832)	This study
YP340	YP147, pIB1, P$_{LtetO-1}$::*mRuby2* (integrated between YPK_3294 and YPK_3295; genome position 3606960-3607832)	This study

Y. pseudotuberculosis YPIII re-isolates and their isolation source after one passage through BALB/c mice (2.5.10) are given in Table 2.10.

Table 2.10 *Y. pseudotuberculosis* YPIII re-isolates

No.	Isolation source	Mouse no.
Acute colonization phase, 6 dpi		
1	Cecum	1
2	Cecum	1
3	Cecum	1
4	Cecum	2
5	Cecum	2
6	Cecum	2
7	Cecum	3
8	Cecum	3
9	Cecum	3
10	Cecal content	1
11	Cecal content	1
12	Cecal content	1
13	Cecal content	2
14	Cecal content	2
15	Cecal content	2
16	Cecal content	3
17	Cecal content	3
18	Cecal content	3
19	Spleen	1
20	Spleen	1
21	Spleen	1
22	Spleen	2
23	Spleen	2
24	Spleen	2
25	Spleen	3
26	Spleen	3
27	Spleen	3
28	Liver	1
29	Liver	1
30	Liver	1

No.	Isolation source	Mouse no.
31	Liver	2
32	Liver	2
33	Liver	2
34	Liver	3
35	Liver	3
36	Liver	3
37	PP (small intestine)	2
38	PP (small intestine)	2
39	PP (small intestine)	2
40	PP (small intestine)	2
Persistent colonization phase, 42 dpi		
41	Spleen	4
42	Spleen	4
43	Spleen	4
44	Spleen	4
45	Spleen	4
46	Spleen	4
47	Liver	4
48	Liver	4
49	Liver	4
50	PP (small intestine)	4
51	PP (small intestine)	4
52	PP (small intestine)	4
53	PP (small intestine)	4
54	PP (small intestine)	5
55	PP (small intestine)	5
56	PP (small intestine)	5
57	PP (small intestine)	5
58	Cecal content	4
59	Cecal content	4
60	Cecal content	4
61	Cecal content	5
62	Cecal content	5

No.	Isolation source	Mouse no.
63	Cecal content	5
64	Cecal content	6
65	Cecal content	6
66	Cecal content	6
67	Cecum	4
68	Cecum	4
69	Cecum	4
70	Cecum	4
71	Cecum	6
72	Cecum	6
73	Cecum	6
74	Cecum	6

2.1.7 Mice

In this study, several mouse strains of different backgrounds, origins and ages at the beginning of the experiment were used for *Y. pseudotuberculosis* infection (Table 2.11).

Table 2.11 Mice

Background	Strain	Origin	Age (weeks)	Section	Reference/ origin
BALB/c	Wild type	Janvier	8	3.1 - 3.5	Zentralinstitut für Versuchstierzucht (Hannover)-1988(F172)
C57BL/6N	Wild type	Janvier	8-9	3.6.1; 3.6.3	National Institutes of Health (USA)-1999
C57BL/6N	Wild type	HZI	8-9	3.6.2; 3.6.4	In house breeding
C57BL/6N	Caspase-$1^{-/-}$	HZI	9-11	3.6.4	Kayagaki *et al*., 2011
C57BL/6N	Caspase-$11^{-/-}$	HZI	8-10	3.6.4	Kayagaki *et al*., 2011
C57BL/6N	Caspase-$1/11^{-/-}$	HZI	8-10	3.6.4	Kuida *et al*., 1995; Li *et al*., 1995
C57BL/6N	Il-$1\alpha^{-/-}$	HZI	8-10	3.6.4	Horai *et al*., 1998
C57BL/6N	Il-$1\beta^{-/-}$	HZI	8-10	3.6.4	Horai *et al*., 1998
FVB/N	Wild type	Janvier	8	Appendix	National Institutes of Health (USA)-1996

2.1.8 Software and databases

In this study, the following applications were used: Adobe Illustrator CS4 (Adobe Systems Software Ireland Ltd.), Adobe Photoshop CS4 (Adobe Systems Software Ireland Ltd.), A plasmid Editor (ApE), FACSDiva™ (BD Biosciences), FlowJo v9.9.4 (Treestar Inc.), Graph Pad PRISM 6.0 (Graphpad Software, Inc.), Image Lab 2.0.1 (BioRad), LEGENDplex™ V7.0 (VigeneTech), Microsoft® Excel® 14.4.1 (Microsoft), Rotor-Gene Q Series Software 2.0.2 (QIAGEN), SkanIt Software 2.4.3 Research edition Varioskan Flash (Thermo Scientific), VisRseq (Younesy *et al.*, 2015), ZEN 2012 (Zeiss). Furthermore, the following databases were employed: Kyoto Encyclopedia of Genes and Genomes (KEGG), Immunological Genome Project (ImmGen), National Center for Biotechnology Information (NCBI), Universal Protein Resource (UniProt).

2.2 Microbiological methods

2.2.1 Sterilization

Media and solutions were moist heat sterilized in an autoclave for 20 min at 121 °C with 1 bar overpressure. Not heat sterilizable solutions (*e.g.* antibiotics or sucrose) were filter sterilized using a pore diameter of 0.2 µm. Dry heat sterilization at 180 °C was employed for glassware such as pipettes or flasks.

2.2.2 Growth conditions and bacterial storage

Y. pseudotuberculosis and *E. coli* strains (Table 2.9) were aerobically grown in appropriate volumes of broth or solidified broth. Medium additives were added if necessary (Table 2.2; Table 2.3). If not differently stated, *Y. pseudotuberculosis* strains were cultivated at 25 °C and *E. coli* at 37 °C, respectively. Liquid cultures were incubated in a shaking incubator at 200 rpm. For long-term storage, bacteria were stocked with 30 % (v/v) glycerol at -80 °C.

2.2.3 Cell density determination

Cell densities of liquid bacterial suspensions were determined by measurement of the optical density (OD) with a spectral photometer (Amersham Biosciences) at 600 nm. It was assumed that an OD_{600} corresponds to a cell density of $1x10^9$ colony-forming units (CFU) per milliliter.

2.2.4 Growth curves

To analyze and compare the growth behavior of different *Y. pseudotuberculosis* strains, an overnight culture of the respective strain was diluted into 5 ml LB broth to $OD_{600} = 0.1$. At several time points, the optical density at 600 nm was measured in a black 96 well clear bottom plate (Becton Dickson) using the Varioskan Flash plate reader (Thermo Scientific; bandwidth 5 nm; measurement time 100 ms).

2.2.5 Fixation of bacteria and fluorescence microscopy

For fluorescence microscopic analysis, yersiniae stably-labeled with *mRuby2* were grown to exponential growth phase (5 h), early stationary growth phase (8 h) or late stationary growth phase (24 h). At the respective time points, 500 µl of the bacterial culture were harvested by centrifugation (5.000 rpm, 2 min) and fixed in 500 µl 4 % paraformaldehyde (PFA) (w/v) for 20 min in the dark. After that, bacteria were washed twice and resuspended in 1x PBS (Table 2.1) for microscopic analysis.
Fluorescence microscopy was performed with the Axiovert II fluorescence microscope (Zeiss) using the Axiocam HR digital charge-coupled device (CCD) camera (Zeiss) and the software ZEN 2012 (Zeiss). For analysis of fixed bacteria under the microscope, bacteria were spotted on a glass slide. Images were processed utilizing Adobe Photoshop CS4 (Version 11.0; Adobe Systems Incorporated).

2.3 Genetic and molecular biological methods for DNA

2.3.1 Polymerase chain reaction

The polymerase chain reaction (PCR) was used to amplify specific DNA fragments with heat-stable polymerases. The annealing temperature depends on the length and nucleotide contents of the primer pairs, whereas the elongation time and temperature are dependent on the polymerase and the size of the amplified DNA fragment.
The Phusion High-Fidelity (HF) DNA polymerase is one of the most accurate polymerases, which possesses high processivity, and low error rates combined with proofreading capability. Therefore, it was used for cloning and sequencing applications. Amplification of DNA fragments for test-PCRs or colony-PCRs was performed using the MangoTaq^{TM} polymerase.
PCR reactions and conditions were composed according to the manufacturer's instructions in volumes ranging from 10 to 50 µl.

2.3.2 Agarose gel electrophoresis

Agarose gel electrophoresis separates DNA fragments depending on their size. The principle is based on the natural negative charge of DNA, which drives the migration of DNA in the agarose gel by the applied electric field. Routinely, 1x TAE gels (Table 2.1) containing agarose ranging from 1 to 2 % (w/v) were employed. DNA samples were mixed with 6x loading dye and separated at 100-120 V for 45 to 60 min. The GeneRuler DNA Ladder Mix (Thermo Scientific) was used as DNA fragment standard. Subsequently, the DNA was visualized by ethidium bromide staining and detected upon UV-light excitation. Gel images were documented with the BioRad Gel Doc XR+ gel documentation system.

2.3.3 Determination of DNA concentration and purity

The DNA concentration and purity was measured with the NanoDrop spectral photometer (Peqlab) by assessing the absorption of the solution at 230, 260 and 280 nm. For concentration calculation it was expected that A_{260} of 1 corresponds to a DNA concentration of 50 µg/ml.
Furthermore, the ratios of A_{260}/A_{280} and A_{260}/A_{230} were calculated to estimate the purity of the DNA samples.

2.3.4 DNA sequencing

To ensure the quality of the cloned plasmids and PCR fragments, the respective DNA was sequenced by the genome analytics in-house sequencing platform.

2.3.5 Isolation of DNA

Plasmid preparation

Plasmid DNA was isolated using the QIAprep® Spin Miniprep kit according to the manufacturer's instructions. The obtained plasmid DNA was eluted in dist. water.

Genomic DNA isolation

For genomic DNA isolation, 750 µl of a bacterial overnight culture was gently mixed with one volume of phenol/chloroform/isoamyl alcohol (25:24:1) and centrifuged (13,000 rpm; 2 min; room temperature (RT)). Subsequently, the watery supernatant was transferred to a clean reaction tube and was mixed with one volume chloroform. After centrifugation at 13,000 rpm for 2 min at RT, the watery supernatant was transferred to a clean reaction tube. This purification step was repeated. The extracted DNA in the watery supernatant was precipitated by addition of two volumes 100 % ethanol and subsequent centrifugation at 13,000 rpm for 20 min at RT. The obtained DNA was washed twice with 70 % ethanol and air-dried. The genomic DNA was resuspended in 100 to 200 µl of dist. water.

Genomic DNA isolation for *Yersinia* colony PCR

To perform colony-PCR with *Y. pseudotuberculosis*, colony material was resuspended in 30 to 50 µl of dist. water and heated at 95 °C for 10 min. 1 to 4 µl of the supernatant were further used as template for PCR.

2.3.6 Purification of DNA fragments

Gel extraction

For DNA fragment exclusion and purification of DNA fragments, DNA was separated with agarose gel electrophoresis and visualized (2.3.2). Subsequently, the fragment of choice was excised and extracted from the gel using the QIAquick® Gel Extraction kit (QIAGEN) according to the manufacturer's instructions. The obtained DNA was eluted in dist. water.

PCR purification

To remove excess primers from PCR reactions (2.3.1), the DNA was purified with the QIAquick® PCR Purification Kit (QIAGEN) following the manufacturer's instructions. The purified PCR reaction was recovered in dist. water.

2.3.7 16S DNA Sequencing

To isolate the crude DNA of the microbial community (sampled in 2.5.11), 500 µl of 0.1 mm zirconia/silica, 700 µl of buffer A with SDS (Table 2.1) and 500 µl phenol/chloroform/isoamyl alcohol (25:24:1, pH 7.9) were added to the feces and chilled on ice. Thereafter, the samples were homogenized twice with a bead-beater (BioSpec) for 2 min and centrifuged (3 min, 8,000 rpm, 4 °C). The supernatant was transferred into a new reaction tube for phenol-chloroform extraction. To do this, one volume phenol/chloroform/isoamyl alcohol was mixed with the supernatant by inversion and centrifuged (5 min, 13,000 rpm, RT). The aqueous phase was precipitated with 0.1 volumes of 3 M sodium acetate (pH 5.5) and 1 volume of

isopropanol. For precipitation, the samples were incubated at -20 °C for 1 h. Subsequently, the DNA was pelleted by centrifugation (20 min, 13,000 rpm, 4 °C). The DNA pellet was washed once with 70 % ethanol, dried using the Speedvac (15 min, no heat, auto run) and dissolved in 200 µl TE buffer (Table 2.1) by incubation at 50 °C for 30 min. The DNA was further purified by treating the dissolved DNA with 100 µg/ml RNase A (2 min, RT) followed by purification with spin columns (BioBasic) according to the manufacturer's specifications. The DNA extracts were eluted with 52 µl EB (BioBasic) delivered with the kit. The DNA extracts were adjusted to 25 ng/µl in EB (BioBasic).
16S DNA amplification was performed at the HZI by the group Microbial Immune Regulation. Briefly, the 16S DNA V4 region (F515/R806) was amplified in triplicates by PCR using Phusion DNA Polymerase and 3' end labeled barcode primers for the 16S DNA. Thereafter, the triplicates were pooled together checked on an agarose gel and quantified using PicoGreen®. The dsDNA was adjusted to 10 nM and samples were pooled. The pooled 16S libraries were quantified with KAPA Library Quantify Kit and handed in for sequencing on the Illumina MiSeq platform (PE250) at the HZI to the Genome Analytics group. Data set analysis was again performed at the HZI by the group of Microbial Immune Regulation. Briefly, filtering of sequences for low quality reads and barcode-based binning was carried out with QIIME v1.8.0 (Caporaso *et al*., 2010). The obtained reads were clustered into 97 % ID operational taxonomic units (OTUs) using UCLUST and taxonomic classification using RDP Classifier (80 % bootstrap confidence cut off) (Edgar, 2010; Wang *et al*., 2007). Sequences without matching reference dataset, were sorted as *de novo* using UCLUST. The phylogenetic relationships between the OTUs were set with FASTTREE to the PyNAST alignment (Price *et al*., 2010). The OTU absolute abundance table and mapping file were utilized for analysis and data visualization.

2.3.8 Cloning techniques

Restriction digestion

For DNA fragment insertion into a specific plasmid site, plasmid and DNA fragment were digested with endonucleases (Table 2.4) to gain compatible 5' and 3' ends. The digestion reactions were carried out following the manufacturer's advice. The restriction enzymes were heat inactivated at 65 °C for 20 min, if recommended.

Dephosphorylation

The 5'-phosphate groups of linearized vector DNA were removed in order to decrease the re-ligation rate of the vector DNA. To this purpose, the Antarctic phosphatase (NEB) was employed according to the manufacturer's advice. The phosphatase was heat inactivated at 70 °C for 5 min.

Ligation

DNA ligases are commonly applied to join two DNA sequences by exploiting their property to form phosphodiester bonds between the 5'-phosphate and the 3'-hydroxylgroup of DNA 5'- and 3'-ends. This technique was utilized to integrate a desired DNA fragment into a vector DNA using the T4 Ligase (NEB) according to the manufacturer's instructions.

2.3.9 DNA transfer

To transfer DNA into bacterial cells different methods were applied. For direct transfer, chemical transformation, and for cell-contact mediated transfer, conjugation was employed.

Chemocompetent *E. coli* and transformation

For production of chemocompetent *E. coli*, bacteria were grown in LB broth supplemented with 20 mM $MgSO_4$ until the culture reached an OD_{600} of 0.5 to 0.8. The bacterial culture was harvested by centrifugation (2,755 g; 10 min; 4 °C) and resuspended in 0.4 volumes of ice-cold TFBI (Table 2.1). The suspension was chilled on ice for 10 min and was subsequently centrifuged for 10 min (2,755 g; 4 °C). The pellet was resuspended in 0.04 volumes of TFBII (Table 2.1) and kept on ice for 60 min. After that, the chemocompetent cells were stored in 100 µl aliquots at -40 °C.
For heat shock transformation of a desired plasmid, 50 to 100 µl of chemocompetent *E. coli* were mixed with 1 to 10 µl of plasmid DNA and incubated for 30 min on ice. Thereafter, bacteria were heat-shocked at 42 °C for 45 to 60 s and immediately chilled on ice for 2 min. Subsequently, 400 µl SOC broth was added and bacteria were incubated at 37 °C for 1 h. The bacterial suspension was streaked onto LB agar plates containing the appropriate antibiotic and incubated overnight.

Conjugation

The mechanisms of conjugation, also named mating, describes the cell-contact mediated horizontal gene transfer via fertility pili (F pili). During the conjugation process, a donor strain (*E. coli* S17-1λpir) harboring conjugal traits (based on RP4) transfers genetic mobilizable material to the acceptor strain. For conjugation, an overnight culture of *E. coli* S17-1λpir carrying the appropriate mobilizable plasmid and *Y. pseudotuberculosis* were inoculated into 10 ml LB broth in 1:100 or 1:50 dilutions, respectively. After 2.5 h of incubation, *E. coli* were shifted to 37 °C without shaking for 0.5 h, allowing the F pili to build up. Thereafter, 300 µl of *E. coli* were harvested by centrifugation (5,000 rpm; 1 min) and washed twice with LB broth to remove the remaining antibiotics. Subsequently, 900 µl of *Y. pseudotuberculosis* were mixed with the *E. coli* S17-1λpir and centrifuged (5,000 rpm; 2 min). The bacterial mixture was resuspended in 200 µl LB and incubated on a nitrocellulose membrane (0.22 µm, Millipore) placed on solid LB broth for 4 h at 25 °C. After that, bacteria were detached from the filter and plated on *Yersinia* selective agar plates supplemented with the appropriate antibiotics.

2.3.10 Construction of plasmid pWH14

For stable integration of *mRuby2* under the control of the $P_{LtetO-1}$ promoter into the *Y. pseudotuberculosis* genome, the mobilizable suicide plasmid pWH14 based on pAKH3 was created. To construct a backbone vector that enables integration of different genetic elements into the desired *Y. pseudotuberculosis* genomic site (NCBI accession path >gi|170022262|ref|NC_010465.1|:3606960-3607832; *Y. pseudotuberculosis* YPIII, complete genome), the genomic region was amplified as an upstream fragment with primer pairs VI392 and VI394 and a downstream fragment with primer pairs VI393 and VI395. To fuse the up- and downstream fragments creating an *Xho*I and *Not*I cloning site in between, the two fragments were fused by PCR using primers VI392 and VI395. Subsequently, pWH9 was generated by digestion of the created fusion DNA and pAKH3 with *Sac*I and ligation of the fragments as described in 2.3.8. The sequence was verified by sequencing with primers III981, III982, VI392 and VI395.

To integrate *mRuby2* under the control of the $P_{LtetO-1}$ promoter into pWH9, the $P_{LtetO-1}$ promoter and the Shine-Dalgarno sequence from pFS43 were amplified with VI545 and VI556 and *mRuby2* (supplied by Marc Erhardt, HZI) with VI557 and VI548. The two fragments were fused by PCR using the primers VI545 and VI548. The resulting fragment and pWH9 were digested with *Xho*I and *Not*I. Following dephosphorylation of pWH9 and ligation with the fusion DNA fragment, pWH14 was generated.

2.3.11 Construction of *Y. pseudotuberculosis* strains YP339 and YP340

The *Y. pseudotuberculosis* strains YPIII *mRuby2* (YP339) and YPIII Δ*cnfY mRuby2* (YP340) were constructed by introduction of pWH14 into *Y. pseudotuberculosis* YPIII and YPIII Δ*cnfY* by conjugation (2.3.9). The plasmid was integrated via homologous recombination into the *Yersinia* genome. To obtain colonies that spontaneously lost the integrated plasmid (including *sacB* and amp^R) leaving $P_{LtetO-1}$::*mRuby2* inserted into the genomic locus, a counter selection on LB solid medium containing 10 % sucrose was employed. This technique exploits the expression of the *sacB* from the integrated plasmid, which leads to the production of toxic compounds out of sucrose thereby inducing selective pressure on the bacterium to lose the integrated plasmid. Thereafter, the selected colonies were patched on antibiotic plates to select for plasmid loss. The obtained colonies were further subjected to colony-PCR to screen for integration of *mRuby2* under the control of the $P_{LtetO-1}$ promoter. The correct integration was further validated by sequencing using primers VI504, VI505, VI545 and VI548.

2.4 Molecular biological methods for RNA

2.4.1 Determination of RNA concentration, purity and quality

The RNA concentration and purity was measured with the NanoDrop spectral photometer by assessing the absorption of the solution at 230, 260 and 280 nm. For concentration calculation it was expected that A_{260} of 1 corresponds to a RNA concentration of 40 µg/ml. Furthermore, the ratios of A_{260}/A_{280} and A_{260}/A_{230} were calculated to estimate the purity of the DNA samples.

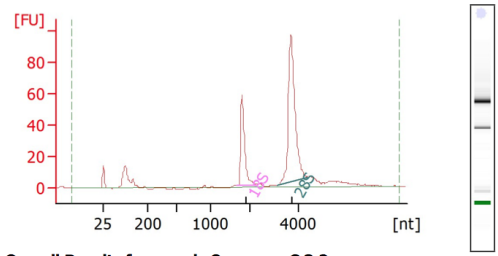

Overall Results for sample 8 : C 3.2

RNA Area:	440,4
RNA Concentration:	148 ng/µl
rRNA Ratio [28s / 18s]:	2,4
RNA Integrity Number (RIN):	10 (B.02.08)
Result Flagging Color:	
Result Flagging Label:	RIN:10

Fragment table for sample 8 : C 3.2

Name	Start Size [nt]	End Size [nt]	Area	% of total Area
18S	1.659	2.213	87,4	19,9
28S	3.116	4.390	206,3	46,8

Figure 2.1 RNA electropherogram.
RNA electropherogram obtained from an Agilent RNA 6000 Nano kit using Expert Software B02.08 (Agilent Technologies).

To evaluate the RNA integrity and quality, appropriate concentrations of RNA were analyzed at the in-house genome analytics platform with the Agilent 2100 Bioanalyzer using either the Agilent RNA 6000 Nano kit or Pico kit or by denaturating urea polyacrylamide gel electrophoresis (2.4.2). Using the Aligent 2100 Bioanalyzer, the quality of the RNA (RNA integrity number; RIN) was calculated by the obtained electropherograms (Figure 2.1) utilizing the Expert Software B02.08 (Agilent Technologies).

2.4.2 Denaturating urea polyacrylamide gel electrophoresis (Urea PAGE)

To evaluate the integrity of isolated RNA from *in vitro* cultures, RNA was checked on denaturating urea polyacrylamide gels (7 M urea, 10% acrylamide):

4.2	g	Urea
0.6	ml	10x TBE
2.5	ml	Acrylamide/bisacrylamide (40%)
3.75	ml	Dist. water
6	µl	Tetramethylethylenediamine (TEMED)
60	µl	10 % ammonium persulfate (APS)
10	ml	1 gel

RNA loading buffer (2x, Table 2.1) was added to 1 µg RNA, boiled 10 min at 70 °C and chilled for 2 min on ice before loading. The RNA was subsequently separated at 140 V for 2.5 h in 1x TBE (Table 2.1). RNA was visualized by ethidium bromide staining.

2.4.3 RNA isolation

Total RNA isolation from bacterial cultures

To analyze bacterial expression patterns by qRT-PCR, RNA of bacterial *in vitro* cultures was isolated. For this purpose, *Y. pseudotuberculosis* grown at 25 °C or 37 °C for 16 h, were pooled from 3 independent biological replicates, resuspended in 0.2 volumes stop solution (5 % (v/v) water-saturated phenol in ethanol) and snap-frozen in liquid nitrogen. The suspension was thawed on ice and centrifuged (14.000 g; 4 °C; 2 min). Subsequently, the pellet was resuspended in lysozyme-TE buffer (50 mg/ml, Table 2.1) and incubated for 10 min at RT. The RNA of the sample was purified with the SV Total RNA-Isolation kit following the manufacturer's advice. The RNA was eluted into a reaction tube in 100-200 µl RNase-free water. The quality of the RNA was determined as described in 2.4.1 and stored at -80 °C.

Total RNA extraction from mouse tissue and sample pooling

For total RNA extraction, 4 ml solution D (Table 2.1), freshly supplemented with β-mercaptoethanol, were added to the snap frozen cecum (2.5.9) and subsequently transferred to a pre-cooled 14 ml tube (Greiner) on ice. The cecum was homogenized on ice with the Polytron PT 2100 homogenizer (Kinematica) at 11,000 rpm for 10 s. The homogenate was split to three 750 µl aliquots into pre-cooled 2 ml reaction tubes with previously added 0.1 mm and 1 mm acid washed glass beads (Sigma). Afterwards, the bacterial cells in the samples were disrupted using the bead beater (TissueLyser II, QIAGEN) for 1 min with a frequency of 30 beats per second and immediately cooled on ice for 1 min. This cell disruption procedure was repeated for three times. Subsequently, 500 µl of the homogenate were transferred to a pre-cooled 2 ml reaction tube and the following solutions were sequentially mixed with the homogenate:

0.1	volumes	2 M sodium acetate, pH 4
1	volume	Water-saturated phenol
0.2	volumes	Chloroform/isoamyl alcohol (24:1)

Thereafter, the tubes were vigorously shaken by hand for 10 s, cooled on ice for 15 min and centrifuged (10,000 g; 4 °C; 20 min). The watery supernatant was transferred to a new 1.5 ml reaction tube. For extraction of phenol, 1 volume chloroform/isoamyl alcohol was added, vortexed for 30 s and centrifuged (10,000 g; 4 °C; 3 min). Subsequently, the watery supernatant was transferred to a fresh reaction tube. The extraction step was repeated. Thereafter, the RNA extract in the watery supernatant was precipitated with 0.1 volumes of 2 M sodium acetate pH 4.0 and 2.5 volumes of ethanol. The samples were incubated overnight at -20 °C. The RNA was recovered by centrifugation (10,000 g; 4 °C; 30 min), washed with 70 % (v/v) ethanol and air-dried. The RNA pellet was dissolved in 50 µl TE buffer (Table 2.1) or RNase and DNase free water. The quality and concentration of the RNA extracts was assessed as mentioned in 2.4.1 and stored at -80 °C.
To receive a robust data set, equal amounts of the RNA extracts of 3 to 4 ceca (5 days post infection (dpi)) or 5 ceca (42 dpi) of one experiment were pooled. In the end, three independent pools of each condition were obtained.

2.4.4 DNA digestion

The TURBO™ DNase (Ambion) is a genetically engineered DNA endonuclease derived from the bovine DNase I that harbors increased catalytic efficiency at higher salt and lower DNA concentrations. The TURBO™ DNase was applied to remove contaminating trace DNA from RNA total extracts for qRT-PCR or RNA sequencing. A standard DNA digestion for 10 µg total RNA extract or 40 µg of the total RNA pools was composed of:

2	µl	TURBO™ DNase
24	µl	10x TURBO™ DNase buffer
1	µl	RiboLock™ RNase Inhibitor (40 U/µl)
213	µl	RNA
240	µl	Final volume

The digestion was incubated at 37 °C for 1 h. To inactivate the TURBO™ DNase phenol/chloroform/isoamyl alcohol extraction (2.4.5) was performed.

2.4.5 Phenol/chloroform/isoamyl alcohol purification

For removal and inactivation of proteins from RNA solutions, the RNA solution volume was increased to 300 µl with RNase-free water. Subsequently, 1 volume of phenol/chloroform/isoamyl alcohol (25:24:1) was added and vortexed. After that, the samples were centrifuged (>10.000 g; 10 min; 4 °C) and the supernatant was extracted twice with 1 volume chloroform/isoamyl alcohol. The supernatant was precipitated with 0.1 volumes of 3 M sodium acetate and 2.5 volumes of ethanol at -20 °C. The RNA was recovered by centrifugation (>10.000 g; 30 min; 4 °C), washed with 70 % (v/v) ethanol, air-dried and resuspended in 20-50 µl RNase-free water.

2.4.6 Quantitative real-time PCR

Quantitative real-time PCR (qRT-PCR) was employed to assess bacterial expression patterns using the SensiFast™ SYBR® No-ROX One-Step kit (Bioline). During qRT-PCR, total RNA was reverse-transcribed by a reverse transcriptase into complementary DNA (cDNA). Subsequently, the desired cDNA was amplified via PCR. After each PCR-cycle, fluorescence intensity of the green fluorescent dye SYBR®, which intercalates into double-stranded DNA, was monitored. The measured fluorescence intensity was used for relative quantification of transcript abundance.

For qRT-PCR, DNA-depleted RNA (2.4.4) was adjusted to a final concentration of 25 ng/µl. A typical qRT-PCR reaction was composed of:

6.25	µl	2x SensiFast™ SYBR No-ROX One-Step Mix
0.5	µl	10 µM forward primer
0.5	µl	10 µM reverse primer
0.125	µl	Reverse transcriptase
0.25	µl	RiboSafe RNase inhibitor
2.375	µl	RNase-free water
2.5	µl	RNA (25 ng/µl)
12.5	µl	Final volume

Reverse transcription and subsequent qRT-PCRs were performed in the Rotor-Gene Q real-time PCR cycler (QIAGEN) in technical duplicates. A 3-step-cycling program with subsequent melt-profile analysis to monitor product specificity was applied (Table 2.12).

Table 2.12 qRT-PCR program design

Step	Cycles	T °C	Time	Description
1. cDNA generation	1	45	20 min	Reverse transcription
2. Polymerase activation	1	95	5 min	
3. PCR	<50	95	10 s	Denaturation
		52-62	20 s	Annealing
		72	10-30 s	Extension and acquisition
	1	72	5 min	Final extension
Melt profile analysis		58-99		Ramp heating and fluorescence detection

The acquired data was further processed with the Gene-Rotor Q Series software. The normalization method was typically set to dynamic tube normalization and normalization was user-defined starting from cycle 1-10. The cycle threshold (Ct) was determined by setting the threshold routinely to 0.005. This threshold reflects the lower fluorescence detection limit of the instrument and constitutes the baseline of the amplification plot. The exceedance of the threshold indicates the accumulation of PCR product and determines the Ct of the sample.

The melt profile was analyzed by setting the threshold to >2. The obtained melt profile and PCR product melt temperatures were used to determine product specificity and to exclude the abundance of primer dimers.

To calculate the relative expression of a target gene compared to a reference gene, the relative quantification method described by Pfaffl was used (Pfaffl, 2001) (Formula 1 to 4). According to formula 4, an ideal primer efficiency of 2 (one duplication per cycle) was assumed. As it

was shown that normalization to a single gene while comparing different conditions could be instable (Vandesompele *et al*., 2002), the total RNA samples were normalized to *sopB* and *if-3* in order to get more stable normalization of relative gene expression. To this end, the mean of the calculated ΔCt $_{\text{reference gene}}$ (Formula 2) was calculated (Formula 3).

$$\Delta Ct_{gene\ of\ interest} = mean\ Ct_{\ gene\ of\ interest_{reference\ condition}} - Ct_{gene\ of\ interest_{test\ condition}} \quad (1)$$

$$\Delta Ct_{reference\ gene} = mean\ Ct_{\ reference\ genes_{reference\ condition}} - Ct_{reference\ gene_{test\ condition}} \quad (2)$$

$$\Delta Ct_{reference\ genes} = mean\ \Delta Ct_{reference\ gene\ 1\&2} \quad (3)$$

$$relative\ expression = \frac{2^{\Delta Ct_{gene\ of\ interest}}}{2^{\Delta Ct_{reference\ gene(s)}}} \quad (4)$$

2.4.7 RNA transcriptomics (ScriptSeq™)

To assess and compare the murine transcriptome during different stages of infection, the total RNA extract pools (2.4.3) were send to the in-house genome analytics platform for library preparation. The libraries were generated with the epicenter ScriptSeq™ complete kit (human/mouse/rat). For this purpose, 1 µg of DNA-depleted total RNA (2.4.4) was depleted for murine rRNA with the Ribo-Zero™ kit (human/mouse/rat) following the manufacturer's specifications. To determine the dynamic range, the lower detection limit and to evaluate the accuracy of the libraries, External RNA Controls Consortium (ERCC) Spike-In control mixes (Ambion) were added. Subsequently, library preparations were performed following the manufacturer's advice. Briefly, the RNA was fragmented and random 5'-end tagged cDNA primers were annealed. Thereafter, cDNA was synthesized with the StarScript reverse transcriptase delivered with the kit. The RNA was removed and the cDNA was labeled with a 3'-terminal-tag. For 5'-end bar code labeling, the di-tagged cDNA library was purified and amplified by PCR. The finalized libraries were sequenced using an Illumina cluster station (HiSeq, short reads, strand specific). The obtained data was processed as described in Nuss *et al*., 2015 and Nuss *et al*., 2017). After demultiplexing, quality assessment and *in silico* adaptor clipping, the remaining reads were mapped with Tophat to the mm10 genome. To identify differential expression profiles in the cecum of the mouse, DESeq2 analysis package was applied (Love *et al*., 2014).

2.5 Mouse experiments

All experiments involving mice were carried out in strict accordance to the European Health Law of the Federation of Laboratory Animal Science Associations (FELASA) and the German Recommendations of the Society of Laboratory Animal Science (GV-SOLAS). Mice were housed under specific pathogen-free conditions in the animal facility of the Helmholtz Centre for Infection Research, Braunschweig. The animal protocol was approved by the Niedersächsisches Landesamt für Verbraucherschutz und Lebensmittelsicherheit: animal licensing committee permission No. 33.9-42502-04-13/1166.
All mouse strains of this study are listed in Table 2.11. Purchased mice were allowed to acclimatize to the new housing conditions for one week prior to infection. Every effort was made to minimize suffering.

2.5.1 Infection of mice

Mice were challenged with bacterial loads via the gastro-intestinal route using a ball-tipped feeding needle to mimic natural infection or by intravenous administration to provoke a systemic infection. For gastrointestinal infections, 200 µl of the appropriate *Y. pseudotuberculosis* strain and dosage suspended in PBS (Table 2.1) were fed, whereas for intravenous infections 100 µl were injected via the tail vein.
For both infection routes, bacteria were prepared as follows: 20 ml LB broth of a bacterial overnight culture was washed twice with 1x PBS and suspended in 10 ml 1x PBS. Subsequently, the optical density was determined (2.2.3) and adjusted according to the desired bacterial loads by dilution (intra-gastric infections: $1x10^6$, $2x10^7$ or $2x10^8$ CFU per mouse; intravenous infections: $5x10^4$ CFU per mouse). Revision of the infection loads was achieved by plating appropriate dilutions of the bacterial suspensions on LB agar.

2.5.2 Survival experiments

To evaluate the role of certain bacterial and host factors on the survival of the host, mice (Table 2.11) were challenged either intra-gastrically ($2x10^8$ CFU per mouse) or intravenously ($5x10^4$ CFU per mouse) with *Y. pseudotuberculosis* bacterial suspensions (2.5.1). The fitness of the mice was monitored daily for two to three days prior to infection to determine the baseline and up to 14 days post infection to assess infection progression. The mice were sacrificed painlessly and were considered as dead for the ongoing experiment if they showed one or both of the following abort criteria: (a) mice that lost more than 20 % of their initial bodyweight, (b) mice with a health scoring with less than three (according to Table 2.13).

Table 2.13 Mouse health scores

Score	Health status
6	Vigorous, curious, very active, shiny clean fur
5	Curious, active, some resting
4	Reacts to care, frequently resting, some untended fur
3	Dozy, rare activity, reduced food intake
2	Little activity, resting, no food intake, hunchback
1	No activity, hunchback, expected death, no social interactions

2.5.3 Chemokine and cytokine profiling

To analyze chemokine and cytokine concentrations in the serum and tissues of untreated and *Y. pseudotuberculosis* infected mice ($1x10^6$ or $2x10^8$ CFU per mouse), serum and tissue samples were taken and subjected to a multiplex immunoassay, or enzyme-linked immunosorbent assay (ELISA).

Serum isolation

At certain time points post infection (*e.g.* 3, 9, 14 dpi, etc.), uninfected and *Y. pseudotuberculosis* infected mice were euthanized via CO_2 asphyxiation. Immediately, 300 to 500 µl heart blood were isolated via cardiac puncture and transferred to Microvette® 500 Z-Gel tubes (Sarstedt). The blood samples were centrifuged (5 min, 10.000 g, 20 °C) and the separated serum was frozen at -80 °C.

Tissue lysates from C57BL/6N mice

Tissue lysates of small intestines, MLNs, spleens, and livers at 3 dpi were generated to assess the cytokine concentration of IL-1α, IL-1β and IL-12p70 with ELISA. To this end, uninfected and *Y. pseudotuberculosis*-infected C57BL/6N mice were sacrificed via CO_2 asphyxiation. The tissues were excised, weighed and snap frozen in liquid nitrogen. Subsequently, the tissues were placed on ice and tissue protein extraction reagent (T-PER; Thermo Scientific) supplemented with phosphatase and protease inhibitors was added. The tissues were homogenized and centrifuged for 15 min, 14,000 g at 4 °C to remove remaining debris. Thereafter, homogenates were aliquoted and stored at -80 °C until further analysis.

Tissue lysates from BALB/c mice

Tissue lysates from the cecum were generated at 3, 9, 14, 21, 30 and 42 dpi to assess the global cytokine profiles with LEGENplex™ bead-based immunoassays (BioLegend). For this purpose, uninfected and *Y. pseudotuberculosis*-infected BALB/c mice were sacrificed via CO_2 asphyxiation. The cecum was isolated, flushed, weighted and snap-frozen in liquid nitrogen. The cecal contents were plated in serial dilutions to determine the *Y. pseudotuberculosis* load (2.5.4). The ceca were stored at -80°C until further processing. For protein isolation, frozen ceca were transferred to 2 ml ice-cold NP-40 buffer (Table 2.1) containing 1 mM PMSF (Table 2.1). Thereafter, ceca were homogenized (15,000 rpm, Polytron PT 2100) on ice and centrifuged (4 °C, 1,000 g, 5 min) to reduce foam and to pellet large debris. The homogenate was aliquoted and frozen at -80 °C until assays were carried out. The protein concentrations were determined with the Pierce™ BCA protein assay kit (Thermo Fisher Scientific) according to the manufacturer's recommendations.

Enzyme-linked immunosorbent assay - ELISA

In order to determine the IL-1α, IL-1β and IL-12p70 protein levels in tissue homogenates, ELISAs for the respective cytokines were performed. For this purpose, tissue homogenates were thawn on ice and analyzed on ELISA plates (Table 2.6) according to the manufacturer's instructions. Subsequently, the absorbance at 450 nm was determined utilizing the Varioskan Flash plate reader (Thermo Scientific). The cytokine concentrations were calculated using a standard curve (Prism 6.0).

Multiplex immunoassay (ProcartaPlex®)

To determine the chemokine and cytokine concentrations in the serum samples, the ProcartaPlex® Mouse Cytokine & Chemokine Panel 1A (36-plex) magnetic bead based kit (eBioscience) was used. The kit included the analytes: ENA-78/CXCL5, eotaxin, G-CSF, GM-CSF, GROα, IFNα, IFNγ, IL-1α, IL-1β, IL-2, IL-3, IL-4, IL-5, IL-6, IL-9, IL-10, IL12p70, IL-13, IL-15/IL-15R, IL-17A, IL-18, IL-22, IL-23, IL-27, IL-28, IL-31, IP-10, LIF, MCP-1; MCP-3, M-CSF, MIP-1α, MIP-1β, MIP-2, RANTES, and TNFα.

The assay was performed according to the manufacturer's instructions. Briefly, the color-coded bead mix coated with its respective analyte-specific antibody was incubated with the serum samples or the standard. Subsequently, biotinylated detection antibody mix specific for the analyte (antibody-antigen sandwich) and phycoerythrin (PE)-conjugated streptavidin (SA), which specifically binds to biotin (Figure 2.2), was added.

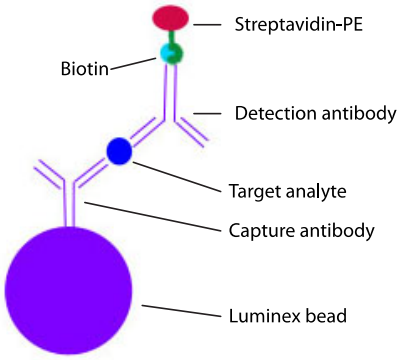

Figure 2.2 Multiplex assay principle.
The analyte binds to the capture antibody coated cytokine/chemokine-specific Luminex bead. Thereafter, biotinylated-detection antibody and streptavidin are added to detect the analyte concentration.

The beads were detected with the Luminex® 100™ system, which is able to detect and quantify multiple analytes in parallel. To this purpose, the single beads were (1) classified (*e.g.* TNFα-Luminex bead) and (2) the intensity of PE-derived signal of this bead was detected. This signal is proportional to the amount of bound analyte. The cytokine concentrations were calculated with best-fit curves of the supplied standards.

Multiplex Immunoassay (LEGENDplex™)

To determine the cytokine and chemokine concentrations in serum samples and tissue homogenates at different time points post infection, the LEGENDplex™ Mouse T_H Cytokine Panel and the Mouse Cytokine Panel 2 bead-based immunoassay (BioLegend) were used. The kits included the analytes: IL-2, IL-4, IL-5, IL-6, IL-9, IL-10, IL-13, IL-17A, IL-17F, IL-21, IL-22, IFNγ, TNFα, GM-CSF, IFNβ, IL-1α, IL-1β, IL-3, IL-7, IL-11, IL-12 (p40), IL-12 (p70), IL-23, IL-27, IL-33 and TSLP.
The assay was performed according to the manufacturer's instructions with the following optimizations. Standard or sample was incubated for 1.5 h at RT with shaking as listed below:

20	µl	Assay buffer
20	µl	Standard/sample
20	µl	Mixed beads (1:4)
12.5	µl	Detection antibodies

Thereafter 12.5 µl of SA-PE (LEGENDplex™) were added and incubated for 30 min. The beads were washed twice with washing buffer and finally suspended in 100 µl of washing buffer.
The beads were detected with the flow cytometer (LSRFortessa™, BD Biosciences) following the assay requirements for flow cytometer setups and acquisition. Data analysis was performed with the LEGENDplex™ Data Analysis Software V7.0 (BioLegend).

2.5.4 Bacterial burden assay

To assess the *Y. pseudotuberculosis* loads in particular tissues bacterial burden assays were performed. For this purpose, infected mice (2.5.1; $5x10^4$, $1x10^6$ or $2x10^8$ CFU per mouse) were sacrificed at different days and stages post infection by CO_2 asphyxiation. Depending on the experimental setup the cecum, small intestine, PP (of small intestine), MLNs, spleen and liver were removed, flushed if applicable, weighted and homogenized in sterile PBS (Table 2.1) with the Polytron PT 2100 (Kinematica) homogenizer at 22.000 rpm for 10 s. Contents of gut compartments like cecum and small intestine were flushed out with a defined volume of sterile 1x PBS and also homogenized. Heart blood was isolated via cardiac puncture with a 0.60x25 mm needle and mixed with 500 mM EDTA (1:2) to prevent clotting. To determine the bacterial loads in the different organs or compartments, the homogenates were plated in appropriate 10-fold serial dilutions onto LB medium plates containing irgasan.

2.5.5 Detection of colonizing *Yersinia*

To follow bacterial long-term colonization of infected mice ($1x10^6$ CFU per mouse) by quantification of *Yersinia* loads and assessment of colonization qualities in the feces (positive or negative for colonization), fecal samples from individual mice were analyzed. To this end, approximately 10 to 50 mg feces were sampled directly from the mice, weighted and homogenized in 1 ml BHI broth supplemented with 1 µg/ml irgasan. For determination of bacterial quantities in the feces 10-fold serial dilutions were plated on LB medium plates containing irgasan. The remaining homogenate was cold-enriched overnight at 25°C with shaking and plated on LB medium containing irgasan to evaluate the colonization quality.

2.5.6 Severity of diarrhea

In order to document severity of diarrhea during the course of long-term infection experiments with *Y. pseudotuberculosis*, diarrheal severity was evaluated. At different time points after *Y. pseudotuberculosis* infection ($1x10^6$ CFU) feces of individual mice were sampled and analyzed with the following scoring system (Table 2.14) (Pearson *et al*., 2013).

Table 2.14 Diarrheal scoring

Score	Description
0	**No diarrhea** Solid stool with no signs of soiling around the anus; stool is very firm when subjected to pressure with tweezers
1	**Very mild diarrhea** Formed stools appear moist on the outside and no signs of soiling around the anus; stool is less firm when considerable pressure is applied with tweezers
2	**Mild diarrhea** Formed stools appear moist on the outside and some signs of soiling around the anus; stool will easily submit to pressure applied with tweezers
3	**Diarrhea** No formed stools with mucus-like appearance; considerable soiling around the anus and the fur around the tail; mouse takes long to pass stool
4	**Severe, watery diarrhea** Mostly clear or mucus-like liquid stool containing very minimal solids and considerable soiling around the anus; mouse may not be able to pass stool at all and may have hunched appearance; occasionally blood may be observed in the stool

2.5.7 Histology

Scoring of tissue alterations during and after *Y. pseudotuberculosis* infection, were performed in cooperation with the in-house mouse pathology platform. For this purpose mice infected with *Y. pseudotuberculosis* were sacrificed via CO_2 asphyxiation at either 3 or 5 dpi (infected with $2x10^8$ CFU per mouse) or at 42 dpi (infected with $1x10^6$ CFU per mouse). Subsequently, organs of interest were removed, fixed in 4 % formalin for 24 to 48 h and paraffin embedded. Sections of the organs were stained with hematoxylin & eosin (H&E stain). Organs of 3 to 5 mice were blindly analyzed by light microscopy and scored by a histopathologist (Ulrike Heise (BALB/c) or Marina Pils (C57BL/6N)).

2.5.8 Cryo-sections of infected murine ceca

To localize bacteria and analyze bacterial colonization patterns inside the infected tissue, mice infected with fluorescently labeled *Y pseudotuberculosis* (2.3.11) were euthanatized at either 3 dpi (infected with $2x10^8$ CFU per mouse) or 42 dpi (infected with $1x10^6$ CFU per mouse). Immediately, the cecum was excised, vigorously flushed with 1x PBS (Table 2.1) and filled with a mixture of 1x PBS and Tissue-Tek OCT freezing medium (Sakurma Finetek; 1:2 dilution). Subsequently, the organ was frozen in Tissue-Tek OCT Medium on dry ice. Sections of 7 µm thickness were trimmed with the Microm HM 560 cryostat (Thermo Scientific), recovered on SuperFrost Plus slides (Thermo Scientific) and fixed in ice-cold 4 % PFA (w/v) for 20 min. The fixed sections were washed twice in 1x PBS and air-dried. To stain the nuclear DNA and for section mounting, Roti-Mount FluorCare (Roth) was employed. The cryo-sections were examined with the Axiovert II fluorescence microscope (Zeiss) using the Axiocam HR digital CCD camera (Zeiss) and the software ZEN 2012 (Zeiss). Multiple fields of multiple sections were scored for bacterial colonization grades and patterns. The scoring criteria are listed in Table 2.15. The obtained images were further processed using Adobe Photoshop CS4 (version 11.0; Adobe Systems Incorporated).

Table 2.15 Bacterial colonization scores

Score	Description
Microcolony	
0	No microcolony
1	Small microcolony >20 µm, <50 µm diameter
2	Medium microcolony <100 µm diameter
3	Large microcolony >100 µm diameter
Lesion	
0	No lesion
1	Small lesion
2	Large lesion
Small bacterial foci <20 µm	
0	No colonization
1	<25 % of the PP colonized
2	<50 % of the PP colonized
3	>50 % of the PP colonized
Bacterial localization in the intracellular space around whole cells	
0	No associations
1	<25 % of small bacterial foci associated
2	<50 % of small bacterial foci associated

Score	Description
3	>50 % of small bacterial foci associated
Lamina propria colonization	
0	No colonization
1	Partially colonized, single colonized areas of the lamina propria within the entire section
2	Moderate colonized, single to dense colonized areas of the lamina propria within the entire section
3	Highly colonized, dense colonization of the lamina propria within the entire section

2.5.9 Isolation of cecal tissue for total RNA extraction

For total RNA extraction (2.4.3) of murine ceca, uninfected equally aged mice and mice infected with either *Y. pseudotuberculosis* YPIII or YPIII Δ*cnfY* were sacrificed at 5 or 42 dpi (infection doses: day 5: $2x10^7$ CFU per mouse of *Y. pseudotuberculosis* YPIII, $2x10^8$ CFU per mouse of *Y. pseudotuberculosis* YPIII Δ*cnfY*; day 42: $1x10^6$ CFU per mouse of *Y. pseudotuberculosis* YPIII or YPIII Δ*cnfY*, respectively). Immediately, the cecum of uninfected or colonized mice (as determined in 2.5.5) was removed, extensively flushed with a defined volume of 1x PBS (Table 2.1) and snap frozen in liquid nitrogen. The organs were stored at -80 °C until further processing. Additionally, the contents of the flushed ceca were analyzed for *Y. pseudotuberculosis* loads as described in 2.5.4 to determine the severity of colonization.

2.5.10 Re-isolation

To determine presence of the virulence plasmid in bacteria during different stages post *Y. pseudotuberculosis* infection, *Y. pseudotuberculosis* YPIII was re-isolated from cecum, cecal content, PP (of the small intestine), spleen and liver of infected mice at 6 dpi ($2x10^7$ CFU per mouse) or 42 dpi ($1x10^6$ CFU per mouse). For this purpose, mice were euthanized via CO_2 asphyxiation and the desired organs were removed. Organ homogenates were prepared as described in 2.5.4. Thereafter, randomly chosen colonies of each organ (3 to 6) and mouse were stocked. The re-isolates are listed in Table 2.10 und were used for further experiments.

2.5.11 Composition of the microbiota

To assess the microbial composition of mice during persistency and its development, 16S DNA Sequencing was used. To this purpose 10 to 70 mg feces were directly sampled from individual mice. The feces were weighed, homogenized in 1 ml BHI and plated as mentioned in 2.5.5 to assay the *Y. pseudotuberculosis* loads. The rest of the homogenate was pelleted in 2 ml micro tubes (Sarstedt). The supernatant was discarded and the pellet was frozen at -20°C until further processing (2.3.7).

2.6 Flow cytometry

2.6.1 Single cell suspensions and cell counting

In order to assess the immune cell dynamics upon *Y. pseudotuberculosis* infection in C57BL/6N mice, the animals were challenged with $2x10^8$ CFU. At 3 dpi, mice were sacrificed by CO_2 asphyxiation and the PP, MLN and spleen were dissected. Single cell suspensions were obtained by passage through a cell strainer (100 µm, BD Biosciences) using 10 ml PBS/BSA (Table 2.1). For erythrocyte lysis, splenocytes were resuspended in 2 ml ammonium-chloride-potassium (ACK) buffer (Table 2.1) and incubated for 5 min at RT. The reaction was stopped with 20 ml PBS/BSA. The splenocytes were pelleted (5 min, 400 g, 4 °C) and resuspended in 2 ml PBS/BSA. To assess cellular concentrations, the cell suspensions were counted at the Beckman Coulter Counter.

2.6.2 Antibody titration

To titrate the optimal antibody concentration for flow cytometry stainings, splenic single cell suspensions of uninfected mice were generated (2.6.1). For each titration $1x10^6$ cells were used. To block the Fc receptor, the cells were incubated with 10 µg/ml CD16/CD32 (5 min, 4 °C). Subsequently, cells were stained for 15 min at 4 °C with different dilutions of the antibody ranging between 1:100 and 1:2000. Thereafter, cells were washed using PBS/BSA (Table 2.1), resuspended and detected at the flow cytometer (LSRFortessa™, BD Biosciences). The optimal antibody working concentrations are depicted in Table 2.5.

2.6.3 Flow cytometry staining

Flow cytometry analysis was performed employing two different antibody panels, which were denoted "innate" and "adaptive" panel. Single antibody and fluorescence minus one (all antibodies except one) control stainings for both multi-color panels were performed with splenocytes. In the "innate" panel $2.5x10^6$ cells and in the "adaptive" panel $1x10^6$ cells were stained. After two washes with PBS, the Fc receptor was blocked using 10 µg/ml CD16/CD32 (15 min, 4 °C). Thereafter, the "innate" and "adaptive" panel stainings followed different protocols.

"Innate" panel

To discriminate T cells, B cells and NK cells from the innate immune cells, the biotinylated antibody mix (CD3, CD19, NKp46; Table 2.5) was added to the blocking antibodies and incubated for 20 min. Subsequently, the cells were washed two times with PBS, resuspended with the antibody mix (CD11b, Streptavidin, F4/80, Ly6G, Ly6C, CD11c, LIVE/DEAD, Table 2.5) and incubated for 30 min at 4 °C. After washing with PBS, the cells were fixed with 4 % PFA (w/v) (20 min, 4 °C). For the acquisition at the flow cytometer (LSRFortessa™, BD Biosciences), cells were washed and resuspended in PBS/BSA (Table 2.1).

"Adaptive" panel

To stain for T cells, B cells and NK cells, the antibody mix containing CD3, CD19, NKp46 and LIVE/DEAD was added to the cells (30 min, 4°C). After two washes with PBS, cells were fixed with 4 % PFA (20 min, 4 °C). Subsequently, cells were washed and resuspended in PBS/BSA (Table 2.1) for the acquisition at the flow cytometer (LSRFortessa™, BD Biosciences)

2.6.4 Flow cytometry data analysis

The acquired flow cytometry data was analyzed using FlowJo (v9.9.4). Single stainings were employed to compensate fluorescence leaking into other detection channels. The FMO control staining was used to discriminate the cell populations from each other. Cell populations of both panels were evaluated by two distinct gating strategies (Figure S1 & Figure S2). In either gating strategy, dead cells (Figure S1A & Figure S2A), doublets (Figure S1B/C & Figure S2B/C) and cell debris (Figure S1D, Figure S2D) were excluded.
The "innate" panel was gated as follows: For exclusion of lymphocytes and NK cells, streptavidin negative cells were gated (Figure S1E). Subsequently, F4/80^{hi} cells were considered to be macrophages (Figure S1F). The remaining cells were cleared for auto-fluorescent cells (Figure S1G). Thereafter, CD11c^{+} Ly6G^{-} cells were identified as DCs (Figure S1H) and Ly6G^{+} cells as PMNs (Figure S1I). Finally, CD11b^{+} Ly6C^{-} cells were denoted as monocytes (Figure S1J).
After cell debris removal from the "adaptive" panel, auto-fluorescent cells were excluded (Figure S2E). Thereafter, CD19^{+} cells were identified as B cells and CD3^{+} cells as T cells (Figure S2F). The remaining cells were gated for NKp46^{+} NK cells (Figure S2G). To calculate the absolute cell numbers, the population percentage was multiplied by the cell numbers (2.6.1).

2.7 Statistical analyses

Statistical analyses were performed with Graph Pad PRISM 6.0 (2.1.8). For comparison of two groups the Mann-Whitney U test was implemented. Column based data containing more than 2 groups was compared employing One-way ANOVA or the non-parametric Kruskal-Wallis test. To compare two groups at different time points, the data was analyzed with multiple t-tests. All multiple comparisons were p-value-adjusted utilizing Holm-Šídák's method or Dunn's correction (Kruskal-Wallis test). Correlation analysis was executed using the Spearman correlation method. Survival data was statistically evaluated with the Mantel-Cox log-rank test. Sequencing data was statistically analyzed by Dr. Michael Beckstette and is provided in the appendix (Table S1-S10).

3 Results

The *Y. pseudotuberculosis* strains YPIII and IP2666 encode the cytotoxic necrotizing factor CNF_Y, which is a homologue of CNF1 of UPEC (Lockman *et al.*, 2002; Caprioli *et al.*, 1983). Deletion of *cnf1* in UPEC leads to attenuation in colonization abilities in the urine, bladder and kidney in a murine UTI model (Rippere-Lampe *et al.*, 2001b). Additionally, presence of CNF1 results in higher inflammatory states and tissue damage in mice and rats (Rippere-Lampe *et al.*, 2001a; Rippere-Lampe *et al.*, 2001b).
Previous work by Schweer and colleagues elucidated that the lack of CNF_Y also reduces pathogenicity of *Y. pseudotuberculosis* YPIII and completely abolishes its ability to cause lethal infections (Schweer *et al*., 2013). When using lethal infection doses, deletion of *cnfY* in *Y. pseudotuberculosis* YPIII led to asymptomatic colonization of the gut compartments (small intestine, cecum) and associated lymphoid tissues (*i.e.* PPs) (Schweer *et al*., 2013).
In 2014, it was discovered that *Y. pseudotuberculosis* YPIII (*cnfY*$^+$) is able to persist in mice after oral infection with sub-lethal infection doses for up to 115 days (Fahlgren *et al.*, 2014). However, there is little known about the influence of *Yersinia* encoded virulence factors, especially CNF_Y, on the establishment and manifestation of persistent *Y. pseudotuberculosis* infection.
Preliminary infection experiments with high infection doses ($2x10^8$ CFU) of *Y. pseudotuberculosis* strain YPIII Δ*cnfY* demonstrated that the *cnfY* mutant is able to cause long-lasting infections in the gut and its associated lymphoid tissues (small intestine, PPs, cecum, colon) (Janina Schweer, unpublished data). Moreover, Avican and colleagues showed that the *cnfY*-expression is down-regulated during persistent infection (Avican *et al*., 2015). Thus, it was hypothesized that the avirulent *Y. pseudotuberculosis* strain YPIII Δ*cnfY* might more effectively cause prolonged infections than the wild type.

This study addresses the influence of CNF_Y on *Y. pseudotuberculosis* pathogenesis during acute and persistent infection.

3.1 Uncoupling of CNF_Y increases the establishment of asymptomatic, persistent infections

To test the assumption that CNF_Y influences the development of persistent *Yersinia* infections, the persistence abilities of *Y. pseudotuberculosis* YPIII and YPIII Δ*cnfY* in BALB/c mice after sub-lethal challenge were compared. Therefore, BALB/c mice were intra-gastrically infected with $1x10^6$ CFU of YPIII or YPIII Δ*cnfY* and disease progression was monitored over a period of 40 days (Figure 3.1).
About 40 % of YPIII infected mice succumbed to the infection between 5 and 21 dpi (data not shown). Weight loss analysis of the surviving mice demonstrated that YPIII infected mice displayed a weight loss of almost 3 % of their initial weight in the first 12 dpi (Figure 3.1A). However, the mice recovered weight beginning at day 9 to 16 post infection (data not shown). In contrast, YPIII Δ*cnfY* infected mice presented no weight loss during the course of the experiment: despite the infection, these mice constantly gained weight (Figure 3.1A, data not shown).
To get more information about the *Yersinia* colonization status and diarrheal severity during the progress of the experiment, fecal egesta of individual mice were analyzed for their *Yersinia*

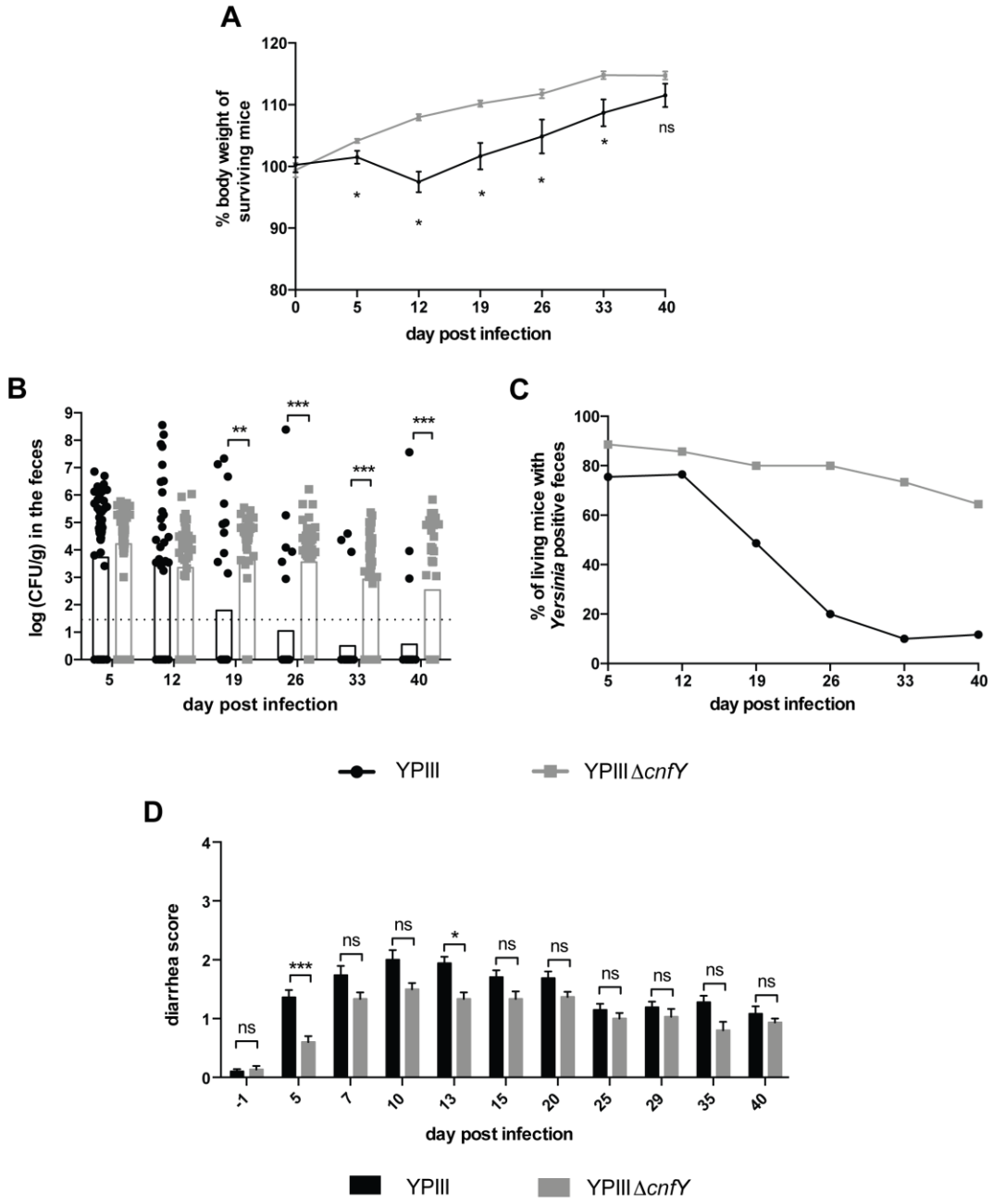

Figure 3.1 Uncoupling of *cnfY* leads to mild disease with enhanced persistence rates in the gut of BALB/c mice.

BALB/c mice were intra-gastrically infected with $1x10^6$ CFU of *Y. pseudotuberculosis* YPIII or YPIII Δ*cnfY*. At indicated time points, body weight, diarrhea score and *Yersinia* colonization in the feces were monitored. (A) Relative body weights of surviving mice after infection. The data represent the mean ±SEM of one independent experiment, the experiment was conducted in triplicate; YPIII n=15; YPIII Δ*cnfY* n=30. The data were analyzed with multiple t-test's utilizing Holm-Šídák's correction: * $p<0.05$; ns, not significant. (B) Individual *Yersinia* loads in the feces. The *Yersinia* burden was determined in the egesta of infected mice at indicated time points. The bar represents the geometric mean. The dotted line indicates the detection limit. The graph shows combined data from two independent experiments; YPIII n=50, YPIII Δ*cnfY* n=35. The data were statistically analyzed with the Mann-Whitney U test: ** $p<0.01$, *** $p<0.001$. (C) Number of BALB/c mice positively tested for *Yersinia* after culture enrichment of yersiniae from egesta samples. Rates were calculated using data of YPIII n=50 and YPIII Δ*cnfY* n=35 from two independent experiments. (D) Diarrheal severity scores: 0: no diarrhea; 1: very mild diarrhea; 2: mild diarrhea; 3: diarrhea; 4: severe, watery diarrhea. The bar represents the mean ±SEM of one representative experiment. The experiment was repeated two times. The data were analyzed with One-way ANOVA employing Holm-Šídák's correction: * $p<0.05$, *** $p<0.001$; YPIII n=50, YPIII Δ*cnfY* n=30.

burden and diarrheal status. While the global YPIII loads decreased starting from 12 dpi, the burden of YPIII Δ*cnfY* remained at the same level (Figure 3.1B). The observed global decrease of wild type *Yersinia* burdens was mostly due to the bacterial load decreasing below the detection limit (Figure 3.1B). Culture enrichment of the fecal sample material further revealed that the overall reduction of YPIII below the detection limit was accompanied by bacterial clearance from the feces (Figure 3.1C). Of 75.5 % initially YPIII positively tested mice (5 dpi) only 11.7 % of the surviving mice were still colonized at 40 dpi (Δ63.8 %). In turn, clearance events were rarely observed upon YPIII Δ*cnfY* infection; of 88.6 % initially colonized mice, 64.4 % were still colonized at 40 dpi (Δ24.2 %). This accounts for an almost 3-fold increase of persistence events upon deletion of *cnfY* (Figure 3.1C). Moreover, diarrheal severity greatly differed between the two *Y. pseudotuberculosis* strains at the beginning of the infection (Figure 3.1D). Mice infected with YPIII Δ*cnfY* on average displayed no- to very mild-diarrhea, whereas mice infected with the wild type demonstrated very mild- to mild-diarrhea at 5 dpi (Figure 3.1D; data not shown). The severity of diarrhea further increased, reaching the highest overall scores between 10 and 13 dpi for both strains. Up to 20 dpi the diarrheal severity scores

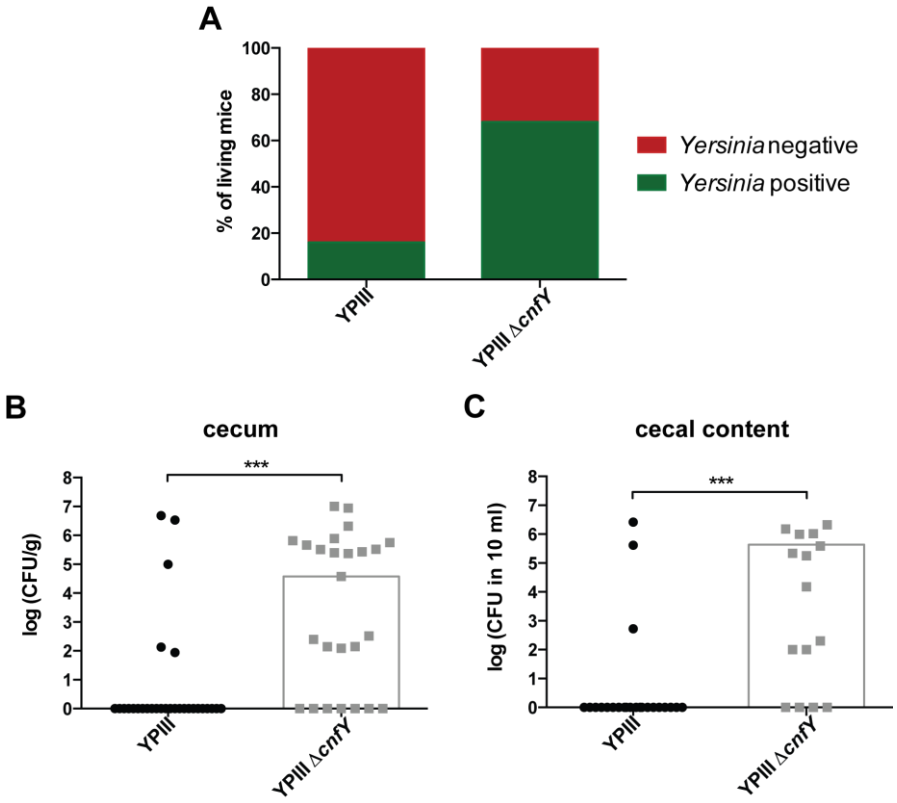

Figure 3.2 Deletion of *cnfY* drastically enhances persistency and colonization rates in the cecum of BALB/c mice.

Mice were intra-gastrically infected with $1x10^6$ CFU of *Y. pseudotuberculosis* YPIII or YPIII Δ*cnfY*. At 42 dpi, *Yersinia* colonization levels in the cecum and the luminal content of the cecum were determined. (A) *Yersinia* colonization in the cecum of surviving mice. The rates were calculated using bacterial burden data of the cecum: YPIII n= 31, YPIII Δ*cnfY* n=25. (B) *Yersinia* loads in the cecum. The presented data were obtained from three combined experiments: YPIII n= 31, YPIII Δ*cnfY* n= 25. The detection limit was ca. 125 CFU/g. (C) *Yersinia* burdens in the luminal content of the cecum. The data were combined from two independent experiments: YPIII n=23, YPIII Δ*cnfY* n=15. The detection limit was at 50 CFU. (B-C) The plots show bacterial burdens of individual mice. The bar represents the median. The data were statistically analyzed with the Mann-Whitney U test: *** $p<0.001$.

were slightly more pronounced upon YPIII infection compared to YPIII Δ*cnfY* infection (Figure 3.1D). Thereafter, all mice displayed very mild diarrhea, which did not differ between the two groups. Interestingly, the majority of mice still displayed very mild diarrhea until the end of the experiment (Figure 3.1D). Taken together, these results support the assumption that YPIII Δ*cnfY* initiates a more frequent long-term infection and is less frequently cleared from the gut luminal compartment than the wild type after intra-gastric challenge with sub-lethal infection doses.

To corroborate that YPIII Δ*cnfY* indeed persists more efficiently, bacterial burden assays in the persistency niche, the cecum, were performed at 42 dpi. About 68 % of the analyzed ceca were still colonized with YPIII Δ*cnfY*, whereas only 16 % of the ceca were inhabited by YPIII (Figure 3.2A). Moreover, around 52 % of YPIII Δ*cnfY* infected mice presented *Yersinia* burdens higher than 10^4 CFU/g, while the same was true for only 9.7 % of YPIII infected mice (Figure 3.2B). This tendency was verified for the luminal contents of the cecum (53.3 % YPIII Δ*cnfY*; 8.7 % YPIII) (Figure 3.2C). In addition, correlation analysis revealed that cecal tissue loads highly correlated with luminal loads (Figure S3A). Therefore, it was undistinguishable if the persistence reservoir is mainly located in the cecal tissue or the luminal contents. This suggests that both compartments might constitute a persistence reservoir, which enables bacterial shedding into the environment. In addition, cecal tissue burdens strongly correlated with the fecal loads (Figure S3B). Taken together, fecal and cecal content screenings provided a reliable means to screen for highly colonized ceca.

The analysis of the small intestinal colonization, *i.e.* small intestinal tissue, luminal contents and PPs, revealed that YPIII Δ*cnfY*, like YPIII, primarily persists in the cecum after sub-lethal infection (Figure S4; Fahlgren *et al*., 2014). Remarkably, enhanced persistence ability of YPIII Δ*cnfY* compared to YPIII was also confirmed using a different mouse strain, *i.e.* FVB/N (Figure S5).

In summary, these experiments indicated that the absence of *cnfY* expression strongly promotes persistence of *Y. pseudotuberculosis* in the cecum. Moreover, long-term cecal colonization was accompanied by continuous shedding of *Yersinia*, which reflected the colonization levels.

3.2 Cecal pathology is linked to the stage of infection

In general, the delivery of toxins and/or effector proteins contributes to tissue destruction and inflammation during acute bacterial infections (Pothoulakis, 2000; Geiser *et al*., 2001). Also CNF toxins were shown to increase tissue inflammation and destruction during infection (Rippere-Lampe *et al*., 2001a; Schweer *et al*., 2013). Until now, nothing is yet known about the impact of CNF_Y on tissue architecture and inflammation during persistent *Yersinia* infections, which might account for the rate of prolonged infection manifestation. Thus, the pathologic appearance of cecal tissue architecture and colonization upon acute and persistent infection was examined.

3.2.1 Histopathology of the cecum during acute and persistent infection stage

To examine the inflammatory reactions and tissue architecture of the cecum during acute (3 dpi) and persistent (42 dpi) infection, the histopathologic presentation of cecal tissue sections was studied. To this end, mice were intra-gastrically infected with either $2x10^8$ CFU per mouse (3 dpi) or $1x10^6$ CFU per mouse (42 dpi) of YPIII and YPIII Δ*cnfY*, respectively. The histopathologic analysis was performed by Ulrike Heise of the Mouse Pathology, Animal Experimental Unit at the Helmholtz Centre for Infection Research.

During acute infection, YPIII caused more severe tissue alterations of the cecal lamina propria than YPIII Δ*cnfY*. The villi of YPIII infected ceca were heavily elongated and high-grade edema formation occurred at the basal site of the lamina propria. Infiltrated lymphocytes dominated in the basal parts of the lamina propria, while only few infiltrated PMNs were detected. Additionally, the lumen was filled with scaled-off epithelial cells and infiltrated PMNs. This luminal pathology quality was also observed upon YPIII Δ*cnfY* infection to comparable extents (Figure 3.3 upper panel). On the other hand, YPIII Δ*cnfY* infected animals

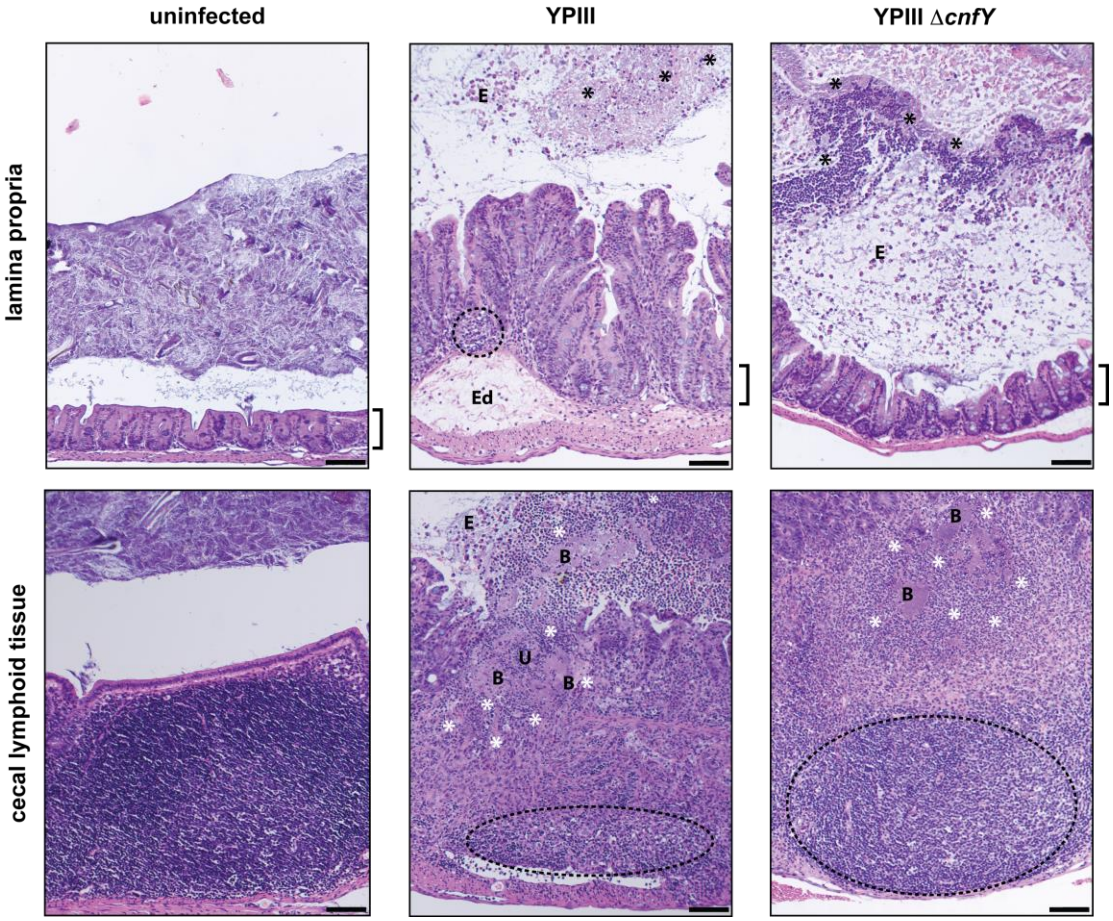

Figure 3.3 Acute *Y. pseudotuberculosis* infection in the cecum causes severe tissue inflammation with CNF_Y-dependent qualities.

BALB/c mice were intra-gastrically infected with $2x10^8$ CFU of *Y. pseudotuberculosis* YPIII or YPIII Δ*cnfY*. Three days post infection, the cecum was removed and sections were stained with H&E. The lamina propria (upper panel) and cecal lymphoid tissue (lower panel) of uninfected and infected mice were analyzed for inflammatory alterations. The microscopic pictures are representatives of multiple microscopic areas (>10) of groups of four mice. B: bacterial microcolony, E: epithelial cells, Ed: edema, U: ulcus, black/white asterisks: mixed inflammatory infiltrate, dashed halo: lymphocytes, parenthesis: length of villi of uninfected mice. The bar represents 100 µm.

displayed medium to high inflammation of the cecal lamina propria with mild villi elongation. Also in contrast to YPIII infection, diffusely distributed PMNs dominated in the lamina propria and quite rare edema formation in the basal part of the lamina propria was observed (Figure 3.3 upper panel). The lymphoid tissue of the cecum in YPIII infected mice also showed more severe tissue remodeling than YPIII Δ*cnfY* infected mice. This included massive necrosis with strong lymphocyte reduction, vast granulocyte infiltration and partial ulcus formation (Figure 3.3 lower panel). Compared to that, the cecal lymphoid tissue of YPIII Δ*cnfY* infected mice showed medium to high grades of inflammation. The tissue remodeling comprised partial necrosis with slight lymphocyte reduction, a high degree of granulocyte infiltration and rare edema formation in the crypts above the cecal lymphoid tissue. In both experimental groups, comparable numbers of bacterial microcolonies surrounded by mixed inflammatory infiltrates were detected inside the cecal lymphoid tissue (Figure 3.3 lower panel).

Only very mild to no alterations of the lamina propria were identified in YPIII and YPIII Δ*cnfY* infected mice at 42 dpi (Figure S6A; data not shown). In contrast to acute infection, only isolated diffuse infiltration of PMNs was observed in the basal parts of the lamina propria in both groups (Figure 3.4 upper panel). Strikingly, no histological alterations of the cecal lymphoid tissue were observed when compared to equally-aged uninfected mice (Figure 3.4 lower panel; Figure S6B). Although high *Yersinia* colonization levels were expected, no bacterial colonization was detectable by H&E staining at 42 dpi.
This suggests that enhanced persistence of YPIII Δ*cnfY* compared to YPIII was not associated with divergent inflammatory reactions during persistent infection phase (42 dpi), but demonstrated that *Yersinia* persists in the cecal tissue without eliciting strong immune responses. However, CNF_Y-dependent tissue inflammation during acute infection might affect persistence development.

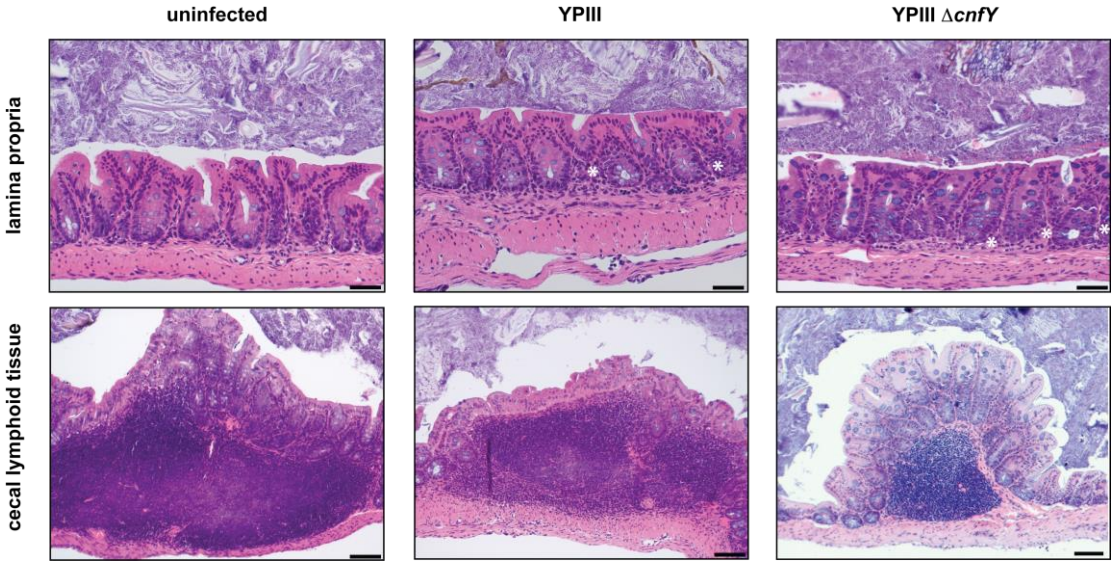

Figure 3.4 Persistent *Y. pseudotuberculosis* infection in the cecum displays no to very mild inflammation independent of CNF_Y.

BALB/c mice were intra-gastrically infected with $1x10^6$ CFU of *Y. pseudotuberculosis* YPIII or YPIII Δ*cnfY*. At 42 dpi, the ceca of highly colonized mice were isolated and sections were stained with H&E. Persistently colonized mice (YPIII middle panel; YPIII Δ*cnfY*: right panel) and uninfected mice of the same age (left panel) were analyzed for inflammatory alterations in the lamina propria (upper panel) and cecal lymphoid tissue (lower panel) at 42 dpi. The shown microscopic pictures are representatives of multiple microscopic areas (>10) of groups of 4 to 5 mice. White asterisks: mixed inflammatory infiltrate. The bar represents 50 µm (upper panel) or 100 µm (lower panel).

3.2.2 Stable expression of *mRuby2* is suitable for *in vivo* localization studies

The previous results indicated a divergent bacterial localization and/or distribution during persistent *Yersinia* infection compared to acute infection phase. To uncover and compare the distinct colonization patterns of *Y. pseudotuberculosis* especially during persistent infection in mice, a straightforward tool was designed and evaluated to study *Y. pseudotuberculosis* localization inside the cecal tissue. Here, the red fluorescent protein mRuby2 under the control of the tetracyclin promoter ($P_{LtetO-1}$) was integrated into a transcriptionally silent locus of the *Y. pseudotuberculosis* chromosome between YPK_3294 (LysR family transcriptional regulator) and YPK_3295 (*pepD*, aminoacyl-histidine dipeptidase) (Figure 3.5) (Nuss *et al.*, 2015; Nuss *et al.*, 2017).

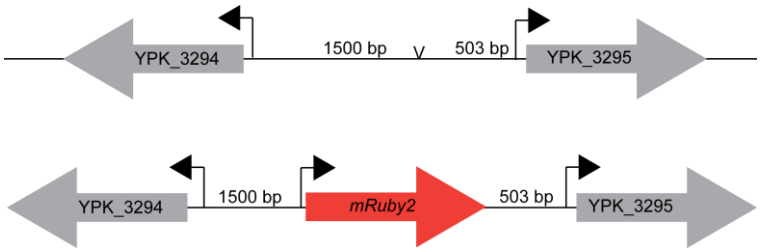

Figure 3.5 $P_{LtetO-1}$*::mRuby2* integration site into the *Y. pseudotuberculosis* YPIII chromosome.

$P_{LtetO-1}$*::mRuby2* was introduced into the *Y. pseudotuberculosis* YPIII genome between YPK_3294 (LysR family transcriptional regulator) and YPK_3295 (*pepD*, aminoacyl-histidine dipeptidase). The distances to the neighboring genes are depicted in the picture.

As the integration of a new and energy demanding genetic element into the *Yersinia* chromosome could impact energy consumption and affect polar genes, the transgenic *Y. pseudotuberculosis* strains YPIII (*mRuby2*) and YPIII Δ*cnfY* (*mRuby2*) were characterized for their growth behavior and *mRuby2* expression patterns *in vitro*. The analysis revealed no growth defects at neither 25 °C nor 37 °C (Figure 3.6). Moreover, fluorescence microscopy of the *mRuby2* expressing *Yersinia* strains at 25 °C and 37 °C during different growth phases

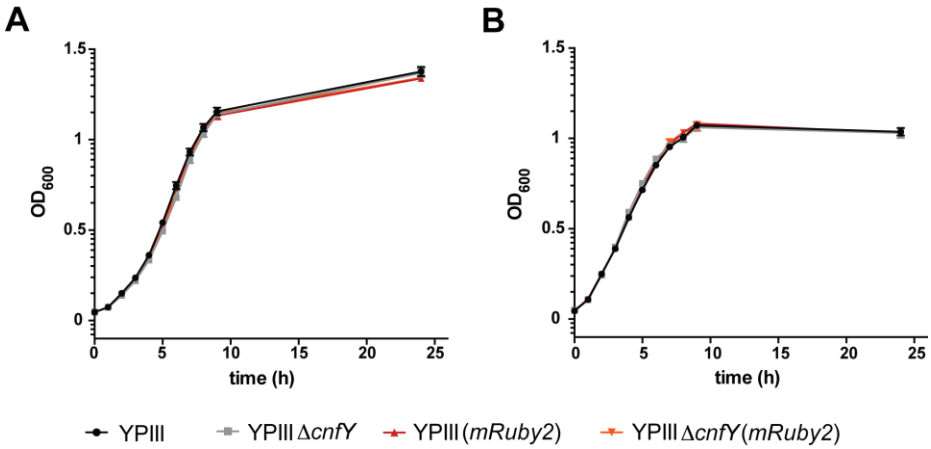

Figure 3.6 Chromosomal integration of $P_{LtetO-1}$*::mRuby2* does not impact *Y. pseudotuberculosis* growth.

Bacterial cultures were grown in LB medium at (A) 25 °C or (B) 37 °C for 24 h. At several time points, optical density at 600 nm (OD_{600}) was determined. The data show the mean ±SEM of three combined independent experiments performed in duplicates.

(exponential, early stationary, late stationary) demonstrated *mRuby2* expression during all assessed conditions (Figure S7-S8). As expected, no red fluorescence was detectable in YPIII and YPIII Δ*cnfY* without the fusion constructs (Figure S9). Thus, the genomic modification at the desired genomic region did yield stable *mRuby2* expressing *Y. pseudotuberculosis* without a growth defect.

The *Y. pseudotuberculosis* mRuby2-labeled strains were further evaluated for their *in vivo* phenotypes during lethal and sub-lethal infections. To assess the virulence and colonization

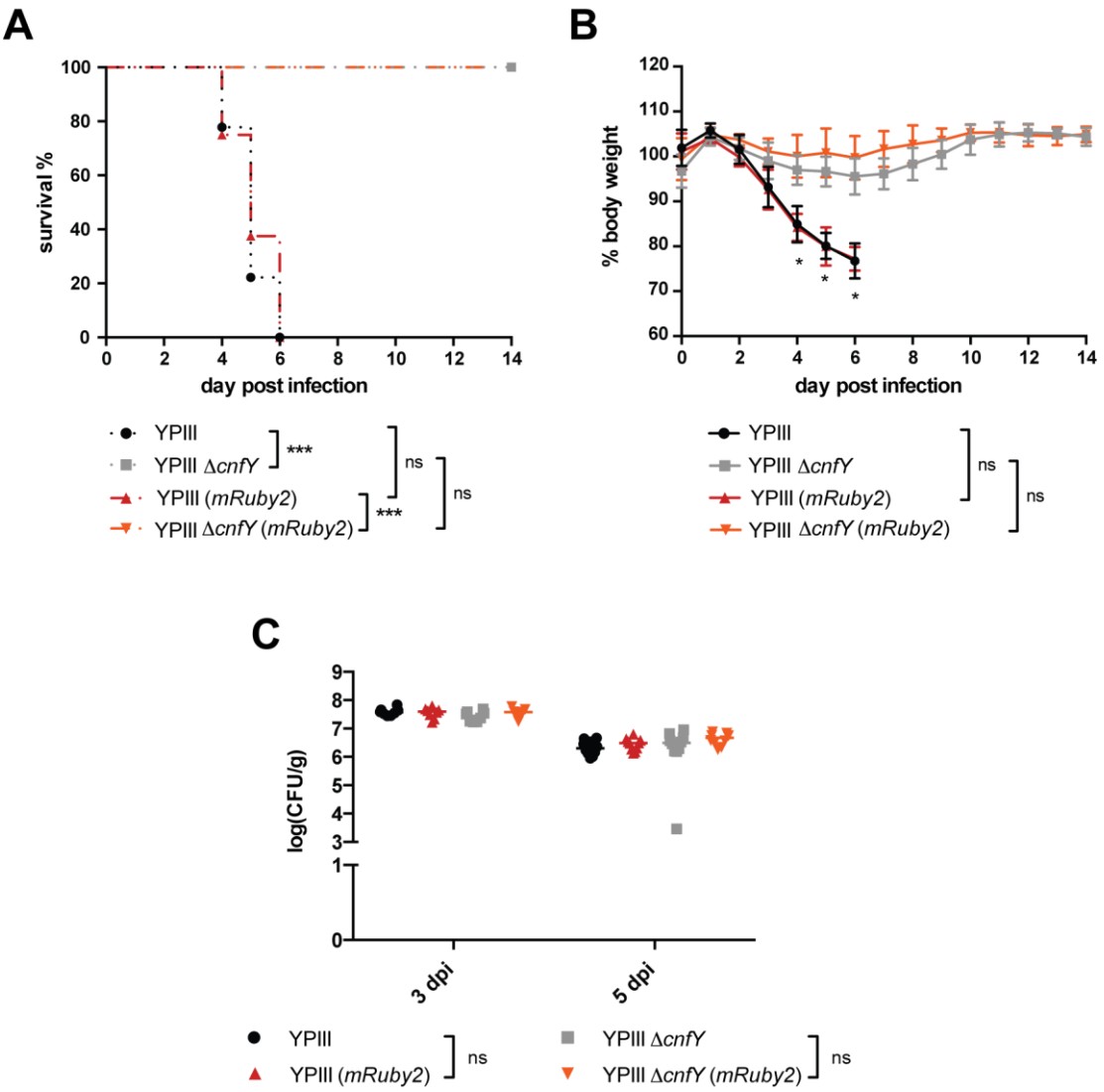

Figure 3.7 Chromosomal Integration of $P_{LtetO-1}$::*mRuby2* does not alter virulence and colonization of the cecum.

BALB/c mice were intra-gastrically infected with $2x10^8$ CFU of *Y. pseudotuberculosis* YPIII, YPIII Δ*cnfY* or the isogenic *mRuby2* labeled strains. (A-B) Health status and survival were monitored over 14 days. The presented data were combined from two independent experiments: YPIII n=9, YPIII Δ*cnfY* n=8, YPIII (*mRuby2*) n=8, YPIII Δ*cnfY* (*mRuby2*) n=9. (A) Survival of BALB/c mice. Survival data were statistically analyzed with the log-rank (Mantel-Cox) test: ns, not significant: *** $p<0.001$. (B) Weight loss curves. Mice that lost more than 20 % of their initial body weight or reached a health score of lower than three were sacrificed and recorded as dead (2.5.2; Table 2.13). The graphs represent the mean ± SD. The data were statistically analyzed with multiple t-tests using Holm-Šídák's correction: * $p<0.05$. (C) *Yersinia* burden in the cecum at 3 and 5 dpi. The presented data were combined from two independent experiments with 8 to 10 mice per group. Statistical analysis was performed using the Kruskal-Wallis test and Dunn's correction: ns, not significant.

abilities upon lethal infections, mice were intra-gastrically challenged with $2x10^8$ CFU of YPIII, YPIII Δ*cnfY* or their isogenic *mRuby2* mutants, respectively. Thereafter, survival, weight loss and the cecal bacterial colonization levels were recorded (Figure 3.7). Similar to the parental strain YPIII Δ*cnfY*, YPIII Δ*cnfY* (*mRuby2*) did not cause mortality in BALB/c mice (Figure 3.7A). Comparison of the weight loss between YPIII Δ*cnfY* and YPIII Δ*cnfY* (*mRuby2*) further revealed that both groups lost about 1-10 % of their body weight until 6 dpi, but recovered quickly until 11 dpi and did not differ significantly from each other (Figure 3.7B, data not shown). On the other hand, YPIII and YPIII (*mRuby2*) infected mice succumbed to the infection around 6 dpi, displaying no significant differences in virulence (Figure 3.7A). Accordingly, there were also no significant differences in body weight between YPIII and YPIII (*mRuby2*). Both groups of mice rapidly lost similar amounts of body weight starting from 2 dpi (Figure 3.7B). YPIII and YPIII Δ*cnfY* differed significantly in virulence and body weight loss, irrespective of the chromosomal integration of $P_{LtetO-1}$*::mRuby2* (Figure 3.7A, B). Therefore, the chromosomal integration of $P_{LtetO-1}$*::mRuby2* did not alter neither virulence (Figure 3.7A) nor disease progression (Figure 3.6B) upon lethal infection.

Comparison of the colonization abilities in the cecum revealed, that the mRuby2-producing strains YPIII (*mRuby2*) and YPIII Δ*cnfY* (*mRuby2*) colonized the cecal tissue to the same extend as their parental strains with approximately $3\text{-}4x10^7$ CFU/g at 3 dpi and $2\text{-}4x10^6$ CFU/g at 5 dpi (Figure 3.7C). In the other organs no significant differences were observed due to integration of $P_{LtetO-1}$*::mRuby2* into the chromosome of YPIII or YPIII Δ*cnfY* at 3 and 5 dpi (Figure S10). Hence, lethal infections with YPIII and YPIII Δ*cnfY* were not affected by the integration and expression of *mRuby2*.

To exclude that chromosomal integration of $P_{LtetO-1}$*::mRuby2* impacts persistence development, long-term colonization of YPIII (*mRuby2*) and YPIII Δ*cnfY* (*mRuby2*) were also tested in the persistent BALB/c infection model. To this end, mice were intra-gastrically infected with $1x10^6$ CFU of YPIII (*mRuby2*), YPIII Δ*cnfY* (*mRuby2*) or their parental strains. Subsequently, disease progression was monitored for up to 42 dpi. As for acute infections, no alterations of disease progression upon sub-lethal infections with the transgenic *Y. pseudotuberculosis mRuby2* strains were detected compared to the parental strains YPIII and YPIII Δ*cnfY* (Figure 3.8A). Like YPIII infected mice, YPIII (*mRuby2*) infected mice lost about 10 % of their initial body weight in the first 9 to 12 dpi, but regained it over the following two weeks. Similarly, YPIII Δ*cnfY* (*mRuby2*) infected mice did not lose any body weight but constantly gained body weight like YPIII Δ*cnfY* infected mice. In addition, the bacterial loads in the feces of YPIII (*mRuby2*) and YPIII Δ*cnfY* (*mRuby2*) infected mice did not differ significantly from the bacterial burden of the respective parental strain at all indicated time points (Figure 3.8B, C). In line with the previous results, broth enrichment revealed the same rates/number of persistent YPIII (*mRuby2*) and YPIII Δ*cnfY* (*mRuby2*) in the feces of mice as their parental strains (Figure S11). Therefore, chromosomal integration of $P_{LtetO-1}$*::mRuby2* did not impact prolonged infection abilities and phenotypes in the persistent infection model.

To confirm that YPIII (*mRuby2*) and YPIII Δ*cnfY* (*mRuby2*) persist in the cecum like their parental strains, the colonization rates and bacterial burden were assayed at 42 dpi (Figure 3.8D, Figure S12). YPIII (*mRuby2*) still colonized about 18.2 % of the ceca and YPIII Δ*cnfY* (*mRuby2*) about 60 % of the ceca, thereby reproducing the persistence frequencies of YPIII (16 %) and YPIII Δ*cnfY* (68 %) in the cecum (Figure 3.8D, 3.1). Moreover, the YPIII (*mRuby2*) and YPIII Δ*cnfY* (*mRuby2*) loads in the cecal tissue and the cecal luminal contents also resembled those obtained with the unlabeled strains (Figure S12, 3.1), indicating

that integration of $P_{LtetO-1}$*::mRuby2* into the YPIII and YPIII Δ*cnfY* chromosome did not impact persistence and long term colonization abilities in the cecum. Notably, the recovered bacteria from the egesta exhibited mRuby2-derived red fluorescence at all analyzed time points (data not shown).

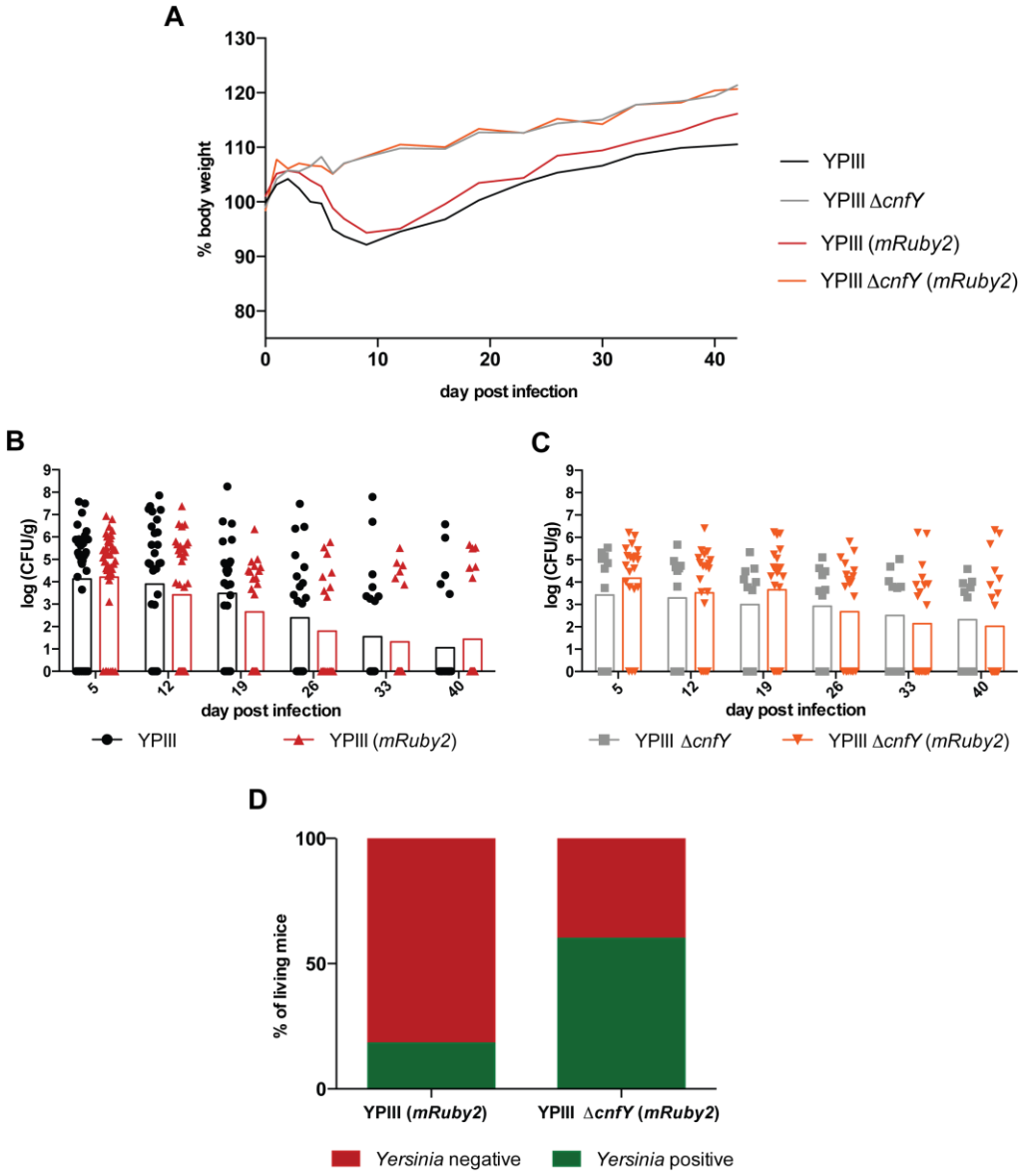

Figure 3.8 Chromosomal integration of $P_{LtetO-1}$*::mRuby2* does not affect *Yersinia* persistency phenotypes.

BALB/c mice were intra-gastrically infected with $1x10^6$ CFU of *Y. pseudotuberculosis* YPIII, YPIII Δ*cnfY* or the isogenic *mRuby2* encoding strains. Health status and bacterial colonization in the egesta were monitored during 40 days. (A) Relative body weights compared to the initial weight. The data show the mean: YPIII n=20; YPIII Δ*cnfY* n=10, YPIII (*mRuby2*) n=40, YPIII Δ*cnfY* (*mRuby2*) n=20. The data were statistically analyzed with multiple t-test's employing Holm-Šídák's correction. Results were not significant. (B, C) Individual *Yersinia* loads in the feces of mice at indicated time points post infection. The bar represents the geometric mean. The data were combined from two experiments and statistically analyzed with Mann-Whitney U test. The results were not significant. YPIII n=40; YPIII Δ*cnfY* n=10, YPIII (*mRuby2*) n=40, YPIII Δ*cnfY* (*mRuby2*) n=20. (D) *Yersinia* colonization frequencies in the cecum of surviving mice. The frequencies were calculated using bacterial burden data of the cecum: YPIII (*mRuby2*) n=11; YPIII Δ*cnfY* (*mRuby2*) n=10.

These data confirm that chromosomal integration of P_{LetO-1}*::mRuby2* yielded stable *mRuby2*-expressing *Y. pseudotuberculosis* that phenotypically behave like the parental strains during lethal and sub-lethal infections *in vivo*.

3.2.3 *Yersinia* colonization patterns during acute and persistent infection phase

Yersiniae are classical extracellular located pathogens that grow in large bacterial foci, referred to as microcolonies, inside infected tissues during early infection (Simonet *et al*., 1990; Autenrieth and Firsching, 1996; Balada-Llasat and Mecsas, 2006). In contrast to the acute infection, no bacterial microcolonies were detected during persistent infection with *Y. pseudotuberculosis* by H&E staining (3.2.1) in BALB/c mice, suggesting divergent localization and/or distribution during persistent infection compared to acute infection. *Y. pseudotuberculosis* YPIII (*mRuby2*) and YPIII Δ*cnfY* (*mRuby2*) were employed to elucidate the localization and colonization patterns during acute (3 dpi; $2x10^8$ CFU/mouse) and persistent (42 dpi; $1x10^6$ CFU/mouse) infection. To this end, the ceca of the infected mice were sectioned and subsequently analyzed using fluorescence microscopy.

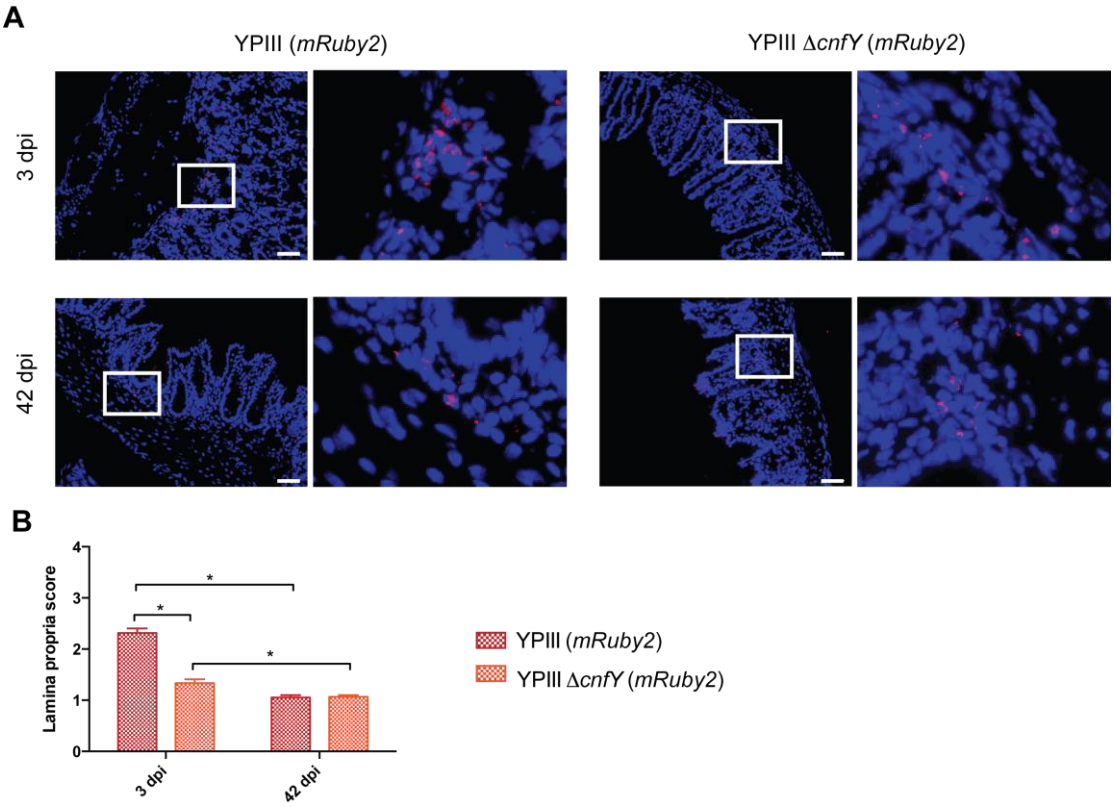

Figure 3.9 *Yersinia* colonization in the lamina propria is dependent on infection stage and *cnfY*.

Groups of three BALB/c mice were intra-gastrically infected with either $2x10^8$ CFU (acute) or $1x10^6$ CFU (persistent) of *Y. pseudotuberculosis* YPIII (mRuby2) or YPIII Δ*cnfY* (mRuby2). At 3 dpi (acute) or 42 dpi (persistent), sections of highly colonized ceca (data not shown) were prepared, fixed, stained and analyzed under the fluorescence microscope. (A) The microscopy pictures are representatives of multiple microscopic areas (>15) of the lamina propria. Red: *Y. pseudotuberculosis* (*mRuby2*), Blue: DAPI stained host cell nuclei. (B) Lamina propria colonization score (Table 2.15). The sections were scored for bacterial colonization by analyses of n sections of multiple fields; 3 dpi: YPIII n=51, YPIII Δ*cnfY* n=45; 42 dpi: YPIII n=56, YPIII Δ*cnfY* n=58; * $p<0.01$. The data show the mean scores ±SEM combined from 3 mice per group. Statistical analyses were performed using multiple t-tests with Holm-Šídák's correction.

Upon acute infection, YPIII (*mRuby2*) and YPIII Δ*cnfY* (*mRuby2*) colonized the basal site of the cecal lamina propria in small single or multi-cell aggregates (Figure 3.9A; upper panel), whereby the lamina propria was significantly stronger colonized by YPIII (*mRuby2*) than YPIII Δ*cnfY* (*mRuby2*), as determined by scoring of the colonization grades (Figure 3.9B).
As during acute infection, YPIII (*mRuby2*) and YPIII Δ*cnfY* (*mRuby2*) also colonized the basal site of the cecal lamina propria at 42 dpi (Figure 3.9A; lower panel). The colonization scores in the lamina propria of both *Yersinia* strains were lower during persistent infection compared to acute infection. However, they did not differ between YPIII (*mRuby2*) and YPIII Δ*cnfY* (*mRuby2*) during prolonged infection (Figure 3.9B).

In the cecal lymphoid tissue two distinct *Yersinia* colonization patterns were observed during acute infection. YPIII (*mRuby2*) and YPIII Δ*cnfY* (*mRuby2*) were either found in large bacterial aggregates (microcolonies) with a diameter greater than 20 µm (Figure 3.10A; upper panel) or in dispersely-distributed small single to multi-cell aggregates that had a maximal diameter of 20 µm (Figure 3.10B; upper panel).
The microcolony sizes did not differ significantly between YPIII (*mRuby2*) and YPIII Δ*cnfY* (*mRuby2*) (Figure 3.10C) and the vast majority of YPIII (*mRuby2*) and YPIII Δ*cnfY* (*mRuby2*) microcolonies caused small to large tissue lesions, which did not differ between the groups (Figure S13, data not shown). However, the area covered with small single and multi-cell aggregates of YPIII (*mRuby2*) was slightly greater in the cecal lymphoid tissue than in YPIII Δ*cnfY* (*mRuby2*)-infected mice (Figure 3.10D).
Interestingly, both *Yersinia* strains colonized the cecal lymphoid tissue in a completely different pattern during persistent infection (Figure 3.10). Densely packed microcolonies were found only very rarely (Figure 3.10A; lower panel). In the vast majority of the analyzed cecal lymphoid tissues no bacterial microcolonies were visible (Figure 3.10C). The yersiniae were generally located in dispersely distributed small multi-cell aggregates (Figure 3.9B; lower panel). Nevertheless, the grade of cecal lymphoid tissue colonization was comparable to acute infection and did not differ between YPIII (*mRuby2*) and YPIII Δ *cnfY* (*mRuby2*) (Figure 3.10D). Furthermore, most bacteria were found in the intercellular space, forming halo-like structures around single lymphocytes (Figure 3.10B; lower panel). This cell-association was significantly stronger during persistent infection compared to acute infection, but did not differ between YPIII (*mRuby2*) and YPIII Δ*cnfY* (*mRuby2*) (Figure 3.10E). Strikingly, during the persistent stage no differences in the colonization patterns of YPIII (*mRuby2*) and YPIII Δ*cnfY* (*mRuby2*) were observed.
Altogether, *Y. pseudotuberculosis* localizes to the basal parts of the lamina propria and inside the cecal lymphoid tissue, displaying different colonization patterns during the acute and persistent phase inside the cecal lymphoid tissue: During acute infection, bacteria localize in large microcolonies and dispersely distributed as single to small multi-cell aggregates. However, upon persistent bacterial infection, discovery of densely-packed small bacterial microcolonies was an exception. Yersiniae localized predominantly as dispersely distributed small multi-cell aggregates in the intercellular space, forming a halo-like structure around single lymphocytes. In contrast to persistent infection, YPIII (*mRuby2*) seemed to colonize larger tissue areas of the lamina propria and the cecal lymphoid tissue during the acute infection than YPIII Δ*cnfY* (*mRuby2*) during the acute phase.

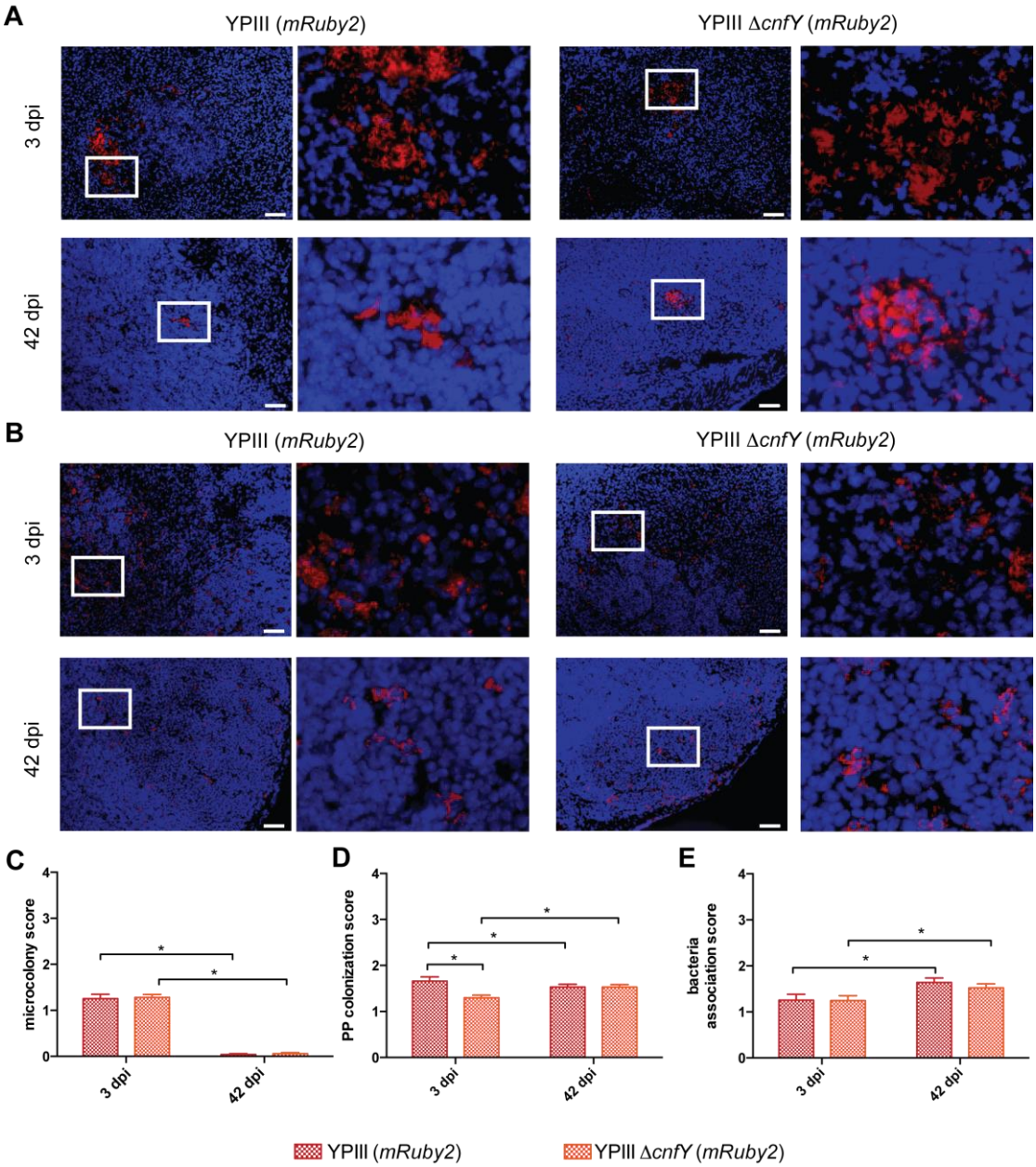

Figure 3.10 The *Yersinia* colonization patterns in the cecal lymphoid tissue differ independently of CNF_Y between the infection stages.

BALB/c mice were intra-gastrically infected with either $2x10^8$ CFU (3 dpi) or $1x10^6$ CFU (42 dpi) of *Y. pseudotuberculosis* YPIII (*mRuby2*) or YPIII Δ*cnfY* (*mRuby2*). At 3 dpi (acute) or 42 dpi (persistent), sections of highly colonized ceca were prepared, fixed, and stained. (A) Microcolonies in the cecal lymphoid tissue. (B) Dispersely distributed small multi-cell aggregates in the cecal lymphoid tissue. The microscopy pictures are representatives of multiple microscopic areas (>15). Red: *Y. pseudotuberculosis* (*mRuby2*), Blue: DAPI stained host cell nuclei. (C-E) The sections were scored for bacterial colonization by the analyses of multiple sections (>15) of n fields. The data show the mean scores ±SEM combined from 3 mice per group. Statistical analyses were performed using multiple t-tests with Holm-Šídák's correction. (C) Microcolony size score (Table 2.15). 3 dpi: YPIII n=141, YPIII Δ*cnfY* n=237; 42 dpi: YPIII n=166, YPIII Δ*cnfY* n=167; * $p<0.001$. (D) Disperse small multi-cell aggregate scores in the cecal lymphoid tissue (Table 2.15). 3 dpi: YPIII n=150, YPIII Δ*cnfY* n=167; 42 dpi: YPIII n=141, YPIII Δ*cnfY* n=237; * $p<0.01$. (E) Association of bacteria in the intercellular space around cells in the cecal lymphoid tissue (Table 2.15). 3 dpi: YPIII n=78, YPIII Δ*cnfY* n=127; 42 dpi: YPIII n=149, YPIII Δ*cnfY* n=165; * $p<0.05$.

3.3 Microbial community composition upon *Y. pseudotuberculosis* infection

Up to date, many research groups described alterations in the commensal community composition upon inflammation and infection that might influence outcome and chronicity (McKenney and Pamer, 2015; Iizasa *et al*., 2015; Hawrelak and Myers, 2004). Recent studies also showed that *Yersinia* infection can lead to global alterations of the commensal microbial community, which might alter infection outcomes (Avican *et al*. 2015; Fonseca *et al*., 2015; Kamdar *et al*., 2016).

Since stronger inflammatory reactions were observed due to *Y. pseudotuberculosis* YPIII infection than upon infection with *Y. pseudotuberculosis* YPIII Δ*cnfY* (3.2.1), it was hypothesized that this could lead to more pronounced alterations in the commensal microbial community. In order to analyze this, the commensal microbial composition was assessed via 16S rDNA sequencing of acute and persistently colonized mice after intra-gastric challenge with $1x10^6$ CFU of *Y. pseudotuberculosis* YPIII or YPIII Δ*cnfY* at various time points post infection. These experiments were performed in collaboration with Sophie Thiemann of the Microbial Immune Regulation group at the Helmholtz Center for Infection Research. Further analysis of the relative abundances of phyla demonstrated that both groups initially displayed comparable relative abundances of phyla, which did not change drastically over the first 3 days of infection (Figure 3.11A). However, YPIII infected animals showed pronounced alterations of the commensal microbial composition at 9 dpi (Figure 3.11). This was also visible in the principal coordinates analysis, which revealed clustering of the feces samples of YPIII at 9 dpi which was distinct from the others (Figure S14). At 9 dpi, there was a relative increase in the abundance of Proteobacteria (particularly Desulfovibrionales), Firmicutes (in particular Clostridiales and Lactobacillales), and Cyanobacteria (YS2), as well as a strong decrease of Bacteroidetes (Bacteroidales) (Figure 3.11A, B). Nevertheless, the relative abundances of the commensal microbiota recovered after acute infection and were completely restored to the initial state at 42 dpi. Interestingly, the relative abundance of Lactobacillales slightly increased, whereas the relative abundance of Bacteroidales decreased during persistent YPIII infection (42 dpi; Figure 3.11B).

Strikingly, no such drastic changes were observed during YPIII Δ*cnfY* infection (Figure 3.11A). There was only a slight increase in Verrucomicrobiota (Verrucomicrobiales) and a minor decrease in Bacteroidetes (Bacteroidales) at 9 and 21 dpi (Figure 3.11). Within the Firmicutes the Clostridiales decreased in their relative abundance whereas there was an increase in Erysipelotrichales at 21 dpi (Figure 3.11B). Nonetheless, at 42 dpi the relative abundances of all phyla recovered to the initial composition (Figure 3.11A).

In mice and humans, the phyla Firmicutes and Bacteroidetes make up the majority of commensal bacteria (Lei *et al*., 2005). Since the relative abundances of both phyla were altered during *Y. pseudotuberculosis* infection, the relative abundance of the single families in the phyla was subjected to detailed analysis (Figure 3.12).

Upon YPIII Δ*cnfY* infection, the proportions of the families within the Firmicutes remained fairly stable over the whole course of infection (Figure 3.12). Only within the Bacteroidetes the relative abundances of *Prevotellaceae* and *Rikenellaceae* (both Bacteroidales) reduced at 9 dpi.

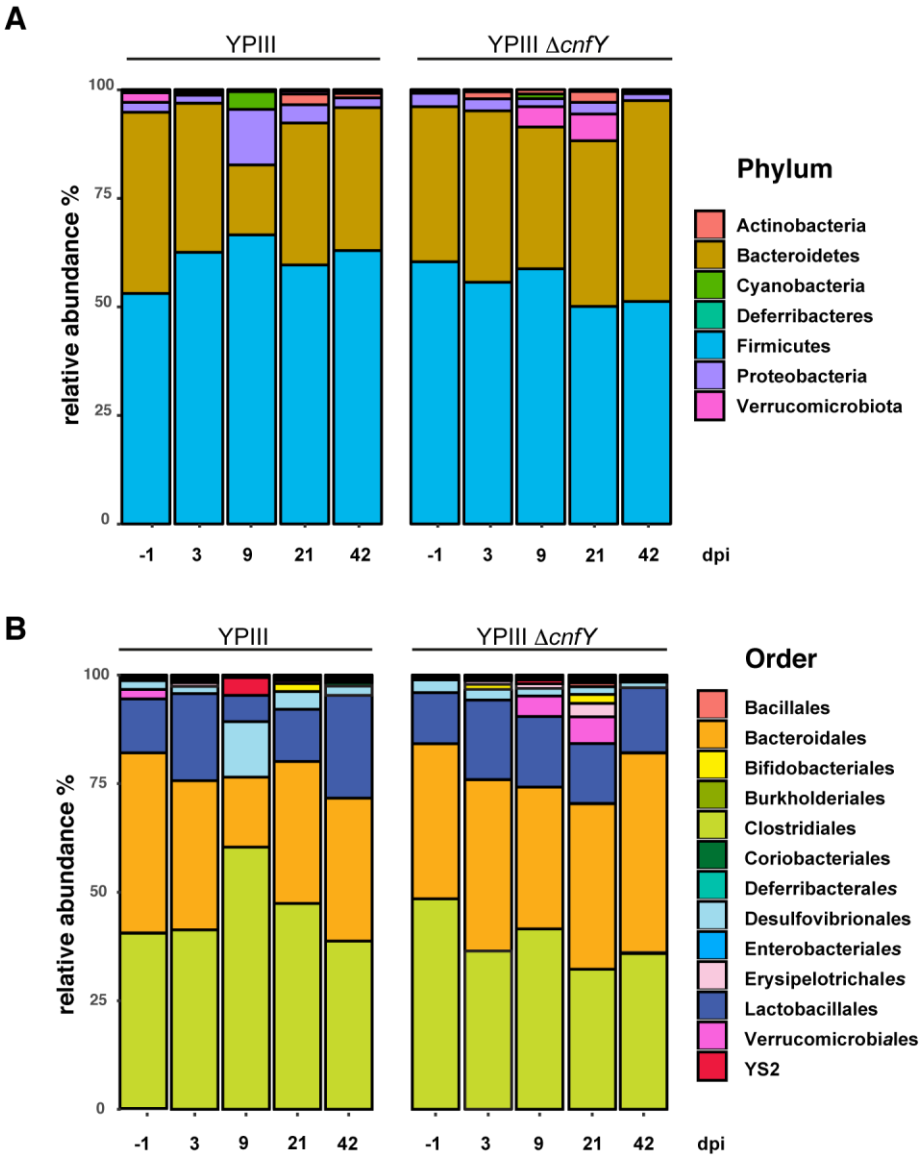

Figure 3.11 *Y. pseudotuberculosis* infection leads to an altered commensal composition.

BALB/c mice were infected with $1x10^6$ CFU of *Y. pseudotuberculosis* YPIII or YPIII Δ*cnfY*, respectively. At indicated time points post infection fresh feces was sampled from individual mice and screened for *Yersinia* colonization. Mice with persistent *Yersinia* infection were analyzed for their commensal microbial composition by 16S rDNA analysis. Each time point includes the average relative abundance from data of 5 to 6 mice. (A) Relative abundance of detected microbial phyla in the feces of persistently colonized mice over time. (B) Relative abundance of detected microbial orders in the feces of persistently colonized mice over time.

While the relative abundance of *Prevotellaceae* recovered quickly after the late acute infection phase, the relative abundance of *Rikenellaceae* remained as low. Instead, the relative abundance of S24-7 (Bacteroidales) continuously increased starting from 9 dpi.
In contrast, a massive remodeling of commensal relative abundances was observed within the Firmicutes and particularly within the Bacteroidetes upon a YPIII infection (Figure 3.12). Within the Firmicutes the relative abundance of *Lachnospiraceae* (Clostridiales), *Ruminococcaceae* (Clostridiales), *Eubacteriaceae* (Clostridiales), other Clostridiales, *Enterococcaceae* (Lactobacillales) and *Streptococcaceae* (Lactobacillales) increased at 9 dpi. On the other hand, the relative abundance of *Lactobacillaceae* (Lactobacillales) drastically decreased (Figure 3.12). Later during the infection course, all of these families normalized to initial levels, whereas the relative abundance of the *Lachnospiraceae* kept rather stable. In the

phylum Bacteroidetes, more drastic alterations of microbial relative abundances were observed (Figure 3.12). Similar to YPIII Δ*cnfY* infection, the relative abundance of *Prevotellaceae* decreased to comparable amounts at 9 dpi. In particular, the relative abundance of S24-7 decreased in the late acute YPIII infection (Figure 3.12). Interestingly, the *Odoribacteraceae* (Bacteroidales) were the exclusive family, which increased in their relative abundance within the Bacteroidetes at 9 dpi. At later time points post infection, the relative abundances of the mentioned families restored to their initial levels of relative abundances, except the *Prevotellaceae* (Figure 3.12).

Altogether, these results suggest that infection-triggered inflammation might cause alteration of commensal composition. Especially, the exacerbated inflammatory reaction upon YPIII infection might strongly impact the composition of the intestinal microbiota.

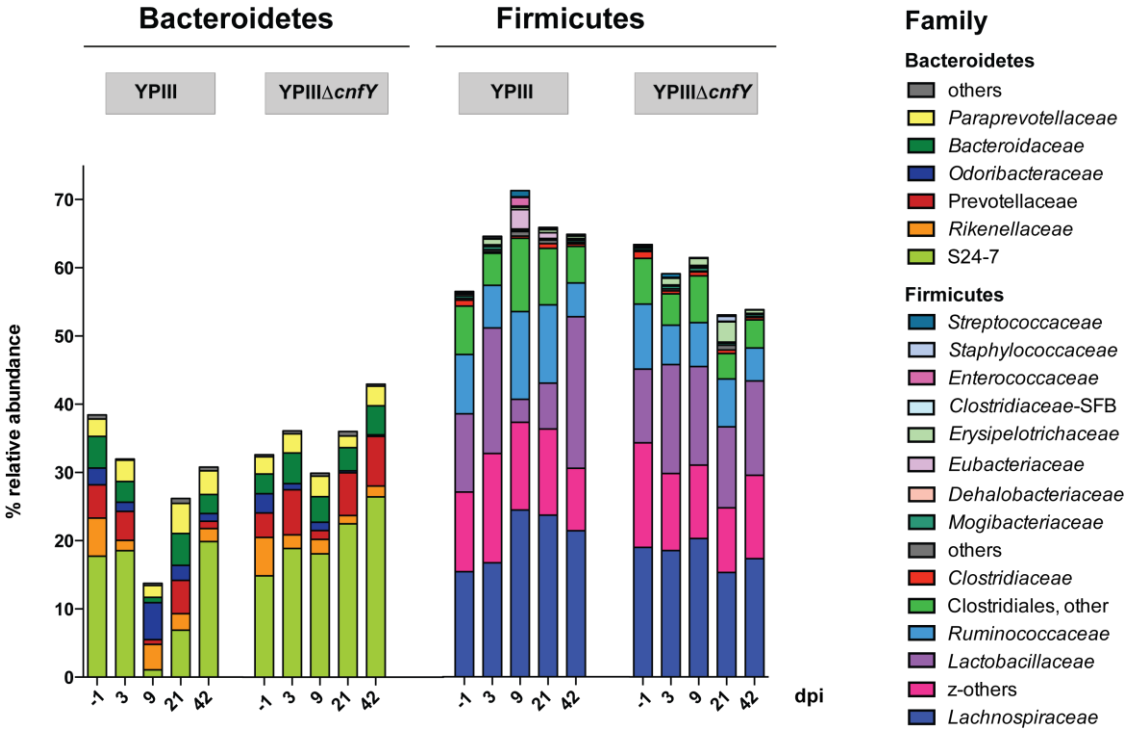

Figure 3.12 *Y. pseudotuberculosis* infection triggers remodeling of the commensal relative abundance in the phyla Firmicutes and Bacteroidetes.

BALB/c mice were infected with $1x10^6$ CFU of *Y. pseudotuberculosis* YPIII or YPIII Δ*cnfY*, respectively. At indicated time points post infection fresh feces was sampled from individual mice and screened for *Yersinia* colonization. Mice with persistent *Yersinia* infection were analyzed for their commensal microbial composition by 16S rDNA analysis. Every time point includes the average relative abundance of families within the Bacteroidetes and Firmicutes. The averages were calculated from data of 5 to 6 mice at each time point.

3.4 Study of infection stage dependent host-pathogen interactions

In contrast to acute bacterial infections, the comprehension of host immune responses and host-pathogen interactions during chronic infections has just started to be obtained. In order to explore the global immune mechanisms underlying the development of *Yersinia* persistence and its characteristics during acute (5 dpi) and persistent (42 dpi) infection, the global host transcriptome of the cecum upon *Y. pseudotuberculosis* YPIII or YPIII Δ*cnfY* infection was evaluated by employing strand-specific RNA sequencing (Figure 3.13A).

To this purpose, high quality RNA pools (Figure S15A) obtained from ceca of equally-aged and equally-colonized mice (Figure S15B) were depleted for mouse ribosomal RNA (rRNA) in order to raise the informative mouse transcript coverage, as described by Nuss *et al*., 2017 (Figure 3.13A). Commercial ERCC (external RNA controls consortia) spike-in controls comprising a 10^6-fold concentration range, were added to determine sequencing precision and platform performance (Figure 3.13A). For strand specific deep sequencing, cDNA libraries were generated with the Illumina ScriptSeq™ kit (Figure 3.13A). The cDNA library deep sequencing produced around 26 million reads of which approximately 16 million mapped to the murine mm10 genome, achieving sufficient coverage. Moreover, of the 16 million genomic mappings, an average of 11 million reads mapped to genes (Table S1). The dynamic range of the sequencing run was calculated to be about 18 $\log_2$-units of concentration (Figure S16A) and the assessment of the fold change estimates revealed high platform accuracy, which was adequate to reliably determine and compare transcript abundance across a broad dynamic range (Figure S16B). Additionally, all replicates strongly correlated to the replicates of the same group with a Pearson correlation coefficient of $r > 0.97$ (Figure S17). As high quality data were obtained, reliable transcript quantification, global host expression profile analysis and comparison was conducted.

The global gene expression profiles (GGEPs) of the nine different conditions were distinct and each condition clustered well together (Figure 3.13B, C). The GGEPs of acute infected ceca were both most distant to the GGEPs of uninfected ceca (Figure 3.13B, C). This most probably reflects the induction of inflammatory immune responses by epithelial cells and infiltrating immune cells that, in all likelihood, are the main drivers of altered gene expression profiles during acute infection. However, the GGEPs of acute YPIII- and YPIII Δ*cnfY*-infected ceca were distinct and clustered hierarchically distant from each other emphasizing that the host tissue reactions are distinct in response to YPIII and YPIII Δ*cnfY* acute infections (Figure 3.13C). Interestingly, the GGEPs of persistently YPIII-colonized ceca also clustered separately from those of uninfected and chronically YPIII Δ*cnfY*-infected ceca (Figure 3.13C). These results show that the host gene expression profile is somewhat more altered in response to YPIII than YPIII Δ*cnfY* during the persistent infection stage.

To gain further knowledge about the *Yersinia*-triggered gene expression changes during acute and persistent infection, which might impact the development and maintenance of persistent *Y. pseudotuberculosis* infection, the differential expression analysis package DESeq2 was applied (Love *et al*., 2014). The results of these analyses are described in the following sections.

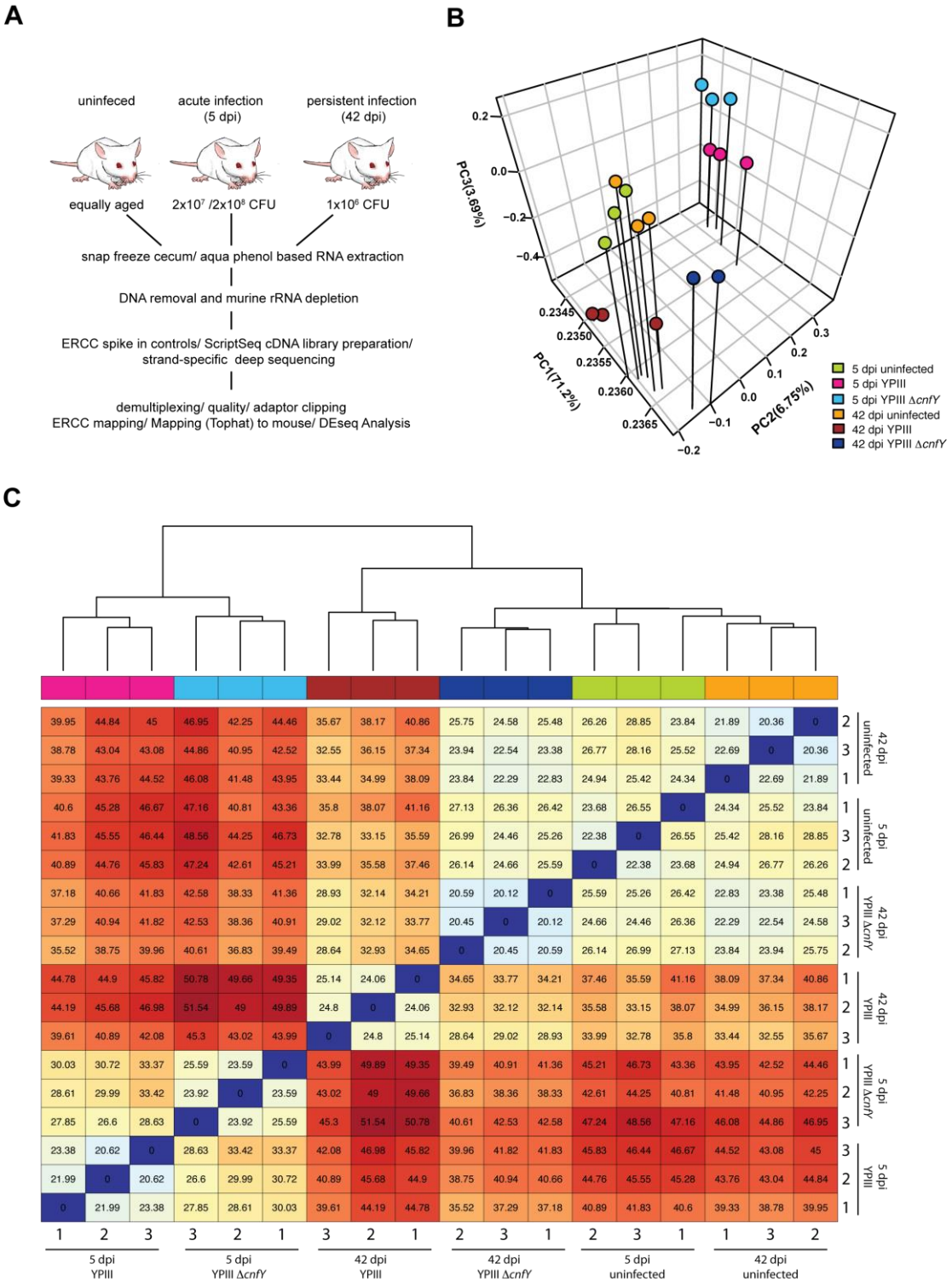

Figure 3.13 The host expression profile during acute and persistent *Y. pseudotuberculosis* infections in the cecum.

BALB/c mice were intra-gastrically infected with either $2x10^7$ CFU (5 dpi)/$1x10^6$ CFU (42 dpi) of *Y. pseudotuberculosis* YPIII or $2x10^8$ CFU (5 dpi)/$1x10^6$ CFU (42 dpi) of *Y. pseudotuberculosis* YPIII Δ*cnfY*. (A) Work flow for murine expression profile assessment. At the indicated time points, ceca of highly colonized mice or equally aged uninfected mice were snap frozen. The complete RNA was extracted using a water-saturated phenol-based extraction protocol. Subsequently, the isolated RNA was pooled together using material from three to five mice. After the removal of contaminating DNA and the depletion of ribosomal RNA (rRNA), ERCC spike in control mixes were added to control the platform performance. Thereafter, complementary DNA (cDNA) libraries were prepared and subjected to strand specific deep sequencing. The assessed reads were demultiplexed, the quality

of the sequences libraries was assessed and adaptors were clipped of the fragments *in silico*. The remaining reads were mapped to the ERCC spike in controls and platform-performance control parameters were calculated. Finally, the remaining reads were mapped with Tophat to the murine genome and submitted to differential expression analysis for sequencing data (DESeq2). (B) Three dimensional principle component analysis of the replicates. The third replicate of YPIII Δ*cnfY* at 42 dpi clusters closely with the first replicate. See also (C). (C) Euclidian sample-to-sample distances calculated for the single replicates.

3.4.1 Host gene expression profiling during acute infection in the cecum

At first, the host gene-expression profiles during acute infection were analyzed. Upon acute infection, 16,974/15,609 (YPIII/YPIII Δ*cnfY*) murine genes were profiled by comparison of the infected to the uninfected group, respectively (data not shown). Of those genes, 75/120 (YPIII/YPIII Δ*cnfY*) were more abundant (induced) with a corresponding $\log_2$-fold change (FC) > 2. Furthermore, 26/16 genes were less abundant (repressed) owing a $\log_2$ FC < -2 (Table S2; Table S3). Gene ontology (GO) enrichment analysis revealed that *Yersinia* infection significantly altered the host transcriptome. Many of the most highly regulated genes were connected to inflammatory responses, immune cell chemotaxis, and acute phase response (data not shown). Comparison of both expression profiles (YPIII/YPIII Δ*cnfY* vs. uninfected) revealed three groups of genes: those that where commonly highly (up-) regulated (Figure 3.14C), or only highly (up-) regulated upon the respective infection (YPIII

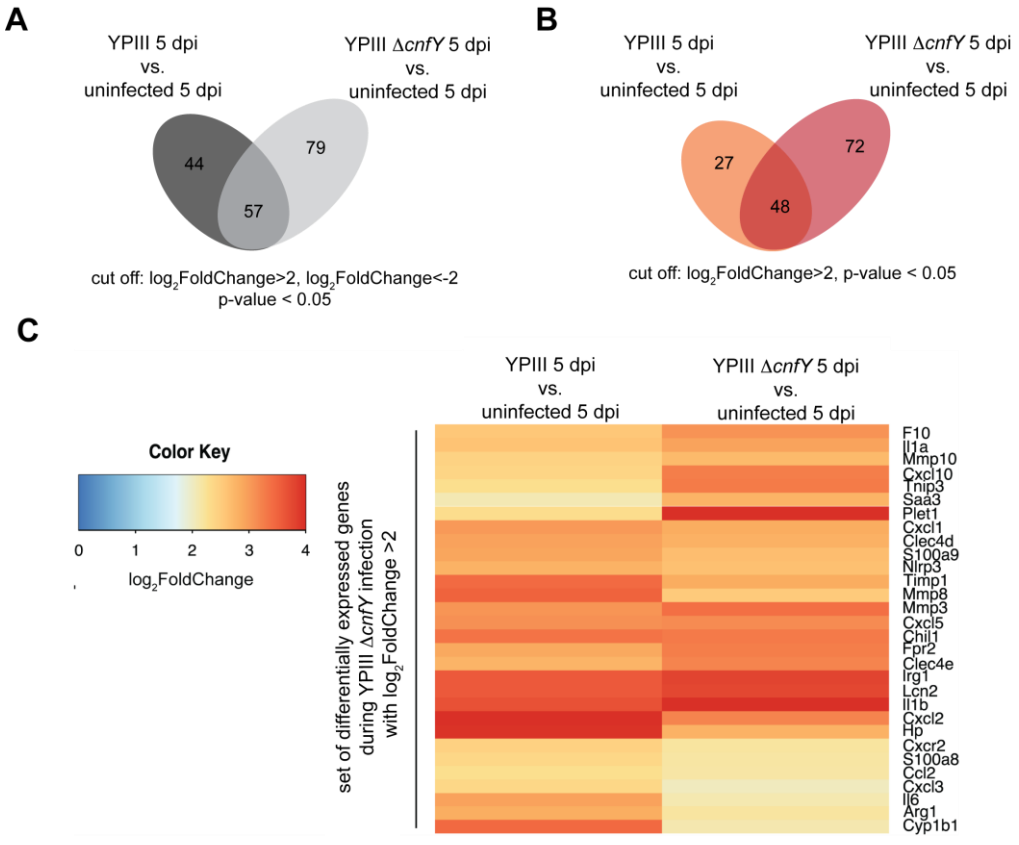

Figure 3.14 Differentially expressed genes upon acute infection with *Y. pseudotuberculosis* in the cecum

Venn diagram of the differentially expressed genes during acute infection (5 dpi) comparing *Y. pseudotuberculosis* infected ceca to uninfected. (B) Venn diagram of induced genes comparing *Y. pseudotuberculosis* infected ceca to uninfected. (C) Heat map of *Yersinia*-increased transcripts ($\log_2$ FC > 2; $p < 0.05$) at 5 dpi comparing *Y. pseudotuberculosis* infected ceca to uninfected samples (YPIII left column; YPIII Δ*cnfY* right column).

or YPIII Δ*cnfY*) compared to gene expression levels of uninfected mice (Figure 3.14A, B). Interestingly, YPIII Δ*cnfY* infection caused the up-regulation of about 2-fold more genes than YPIII infection in comparison to the uninfected samples (Figure 3.14B).
Among the commonly highly up-regulated genes were several metal ion scavenging proteins that limit metal ion availability (*i.e. lcn2*, *hp*, s*100a9*, *s100a8*), cytokines and chemokines (*i.e. il-6*, *cxcl3*, *ccl2*, *cxcl2*, *il-1β*, *cxcl5*, *cxcl1*, *cxcl10*, *il-1α*), acute-phase response proteins (*chil1*, *saa3*), an inflammasome component (*i.e. nlrp3*), genes involved in reactive compound protection/detoxification (*i.e. cyp1b1*, *arg1*) (Popovic *et al*., 2007; Jaeger *et al*., 2015), and a versatile g-protein coupled receptor *fpr2* that triggers multiple cellular events after activation, such as activation/inhibition of NFκB, chemotaxis, superoxide generation, healing and cell proliferation (Cattaneo *et al*., 2013) (Figure 3.14C). Furthermore, matrix metalloproteinases and inhibitors (*mmp3*, *mmp8*, *mmp10*, *timp1*, *hp*), controlling multiple immune functions, *e.g.* cytokine in-/activation, tissue permeability, cytokine gradients, and antimicrobial peptide or defensin activation (Elkington *et al*., 2005), were induced upon *Y. pseudotuberculosis* infection (Figure 3.14C). The analysis also revealed increased expression of *irg1*, which produces bactericidal and immune modulatory itaconate (Luan and Medzhitov, 2016) and the endocytic receptors, *clec4d* and *clec4e*, involved in bacterial recognition and uptake (Wilson *et al*., 2015; Sharma *et al*., 2014) (Figure 3.14C). Although these genes were commonly induced upon both *Yersinia* infections, a stronger induction of *il-6*, *cxcl2*, *mmp8*, haptoglobin (*hp*) and cytochrome P450 (*cyp1b1*) expression was detected upon YPIII infection (Figure 3.14C).

As the comparison of the GGEPs suggested differential gene expression between the two *Y. pseudotuberculosis* stains (3.4), the gene expression profiles of acute infected mice were compared to each other. This analysis yielded detection of 14,244 genes, of which two genes were induced with a $\log_2$ FC > 2, and 113 genes with a $\log_2$ FC > 1. Moreover, two genes were repressed with a $\log_2$ FC < -2 and 36 genes demonstrated a $\log_2$ FC < -1 upon acute YPIII Δ*cnfY* infection in comparison to acute YPIII infection (Table S4). GO enrichment analysis and GAGE KEGG gene perturbation analysis showed that *cnfY*-deficiency significantly altered the host transcriptome, with many of the up-regulated pathways involved in the regulation of immune responses (data not shown). Moreover, the majority of differentially regulated genes ($\log_2$FC > 1, $\log_2$FC < -1) between YPIII and YPIII Δ*cnfY* infection at 5 dpi were also differentially regulated by comparison to uninfected mice, respectively (Figure 3.15A).
The direct comparison of the two gene expression profiles revealed that genes acting on iron depletion from tissue, *i.e. scara5* and *hp*, and reactive compound protection (*cyp1b1*) are more strongly induced during acute YPIII infection compared to acute YPIII Δ*cnfY* infection (Figure 3.15B). Moreover, the expression of the LPS detoxifying tissue non-specific alkaline phosphatase *alpl* and the PMN chemoattractant during barrier immune responses *chil3* was highly induced (Bender *et al*., 2015; Muallem and Hunter, 2014). The data analysis also revealed stronger induction of genes associated with tissue turn-over/architecture modifications, such as *wisp2*, *has2*, *adam12*, *adamts5*, *adamts4*, *thbs1*, *csgalnact1*, and *cdh3* (Maytin, 2014; Nyren-Erickson *et al*., 2013; Lin and Liu, 2010; Kintakas and McCulloch, 2011; Sabbah *et al*., 2011; Kelwick *et al*., 2015; Masli *et al*., 2014; Sato *et al*., 2011; Hubmacher and Apte, 2015). In addition, there was an up-regulation of a couple of genes

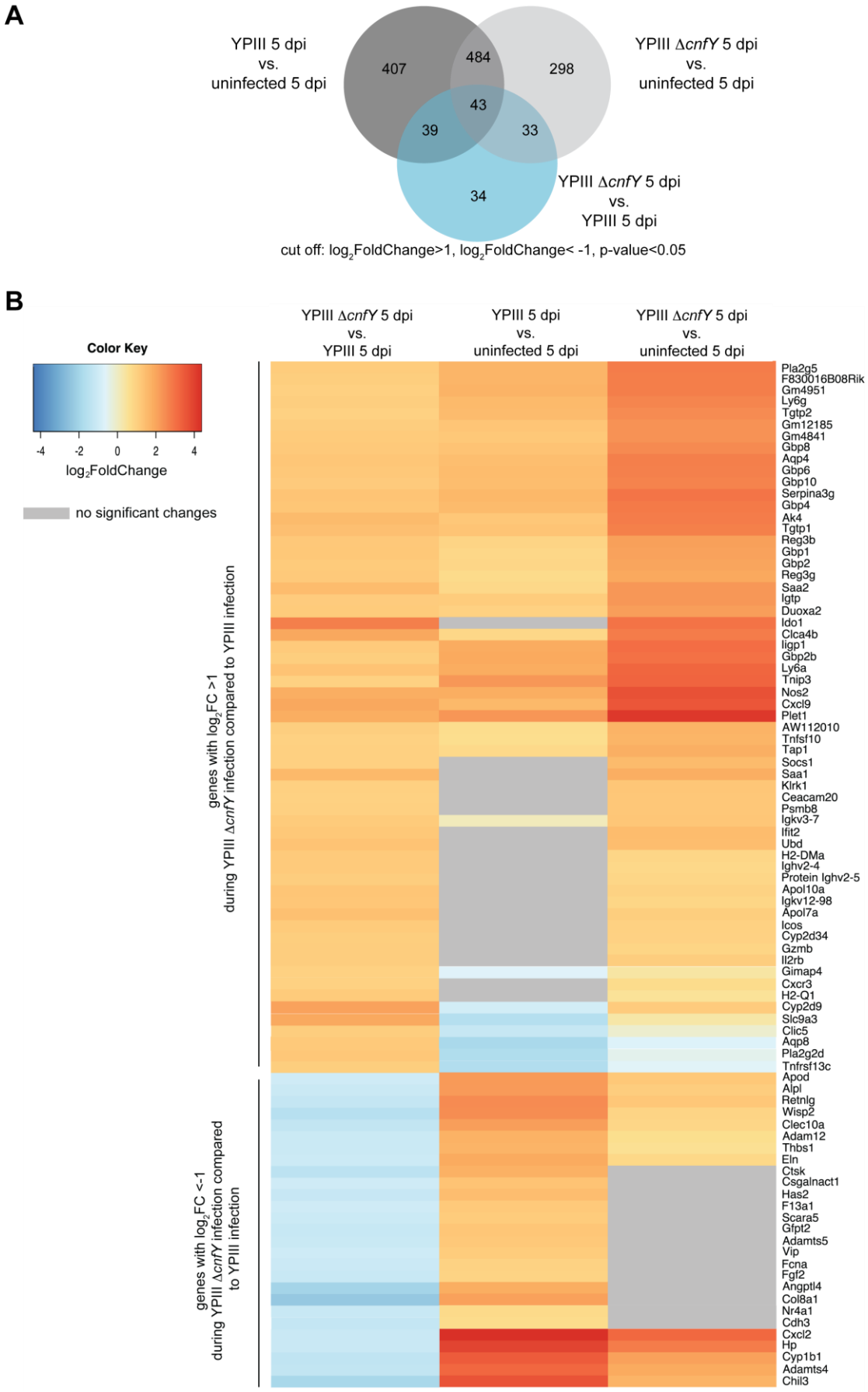
A
YPIII 5 dpi
vs.
uninfected 5 dpi
YPIII ΔcnfY 5 dpi
vs.
uninfected 5 dpi
YPIII ΔcnfY 5 dpi
vs.
YPIII 5 dpi
407
484
298
43
39
33
34
cut off: log2FoldChange>1, log2FoldChange< -1, p-value<0.05
B
Color Key
-4
-2
0
2
4
log2FoldChange
no significant changes
YPIII ΔcnfY 5 dpi
vs.
YPIII 5 dpi
YPIII 5 dpi
vs.
uninfected 5 dpi
YPIII ΔcnfY 5 dpi
vs.
uninfected 5 dpi
genes with log2FC >1
during YPIII ΔcnfY infection compared to YPIII infection
genes with log2FC <-1
during YPIII ΔcnfY infection compared
to YPIII infection
Pla2g5
F830016B08Rik
Gm4951
Ly6g
Tgtp2
Gm12185
Gm4841
Gbp8
Aqp4
Gbp6
Gbp10
Serpina3g
Gbp4
Ak4
Tgtp1
Reg3b
Gbp1
Gbp2
Reg3g
Saa2
Igtp
Duoxa2
Ido1
Clca4b
Iigp1
Gbp2b
Ly6a
Tnip3
Nos2
Cxcl9
Plet1
AW112010
Tnfsf10
Tap1
Socs1
Saa1
Klrk1
Ceacam20
Psmb8
Igkv3-7
Ifit2
Ubd
H2-DMa
Ighv2-4
Protein Ighv2-5
Apol10a
Igkv12-98
Apol7a
Icos
Cyp2d34
Gzmb
Il2rb
Gimap4
Cxcr3
H2-Q1
Cyp2d9
Slc9a3
Clic5
Aqp8
Pla2g2d
Tnfrsf13c
Apod
Alpl
Retnlg
Wisp2
Clec10a
Adam12
Thbs1
Eln
Ctsk
Csgalnact1
Has2
F13a1
Scara5
Gfpt2
Adamts5
Vip
Fcna
Fgf2
Angptl4
Col8a1
Nr4a1
Cdh3
Cxcl2
Hp
Cyp1b1
Adamts4
Chil3

Figure 3.15 The host induces bacterial defense mechanisms upon *Y. pseudotuberculosis* YPIII Δ*cnfY* acute infection.

(A) Venn diagram of the differentially expressed genes during acute infection (5 dpi). (B) Heat map of a selection of more/less abundant transcripts ($-1 < \log_2 FC > 1$; $p < 0.05$) at 5 dpi comparing YPIII Δ*cnfY* to YPIII infection (left column). The respective $\log_2$ FC of each gene compared to uninfected mice are displayed: YPIII infected mice 5 dpi compared to uninfected (middle column) and YPIII Δ*cnfY* infected mice 5 dpi compared to uninfected (right column). Grey fields indicate no significant changes ($p \geq 0.05$) compared to uninfected mice.

involved in angiogenesis, *i.e. col8a1*, *eln*, *fgf2*, *cyp1b1*, *angptl4*, and *vip* (Iruela-Arispe *et al*., 1991; Delgado *et al*., 2001; Jiang *et al*., 2016; Li *et al*., 1998; Liu *et al*., 2013a; Bäckhed *et al*., 2007; Palenski *et al*., 2013) (Figure 3.15B).
Altogether, these findings lead to the assumption that massive tissue remodeling occurs during acute YPIII infection due to high induction of inflammation, which is not observed during acute YPIII Δ*cnfY* infection.

In contrast to YPIII infection, many immune response-associated GTPases and interferon-inducible genes (*e.g. gbp1*, *gbp2*, *gbp2b*, *gbp4*, *gbp6*, *gbp8*, *gbp10*, *igtp*, *iigp*, *Ifgga2* (Gm4951), *Ifgga3* (Gm4841), Ifgga*4* (F830016B08Rik)) involved in cell-autonomous immune responses (Meunier and Broz, 2016) were up-regulated during YPIII Δ*cnfY* infection compared to YPIII infected samples (Figure 3.15B). Furthermore, the expression of genes encoding bactericidal gene products like the reactive oxygen producing enzyme Nos2 and the Duox2 maturation factor Duoxa2 (Gogoi *et al*., 2016; Leto and Geiszt, 2006; Hoste *et al*., 2012), the defensins RegIIIβ, RegIIIγ, and Pla2g5 (Dann and Eckmann, 2007; van Ampting *et al*., 2012; Grönroos *et al*., 2001), the bactericidal chemokine Cxcl9 (Cole *et al*., 2001), and the acute phase proteins Saa1/2 were more strongly induced compared to acute YPIII infection. The expression of genes associated with phagosome maturation and antigen processing (*i.e. rab39*, *tap1*, *psmb8*, *h2-dma*, *h2-q1*) was also more highly induced upon acute YPIII Δ*cnfY* infection (Kasmapour *et al*., 2012; Abele and Tampé, 2011; Joeris *et al*., 2012; Russell *et al*., 1999; Zeng *et al*., 2012). In accordance with that, the expression of loci encoding for immunoglobin variable chains (*e.g. ighv2-4*, *igkv12-98*) was strongly up-regulated in comparison to YPIII infection at 5 dpi. Interestingly, upon acute YPIII Δ*cnfY* infection the expression of T cell associated genes such as *ido1*, involved in suppression of T cell proliferation and development of Tregs (Murakami *et al*., 2013), *ly6a*, which is up-regulated in activated T cells (Holmes and Stanford, 2007), *cd274* an immune-inhibitory receptor on activated T cells important for peripheral tolerance (Freeman *et al*., 2000) and the T cell chemoattractants *cxcl9/11* were highly induced (Figure 3.14C). Moreover, the expression of *icos*, which is involved in multiple T and B cell activities, for instance enhancement of T cell responses to a foreign antigen and assistance of antibody secretion by B cells (Wikenheiser and Stumhofer, 2016), was increased during acute infection with YPIII Δ*cnfY*. On the other hand, there was a profound up-regulation of genes encoding proteins that modulate and limit inflammation and the immune response: *ubd*, which regulates activation of NFκB (Gong *et al*., 2010), *socs1* that inhibits the JAK pathway and plays a key role in Treg stability (Ahmed *et al*., 2015), *tnip3* that inhibits NFκB activation (Verstrepen *et al*., 2009), *pla2g5* that is involved in the regulation of inflammation (Ohta *et al*., 2013; Giannattasio *et al*, 2010; Lapointe *et al*., 2010; Munoz *et al*., 2009; Balestrieri *et al*., 2009), and *pla2g2d* that drives production of anti-inflammatory factors (Miki *et al*., 2013; Seroussi *et al*., 2013).
These data suggest that YPIII Δ*cnfY* infection elicits a regulated immune response encompassing cell autonomous immunity, antigen processing/presentation, antibody maturation and immune modulation, implicating that YPIII Δ*cnfY* has to deal with harsher host environmental stresses during acute infection than YPIII.

All in all, these data indicate that *Y. pseudotuberculosis* infection induces a common acute inflammatory host immune response, which also differs between the two strains: YPIII acute infection drives massive tissue remodeling, whereas YPIII Δ*cnfY* acute infection induces cell autonomous and adaptive immune responses.

3.4.2 Host expression pattern reprogram from acute to persistent *Yersinia* infection

Next, the murine gene expression pattern changes from acute to persistent infection were analyzed. To this purpose, DESeq2 analysis was applied to compare acute to persistently infected mice or uninfected mice at the respective age (Table S5-Table S7).

By comparing persistently YPIII-infected mice to acute YPIII-infected mice, 354 genes displayed a $\log_2$FC greater than 1.5 or less than -1.5. Of these genes, 134 genes overlapped with genes that were also differentially regulated upon YPIII infection at either infection stage ($\log_2$ fold change > 1.5; $\log_2$ fold change < -1.5; p-value < 0.05) (Figure 3.16A). The following analysis was concentrated on these 134 genes (Figure 3.16A). The 134 genes could be divided into four different groups. The first group comprises genes, which were down-regulated in the acute phase and then again up-regulated to the level of uninfected mice during the persistent infection stage (Figure 3.16B). These genes included transporter, channels and pores (*i.e. slc20a1*, *slc30a10*, *slc37a2*, *slc9a3*, *abcb1a*, *aqp8*, *slc22a4*, *kcnf1*, *trpm6*) and genes involved in diverse biosynthetic pathways (*e.g.* acetyl-CoA desaturase 1 (*scd1*), carboxylesterases (*ces1c/d/f*), cytochrome P450 2c55 (*cyp2c55*), alanine aminotransferase 1 (*gpt*), phosphoenolpyrovate carboxykinase (*pck1*), or galactose-3-O- sulfotransferase 2 (*gal3st2*)). This expression increase effect during persistent YPIII infection is most likely due to decreased relative abundance of immune cell-derived transcripts and the regeneration of the tissue in the persistent infection phase.

The second group encompasses genes that were more abundant upon persistent YPIII infection compared to acute phase, and were more abundant during persistent infection compared to uninfected mice (Figure 3.16B). The majority of these genes is associated with the induction of immune responses. Those are described in section 3.4.3 in more detail.

The third group includes genes that were less abundant during persistent YPIII infection compared to acute infection but were still slightly induced during persistent YPIII infection (Figure 3.16B): iron sequestration (*lcn2*, *hp*), chemokines and cytokines (*e.g. cxcl5*, *il-1α*, *cxcl1*, *cxcl2*, and *il1f9*), endocytic receptors (*clec4d*, *clec4e*), metalloproteinases and their inhibitors (*mmp8*, *timp1*) and inflammation modulators (*chil1*, *chil3*, *irg1*).

In the fourth group, few genes were detected. This group encompasses genes that were down-regulated upon persistent YPIII infection compared to acute YPIII infection and were not significantly altered during persistent YPIII infection in comparison to uninfected mice (Figure 3.16B). These genes were *il-6*, *ly6g* and *saa3*.

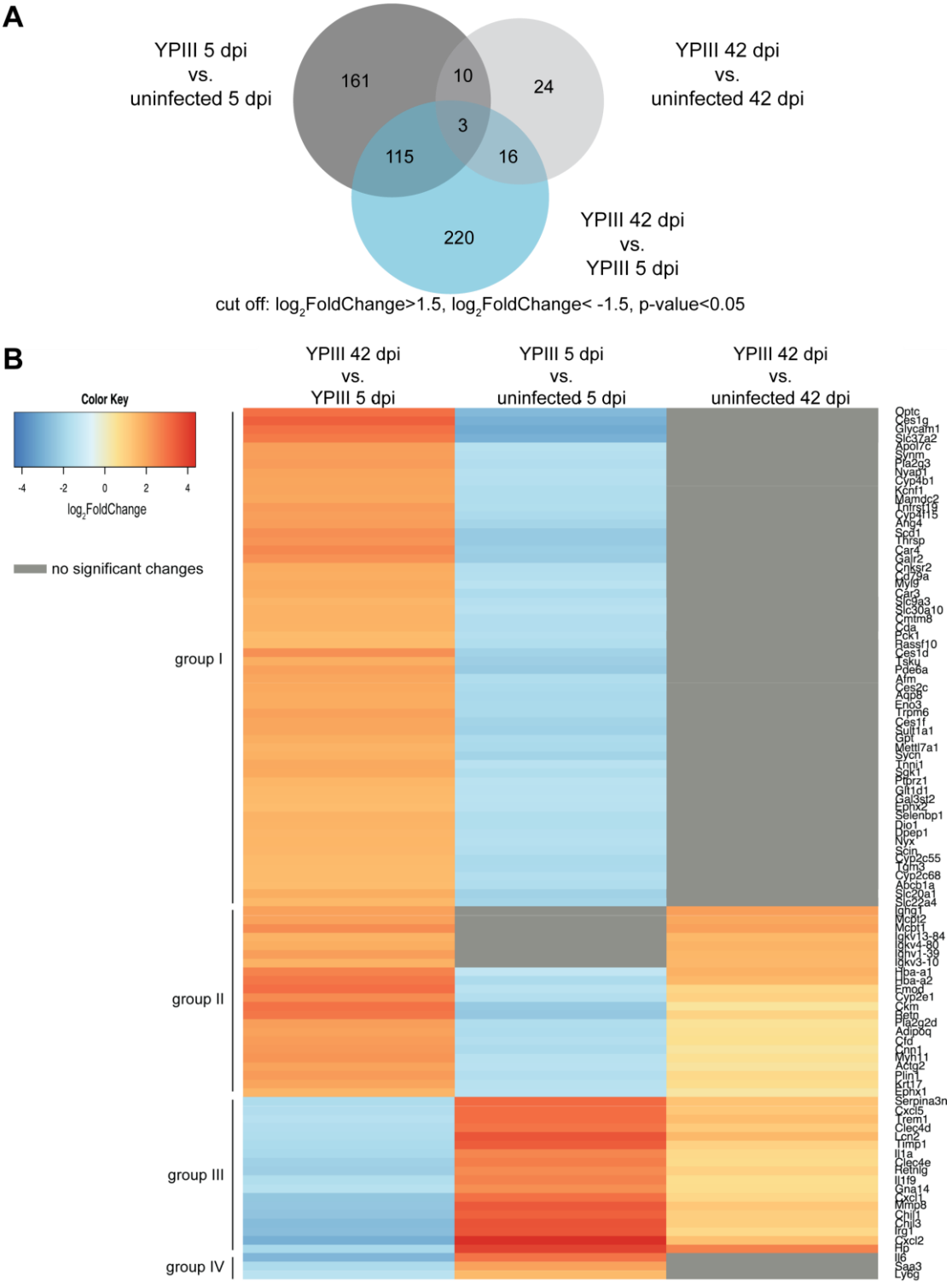

Figure 3.16 The host remodels its gene expression upon persistent *Y. pseudotuberculosis* YPIII infection

(A) Venn diagram of the differentially expressed genes during persistent infection (42 dpi) compared to acute infection during YPIII challenge. (B) Heat map of a selection of differentially abundant transcripts ($-1.5 < \log_2 FC > 1.5$; $p < 0.05$) upon YPIII infection at 42 dpi compared to 5 dpi (left column). The respective $\log_2$ FC of each gene compared to uninfected mice at the respective time point are displayed: YPIII-infected mice at 5 dpi (middle column) and at 42 dpi (right column) compared to uninfected mice. Grey fields indicate no significant changes ($p \geq 0.05$) compared to uninfected mice.

By comparing persistently YPIII Δ*cnfY*-infected mice to acute YPIII Δ*cnfY*-infected mice 177 genes displayed a log_2FC greater than 1.5 or less than -1.5. 155 of these genes overlapped with genes that were also differentially regulated at either infection stage (log_2 fold change > 1.5; log_2 fold change < -1.5; p-value < 0.05) (Figure 3.17A). As for YPIII, a similar set of four differentially expressed transcript groups was observed. The first group includes genes that were more abundant during persistent stage but did not display a significant different expression upon persistent YPIII Δ*cnfY* infection compared to uninfected mice. These genes also encompassed transporters and channels (*i.e. trpm6*, *slc30a10*) and genes involved in diverse biosynthetic pathways, for instance cytochrome P450 2c55 (*cyp2c55*), carboxyltransferase (*ces1d*), creatine kinase M-type (*ckm*), and hydroxymethylglutaryl-CoA synthase (*hmgcs2*) (Figure 3.17B). Once more, this increased expression during persistent YPIII Δ*cnfY* infection is also most likely due to the reduction of immune cell-derived transcripts and the regeneration of the tissue in the persistent infection stage.

In contrast to YPIII infection, the second group of this analysis comprises only one gene, which was more abundant during persistent YPIII Δ*cnfY* infection phase compared to acute infection and was also more abundant during persistent infection compared to uninfected mice, *i.e.* mast cell protease 1 (*mcpt1*).

The third group encompasses genes that were down-regulated during persistent YPIII Δ*cnfY* infection compared to acute YPIII Δ*cnfY* infection, but were still slightly induced during persistent YPIII Δ*cnfY* infection (Figure 3.17B): iron scavenger (*hp*), chemokines and cytokines (*i.e. cxcl2*, *cxcl5*, *cxcl9*, *il-1α*, *il-1β*), bactericidal effectors (*e.g. cxcl9*, *duox2*, *nos2*), proteins that contribute to inflammation or its modulation (*i.e. trem1*, *socs3*, *chil1*, *pla2g5*), matrix metalloproteinase *mmp3*, T cell activation marker *ly6a* and the endocytic receptors (*clec4d*/*e*).

In the fourth group, plenty of genes were detected that were down-regulated upon persistent YPIII Δ*cnfY* infection compared to acute YPIII Δ*cnfY* infection and demonstrated no significant changes in their expression compared to uninfected mice during persistent YPIII Δ*cnfY* infection (Figure 3.17B). These included the cell autonomous immunity associated GTPases (*i.e. gbp2/2b/4/6/7/8*, *Ifgga2/3*, *igtp*, *iigp1*), metal ion scavengers (*i.e. s100a8/9*, *lcn2*), acute phase response genes (*saa1/2/3*), matrix metalloproteinases (*mmp8/10*, *pappa2*), immune response modulators (*e.g. ido1*, *irg1*, *tnip3*, *tifa*, *tnfaip2*), chemokines and cytokines (*i.e. ccl3*, *cxcl1*, *cxcl10*, *cxcl11*, *il-6*, *tnf*), bactericidal or bacteriostatic proteins (*regIIIα*, *regIIIβ*, *regIIIγ*, *ido1*, *irg1*), and the granulocyte marker *ly6g*.

In conclusion, the analysis of the switch of the host transcriptome profiles from acute to persistent *Y. pseudotuberculosis* infection demonstrated that the initial disruption of the tissue homeostasis during the acute infection phase is restored to almost homeostatic conditions at 42 dpi. However, it appears that persistent YPIII infection still triggers stronger immune responses than persistent YPIII Δ*cnfY* infection, as (1) more immune response-associated genes are up-regulated during persistent YPIII infection than in YPIII Δ*cnfY*-infected cecal tissue, and (2) more immune response-linked genes in persistently YPIII Δ*cnfY* infected mice are expressed at levels as in the uninfected cecal tissue.

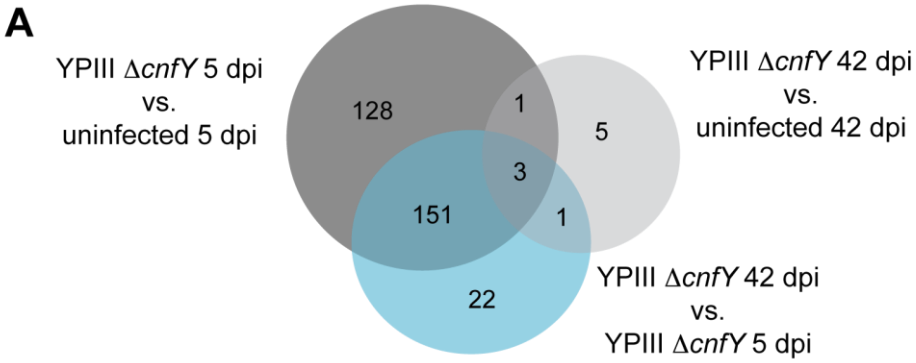

cut off: $\log_2$ FoldChange>1.5, $\log_2$ FoldChange< -1.5, p-value<0.05

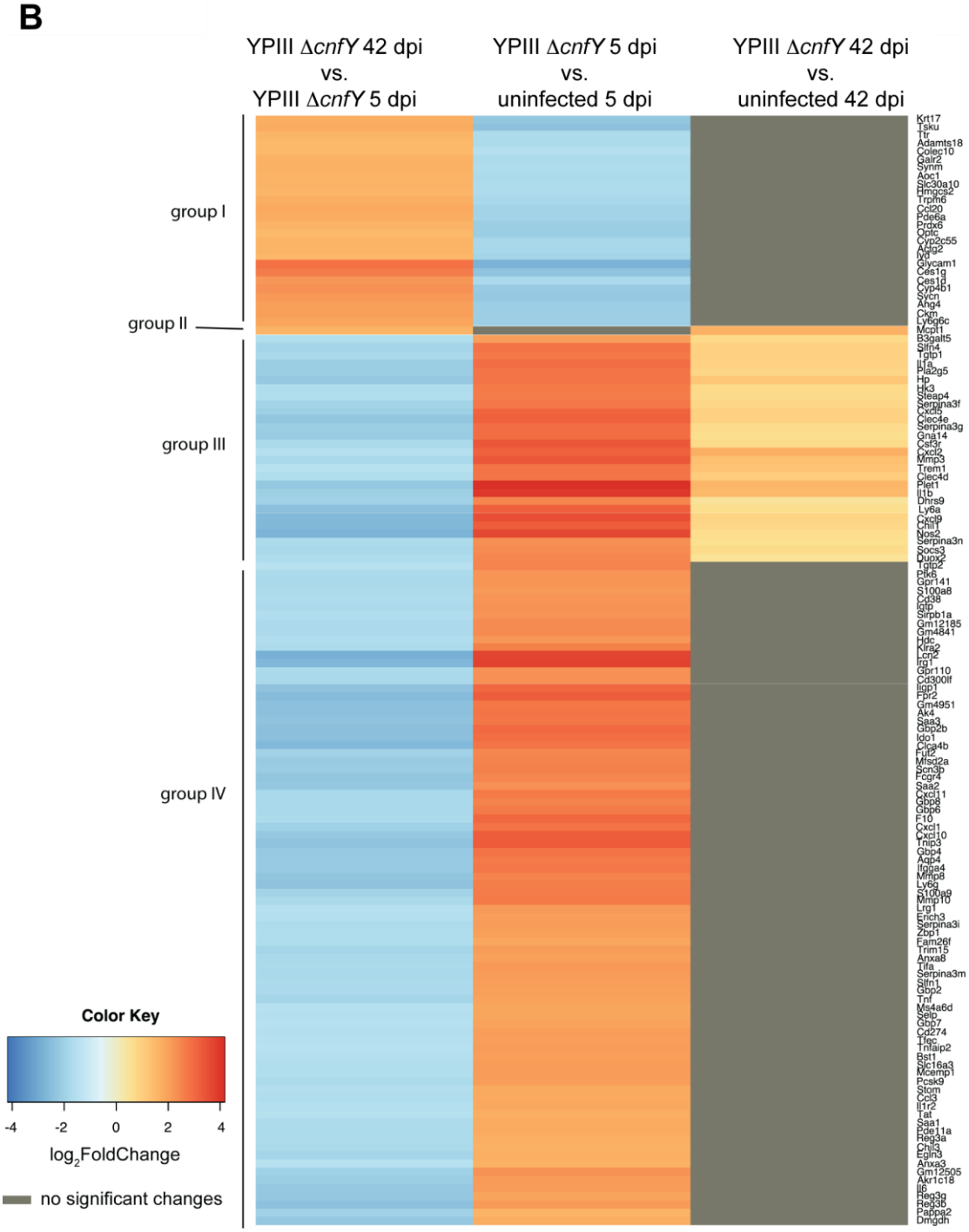

Figure 3.17 The murine gene expression patterns upon *Y. pseudotuberculosis* YPIII Δ*cnfY* infection reprogram from acute to persistent infection and resemble gene expression profiles of uninfected mice.

(A) Venn diagram of the differentially expressed genes during persistent infection (42 dpi) compared to acute infection during YPIII Δ*cnfY* challenge. (B) Heat map of a selection of increased transcripts ($-1.5 < \log_2 FC > 1.5$; $p < 0.05$) upon YPIII Δ*cnfY* infection at 42 dpi compared to 5 dpi (left column). The respective $\log_2$ FC of each gene compared to uninfected mice at the respective time point are displayed: YPIII Δ*cnfY* infected mice at 5 dpi (middle column) and at 42 dpi (right column) compared to uninfected. Grey fields indicate no significant changes ($p \geq 0.05$) compared to uninfected mice.

3.4.3 *Y. pseudotuberculosis* dependent host gene expression profiles during persistent infection

Lastly, the host gene-expression patterns during persistent *Y. pseudotuberculosis* infection were compared using DESeq2 analysis. Upon persistent infection (42 dpi), 14,244/22,434 (YPIII/YPIII Δ*cnfY*) murine genes were profiled by comparison of the infected to the uninfected group, respectively (data not shown). During persistent YPIII infection, 178 of these genes were induced with a $\log_2$ FC > 1 (5 genes with $\log_2$ FC > 2) and 112 genes were repressed with a $\log_2$ FC < -1 (4 genes with $\log_2$ FC < -2) compared to uninfected, equally-aged mice (Table S8). On the other hand, the analysis of persistent YPIII Δ*cnfY* infection compared to uninfected, equally-aged mice demonstrated that 19 genes were induced with a $\log_2$ FC > 1 (no genes with $\log_2$ FC > 2), and 19 genes were repressed with a $\log_2$ FC < -1 (no genes with $\log_2$ FC < -2) (Table S9). Noteworthy, these data demonstrate that there were almost 8-times more genes differentially (up-)regulated upon persistent YPIII infection compared to persistent YPIII Δ*cnfY* infection (Figure 3.18A, B).

The following analysis was concentrated on the genes that were induced during persistent *Y. pseudotuberculosis* infection. Comparison of both expression profiles (YPIII/YPIII Δ*cnfY* vs. uninfected) revealed three groups of genes: those that where commonly up-regulated, or only up-regulated upon the respective infection (YPIII or YPIII Δ*cnfY*) compared to cecal tissue of uninfected mice (Figure 3.18A, B). Among the commonly up-regulated genes were the iron scavenger haptoglobin (*hp*), the immunoglobin C-regions (*i.e. ighg1* and *ighg2c*), the mast cell proteases 1 and 2 (*mcpt1/2*), the cytokine *il-1β*, the chemokine *cxcl2*, the endocytic receptor *clec4d*, the matrix metalloproteinase *mmp3*, the immune-modulatory arginase-1 (*arg1*) (Popovic *et al.*, 2007), the pro-inflammatory receptor Trem-1, which induces inflammatory responses such as cytokine production and phagocytosis (Arts *et al.*, 2013), and the immune regulatory and anti-microbial protein secretory leukocyte protease inhibitor (*slpi*) (Weldon and Taggart, 2007) (Figure 3.18C).

As the comparison of the GGEPs suggested differential gene expression between the two *Y. pseudotuberculosis* stains (3.4), the gene expression profiles of persistently infected mice were compared to each other. The direct comparison revealed that there were two large classes of genes: (1) immune response related (Figure 3.19) and (2) tissue organization/repair related genes (Figure S18).

Further analysis showed that the metal ion scavenger systems, haptoglobin (*hp*), lactotransferrin (*ltf*), the ferritin receptor Scara5, and metallotheonein-1 and -2 (*mt1/2*) were significantly more strongly induced upon persistent YPIII infection compared to persistent YPIII Δ*cnfY* infection (Figure 3.19B). Interestingly, haptoglobin was the only gene among all genes that was also differentially expressed during persistent YPIII Δ*cnfY* infection compared

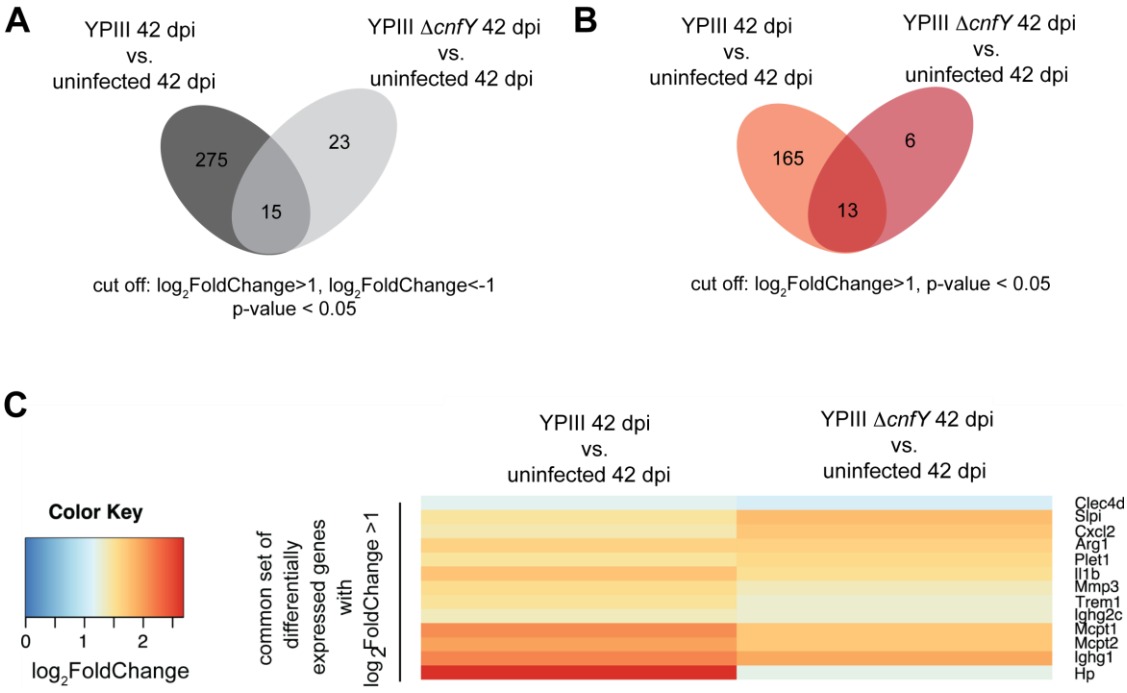

Figure 3.18 Host differentially expressed genes during persistent infection with *Y. pseudotuberculosis*

(A) Venn diagram of the differentially expressed genes during persistent infection (42 dpi) comparing *Y. pseudotuberculosis* infected ceca to uninfected. (B) Venn diagram of induced genes comparing persistently *Y. pseudotuberculosis* infected ceca to uninfected. (C) Heat map of induced transcripts (log_2 FC > 1; p < 0.05) at 42 dpi comparing *Y. pseudotuberculosis* infected ceca to uninfected samples (YPIII left column; YPIII Δ*cnfY* right column).

to uninfected mice (Figure 3.19B). Moreover, the complement system, *i.e. c7*, *c3*, *c1rb* and *c4b*, and PAMP receptors (*i.e. spon2*, *lbp* and *tlr9*) (He *et al.*, 2004b; Lengacher *et al.*, 1995) were more highly up-regulated during persistent YPIII infection compared to YPIII Δ*cnfY*-infected cecal tissue (Figure 3.19B). The persistent YPIII infection also induced the expression of matrix metalloproteinases (*i.e. mmp8*, *mmp10*, *mmp11*, *mmp19*), the defensin and immune regulatory gene *pla2g5* (Table S8), and genes involved in antigen presentation or antibody production (*e.g. h2-k2*, *lilra4*, *lilra6*, *igkv3-10*, *igkv3-1*, *ighv1-39*, *ighv1-74*) (Figure 3.19B; Table S8). Additionally, there was an induction of genes that are involved in reactive metabolite/oxygen production (*i.e. duoxa2* and *cyp2e1*), reactive metabolite/oxygen protection (*i.e. sod3*, *gpx3* and *cygp*), and immune modulation, such as *card10*, *aebp1*, *nr4a1*, *c1qtnf3*, *s100a9*, *cd300lf*, *socs3*, *alox5*, *il12b*, *chil1* and *chil3* (Grabiner *et al.*, 2007; Majdalawieh *et al.*, 2007; Wu *et al.*, 2016; Schmid *et al.*, 2014), compared to uninfected and/or YPIII Δ*cnfY*-infected cecal samples (Figure 3.19B; Table S8). Interestingly, the comparison of the cecal tissue expression profile of YPIII-infected mice with YPIII Δ*cnfY*-infected mice also revealed that persistent YPIII infection more strongly triggered the expression of genes connected with adaptive immunity: Ccl21a that is important to recruit T cells to the periphery (Lo *et al.*, 2003), the nuclear factor of activated T-cells Nfatc4 that is involved in expression of T cell cytokines (Rao *et al.*, 1997), Chst1 that is important for lymphocyte homing in lymph nodes (Hemmerich and Rosen, 2000), and the T_H1-specific transcription factor Hlx that interacts with the T_H1-specific transcription factor T-bet to optimally induce IFNγ expression (Mullen *et al.*, 2002) (Figure 3.19B).

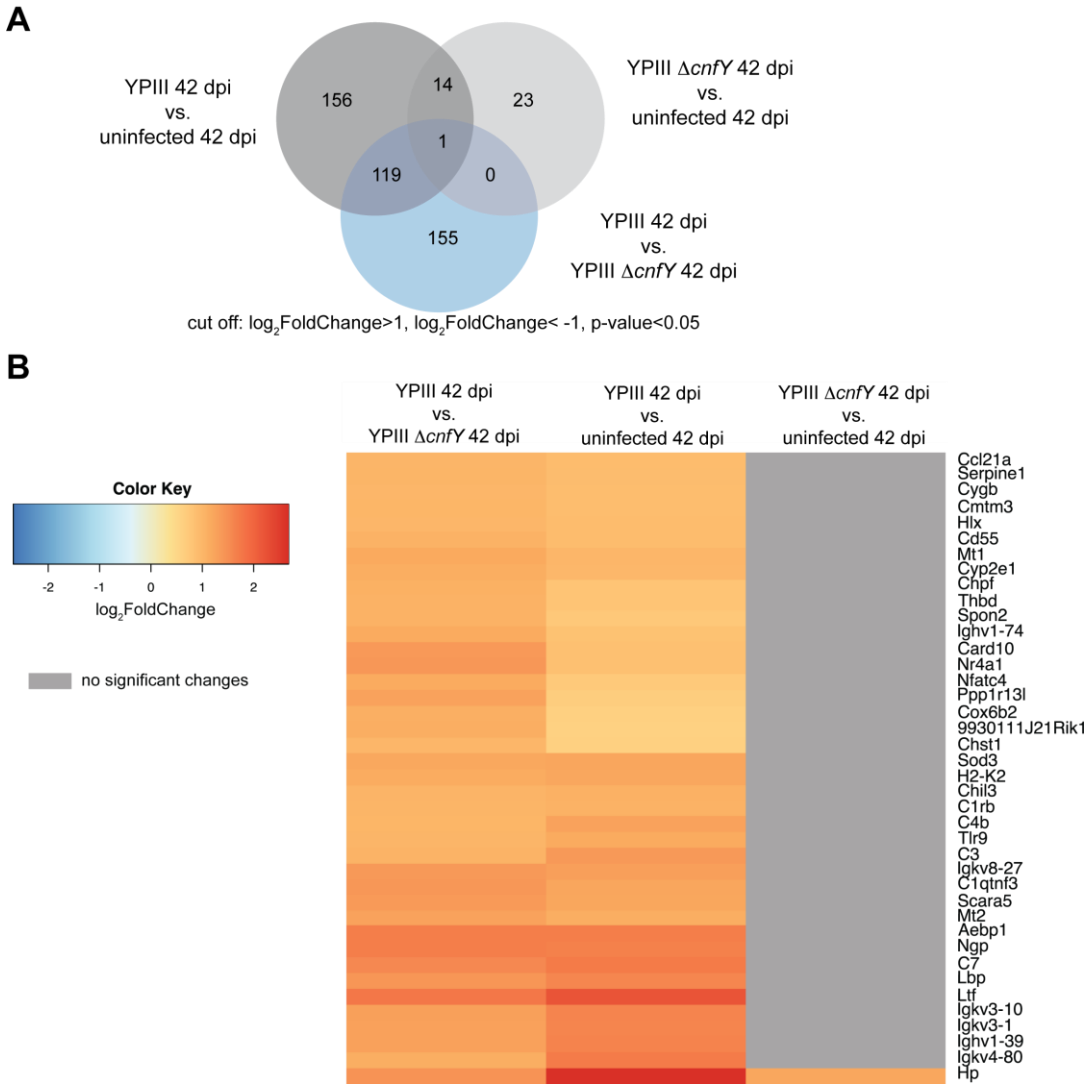

Figure 3.19 The host still responds to *Y. pseudotuberculosis* YPIII persistent infection

(A) Venn-diagram of the differentially expressed genes during persistent infection (42 dpi). (B) Heat map of more abundant transcripts (log_2FC>1; p-value<0.05) at 42 dpi comparing YPIII to YPIII Δ*cnfY* infection (left column). The respective log_2FC of each gene compared to uninfected mice are displayed: YPIII infected mice 42 dpi compared to uninfected (middle column) and YPIII Δ*cnfY* infected mice 42 dpi compared to uninfected (right column). Grey fields indicate no significant changes (p>0.05) compared to uninfected mice.

In contrast, persistent YPIII Δ*cnfY* infection induced the expression of only six genes with a log_2FC>1 that were not increased during YPIII infection by comparison to uninfected cecal tissue transcription profiles: immunoglobin heavy variables 1-78 and 5-2, immunoglobin kappa variable 2-116, the important neutrophil chemoattractant *cxcl1* (Kobayashi, 2008), and two mast cell proteases, *i.e. mcpt9* and *cma2* (Table S9).

In summary, persistent YPIII infection drives pronounced immune reactions and tissue organization/repair, while changes of the host expression profile in response to persistent YPIII Δ*cnfY* infection are restricted.

3.4.4 *In vivo*-characterization of *Y. pseudotuberculosis* gene expression

Recently, an *in vivo* deep sequencing approach demonstrated that *Y. pseudotuberculosis* reprograms its transcription profile from acute to persistent infection inside the cecal lymphoid tissue. The transcriptional remodeling encompassed the repression of virulence genes and induction of flagellar, anaerobiosis, oxidative and acid stress gene expression during persistent *Y. pseudotuberculosis* YPIII infection compared to acute infection. Furthermore, important virulence and metabolic regulators, *i.e. crp*, *csrA*, *rovA*, were induced during persistent infection (42 dpi) unlike during acute infection (2 dpi) (Avican *et al.*, 2015).
In order to compare the gene expression patterns of *Y. pseudotuberculosis* during the infection of the cecum, relative expression of *Y. pseudotuberculosis* genes in the total RNA extracts of acute (5 dpi) and chronically (42 dpi) infected ceca was evaluated employing qRT-PCR. The obtained expression levels were normalized to the gene expression levels of acute YPIII infected ceca (Figure 3.20; Figure 3.21).
Upon persistent infection, YPIII and YPIII Δ*cnfY* induced the expression of the anaerobiosis genes (*i.e. arcA*, *frdA*, *napA*). ArcA (aerobic respiration control protein A) represses aerobic genes under anaerobic conditions, whereas FrdA (fumarate reductase flavoprotein subunit A) and NapA (periplasmic nitrate reductase) participate in anaerobic respiration (Figure 3.20A). Interestingly, the expression of the anaerobic respiration regulator Fnr (fumarate and nitrate reduction regulatory protein) and CspC (cold shock-like protein), which is involved in acid and salt stress responses were not infection phase regulated in either *Yersinia* strains (Figure 3.20A, B). Moreover, expression of flagellin (*fliC*), the acid stress chaperone *hdeB* required for acid stress protection, the transcription antitermination protein *rfaH* involved in increased lipopolysaccharide expression, the NAD(P)H dehydrogenase *wrbA* involved in oxidative stress response and the superoxide dismutase *sodB*, which removes superoxide radicals, were up-regulated during persistent YPIII and YPIII Δ*cnfY* infection (Figure 3.20B). The universal stress protein A (*uspA*), which is needed to protect against DNA damage was more strongly induced upon persistent YPIII Δ*cnfY* infection than during persistent YPIII infection (Figure 3.20B). In addition, YPIII Δ*cnfY* induced the expression of flagellin more pronounced than YPIII at 42 dpi.
The expression of virulence genes like *yscF* (TTSS needle), *yadA* (adhesin), *cnfY* and the TTSS regulator *lcrF* were down-regulated during persistent *Yersinia* infection (Figure 3.21A, B). Intriguingly, the expression of the TTSS effector *yopJ* was up-regulated during persistent YPIII and YPIII Δ*cnfY* infection (Figure 3.21A). Additionally, the *ail* (adhesin) expression levels were independent of the infection stage, but were more strongly induced upon YPIII Δ*cnfY* infection than YPIII infection at both, 5 dpi and 42 dpi (Figure 3.21A). On the other hand, the expression of the metabolism and virulence regulators, *i.e.* cAMP-activated global transcriptional regulator gene (*crp*), the carbon storage regulator (*csrA*) and the regulator of virulence A (*rovA*), was induced during persistent *Yersinia* infection compared to acute infection (Figure 3.21B) as previously described.

Remarkably, relative gene-expression analysis at 5 dpi revealed that anaerobiosis genes (*arcA*, *frdA*, *napA*), stress genes (*hdeB*, *rfaH*, *sodB*, *wrbA*), *yopJ*, and the regulators *crp* and *rovA* were more strongly induced upon acute YPIII Δ*cnfY* infection compared to YPIII. The relative transcript levels of those genes during acute YPIII Δ*cnfY* infection ranged between the lowest

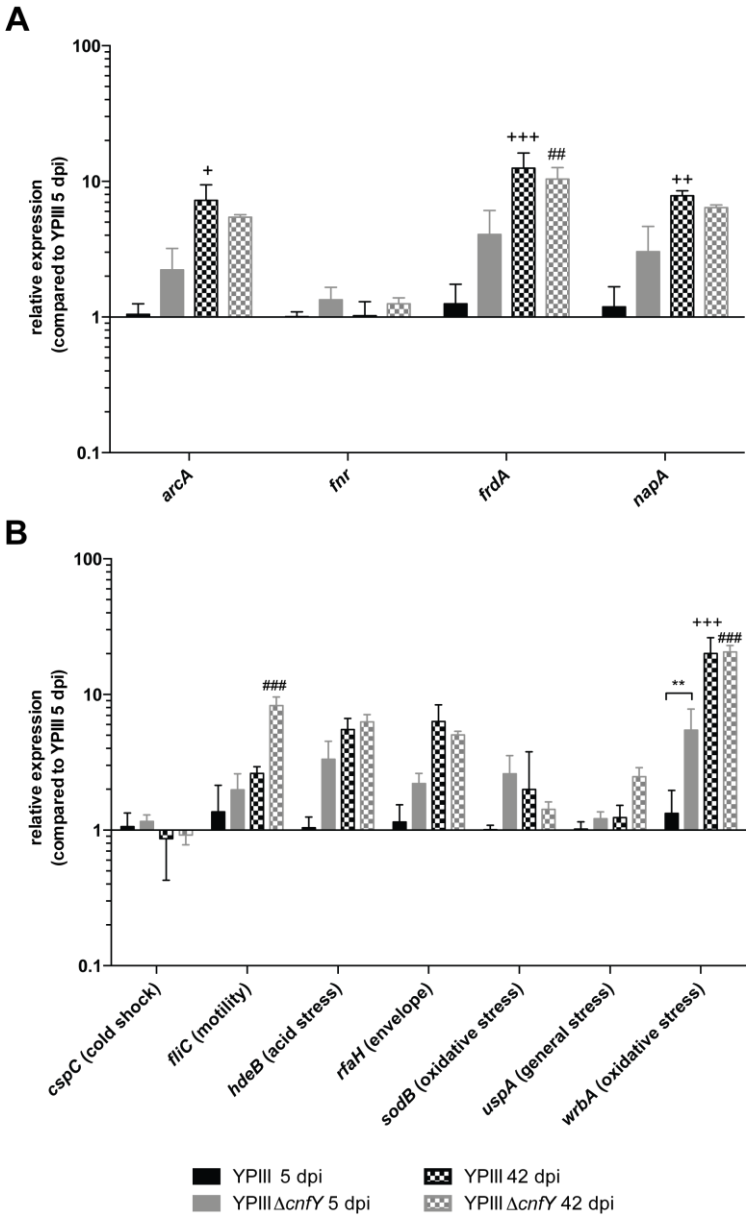

Figure 3.20 *Y. pseudotuberculosis* reprograms anaerobiosis and stress gene expression dependent on *cnfY* and infection stage.

BALB/c mice were intra-gastrically infected with either $2x10^7$ CFU (acute infection, 5 dpi)/$1x10^6$ CFU (persistent, 42 dpi) of *Y. pseudotuberculosis* YPIII or $2x10^8$ CFU (acute infection, 5 dpi)/$1x10^6$ CFU (persistent infection, 42 dpi) of *Y. pseudotuberculosis* YPIII Δ*cnfY*. Total RNA of highly infected ceca were isolated, DNA depleted and analyzed for *Yersinia* transcript expression levels using qRT-PCR. The relative expression levels were normalized to *sopB* and *if-3* expression levels and calculated relative to YPIII 5 dpi. (A) Anaerobiosis genes. (B) Stress genes reacting to environmental cues. The data show the mean ±SEM and was statistically analyzed with multiple t-tests employing Holm-Šídák's correction: *, comparison between YPIII and YPIII Δ*cnfY*: ** $p<0.01$; +, comparison between 5 dpi and 42 dpi upon YPIII infection: + $p<0.05$, ++ $p<0.01$, +++ $p<0.001$; #, comparison between 5 dpi and 42 dpi upon YPIII Δ*cnfY* infection: ## $p<0.01$, ### $p<0.001$.

induction during acute YPIII infection and the highest upon persistent *Y. pseudotuberculosis* infection (both YPIII and YPIII Δ*cnfY*). These expression differences between the two *Y. pseudotuberculosis* strains are specific for *in vivo* since *in vitro* expression analysis showed no gene expression differences at 25 °C and 37 °C (Figure S19, Figure S20). Strikingly, comparison of *in vivo cnfY* transcript levels during acute and persistent infection to *in vitro cnfY* transcript levels revealed that the *cnfY* mRNA is less increased during murine infection at

the assessed time points than *in vitro* (Figure S21). All in all, these data suggest that both *Y. pseudotuberculosis* strains exhibit comparable RNA expression profiles during persistent infection in the cecum. Nevertheless, slightly different host-derived environmental challenges that depend on the presence of *cnfY* might drive slightly altered *Yersinia* gene expression (*e.g.*

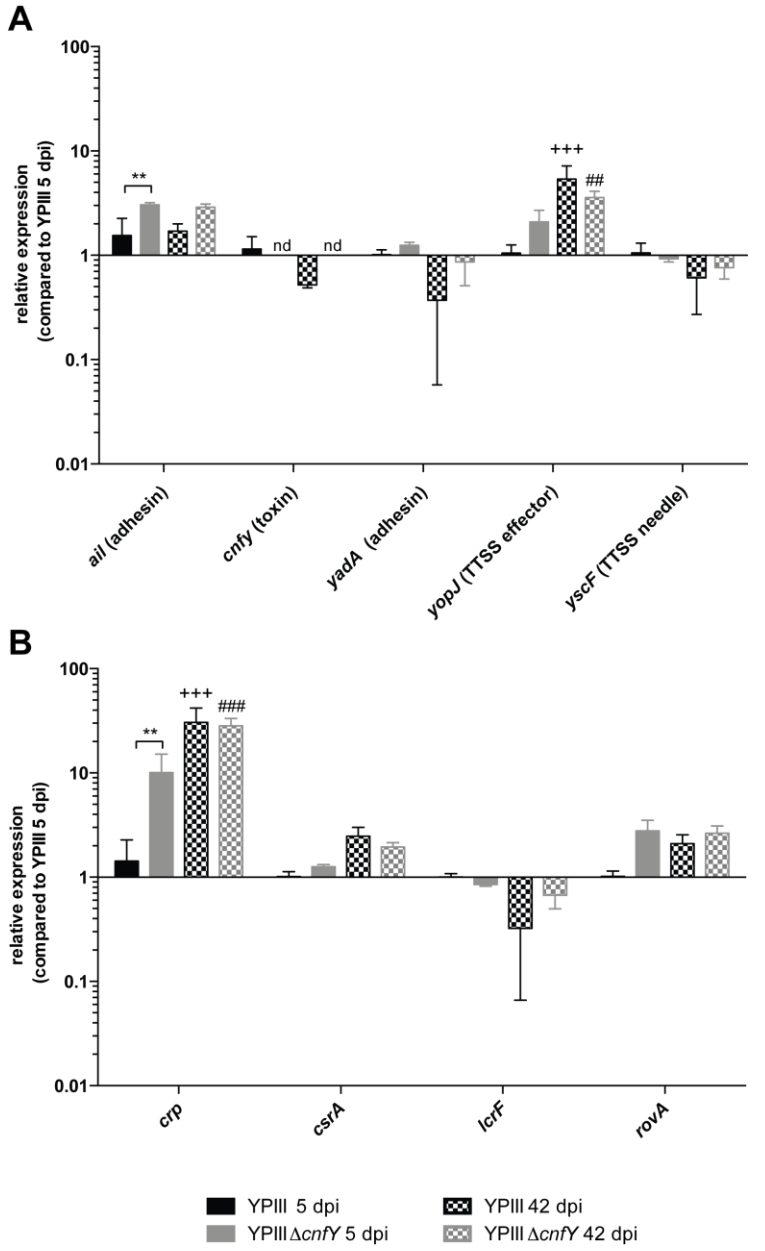

Figure 3.21 *Y. pseudotuberculosis* adapts virulence and regulator gene expression dependent on *cnfY* and infection stage.

BALB/c mice were intra-gastrically infected with either $2x10^7$ CFU (acute infection, 5 dpi)/$1x10^6$ CFU (persistent, 42 dpi) of *Y. pseudotuberculosis* YPIII or $2x10^8$ CFU (acute infection, 5 dpi)/$1x10^6$ CFU (persistent infection, 42 dpi) of *Y. pseudotuberculosis* YPIII Δ*cnfY*. Total RNA from highly infected ceca were isolated, DNA depleted and analyzed for *Yersinia* transcript expression levels using qRT-PCR. The relative expression levels were normalized to *sopB* and *if-3* expression levels and calculated relative to YPIII 5 dpi. (A) Virulence genes. (B) Metabolic and virulence regulators. The data show the mean ±SEM and was statistically analyzed with multiple t-tests employing Holm-Šídák's correction: *, comparison between YPIII and YPIII Δ*cnfY*: ** $p<0.01$; +, comparison between 5 dpi and 42 dpi upon YPIII infection: +++ $p<0.001$; #, comparison between 5 dpi and 42 dpi upon YPIII Δ*cnfY* infection: ## $p<0.01$, ### $p<0.001$. nd: not detected.

fliC, *uspA*, *ail*) during persistent infection (Figure 3.20; Figure 3.21). Moreover, the analysis of relative gene expression at 5 dpi strongly implies that YPIII Δ*cnfY* is confronted with other host-mediated stresses and cues than YPIII, which triggers different transcriptional adaptations during the acute infection stage.

3.4.5 Virulence plasmid stability in *Y. pseudotuberculosis* during long-term infection

The virulence plasmid pYV of *Yersinia* is crucial for virulence (Ben-Gurion and Shafferman, 1981). However, it was reported that *Y. pseudotuberculosis* lacking the virulence plasmid was isolated from diseased patients (Fukushima *et al*., 1991; Eppinger *et al*., 2007). Moreover, it is assumed that pYV is the least stable virulence factor of *Yersinia* in comparison to the iron-scavenging high-pathogenicity island (HPI) and the *Y. pseudotuberculosis*-derived mitogens (YPM) (Ch'ng *et al*., 2011). Accordingly, a *Y. pseudotuberculosis* heterogeneity study analyzing isolates from multiple sources (human, animals and environment) in 2001 found that the *Yersinia* virulence plasmid was lacking in around 25 % of virulent serotypes (Fukushima *et al*., 2001). All in all, this implicates that the presence of the virulence plasmid is not sufficient to determine pathogenicity and colonization abilities of *Y. pseudotuberculosis*, which is further supported by a study showing that the virulence plasmid is not required for colonization of the mesenteric lymph nodes in mice (Balada-Llasat and Mecsas, 2006).

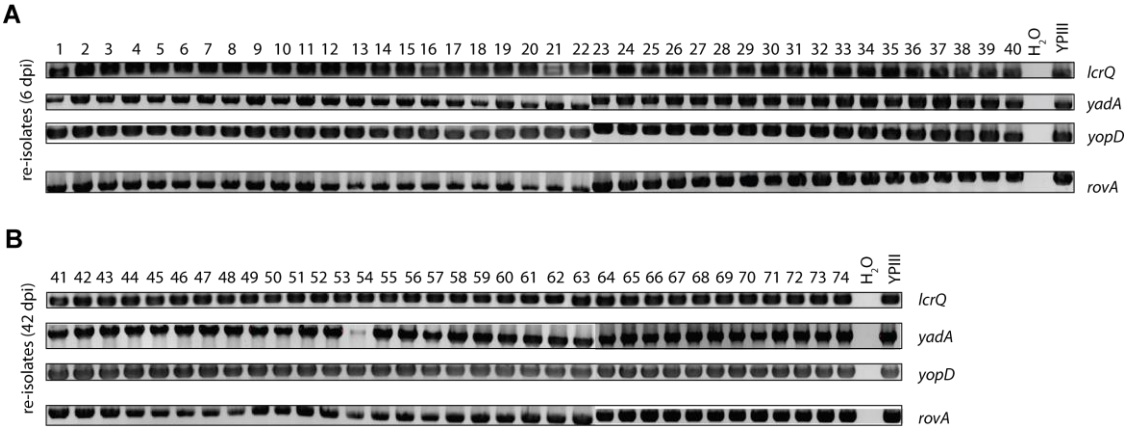

Figure 3.22 The virulence plasmid is stable during persistency.

BALB/c mice were infected with $2x10^7$ CFU (acute infection, 6 dpi) or $1x10^6$ CFU (persistent infection, 41 dpi) of *Y. pseudotuberculosis* YPIII. At the indicated time points, *Y. pseudotuberculosis* was re-isolated from the cecum, the luminal content of the cecum, PPs of the small intestine, spleen and liver. The re-isolated bacteria were further tested for plasmid loss by PCR. Genes located on pIB: *lcrQ*, *yadA*, *yopD* genomic control: *rovA* (A) Re-isolates at 6 dpi. (B) Re-isolates at 42 dpi.

Hence, it was hypothesized that *Y. pseudotuberculosis* might undergo a heterogenic selection during long-term infection, which triggers virulence plasmid loss in a fraction of the population. This, in turn, could lead to decreased virulence gene expression as observed in 3.3.4 and by Avican and colleagues in 2015 (Avican *et al*., 2015). To analyze this further, re-isolated *Y. pseudotuberculosis* YPIII from different tissue localizations were screened for virulence plasmid loss during acute (Figure 3.22A) and persistent infection (Figure 3.22B). To this purpose, single colonies were tested for the virulence plasmid encoded genes *lcrQ*, *yadA* and *yopD*. The chromosomally encoded virulence regulator *rovA* was used as control.
Single colony analysis revealed that neither re-isolates of *Y. pseudotuberculosis* YPIII from acute infection phase nor from persistent infection phase demonstrated virulence plasmid loss

(Figure 3.22). Therefore, *Y. pseudotuberculosis* YPIII shows strong virulence plasmid stability during persisting infection.

3.5 Cytokine profiling over the course of persistent *Yersinia* infection

In this study, distinctive immune and inflammatory responses were detected by histopathological analysis (3.2.1) and host transcriptome profiling (3.4.1 to 3.4.3) during *Y. pseudotuberculosis* YPIII and YPIII Δ*cnfY* infection. To identify the cytokine levels in the serum and in the cecum of *Yersinia*-colonized mice, BALB/c mice were intra-gastrically challenged with $1x10^6$ CFU of *Y. pseudotuberculosis* YPIII or YPIII Δ*cnfY*. Thereafter, the cytokine levels of 26 cytokines in *Yersinia*-colonized mice (Figure S22) were assessed.

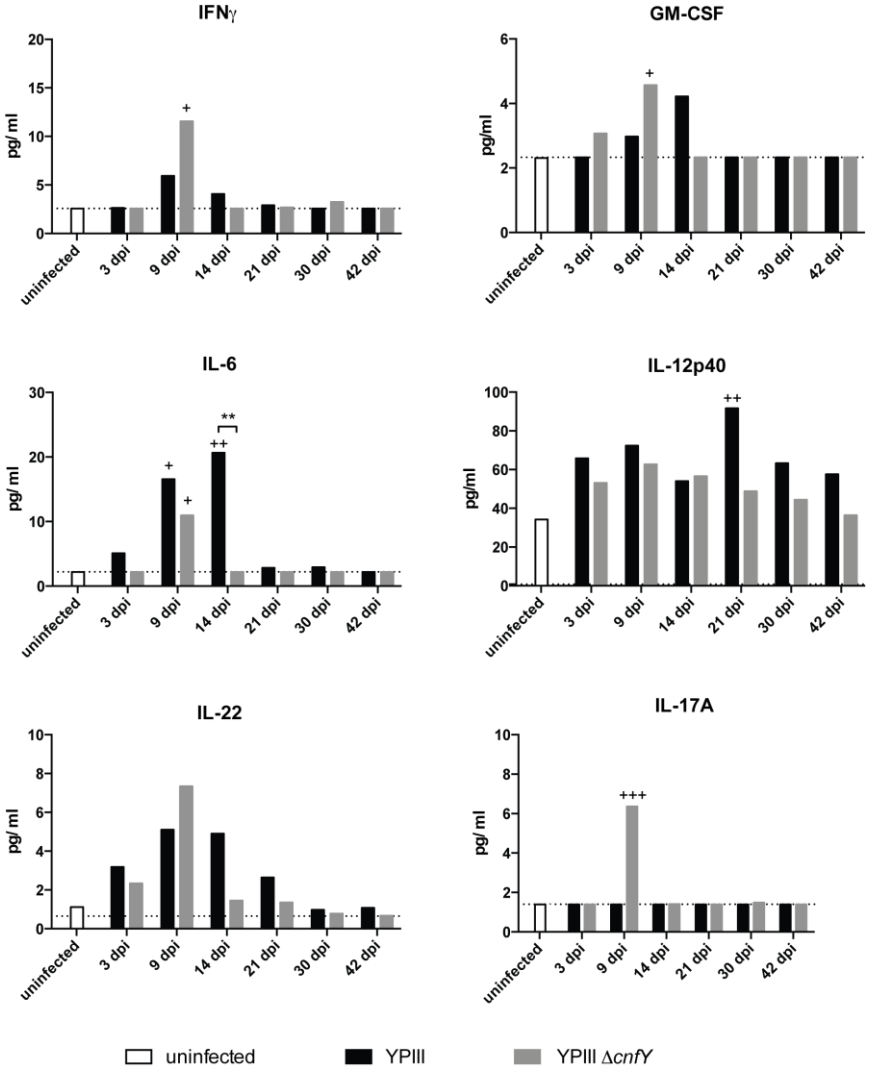

Figure 3.23 Systemic cytokine response to *Yersinia* infection.

BALB/c mice were intra-gastrically challenged with $1x10^6$ CFU of *Y. pseudotuberculosis* YPIII or YPIII Δ*cnfY*, respectively. At indicated time points post infection the mice were sacrificed and the cytokines in serum of *Yersinia* colonized mice were measured: uninfected n=10; YPIII n=8 (3-30 dpi); n=3 (42 dpi); YPIII Δ*cnfY* n≥7. The bars represent the geometric mean and the dotted lines the detection limits. The data were statistically analyzed with the Kruskal-Wallis test employing Dunn's correction; + indicates comparison to uninfected samples and * indicates comparison of YPIII to YPIII Δ*cnfY*: + $p<0.05$; **, ++ $p<0.01$; +++ $p<0.001$.

In the serum of *Yersinia* colonized mice, the abundance of only few pro-inflammatory cytokines was detected compared to uninfected mice and further analysis revealed CNF_Y-dependent cytokine abundances (Figure 3.23). Among the *Yersinia*-induced cytokines in the serum were IFNγ, GM-CSF, IL-12p40, IL-17A and IL-22.

IFNγ and **IL-17A** were significantly more abundant in the serum of YPIII Δ*cnfY*-infected mice compared to uninfected mice at 9 dpi, and the geometric mean of IFNγ was about 2-fold higher than upon YPIII infection (Figure 2.23). **GM-CSF** was also significantly induced in the serum of YPIII Δ*cnfY*-infected mice at 9 dpi compared to uninfected mice, while the GM-CSF level was higher in YPIII-infected mice at 14 dpi (Figure 3.23). Moreover, the **IL-6** level was strongly increased in the serum of YPIII-infected mice during acute infection phase and also higher by comparison to YPIII Δ*cnfY* infection (Figure 3.23). **IL-12p40** is a subunit of IL-12p70 and IL-23**,** but it is also able to form homodimers (IL-12p80) (Gee *et al*., 2009). This cytokine was more abundant in the serum of both *Y. pseudotuberculosis* infections in comparison to uninfected mice (Figure 3.23). While the levels of IL-12p40 in YPIII Δ*cnfY* infected mice were reduced at 42 dpi, they remained at increased levels upon YPIII infection compared to YPIII Δ*cnfY* infected mice (Figure 3.23). In YPIII-colonized mice**, IL-22** was more abundant from 3 to 21 dpi compared to uninfected mice (Figure 3.23), whereas the IL-22 level in the serum of YPIII Δ*cnfY*-infected mice was only increased at 3 and 9 dpi. Strikingly, the IL-22 levels in YPIII Δ*cnfY*-infected mice were somewhat higher than in YPIII-colonized mice at 9 dpi (Figure 3.23).

Taken together, divergent systemic cytokine dynamics and inflammatory responses were observed in the serum of *Yersinia*-colonized mice during the course of infection. In particular at the early stages of infection, pro-inflammatory cytokine circulation in the serum of infected mice was observed, while there were no cytokines detected at later stages of the infection (≥30 dpi).

In the cecum of *Yersinia* colonized mice a couple of cytokines were differentially produced (Figure 3.24). As it was already observed in the serum, **IL-6** and also **IL-33** were significantly more abundant in *Yersinia*-infected ceca compared to uninfected ceca. The IL-6 and IL-33 levels were also higher in YPIII-infected than in YPIII Δ*cnfY*-infected ceca during the acute infection (Figure 3.24). The **IL-1α** levels were increased at all assessed time points post infection in *Yersinia*-infected ceca compared to uninfected ceca (Figure 3.24), however the IL-1α levels were higher in YPIII Δ*cnfY*-infected than in YPIII-infected ceca during early infection stages (Figure 3.24). Moreover, the cytokines **IL-17A, IL-22, IL-7, IL-12p70, IL-23** and the anti-inflammatory cytokine **IL-11** were increased during the early to late acute infection phase in *Yersinia*-infected ceca compared to uninfected ceca (Figure 3.24). Furthermore, two other anti-inflammatory cytokines IL-10 and IL-13 were also more strongly induced at 3 dpi in YPIII-infected ceca compared to uninfected and YPIII Δ*cnfY*-colonized ceca (data not shown). Remarkably, the IL-22, IL-7, IL-12p70 and IL-23 levels in *Y. pseudotuberculosis*-infected ceca were lower during the late infection phase by comparison to uninfected ceca, while the **IL-12p40** levels were continuously increased during *Yersinia* infection (Figure 3.24).

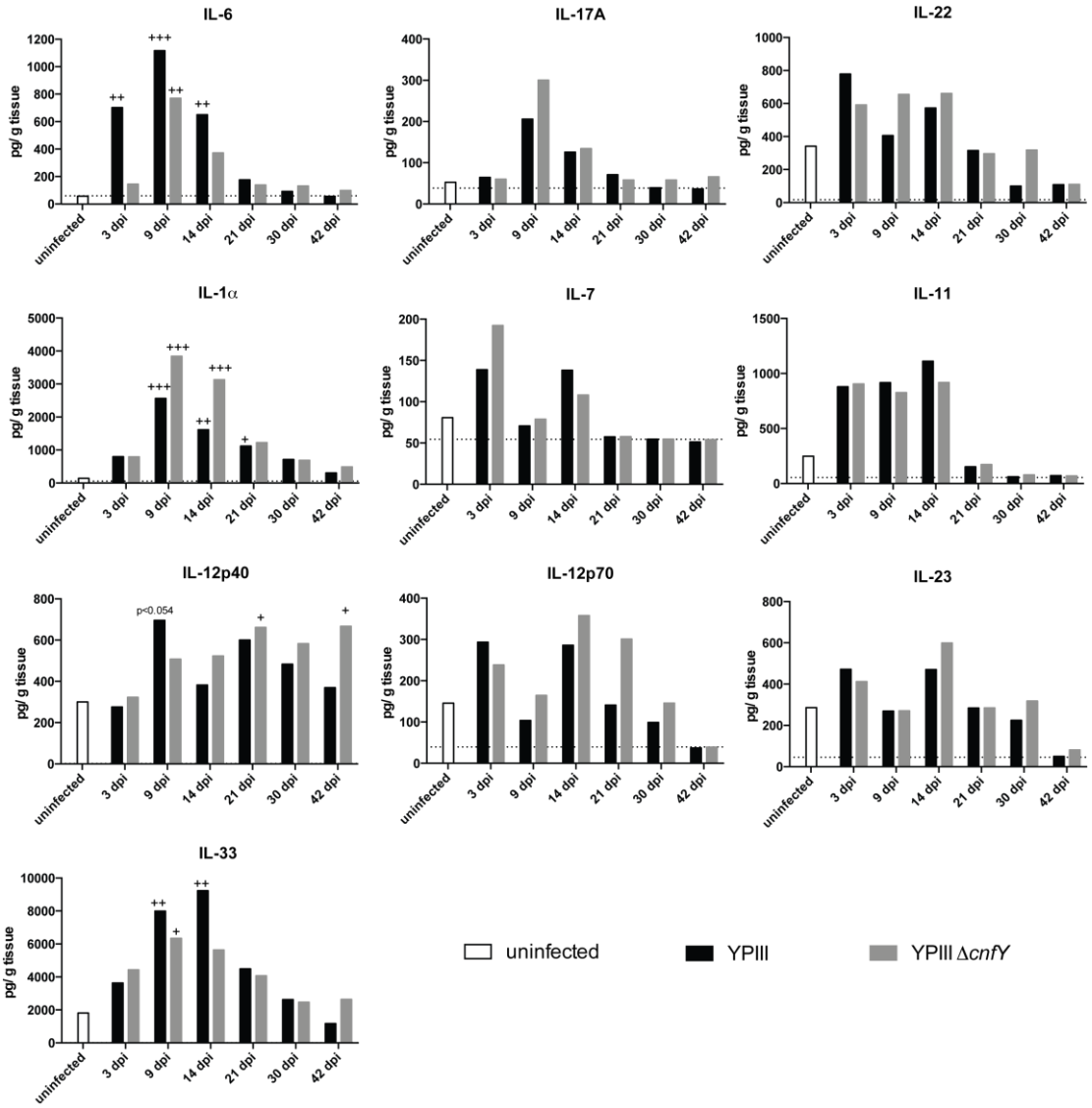

Figure 3.24 Local cytokine response in the cecum during *Yersinia* infection.

BALB/c mice were intra-gastrically infected with $1x10^6$ CFU of *Y. pseudotuberculosis* YPIII or YPIII Δ*cnfY*, respectively. At the indicated time points post infection the mice were sacrificed and the cytokines in the tissue of colonized ceca (Figure S22) were determined: uninfected n=10, YPIII n=8 (3-30 dpi); n=3 (42 dpi); YPIII Δ*cnfY* n≥7. The bars represent the geometric mean and the dotted lines the detection limits. The data were statistically analyzed with the Kruskal-Wallis test employing Dunn's correction; + indicates comparison to uninfected samples: + $p<0.05$; ++ $p<0.01$; +++ $p<0.001$.

As in the serum, diverging cytokine dynamics and profiles were detected in the cecum of YPIII- and YPIII Δ*cnfY*-infected mice. YPIII infection was found to predominantly trigger the production of IL-6 and IL-33, while YPIII Δ*cnfY* infection induced the production of IL-1α. During the onset of the infection until 14 dpi, pro-inflammatory cytokine production was observed upon either *Yersinia* infection. However, the production of IL-22, IL-7, IL-12p70 and IL-23 was reduced in the cecum upon persistent *Yersinia* infection compared to uninfected mice indicating suppression of inflammation.

3.6 The influence of CNF_Y on inflammation in the C57BL/6N mouse model

As the inflammasome-interleukin-1 axis is associated with resistance to bacterial infections and bacterial clearance, bacterial pathogens have evolved mechanisms to control inflammasome activities. These mechanisms include LPS modification, down-regulation of flagella gene expression, altered flagellin, metabolite regulation and expression of bacterial effectors proteins that interfere with inflammasome activation and function (Shin and Brodsky, 2015; Stewart and Cookson, 2016). *Yersinia* spp. also manipulate the inflammasome by multiple means. The effectors YopE and YopT are known to inhibit caspase-1 activation via interference with small Rho-GTPase activity (Schotte *et al*., 2004), whereas YopM directly binds to caspase-1, preventing its activation (LaRock and Cookson, 2012). In turn, YopK regulates the amount of translocated Yop effector proteins, thereby limiting inflammasome activation (Holmström *et al*., 1997; Brodsky *et al*., 2010). Interestingly, translocation of YopJ into naïve macrophages induces cell death and activates caspase-1, while it synergizes with YopM in activated macrophages in order to restrain caspase-1 activation (Philip *et al.*, 2014; Weng *et al.*, 2014; Ratner *et al.*, .2016; Schoberle *et al.*, 2016). However, whether the Yop translocation-enhancing toxin CNF_Y influences the activity of the inflammasome remains to be determined.

In this study, previous analysis showed high up-regulation of *il-1α*, *il-1β* and *nlrp3* gene expression during acute *Yersinia* infection (3.4.1). *il-1β* was also still significantly up-regulated during persistent *Y. pseudotuberculosis* infection (3.4.2, 3.4.3). Cytokine profiling in the cecum of YPIII Δ*cnfY*-infected mice showed high IL-1α levels in the cecal tissue during the early infection stage and slightly increased IL-1α levels during persistent infection phases. Hence, the influence of the inflammasome on *Y. pseudotuberculosis* infections was examined.

3.6.1 C57BL/6N mice develop patho-physiologies resembling those of BALB/c mice

As caspase-1, caspase-11 and IL-1 knockout mice are of the C57BL/6N genetic background, the *Y. pseudotuberculosis* YPIII Δ*cnfY* infections were performed in C57BL/6N mice. In order to review the phenotypes observed in BALB/c mice, the survival, histopathology, immune and cytokine response in *Y. pseudotuberculosis* YPIII- or YPIII Δ*cnfY*-infected C57BL/6N mice ($2x10^8$ CFU/mouse) were assessed.

The analysis of the survival of C57BL/6N mice revealed that 80 % of the YPIII-infected mice succumbed to the infection until 12 dpi, whereas all YPIII Δ*cnfY*-infected mice survived the infection (Figure 3.25A). Body weight analysis further demonstrated that YPIII-infected mice started to lose weight from 2 dpi and on average lost 14 % of their body weight until 6 dpi (Figure 3.25B). Interestingly, YPIII Δ*cnfY* infection of C57BL/6N mice did not cause any body weight loss during the assessed time period (Figure 3.25B). Despite the fact that C57BL/6N

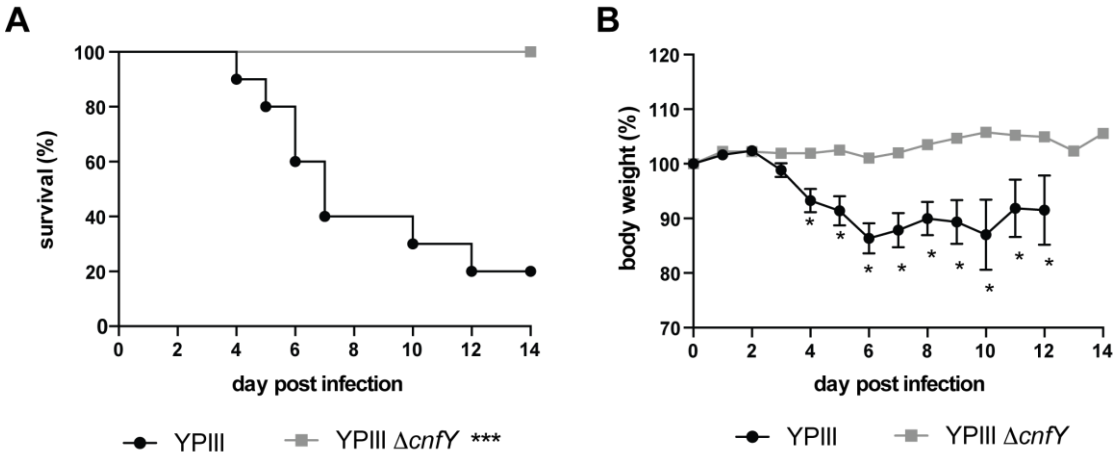

Figure 3.25 C57BL6/N mice are more resistant to *Y. pseudotuberculosis* infection.

C57BL/6N mice were intra-gastrically challenged with $2x10^8$ CFU of *Y. pseudotuberculosis* YPIII or YPIII Δ*cnfY*. The health status of the mice was monitored for 14 days. The presented data were combined from two experiments: YPIII n=10, YPIII Δ*cnfY* n=10. (A) Survival of C57BL/6N mice. Survival data were statistically analyzed with the log-rank (Mantel-Cox) test: *** $p<0.001$. (B) Body weight-loss curves. Mice that lost more than 20 % of their initial body weight or reached a health score lower than three were sacrificed and recorded as dead. The graphs represent the mean ±SEM. The data were statistically analyzed with multiple t-tests using Holm-Šídák's correction: * $p<0.001$.

mice were more resistant to *Y. pseudotuberculosis* infection compared to BALB/c mice (see Figure 3.7A, B), deletion of *cnfY* still rendered the bacteria avirulent.

The increased resistance of C57BL/6N mice might possibly be due to decreased inflammation compared to BALB/c mice. Thus, Marina Pils of the Mouse Pathology, Animal Experimental Unit at the Helmholtz Center for Infection Research performed histopathologic analysis of the infected C57BL/6N mice. At 5 dpi in C57BL/6N mice, histopathologic analysis of the ileum demonstrated the same observations, as were made in BALB/c mice (Schweer *et al*., 2013): inflammation of YPIII Δ*cnfY*-infected ilea was restricted to multifocal areas accompanied by hyperplasia of the epithelium, whereas YPIII-infected ilea showed diffuse inflammation along the entire ileum (Figure 3.26A).

In the spleen of YPIII infected animals, mild to severe depletion of the white pulp and severe depletion of the red pulp were detected, similar to spleens of YPIII-infected BALB/c mice. Moreover, spleens of YPIII Δ*cnfY*-infected C57BL/6N mice displayed mild hyperplasia of the white and red pulp (Figure 3.26B), which resembled the observations made in BALB/c mice (Schweer *et al*., 2013). As indicated by histopathologic analysis, depletion of the white and red pulp in the spleen led to decreased spleen sizes in C57BL/6N mice, whereas hyperplasia in the spleen of YPIII Δ*cnfY*-infected mice resulted in increased organ sizes (data not shown). This phenotype was also observed in BALB/c mice (Schweer *et al.*, 2013).

In summary, both YPIII and YPIII Δ*cnfY* elicit histopathologic phenotypes in the spleen and ileum of C57BL/6N mice comparable to BALB/c mice.

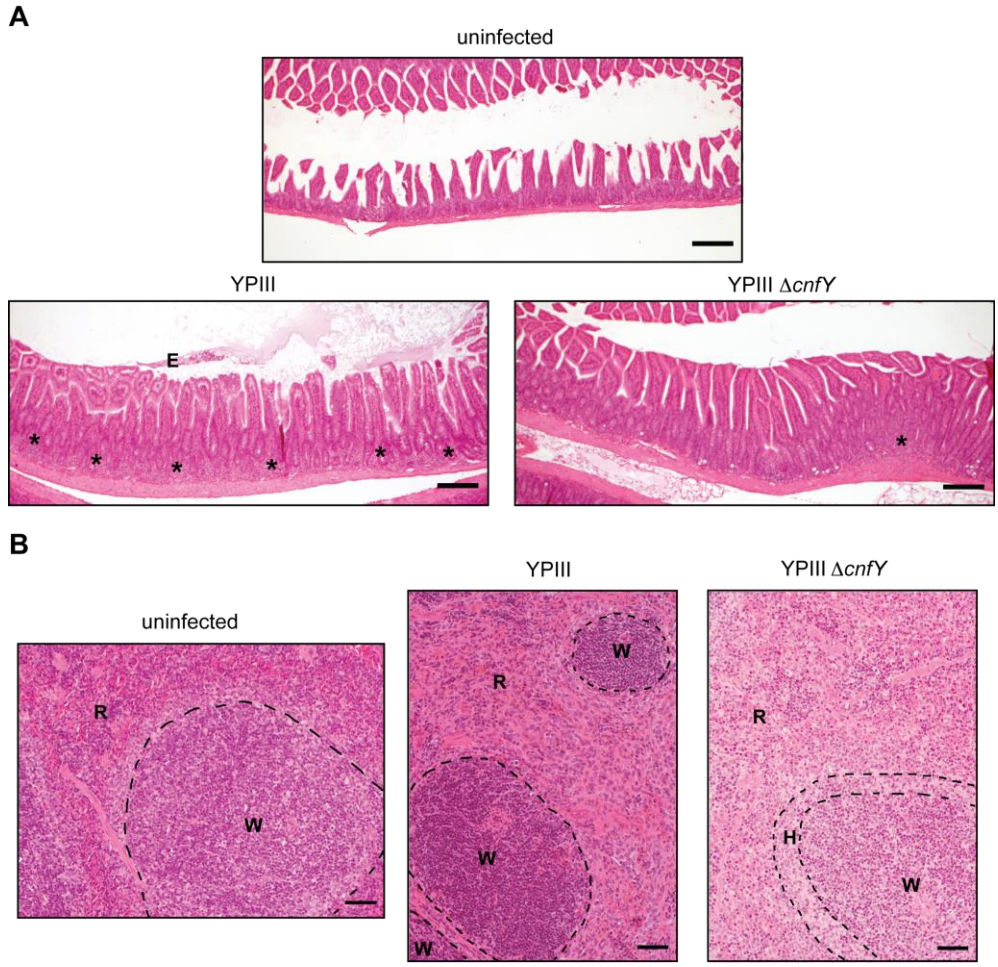

Figure 3.26 CNF_Y enhances inflammation and necrosis in C57BL/6N mice.

C57BL/6N mice were intra-gastrically infected with $2x10^8$ CFU of *Y. pseudotuberculosis* YPIII or YPIII Δ*cnfY*. At 5 dpi mice were sacrificed, the small intestine and spleen were excised, fixed, and paraffin embedded. Sections were stained with H&E and analyzed with the light microscope. The shown pictures are representatives of multiple microscopic fields (>15) of groups of 5 mice. (A) Ileum. Bar: 200 µm. E: epithelial cells; *: mixed inflammatory infiltrate (B) Spleen. Bar: 100 µm. R: red pulp; W: white pulp; H: hyperplasia.

Previously, CNF_Y was found to fine tune the immune response in the lymphatic organs (PPs, MLNs, and especially in the spleen) during *Y. pseudotuberculosis* YPIII infection of BALB/c mice (Schweer *et al*., 2013; Janina Schweer, PhD thesis). As infection in different mouse models and even using different infection conditions could greatly impact immune cell numbers (Figure S23), the relative abundance of immune cells in the PPs, MLNs and spleen at 3 dpi were analyzed (Figure 3.27). Like in BALB/c mice, CNF_Y was found to modulate the immune cell composition in the PPs, MLNs and especially in the spleen during *Y. pseudotuberculosis* YPIII infection in C57BL/6N mice (Figure S24; Schweer et al., 2013; PhD thesis Janina Schweer). However, some differences between C57BL/6N mice and BALB/c mice during *Yersinia* infection were observed: in the PPs of *Y. pseudotuberculosis*-infected C57BL/6N mice, the relative abundance of neutrophils was generally more pronounced compared to uninfected C57BL/6N and *Yersinia* infected BALB/c mice. As the intestine and its lumen are the largest reservoirs of *Yersinia* during infection, the increased relative abundance of neutrophils in the PPs of C57BL/6N mice compared to BALB/c mice (ca. 10% vs. ca. 3 %) might constitute an improved barrier defense against *Yersinia* infection, that might result in decreased susceptibility of C57BL/6N mice compared to BALB/c mice.

Moreover, the relative abundance of neutrophils in the spleens of YPIII infected C57BL/6N mice compared to uninfected mice was higher (2.6-fold) than during BALB/c infection (1.4-fold). As mentioned previously, this might also result in increased resistance to *Y. pseudotuberculosis* YPIII infection in C57BL/6N mice in comparison with BALB/c mice. However, the relative abundance of neutrophils, and monocytes/macrophages upon YPIII Δ*cnfY* infection in the spleen of C57BL/6N mice was reduced compared to BALB/c mice, which might account for the reduced dissemination of YPIII Δ*cnfY* to the spleen in C57BL/6N mice at 3 dpi compared to BALB/c mice (3.6.2, Schweer *et al.*, 2013).

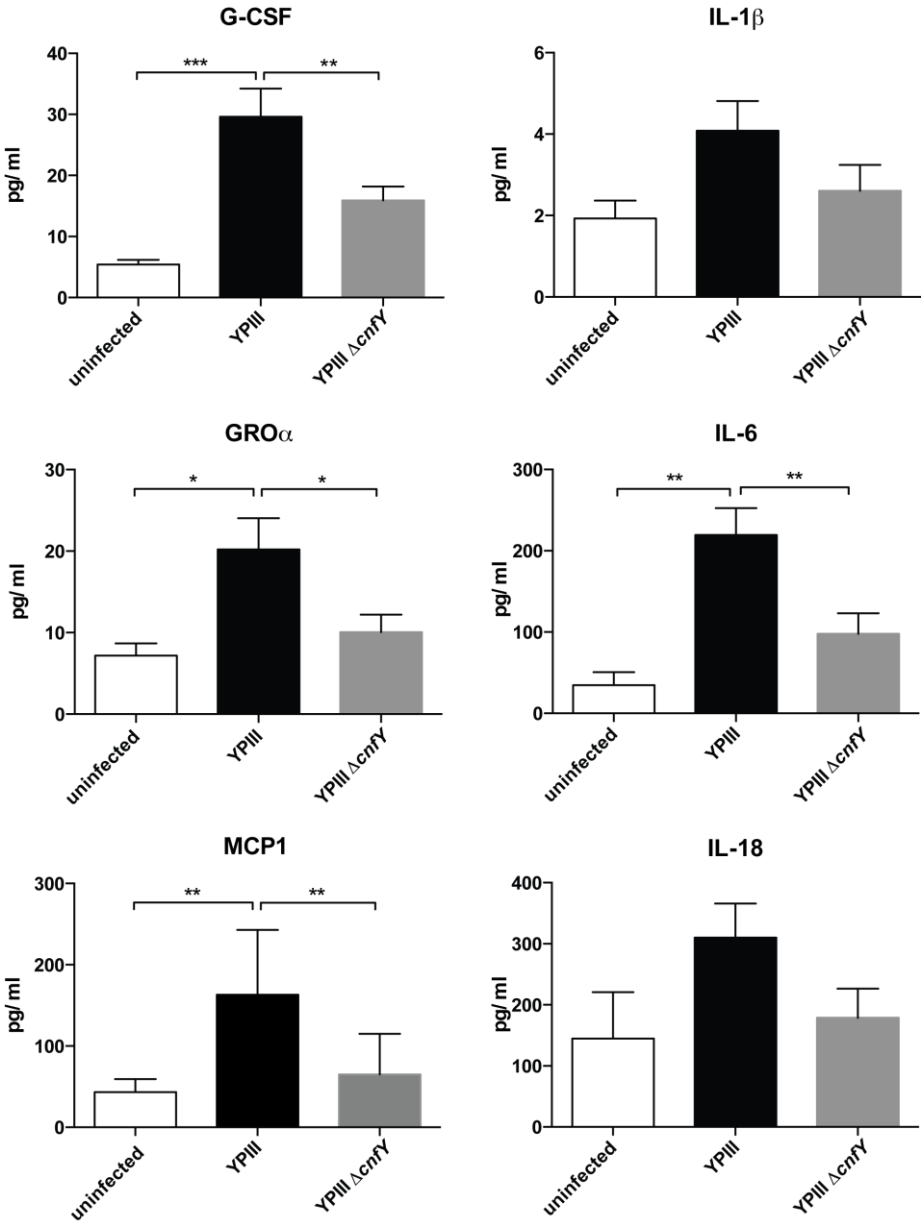

Figure 3.27 CNF_Y affects pro-inflammatory cytokine and chemokine circulation in the serum at 3 dpi.

C57BL/6N mice were intra-gastrically infected with $2x10^8$ CFU of *Y. pseudotuberculosis* YPIII or YPIII Δ*cnfY*. At 3 dpi, serum from heart blood of mice was isolated and analyzed for pro-inflammatory chemokine and cytokine levels. The bars represent the mean ±SEM. The data were combined from two independent experiment: uninfected n=4, YPIII n=10, YPIII Δ*cnfY* n=10. Statistical analysis was performed employing Fisher's LSD test: * $p<0.05$, ** $p<0.01$, * $p<0.001$.

Although the histopathological analysis suggested similar inflammatory responses in C57BL/6N and BALB/c mice, immune cell composition analysis showed that there are some minor differences in the relative abundance of immune cells. Thus, it was interesting to assess the cytokine profiles of C57BL/6N mice after *Y. pseudotuberculosis* challenge (Figure 3.27). In order to analyze this, C57BL/6N mice were intra-gastrically infected with $2x10^8$ CFU of *Y. pseudotuberculosis* YPIII or YPIII Δ*cnfY* and the chemokine and cytokine levels of 32 cytokines were determined in the serum at 3 dpi.

As suggested by the slight differences in the immune cell composition in the assessed organs of C57BL/6N mice, the *Yersinia*-affected cytokine and chemokine levels in the serum differed between BALB/c and C57BL/6N mice. However, YPIII infection generally induced the production of more different types of cytokines and chemokines in the serum of mice than YPIII Δ*cnfY* infection (Figure 3.27; Pisano *et al*., 2014; unpublished data from Janina Schweer). Accordingly, the cytokine and chemokine levels affected by *Yersinia* infection were also generally higher in the serum of YPIII-infected mice by comparison to YPIII Δ*cnfY*, irrespective of the mouse strain (Figure 3.27; Pisano *et al*., 2014; unpublished data from Janina Schweer). This suggests that YPIII infection generally and independently of the mouse strain induces a stronger pro-inflammatory response than YPIII Δ*cnfY* infection. Moreover, *Y. pseudotuberculosis* infection in BALB/c mice increased the production of more different pro-inflammatory cytokines and chemokines than *Y. pseudotuberculosis* infection in C57BL/6N mice (data not shown), indicating that *Y. pseudotuberculosis* infection is less severe in C57BL/6N mice.

The analysis of the cytokine levels in the serum of C57BL/6N mice also revealed that IL-6, G-CSF, GROα/KC, IL-1β, IL-18, IP-10, and MCP1 were differentially regulated during YPIII infection in comparison to YPIII Δ*cnfY* infection (Figure 3.27; data not shown), implicating that there is a strong induction of inflammasome activity, and recruitment/activation of leukocytes, especially neutrophils, in YPIII-infected C57BL/6N mice compared to YPIII Δ*cnfY*-infected wild type mice. On the other hand, IL-6, eotaxin, GM-CSF, and MIP-1β were more abundant during YPIII infection than during YPIII Δ*cnfY* infection of BALB/c mice (Pisano *et al*., 2014; PhD thesis of Janina Schweer), suggesting stronger phagocyte activation/maturation and eosinophil, neutrophil, DC, NK cell and monocyte recruitment in YPIII- compared to YPIII Δ*cnfY*-infected BALB/c mice. This data, together, indicates that C57BL/6N mice might elicit a stronger neutrophil-driven immunity in response to YPIII infection than BALB/c mice and thus are more resistant to YPIII infection, while YPIII infection of BALB/c mice triggers the recruitment of several immune cells.

Although the *Yersinia*-affected cytokines and chemokines differ between C57BL/6N and BALB/c mice, the data propose that CNF_Y induces the production of pro-inflammatory chemokines and cytokines in C57BL/6N mice as it does in BALB/c mice. However, there are some differences in the abundance of the cytokines and chemokines in the serum of the mice that might contribute to C57BL/6N resistance and BALB/c susceptibility.

In conclusion, C57BL/6N mice are more resistant to *Y. pseudotuberculosis* infection, which is possibly caused by an improved immune response in C57BL/6N compared to BALB/c mice, but C57BL/6N mice still display a pathophysiology resembling that of BALB/c mice.

3.6.2 *Y. pseudotuberculosis* YPIII Δ*cnfY* is defective in effective systemic organ colonization in C57BL/6N mice

In the previous sections, it was found that C57BL/6N mice are more resistant to *Y. pseudotuberculosis* infection than BALB/c mice, which might be due to divergent inflammatory immune reactions (3.6.1). These differences might also impact the organ colonization abilities of both *Yersinia* strains. To study this, C57BL/6N mice were intra-gastrically challenged with $2x10^8$ CFU of *Y. pseudotuberculosis* YPIII or YPIII Δ*cnfY*. After

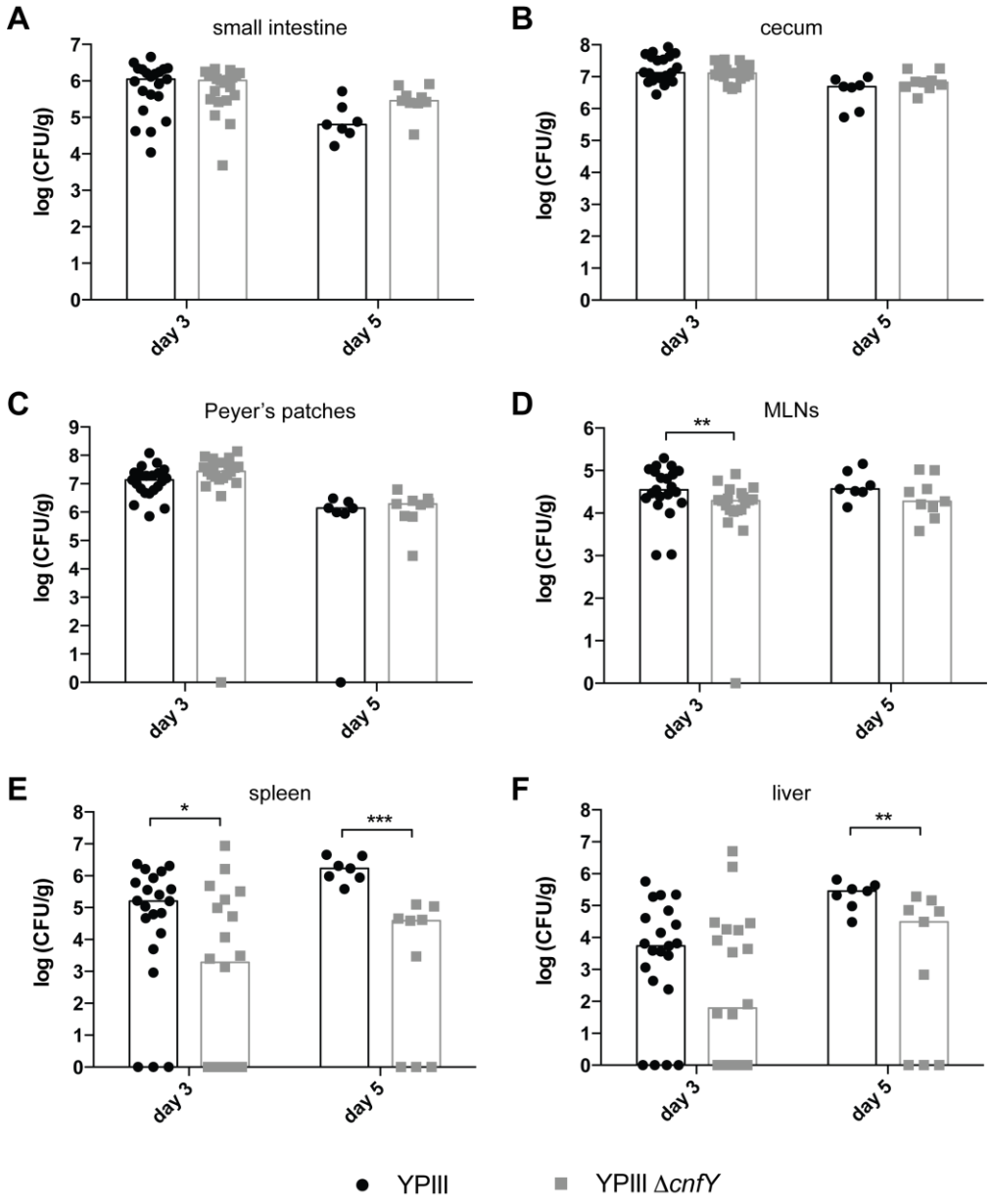

Figure 3.28 Deletion of *cnfY* results in colonization defects in the MLNs, spleen and liver during early infection stages.

C57BL/6N mice were intra-gastrically infected with $2x10^8$ CFU of *Y. pseudotuberculosis* YPIII or YPIII Δ*cnfY*. At indicated time points post infection, the *Yersinia* burden in (A) small intestine, (B) cecum, (C) PPs, (D) MLNs, (E) spleen, and (F) liver was determined. The data were combined from four (3 dpi) or two (5 dpi) independent experiments: YPIII, n=21 (3 dpi) n=7 (5 dpi); YPIII Δ*cnfY*, n=20 (3 dpi) n=9 (5 dpi). The bars represent the median. The data were statistically analyzed with t-tests (A-D) or Mann-Whitney U tests (E & F): * $p<0.05$, ** $p<0.01$, *** $p<0.001$.

3 and 5 dpi the *Yersinia* burdens in the small intestine, cecum, PPs, MLNs, spleen and liver were determined (Figure 3.28). The obtained *Yersinia* burden data demonstrate that the colonization levels in the small intestine (Figure 3.28A), the cecum (Figure 3.28B), and the PPs (Figure 3.28C) of YPIII and YPIII Δ*cnfY* at 3 and 5 dpi were comparable to those obtained for BALB/c mice (Schweer *et al*., 2013). In the MLNs of the C57BL/6N mice, the colonization levels of YPIII and YPIII Δ*cnfY* were also comparable to those of BALB/c mice (Figure 3.28D, Schweer *et al*., 2013). However, YPIII loads in the MLNs of C57BL/6N mice did not increase at 5 dpi as they did in BALB/c mice, emphasizing that C57BL/6N mice are more resistant to *Y. pseudotuberculosis* YPIII infection (Figure 3.28D, Schweer *et al*., 2013). While 86 % and 81 % of the C57BL/6N spleens and livers were colonized by YPIII at 3 dpi, only 55 % and 60 % of C57BL/6N spleens and livers were populated by YPIII Δ*cnfY* at 3 dpi (Figure 3.28E, F). This colonization/dissemination defects during acute YPIII Δ*cnfY* infection were not observed in BALB/c mice at 3 dpi (Figure S10, Schweer *et al*., 2013), and were still somewhat present in the spleen and liver of C57BL/6N mice at 5 dpi.

In conclusion, the gut-associated tissues of C57BL/6N mice, *i.e.* small intestine, cecum and PPs, were as highly colonized by YPIII and YPIII Δ*cnfY* as observed in BALB/c mice. During C57BL/6N infection, YPIII burdens did not increase in the MLNs at 5 dpi and YPIII Δ*cnfY* was defective in early systemic organ colonization (spleen and liver) in C57BL/6N mice compared to BALB/c mice, which was somewhat compensated at later infection stages.

3.6.3 *Y. pseudotuberculosis* YPIII Δ*cnfY* is defective in systemic dissemination in C57BL/6N mice

During intra-gastric *Y. pseudotuberculosis* infection in C57BL/6N mice, an early dissemination and/or colonization defect was detected, which could be due to bacterial elimination of YPIII Δ*cnfY* in comparison to the wild type. In order to dissect this, intra-venous infections with 5,000 CFU of *Y. pseudotuberculosis* YPIII or YPIII Δ*cnfY* were performed in C57BL/6N mice. Strikingly, YPIII Δ*cnfY* was also severely attenuated upon systemic infection, suggesting that there might also be differences in organ colonization abilities compared to YPIII (Figure S25). Organ colonization analysis of the spleen and liver at 1 dpi, when mice still shared the same relative body weight (Figure S25B), revealed that both, YPIII and YPIII Δ*cnfY*, efficiently colonize the organs to the same amounts (Figure 3.29A, B). During the ongoing infection (3 dpi), when the relative body weights of both infection groups differed by approximately 10 %, the *Yersinia* burdens in the spleen remained stable and increased to comparable levels in the liver (Figure 3.29A, B). Interestingly, the YPIII Δ*cnfY* levels in the spleen were slightly reduced and in the liver slightly increased compared to YPIII at 3 dpi (Figure 3.29A, B). The analysis of the bacterial loads in the blood at 3 dpi, revealed that 60 % of YPIII-infected mice suffered from bacteremia, while only 10 % of YPIII Δ*cnfY*-infected mice did (Figure 3.29C).

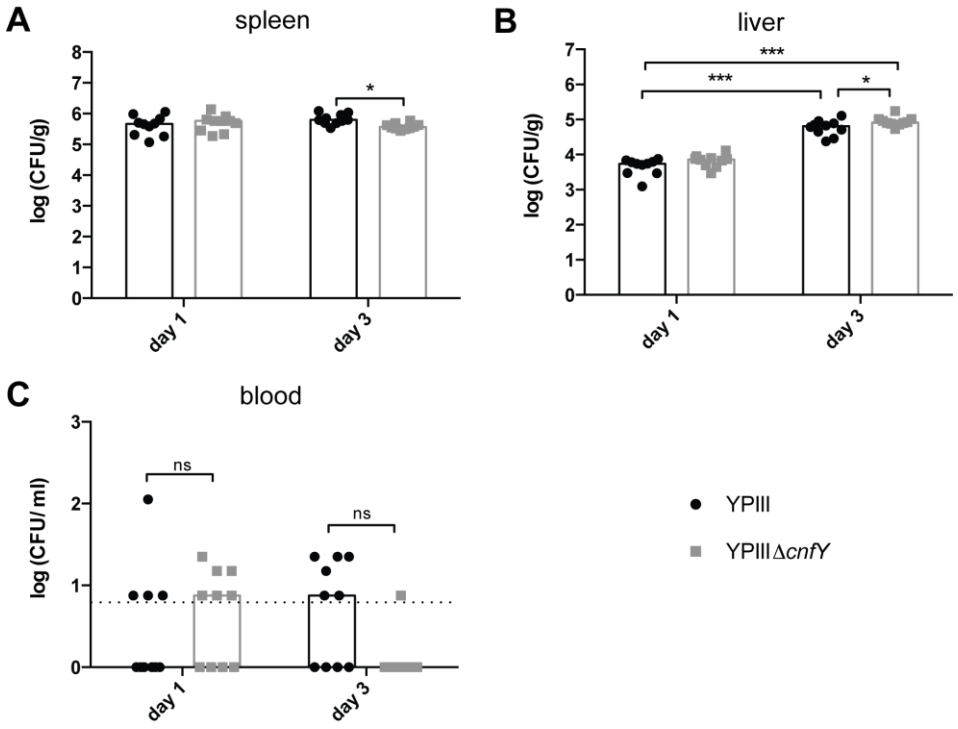

Figure 3.29 Deletion of *cnfY* does not impact *Y. pseudotuberculosis* colonization abilities during systemic infection.

C57BL/6N mice were intra-venously infected with 5,000 CFU of *Y. pseudotuberculosis* YPIII or YPIII Δ*cnfY*. At indicated time points post infection, the *Yersinia* loads in the (A) spleen, (B) liver, and (C) blood were assessed. The data were combined from two independent experiments: YPIII n=10; YPIII Δ*cnfY* n=10. The bars indicate the median and the dashed line the detection limit (7 CFU/ml). The statistical analysis was performed with two-way ANOVA employing Holm-Šídák's correction: * $p<0.05$, *** $p<0.001$; ns: not significant.

These results suggest that YPIII Δ*cnfY* might primarily experience a dissemination defect to systemic organs during early infection, since initial systemic organ colonization after intra-venous challenge is not affected by a loss of *cnfY*. This assumption is supported by detection of bacteremia, which is 6-fold higher in wild type *Y. pseudotuberculosis* expressing *cnfY*. Nevertheless, bacterial clearance from the organs, especially the spleen, might have a more important impact during later infection stages.

3.6.4 The inflammasome network plays divergent roles in early *Y. pseudotuberculosis* dissemination and depends on CNF_Y

In section 3.6, the modulation of the inflammasomes by *Y. pseudotuberculosis* was introduced. Although there are plenty of *in vitro* studies in bone marrow derived macrophages concerning the influence of Yops and the TTSS on the activity of the inflammasome, little is known about the impact during the oral infection route *in vivo*. Moreover, the CNF_Y toxin, which is known to constitutively activate small Rho GTPases, thereby increasing Yop translocation into immune cells, could impact inflammasome-dependent infection outcomes with *Y. pseudotuberculosis*. However, it has to be considered that YPIII and YPIII Δ*cnfY* elicit different immune responses and levels of inflammation during acute infection (3.4, 3.6.1), which proposes that the induction of the inflammasome could differently impact *Y. pseudotuberculosis* infection. Thus, the direct comparison of YPIII to YPIII Δ*cnfY* infection should carefully be drawn and the comparison should be focused on each strain's colonization abilities in the different knockout mouse strains.

In order to analyze the impact of caspase-1 and caspase-11 on either *Y. pseudotuberculosis* YPIII or YPIII Δ*cnfY* infection after intra-gastric challenge, caspase-1, caspase-11 and caspase-1/11-knockout mice were infected with $2x10^8$ CFU of *Y. pseudotuberculosis*. The caspase-1- and caspase-1/11-knockout mice were as susceptible as C57BL/6N mice to YPIII infection (Figure S26), but the caspase-11-knockout mouse strain was slightly more resistant against YPIII infection. However, this difference was not significant. Upon YPIII Δ*cnfY* infection, the caspase-1-, caspase-11- and caspase-1/11-knockout mice were as resistant as wild type mice (C57BL/6N) (Figure S26). This data suggests that the inflammasome and/or pyroptosis have no/minor influence on resistance/susceptibility to *Y. pseudotuberculosis* infection by the oral infection route.

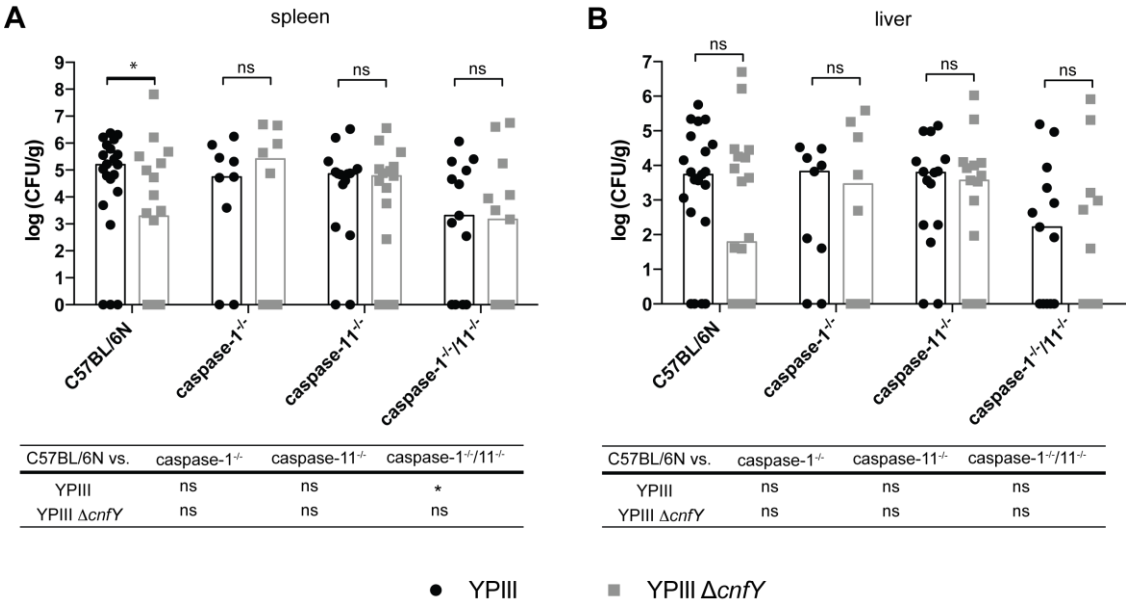

Figure 3.30 The pro-inflammatory caspases modulate systemic *Y. pseudotuberculosis* dissemination depending on *cnfY*.

C57BL/6N, caspase-1-, caspase-11- or caspase-1/11-knockout mice were intra-gastrically infected with $2x10^8$ CFU of *Y. pseudotuberculosis* YPIII or YPIII Δ*cnfY*. At 3 dpi, spleen (A) and liver (B) were analyzed for *Yersinia* colonization levels. The data were combined from two to four independent experiments: C57BL/6N mice, YPIII n=21, YPIII Δ*cnfY* n=20; caspase-$1^{-/-}$ mice, YPIII n=9, YPIII Δ*cnfY* n=8; caspase-$11^{-/-}$ mice, YPIII n=15, YPIII Δ*cnfY* n=15; caspase-$1^{-/-}/11^{-/-}$ mice, YPIII n=13, YPIII Δ*cnfY* n=13. The bar represents the median. The detection limit was at 300 CFU/g in the spleen and 50 CFU/g in the liver. The statistical analysis was performed with the Mann-Whitney U test: ns: not significant; * $p<0.05$.

As cell death and the release of pro-inflammatory cytokines are associated with bacterial resistance and clearance (Lebeis *et al.*, 2009; Aachoui *et al.*, 2013; Barry *et al.*, 2013; Lemon *et al.*, 2015), the influence of caspase-1 and -11 on bacterial organ colonization during early infection stage was assessed. To this end, wild type mice or the respective caspase-knockout mutants were intra-gastrically challenged with $2x10^8$ CFU of *Y. pseudotuberculosis* YPIII or YPIII Δ*cnfY*. Bacterial burdens in the small intestine, cecum, PPs, and MLNs of the caspase-knockout mutants did not differ from those in wild type mice (data not shown). In contrast, *Yersinia* dissemination and/or colonization of spleen and liver were slightly altered (Figure 3.30). Although the *Y. pseudotuberculosis* wild type and the isogenic *cnfY* mutant colonized caspase-1, caspase-11 and caspase-1/11- knockout mice to comparable amounts as C57BL/6N mice, the median colonization efficiency of *Y. pseudotuberculosis* was *cnfY* and caspase-dependent (Figure 3.30): while the bacterial loads in the spleen of the colonized mice

ranged between 10^2 to 10^7 CFU/g (Figure 3.30A) and in the liver between $1.5x10^1$ to 10^6 CFU/g (Figure 3.30B), YPIII colonization of caspase1/11-knockout mice was slightly reduced. In contrast, the median systemic colonization levels of YPIII in caspase-1- and caspase-11-knockout mice were not altered (Figure 3.30). Moreover, the YPIII Δ*cnfY* bacterial load was reduced compared with YPIII in C57BL/6N mice but not when caspase-1 and/or -11 were absent, however these differences were not significant (Figure 3.30).

Table 3.1 Comparison of dissemination/manifestation efficiency in systemic organs of caspase-1 and caspase-11-knockout mice.

Yersinia strain	Mouse strain	Relative dissemination/manifestation effectiveness at 3 dpi[11]	
		spleen	liver
YPIII	C57BL/6N	86 % (18/21)	81 % (17/21)
	Caspase-$1^{-/-}$	78 % (7/9)	89 % (8/9)
	Caspase-$11^{-/-}$	87 % (13/15)	87 % (13/15)
	Caspase-$1/11^{-/-}$	**69 % (9/13)**	**62 % (8/13)**
YPIII Δ*cnfY*	C57BL/6N	55 % (11/20)	60 % (12/20)
	Caspase-$1^{-/-}$	63 % (5/8)	63 % (5/8)
	Caspase-$11^{-/-}$	**80 % (12/15)**	**73 % (11/15)**
	Caspase-$1/11^{-/-}$	54 % (7/13)	46 % (6/13)

As YPIII Δ*cnfY* is impaired in systemic dissemination (3.6.2 & 3.6.3), the dissemination efficiencies of YPIII or YPIII Δ*cnfY* to the spleen and liver between the different mouse strains were compared (Table 3.1). In line with the assumption at the top of the chapter, the caspases differently influenced the dissemination to the systemic organs. While YPIII was partly impaired in dissemination to the spleen and liver of caspase-1/11-knockout mice (69 %/62 % vs. 86 %/81 % in C57BL/6N mice), YPIII Δ*cnfY* was improved in systemic dissemination in caspase-11-knockout mice (80 %/73 % vs. 55 %/60 % in C57BL/6N mice) (Table 3.1). This proposes that pyroptosis-deficient caspase-1/-11-knockout mice are slightly more protected from systemic dissemination of YPIII, whereas caspase-1/11-sufficiency is not as important for YPIII Δ*cnfY* dissemination. Moreover, caspase-11 activity hinders systemic dissemination of YPIII Δ*cnfY* in wild type mice, while this is not important for YPIII infections. In conclusion, the data suggest different roles of the caspases during YPIII and YPIII Δ*cnfY* infection due to the induction of different immune reactions in response to each infection.

The inflammasome not only mediates pyroptosis, but also facilitates pro-inflammatory cytokine production and release. Thus, the influence of IL-1α and IL-1β cytokines on bacterial colonization was tested (Figure 3.31). The *Yersinia* burden in the PPs, cecum and small intestine was not altered during the infection of IL-1-knockout mice compared to C57BL/6N wild type mice (data not shown). In the spleen and liver, YPIII was severely impaired in systemic dissemination and colonization of IL-1α knockout mice after intra-gastric challenge with $2x10^8$ CFU (Figure 3.31; Table 3.2): YPIII bacteria systemically disseminated to only

[11] relative proportion of colonized systemic organs among *Y. pseudotuberculosis* infected animals (total amount of colonized spleens or livers per the total amount of *Y. pseudotuberculosis* infected mice)

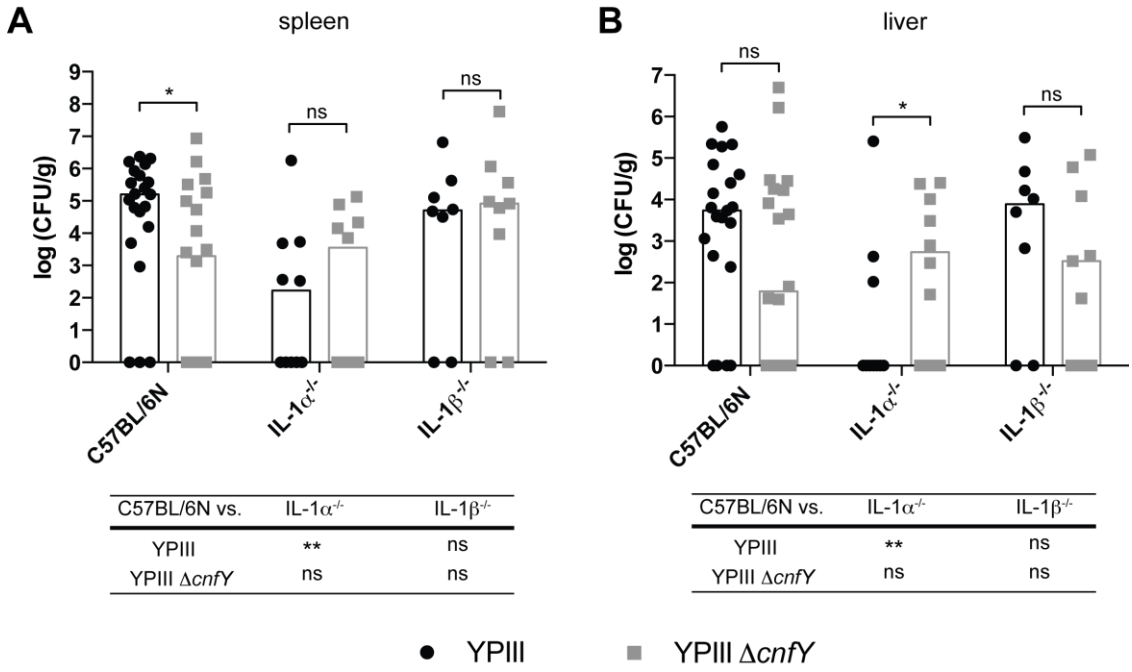

Figure 3.31 The pro-inflammatory cytokines IL-1α and IL-1β modulate systemic *Y. pseudotuberculosis* dissemination depending on *cnfY*.

C57BL/6N, IL-1α-, or IL-1β-knockout mice were intra-gastrically infected with $2x10^8$ CFU of *Y. pseudotuberculosis* YPIII or YPIII Δ*cnfY*. At 3 dpi, spleen (A) and liver (B) were analyzed for *Yersinia* burdens. The data were combined from two (IL-1-knockout mice) or four (C57BL/6N mice) independent experiments: C57BL/6N mice, YPIII n=21, YPIII Δ*cnfY* n=20; IL-$1\alpha^{-/-}$ mice, YPIII n=10, YPIII Δ*cnfY* n=10; IL-$1\beta^{-/-}$ mice, YPIII n=8, YPIII Δ*cnfY* n=9. The bar represents the median. The detection limit was at approximately 300 CFU/g in the spleen and at ca. 50 CFU/g in the liver. The statistical analysis was performed with the Mann-Whitney U test: ns: not significant; * $p<0.05$, ** $p<0.01$.

50 % of the spleens and 30 % of the livers of IL-1α-knockout mice (Table 3.2). This dissemination defect was even stronger than in caspase-1/11 knockout mice, indicating that IL-1α is more crucial than caspase-1/11-sufficiency for YPIII dissemination. However, IL-1α did not influence systemic dissemination/colonization of YPIII Δ*cnfY* (Figure 3.31; Table 3.2).
Interestingly, IL-1β-deficiency did not have a similar impact on systemic dissemination of YPIII, though IL-1β-deficiency caused slightly increased systemic dissemination of YPIII Δ*cnfY* to the spleen (78 % vs. 55 % in C57BL/6N mice) (Table 3.2; Figure 3.31A). This increase of YPIII Δ*cnfY* dissemination in IL-1β-knockout mice suggests that IL-1β secretion might prevent dissemination/manifestation of YPIII Δ*cnfY* in the spleen. However, IL-1β did not prevent YPIII Δ*cnfY* dissemination to/manifestation in the liver. These results again support the assumption that YPIII and YPIII Δ*cnfY* elicit different immune responses during the infection resulting in divergent influences of caspases and IL-1 cytokines on bacterial dissemination to systemic organs.

Table 3.2 Comparison of dissemination/manifestation efficiency in systemic organs of IL-1-knockout mice.

Yersinia strain	Mouse strain	Relative dissemination/manifestation effectiveness at 3 dpi[12]	
		spleen	liver
YPIII	C57BL/6N	86 % (18/21)	81 % (17/21)
	IL-1α$^{-/-}$	**50 % (5/10)**	**30 % (3/10)**
	IL-1β$^{-/-}$	75 % (6/8)	75 % (6/8)
YPIII Δ*cnfY*	C57BL/6N	55 % (11/20)	60 % (12/20)
	IL-1α$^{-/-}$	50 % (5/10)	70 % (7/10)
	IL-1β$^{-/-}$	**78 % (7/9)**	67 % (6/9)

In order to test whether YPIII and YPIII Δ*cnfY* elicit different IL-1 cytokine responses in the infected tissues, C57BL/6N mice were intra-gastrically infected with 2x10^8 CFU of *Y. pseudotuberculosis* YPIII or YPIII Δ*cnfY*. At 3 dpi, the cytokine responses of IL-1α, IL-1β and IL-12p70 (a caspase independent cytokine) were tested in the small intestine, MLNs, spleen and liver. As shown in Figure 3.32, the IL-1α level was ~10-fold higher in the MLNs of YPIII infected mice compared to uninfected and YPIII Δ*cnfY*-infected mice, suggesting that IL-1α secretion in the MLNs could ease bacterial spread to spleen and liver (Figure 3.32A). This is further supported by the observation that YPIII Δ*cnfY* does not elicit elevated IL-1α levels in the MLNs and is simultaneously impaired in systemic spread in C57BL/6N mice (3.6.2 & 3.6.3). The IL-1β levels were significantly increased upon YPIII infection in the MLNs and spleen in comparison to uninfected and YPIII Δ*cnfY*-infected C57BL/6N mice (Figure 3.32B). Moreover, YPIII Δ*cnfY* caused significantly increased IL-1β levels in the spleen compared to uninfected C57BL/6N mice (Figure 3.32B). Although the IL-1β level was slightly more induced during YPIII infection than upon YPIII Δ*cnfY* infection, IL-1β was dispensable for systemic dissemination of YPIII (Table 3.2). The IL-1β cytokine more likely prevents dissemination to/ colonization in the spleen of YPIII Δ*cnfY* infected mice and confers protection. Interestingly, *Y. pseudotuberculosis*-mediated IL-12p70 levels were unaffected by CNF_Y.

Altogether, the data indicate that YPIII favors pyroptosis and IL-1α production in order to establish efficient systemic infections in early infection phase, whereas the activities of caspase-11 and IL-1β contribute to systemic dissemination-resistance during early YPIII Δ*cnfY* infection.

[12] relative proportion of colonized systemic organs among *Y. pseudotuberculosis* infected animals (total amount of colonized spleens or livers per the total amount of *Y. pseudotuberculosis* infected mice)

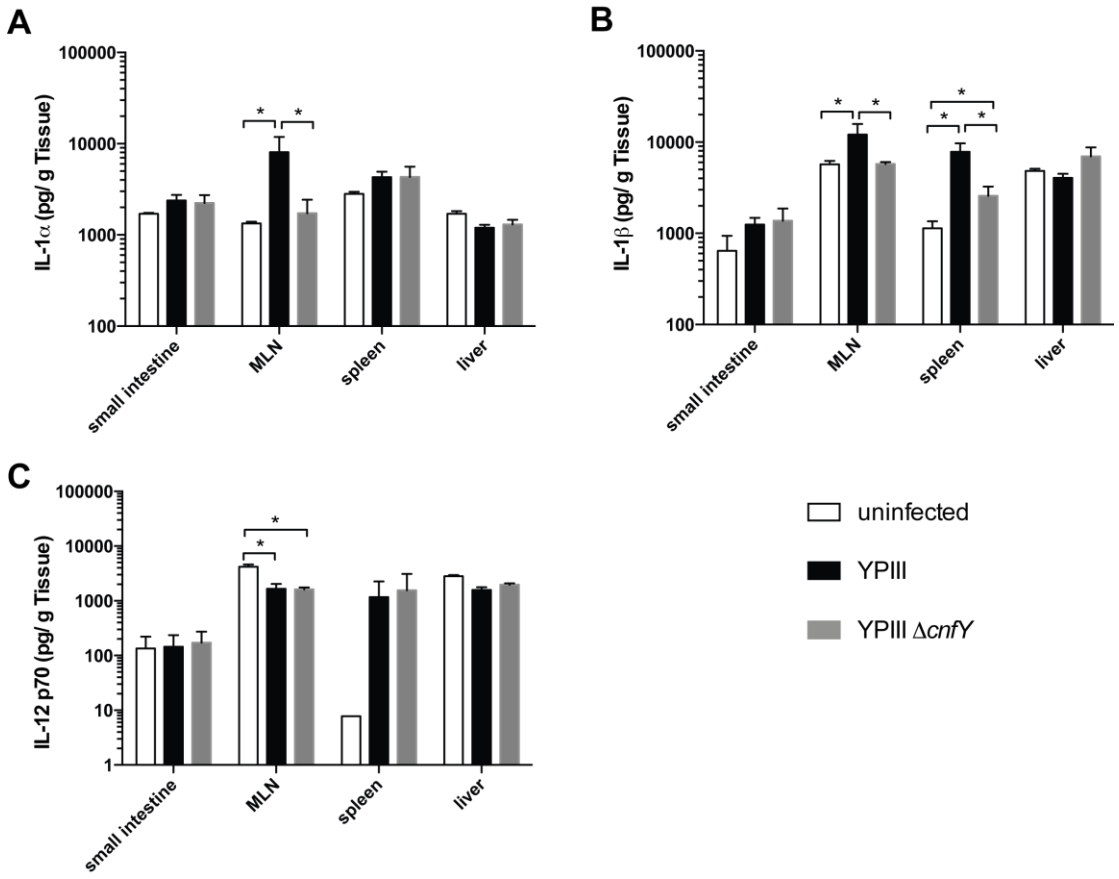

Figure 3.32 *Y. pseudotuberculosis* infection causes *cnfY*-dependent IL-1 production in C57BL/6N tissues.

C57BL/6N mice were intra-gastrically challenged with $2x10^8$ CFU of *Y. pseudotuberculosis* YPIII or YPIII Δ*cnfY*. At 3 dpi, small intestine, MLNs, spleen and liver were monitored for (A) IL-1α, (B) IL-1β and (C) IL-12p70 levels with ELISA. The data are combined from two independent experiments. The bar represents the mean ±SEM. The data were statistically analyzed with multiple t-tests employing Holm-Šídák's correction: * $p<0.05$.

4 Discussion

In the past, bacterial pathogens have been increasingly recognized to possess the ability of causing long-lasting infections that may lead to morbidity and mortality (1.4). *Y. pseudotuberculosis* is known to elicit gastrointestinal diseases but also holds the potential to cause relapsing and autoimmune diseases, *i.e.* erythema nodosum and reactive arthritis (1.2). Hoogkamp-Korstanje and colleagues demonstrated that *Yersinia* is able to persist in the colon and lymph nodes after initial infection in patients developing chronic arthritis and ileitis (Hoogkamp-Korstanje *et al*., 1988). Moreover, the prolonged presence of *Yersinia*-specific short-lived IgA antibodies indicates chronic stimulation by *Yersinia*-derived antigens in the gut-associated lymphoid tissue (Granfors and Toivanen, 1986; Hoogkamp-Korstanje *et al*., 1988). The circulation of *Yersinia*-specific antigens in peripheral blood cells is detectable even years after *Yersinia* infection in reactive arthritis patients (Granfors *et al*., 1998). Recently, it was discovered that *Y. pseudotuberculosis* YPIII is able to persistently infect BALB/c and FVB/N mice, leading to asymptomatic infection in the cecum (Fahlgren *et al*., 2014). The importance of *Yersinia* virulence factors in the development and maintenance of persistence was not yet intensively studied.

The virulence factor, CNF_Y, of the *Y. pseudotuberculosis* isolate YPIII is expressed during the infection of mice (Schweer *et al*., 2013). It significantly contributes to the pathogenesis of *Y. pseudotuberculosis* YPIII infection in BALB/c mice, since a *cnfY* mutant is attenuated in virulence and tissue colonization (Schweer *et al.*, 2013). Furthermore, CNF_Y fosters increased inflammation and enhances the translocation of Yop effector proteins into host immune cells, especially neutrophils (Schweer *et al*., 2013).

This study investigated the impact of *cnfY* on the pathogenesis of *Y. pseudotuberculosis* infections. In order to characterize its role in *Yersinia* persistence, the influence of *cnfY* on persistence establishment, host inflammation and host transcriptome alterations during the switch from acute to persistent asymptomatic gastrointestinal infection was studied.

4.1 Relevance of CNF_Y for the development of persistent *Y. pseudotuberculosis* infection

Bacterial pathogens that establish persistent infection encode for a variety of virulence and metabolic factors that influence and contribute to persistence ability. For this, these genes trigger or reduce the development of persistent infection. Studies to elucidate the mechanisms of bacterial persistence uncovered numerous genetic factors, which are involved in establishing colonization and persistence in the niche of the pathogen. The genetically highly variable *H. pylori* encodes several virulence factors that contribute to virulence and colonization, enabling the pathogen to establish long-lasting infections in the hostile environment of the stomach (Cellini *et al*., 2003; Kao *et al*., 2015): Urease activity, chemotaxis and motility are essential to establish infection by *H. pylori* since their inactivity led to the inability to establish long-lasting colonization of the gastric epithelium (Eaton *et al*., 1991; Eaton *et al*., 1996; Schoep *et al*., 2010; Howitt *et al*., 2011). VacA of *H. pylori*, which permeabilizes host membranes, induces apoptosis and triggers inflammation, is also necessary for long-term colonization of the stomach (Kao *et al*., 2015; Oertli *et al*., 2013). Interestingly, the natural competence of *H. pylori* that facilitates inter-strain genetic exchange, is dispensable for initial infection but important for long-term persistence in the murine infection model (Dorer *et al*., 2013).

In contrast to *H. pylori*, *S.* Typhimurium normally does not persist in wild-type mice (Rhen *et al*., 2003). However, the analysis of several attenuated *S.* Typhimurium mutants demonstrated their ability to persist in systemic organs after oral and/or intra-peritoneal infection. Those attenuated *S.* Typhimurium strains include *ompR* (transcriptional regulator), *aroAC* (aromatic amino acid biosynthesis) *agfA* (fimbrium) and *surA* (chaperone) mutants (Dorman *et al*. 1989; Chatfield *et al*., 1992; Sukupolvi .*et al*., 1997; Sydenham *et al*., 2000). Moreover, *S.* Typhimurium persistence particularly requires the *Salmonella* pathogenicity islands (SPI) -1 and SPI-2 for persistence. A *S.* Typhimurium *clpXP* protease mutant that produces increased amounts of SPI-1 proteins, was able to persistently colonize spleen and liver after intra-peritoneal infection (Yamamoto *et al*., 2001; Kage *et al*., 2008). Likewise, PNPase mutants of *S.* Typhimurium show increased expression of SPI-1 and SPI-2, which leads to persistence of *Salmonella* in the spleen, liver and gall bladder after intra-gastric challenge (Clements *et al*., 2002). A more direct link of SPI-1 and SPI-2 involvement in persistent *Salmonella* infection was shown in studies by Lawley *et al*. and McLaughlin *et al*. in Nramp1$^{+/+}$ mice, which develop persistent infections with *Salmonella* wild type bacteria (Monack *et al*., 2004a; Johanns *et al*., 2010). In these studies, co-infection experiments demonstrated that SPI-1, some SPI-1 effectors, and the SPI-2 effector SseI are necessary for effective long-term colonization by *Salmonella*, thereby implicating that the pathogenicity islands and effectors are required to reinvade and modulate immunity to prevent clearance during persistence (Lawley *et al*., 2006; Lawley *et al*., 2008; McLaughlin *et al*., 2009).

The virulence factor CNF$_Y$ decreases *Yersinia* persistence

This work demonstrates that deletion of *cnfY* enhances *Y. pseudotuberculosis* persistence events in the murine cecum after intra-gastric infection. Avican and co-workers showed that *cnfY* expression is down-regulated in *Y. pseudotuberculosis* YPIII during the persistent infection of FVB/N mice, suggesting that *cnfY* expression might impair or reduce persistence at later infection stages (Avican *et al*., 2015). This expression profile was confirmed during this study in BALB/c mice (3.4.4). Remarkably, the data in this study showed that *cnfY* expression was generally lower *in vivo* than *in vitro*, indicating the necessity to adjust *cnfY* expression to achieve ideal virulence and growth properties depending on the bacterial environment. Although there is little data on genetic factors of *Y. pseudotuberculosis* that influence the ability to establish and maintain infection, the impact of some virulence, regulator and metabolic genes on *Yersinia* persistence are described. Most of these genes were shown to reduce the ability of *Y. pseudotuberculosis* to either establish or maintain prolonged infection. Anaerobiosis and oxidative stress mutants of *Y. pseudotuberculosis* YPIII (*i.e.* Δ*arcA*, Δ*fnr*, Δ*frdA* and Δ*wrbA*) showed reduced ability to maintain prolonged infection after they passed the initial infection phase (Avican *et al*., 2015). Furthermore, YPIII Δ*hdeB* (acid stress protection) caused more severe disease than the wild type, leading to complete clearance and inability to establish long-lasting infections (Avican *et al*., 2015). The analysis of disease severity upon persistent *Yersinia* infection by survival, body weights and diarrhea scores also showed that YPIII Δ*cnfY* caused less severe disease during initial infection than YPIII (3.1). Altogether, this suggests that less severe forms of yersiniosis might assist the establishment of persistent infection, since most of the studies analyzing other persistent bacteria show that persistent pathogens harbor reduced virulence properties and emerged from virulent bacteria through gene loss (Dorman *et al*. 1989; Chatfield *et al*., 1992; Sukupolvi .*et al*., 1997; Sydenham *et al*., 2000; Zdziarski *et al*., 2007; Dobrindt *et al*., 2010). However, bacteria must retain virulence genes to guarantee long-term colonization, as shown for SPI-1 of *S.* Typhimurium (Lawley *et al*., 2006; Lawley *et al*., 2008).

Studies on persistent bacterial infections regularly report on genes that are essential to facilitate persistent colonization (Zahrt, 2003; Monack, 2013). However, there are few publications that demonstrate enhanced bacterial persistence after gene mutagenesis, as described in this work. In *P. aeruginosa*, it was found that inactivation of *hmgA* (phenylalanine and tyrosine catabolism), which leads to hyperproduction of pyomelanin, increases persistence in the lungs of mice, most likely by increasing resistance to hydrogen peroxide (Rodríguez-Rojas *et al*., 2009). This pyomelanin hyperproducing-phenotype is also frequently observed in isolates of cystic fibrosis and chronic obstructive pulmonary disease (COPD) patients (Rodríguez-Rojas *et al*., 2009). In *Brucella suis*, inactivation of the ATP-dependent Clp protease subunit A (ClpA) led to prolonged colonization of liver and spleen of infected mice. The authors suggested that the growth defect of the *clpA* mutant might contribute to enhanced persistence through delayed induction of an inflammatory response (Ekaza *et al*., 2000). However, the *cnfY* mutant of *Y. pseudotuberculosis* does not display a growth defect *in vitro* (3.2.2). Interestingly, deletion of the DNA-damage protecting gene *uspA* in *Y. pseudotuberculosis* strain YPIII, also caused increased persistence. Genomic mutations that are more frequent in *uspA* mutants may decrease bacterial fitness and thus induction of inflammation (Diez *et al*., 2000; Avican *et al*., 2015).

CNF_Y-dependent Yop secretion efficiency might modulate *Yersinia* persistence

Fahlgren and co-workers showed that YopE and YopH are necessary to develop and maintain a persistent *Y. pseudotuberculosis* infection (Fahlgren *et al*., 2014). In the present work, it was also shown that persisting *Y. pseudotuberculosis* YPIII maintain the virulence plasmid during persistent infection, although it is the least stable virulence factor of *Y. pseudotuberculosis* (Fukushima *et al*., 1991; Eppinger *et al*., 2007; Ch'ng *et al*., 2011). While it was shown that *Y. pseudotuberculosis* increases its virulence plasmid copy numbers during the acute infection (Wang *et al*., 2016a), it can be speculated that *Yersinia* virulence plasmid copy numbers are down-regulated at the persistent infection stage compared to early infection. This is supported by the study of Avican and co-workers, who demonstrated that virulence plasmid encoded genes are expressed at lower levels during persistent *Yersinia* infection compared to acute infection (Avican *et al*., 2015), which is possibly accomplished by gene-dose reduction through decreased plasmid copy numbers. Whether *Y. pseudotuberculosis* harbors reduced plasmid copy numbers during persistent infection remains to be clarified. As the main function of CNF_Y appears to increase Yop translocation into host immune cells (Janina Schweer, PhD thesis; Schweer *et al*., 2013), fine-tuning of Yop translocation *in vivo* seems important for the development of a persistent infection.

The evolutionary relevance of CNF_Y for infection and persistence

In many *Y. pestis* and other *Y. pseudotuberculosis* isolates excluding YPIII and IP2666, the *cnfY* locus is truncated and therefore non-functional due to a deletion in the *cnfY* locus in HPI^- strains or two deletions in HPI^+ strains (Lockman *et al*., 2002). These data suggests that deletion of the *cnfY* gene may be beneficial. In this work, the deletion of the *cnfY* gene not only caused long-term colonization of a protected niche, it also conferred continuous shedding of the organisms into the environment. This potentially improves fecal-oral dissemination to other animals, and ensures host reservoir maintenance and zoonotic infections.

Similar to *Yersinia*, not all UPEC isolates are *cnf1* positive. A couple of studies analyzing the *cnf1* prevalence in UTI caused by UPEC and uroseptic *E. coli* revealed that *cnf1* was present in 3-37 % of the isolates (Caprioli *et al*., 1987; Bingen-Bidois *et al*., 2002; Tarchouna *et al*., 2013). In contrast, *cnf1* positive *E. coli* strains were infrequently isolated from stool samples of

healthy people (Caprioli *et al*., 1987), indicating that *cnf1* is specifically required during UTI. This is supported by a study of Rippere-Lampe and colleagues who showed that *cnf1* permits UPEC to long-term colonize the urine, bladder and kidneys of mice (Rippere-Lampe *et al*., 2001b). Moreover, the presence of *cnf1* mediates apoptosis of cells in the bladder epithelium and bacterial invasion into bladder cells (Mills *et al*., 2000b; Doye et al., 2002; Bower *et al*., 2005). This might provide UPEC access to deeper tissues, which is an important step to establish UPEC persistence (Hannan *et al*., 2012). These reports emphasize that homologous virulence factors, such as CNF_Y and CNF1, might confer different virulence abilities in distinct pathogens that are important to their evolution and access to different host niches. While the presence of *cnfY* facilitates systemic colonization during acute *Yersinia* infection (Schweer *et al*., 2013), it impairs persistent infection in the cecum. To further extend this hypothesis, it was shown that the *Salmonella* TTSS effector AvrA improves persistence in the cecal lumen of young chicken by improving bacterial invasion, yet persistence of an *avrA* mutant was decreased during murine infection (Lu *et al*., 2010; Arsenault *et al*., 2016), suggesting that persistence related genes might also depend on the host organism.

4.2 The contribution of inflammation on pathogenesis and development of persistent *Yersinia* infection

Some studies show that pathogens induce initial inflammation to initiate and establish effective colonization (Mahdavi *et al*., 2002; Stecher *et al*., 2007; Winter *et al*., 2010; Sasindran and Torrelles, 2011). However, bacterial pathogens have also evolved strategies to avoid extensive immune recognition and induction of inflammation to promote long-term infections. *H. pylori* has developed multiple strategies for this, for instance modification of lipid A via acetylation to avoid TLR4 recognition (Moran *et al*., 1997; Salama *et al*., 2013). This is important for *H. pylori* colonization in the long term, since increased inflammation was associated with increased clearance of the bacterium (Blanchard *et al*., 2003; Ismail *et al*., 2003). It is accepted that the presence of *cnfY/1* enhances inflammation and tissue damage (Rippere-Lampe *et al*., 2001a; Schweer *et al*., 2013). The histopathologic analysis of the cecal tissue during acute *Yersinia* infection in this work also showed increased inflammation of the lamina propria (LP) and the lymphoid tissue of the cecum with *cnfY*$^+$ YPIII, yet YPIII Δ*cnfY* infected ceca still presented inflammation (3.2.1). Interestingly, presence of *cnfY* caused massive edema formation, which was also observed during infection with *cnf1*$^+$ *E. coli* (Rippere-Lampe *et al*., 2001; Smith *et al*., 2015). The exacerbated inflammation upon YPIII infection compared to the *cnfY* mutant might also be reinforced by dampened wound repair through secretion of CNF_Y, since CNF1 was described to impair wound healing in bladder, intestinal and fibroblast cell layers (Island *et al*., 1999; Brest *et al*., 2004). This might facilitate barrier breaching for systemic dissemination of *Y. pseudotuberculosis* YPIII, but the sustained inflammatory response during the infection might foster bacterial clearance. Thus, reduced inflammation by YPIII Δ*cnfY* might contribute to enhanced persistence.

CNF_Y-mediated IL-6 production might foster tissue destruction and inflammation through neutrophils and bacterial clearance via the development of T cell immunity

Acute YPIII infection triggered massive infiltration of lymphocytes into the LP of the cecum, whereas acute YPIII Δ*cnfY* infection caused diffuse infiltration of PMNs into the LP, indicating a dampened inflammatory response and a reduced immunogenicity of YPIII Δ*cnfY*. Necrosis was also more pronounced in the cecal lymphoid tissue of YPIII-infected mice compared to those infected with the *cnfY* mutant and infiltrating neutrophils surrounded

bacterial microcolonies. Cytokine analysis of the cecal tissue also revealed that IL-6 levels were more strongly elevated in the cecal tissue and serum of YPIII-infected mice than in mice infected with YPIII Δ*cnfY* (3.5). IL-6 contributes to neutrophil attraction during early infection, triggers monocyte recruitment at later stages, and regulates adaptive immunity by mediating lymphocyte recruitment (as observed in histopathologic sections), effector T cell differentiation and proliferation (Scheller *et al*., 2011; Araie-Kachoie *et al*., 2014; Hunter and Jones, 2015), suggesting a potential role in enhanced clearance of YPIII from the cecum. In line with that, a previous study showed that *Y. pseudotuberculosis* YPIII infection of BALB/c mice caused more enhanced infiltration of neutrophils into the PP than YPIII Δ*cnfY* (Schweer *et al*., 2013). The increased infiltration of neutrophils can lead to massive tissue destruction by conglomeration of secreted proteases and ROS (Borregaard *et al*., 2007; El-Benna *et al*., 2016). Interestingly, CNF1 was also connected to enhanced ROS production from neutrophils (Davis *et al*., 2005).

Mild inflammation during persistent *Yersinia* infection is independent of CNF_Y but dependent on the mouse strain

Histopathologic analysis revealed *cnfY*-independent, low inflammation in the LP of the cecum during persistent *Y. pseudotuberculosis* infection, eliciting diffuse and isolated neutrophil infiltration into the LP of the cecum. One possible reason for the *cnfY*-independency might be that *cnfY* is only lowly expressed in the persistent infection stage compared to acute infection (Avican *et al*., 2015; this study). Notably, the clinical study of Hoogkamp-Korstanje presented *Yersinia*-driven, nonspecific inflammation of the colon during acute ileitis or colitis, which encompassed tissue destruction and recruitment of mononuclear cells, whereas colon biopsies of chronically *Yersinia* infected patients demonstrated no tissue destruction (Hoogkamp-Korstanje *et al*., 1988). In contrast, persistently *Y. pseudotuberculosis*-infected FVB/N mice had disrupted epithelium and a profound influx of neutrophils that surrounded the *Y. pseudotuberculosis* foci (Fahlgren *et al*., 2014; Avican *et al*., 2015). This discrepancy compared to the results in this work might be due to genetic differences between FVB/N and BALB/c mice. The genetic backgrounds that cause these differences are still not fully understood, yet the myeloid transmembrane receptor Gpr84 is truncated in FVB/N mice, whereas it is functional in BALB/c mice (Perez *et al*., 2013). Moreover, BALB/c mice produce complement component C5, whereas FVB/N mice are deficient (Radovanovic *et al*., 2011). The MHC class I haplotypes of H-2 also differ between the two strains, which was associated with different susceptibilities to bacterial infection (Curtis *et al*., 1982; Goldmann *et al*., 2005). This proposes that the murine genetic background might be involved in controlling inflammation during persistent *Y. pseudotuberculosis* infection.

***Yersinia* might exploit neutrophil transmigration to establish a bacterial reservoir in the lamina propria**

The histopathologic analysis showed neutrophil accumulation in the intestinal lumen during acute *Yersinia* infection, which is known to occur in the inflamed gut through neutrophil trans-epithelial migration (Reaves *et al*., 2005). A sophisticated study by McCormick and colleagues with *Y. pseudotuberculosis* established that this event in particular disrupts barrier polarization, thereby exposing β_1 integrins at the apical site. This enables *Y. pseudotuberculosis* to cross the epithelial layer by engaging InvA with the apical β_1 integrins and thus colonizing the basolateral side (McCormick *et al*., 1997). Considering the obtained histopathologic and *Yersinia*-localization data, this mechanism explains (1) *Yersinia* colonization at the basal site of the epithelium and (2) that increased neutrophil infiltration and transmigration in YPIII-

infected animals might lead to augmented invasion of YPIII into the lamina propria compared to YPIII Δ*cnfY*. In the persistent colonization state, *Yersinia* can exploit this basolateral localization to re-enter the lumen by engaging with β_1 integrins at the basolateral site, allowing dissemination into the environment and re-invasion. This assumption proposes circulation of *Yersinia* in the cecum to maintain environmental shedding and reservoir colonization.

Re-distributed colonization patterns of *Y. pseudotuberculosis* might protect the bacteria from elimination

Analysis of the colonization patterns of *Y. pseudotuberculosis* during persistent infection revealed that the colonization pattern greatly differs from acute infection and the patterns observed during persistent *Y. pseudotuberculosis* infection in FVB/N mice (Fahlgren *et al*., 2014; Avican *et al*., 2015). *Yersinia* was found to localize in small to large microcolonies in the cecal lymphoid tissue during acute BALB/c infection and persistent infection in FVB/N mice (3.2.3; Fahlgren *et al*., 2014; Avican *et al*., 2015), whereas *Y. pseudotuberculosis* was widely distributed as single to multiple-cell aggregates during persistent infection of BALB/c mice.

M. tuberculosis, *P. aeruginosa*, *H. pylori* and UPEC are biofilm-forming bacteria that cause persisting infections (Singh *et al*., 2000; Anderson *et al*., 2004; Ojha *et al*., 2008; Percival and Suleman, 2014). The ability to form a biofilm and to undergo phenotypic switches is correlatable to bacterial persistence and important for reservoir maintenance (Balaban *et al*., 2004; Chen and Wen, 2011). In *Y. pseudotuberculosis*, PhoP represses the production of *Yersinia* biofilms (Sun *et al*., 2009). However, *Y. pseudotuberculosis* YPIII carries naturally a non-functional *phoP* gene (Grabenstein *et al*., 2004), and was thus shown to be capable of forming biofilms at abiotic and biotic surfaces (Joshua *et al*., 2003; Sun *et al*., 2009). In the study by Avican *et al*., it was also shown that biofilm and quorum-sensing genes are up-regulated during persistent infection (Avican *et al*., 2015). As biofilm formation is induced upon iron starvation in *Y. pestis*, iron limitation in the host during *Y. pseudotuberculosis* infection might also induce biofilm formation (3.4.3) (Perry and Fetherston, 1997; Liu *et al*., 2009; Nuss *et al*., 2017). However, the localization studies of the cecal lymphoid tissue during persistent infection showed that *Y. pseudotuberculosis* was almost exclusively found in the intercellular space, and in close and dense association to lymphocytes. These results lead to the hypothesis that the bacteria adhere tightly as aggregates on the surface of lymphocytes and/or in the intracellular space. As bacterial adherence and the formation of aggregates protect pathogens from phagocytosis (Galdiero *et al.*, 1988; Ribet and Cossart, 2015), the aggregation and/or adherence to cells might protect the bacteria from phagocytic elimination.

The cytokine production is dependent on CNF_Y and might contribute to disease progression

Cytokine profiling in the serum of *Y. pseudotuberculosis*-infected mice showed a mild systemic inflammation in both infection groups during acute infection ($\leq$ 14 dpi), whereas almost no systemic cytokine response was observed during persistent *Yersinia* infection ($\geq$ 21 dpi) (3.5). Only IL-12p40 was more abundant in the serum of persistently YPIII colonized mice, which enhances innate immune responses by recruiting macrophages, fostering activated dendritic cells migration and IFNγ production (Piccotti *et al*., 1997; Ha *et al*., 1999; Kahder *et al*., 2006; Cooper and Khader, 2007). In persistent *Salmonella* and *Mycobacteria* infection, IL-12 signaling is a key pathway to control the infection (Cooper *et al*., 1997; Lehmann *et al*., 2006). This suggests that replication of YPIII might be more easily controlled through long-term immune system stimulation.

Interestingly, pro-inflammatory cytokines such as IFNγ, GM-CSF, and IL-17A were more abundant in the serum of YPIII Δ*cnfY* infected mice during the late phase of acute infection (9 dpi), indicating that antigen presentation, pathogen elimination and defense mechanisms, *e.g.* phagocyte activation and antimicrobial peptides, against YPIII Δ*cnfY* infection are more active (Teixeira *et al*., 2005; Iwakura *et al*., 2008; Manni *et al*., 2014; Becher *et al*., 2016; Song *et al*., 2016). In contrast, YPIII induces a massive systemic inflammation, as indicated by a prolonged and/or elevated abundance of IL-22 and the pleiotropic cytokine IL-6 in the serum of mice (3.5).

As shown in this study, acute *Yersinia* infection led to a pro-inflammatory cytokine response in the cecum by increased production of IL-6, Il-12 family cytokines (IL-12p40, IL-12p70, IL-23), IL-1α and IL-33. These cytokines recruit leukocytes and lymphocytes, increase pro-inflammatory cytokine production, induce acute phase response and act during T cell polarization/differentiation and tissue repair (Gee *et al*., 2009; Vignali and Kuchroo, 2012; Yazdi and Drexler, 2013; Rider *et al*., 2013; Ataie-Kachoie *et al.*, 2014; Molofsky *et al*., 2015; Martin and Martin, 2016). The enhanced abundance of the alarmins IL-33 and IL-1α indicates increased cell destruction (Garlanda *et al.*, 2013; Rider *et al*., 2013; Martin and Martin, 2016). Interestingly, IL-1α and IL-33 levels were slightly oppositionally produced between the two *Y. pseudotuberculosis* strains at 9 and 14 dpi, with higher levels of IL-33 in YPIII-infected mice and greater IL-1α production in YPIII Δ*cnfY*-infected animals. This suggests different cellular sources and/or activated pathways during infection. Epithelial cells constitutively express IL-33 and release it upon disruption (Moussion *et al*., 2008; Pichery *et al*., 2012). The more pronounced production of IL-33 during YPIII infection could indicate that more tissue destruction occurs, which is also supported by histopathology. Moreover, intracellular IL-33 induces the expression of IL-6 (Shan *et al*., 2015), explaining that YPIII-infected mice more highly expressed IL-6 in the cecum (3.4.1). *il-1α* is constitutively expressed in epithelial cells, though expression of *il-1α* in myeloid cells requires TLR activation (Dinarello, 2009; Yazdi and Drexler, 2013). Furthermore, IL-1α release from myeloid cells requires the activation of either caspase-1 or caspase-11 (Viganò and Mortellaro, 2013), which, taken together, might imply different phagocyte-activation states during YPIII and YPIII Δ*cnfY* infection. Given these assumptions, it is noteworthy that caspase-1 seems to inactivate IL-33, thereby reducing the severity of inflammation (Madouri *et al*., 2015). This might indicate that caspase-1 activation during YPIII Δ*cnfY* infection could also decrease IL-33 levels and thus IL-33-mediated inflammation.

The abundance of IL-7, IL-12p70, IL-23 and IL-6 during acute *Yersinia* infection further proposes the development of adaptive immune responses, *i.e.* recruitment of T cells, B cell maturation, and T cell survival, development and differentiation (Stetsko and Sauder, 2008; Ceredig and Rohlink, 2012; Kang and Coles, 2012; Hunter and Jones, 2015). The highly elevated IL-6 levels during YPIII infection compared to YPIII Δ*cnfY* infection indicate development of T_H17 immunity and maturation of plasma blasts into antibody-secreting plasma cells in response to YPIII infection (Hunter and Jones, 2015). This supports the assumption that the strong inflammatory immune response during YPIII infection might trigger clearance and thereby impairs persistence. Additionally, the abundance of pro-inflammatory cytokines such as IL-6 IL-17A, IL-22, IL-1α, IL-7, IL-12, and IL-23, implicated the development of a T_H1/T_H17 dominated immune response in the cecum (Figure 1.3). Nuss and co-workers also observed increased expression of pro-inflammatory cytokines that contribute to T_H1/T_H17 development and T_H1/T_H17 immune responses in the PP of BALB/c mice after infection with *Y. pseudotuberculosis* IP32953 (Nuss *et al.*, 2017).

Moreover, acute *Yersinia* infection triggered the production of cytokines involved in barrier defense (IL-17A, IL-22), maintenance (IL-22, IL-11) and regeneration (IL-22, IL-11, IL-33) (Iwakura *et al*., 2008; Garbers and Scheller, 2013; Dudakov *et al*., 2015; Molofsky *et al*., 2015; Parks *et al*., 2016), contributing to the restoration of tissue homeostasis after its disruption. The majority of affected and elevated cytokine levels decline after 14 dpi, suggesting restoration of tissue homeostasis, thereby allowing establishment of bacterial persistence. Interestingly, the anti-inflammatory cytokine levels, *i.e.* IL-10 and IL-13, were increased in the cecum of YPIII-infected mice 3 dpi compared to uninfected and YPIII Δ*cnfY* infected mice. *Y. pseudotuberculosis* is known to stimulate anti-inflammatory cytokine production during early infection, which is important for virulence (McPhee *et al*., 2012). The lack of early anti-inflammatory cytokine production in the cecum might lead to an accelerated onset of the immune response against YPIII Δ*cnfY*, thereby reducing virulence and improving persistence.

CNF_Y-dependent inflammation during *Yersinia* infection triggers dysbiosis of the microbial community in the gut

Inflammation due to invading pathogens is able to alter the composition of the symbiotic microbial community in the intestinal compartment, a mechanism named dysbiosis, and leads mostly to a bloom of Proteobacteria (Zeng *et al*., 2016). This Proteobacteria bloom is often associated with increased susceptibility to bacterial infection (Buffie *et al*., 2012; Ayres *et al*., 2012; Dicksved *et al*., 2014). Furthermore, *Citrobacter rodentium* and *Salmonella* initiate inflammation in the gut to gain a growth advantage compared with the commensal microbiota (Lupp *et al*., 2007; Barman *et al*., 2008; Kamada *et al*., 2012). Upon *Yersinia* infection, Avican and colleagues detected a decrease in the relative abundance of Bacteroidetes during acute infection, however they did not observe the described bloom of Proteobacteria (Avican *et al*., 2015). The data of this work show that YPIII-induced inflammation but not YPIII Δ*cnfY*-triggered inflammatory reactions caused dysbiosis during late acute *Yersinia* infection with an associated increase of the relative abundance of Proteobacteria, *i.e.* Desulfovibrionales, and a massive decrease in the Bacteroidetes (S24-7). Kamdar *et al*. also observed an outgrowth of Desulfovibrionales upon *Y. enterocolitica* infection in $TLR1^{-/-}$ mice. They revealed, that *Y. enterocolitica*, similar to *S.* Typhimurium, utilizes tetrathionate, which is generated through the reaction of ROS with intestinal thiosulfate in the inflamed gut, thereby mediating the outgrowth of Desulfovibrionales (Winter *et al*., 2010; Kamdar *et al*., 2016). It can be speculated that YPIII Δ*cnfY*-driven inflammation leads to no or decreased tetrathionate production in the inflamed gut, which prevents tetrathionate respiration of YPIII Δ*cnfY* and dysbiosis. Furthermore, outgrowth of Proteobacteria could also be reinforced by higher oxygen concentrations in the inflamed intestine, which inhibits growth of obligate anaerobes, such as Bacteroidetes, but fosters the growth of facultative aerobes, such as Proteobacteria (Zeng *et al*., 2016). This might also indicate that the dampened inflammation during YPIII Δ*cnfY* infection might circumvent dysbiosis and clearance.

Similar to the present study, the relative abundance of *Lactobacillaceae* was also decreased in the work of Kamdar and colleagues and therapy with *Lactobacillus* species prevented Desulfovibrionales outgrowth and improved *Y. enterocolitica* clearance (Kamdar *et al*., 2016). Whether this effect could be reproduced using the infection model described in this work and whether *Lactobacillus* transfer influences *Y. pseudotuberculosis* persistence remains to be determined.

The gut-associated microbial genus *Akkermansia* belongs to the Verrucomicrobiota. *Akkermansia* was specifically associated with increased barrier integrity and protection upon administration as a probiotic, suggesting that it might protect against microbial encroachment

(Everard *et al*., 2013). However, upon *S*. Typhimurium infection, the presence of *Akkermansia* has been found to increase tissue inflammation. The same study also showed that *Akkermansia* degrades mucin, in response most likely enabling increased access of *Salmonella* to host tissue and its overgrowth (Ganesh *et al*., 2013). Thus, the increased abundance of the Verrucomicrobiota upon YPIII Δ*cnfY* infection might support colonization.

***Yersinia* infection might trigger long-term gut dysfunction**

Interestingly, very mild diarrhea was still observed during persistent infection phase in both *Y. pseudotuberculosis* infection groups. The grade of inflammation and dysbiosis correlated with the severity of diarrhea during early infection, whereas sustained diarrhea during late infection was not associated with altered microbial community composition or pathologic tissue alterations. In a study by Fonseca and co-workers, it was demonstrated that *Y. pseudotuberculosis* is able to elicit long-term impairment of mucosal immune functions even after its clearance (Fonseca *et al*., 2015): They showed that the intestinal microbiota was able to infiltrate the deeper-lying tissue, thereby debilitating tolerance and immunity (Fonseca *et al*., 2015), indicating that not only *Yersinia* by itself but also dislocated microbiota might foster prolonged gut dysfunction. Infections with *Yersinia* spp. have also been linked to inflammatory complications after acute gastroenteritis, encompassing Crohn's disease, ulcerative colitis, irritable bowel syndrome, intestinal malabsorption and non-infective colitis (Ternhag *et al*., 2008), suggesting that tissue impairment might contribute to the development of sequelae. In patients suffering from irritable bowel syndrome, only subtle changes in immune cell composition are observed: especially mast cells are significantly more abundant in the gut tissue (Weston *et al*., 1993; O'Sullivan *et al*., 2000; Bercik *et al*., 2005) and a higher abundance and/or an activation of mast cells are clearly connected with chronic diarrhea (Yen and Pardi, 2011). Moreover, the *il-1β* expression in tissue biopsies from patients suffering from irritable bowel disease is also significantly increased in comparison to healthy persons (Gwee *et al*., 2003). Similar to that, only mild inflammation was observed during persistent *Yersinia* infection visible by diffuse infiltration of neutrophils into the LP of the cecum (3.2.1). Additionally, up-regulation of mast cell proteases (*mcpt1/2*) and *il-1β* expression during persistent *Yersinia* infection (both YPIII and YPIII Δ*cnfY*) was observed (3.4.3). Together, this suggests that prolonged diarrhea after and during *Y. pseudotuberculosis* infection in BALB/c mice, might be due to subtle alterations in the gut tissue, which resembles those connected with irritable bowel syndrome.

In conclusion, YPIII-driven inflammation results in severe pathogenesis encompassing dysbiosis, severe tissue pathology, and enhanced IL-6 production. This might result in development of adaptive immunity and bacterial clearance events. On the other hand, YPIII Δ*cnfY* elicits milder inflammation, which is associated with enhanced persistence, a lack of dysbiosis and decreased IL-6 levels in comparison to YPIII. Together these results suggest that acute inflammation and host immune responses to the respective *Y. pseudotuberculosis* infection influence the development of persistent infection.

4.3 Crosstalk of genomes - complex host-pathogen interactions

Infection with a pathogen challenges the host to mount innate and adaptive immune responses against the invader. Also, the intruding pathogen is confronted with harsh and hostile conditions in the host and has to employ its virulence strategies. This demands readjustment of both, host and pathogen, transcriptional expression profiles, which are interconnected through complex host-pathogen interaction networks. Studies analyzing this issue *in vivo* are realized via different means, such as knockout mutant analysis or more global approaches, for instance proteome and transcriptome analysis. In this study, the global mRNA transcriptome of the host and the expression of important factors for *Yersinia* virulence and persistence during acute and persistent *Y. pseudotuberculosis* infection in BALB/c mice were assessed. The data are discussed in the following sections.

4.3.1 CNF_Y sufficiency and deficiency shapes the host transcriptome during acute and persistent infection

The deletion of a single virulence gene is generally not expected to strongly impact overall immune signaling. This is supported by the study of Arsenault and co-workers, who showed that the deletion of the kinase inhibitor AvrA of *Salmonella* caused similar phosphorylation patterns on immune signaling proteins as the wild type (Arsenault *et al*., 2016). This is reinforced by the work of Price and Abu Kwaik, who showed that AnkB, which confers intracellular *Legionella pneumophila* replication, does not alter the transcription profile of human macrophages (Price and Abu Kwaik, 2014). However, a study by Wang *et al*. analyzed the impact of SpeG of *Salmonella* on Caco-2 and M-cells. They found that SpeG alters immune signaling, resulting in different immune responses (Wang *et al*., 2016b).
The virulence factor CNF_Y of *Y. pseudotuberculosis* mainly functions to enhance translocation of the Yop effectors into host immune cells (Wolters *et al*., 2013; Schweer *et a*l., 2013; Janina Schweer, PhD thesis), which might manipulate Yop effector functions during the infection. Thus, it was not surprising that the transcriptional profiles differed between the *Y. pseudotuberculosis* strains YPIII and YPIII Δ*cnfY*.

Analysis of the acute infection phase reveals regulation of inflammation and immune responses after challenge with *Y. pseudotuberculosis*
It is well known that *Y. pseudotuberculosis* infection triggers inflammation. As expected several inflammatory modulators, acute phase proteins, metal ion sequestration, and proteins involved in bacterial killing and growth restriction were up-regulated during *Y. pseudotuberculosis* infection irrespective of the presence of CNF_Y. Almost all of these commonly up-regulated genes were also found to be most highly induced during *Y. pseudotuberculosis* IP32953 infection of the PP in BALB/c mice (Nuss *et al*., 2017). This suggests that a common core regulon is triggered by infection with *Y. pseudotuberculosis* in the gut associated tissues. Similar to the work of Nuss and colleagues, most of the detected, highly induced transcripts are specific for neutrophils (Nuss *et al.*, 2017), emphasizing that the immune response to *Y. pseudotuberculosis* YPIII/YPIII Δ*cnfY* is also dominated by infiltrating neutrophils.

YPIII triggers expression of IL-6-inducible genes
The analysis of host genes that are *cnfY*-dependent, demonstrated distinct tissue and immune reactions. In accordance to the cytokine levels observed in the cecum, YPIII infection drove a stronger induction of *il-6* gene expression and expression of genes related to IL-6-induced

pathways, for instance acute phase proteins, haptoglobin, matrix metalloproteinases, and angiogenesis (Heinrich *et al*., 1990; Cronstein, 2007; Nagasaki *et al*., 2014; Kelwick). Remarkably, the matrix metalloproteinase pathway is linked to tissue destruction (Birkedal-Hansen, 1993; Elkington *et al*., 2005), which might also contribute to increased tissue pathology upon YPIII infection. Moreover, the acute phase proteins Chil3 and Cxcl2, which attract neutrophils, and the neutrophil derived matrix metalloproteinase MMP8 that facilitates chemokine gradients to attract neutrophils, were more strongly induced during YPIII than during YPIII Δ*cnfY* infection. This supports the assumption that YPIII drives massive neutrophil infiltration, which results in exacerbated immune responses and uncontrolled tissue destruction and reorganization (Figure 4.1).

YPIII Δ*cnfY* drives expression of IL-22 and IFN-inducible genes

In contrast to YPIII, an increased expression of IL-22-inducible genes, such as fucosyltransferase 2, dual oxidase 2, RegIII and other defensins, was observed during YPIII Δ*cnfY* infection (3.4.1; Mizoguchi, 2012; Grasberger *et al*., 2015; Parks *et al*., 2016). In *Citrobacter* intestinal infections, IL-22 was associated with reduction of colitis severity, while IL-22 is also necessary to avoid systemic inflammation and bacterial admittance to lymphatic tissues (Zheng *et al*., 2008; Sonnenberg *et al*., 2011; Sonnenberg *et al*., 2012; Grasberger *et al*., 2015). A study on *Y. pseudotuberculosis* also demonstrated that RegIIIβ decreases *Yersinia* encroachment of the PP (Dessein *et al*., 2009). Hence, increased expression of IL-22-inducible genes during YPIII Δ*cnfY* infection might contribute to decreased disease severity and tissue invasion compared to YPIII infection (Figure 4.1). In addition, increased IFNγ production and enhanced expression of many interferon-inducible genes, such as genes for antigen presentation, the inducible nitric oxide synthase, and the interferon-inducible GTPases, were detected during YPIII Δ*cnfY* infection (3.4.1 & 3.5) (Boehm *et al*., 1997; MacMicking, 2012). The latter are associated with the control of bacterial infections involving antimicrobial activities, such as promotion of canonical and non-canonical inflammasome activation (Taylor *et al*., 2000; Tietzel *et al*., 2009; Al-Zeer *et al*., 2013; Meunier and Broz, 2015; Pilla *et al*., 2014; Man *et al*., 2015; Finethy *et al*., 2015; Meunier *et al*., 2015). To foster inflammasome activation, the GTPases destabilize the phagosome or pathogen-containing vacuole, thereby releasing LPS into the host cytosol (Meunier *et al*., 2014). Caspase-11 directly binds the cytosolic LPS and becomes activated, triggering pyroptosis and release of pro-inflammatory cytokines, such as IL-1α (Yazdi and Drexler, 2012; Shi *et al*., 2014). The detected cytokines and RNA-profiles of the cecal samples support that YPIII Δ*cnfY* infection induces pyroptotic cell death of activated phagocytes, triggering increased amounts of IL-1α.

Some pathogens exploit lytic host cell death to escape the host cell and to colonize the extracellular space (Traven and Naderer, 2014; Chow *et al*., 2016). Particularly, caspase-11-mediated pyroptosis is able to trigger *Salmonella* proliferation and dissemination (Broz *et al*., 2012). Moreover, *S.* Typhimurium and *L. monocytogenes* exploit the type I IFN pathway to establish infection (Auerbuch *et al*., 2004, Robinson *et al*., 2012). Previously, pathogenic yersiniae have also been detected inside phagocytes *in vivo* and *in vitro* (Rosqvist *et al*., 1988; Pujol and Bliska, 2003). Furthermore, decreased Yop translocation of YPIII Δ*cnfY* might impair the blockage of phagocytosis, allowing bacterial uptake and pro-inflammatory signaling (Rosqvist *et al*., 1988; Pha and Navarro, 2016; Zhang *et al*., 2016a) This, altogether, indicates that cell lysis and/or IFN-mediated signaling during YPIII Δ*cnfY* infection might similarly support bacterial colonization of the host (Figure 4.1).

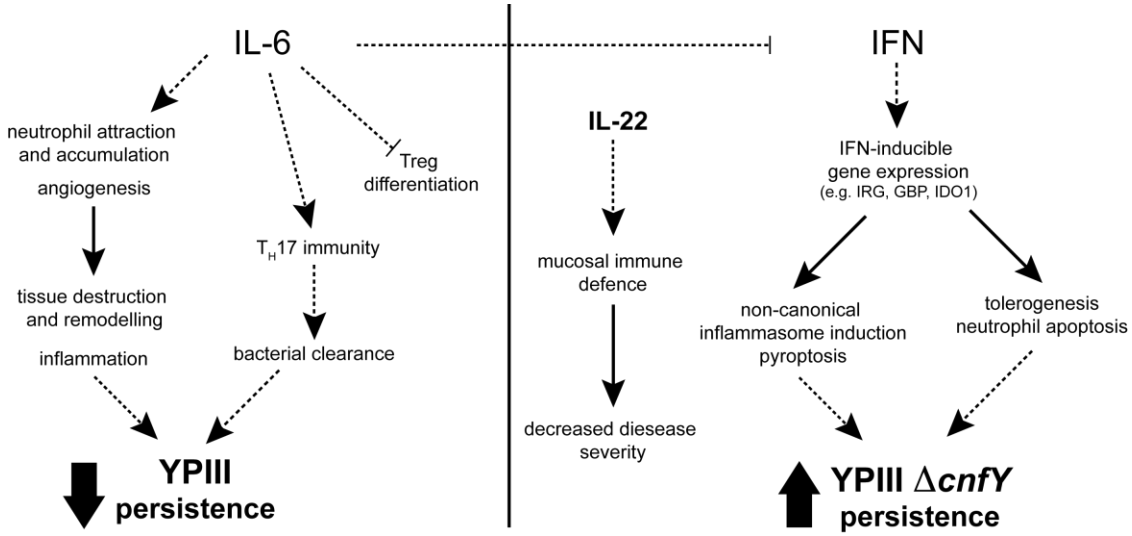

Figure 4.1 CNF_Y-dependent cytokine signaling shapes the host transcriptional landscape during acute *Yersinia* infection.

Prevalence of IL-6 levels during *Y. pseudotuberculosis* YPIII infection drives immunopathology, IFN signaling suppression and clearance of *Yersinia* (left site), whereas reduced IL-6 levels during YPIII Δ*cnfY* infection allow IFN pathway induction, tolerogenesis and decreased clearance of *Yersinia*. Induction of IL-22 associated genes might contribute to host barrier protection and decreased disease severity.

IFN-induced *ido1* expression might facilitate YPIII Δ*cnfY* persistence

The IFN-inducible indoleamine 2,3-dioxygenase (*ido1*) was the most highly induced gene during YPIII Δ*cnfY* infection compared to YPIII infection. IDO1 is a multifaceted enzyme of the tryptophan catabolism that locally regulates immunity, thereby mediating either protection or disease (Zelante *et al*., 2009; Carlin *et al*., 1989). Through the depletion of tryptophan and the generation of kynurenine metabolites, IDO1 inhibits T cell proliferation, induces T cell apoptosis (Frumento *et al*., 2002; Murakami *et al*., 2013) and triggers the differentiation of Tregs, which inhibit effector T cells (Fallarino *et al*., 2006; von Boehmer, 2005). Moreover, induction of *ido1* in DCs promotes immune tolerance and restricts immunity (Mellor and Munn, 2004; Romani *et al*., 2006), which benefits parasitic, viral and bacterial persistent infections (Sanchez and Yang, 2011; Mellor and Munn, 2008). Notably, *ido1* expression was implicated in infections with pathogens causing persistent infections (Pantoja *et al*., 2001; Desvignes and Ernst, 2009; Loughman and Hunstad, 2012; Larussa *et al*., 2014). During human immunodeficiency virus (HIV) infection, *ido1* over-expression is linked to the impairment of T cell immunity, which dampens HIV-specific immune responses (Favre *et al*., 2010; Boasso *et al*., 2008). During bacteria-induced granulomatous disease, a significant amount of the ring structure cells are IDO1-positive, which possibly prevents clearance of the granulomas (Popov *et al*., 2006, Popov *et al*., 2008, Desvignes and Ernst 2009, Barth and Raghuraman, 2014). Moreover, IDO1 restricts pathology during *C. difficile* intestinal infections by inducing neutrophil apoptosis (El-Zaatari *et al*., 2014). As acute pathology in the YPIII Δ*cnfY*-infected cecum is less severe than during YPIII infection, these data propose a similar mechanism during YPIII Δ*cnfY* infection. In summary, IDO1 induced tolerogenesis is a possible mechanism that might foster YPIII Δ*cnfY* long-term infection and protection from the immune system (Figure 4.1). Whether IDO1 inhibition by administration of 1-methyl-D-tryptophan prevents the development of persistent *Yersinia* infection should be addressed in the future.

Increased IL-6 levels might inhibit immune suppression

It is noteworthy that the tolerogenic function of *ido1*-expressing DCs is abrogated by IL-6 (Grohmann *et al*., 2001). A study on *M. tuberculosis* showed that IL-6 expression inhibits type I interferon signaling by down-regulating the expression of type I interferon-inducible genes, such as *irg1* (Martinez *et al*., 2013), proposing that reduced IL-6 production during YPIII Δ*cnfY* infection might facilitate IFN signaling, whereas a high level of IL-6 prevents IFN signaling and immune regulation upon YPIII infection. As IL-6 protects against *Y. enterocolitica* infection and facilitates bacterial clearance (Dube *et al*., 2004), production of high IL-6 levels during YPIII infection might induce T_H17 immunity and confer potent clearance, while impairing Treg differentiation (Kimura and Kishimoto, 2010) (Figure 4.1). Whether administration of IL-6 during YPIII Δ*cnfY* infection decreases persistence, should be addressed in the future. Interestingly, human IL-6 polymorphisms, that cause increased production of IL-6 are more prevalent in regions with a high pathogen burden, suggesting increased IL-6 levels are necessary to confer pathogen clearance (Napolioni and MacMurray, 2016).

Altogether, this data suggests, that CNF_Y-dependent cytokine responses drive the transcription of different signaling cascades, which favor either bacterial clearance or benefit bacterial long-term colonization (Figure 4.1).

Persistent *Yersinia* infection is marked by a mélange of immune suppression and infection control

The comparison of the gene expression profiles of persistent *Yersinia*-infected mice to uninfected mice suggested that the infection triggers chronic gut dysfunction and diarrhea (discussed in 4.2). The persistent *Yersinia* infection induced expression of immunoglobins and mobilization of neutrophils by Cxcl2 expression (Day and Link, 2012), which resulted in the attraction of neutrophils and increased abundance of neutrophil associated genes, *i.e. clec4d, il-1β, hp, slpi*, and *trem1*. This indicates that development of B cell immunity and recruitment of neutrophils are involved in the containment of persistent *Yersinia* infection (Figure 4.2). The induction of *mmp3* expression during persistent *Yersinia* infection might also foster T_H recruitment and infection control (Li *et al*., 2004). Interestingly, the secretory leukocyte protease inhibitor SLPI harbors not only antimicrobial activity (Hiemstra *et al*., 1996), but also suppresses immune signaling and responses, such as the NFκB pathway and the formation of neutrophil extracellular traps (Weldon and Taggart, 2007; Zabieglo *et al*., 2015). Thus, *slpi* expression might contribute to suppression of inflammation during persistent bacterial colonization, thereby preventing tissue damage but also enhancing bacterial persistence. In addition to *slpi* expression, the arginase-1 transcript, which is associated to the abundance of myeloid suppressor cells (Popovic *et al*., 2007), was induced during persistent *Yersinia* infection. Arginase-1 depletes arginine in the host environment and thereby impairs NO production and T cell immunity by inhibiting T cell proliferation, T cell receptor expression and T cell memory (Bronte *et al*., 2003). During chronic colitis, the induction of arginine metabolism is a protective mechanism against exacerbated T cell activities (Kurmaeva *et al*., 2014). Moreover, activation of arginase-1 during viral and bacterial infections is connected with immune evasion and chronic infection (Lewis *et al*., 2011; Burrack *et al*., 2015; Knippenberg *et al*., 2015; Goh *et al*., 2016). Remarkably, *H. pylori* also actively evades T cell immunity in the host by expressing a *Helicobacter*-encoded arginase (Zabaleta *et al*., 2004). This indicates that *Yersinia* persistence might be fostered by *arg1* expression, similar to IDO1 induction during acute YPIII Δ*cnfY* infection.

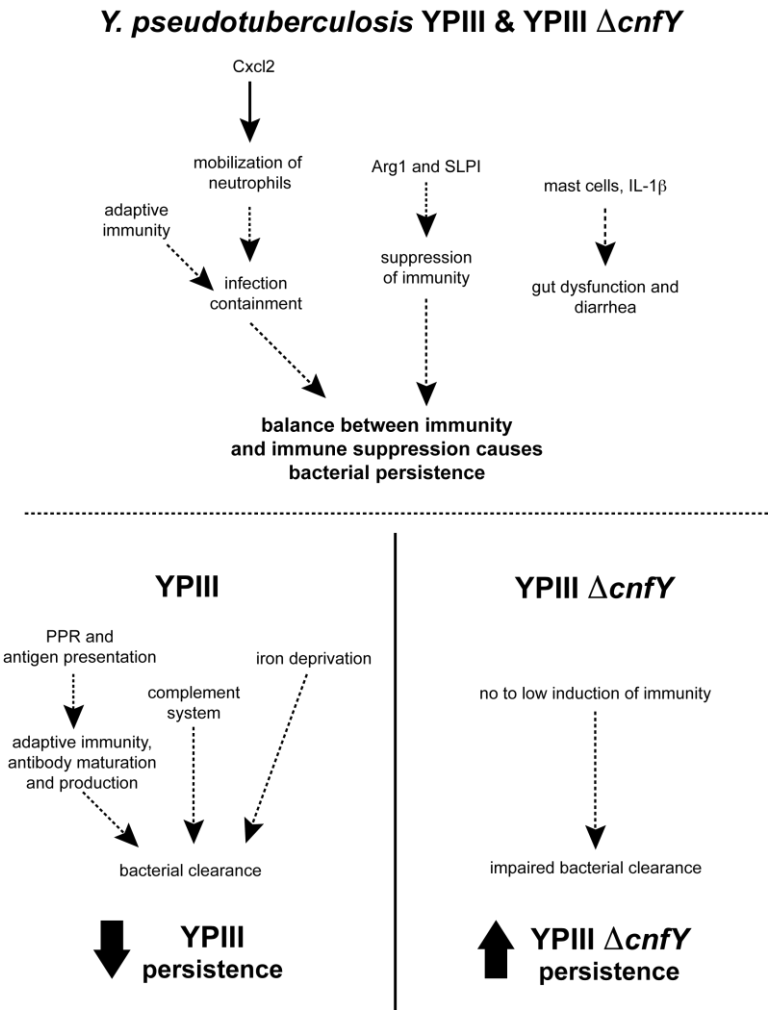

Figure 4.2 Dampened host immunity benefits persistence of *Y. pseudotuberculosis* YPIII Δ*cnfY*.
Yersinia persistence is a balance between immune responses that confer infection containment and suppression of immune responses (upper panel). The strong induction of immune responses during persistent YPIII infection shifts the balance towards pathogen clearance. In contrast, diminished immune responses to YPIII Δ*cnfY* infection prevent effective pathogen elimination (lower panel).

Interestingly, chronic stimulation of the immune system with type I interferon and IL-1β is associated with the generation of myeloid suppressor cells, which are also more frequently observed in *H. pylori*-infected patients (Mesali *et al*., 2016; Tu *et al*., 2008; Taleb *et al*., 2017). The sequencing data of this thesis also indicated the presence of myeloid suppressor cells by detection of arginase-1 transcript, yet this remains to be verified.
In summary, persistent *Yersinia* infection encompasses the balance between infection containment and inhibition of immunity that prevents pathology but also facilitates pathogen long-term infection (Figure 4.2).

Presence of CNF_Y might stimulate clearance by the immune system
Similar to acute *Y. pseudotuberculosis* infection, persistent YPIII infection triggered stronger and/or varying tissue and immune response reactions in the cecum, which are linked to host defense and pathogen clearance, *e.g.* the complement system, T cell immunity, antigen presentation and antibody maturation. This analysis supports the hypothesis that YPIII activates host immunity during persistent infection resulting in a shift of the balance between persistence and clearance towards pathogen elimination (Figure 4.2). In contrast, persistent

YPIII Δ*cnfY* infection only very mildly induced expression of host immune response associated transcripts, which might impair YPIII Δ*cnfY* elimination (Figure 4.2). Persistence of other pathogens is also fostered by impaired or lacking immune responses (Gercken *et al*., 1994; Stevens *et al*., 1994; Knipp *et al*., 1994; Molinari *et al*., 1998). The best studied among them is *H. pylori* that evolved several sophisticated mechanisms to avoid the development of effective immunity: *Helicobacter* secretes factors that impair IL-12 expression and release during infection, which avoids mounting of effective T_H1-derived immunity, and prevents the proliferation of T cells (Ishii *et al*., 2008; Kao *et al*., 2006; Weiss *et al*., 2013). Moreover, *H. pylori* manipulates DC maturation and induces the development of tolerogenic DCs, which drives differentiation of immune-suppressive Tregs (Oertli *et al*., 2012; Zhang *et al*., 2010). Further experiments should address the adaptive immune evasion strategy of *Y. pseudotuberculosis*. Especially, the evasion strategy of YPIII Δ*cnfY*, which suppresses protective immune responses during persistent YPIII Δ*cnfY* infection, should be analyzed.

4.3.2 The transcriptional adaptation strategy of *Y. pseudotuberculosis* during infection

Studies on *Yersinia* transcription profiles during acute infection *in vivo*, showed that the transcriptional profile is distinct from virulence-relevant *in vitro* culture conditions, highlighting that the host environment confronts the bacterium with complex growth conditions that drive transcriptional adaptation programs that are either not or only partly experienced in an *in vitro* culture (Lathem *et al*., 2005; Avican *et al*., 2015; Nuss *et al*., 2017). The study of Avican and co-workers in 2015 on *Y. pseudotuberculosis* transcriptional programming during acute and persistent infection in FVB/N mice elucidated that *Yersinia* undergo a transcriptional adaptation process that reduces virulence traits, enhances overall stress resistance, and induces anaerobic growth (1.4.2; Avican *et al*., 2015). Although this transcriptional adaption process was mainly also detected during the infection in the present study, some differences in the gene transcription profiles of *Y. pseudotuberculosis* were observed compared to those detected in FVB/N mice. Unlike to FVB/N mice, *fnr* and *cspC* were not induced during persistent *Yersinia* infection. *fnr* mutants persist like the wild type *Y. pseudotuberculosis* in FVB/N mice (Avican *et al*., 2015), demonstrating that *fnr* is not necessarily needed for establishment of persistent infection. As the RNA chaperone CspC stabilizes the alternative sigma factor σ^S (*rpoS*), *cspC* expression is important for salt and acid induced stress responses (Cohen-Or *et al*., 2010; Derman *et al*., 2015). This suggests that *Yersinia* infection in FVB/N mice mounts other stresses, *e.g.* stronger neutrophil recruitment, that demand stable stress responses (Cohen-Or *et al*., 2010; Avican e*t al*., 2015).

Expression of *yopJ, ail, cnfY* and *uspA* might modulate *Yersinia* persistence and host immunity

The expression of the virulence factors *yopJ* and *ail* was not down-regulated during persistent infection of BALB/c mice compared to the expression profile in FVB/N mice. YopJ was previously shown to be dispensable for the establishment of persistent infection in FVB/N mice (Fahlgren *et al*., 2014); nevertheless the results of the present work strongly indicate that YopJ might play a crucial role during persistent *Y. pseudotuberculosis* infection. As YopJ inhibits the MAPK and NFκB pathways, induces apoptosis, and is important for intestinal epithelium disruption and dissemination from the gut intestinal epithelium (Monack *et al*., 1997; Monack *et al*., 1998; Meinzer *et al*., 2012; Zhang *et al*., 2016a), enhanced transcription of *yopJ* might confer (1) immune suppression and reduced clearance and (2) a possible mechanism to allow continuous dissemination and colonization of the cecum (Figure 4.3).

Together this suggests that *yopJ* might be crucial for persistent colonization of the cecum in BALB/c in contrast to FVB/N mice. The adhesin Ail is responsible for serum resistance, adherence to cells and autoaggregation of *Yersinia* (Biedzka-Sarek *et al*., 2005; Felek and Krukonis, 2009; Rebecca Geyer, PhD thesis), which proposes that *ail* expression during persistent infection, is important to defend against humoral immunity. Enhanced *ail* expression might also promote increased protection against phagocytosis and elimination by the formation of multi-cell aggregates. Moreover, increased expression of *ail* during persistent infection might support tight cellular adherence and dense bacterial packaging, as observed in cecal tissue preparations (3.2.3).

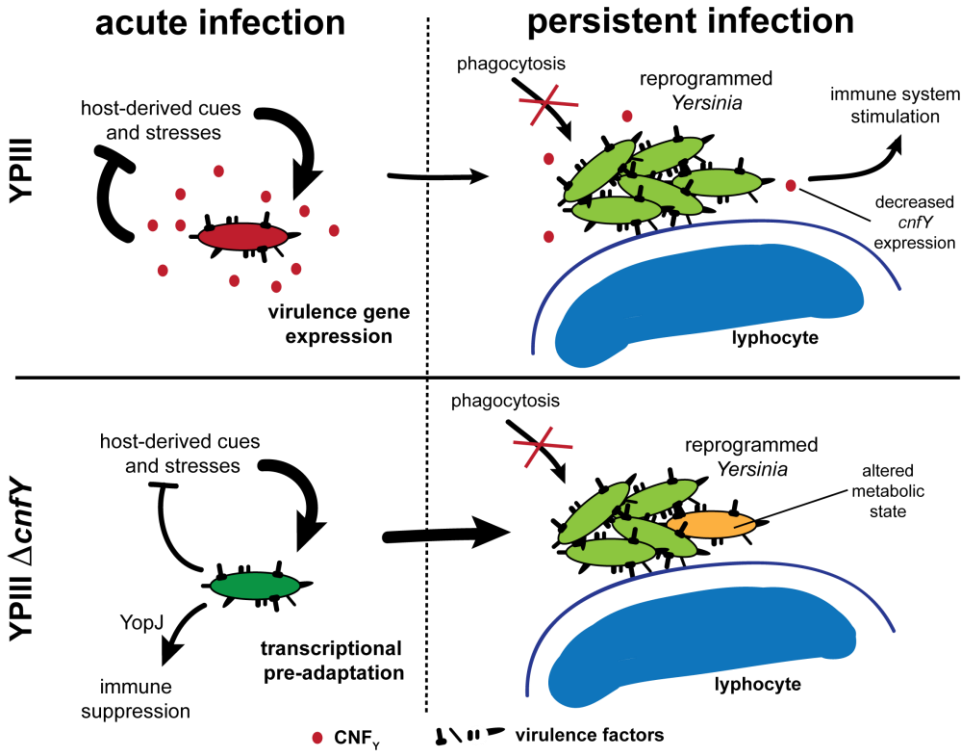

Figure 4.3 Model of the *Y. pseudotuberculosis* gene expression strategy during acute and persistent infection.

cnfY expression during the acute phase of the infection enhances translocation of Yop effectors into host immune cells (Schweer *et al*., 2013), thereby suppressing host-derived stresses and bacterial elimination. Inflammation-driven recruitment of neutrophils stimulates ongoing virulence-gene expression. Deletion of CNF_Y provokes enhanced abundance of host-derived cues and stresses, which fosters transcriptional adaptation causing pre-adaptation for transcriptional reprogramming. This enables transition to persistent infection compared to CNF_Y-expressing *Yersinia*. The sustained expression of *ail* and *yopJ* during persistent *Yersinia* infection are likely to contribute to an anti-inflammatory environment, resistance against phagocytosis, and enables dissemination and re-colonization. Increased *uspA* expression in the YPIII Δ*cnfY* population might indicate that at least a part of the bacteria reside in an altered metabolic state, as known for persister cells, while sustained secretion of CNF_Y might stimulate immune responses.

Remarkably, the stress protein UspA was differentially expressed between the two *Y. pseudotuberculosis* strains during persistent infection. *uspA* expression is induced upon metabolic, oxidative, and temperature stress. Moreover, *uspA* is highly expressed in cells that enter stationary phase or are growth-arrested (Liu *et al.*, 2007). As YPIII Δ*cnfY* is confronted with decreased host-derived stresses compared to YPIII, this suggests that at least a part of the YPIII Δ*cnfY* population could be in a different metabolic state than persistent YPIII bacteria

(Figure 4.3), allowing persistence over long periods of time with rare clearance events, as observed in this thesis.
Although *cnfY* expression is down-regulated during persistent infection, low but sustained production of CNF_Y might stimulate the immune system to clear the infection (Figure 4.3, 4.3.1). This hypothesis is supported by recent publications, which recognized CNF_Y and CNF1 as potent immunogens and immunoadjuvants (Mou *et al*., 2012; Michel *et al*., 2016).

YPIII Δ*cnfY* undergoes a transcriptional pre-adaption process during acute infection
Recently, a study on *S. aureus* showed that a differential immune response of the host affects the transcriptional landscape of the bacterium (Thänert *et al*., 2017). Noteworthy, the expression profiles of important *Yersinia* persistence and virulence factors from YPIII Δ*cnfY* during acute infection were different to those observed during acute YPIII infection. In YPIII Δ*cnfY*, increased expression of anaerobiosis genes (*arcA*, *frdA*, *napA*), stress response genes (*hdeB*, *rfaH*, *sodB*, *wrbA*), virulence factors (*i.e. ail* and *yopJ*), *crp* and *rovA* was observed. This expression pattern suggested that host-derived environmental cues and stresses, which are discussed above, trigger a transcriptional pre-adaptation of YPIII Δ*cnfY*, which might ease the transition to persistent colonization of the host (Figure 4.3). One can speculate that this transcriptional pre-adaptation confers an advantage to YPIII Δ*cnfY* bacteria in comparison to YPIII: wild type *Y. pseudotuberculosis* has to undergo stronger transcriptional reprogramming, thereby impairing effective and accurately-timed transcriptional switches (Figure 4.3). This hypothesis is reinforced by the study by Avican and colleagues that showed that *Y. pseudotuberculosis arcA*, *frdA*, and *wrbA* mutants are somewhat impaired in the establishment of persistent infection (Avican *et al*., 2015). Increased expression of *yopJ* during the acute infection with YPIII Δ*cnfY* might further foster persistent infection by suppression of immune responses.

4.4 CNF_Y-dependent host-pathogen interactions – a decision between immune suppression and clearance

The results of this work provide a new understanding of the host-pathogen interactions during acute and persistent *Y. pseudotuberculosis* infection and illustrate the dominant role of CNF_Y in *Y. pseudotuberculosis* YPIII pathogenesis. Adapted from these data, a multifaceted model of the acute and persistent infection can be proposed (Figure 4.4).

Consistent with the studies by Schweer and colleagues, secretion of CNF_Y during the acute stage of infection triggers a pro-inflammatory cascade that leads to a strong inflammatory reaction, which encompasses enhanced production of IL-6 and IL-6-dependent genes, enhanced neutrophil recruitment, dysbiosis and tissue destruction (Schweer *et al*., 2013; Janina Schweer, PhD thesis; 4.2; 4.3.1). This pro-inflammatory milieu supports the development of protective immunity by T_H17 cells and impairs the differentiation of Tregs, which, together, mediate bacterial clearance (Figure 4.4 upper left). In the absence of CNF_Y, this proinflammatory cascade is less induced, which results in decreased IL-6 levels and the induction of interferon- and IL-22-dependent genes. This leads to a transcriptional pre-adaptation of YPIII Δ*cnfY* and an IDO1-mediated suppression of effector T cells and induction of tolerogenesis. These events allow expedited transcriptional reprogramming in *Yersinia* and impair innate and adaptive immunity, thereby mediating enhanced bacterial persistence (Figure 4.4 upper right).

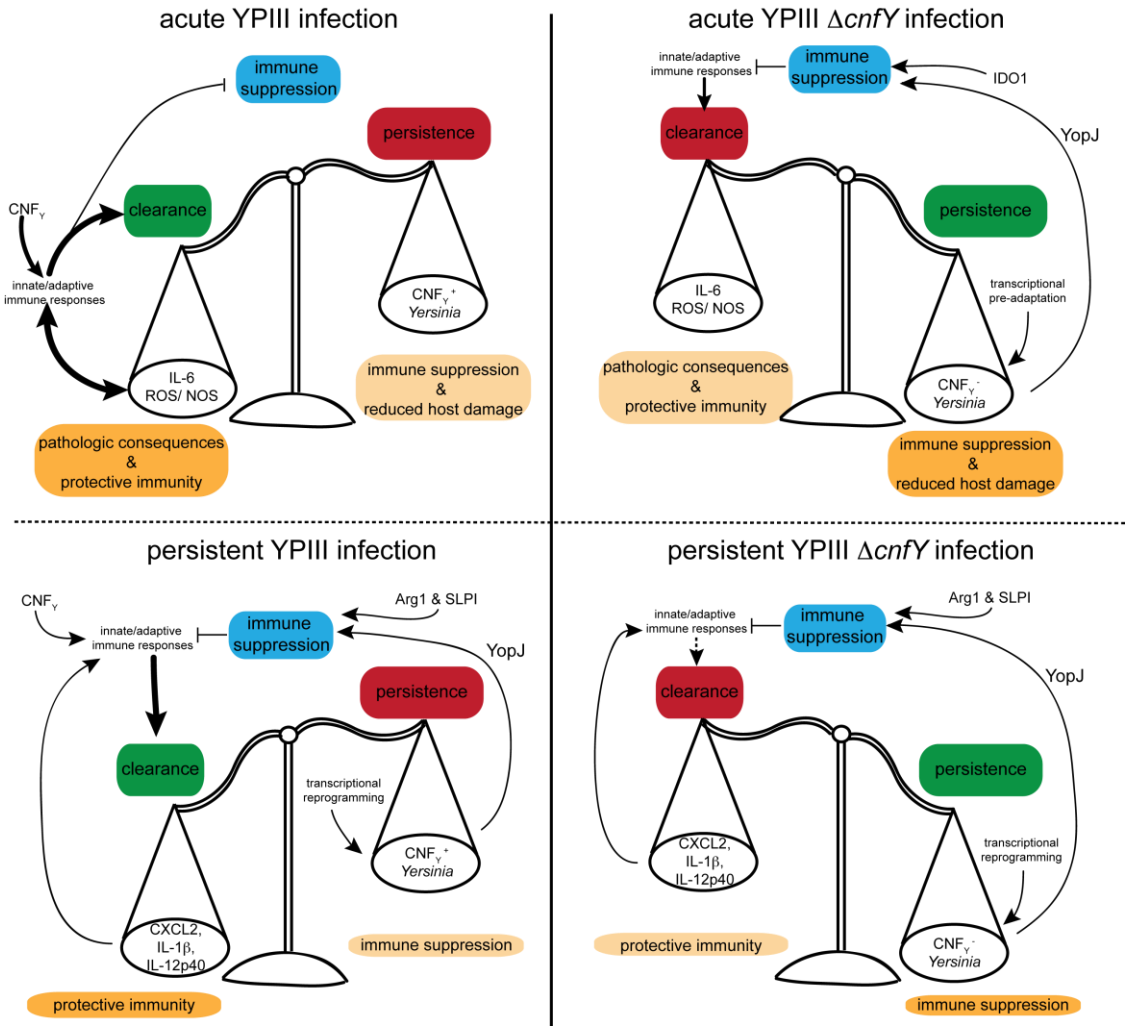

Figure 4.4 The decision between *Y. pseudotuberculosis* clearance and persistence is dependent on CNF_Y.

Model of the CNF_Y-dependent host-pathogen interactions during acute and persistent infection. Bacterial and host-derived genetic factors dictate immune response development or its suppression resulting in either enhancement of bacterial clearance/elimination or development/maintenance of bacterial persistence.

At the persistent stage of the infection, the immune system is balanced between infection containment by the immune system and immune suppression through Arg1 and SLPI (Figure 4.4 lower panels). Moreover, *Yersinia* has reprogrammed its gene expression from virulent to a stress-adapted phenotype and the expression of *yopJ* and *ail* facilitates immune evasion (Figure 4.4 lower panels). However, YPIII is more strongly impaired in maintaining persistent infection of mice in comparison to YPIII Δ*cnfY*: persistent YPIII infection induces sustained activation of the immune system that is most likely triggered by the production of CNF_Y, causing decreased persistence and elimination of YPIII infection (Figure 4.4 lower left). In contrast, the stimulation of the immune system is decreased during persistent YPIII Δ*cnfY* infection, resulting in enhanced persistence of YPIII Δ*cnfY* infection (Figure 4.4 lower right).

4.5 Murine genetics and the inflammasome network influence systemic *Y. pseudotuberculosis* dissemination

Host susceptibility is linked to genetic predispositions

Resistance to an infection is not determined by the pathogen alone but also by the genetic predisposition of the host (Casanova, 2015a,b; Shukla *et al*., 2015; Wu and Holland, 2016; Thänert *et al*., 2017). Many studies have shown that C57BL/6 mice are more resistant against bacterial infections than BALB/c mice (Murphy *et al*., 2001; Hancock *et al*., 1986; Arko-Mensah *et al*., 2009; Jiang *et al*., 2010). This is linked to the genetic background of these two mouse strains. C57BL/6 mice favor the development of T_H1-dominated immune responses, whereas BALB/c mice develop T_H2-dominated immunity (Hsieh *et al*., 1995; Mills *et al*., 2000a). During *Y. enterocolitica* infections the major T_H1-cytokine IFNγ determines susceptibility to the infection and is crucial for mediating bacterial clearance, thus explaining why BALB/c mice are more susceptible to *Yersinia* infection than C57BL/6 mice (Autenrieth *et al*., 1994). Moreover, the macrophages of C57BL/6 mice exhibit effective bactericidal activities and display M1 macrophage polarization, while BALB/c mice mount primarily M2 macrophage polarization, which is associated with impairment in bacterial clearance and susceptibility to *Yersinia* infection (Mills *et al*., 2000a; Watanabe *et al*., 2004; van Erp *et al*., 2006; Tumitan *et al*., 2007). The current study also confirms that C57BL/6N mice are more resistant against *Y. pseudotuberculosis* YPIII infection. However, the survival of C57BL/6N mice after *Y. pseudotuberculosis* YPIII Δ*cnfY* infection is still significantly increased compared to a *Y. pseudotuberculosis* YPIII infection, demonstrating a crucial role for CNF_Y in the pathogenicity in both mouse models.

Decreased Yop translocation efficiencies might impair systemic dissemination through the action of neutrophils

Similarly to BALB/c mice (Schweer *et al*., 2013; Janina Schweer, PhD thesis), the histopathology, cytokine levels and immune response were dependent on CNF_Y. The increased relative abundance of neutrophils in C57BL/6N mice compared to BALB/c mice might contribute to increased resistance against *Y. pseudotuberculosis* infection since neutrophils were found to protect against human pathogenic *Yersinia* infection (Conlan, 1997; Laws *et al*., 2010; Westermark *et al*., 2014; Vagima *et al*., 2015). As a consequence, the human pathogenic *Yersinia* spp. successfully developed defense mechanisms against neutrophils and their functions. Via injection of Yop effectors into neutrophils, yersiniae prevent their recruitment, block degranulation, inhibit the respiratory burst, and avoid killing and phagocytosis by neutrophils (Ruckdeschel *et al*., 1996; Spinner *et al*., 2008; Laws *et al*., 2011; Dave *et al*., 2016; Taheri *et al*., 2016). As neutrophils are preferentially targeted by *Y. pseudotuberculosis* TTSS *in vivo* (Schweer *et al*., 2013), it seems reasonable that impaired Yop effector translocation into neutrophils by the *Y. pseudotuberculosis cnfY* mutant might result in impaired escape from neutrophils and decreased dissemination. This assumption is reinforced by a study by Westermark and co-workers. They demonstrated that *yopE* and *yopH* mutants are impaired in early dissemination to the MLNs and that this effect is dependent on neutrophils (Westermark *et al*., 2014). Additionally, a functional TTSS and two other Yop effectors have been shown to be important for *Yersinia* dissemination after intra-gastric challenge: the TTSS is indispensable for systemic dissemination (Balada-Llasat and Mecsas, 2006), YopJ is important for barrier breaching, virulence and colonization of MLNs and spleen (Meinzer *et al*., 2012) and deletion of *yopM* is connected to impaired dissemination to systemic organs and reduced virulence (McPhee *et al*., 2010). This suggests that, overall, decreased Yop

translocation might be responsible for impaired dissemination in C57BL/6N mice. Moreover, YPIII Δ*cnfY* is able to colonize systemic organs after intra-venous administration but is less effective entering the blood stream during the progression of the disease as opposed to the wild type, which, supports this hypothesis. The observed inability of YPIII Δ*cnfY* to effectively cause bacteremia might be also a possible reason for its avirulence during intra-venous infection, since bacteremia could cause sepsis and/or colonization of multiple systemic organs leading to multi-organ failure (Schlag *et al*., 1991; Tsiotou *et al*., 2005; Shah and Reed, 2014).

The inflammasome network is involved in the modulation of CNF_Y-dependent systemic *Y. pseudotuberculosis* dissemination

During bacterial infections NLRs (NOD-and leucine-rich repeat-containing receptor) recognize bacterial derived molecular patterns (*e.g.* flagellin, LPS, secretion system proteins) and assemble together with ASC (apoptosis-associated speck-like protein containing CARD) and pro-caspase-1 to a multi-protein platform called the inflammasome (Man and Kanneganti, 2016). After the assembly, activated caspase-1 is able to cleave pro-IL-1β, pro-IL-18, and gasdermin D that triggers pyroptosis (van de Veerdonk *et al.*, 2011). Procaspase-11 is activated by cytosolic LPS that is released by guanylate-binding proteins (GBPs) from bacteria containing vacuoles (Meunier *et al*., 2014). Thereafter, activated caspase-11 drives non-canonical inflammasome activation via NLRP3 as well as pyroptosis by cleaving gasdermin D (Broz and Dixit, 2016).

At the molecular level, pathogens have evolved strategies to prevent the activation of the inflammasome, for instance IcaA of *Coxiella burnetii*, which inhibits caspase-11 and ExoU of *P. aeruginosa*, which prevents caspase-1 activation (Shin and Brodsky, 2015; Stewart and Cookson, 2016). In *Yersinia*, the TTSS and the Yops also interact with the inflammasome network (Auerbuch *et al*., 2009; Zheng *et al*., 2011; Casson *et al*., 2013; Zwack *et al*., 2015). While the formation of a translocation pore and/or the translocation of the translocon proteins YopB and YopD into the host cell cytosol activate the inflammasome (Auerbuch *et al*., 2009; Casson *et al*., 2013; Zwack *et al*., 2015), YopE/YopH coordinately inhibit integrin-mediated inflammasome activation in intestinal epithelial cells (Thinwa *et al*., 2014). Additionally, YopJ/YopM inhibit the activity of the caspase-1 inflammasome in phagocytes (LaRock and Cookson, 2012; Chung *et al*., 2014; Chung *et al*., 2016; Schoberle *et al*., 2016; Ratner *et al*., 2016). Remarkably, YopJ also prevents pro-inflammatory NFκB and MAPK signaling, thereby favoring caspase-8 activation and apoptotic cell death (Philip and Brodsky, 2012). Activated caspase-8 in turn can also trigger caspase-1 activation in the targeted host cell, which initiates pro-inflammatory immune responses and pyroptosis (Weng *et al*., 2014; Philip *et al*., 2014). This mechanism is particularly important for dissemination from the intestinal compartment (Meinzer *et al*., 2012). In UPEC, CNF1 was also found to activate the inflammasome and induce the release of IL-1β, which elicits protective immune responses (Diabate *et al*., 2015). The cytokine data of the serum revealed that YPIII infection triggered the production of IL-1β and IL-18 and bacterial load determination showed that YPIII was more effectively disseminating to systemic organs compared to the *cnfY* mutant (3.6.1 & 3.6.2). This suggested that CNF_Y-enhanced Yop translocation and/or the CNF_Y toxin itself might facilitate bacterial dissemination, which might be influenced by the inflammasome activity. However, the inflammasome and caspase-1/-11 differently affected the *Y. pseudotuberculosis* dissemination. While coordinated caspase-1/-11 activity and IL-1α-sufficiency were important to foster systemic dissemination of *Y. pseudotuberculosis* YPIII, caspase-11 and IL-1β were important to restrict systemic dissemination of YPIII Δ*cnfY* (3.6.4). Interestingly, the transcriptional profiling in BALB/c mice also suggested that YPIII Δ*cnfY* infection is controlled by the

induction of the non-canonical caspase-11 inflammasome, supporting the assumption that caspase-11 activity might protect against the systemic dissemination of YPIII Δ*cnfY*. This is supported by studies with other pathogens such as *Listeria monocytogenes*, *L. pneumophila*, *Burkholderia thailandensis*, and *Burkholderia pseudomallei*, where the inflammasome activity assists pathogen elimination (Miao *et al*., 2010; Menu and Vince, 2011; Ceballos-Olvera *et al*., 2011; Aachoui *et al*., 2013). Yet, YPIII Δ*cnfY* does not excessively activate IL-1β and IL-18 production in the serum, indicating that diminished inflammasome activity during YPIII Δ*cnfY* infection might also protect against systemic *Yersinia* infections. In contrast, YPIII-induced inflammasome activities, namely pyroptosis and the production of IL-1α, support systemic dissemination. This is reinforced by previous work, which revealed that IL-1α is associated with intestinal inflammation, pathology development and bacterial dissemination upon *Y. enterocolitica* infection (Dube *et al*., 2001). Moreover, pyroptosis was previously connected to *Salmonella* dissemination (Broz *et al.*, 2012; Knodler et al., 2010). Hence, the IL-1α/pyroptosis-axis might support systemic dissemination of YPIII. Interestingly, LPS induced sepsis requires caspase-11 (Wang *et al*., 1998; Kayagaki *et al*., 2011) and the survival experiments in the present work showed that the caspase-11-knockout mice were slightly more resistant against YPIII infection (3.6.4), indicating that caspase-11 might contribute to YPIII infection-mediated pathological consequences. Although epithelial and endothelial cell death are clearly connected with the progression of systemic infections, which presumably lead to sepsis, it is challenging to dissect this process since caspase-1 has several functions beyond pyroptosis and pro-inflammatory cytokine secretion (Labbé and Saleh, 2008; Denes *et al*., 2012). Thus, further experiments in C57BL/6N wild type mice testing whether the administration of caspase inhibitors and/or anti-IL1α/β antibodies impact *Y. pseudotuberculosis* dissemination abilities are needed to verify these assumptions.

Host genetic polymorphisms might contribute to disease progression after *Y. pseudotuberculosis* infection

As IL-1β and inflammasome-associated polymorphisms in humans determine development of sepsis, severity of infectious disease, sequelae of infection (*e.g.* cancer development), and chronic disease/infection (Azad *et al*., 2012; Liu *et al*., 2013b; Opipari and Franchi, 2015; Hong *et al*., 2016; Jiménez-Sousa *et al*., 2017), genetic properties of the host are highly likely to determine the susceptibility to *Yersinia* infection. This is supported by a case report of chronic yersiniosis that was caused by defects in TLR5 and NOD2 recognition due to polymorphisms in these receptors (Netea *et al*., 2010). The present work further reinforces this hypothesis by showing that the bacterial and host genetic predispositions modulate inflammation and infection outcome during acute and persistent *Y. pseudotuberculosis* infection. It will be interesting to analyze whether there are additionally unidentified genetic predispositions that have an impact on disease severity and chronicity of yersiniosis

5 Perspectives

In this work, it was demonstrated that CNF_Y-deficiency increases *Y. pseudotuberculosis* persistence in its preferred niche, the cecum of mice. This is due to altered host-pathogen interactions during acute *Y. pseudotuberculosis* YPIII Δ*cnfY* infection, which favor the switch for bacterial transcriptional reprogramming and host immune suppression. However, the initiating signals that induce the transcriptional re-adaptation in *Y. pseudotuberculosis* YPIII are still unknown. Next experiments should analyze the host's transcriptional profile in a time series after the infection, to identify which host-derived signals drive transcriptional reprogramming of *Y. pseudotuberculosis* YPIII. This will help to identify more putative treatment targets that could be applied to avoid the development of chronic disease. Moreover, inhibitors against the putative treatment targets, IDO1 and Arginase-1, to treat persistent bacterial infections should be tested in the mouse model.

The colonization-pattern analysis suggested that *Y. pseudotuberculosis* forms biofilms and/or aggregates as well as persister cells during persistent infection. To gain reliable data on this, the expression and presence of proteins known for biofilm, aggregate and persister cell formation should be analyzed. This is of particular interest for treatment strategies against persistent *Yersinia* infections, since all these colonization states potentially protect the bacteria against the host immune system and antimicrobial treatment (Mihai *et al*., 2015). The results of these analyses should provide new approaches to design treatment strategies against persistent *Yersinia* infection.

It remains unclear whether persistent *Y. pseudotuberculosis* infection in the murine model also elicits development of reactive arthritis. To evaluate this model to study reactive arthritis, further experiments should assess whether bacterial antigens and *Yersinia*-specific IgA antibodies circulate in the blood stream of persistently infected mice and whether the persistent infection elicits a local inflammatory reaction in the joints of the mice. In this respect, it is also interesting to study whether reactive arthritis development is CNF_Y-dependent.

6 Summary

The bacterial cytotoxic necrotizing factor toxin CNF_Y is important for *Y. pseudotuberculosis* virulence and modulates pathogenesis. This study set forth to characterize the complexity of the CNF_Y-dependent pathogenesis and host-pathogen interactions during acute and persistent *Y. pseudotuberculosis* infection.

The results of this work demonstrated that presence of CNF_Y impaired the development of persistent *Y. pseudotuberculosis* infection. The enhanced persistence of the YPIII Δ*cnfY* was linked to decreased inflammatory tissue alterations, reduced production of IL-6, and lower disease severity during acute infection. Moreover, dysbiosis in the gut during late acute infection was CNF_Y-dependent but eliminated during persistent *Y. pseudotuberculosis* infections.

Analysis of the bacterial colonization patterns using newly engineered, stable red-fluorescent *Y. pseudotuberculosis* enabled the detection of bacterial re-distribution in the cecal lymphoid tissue from acute to persistent infection. The re-distribution during the switch from acute to persistent infection stage was characterized by the absence of microcolonies and increased formation of dense bacterial aggregates during persistent *Yersinia* infection. Mild inflammatory responses in the cecum during persistent *Y. pseudotuberculosis* YPIII and YPIII Δ*cnfY* infection were accompanied by no- to low inflammatory cytokine production.

The results of the host transcription profile analysis demonstrated that acute *Y. pseudotuberculosis* infection induced a common pro-inflammatory immune response in the cecum. However, YPIII infection resulted in the increased transcription of IL-6 induced genes, such as acute phase response proteins, and YPIII Δ*cnfY* infection triggered the transcription of interferon- and IL-22-induced genes, such as IDO1, GTPases and RegIII defensins. In comparison to uninfected cecal tissue, persistent *Y. pseudotuberculosis* infection caused sustained neutrophil recruitment and expression of *il-1β*, mast cell-associated proteases, and arginase-1. Although the acute inflammatory immune response was strongly down-regulated during persistent YPIII Δ*cnfY* infection, persistent YPIII infection fostered the expression of the complement system, antigen presentation and antibody maturation-associated genes.

Transcriptional profiling of selected *Y. pseudotuberculosis* genes that are important for virulence and persistence showed that *Y. pseudotuberculosis* undergoes a transcriptional reprogramming from acute to persistent infection in BALB/c mice and retains the virulence plasmid during persistent infection. The analysis also revealed that the YPIII Δ*cnfY* gene expression profile upon acute infection was distinct from that of the wild type and strongly resembled the gene expression profile during persistent infection.

Detailed analysis of *Y. pseudotuberculosis* CNF_Y-dependent pathogenesis in C57BL/6 mice revealed a similar modulation of virulence and disease progression compared to BALB/c mice. In this study it was also shown that systemic dissemination efficiency of *Yersinia* in C57BL/6N mice was CNF_Y-dependent. The dissemination of YPIII Δ*cnfY* was controlled by IL-1β and caspase-11, whereas YPIII systemic dissemination was supported by IL-1α and collective caspase-1/-11 activity.

In conclusion, this study highlights CNF_Y as a crucial modulator during *Y. pseudotuberculosis* infection. It is a potent modulating factor of immune responses and inflammation that controls pathogenesis and infection outcome. Through its secretion, the toxin triggers strong pro-inflammatory reactions that cause severe acute infection, while CNF_Y-deficiency reduces *Yersinia* virulence and pathology, but causes effective long-term infections that ensure environmental dissemination and reservoir maintenance.

References

Aachoui, Y., Sagulenko, V., Miao, E. A., & Stacey, K. J. (2013). Inflammasome-mediated pyroptotic and apoptotic cell death, and defense against infection. *Current Opinion in Microbiology*. http://doi.org/10.1016/j.mib.2013.04.004

Abele, R., & Tampé, R. (2011). The TAP translocation machinery in adaptive immunity and viral escape mechanisms. *Essays in Biochemistry*, *50*(1), 249–64. http://doi.org/10.1042/bse0500249

Åberg, M., & Siegbahn, A. (2013, May). Tissue factor non-coagulant signaling - molecular mechanisms and biological consequences with a focus on cell migration and apoptosis. *Journal of Thrombosis and Haemostasis*. http://doi.org/10.1111/jth.12156

Abu Kwaik, Y., & Bumann, D. (2013). Microbial quest for food *in vivo*: "Nutritional virulence" as an emerging paradigm. *Cellular Microbiology*, *15*(6), 882–890. http://doi.org/10.1111/cmi.12138

Achtman, M., Zurth, K., Morelli, G., Torrea, G., Guiyoule, A., & Carniel, E. (1999). *Yersinia pestis*, the cause of plague, is a recently emerged clone of *Yersinia pseudotuberculosis*. *Proceedings of the National Academy of Sciences of the United States of America*, *96*(24), 14043–8.

Ahmed, C. M. I., Larkin, J., & Johnson, H. M. (2015). Socs1 mimetics and antagonists: a complementary approach to positive and negative regulation of immune function. *Frontiers in Immunology*, *6*(April), 183.

Akhiani, A. a, Pappo, J., Kabok, Z., Schön, K., Gao, W., Franzén, L. E., & Lycke, N. (2002). Protection against *Helicobacter pylori* infection following immunization is IL-12-dependent and mediated by Th1 cells. *Journal of Immunology (Baltimore, Md. : 1950)*, *169*(12), 6977–84.

Akhshi, T. K., Wernike, D., & Piekny, A. (2014, January). Microtubules and actin crosstalk in cell migration and division. *Cytoskeleton*. http://doi.org/10.1002/cm.21150

Aktories, K., Weller, U., & Chhatwal, G. S. (1987). *Clostridium botulinum* type C produces a novel ADP-ribosyltransferase distinct from botulinum C2 toxin. *FEBS Letters*, *212*(1), 109–113.

Al-Zeer, M. A., Al-Younes, H. M., Lauster, D., Lubad, M. A., & Meyer, T. F. (2013). Autophagy restricts *Chlamydia trachomatis* growth in human macrophages via IFNγ-inducible guanylate binding proteins. *Autophagy*, *9*(1), 50–62.

Alcorn, J. M., Fierer, J., & Chojkier, M. (1992). The acute-phase response protects mice from D-galactosamine sensitization to endotoxin and tumor necrosis factor-alpha. *Hepatology (Baltimore, Md.)*, *15*(1), 122–129.

Aleksic, S., Steigerwalt, A. G., Bockemuhl, J., Huntley-Carter, G. P., & Brenner, D. J. (1987). *Yersinia rohdei* sp. nov. Isolated from Human and Dog Feces and Surface Water. *International Journal of Systematic Bacteriology*, *37*(4), 327–332.

Alto, N. M., Shao, F., Lazar, C. S., Brost, R. L., Chua, G., Mattoo, S., … Dixon, J. E. (2006). Identification of a bacterial type III effector family with G protein mimicry functions. *Cell*, *124*(1), 133–145.

Amerongen, H. M., & Langermann, S. (1992). Antigen transport by intestinal M cells. *Current Opinion in Gastroenterology*, *8*, 983–987.

Amieva, M. R., & El-Omar, E. M. (2008). Host-bacterial interactions in *Helicobacter pylori* infection. *Gastroenterology*, *134*(1), 306–323.

Andersen-Nissen, E., Hawn, T. R., Smith, K. D., Nachman, A., Lampano, A. E., Uematsu, S., … Aderem, A. (2007). Cutting edge: Tlr5-/- mice are more susceptible to *Escherichia coli* urinary tract infection. *Journal of Immunology (Baltimore, Md. : 1950)*, *178*(8), 4717–4720.

Anderson, G. G., Palermo, J. J., Schilling, J. D., Roth, R., Heuser, J., & Hultgren, S. J. (2003). Intracellular bacterial biofilm-like pods in urinary tract infections. *Science*, *301*(5629), 105–107.

Anderson, G. G., Dodson, K. W., Hooton, T. M., & Hultgren, S. J. (2004). Intracellular bacterial communities of uropathogenic *Escherichia coli* in urinary tract pathogenesis. *Trends in Microbiology*. http://doi.org/10.1016/j.tim.2004.07.005

Arko-Mensah, J., Rahman, M. J., Dégano, I. R., Chuquimia, O. D., Fotio, A. L., Garcia, I., & Fernández, C. (2009). Resistance to mycobacterial infection: A pattern of early immune responses leads to a better control of pulmonary infection in C57BL/6 compared with BALB/c mice. *Vaccine*, *27*(52), 7418–7427.

Arsenault, R. J., Genovese, K. J., He, H., Wu, H., Neish, A. S., & Kogut, M. H. (2016). Wild-type and mutant AvrA- *Salmonella* induce broadly similar immune pathways in the chicken ceca with key differences in signaling intermediates and inflammation. *Poultry Science*, *95*(2), 354–63.

Arthur, J. S., & Ley, S. C. (2013). Mitogen-activated protein kinases in innate immunity. *Nat Rev Immunol*, *13*(9), 679–692.

Arts, R. J. W., Joosten, L. A. B., van der Meer, J. W. M., & Netea, M. G. (2013). TREM-1: intracellular signaling pathways and interaction with pattern recognition receptors. *Journal of Leukocyte Biology*, *93*(2), 209–15.

Ashida, H., Mimuro, H., Ogawa, M., Kobayashi, T., Sanada, T., Kim, M., & Sasakawa, C. (2011, December 12). Cell death and infection: A double-edged sword for host and pathogen survival. *Journal of Cell Biology*. Rockefeller University Press. http://doi.org/10.1083/jcb.201108081

Ataie-Kachoie, P., Pourgholami, M. H., Richardson, D. R., & Morris, D. L. (2014). Gene of the month: Interleukin 6 (IL-6). *Journal of Clinical Pathology*, *6*, 1–6.

Atkinson, S., & Williams, P. (2016). *Yersinia* virulence factors - a sophisticated arsenal for combating host defences. *F1000Research*, *5*, 1370.

Auerbuch, V., Brockstedt, D. G., Meyer-Morse, N., O'Riordan, M., & Portnoy, D. A. (2004). Mice lacking the type I interferon receptor are resistant to *Listeria monocytogenes*. *The Journal of Experimental Medicine*, *200*(4), 527–33.

Auerbuch, V., Golenbock, D. T., & Isberg, R. R. (2009). Innate immune recognition of *Yersinia pseudotuberculosis* type III secretion. *PLoS Pathogens*, *5*(12), e1000686.

Autenrieth, I. B., Tingle, A., Reske-Kunz, A., & Heesemann, J. (1992). T lymphocytes mediate protection against *Yersinia enterocolitica* in mice: Characterization of murine T-cell clones specific for *Y. enterocolitica*. *Infection and Immunity*, *60*(3), 1140–1149.

Autenrieth, I. B., Vogel, U., Preger, S., & Heymer, B. (1993). Experimental *Yersinia enterocolitica* Infection in Euthymic and T-Cell-Deficient Athymic Nude C57BL / 6 Mice : Comparison of Time Course , Histomorphology , and Immune Response. *Infection and Immunity*, *61*(6), 2585–2595.

Autenrieth, I. B., Beer, M., Bohn, E., Kaufmann, S. H. E., & Heesemann, J. (1994). Immune responses to *Yersinia enterocolitica* in susceptible BALB/c and resistant C57BL/6 mice: An essential role for gamma interferon. *Infection and Immunity*, *62*(6), 2590–2599.

Autenrieth, I., & Firsching, R. (1996). Penetration of M cells and destruction of Peyer's patches by *Yersinia enterocolitica* : an uItrastructuraI and histological study. *Journal of Medical Microbiology*, *44*(4), 285–294.

Avican, K., Fahlgren, A., Huss, M., Heroven, A. K., Beckstette, M., Dersch, P., & Fällman, M. (2015). Reprogramming of *Yersinia* from Virulent to Persistent Mode Revealed by Complex *In Vivo* RNA-seq Analysis. *PLoS Pathogens*, *11*(1), 1–28.

Ayres, J. S., Trinidad, N. J., & Vance, R. E. (2012). Lethal inflammasome activation by a multidrug-resistant pathobiont upon antibiotic disruption of the microbiota. *Nature Medicine*, *18*(5), 799–806.

Azad, A. K., Sadee, W., & Schlesinger, L. S. (2012, October). Innate immune gene polymorphisms in tuberculosis. *Infection and Immunity*. American Society for Microbiology (ASM). http://doi.org/10.1128/IAI.00443-12

Azizi, A., Kumar, A., Diaz-Mitoma, F., & Mestecky, J. (2010). Enhancing oral vaccine potency by targeting intestinal M cells. *PLoS Pathogens*. http://doi.org/10.1371/journal.ppat.1001147

Backhans, A., Fellström, C., & Lambertz, S. T. (2011). Occurrence of pathogenic *Yersinia enterocolitica* and *Yersinia pseudotuberculosis* in small wild rodents. *Epidemiology and Infection*, *139*(8), 1230–1238.

Bäckhed, F., Crawford, P. A., O'Donnell, D., & Gordon, J. I. (2007). Postnatal lymphatic partitioning from the blood vasculature in the small intestine requires fasting-induced adipose factor. *Proc Natl Acad Sci U S A*, *104*(2), 606–611.

Bacle F, Haeffner-Cavaillon N, Laude M, Couturier C, Kazatchkine MD, Bacle, F., … Kazatchkine, M. D. (1990). Induction of IL-1 release through stimulation of the C3b/C4b complement receptor type one (CR1, CD35) on human monocytes. *Journal of Immunology*, *144*(1), 147–152.

Badolato, R., Wang, J. M., Murphy, W. J., Lloyd, A. R., Michiel, D. F., Bausserman, L. L., … Oppenheim, J. J. (1994). Serum amyloid A is a chemoattractant: induction of migration, adhesion, and tissue infiltration of monocytes and polymorphonuclear leukocytes. *The Journal of Experimental Medicine*, *180*(1), 203–9.

Bahrani-Mougeot, F. K., Buckles, E. L., Lockatell, C. V., Hebel, J. R., Johnson, D. E., Tang, C. M., & Donnenberg, M. S. (2002). Type 1 fimbriae and extracellular polysaccharides are preeminent uropathogenic *Escherichia coli* virulence determinants in the murine urinary tract. *Molecular Microbiology*, *45*(4), 1079–1093.

Balaban, N. Q., Merrin, J., Chait, R., Kowalik, L., & Leibler, S. (2004). Bacterial Persistenceas a Phenotypic Switch. *Science*, *305*(September), 1622–1625.

Balada-Llasat, J. M., & Mecsas, J. (2006). *Yersinia* has a tropism for B and T cell zones of lymph nodes that is independent of the type III secretion system. *PLoS Pathogens*, *2*(9), 0816–0828.

Balestrieri, B., Maekawa, A., Xing, W., Gelb, M. H., Katz, H. R., & Arm, J. P. (2009). Group V secretory phospholipase A2 modulates phagosome maturation and regulates the innate immune response against *Candida albicans*. *Journal of Immunology (Baltimore, Md. : 1950)*, *182*(8), 4891–4898.

Balligand, G., Laroche, Y., & Cornelis, G. (1985). Genetic analysis of virulence plasmid from a serogroup 9 *Yersinia enterocolitica* strain: Role of outer membrane protein P1 in resistance to human serum and autoagglutination. *Infection and Immunity*, *48*(3), 782–786.

Banchereau, J., & Steinman, R. M. (1998). Dendritic cells and the control of immunity. *Nature*, *392*(March), 245–252.

Barbieri, J. T., & Sun, J. (2004). *Pseudomonas aeruginosa* ExoS and ExoT. *Reviews of Physiology, Biochemistry and Pharmacology*, *152*, 79–92.

Barman, M., Unold, D., Shifley, K., Amir, E., Hung, K., Bos, N., & Salzman, N. (2008). Enteric salmonellosis disrupts the microbial ecology of the murine gastrointestinal tract. *Infection and Immunity*, *76*(3), 907–915.

Barr, J. J., Auro, R., Furlan, M., Whiteson, K. L., Erb, M. L., Pogliano, J., … Rohwer, F. (2013). Bacteriophage adhering to mucus provide a non-host-derived immunity. *Proceedings of the National Academy of Sciences of the United States of America*, *110*(26), 10771–6.

Barry, K. C., Fontana, M. F., Portman, J. L., Dugan, A. S., & Vance, R. E. (2013). IL-1α signaling initiates the inflammatory response to virulent *Legionella pneumophila in vivo*. *Journal of Immunology (Baltimore, Md. : 1950)*, *190*(12), 6329–39.

Barth, H., & Raghuraman, S. (2014). Persistent infectious diseases say-IDO. Role of indoleamine-2,3-dioxygenase in disease pathogenesis and implications for therapy. *Critical Reviews in Microbiology*, *40*(4), 360–368.

Barton, G. M., & Kagan, J. C. (2009). A cell biological view of Toll-like receptor function: regulation through compartmentalization. *Nature Reviews. Immunology*, *9*(8), 535–42.

Bates, J. M., Akerlund, J., Mittge, E., & Guillemin, K. (2007). Intestinal Alkaline Phosphatase Detoxifies Lipopolysaccharide and Prevents Inflammation in Zebrafish in Response to the Gut Microbiota. *Cell Host and Microbe*, *2*(6), 371–382.

Baumann, H., & Gauldie, J. (1994). The acute phase response. *Immunology Today*, *15*(2), 74–80.

Baumer, Y., Burger, S., Curry, F. E., Golenhofen, N., Drenckhahn, D., & Waschke, J. (2008). Differential role of Rho GTPases in endothelial barrier regulation dependent on endothelial cell origin. *Histochemistry and Cell Biology*, *129*(2), 179–191.

Bäumler, A., & Fang, F. C. (2013). Host specificity of bacterial pathogens. *Cold Spring Harbor Perspectives in Medicine*, *3*(12), a010041.

Becher, B., Tugues, S., & Greter, M. (2016). GM-CSF: From Growth Factor to Central Mediator of Tissue Inflammation. *Immunity*. http://doi.org/10.1016/j.immuni.2016.10.026

Beermann, S., Behnke, S., Bremer, V., Buchholz, U., Buda, S., Cai, W., … Zimmermann, R. (2016). *Infektionsepidemiologisches Jahrbuch meldepflichtiiger Krankheiten für 2015*. (D. A. Gilsdorf, Ed.). Berlin: Robert Koch-Institut. Retrieved from http://www.rki.de/DE/Content/Infekt/Jahrbuch/Jahrbuch_2015.pdf?__blob=publicationFile

Belkaid, Y. (2007). Regulatory T cells and infection: a dangerous necessity. *Nature Reviews Immunology*, *7*(11), 875–888.

Ben-Gurion, R., & Shafferman, A. (1981). Essential virulence determinants of different *Yersinia* species are carried on a common plasmid. *Plasmid*, *5*(2), 183–187.

Bender, B., Baranyi, M., Kerekes, A., Bodrogi, L., Brands, R., Uhrin, P., & Bösze, Z. (2015). Recombinant human tissue non-specific alkaline phosphatase successfully counteracts lipopolysaccharide induced sepsis in mice. *Physiological Research*, *64*(5), 731–738.

Benvenga, S., & Guarneri, F. (2016). Molecular mimicry and autoimmune thyroid disease. *Reviews in Endocrine and Metabolic Disorders*, *50*, 819–820. http://doi.org/10.1007/s11154-016-9363-2

Bercik, P., Verdu, E. F., & Collins, S. M. (2005). Is irritable bowel syndrome a low-grade inflammatory bowel disease? *Gastroenterology Clinics of North America*. http://doi.org/10.1016/j.gtc.2005.02.007

Bercovier, H., Steigerwalt, A. G., Guiyoule, A., Huntley-Carter, G., & Brenner, D. J. (1984). *Yersinia aldovae* (Formerly *Yersinia enterocolitica*-Like Group X2): a New Species of *Enterobacteriaceae* Isolated from Aquatic Ecosystems. *International Journal of Systematic Bacteriology*, *34*(2), 166–172.

Berger, A. (2000). Science commentary: Th1 and Th2 responses: what are they? *British Medical Journal*, *321*(7258), 424–424.

Bergsbaken, T., & Cookson, B. T. (2007). Macrophage activation redirects *Yersinia*-infected host cell death from apoptosis to caspase-1-dependent pyroptosis. *PLoS Pathogens*, *3*(11), 1570–1582.

Bergsbaken, T., & Cookson, B. T. (2009). Innate immune response during *Yersinia* infection: critical modulation of cell death mechanisms through phagocyte activation. *Journal of Leukocyte Biology*, *86*(5), 1153–1158.

Bergsbaken, T., Fink, S. L., & Cookson, B. T. (2009). Pyroptosis: host cell death and inflammation. *Nature Reviews. Microbiology*, *7*(2), 99–109.

Bergstrom, K. S. B., Kissoon-Singh, V., Gibson, D. L., Ma, C., Montero, M., Sham, H. P., … Vallance, B. A. (2010). Muc2 protects against lethal infectious colitis by disassociating pathogenic and commensal bacteria from the colonic mucosa. *PLoS Pathogens*, *6*(5), e1000902.

Bichowsky-Slomnicky, L., & Ben-Efrain, S. (1963). Biological activities in extracts of "*Pasteurella pestis*" and their relation to the "pH6 antigen." *J. Bacteriol.*, *86*, 101–111.

Biedzka-Sarek, M., Venho, R., & Skurnik, M. (2005). Role of YadA, Ail, and lipopolysaccharide in serum resistance of *Yersinia enterocolitica* serotype O:3. *Infection and Immunity*, *73*(4), 2232–2244.

Biedzka-Sarek, M., Jarva, H., Hyytiäinen, H., Meri, S., & Skurnik, M. (2008a). Characterization of complement factor H binding to *Yersinia enterocolitica* serotype O:3. *Infection and Immunity*, *76*(9), 4100–4109.

Biedzka-Sarek, M., Salmenlinna, S., Gruber, M., Lupas, A. N., Meri, S., & Skurnik, M. (2008b). Functional mapping of YadA- and Ail-mediated binding of human factor H to *Yersinia enterocolitica* serotype O:3. *Infection and Immunity*, *76*(11), 5016–5027.

Bingen-Bidois, M., Clermont, O., Bonacorsi, S., Terki, M., Brahimi, N., Loukil, C., … Bingen, E. (2002). Phylogenetic analysis and prevalence of urosepsis strains of *Escherichia coli* bearing pathogenicity island-like domains. *Infection and Immunity*, *70*(6), 3216–3226.

Birkedal-Hansen, H. (1993). Role of cytokines and inflammatory mediators in tissue destruction. *Journal of Periodontal Research*. http://doi.org/10.1111/j.1600-0765.1993.tb02113.x

Biswas, S. K., Chittezhath, M., Shalova, I. N., & Lim, J. Y. (2012). Macrophage polarization and plasticity in health and disease. *Immunologic Research*, *53*(1–3), 11–24.

Black, S., Kushner, I., & Samols, D. (2004, November 19). C-reactive protein. *Journal of Biological Chemistry*. American Society for Biochemistry and Molecular Biology. http://doi.org/10.1074/jbc.R400025200

Blanchard, T. G., Yu, F., Hsieh, C., & Redline, R. W. (2003). Severe Inflammation and Reduced Bacteria Load in Murine *Helicobacter* Infection Caused by Lack of Phagocyte Oxidase Activity. *The Journal of Infectious Diseases*, *187*(10), 1609–1615.

Blumenthal, B., Hoffmann, C., Aktories, K., Backert, S., & Schmidt, G. (2007). The cytotoxic necrotizing factors from *Yersinia pseudotuberculosis* and from *Escherichia coli* bind to different cellular receptors but take the same route to the cytosol. *Infection and Immunity*, *75*(7), 3344–3353.

Boasso, A., Herbeuval, J. P., Hardy, A. W., Anderson, S. A., Dolan, M. J., Fuchs, D., & Shearer, G. M. (2007). HIV inhibits CD4+ T-cell proliferation by inducing indoleamine 2,3-dioxygenase in plasmacytoid dendritic cells. *Blood*, *109*(8), 3351–3359.

Boehm, U., Klamp, T., Groot, M., & Howard, J. C. (1997). Cellular responses to interferon-γ. *Annu. Rev. Immunol*, *15*(1), 749–95.

Bohn, E., & Autenrieth, I. B. (1996). IL-12 is essential for resistance against *Yersinia enterocolitica* by triggering IFN-gamma production in NK cells and CD4+ T cells. *Journal of Immunology (Baltimore, Md. : 1950)*, *156*(4), 1458–1468.

Bohn, E., Sing, A., Zumbihl, R., Bielfeldt, C., Okamura, H., Kurimoto, M., … Autenrieth, I. B. (1998). IL-18 (IFN- g -inducing factor) regulates early cytokine production in, and promotes resolution of, bacterial infection in mice. *J.Immunol.*, *160*(1), 299–307.

Bokoch, G. M. (2005). Regulation of innate immunity by Rho GTPases. *Trends in Cell Biology*. http://doi.org/10.1016/j.tcb.2005.01.002

Bölin, I., Norlander, L., & Wolf-watz, H. (1982). Temperature-inducible outer membrane protein of *Yersinia pseudotuberculosis* and *Yersinia enterocolitica* is associated with the virulence Temperature-Inducible Outer Membrane Protein of *Yersinia pseudotuberculosis* and *Yersinia enterocolitica* Is Associated. *Infection and Immunity*, *37*(2), 506–512.

Bonizzi, G., & Karin, M. (2004). The two NF-κB activation pathways and their role in innate and adaptive immunity. *Trends in Immunology*. http://doi.org/10.1016/j.it.2004.03.008

Boquet, P. (1999). Bacterial toxins inhibiting or activating small GTP-binding proteins. *Annals of the New York Academy of Sciences*, *886*, 83–90.

Boquet, P., & Lemichez, E. (2003). Bacterial virulence factors targeting Rho GTPases: Parasitism or symbiosis? *Trends in Cell Biology*. http://doi.org/10.1016/S0962-8924(03)00037-0

Borregaard, N., Sørensen, O. E., & Theilgaard-Mönch, K. (2007). Neutrophil granules: a library of innate immunity proteins. *Trends in Immunology*, *28*(8), 340–345.

Bottone, E. J. (1997). *Yersinia enterocolitica*: the charisma continues. *Clinical Microbiology Reviews*, *10*(2), 257–76.

Bourne, H. R., Sanders, D. A., & McCormick, F. (1991). The GTPase superfamily: conserved structure and molecular mechanism. *Nature*, *349*(6305), 117–127.

Bower, J. M., Eto, D. S., & Mulvey, M. A. (2005). Covert operations of uropathogenic *Escherichia coli* within the Urinary Tract. *Traffic*. http://doi.org/10.1111/j.1600-0854.2004.00251.x

Brandtzaeg, P. (2009, December). Mucosal immunity: Induction, dissemination, and effector functions. *Scandinavian Journal of Immunology*. http://doi.org/10.1111/j.1365-3083.2009.02319.x

Braun, J., Yin, Z., Spiller, I., Siegert, S., Rudwaleit, M., Liu, L., … Sieper, J. (1999). Low secretion of tumor necrosis factor alpha, but no other Th1 or Th2 cytokines, by peripheral blood mononuclear cells correlates with chronicity in reactive arthritis. *Arthritis and Rheumatism*, *42*(10), 2039–44.

Brest, P., Turchi, L., Le'Negrate, G., Berto, F., Moreilhon, C., Mari, B., … Hofman, P. (2004). *Escherichia coli* cytotoxic necrotizing factor 1 inhibits intestinal epithelial wound healing *in vitro* after mechanical injury. *Infection and Immunity*, *72*(10), 5733–5740.

Brinkmann, V., Reichard, U., Goosmann, C., Fauler, B., Uhlemann, Y., Weiss, D. S., … Zychlinsky, A. (2004). Neutrophil extracellular traps kill bacteria. *Science*, *303*(5663), 1532–1535.

Brodsky, I. E., Palm, N. W., Sadanand, S., Ryndak, M. B., Sutterwala, F. S., Flavell, R. A., … Medzhitov, R. (2010). A *Yersinia* effector protein promotes virulence by preventing inflammasome recognition of the type III secretion system. *Cell Host and Microbe*, *7*(5), 376–387.

Bronte, V., Serafini, P., Mazzoni, A., Segal, D. M., & Zanovello, P. (2003). L-arginine metabolism in myeloid cells controls T-lymphocyte functions. *Trends in Immunology*. http://doi.org/10.1016/S1471-4906(03)00132-7

Brown, D. L., & Frank, J. E. (2003). Diagnosis and management of syphilis. *American Family Physician*.

Broz, P., & Monack, D. M. (2011). Molecular mechanisms of inflammasome activation during microbial infections. *Immunological Reviews*. http://doi.org/10.1111/j.1600-065X.2011.01041.x

Broz, P., Ruby, T., Belhocine, K., Bouley, D. M., Kayagaki, N., Dixit, V. M., & Monack, D. M. (2012). Caspase-11 increases susceptibility to *Salmonella* infection in the absence of caspase-1. *Nature*, *490*(7419), 288–91.

Broz, P., & Dixit, V. M. (2016). Inflammasomes: mechanism of assembly, regulation and signaling. *Nature Reviews Immunology*, *16*(7), 407–420.

Brubaker, R. R. (1983). The Vwa+ virulence factor of yersiniae: the molecular basis of the attendant nutritional requirement for Ca++. *Rev Infect Dis*, *5 Suppl 4*(October), S748-58.

Brubaker, R. R. (1991). Factors promoting acute and chronic diseases caused by yersiniae. *Clin. Microbiol. Rev.*, *4*(0893–8512 (Print)), 309–324.

Buchsbaum, R. J. (2007). Rho activation at a glance. *Journal of Cell Science*, *120*(Pt 7), 1149–52.

Buffie, C. G., Jarchum, I., Equinda, M., Lipuma, L., Gobourne, A., Viale, A., … Pamer, E. G. (2012). Profound alterations of intestinal microbiota following a single dose of clindamycin results in sustained susceptibility to *Clostridium difficile*-induced colitis. *Infection and Immunity*, *80*(1), 62–73.

Bulgin, R., Raymond, B., Garnett, J. A., Frankel, G., Crepin, V. F., Berger, C. N., & Arbeloa, A. (2010). Bacterial guanine nucleotide exchange factors SopE-Like and WxxxE effectors. *Infection and Immunity*. http://doi.org/10.1128/IAI.01250-09

Burrack, K. S., Tan, J. J. L., McCarthy, M. K., Her, Z., Berger, J. N., Ng, L. F. P., & Morrison, T. E. (2015). Myeloid cell Arg1 inhibits control of arthritogenic alphavirus infection by suppressing antiviral T cells. *PLoS Pathogens*, *11*(10), e1005191.

Burridge, K., & Wittchen, E. S. (2013). The tension mounts: Stress fibers as force-generating mechanotransducers. *Journal of Cell Biology*. http://doi.org/10.1083/jcb.201210090

Burridge, K., & Guilluy, C. (2016). Focal adhesions, stress fibers and mechanical tension. *Experimental Cell Research*. http://doi.org/10.1016/j.yexcr.2015.10.029

Butler, A., & Whitehead, A. S. (1996). Mapping of the mouse serum amyloid A gene cluster by long-range polymerase chain reaction. *Immunogenetics*, *44*(6), 468–74.

Buttó, L. F., Schaubeck, M., & Haller, D. (2015). Mechanisms of microbe-host interaction in Crohn's disease: dysbiosis vs. pathobiont selection. *Frontiers in Immunology*. http://doi.org/10.3389/fimmu.2015.00555

Callan-Jones, A. C., & Voituriez, R. (2016). Actin flows in cell migration: From locomotion and polarity to trajectories. *Current Opinion in Cell Biology*, *38*, 12–17.

Calvet, X., Ramírez Lázaro, M.-J., Lehours, P., & Mégraud, F. (2013). Diagnosis and Epidemiology of *Helicobacter pylori* Infection. *Helicobacter*, *18*(S1), 5–11.

Caporaso, J. G., Kuczynski, J., Stombaugh, J., Bittinger, K., Bushman, F. D., Costello, E. K., … Knight, R. (2010). QIIME allows analysis of high-throughput community sequencing data. *Nature Methods*, *7*(5), 335–6.

Caprioli, A., Falbo, V., Roda, L. G., Ruggeri, F. M., & Zona, C. (1983). Partial purification and characterization of an *Escherichia coli* toxic factor that induces morphological cell alterations. *Infection and Immunity*, *39*(3), 1300–1306.

Caprioli, A., Falbo, V., Ruggeri, F. M., Baldassarri, L., Bisicchia, R., Ippolito, G., … Donelli, G. (1987). Cytotoxic necrotizing factor production by hemolytic strains of *Escherichia coli* causing extraintestinal infections. *Journal of Clinical Microbiology*, *25*(1), 146–149.

Cargnelutti, E., & Di Genaro, M. S. (2013). Reactive Arthritis: From Clinical Features to Pathogenesis. *International Journal of Clinical Medicine*, *4*(12), 20–30.

Carlin, J. M., Borden, E. C., & Byrne, G. I. (1989). Interferon-induced indoleamine 2,3-dioxygenase activity inhibits *Chlamydia psittaci* replication in human macrophages. *Journal of Interferon Research*, *9*(3), 329–337.

Carniel, E., Mazigh, D., & Mollaret, H. H. (1987). Expression of Iron-Regulated Proteins. *Infection and Immunity*, *55*(1), 277–280.

Carniel, E. (2001). The *Yersinia* high-pathogenicity island: An iron-uptake island. *Microbes and Infection*, *3*(7), 561–569.

Carter, P. B. (1975). Pathogenicity of *Yersinia enterocolitica* for mice. *Infection and Immunity*, *11*(1), 164–70.

Carter, R. H., & Fearon, D. T. (1992). CD19: lowering the threshold for antigen receptor stimulation of B lymphocytes. *Science (New York, N.Y.)*, *256*(5053), 105–107.

Casanova, J.-L. (2015a). Severe infectious diseases of childhood as monogenic inborn errors of immunity. *Proceedings of the National Academy of Sciences of the United States of America*, *112*(51), E7128-37.

Casanova, J.-L. (2015b). Human genetic basis of interindividual variability in the course of infection. *Proceedings of the National Academy of Sciences of the United States of America*, *112*(51), E7118-27.

Cassel, D., & Pfeuffer, T. (1978). Mechanism of cholera toxin action: covalent modification of the guanyl nucleotide-binding protein of the adenylate cyclase system. *Proceedings of the National Academy of Sciences of the United States of America*, *75*(6), 2669–73.

Casson, C. N., Copenhaver, A. M., Zwack, E. E., Nguyen, H. T., Strowig, T., Javdan, B., … Shin, S. (2013). Caspase-11 activation in response to bacterial secretion systems that access the host cytosol. *PLoS Pathogens*, *9*(6), e1003400.

Cattaneo, F., Parisi, M., & Ammendola, R. (2013, April 2). Distinct signaling cascades elicited by different formyl peptide receptor 2 (FPR2) agonists. *International Journal of Molecular Sciences*. http://doi.org/10.3390/ijms14047193

Ceballos-Olvera, I., Sahoo, M., Miller, M. A., Barrio, L. del, & Re, F. (2011). Inflammasome-dependent Pyroptosis and IL-18 Protect against *Burkholderia pseudomallei* Lung Infection while IL-1β Is Deleterious. *PLoS Pathogens*, *7*(12), e1002452.

Cellini, L., Di Campli, E., Di Candia, M., & Marzio, L. (2003). Molecular fingerprinting of *Helicobacter pylori* strains from duodenal ulcer patients. *Letters in Applied Microbiology*, *36*(4), 222–6.

Ceredig, R., & Rolink, A. G. (2012). The key role of IL-7 in lymphopoiesis. *Seminars in Immunology*. http://doi.org/10.1016/j.smim.2012.02.004

Ch'ng, S. L., Octavia, S., Xia, Q., Duong, A., Tanaka, M. M., Fukushima, H., & Lan, R. (2011). Population structure and evolution of pathogenicity of *Yersinia pseudotuberculosis*. *Applied and Environmental Microbiology*, *77*(3), 768–775.

Chatfield, S. N., Strahan, K., Pickard, D., Charles, I. G., Hormaeche, C. E., & Dougan, G. (1992). Evaluation of *Salmonella* Typhimurium strains harboring defined mutations in *htrA* and *aroA* in the murine salmonellosis model. *Microbial Pathogenesis*, *12*(2), 145–151.

Chen, L., & Wen, Y. (2011). The role of bacterial biofilm in persistent infections and control strategies. *International Journal of Oral Science*, *3*(2), 66–73.

Chen, F., Liu, Z., Wu, W., Rozo, C., Bowdridge, S., Millman, A., … Gause, W. C. (2012). An essential role for TH2-type responses in limiting acute tissue damage during experimental helminth infection. *Nature Medicine*, *18*(2), 260–266.

Chiba, T., Han, C. Y., Vaisar, T., Shimokado, K., Kargi, A., Chen, M.-H., … Chait, A. (2009). Serum amyloid A3 does not contribute to circulating SAA levels. *Journal of Lipid Research*, *50*(7), 1353–62.

Chow, S. H., Deo, P., & Naderer, T. (2016). Macrophage cell death in microbial infections. *Cellular Microbiology*, *18*(4), 466–474.

Chu, A. J. (2005). Tissue factor mediates inflammation. *Archives of Biochemistry and Biophysics*. http://doi.org/10.1016/j.abb.2005.06.005

Chung, L. K., Philip, N. H., Schmidt, V. A., Koller, A., Strowig, T., Flavell, R. A., … Bliska, J. B. (2014). IQGAP1 is important for activation of caspase-1 in macrophages and is targeted by *Yersinia pestis* type III effector YopM. *mBio*, *5*(4), e01402-14-e01402-14.

Chung, L. K., & Bliska, J. B. (2016). *Yersinia* versus host immunity: How a pathogen evades or triggers a protective response. *Current Opinion in Microbiology*. http://doi.org/10.1016/j.mib.2015.11.001

Chung, L. K., Park, Y. H., Zheng, Y., Brodsky, I. E., Hearing, P., Kastner, D. L., … Bliska, J. B. (2016). The *Yersinia* Virulence Factor YopM Hijacks Host Kinases to Inhibit Type III Effector-Triggered Activation of the Pyrin Inflammasome. *Cell Host and Microbe*, *20*(3), 296–306.

Clark, M. A. N. N., Hirst, B. H., & Jepson, M. A. (1998). M-Cell Surface [illegible] 1 Integrin Expression and Invasin-Mediated Targeting of *Yersinia pseudotuberculosis* to Mouse Peyer's Patch M Cells. *Infection and Immunity*, *66*(3), 1237–1243.

Clements, M. O., Eriksson, S., Thompson, A., Lucchini, S., Hinton, J. C. D., Normark, S., & Rhen, M. (2002). Polynucleotide phosphorylase is a global regulator of virulence and persistency in *Salmonella enterica*. *Proceedings of the National Academy of Sciences of the United States of America*, *99*(13), 8784–9.

Coconnier, M. H., Bernet-Camard, M. F., & Servin, A. L. (1994). How intestinal epithelial cell differentiation inhibits the cell-entry of *Yersinia pseudotuberculosis* in colon carcinoma Caco-2 cell line in culture. *Differentiation*, *58*(1), 87–94.

Cohen-Or, I., Shenhar, Y., Biran, D., & Ron, E. Z. (2010). CspC regulates *rpoS* transcript levels and complements *hfq* deletions. *Research in Microbiology*, *161*(8), 694–700.

Cohen, N. R., Lobritz, M. A., & Collins, J. J. (2013). Microbial persistence and the road to drug resistance. *Cell Host and Microbe*. http://doi.org/10.1016/j.chom.2013.05.009

Cole, a M., Ganz, T., Liese, a M., Burdick, M. D., Liu, L., & Strieter, R. M. (2001). Cutting edge: IFN-inducible ELR- CXC chemokines display defensin-like antimicrobial activity. *Journal of Immunology (Baltimore, Md. : 1950)*, *167*(2), 623–627.

Conlan, J. W. (1997). Critical roles of neutrophils in host defense against experimental systemic infections of mice by *Listeria monocytogenes*, *Salmonella* Typhimurium, and *Yersinia enterocolitica* . Critical Roles of Neutrophils in Host Defense against Experimental Systemic I. *Infection and Immunity*, *65*(2), 630–635.

Contamin, S., Galmiche, a, Doye, a, Flatau, G., Benmerah, a, & Boquet, P. (2000). The p21 Rho-activating toxin cytotoxic necrotizing factor 1 is endocytosed by a clathrin-independent mechanism and enters the cytosol by an acidic-dependent membrane translocation step. *Molecular Biology of the Cell*, *11*(May), 1775–1787.

Cooper, A. M., Magram, J., Ferrante, J., & Orme, I. M. (1997). Interleukin 12 (IL-12) is crucial to the development of protective immunity in mice intravenously infected with *Mycobacterium tuberculosis*. *The Journal of Experimental Medicine*, *186*(1), 39–45.

Cooper, A. M., & Khader, S. A. (2007). IL-12p40: an inherently agonistic cytokine. *Trends in Immunology*. http://doi.org/10.1016/j.it.2006.11.002

Cornelis, G. R., Boland, A., Boyd, A. P., Geuijen, C., Iriarte, M., Neyt, C., … Stainier, I. (1998). The virulence plasmid of *Yersinia*, an antihost genome. *Microbiology and Molecular Biology Reviews : MMBR*, *62*(4), 1315–1352.

Cornelis, G. R. (2002). The *Yersinia* Ysc-Yop "type III" weaponry. *Nature Reviews. Molecular Cell Biology*, *3*(10), 742–752.

Cossart, P., & Sansonetti, P. J. (2004). Bacterial Invasion: The Paradigms of Enteroinvasive Pathogens. *Science*, *304*(5668), 242–248.

Cover, T. L., & Aber, R. C. (1989). *Yersinia enterocolitica*. *The New England Journal of Medicine*, *321*(1), 16–24.

Crawford, R. W., Gibson, D. L., Kay, W. W., & Gunn, J. S. (2008). Identification of a bile-induced exopolysaccharide required for *Salmonella* biofilm formation on gallstone surfaces. *Infection and Immunity*, *76*(11), 5341–5349.

Crawford, R. W., Rosales-Reyes, R., Ramirez-Aguilar, M. d. l. L., Chapa-Azuela, O., Alpuche-Aranda, C., Gunn, J. S., … Gunn, J. S. (2010). Gallstones play a significant role in *Salmonella* spp. gallbladder colonization and carriage. *Proc. Natl. Acad. Sci. U. S. A.*, *107*(9), 4353–4358.

Cronstein, B. N. (2007). Interleukin-6--a key mediator of systemic and local symptoms in rheumatoid arthritis. *Bull NYU Hosp Jt Dis*, *65 Suppl 1*(Suppl 1), S11-5.

Croxen, M. A., Sisson, G., Melano, R., & Hoffman, P. S. (2006). The *Helicobacter pylori* chemotaxis receptor TlpB (HP0103) is required for pH taxis and for colonization of the gastric mucosa. *Journal of Bacteriology*, *188*(7), 2656–2665.

Curfs, J. H., Meis, J. F., Van der Lee, H. A., Mulder, J. A., Kraak, W. A., & Hoogkamp-Korstanje, J. A. (1995). Persistent *Yersinia enterocolitica* infection in three rat strains. *Microbial Pathogenesis*, *19*(1), 57–63.

Curtis, J., Adu, H. O., & Turk, J. L. (1982). H-2 linkage control of resistance to subcutaneous infection with *Mycobacterium lepraemurium*. *Infection and Immunity*, *38*(2), 434–9.

Dann, S. M., & Eckmann, L. (2007). Innate immune defenses in the intestinal tract. *Current Opinion in Gastroenterology*, *23*(2), 115–120.

Dave, M. N., Silva, J. E., Eliçabe, R. J., Jeréz, M. B., Filippa, V. P., Gorlino, C. V., … di Genaro, M. S. (2016). *Yersinia enterocolitica* YopH-deficient strain activates neutrophil recruitment to Peyer's patches and promotes clearance of the virulent strain. *Infection and Immunity*, *84*(11), 3172–3181.

Davis, J. M., Rasmussen, S. B., & O'Brien, A. D. (2005). Cytotoxic necrotizing factor type 1 production by uropathogenic *Escherichia coli* modulates polymorphonuclear leukocyte function. *Infection and Immunity*, *73*(9), 5301–5310.

Davis, J. M., Carvalho, H. M., Rasmussen, S. B., & O'Brien, A. D. (2006). Cytotoxic necrotizing factor type 1 delivered by outer membrane vesicles of uropathogenic *Escherichia coli* attenuates polymorphonuclear leukocyte antimicrobial activity and chemotaxis. *Infection and Immunity*, *74*(8), 4401–4408.

Day, R. B., & Link, D. C. (2012). Regulation of neutrophil trafficking from the bone marrow. *Cellular and Molecular Life Sciences*. SP Birkhäuser Verlag Basel. http://doi.org/10.1007/s00018-011-0870-8

De Koning-Ward, T. F., & Robins-Browne, R. M. (1995). Contribution of urease to acid tolerance in *Yersinia enterocolitica*. *Infection and Immunity*, *63*(10), 3790–3795.

De Rycke, J., Milon, A., & Oswald, E. (1999). Necrotoxic *Escherichia coli* (NTEC): Two emerging categories of human and animal pathogens. *Veterinary Research*.

de Santo, C., Arscott, R., Booth, S., Karydis, I., Jones, M., Asher, R., … Cerundolo, V. (2010). Invariant NKT cells modulate the suppressive activity of IL-10-secreting neutrophils differentiated with serum amyloid A. *Nature Immunology*, *11*(11), 1039–1046.

Delgado, M., Abad, C., Martinez, C., Leceta, J., & Gomariz, R. P. (2001). Vasoactive intestinal peptide prevents experimental arthritis by down-regulating both autoimmune and inflammatory components of the disease. *Nature Medicine*, *7*(5), 563–568.

Dempsey, P. W., Allison, M. E., Akkaraju, S., Goodnow, C. C., & Fearon, D. T. (1996). C3d of complement as a molecular adjuvant: bridging innate and acquired immunity. *Science (New York, N.Y.)*, *271*(5247), 348–350.

den Haan, J. M., Lehar, S. M., & Bevan, M. J. (2000). CD8(+) but not CD8(-) dendritic cells cross-prime cytotoxic T cells *in vivo*. *The Journal of Experimental Medicine*, *192*(12), 1685–96.

Denecker, G., Declercq, W., Geuijen, C. A. W., Boland, A., Benabdillah, R., Van Gurp, M., … Cornelis, G. R. (2001). *Yersinia enterocolitica* YopP-induced Apoptosis of Macrophages Involves the Apoptotic Signaling Cascade Upstream of Bid. *Journal of Biological Chemistry*, *276*(23), 19706–19714.

Denes, A., Lopez-Castejon, G., & Brough, D. (2012). Caspase-1: is IL-1 just the tip of the ICEberg? *Cell Death and Disease*, *3*(7), e338.

Derebe, M. G., Zlatkov, C. M., Gattu, S., Ruhn, K. A., Vaishnava, S., Diehl, G. E., … Hooper, L. V. (2014). Serum amyloid A is a retinol binding protein that transports retinol during bacterial infection. *eLife*, *3*, e03206.

Derman, Y., Söderholm, H., Lindström, M., & Korkeala, H. (2015). Role of *csp* genes in NaCl, pH, and ethanol stress response and motility in *Clostridium botulinum* ATCC 3502. *Food Microbiology*, *46*, 463–470.

Dessein, R., Gironella, M., Vignal, C., Peyrin-Biroulet, L., Sokol, H., Secher, T., … Chamaillard, M. (2009). Toll-like receptor 2 is critical for induction of Reg3 beta expression and intestinal clearance of *Yersinia pseudotuberculosis*. *Gut*, *58*(6), 771–776.

Desvignes, L., & Ernst, J. D. (2009). Interferon-g-responsive non-hematopoietic cells regulate the immune response to *Mycobacterium tuberculosis*. *Immunity*, *31*(6), 974–985.

Diabate, M., Munro, P., Garcia, E., Jacquel, A., Michel, G., Obba, S., … Boyer, L. (2015). *Escherichia coli* α-hemolysin counteracts the anti-virulence innate immune response triggered by the Rho GTPase activating toxin CNF1 during bacteremia. *PLoS Pathogens*, *11*(3), e1004732.

Dicksved, J., Ellström, P., Engstrand, L., & Rautelin, H. (2014). Susceptibility to *Campylobacter* infection is associated with the species composition of the human fecal microbiota. *mBio*, *5*(5), e01212-14.

Diez, A., Gustavsson, N., & Nyström, T. (2002). The universal stress protein A of *Escherichia coli* is required for resistance to DNA damaging agents and is regulated by a RecA/FtsK-dependent regulatory pathway. *Molecular Microbiology*, *36*(6), 1494–1503.

Dinarello, C. A. (2009). Immunological and inflammatory functions of the interleukin-1 family. *Annual Review of Immunology*, *27*, 519–50.

Dobrindt, U., Zdziarski, J., Salvador, E., & Hacker, J. (2010). Bacterial genome plasticity and its impact on adaptation during persistent infection. *International Journal of Medical Microbiology*. http://doi.org/10.1016/j.ijmm.2010.04.010

Dominguez, R., & Holmes, K. C. (2011). Actin structure and function. *Annual Review of Biophysics*, *40*, 169–86

Donadinia, R., & Fields, B. A. (2007). *Yersinia pseudotuberculosis* Superantigens. *Public Health Agency of Canada*, *93*, 77–91.

Dorer, M. S., Cohen, I. E., Sessler, T. H., Fero, J., & Salama, N. R. (2013). Natural Competence Promotes *Helicobacter pylori* Chronic Infection. *Infection and Immunity*, *81*(1), 209–215.

Dorman, C. J., Chatfield, S., Higgins, C. F., Hayward, C., & Dougan, G. (1989). Characterization of porin and *ompR* mutants of a virulent strain of *Salmonella* Typhimurium: *ompR* mutants are attenuated *in vivo*. *Infection and Immunity*, *57*(7), 2136–40.

Dougan, G., John, V., Palmer, S., & Mastroeni, P. (2011). Immunity to salmonellosis. *Immunological Reviews*. http://doi.org/10.1111/j.1600-065X.2010.00999.x

Doye, A., Mettouchi, A., Bossis, G., Clément, R., Buisson-Touati, C., Flatau, G., … Lemichez, E. (2002). CNF1 exploits the ubiquitin-proteasome machinery to restrict Rho GTPase activation for bacterial host cell invasion. *Cell*, *111*(4), 553–64.

Dranoff, G. (2004). Cytokines in cancer pathogenesis and cancer therapy. *Nature Reviews Cancer*, *4*(1), 11–22.

Drechsler-Hake, D., Alamir, H., Hahn, J., Günter, M., Wagner, S., Schütz, M., … Autenrieth, S. E. (2016). Mononuclear phagocytes contribute to intestinal invasion and dissemination of *Yersinia enterocolitica*. *International Journal of Medical Microbiology*, *306*(6), 357–366.

Dube, P. H., Revell, P. A., Chaplin, D. D., Lorenz, R. G., & Miller, V. L. (2001). A role for IL-1 alpha in inducing pathologic inflammation during bacterial infection. *Proceedings of the National Academy of Sciences of the United States of America*, *98*(19), 10880–5.

Dube, P. H., Handley, S. A., Lewis, J., & Miller, V. L. (2004). Protective Role of Interleukin-6 during *Yersinia enterocolitica* Infection Is Mediated through the Modulation of Inflammatory Cytokines. *Infection and Immunity*, *72*(6), 3561.

Dube, P. (2009). Interaction of *Yersinia* with the Gut: Mechanisms of pathogenesis and immune evasion. *Current Topics in Microbiology and Immunology*. http://doi.org/10.1007/978-3-642-01846-6-3

Dudakov, J. A., Hanash, A. M., & van den Brink, M. R. M. M. (2015). Interleukin-22: Immunobiology and Pathology. *Annual Review of Immunology*, *33*(1), 747–85.

Dudziak, D., Kamphorst, A. O., Heidkamp, G. F., Buchholz, V. R., Trumpfheller, C., Yamazaki, S., … Nussenzweig, M. C. (2007). Differential antigen processing by dendritic cell subsets *in vivo*. *Science*, *315*(5808), 107–111.

Dunkelberger, J. R., & Song, W.-C. (2010). Complement and its role in innate and adaptive immune responses. *Cell Research*, *20*(1), 34–50.

Eaton, K. A., Brooks, C. L., Morgan, D. R., & Krakowka, S. (1991). Essential Role of Urease in Pathogenesis of Gastritis Induced by Helicobacter-Pylori in Gnotobiotic Piglets. *Infection and Immunity*, *59*(7), 2470–2475.

Eaton, K. A., Suerbaum, S., Josenhans, C., & Krakowka, S. (1996). Colonization of gnotobiotic piglets by *Helicobacter pylori* deficient in two flagellin genes. *Infection and Immunity*, *64*(7), 2445–2448.

Eckmann, L., & Kagnoff, M. F. (2005). Intestinal mucosal responses to microbial infection. *Springer Seminars in Immunopathology*, *27*(2), 181–196.

Eddy, J. L., Gielda, L. M., Caulfield, A. J., Rangel, S. M., & Lathem, W. W. (2014). Production of outer membrane vesicles by the plague pathogen *Yersinia pestis*. *PLoS ONE*, *9*(9). http://doi.org/10.1371/journal.pone.0107002

Edgar, R. C. (2010). Search and clustering orders of magnitude faster than BLAST. *Bioinformatics*, *26*(19), 2460–2461.

Eitel, J., & Dersch, P. (2002). The YadA Protein of *Yersinia pseudotuberculosis* Mediates High-Efficiency Uptake into Human Cells under Environmental Conditions in Which Invasin Is Repressed. *Infection and Immunity*, *70*(9), 4880–4891.

Ekaza, E., Guilloteau, L., Teyssier, J., Liautard, J. P., & Köhler, S. (2000). Functional analysis of the ClpATPase ClpA of *Brucella suis*, and persistence of a knockout mutant in BALB/c mice. *Microbiology (Reading, England)*, (7), 1605–16.

El Kebir, D., & Filep, J. G. (2010). Role of neutrophil apoptosis in the resolution of inflammation. *TheScientificWorldJournal*, *10*, 1731–1748.

El Tahir, Y., & Skurnik, M. (2001). YadA, the multifaceted *Yersinia* adhesin. *International Journal of Medical Microbiology : IJMM*, *291*(3), 209–18.

El-Benna, J., Hurtado-Nedelec, M., Marzaioli, V., Marie, J. C., Gougerot-Pocidalo, M. A., & Dang, P. M. C. (2016). Priming of the neutrophil respiratory burst: role in host defense and inflammation. *Immunological Reviews*. http://doi.org/10.1111/imr.12447

El-Zaatari, M., Chang, Y.-M., Zhang, M., Franz, M., Shreiner, A., McDermott, A. J., … Kao, J. Y. (2014). Tryptophan Catabolism Restricts IFN-γ-expressing Neutrophils and *Clostridium difficile* Immunopathology. *Journal of Immunology (Baltimore, Md. : 1950)*, *193*(2), 807–816.

Elkington, P. T. G., O'Kane, C. M., & Friedland, J. S. (2005). The paradox of matrix metalloproteinases in infectious disease. *Clinical and Experimental Immunology*, *142*(1), 12–20.

Eppinger, M., Rosovitz, M. J., Fricke, W. F., Rasko, D. A., Kokorina, G., Fayolle, C., … Ravel, J. (2007). The complete genome sequence of *Yersinia pseudotuberculosis* IP31758, the Causative agent of Far East scarlet-like fever. *PLoS Genetics*, *3*(8), 1508–1523.

Erhardt, M., & Dersch, P. (2015). Regulatory principles governing *Salmonella* and *Yersinia* virulence. *Frontiers in Microbiology*, *6*, 949.

Etienne-Manneville, S., & Hall, a. (2002). Rho GTPases in Cell Biology. *Nature*, *420*(December), 629–635.

Evans, D. F., Pye, G., Bramley, R., Clark, a G., Dyson, T. J., & Hardcastle, J. D. (1988). Measurement of gastrointestinal pH profiles in normal ambulant human subjects. *Gut*, *29*(8), 1035–41.

Everard, A., Belzer, C., Geurts, L., Ouwerkerk, J. P., Druart, C., Bindels, L. B., … Cani, P. D. (2013). Cross-talk between *Akkermansia muciniphila* and intestinal epithelium controls diet-induced obesity. *Proceedings of the National Academy of Sciences of the United States of America*, *110*(22), 9066–71.

Ewing, W. H., Ross, A. J., Brenner, D. O. N. J., & Fanning, G. R. (1978). *Yersinia ruckeri* sp.. the Redmouth (RM) Bacterium. *International Journal of Systematic Bacteriology*, *28*(1), 37–44.

Fabbri, A., Travaglione, S., & Fiorentini, C. (2010). *Escherichia coli* cytotoxic necrotizing factor 1 (CNF1): Toxin biology, *in vivo* applications and therapeutic potential. *Toxins*, *2*(2), 283–296.

Fahlgren, A., Avican, K., Westermark, L., Nordfelth, R., & Fällman, M. (2014). Colonization of cecum is important for development of persistent infection by *Yersinia pseudotuberculosis*. *Infection and Immunity*, *82*(8), 3471–3482.

Fallarino, F., Grohmann, U., You, S., McGrath, B. C., Cavener, D. R., Vacca, C., … Puccetti, P. (2006). Tryptophan catabolism generates autoimmune-preventive regulatory T cells. *Transplant Immunology*, *17*(1), 58–60.

Falnes, P. O., & Sandvig, K. (2000). Penetration of protein toxins into cells. *Current Opinion in Cell Biology*. http://doi.org/10.1016/S0955-0674(00)00109-5

Falzano, L., Fiorentini, C., Donelli, G., Michel, E., Kocks, C., Cossart, P., … Boquet, P. (1993). Induction of phagocytic behavior in human epithelial cells by *Escherichia coli* cytotoxic necrotizing factor type 1. *Mol Microbiol*, *9*(6), 1247–1254.

Fang, Y., Xu, C., Fu, Y. X., Holers, V. M., & Molina, H. (1998). Expression of complement receptors 1 and 2 on follicular dendritic cells is necessary for the generation of a strong antigen-specific IgG response. *Journal of Immunology (Baltimore, Md. : 1950)*, *160*(11), 5273–5279.

Favre, D., Mold, J., Hunt, P. W., Kanwar, B., Loke, P., Seu, L., … McCune, J. M. (2010). Tryptophan catabolism by indoleamine 2,3-dioxygenase 1 alters the balance of TH17 to regulatory T cells in HIV disease. *Science Translational Medicine*, *2*(32), 32ra36.

Fehr, D., Burr, S. E., Gibert, M., D'Alayer, J., Frey, J., & Popoff, M. R. (2007). *Aeromonas* exoenzyme T of *Aeromonas salmonicida* is a bifunctional protein that targets the host cytoskeleton. *Journal of Biological Chemistry*, *282*(39), 28843–28852.

Felek, S., & Krukonis, E. S. (2009). The *Yersinia pestis* Ail protein mediates binding and Yop delivery to host cells required for plague virulence. *Infection and Immunity*, *77*(2), 825–836.

Fetherston, J., Bertolino, V., & Perry, R. (1999). YbtP and YbtQ: two ABC transporters required for iron uptake in *Yersinia pestis*. *Molecular Microbiology*, *32*(2), 289–299.

Finethy, R., Jorgensen, I., Haldar, A. K., de Zoete, M. R., Strowig, T., Flavell, R. A., … Coers, J. (2015). Guanylate Binding Proteins Enable Rapid Activation of Canonical and Noncanonical Inflammasomes in *Chlamydia*-Infected Macrophages. *Infection and Immunity*, *83*(12), 4740–4749.

Fiorentini, C., Arancia, G., Caprioli, A., Falbo, V., Ruggeri, F. M., & Donelli, G. (1988). Cytoskeletal changes induced in HEp-2 cells by the cytotoxic necrotizing factor of *Escherichia coli*. *Toxicon*, *26*(11), 1047–1056.

Fiorentini, C., Fabbri, A., Flatau, G., Donelli, G., Matarrese, P., Lemichez, E., … Boquet, P. (1997). *Escherichia coli* cytotoxic necrotizing factor 1 (CNF1), a toxin that activates the Rho GTPase. *Journal of Biological Chemistry*, *272*(31), 19532–19537.

Flatau, G., Lemichez, E., Gauthier, M., Chardin, P., Paris, S., Fiorentini, C., & Boquet, P. (1997). Toxin-induced activation of the G protein p21 Rho by deamidation of glutamine. *Nature*, *387*(6634), 729–733.

Flügel, A., Schulze-Koops, H., Heesemann, J., Kühn, K., Sorokin, L., Burkhardt, H., … Emmrich, F. (1994). Interaction of enteropathogenic *Yersinia enterocolitica* with complex basement membranes and the extracellular matrix proteins collagen type IV, laminin-1 and -2, and nidogen/entactin. *Journal of Biological Chemistry*, *269*(47), 29732–29738.

Fonseca, D. M. Da, Hand, T. W., Han, S. J., Gerner, M. Y., Zaretsky, A. G., Byrd, A. L., … Belkaid, Y. (2015). Microbiota-Dependent Sequelae of Acute Infection Compromise Tissue-Specific Immunity. *Cell*, *163*(2), 354–366.

Foxman, B. (2003). Epidemiology of urinary tract infections: Incidence, morbidity, and economic costs. *Disease-a-Month*. http://doi.org/10.1016/S0011-5029(03)90000-9

Franceschi, F., Zuccalà, G., Roccarina, D., & Gasbarrini, A. (2014). Clinical effects of *Helicobacter pylori* outside the stomach. *Nature Reviews. Gastroenterology & Hepatology*, *11*(4), 234–242.

Fredriksson-Ahomaa, M., Stolle, A., Siitonen, A., & Korkeala, H. (2006). Sporadic human *Yersinia enterocolitica* infections caused by bioserotype 4/O:3 originate mainly from pigs. *Journal of Medical Microbiology*, *55*(6), 747–749.

Freeman, G. J., Long, A. J., Iwai, Y., Bourque, K., Chernova, T., Nishimura, H., … Honjo, T. (2000). Engagement of the PD-1 immunoinhibitory receptor by a novel B7 family member leads to negative regulation of lymphocyte activation. *The Journal of Experimental Medicine*, *192*(7), 1027–1034.

Freeman, S. A., & Grinstein, S. (2014). Phagocytosis: Receptors, signal integration, and the cytoskeleton. *Immunological Reviews*, *262*(1), 193–215.

Frick, I.-M., Akesson, P., Herwald, H., Mörgelin, M., Malmsten, M., Nägler, D. K., & Björck, L. (2006). The contact system--a novel branch of innate immunity generating antibacterial peptides. *The EMBO Journal*, *25*(23), 5569–78.

Frumento, G., Rotondo, R., Tonetti, M., Damonte, G., Benatti, U., & Ferrara, G. B. (2002). Tryptophan-derived catabolites are responsible for inhibition of T and natural killer cell proliferation induced by indoleamine 2,3-dioxygenase. *The Journal of Experimental Medicine*, *196*(4), 459–68.

Fukushima, H., Sato, T., Nagasako, R., & Takeda, I. (1991, June). Acute mesenteric lymphadenitis due to *Yersinia pseudotuberculosis* lacking a virulence plasmid. *Journal of Clinical Microbiology*. American Society for Microbiology.

Fukushima, H., Gomyoda, M., Tsubokura, M., & Aleksic, S. (1995). Isolation of *Yersinia pseudotuberculosis* from river waters in Japan and Germany using direct KOH and HeLa cell treatments. *Int J Med Microbiol Virol Parasitol Infect Dis*, *282*(1), 40–49.

Fukushima, H., Matsuda, Y., Seki, R., Tsubokura, M., Takeda, N., Shubin, F. N., … Xue Bin Zheng. (2001). Geographical heterogeneity between Far Eastern and western countries in prevalence of the virulence plasmid, the superantigen *Yersinia pseudotuberculosis*-derived mitogen, and the high-pathogenicity island among *Yersinia pseudotuberculosis* strains. *Journal of Clinical Microbiology*, *39*(10), 3541–3547.

Furlaneto, C. J., & Campa, A. (2000). A novel function of serum amyloid A: a potent stimulus for the release of tumor necrosis factor-alpha, interleukin-1beta, and interleukin-8 by human blood neutrophil. *Biochemical and Biophysical Research Communications*, *268*(2), 405–8.

Galdiero, F., Carratelli, C. R., Nuzzo, I., Bentivoglio, C., & Galdiero, M. (1988). Phagocytosis of bacterial aggregates by granulocytes. *European Journal of Epidemiology*, *4*(4), 456–460.

Galindo, C. L., Rosenzweig, J. A., Kirtley, M. L., & Chopra, A. K. (2011). Pathogenesis of *Y. enterocolitica* and *Y. pseudotuberculosis* in Human Yersiniosis. *Journal of Pathogens*, *2011*, 1–16.

Ganesh, B. P., Klopfleisch, R., Loh, G., Blaut, M., Derrien, M., Passel, M. van, … Macpherson, G. (2013). Commensal *Akkermansia muciniphila* Exacerbates Gut Inflammation in *Salmonella* Typhimurium-Infected Gnotobiotic Mice. *PLoS ONE*, *8*(9), e74963.

Garbers, C., & Scheller, J. (2013). Interleukin-6 and interleukin-11: Same same but different. *Biological Chemistry*. http://doi.org/10.1515/hsz-2013-0166

Garlanda, C., Dinarello, C. A., & Mantovani, A. (2013). The Interleukin-1 Family: Back to the Future. *Immunity*, *39*(6), 1003–1018.

Gaston, J. S. H., Cox, C., & Granfors, K. (1999). Clinical and experimental evidence for persistent *Yersinia* infection in reactive arthritis. *Arthritis and Rheumatism*, *42*(10), 2239–2242.

Gebert, B., Fischer, W., Weiss, E., Hoffmann, R., & Haas, R. (2003). *Helicobacter pylori* vacuolating cytotoxin inhibits T lymphocyte activation. *Science*, *301*(5636), 1099–1102.

Gee, K., Guzzo, C., Che Mat, N. F., Ma, W., & Kumar, A. (2009). The IL-12 family of cytokines in infection, inflammation and autoimmune disorders. *Inflammation & Allergy Drug Targets*, *8*(April), 40–52.

Geiser, T. K., Kazmierczak, B. I., Garrity-Ryan, L. K., Matthay, M. A., & Engel, J. N. (2001). *Pseudomonas aeruginosa* ExoT inhibits *in vitro* lung epithelial wound repair. *Cellular Microbiology*, *3*(4), 223–36.

Gemski, P., Lazere, J. R., Casey, T., & Wohlhieter, J. A. (1980). Presence of a virulence-associated plasmid in *Yersinia pseudotuberculosis*. *Infection and Immunity*, *28*(3), 1044–1047.

Gercken, J., Pryjma, J., Ernst, M., & Flad, H. D. (1994). Defective antigen presentation by *Mycobacterium tuberculosis*-infected monocytes. *Infection and Immunity*, *62*(8), 3472–8.

Gerhard, M., Schmees, C., Voland, P., Endres, N., Sander, M., Reindl, W., … Prinz, C. (2005). A secreted low-molecular-weight protein from *Helicobacter pylori* induces cell-cycle arrest of T cells. *Gastroenterology*, *128*(5), 1327–1339.

Gerritsen, B., & Pandit, A. (2015). The memory of a killer T cell: models of CD8(+) T cell differentiation. *Immunology and Cell Biology*, *94*(October), 1–27.

Gewirtz, A. T., Yu, Y., Krishna, U. S., Israel, D. a, Lyons, S. L., & Peek, R. M. (2004). *Helicobacter pylori* flagellin evades toll-like receptor 5-mediated innate immunity. *The Journal of Infectious Diseases*, *189*(10), 1914–1920.

Geyer, R. (2014). *Analysis of the molecular function of invasin-like proteins of Yersinia pseudotuberculosis and their role in pathogenesis*. Hannover.

Giannattasio, G., Fujioka, D., Xing, W., Katz, H. R., Boyce, J. A., & Balestrieri, B. (2010). Group V secretory phospholipase A2 reveals its role in house dust mite-induced allergic pulmonary inflammation by regulation of dendritic cell function. *Journal of Immunology (Baltimore, Md. : 1950)*, *185*(7), 4430–4438.

Giannitti, F., Barr, B. C., Brito, B. P., Uzal, F. A., Villanueva, M., & Anderson, M. (2014). *Yersinia pseudotuberculosis* infections in goats and other animals diagnosed at the California Animal Health and Food Safety Laboratory System: 1990-2012. *Journal of Veterinary Diagnostic Investigation : Official Publication of the American Association of Veterinary Laboratory Diagnosticians, Inc*, *26*(1), 88–95.

Goehring, U. M., Schmidt, G., Pederson, K. J., Aktories, K., & Barbieri, J. T. (1999). The N-terminal domain of *Pseudomonas aeruginosa* exoenzyme S is a GTPase-activating protein for Rho GTPases. *The Journal of Biological Chemistry*, *274*(51), 36369–36372.

Gogoi, M., Datey, A., Wilson, K. T., & Chakravortty, D. (2016). Dual role of arginine metabolism in establishing pathogenesis. *Current Opinion in Microbiology*. http://doi.org/10.1016/j.mib.2015.10.005

Goh, C. C., Roggerson, K. M., Lee, H.-C., Golden-Mason, L., Rosen, H. R., & Hahn, Y. S. (2016). Hepatitis C Virus–Induced Myeloid-Derived Suppressor Cells Suppress NK Cell IFN-γ Production by Altering Cellular Metabolism via Arginase-1. *The Journal of Immunology*, *196*(5), 2283–2292.

Goldmann, O., Lengeling, A., Böse, J., Bloecker, H., Geffers, R., Chhatwal, G. S., & Medina, E. (2005). The role of the MHC on resistance to group a streptococci in mice. *Journal of Immunology (Baltimore, Md. : 1950)*, *175*(6), 3862–72.

Golubovskaya, V., & Wu, L. (2016). Different subsets of T cells, memory, effector functions, and CAR-T immunotherapy. *Cancers*. Multidisciplinary Digital Publishing Institute (MDPI). http://doi.org/10.3390/cancers8030036

Gong, P., Canaan, A., Wang, B., Leventhal, J., Snyder, A., Nair, V., … Ross, M. J. (2010). The ubiquitin-like protein FAT10 mediates NF-κB activation. *Journal of the American Society of Nephrology : JASN*, *21*(2), 316–326.

Gonzalez-Rodriguez, D., Maddugoda, M. P., Stefani, C., Janel, S., Lafont, F., Cuvelier, D., … Brochard-Wyart, F. (2012). Cellular dewetting: Opening of macroapertures in endothelial cells. *Physical Review Letters*, *108*(21).

Gordon, S., & Taylor, P. R. (2005). Monocyte and macrophage heterogeneity. *Nature Reviews. Immunology*, *5*(12), 953–64.

Gordon, S., & Martinez, F. O. (2010). Alternative activation of macrophages: Mechanism and functions. *Immunity*. http://doi.org/10.1016/j.immuni.2010.05.007

Goto, Y., & Kiyono, H. (2012, January). Epithelial barrier: An interface for the cross-communication between gut flora and immune system. *Immunological Reviews*. http://doi.org/10.1111/j.1600-065X.2011.01078.x

Grabenstein, J. P., Marceau, M., Pujol, C., Simonet, M., & Bliska, J. B. (2004). The response regulator PhoP of *Yersinia pseudotuberculosis* is important for replication in macrophages and for virulence. *Infection and Immunity*, *72*(9), 4973–4984.

Grabiner, B. C., Blonska, M., Lin, P.-C., You, Y., Wang, D., Sun, J., … Lin, X. (2007). CARMA3 deficiency abrogates G protein-coupled receptor-induced NF- B activation. *Genes & Development*, *21*(8), 984–996.

Granfors, K., & Toivanen, A. (1986). IgA-anti-*Yersinia* antibodies in *Yersinia* triggered reactive arthritis. *Annals of the Rheumatic Diseases*, *45*(7), 561–5.

Granfors, K., Jalkanen, S., von Essen, R., Lahesmaa-Rantala, R., Isomaki, O., Pekkola-Heino, K., … Toivanen, A. (1989). *Yersinia* antigens in synovial-fluid cells from patients with reactive arthritis. *The New England Journal of Medicine*, *320*(4), 216–221.

Granfors, K., Merilahti-palo, R., Luukkainen, R., Mottonen, T., Lahesmaa, R., Probst, P., & Toivanen, P. (1998). Persistence Of *Yersinia* antigens in peripheral blood cells from patients with *Yersinia enterocolitica* O :3 infection with or without reactive arthritis. *Arthritis & Rheumatism*, *41*(5), 855–862.

Grant, S. G. N., Jessee, J., Bloom, F. R., & Hanahan, D. (1990). Differential plasmid rescue from transgenic mouse DNAs into *Escherichia coli* methylation-restriction mutants. *Proceedings of the National Academy of Sciences of the United States of America*, *87*(12), 4645–4649.

Grant, S. S., & Hung, D. T. (2013). Persistent bacterial infections, antibiotic tolerance, and the oxidative stress response. *Virulence*, *4*(4), 273–283.

Grasberger, H., Gao, J., Nagao-Kitamoto, H., Kitamoto, S., Zhang, M., Kamada, N., … Kao, J. Y. (2015). Increased Expression of DUOX2 Is an Epithelial Response to Mucosal Dysbiosis Required for Immune Homeostasis in Mouse Intestine. *Gastroenterology*, *149*(7), 1849–59.

Green, E. R., Clark, S., Crimmins, G. T., Mack, M., Kumamoto, C. A., & Mecsas, J. (2016). Fis is essential for Y*ersinia pseudotuberculosis* virulence and protects against reactive oxygen species produced by phagocytic cells during infection. *PLOS Pathogens*, *12*(9), e1005898.

Grohmann, U., Fallarino, F., Bianchi, R., Belladonna, M. L., Vacca, C., Orabona, C., … Puccetti, P. (2001). IL-6 inhibits the tolerogenic function of CD8α+ dendritic cells expressing indoleamine 2,3-dioxygenase. *The Journal of Immunology*, *167*(2).

Groisman, E. A. Priciples of bacterial pathogenesis. San Diego: Academic Press Inc, 2001. Print. ISBN: 978-0-12-304220-0

Grönroos, J. O., Laine, V. J., Janssen, M. J., Egmond, M. R., & Nevalainen, T. J. (2001). Bactericidal properties of group IIA and group V phospholipases A2. *Journal of Immunology (Baltimore, Md. : 1950)*, *166*(6), 4029–4034.

Gruys, E., Toussaint, M. J. M., Niewold, T. A., & Koopmans, S. J. (2005). Acute phase reaction and acute phase proteins. *Journal of Zhejiang University. Science. B*, *6*(11), 1045–56.

Guidoboni, M., Ferreri, A. J. M., Ponzoni, M., Doglioni, C., & Dolcetti, R. (2006). Infectious agents in mucosa-associated lymphoid tissue-type lymphomas: pathogenic role and therapeutic perspectives. *Clinical Lymphoma & Myeloma*, *6*(4), 289–300.

Gwee, K.-A., Collins, S. M., Read, N. W., Rajnakova, A., Deng, Y., Graham, J. C., … Moochhala, S. M. (2003). Increased rectal mucosal expression of interleukin-1β in recently acquired post-infectious irritable bowel syndrome. *Gut*, *52*(4), 523–6.

Ha, S. J., Lee, C. H., Lee, S. B., Kim, C. M., Jang, K. L., Shin, H. S., & Sung, Y. C. (1999). A novel function of IL-12p40 as a chemotactic molecule for macrophages. *Journal of Immunology (Baltimore, Md. : 1950)*, *163*(5), 2902–8.

Haas, P.-J., & van Strijp, J. (2007). Anaphylatoxins: their role in bacterial infection and inflammation. *Immunologic Research*, *37*(3), 161–175.

Hamburger, Z. A., Brown, M. S., Isberg, R. R., & Bjorkman, P. J. (1999). Integrin-Binding Protein Crystal Structure of Invasin: A Bacterial Crystal Structure of Invasin: A Bacterial Integrin-Binding Protein. *Science*, *286*(5438), 291–295.

Hancock, G. E., Schaedler, R. W., & MacDonald, T. T. (1986). *Yersinia enterocolitica* infection in resistant and susceptible strains of mice. *Infection and Immunity*, *53*(1), 26–31.

Hannan, T. J., Mysorekar, I. U., Hung, C. S., Isaacson-Schmid, M. L., & Hultgren, S. J. (2010). Early severe inflammatory responses to uropathogenic *E. coli* predispose to chronic and recurrent urinary tract infection. *PLoS Pathogens*, *6*(8), 29–30.

Hannan, T. J., Totsika, M., Mansfield, K. J., Moore, K. H., Schembri, M. A., & Hultgren, S. J. (2012). Host-pathogen checkpoints and population bottlenecks in persistent and intracellular uropathogenic *Escherichia coli* bladder infection. *FEMS Microbiology Reviews*. http://doi.org/10.1111/j.1574-6976.2012.00339.x

Hannu, T., Mattila, L., Nuorti, J. P., Ruutu, P., Mikkola, J., Siitonen, A., & Leirisalo-Repo, M. (2003). Reactive arthritis after an outbreak of *Yersinia pseudotuberculosis* serotype O:3 infection. *Annals of the Rheumatic Diseases*, *62*(9), 866–9.

Hansen, J. D., Vojtech, L. N., & Laing, K. J. (2011). Sensing disease and danger: A survey of vertebrate PRRs and their origins. *Developmental and Comparative Immunology*. http://doi.org/10.1016/j.dci.2011.01.008

Hanski, C., Kutschka, U., Schmoranzer, H. P., Naumann, M., Stallmach, A., Hahn, H., … Riecken, E. O. (1989). Immunohistochemical and electron microscopic study of interaction of *Yersinia enterocolitica* serotype O:8 with intestinal mucosa during experimental enteritis. *Infection and Immunity*, *57*(3), 673–8.

Hardt, W. D., Chen, L. M., Schuebel, K. E., Bustelo, X. R., & Galán, J. E. (1998). *S*. Typhimurium Encodes an activator of Rho GTPases that induces membrane ruffling and nuclear responses in host cells. *Cell*, *93*(5), 815–826.

Hargreaves, C. E., Grasso, M., Hampe, C. S., Stenkova, A., Atkinson, S., Joshua, G. W. P., … Banga, J. P. (2013). *Yersinia enterocolitica* provides the link between thyroid-stimulating antibodies and their germline counterparts in Graves' disease. *Journal of Immunology (Baltimore, Md. : 1950)*, *190*(11), 5373–81.

Hawgood, B. J. (2008). Alexandre Yersin (1863-1943): discoverer of the plague bacillus, explorer and agronomist. *Journal of Medical Biography*, *16*(3), 167–172.

Hawn, T. R., Scholes, D., Li, S. S., Wang, H., Yang, Y., Roberts, P. L., … Hooton, T. M. (2009). Toll-like receptor polymorphisms and susceptibility to urinary tract infections in adult women. *PLoS ONE*, *4*(6).

Hawrelak, J. A., & Myers, S. P. (2004). The causes of intestinal dysbiosis: A review. *Alternative Medicine Review*. http://doi.org/10.1016/0965-2299(93)90012-3

He, S. Y., Nomura, K., & Whittam, T. S. (2004a). Type III protein secretion mechanism in mammalian and plant pathogens. *Biochim. Biophys. Acta*, *1694*(1–3), 181–206.

He, Y.-W., Li, H., Zhang, J., Hsu, C.-L., Lin, E., Zhang, N., … Bevan, M. J. (2004b). The extracellular matrix protein mindin is a pattern-recognition molecule for microbial pathogens. *Nature Immunology*, *5*(1), 88–97.

Heasman, S. J., & Ridley, A. J. (2008). Mammalian Rho GTPases: new insights into their functions from *in vivo* studies. *Nature Reviews. Molecular Cell Biology*, *9*(9), 690–701.

Hecht, G., Pothoulakis, C., LaMont, J. T., & Madara, J. L. (1988). *Clostridium difficile* toxin A perturbs cytoskeletal structure and tight junction permeability of cultured human intestinal epithelial monolayers. *Journal of Clinical Investigation*, *82*(5), 1516–1524.

Heesemann, J., & Laufs, R. (1983). Construction of a mobilizable *Yersinia enterocolitica* virulence plasmid. *Journal of Bacteriology*, *155*(2), 761–767.

Heesemann, J., Algermissen, B., & Laufs, R. (1984). Genetically manipulated virulence of *Yersinia enterocolitica*. *Infection and Immunity*, *46*(1), 105–110.

Heesemann, J. (1987). Chromosomal-encoded siderophores are required for mouse virulence of enteropathogenic *Yersinia* species. *FEMS Microbiology Letters*, *48*(1–2), 229–233.

Heesemann, J., Gaede, K., & Autenrieth, I. B. (1993a). Experimental *Yersinia enterocolitica* infection in rodents: a model for human yersiniosis. *APMIS : Acta Pathologica, Microbiologica, et Immunologica Scandinavica*, *101*, 417–429.

Heesemann, J., Hantke, K., Vocke, T., Saken, E., Rakin, A., Stojiljkovic, I., & Berner, R. (1993b). Virulence of *Yersinia enterocolitica* is closely associated with siderophore production, expression of an iron-repressible outer membrane polypeptide of 65,000 Da and pesticin sensitivity. *Molecular Microbiology*, *8*(2), 397–408.

Hein, J., Kempf, V. A. J., Diebold, J., Bücheler, N., Preger, S., Horak, I., … Autenrieth, I. B. (2000). Interferon consensus sequence binding protein confers resistance against *Yersinia enterocolitica*. *Infection and Immunity*, *68*(3), 1408–1417.

Heinrich, P. C., Castell, J. V, & Andus, T. (1990). Interleukin-6 and the acute phase response. *Biochemical Journal*, *265*(3), 621–636.

Helaine, S., Thompson, J. a., Watson, K. G., Liu, M., Boyle, C., & Holden, D. W. (2010). Dynamics of Intracellular Bacterial Replication at the Single Cell Level. *Proceedings of the National Academy of Sciences*, *107*(8), 3746–3751.

Helmy, K. Y., Katschke, K. J., Gorgani, N. N., Kljavin, N. M., Elliott, J. M., Diehl, L., … Van Lookeren Campagne, M. (2006). CRIg: A macrophage complement receptor required for phagocytosis of circulating pathogens. *Cell*, *124*(5), 915–927.

Hemmerich, S., & Rosen, S. D. (2000). MINI REVIEW Carbohydrate sulfotransferases in lymphocyte homing. *Glycobiology*, *10*(9), 849–856.

Heroven, A. K., Sest, M., Pisano, F., Scheb-Wetzel, M., Steinmann, R., Bohme, K., … Dersch, P. (2012). Crp induces switching of the CsrB and CsrC RNAs in *Yersinia pseudotuberculosis* and links nutritional status to virulence. *Front Cell Infect Microbiol*, *2*(December), 158.

Hessey, S. J., Spencer, J., Wyatt, J. I., Sobala, G., Rathbone, B. J., Axon, A. T., & Dixon, M. F. (1990). Bacterial adhesion and disease activity in *Helicobacter* associated chronic gastritis. *Gut*, *31*(2), 134–138.

Hiemstra, P. S., Maassen, R. J., Stolk, J., Heinzel-Wieland, R., Steffens, G. J., & Dijkman, J. H. (1996). Antibacterial activity of antileukoprotease. *Infection and Immunity*, *64*(11), 4520–4.

Hild, G., Bugyi, B., & Nyitrai, M. (2010). Conformational dynamics of actin: Effectors and implications for biological function. *Cytoskeleton*, *67*(10), 609–629.

Hill, D. A., & Artis, D. (2009). Intestinal bacteria and the regulation of immune cell homeostasis. *Annual Review of Immunology*, *28*(1), 623–667.

Hinnebusch, B. J., Chouikha, I., & Sun, Y. (2016). Ecological Opportunity, Evolution, and the Emergence of Flea-Borne Plague. *Infection and Immunity*, *84*(7), 1932–1940.

Hitzler, I., Sayi, A., Kohler, E., Engler, D. B., Koch, K. N., Hardt, W.-D., & Müller, A. (2012). Caspase-1 has both proinflammatory and regulatory properties in *Helicobacter* infections, which are

differentially mediated by its substrates IL-1β and IL-18. *Journal of Immunology (Baltimore, Md. : 1950)*, *188*(8), 3594–602.

Hofman, P., Negrate, G. Le, Mograbi, B., Hofman, V., Brest, P., Alliana-Schmid, A., … Rossi, B. (2000). *Escherichia coli* cytotoxic necrotizing factor-1 (CNF-1) increases the adherence to epithelia and the oxidative burst of human polymorphonuclear leukocytes but decreases bacteria phagocytosis. *Journal of Leukocyte Biology*, *68*(4), 522–528.

Hoiczyk, E., Roggenkamp, A., Reichenbecher, M., Lupas, A., & Heesemann, J. (2000). Structure and sequence analysis of *Yersinia* YadA and Moraxella UspAs reveal a novel class of adhesins. *The EMBO Journal*, *19*(22), 5989–99.

Holmes, C., & Stanford, W. L. (2007). Concise review: stem cell antigen-1: expression, function, and enigma. *Stem Cells*, *25*(6), 1339–1347.

Holmström, A., Petterson, J., Rosqvist, R., Håkansson, S., Tafazoli, F., Fällman, M., … Forsberg, A. (1997). YopK of *Yersinia pseudotuberculosis* controls translocation of Yop effectors across the eukaryotic cell membrane. *Molecular Microbiology*, *24*(1), 73–91.

Hong, J.-B., Zuo, W., Wang, A.-J., & Lu, N.-H. (2016). *Helicobacter pylori* infection synergistic with IL-1β gene polymorphisms potentially contributes to the carcinogenesis of gastric cancer. *International Journal of Medical Sciences*, *13*(4), 298–303.

Hoogkamp-Korstanje, J. a, de Koning, J., & Heesemann, J. (2000). Persistence of *Yersinia enterocolitica* in man. *Infection*, *16*(2), 81–5.

Hopkins, W. J., James, L. J., Balish, E., & Uehling, D. T. (1993). Congenital immunodeficiencies in mice increase susceptibility to urinary tract infection. *J Urol*, *149*(4), 922–925.

Hopkins, A. M., Walsh, S. V, Verkade, P., Boquet, P., & Nusrat, A. (2003). Constitutive activation of Rho proteins by CNF-1 influences tight junction structure and epithelial barrier function. *Journal of Cell Science*, *116*(Pt 4), 725–742.

Horai, R., Asano, M., Sudo, K., Kanuka, H., Suzuki, M., Nishihara, M., … Iwakura, Y. (1998). Production of mice deficient in genes for interleukin (IL)-1α, IL-1β, IL-1α/β, and IL-1 receptor antagonist shows that IL-1β is crucial in turpentine-induced fever development and glucocorticoid secretion. *The Journal of Experimental Medicine*, *187*(9), 1463–1475.

Horinouchi, T., Nozu, K., Hamahira, K., Inaguma, Y., Abe, J., Nakajima, H., … Iijima, K. (2015). *Yersinia pseudotuberculosis* infection in Kawasaki disease and its clinical characteristics. *BMC Pediatrics*, *15*(1), 177.

Hoste, C., Dumont, J. E., Miot, F., & De Deken, X. (2012). The type of DUOX-dependent ROS production is dictated by defined sequences in DUOXA. *Experimental Cell Research*, *318*(18), 2353–2364.

Howitt, M. R., Lee, J. Y., Lertsethtakarn, P., Vogelmann, R., Joubert, L. M., Ottemann, K. M., & Amieva, M. R. (2011). ChePep controls *Helicobacter pylori* infection of the gastric glands and chemotaxis in the ε-proteobacteria. *mBio*, *2*(4).

Hsieh, C. S., Macatonia, S. E., O'Garra, A., & Murphy, K. M. (1995). T cell genetic background determines default T helper phenotype development *in vitro*. *The Journal of Experimental Medicine*, *181*(2), 713–21.

Hu, Y., Lu, P., Wang, Y., Ding, L., Atkinson, S., & Chen, S. (2009). OmpR positively regulates urease expression to enhance acid survival of *Yersinia pseudotuberculosis*. *Microbiology*, *155*(8), 2522–2531.

Huang, Z., Sutton, S. E., Wallenfang, A. J., Orchard, R. C., Wu, X., Feng, Y., … Alto, N. M. (2009). Structural insights into host GTPase isoform selection by a family of bacterial GEF mimics. *Nature Structural & Molecular Biology*, *16*(8), 853–860.

Hubmacher, D., & Apte, S. S. (2015, September). ADAMTS proteins as modulators of microfibril formation and function. *Matrix Biology*. http://doi.org/10.1016/j.matbio.2015.05.004

Hugli, T. E., & Muller-Eberhard, H. J. (1978). Anaphylatoxins: C3a and C5a. *Adv Immunol*, *26*, 1–53.

Hunt, R. H. (1996). The role of *Helicobacter pylori* in pathogenesis: the spectrum of clinical outcomes. *Scandinavian Journal of Gastroenterology. Supplement*, *220*, 3–9.

Hunter, C. a, & Jones, S. a. (2015). IL-6 as a keystone cytokine in health and disease. *Nature Immunology*, *16*(5), 448–457.

Hurst, M. R. H., Becher, S. A., Young, S. D., Nelson, T. L., & Glare, T. R. (2011). *Yersinia entomophaga* sp. nov., isolated from the New Zealand grass grub *Costelytra zealandica*. *International Journal of Systematic and Evolutionary Microbiology*, *61*(4), 844–849.

Idoyaga, J., Cheong, C., Suda, K., Suda, N., Kim, J. Y., Lee, H., … Steinman, R. M. (2008). Cutting edge: Langerin/CD207 receptor on dendritic cells mediates efficient antigen presentation on MHC I and II products *in vivo*. *The Journal of Immunology*, *180*(6), 3647–3650.

Iizasa, H., Ishihara, S., Richardo, T., Kanehiro, Y., & Yoshiyama, H. (2015). Dysbiotic infection in the stomach. *World Journal of Gastroenterology*. http://doi.org/10.3748/wjg.v21.i40.11450

Ilver, D., Arnqvist, a, Ogren, J., Frick, I. M., Kersulyte, D., Incecik, E. T., … Borén, T. (1998). *Helicobacter pylori* adhesin binding fucosylated histo-blood group antigens revealed by retagging. *Science (New York, N.Y.)*, *279*(5349), 373–377.

Iruela-Arispe, M. L., Diglio, C. A., & Sage, E. H. (1991). Modulation of extracellular matrix proteins by endothelial cells undergoing angiogenesis *in vitro*. *Arteriosclerosis, Thrombosis, and Vascular Biology*, *11*(4).

Isberg, R. R., Voorhis, D. L., & Falkow, S. (1987). Identification of invasin: A protein that allows enteric bacteria to penetrate cultured mammalian cells. *Cell*, *50*(5), 769–778.

Ishii, K. J., Koyama, S., Nakagawa, A., Coban, C., Akira, S., Nakagawa, A., … Phuanukoonnon, S. (2008). Host Innate Immune Receptors and Beyond: Making Sense of Microbial Infections. *Cell Host & Microbe*, *3*(6), 352–363.

Island, M. D., Cui, X., & Warren, J. W. (1999). Effect of *Escherichia coli* cytotoxic necrotizing factor 1 on repair of human bladder cell monolayers *in vitro*. *Infection and Immunity*, *67*(7), 3657–61.

Ismail, H. F., Zhang, J., Lynch, R. G., Wang, Y., & Berg, D. J. (2003). Role for complement in development of *Helicobacter*-induced gastritis in interleukin-10-deficient mice. *Infection and Immunity*, *71*(12), 7140–7148.

Iwakura, Y., Nakae, S., Saijo, S., & Ishigame, H. (2008). The roles of IL-17A in inflammatory immune responses and host defense against pathogens. *Immunological Reviews*. http://doi.org/10.1111/j.1600-065X.2008.00699.x

Izoré, T., Job, V., & Dessen, A. (2011). Biogenesis, regulation, and targeting of the type III secretion system. *Structure*. http://doi.org/10.1016/j.str.2011.03.015

Jacquemet, G., Hamidi, H., & Ivaska, J. (2015). Filopodia in cell adhesion, 3D migration and cancer cell invasion. *Current Opinion in Cell Biology*, *36*, 23–31.

Jaeger, A., Bardehle, D., Oster, M., Gunther, J., Murani, E., Ponsuksili, S., … Kemper, N. (2015). Gene expression profiling of porcine mammary epithelial cells after challenge with *Escherichia coli* and *Staphylococcus aureus in vitro*. *Vet Res*, *46*(1), 50.

Jalava, K., Hakkinen, M., Valkonen, M., Nakari, U., Palo, T., Hallanvuo, S., … Nuorti, J. P. (2006). An outbreak of gastrointestinal illness and erythema nodosum from grated carrots contaminated with *Yersinia pseudotuberculosis*. *The Journal of Infectious Diseases*, *194*(9), 1209–1216.

Janeway, C. A., Travers, P., Walport, M., Shlomchik, M. J. Immunobiology, 5th edition. New York: Garland Science, 2001. Print. ISBN-10: 0-8153-3642-X

Jetten, A. M. (2007). Retinoid-related orphan receptors (RORs): critical roles in development, immunity, circadian rhythm, and cellular metabolism. *Nuclear Receptor Signaling*, *4*, e003.

Jepson, M. A., & Clark, M. A. (2001). The role of M cells in *Salmonella* infection. *Microbes and Infection*, *3*(14–15), 1183–1190.

Jiang, X., Shen, C., Yu, H., Karunakaran, K. P., & Brunham, R. C. (2010). Differences in innate immune responses correlate with differences in murine susceptibility to *Chlamydia muridarum* pulmonary infection. *Immunology*, *129*(4), 556–566.

Jiang, W., Wang, H., Li, Y.-S., & Luo, W. (2016). Role of vasoactive intestinal peptide in osteoarthritis. *Journal of Biomedical Science*, *23*(1), 63.

Jiménez-Sousa, M. Á., Medrano, L. M., Liu, P., Almansa, R., Fernández-Rodríguez, A., Gómez-Sánchez, E., … Resino, S. (2017). *IL-1B* rs16944 polymorphism is related to septic shock and death. *European Journal of Clinical Investigation*, *47*(1), 53–62.

Joeris, T., Schmidt, N., Ermert, D., Krienke, P., Visekruna, A., Kuckelkorn, U., … Steinhoff, U. (2012). The proteasome system in infection: Impact of β5 and LMP7 on composition, maturation and quantity of active proteasome complexes. *PLoS ONE*, *7*(6), e39827.

Joffre, O. P., Segura, E., Savina, A., & Amigorena, S. (2012). Cross-presentation by dendritic cells. *Nature Reviews. Immunology*, *12*(8), 557–69.

Johanns, T. M., Ertelt, J. M., Rowe, J. H., & Way, S. S. (2010). Regulatory T cell suppressive potency dictates the balance between bacterial proliferation and clearance during persistent *Salmonella* infection. *PLoS Pathogens*, *6*(8), 31–32.

Johnson, J. R. (1991). Virulence factors in *Escherichia coli* urinary tract infection. *Clinical Microbiology Reviews*, *4*(1), 80–128.

Joiner, K. A., Grossman, N., Schmetz, M., & Leive, L. (1986). C3 binds preferentially to long-chain lipopolysaccharide during alternative pathway activation by *Salmonella montevideo*. *J Immunol*, *136*(2), 710–715.

Jones-Carson, J., Balish, E., & Uehling, D. T. (1999). Susceptibility of immunodeficient gene-knockout mice to urinary tract infection. *Journal of Urology*, *161*(1), 338–341.

Jones, B. D., Ghori, N., & Falkow, S. (1994). *Salmonella* Typhimurium initiates murine infection by penetrating and destroying the specialized epithelial M cells of the Peyer's patches. *The Journal of Experimental Medicine*, *180*(1), 15–23.

Jones, J. W., Kayagaki, N., Broz, P., Henry, T., Newton, K., O'Rourke, K., … Monack, D. M. (2010). Absent in melanoma 2 is required for innate immune recognition of *Francisella tularensis*. *Proceedings of the National Academy of Sciences*, *107*(21), 9771–9776.

Joshua, G. W. P., Karlyshev, A. V., Smith, M. P., Isherwood, K. E., Titball, R. W., & Wren, B. W. (2003). A *Caenorhabditis elegans* model of *Yersinia* infection: Biofilm formation on a biotic surface. *Microbiology*, *149*(11), 3221–3229.

Juhas, U., Ryba-Stanisławowska, M., Szargiej, P., & Myśliwska, J. (2015). Different pathways of macrophage activation and polarization. *Postepy Higieny I Medycyny Doswiadczalnej*. http://doi.org/10.5604/17322693.1150133

Just, I., Selzer, J., Hofmann, F., Green, G. A., & Aktories, K. (1996). Inactivation of Ras by *Clostridium sordellii* lethal toxin-catalyzed glucosylation. *Journal of Biological Chemistry*, *271*(17), 10149–10153.

Justice, S. S., Hung, C., Theriot, J. A., Fletcher, D. A., Anderson, G. G., Footer, M. J., & Hultgren, S. J. (2004). Differentiation and developmental pathways of uropathogenic *Escherichia coli* in urinary tract pathogenesis. *Proceedings of the National Academy of Sciences of the United States of America*, *101*(5), 1333–1338.

Kage, H., Takaya, A., Ohya, M., & Yamamoto, T. (2008). Coordinated regulation of expression of *Salmonella* pathogenicity island 1 and flagellar type III secretion systems by ATP-dependent ClpXP protease. *Journal of Bacteriology*, *190*(7), 2470–8.

Kamada, N., Kim, Y.-G., Sham, H. P., Vallance, B. A., Puente, J. L., Martens, E. C., & Núñez, G. (2012). Regulated virulence controls the ability of a pathogen to compete with the gut microbiota. *Science*, *336*(6086).

Kamdar, K., Khakpour, S., Chen, J., Leone, V., Brulc, J., Mangatu, T., … DePaolo, R. W. (2016). Genetic and metabolic signals during acute enteric bacterial infection alter the microbiota and drive progression to chronic inflammatory disease. *Cell Host & Microbe*, *19*(1), 21–31.

Kampik, D., Schulte, R., & Autenrieth, I. B. (2000). *Yersinia enterocolitica* invasin protein triggers differential production of interleukin-1, interleukin-8, monocyte chemoattractant protein 1, granulocyte-macrophage colony-stimulating factor, and tumor necrosis factor alpha in epithelial cells: implications for understanding the early cytokine network in *Yersinia* infections. *Infection and Immunity*, *68*(5), 2484–92.

Kang, J., & Coles, M. (2012). IL-7: the global builder of the innate lymphoid network and beyond, one niche at a time. *Seminars in Immunology*, *24*(3), 190–7.

Kao, J. Y., Rathinavelu, S., Eaton, K. A., Bai, L., Zavros, Y., Takami, M., … Merchant, J. L. (2006). *Helicobacter pylori*-secreted factors inhibit dendritic cell IL-12 secretion: a mechanism of ineffective host defense. *American Journal of Physiology - Gastrointestinal and Liver Physiology*, *291*(1).

Kao, J. Y., Zhang, M., Miller, M. J., Mills, J. C., Wang, B., Liu, M., … Luther, J. (2010). *Helicobacter pylori* immune escape is mediated by dendritic cell-induced Treg skewing and Th17 suppression in mice. *Gastroenterology*, *138*(3), 1046–1054.

Kao, C.-Y., Sheu, B.-S., & Wu, J.-J. (2016). *Helicobacter pylori* infection: An overview of bacterial virulence factors and pathogenesis. *Biomedical Journal*, *39*(1), 14–23.

Kapatral, V., & Minnich, S. A. (1995). Coordinate, temperature-sensitive regulation of the 3 *Yersinia enterocolitica* flagellin genes. *Molecular Microbiology*, *17*(1), 49–56.

Karin, M., Lawrence, T., & Nizet, V. (2006). Innate immunity gone awry: Linking microbial infections to chronic inflammation and cancer. *Cell*. http://doi.org/10.1016/j.cell.2006.02.016

Kasmapour, B., Gronow, A., Bleck, C. K. E., Hong, W., & Gutierrez, M. G. (2012). Size-dependent mechanism of cargo sorting during lysosome-phagosome fusion is controlled by Rab34. *Proceedings of the National Academy of Sciences of the United States of America*, *109*(50), 20485–90.

Kayagaki, N., Warming, S., Lamkanfi, M., Walle, L. Vande, Louie, S., Dong, J., … Dixit, V. M. (2011). Non-canonical inflammasome activation targets caspase-11. *Nature*, *479*(7371), 117–121.

Kaye, P. M. (1995). Costimulation and the regulation of antimicrobial immunity. *Immunology Today*, *16*(9), 423–427.

Keestra, A. M., Winter, M. G., Auburger, J. J., Frässle, S. P., Xavier, M. N., Winter, S. E., … Bäumler, A. J. (2013). Manipulation of small Rho GTPases is a pathogen-induced process detected by NOD1. *Nature*, *496*(7444), 233–7.

Keller, B., Mühlenkamp, M., Deuschle, E., Siegfried, A., Mössner, S., Schade, J., … Bohn, E. (2015). *Yersinia enterocolitica* exploits different pathways to accomplish adhesion and toxin injection into host cells. *Cellular Microbiology*, *17*(March), 1179–1204.

Kelwick, R., Desanlis, I., Wheeler, G. N., & Edwards, D. R. (2015). The ADAMTS (A Disintegrin and Metalloproteinase with Thrombospondin motifs) family. *Genome Biology*, *16*(1), 113.

Khader, S. A., Partida-Sanchez, S., Bell, G., Jelley-Gibbs, D. M., Swain, S., Pearl, J. E., … Cooper, A. M. (2006). Interleukin 12p40 is required for dendritic cell migration and T cell priming after *Mycobacterium tuberculosis* infection. *The Journal of Experimental Medicine*, *203*(7), 1805–1815.

Khan, N. A., Wang, Y., Kim, K. J., Chung, J. W., Wass, C. A., & Kim, K. S. (2002). Cytotoxic necrotizing factor-1 contributes to *Escherichia coli* K1 invasion of the central nervous system. *Journal of Biological Chemistry*, *277*(18), 15607–15612.

Kim, K. J., Chung, J. W., & Kim, K. S. (2005). 67-kDa laminin receptor promotes internalization of cytotoxic necrotizing factor 1-expressing *Escherichia coli* K1 into human brain microvascular endothelial cells. *Journal of Biological Chemistry*, *280*(2), 1360–1368.

Kimura, A., & Kishimoto, T. (2010). IL-6: Regulator of Treg/Th17 balance. *European Journal of Immunology*, *40*(7), 1830–1835.

Kintakas, C., & McCulloch, D. R. (2011). Emerging roles for ADAMTS5 during development and disease. *Matrix Biology*. http://doi.org/10.1016/j.matbio.2011.05.004

Kiraz, Y., Adan, A., Kartal Yandim, M., & Baran, Y. (2016, April 9). Major apoptotic mechanisms and genes involved in apoptosis. *Tumor Biology*, pp. 1–16. Springer Netherlands.

Kirjavainen, V., Jarva, H., Biedzka-Sarek, M., Blom, A. M., Skurnik, M., & Meri, S. (2008). *Yersinia enterocolitica* serum resistance proteins YadA and Ail bind the complement regulator C4b-binding protein. *PLoS Pathogens*, *4*(8), e1000140.

Klink, B. U., Barden, S., Heidler, T. V., Borchers, C., Ladwein, M., Stradal, T. E. B., … Heinz, D. W. (2010). Structure of *Shigella* IpgB2 in complex with human RhoA: Implications for the mechanism of bacterial guanine nucleotide exchange factor mimicry. *Journal of Biological Chemistry*, *285*(22), 17197–17208.

Knipp, U., Birkholz, S., Kaup, W., Mahnke, K., & Opferkuch, W. (1994). Suppression of human mononuclear cell response by *Helicobacter pylori*: effects on isolated monocytes and lymphocytes. *FEMS Immunology and Medical Microbiology*, *8*(2), 157–66.

Knippenberg, S., Brumshagen, C., Aschenbrenner, F., Welte, T., & Maus, U. A. (2015). Arginase 1 activity worsens lung-protective immunity against *Streptococcus pneumoniae* infection. *European Journal of Immunology*, *45*(6), 1716–1726.

Knodler, L. A., Vallance, B. A., Celli, J., Winfree, S., Hansen, B., Montero, M., & Steele-Mortimer, O. (2010). Dissemination of invasive *Salmonella* via bacterial-induced extrusion of mucosal epithelia. *Proceedings of the National Academy of Sciences of the United States of America*, *107*(41), 17733–8.

Knust, Z., Blumenthal, B., Aktories, K., & Schmidt, G. (2009). Cleavage of *Escherichia coli* cytotoxic necrotizing factor 1 is required for full biologic activity. *Infection and Immunity*, *77*(5), 1835–1841.

Knust, Z., & Schmidt, G. (2010). Cytotoxic necrotizing factors (CNFs)-a growing toxin family. *Toxins*. http://doi.org/10.3390/toxins2010116

Kobayashi, Y. (2008). The role of chemokines in neutrophil biology. *Frontiers in Bioscience : A Journal and Virtual Library*, *13*, 2400–7.

Kohbata, S., Yokoyama, H., & Yabuuchi, E. (1986). Cytopathogenic effect of *Salmonella* Typhi GIFU 10007 on M cells of murine ileal Peyer's patches in ligated ileal loops: an ultrastructural study. *Microbiol Immunol*, *30*(12), 1225–1237.

Köhler, S., Ekaza, E., Guilloteau, L., Liautard, J.-P., & Teyssier, J. (2000). Functional analysis of the ClpATPase ClpA of *Brucella suis*, and persistence of a knockout mutant in BALB/c mice. *Microbiology*, *146*(7), 1605–1616.

Kopf, M., Baumann, H., Freer, G., Freudenberg, M., Lamers, M., Kishimoto, T., … Köhler, G. (1994). Impaired immune and acute-phase responses in interleukin-6-deficient mice. *Nature*, *368*(6469), 339–342.

Kouokam, J. C., Wai, S. N., Fällman, M., Dobrindt, U., Hacker, J., & Uhlin, B. E. (2006). Active cytotoxic necrotizing factor 1 associated with outer membrane vesicles from uropathogenic *Escherichia coli*. *Infection and Immunity*, *74*(4), 2022–2030.

Kraehenbuhl, J.-P. P., & Neutra, M. R. (2000). Epithelial M cells: differentiation and function. *Annual Review of Cell and Developmental Biology*, *16*(1), 301–332.

Krall, R., Schmidt, G., Aktories, K., & Barbieri, J. T. (2000). *Pseudomonas aeruginosa* ExoT is a Rho GTPase-activating protein. *Infection and Immunity*, *68*(10), 6066–6068.

Krych-Goldberg, M., & Atkinson, J. P. (2001). Structure-function relationships of complement receptor type 1. *Immunological Reviews*, *180*, 112–122.

Kuida Lippke, J. A., Ku, G., Harding, M. W., Livingston, D. J., Su, M. S.-S., Flavell, R. A., K. (1995). Altered cytokine export and apoptosis in mice deficient in interleukin-1β converting enzyme. *Science*, *267*(5206), 2000–2003.

Kurmaeva, E., Bhattacharya, D., Goodman, W., Omenetti, S., Merendino, A., Berney, S., … Ostanin, D. V. (2014). Immunosuppressive monocytes: possible homeostatic mechanism to restrain chronic intestinal inflammation. *Journal of Leukocyte Biology*, *96*(3), 377–389.

Labbé, K., & Saleh, M. (2008). Cell death in the host response to infection. *Cell Death and Differentiation*, *15*(9), 1339–1349.

Langford, E. V. (1972). *Pasteurella pseudotuberculosis* infections in western Canada. *The Canadian Veterinary Journal*, *13*(4), 85–87.

Lapointe, S., Brkovic, A., Cloutier, I., Tanguay, J. F., Arm, J. P., & Sirois, M. G. (2010). Group V secreted phospholipase A2 contributes to LPS-induced leukocyte recruitment. *Journal of Cellular Physiology*, *224*(1), 127–134.

LaRock, C. N., & Cookson, B. T. (2012). The *Yersinia* Virulence Effector YopM Binds Caspase-1 to Arrest Inflammasome. *Assembly and Processing*. *Cell Host & Microbe* (Vol. 12).

Larussa, T., Leone, I., Suraci, E., Nazionale, I., Procopio, T., Conforti, F., … Luzza, F. (2015). Enhanced expression of indoleamine 2,3-dioxygenase in *Helicobacter pylori*-infected human gastric mucosa modulates Th1/Th2 pathway and interleukin 17 production. *Helicobacter*, *20*(1), 41–48.

Lathem, W. W., Crosby, S. D., Miller, V. L., & Goldman, W. E. (2005). Progression of primary pneumonic plague: a mouse model of infection, pathology, and bacterial transcriptional activity. *Proceedings of the National Academy of Sciences of the United States of America*, *102*(49), 17786–17791.

Lawley, T. D., Chan, K., Thompson, L. J., Kim, C. C., Govoni, G. R., & Monack, D. M. (2006). Genome-wide screen for *Salmonella* genes required for long-term systemic infection of the mouse. *PLoS Pathogens*, *2*(2), e11.

Lawley, T. D., Bouley, D. M., Hoy, Y. E., Gerke, C., Relman, D. A., & Monack, D. M. (2008). Host transmission of *Salmonella enterica* serovar Typhimurium is controlled by virulence factors and indigenous intestinal microbiota. *Infection and Immunity*, *76*(1), 403–416.

Laws, T. R., Davey, M. S., Titball, R. W., & Lukaszewski, R. (2010). Neutrophils are important in early control of lung infection by *Yersinia pestis*. *Microbes and Infection*, *12*(4), 331–335.

Laws, T. R., Davey, M. S., Green, C., Cooper, I. A. M., Titball, R. W., & Lukaszewski, R. A. (2011). *Yersinia pseudotuberculosis* is resistant to killing by human neutrophils. *Microbes and Infection*, *13*(6), 607–611.

Lebeis, S. L., Powell, K. R., Merlin, D., Sherman, M. A., & Kalman, D. (2009). Interleukin-1 receptor signaling protects mice from lethal intestinal damage caused by the attaching and effacing pathogen *Citrobacter rodentium*. *Infection and Immunity*, *77*(2), 604–614.

Lee, S. H., & Dominguez, R. (2010). Regulation of actin cytoskeleton dynamics in cells. *Molecules and Cells*. http://doi.org/10.1007/s10059-010-0053-8

Lehmann, J., Springer, S., Werner, C., Lindner, T., Bellmann, S., Straubinger, R., … Alber, G. (2006). Immunity induced with a *Salmonella enterica* serovar Enteritidis live vaccine is regulated by Th1-cell-dependent cellular and humoral effector mechanisms in susceptible BALB/c mice. *Vaccine*, *24*(22), 4779–4793.

Lemichez, E., Flatau, G., Bruzzone, M., Boquet, P., & Gauthier, M. (1997). Molecular localization of the *Escherichia coli* cytotoxic necrotizing factor CNF1 cell-binding and catalytic domains. *Molecular Microbiology*, *24*(5), 1061–1070.

Lemichez, E., & Aktories, K. (2013). Hijacking of Rho GTPases during bacterial infection. *Experimental Cell Research*. http://doi.org/10.1016/j.yexcr.2013.04.021

Lemon, J. K., Miller, M. R., & Weiser, J. N. (2015). Sensing of interleukin-1 cytokines during *Streptococcus pneumoniae* colonization contributes to macrophage recruitment and bacterial clearance. *Infection and Immunity*, *83*(8), 3204–3212.

Lengacher, S., Jongeneel, C. V, Le Roy, D., Lee, J. D., Kravchenko, V., Ulevitch, R. J., … Heumann, D. (n.d.). Reactivity of murine and human recombinant LPS-binding protein (LBP) within LPS and gram negative bacteria. *Journal of Inflammation*, *47*(4), 165–72.

Leo, J. C., & Skurnik, M. (2011). Adhesins of Human Pathogens from the Genus *Yersinia*. In *Bacterial Adhesion* (Vol. 715, pp. 1–15).

Lerm, M., Selzer, J., Hoffmeyer, A., Rapp, U. R., Aktories, K., & Schmidt, G. (1999). Deamidation of Cdc42 and Rac by *Escherichia coli* cytotoxic necrotizing factor 1: Activation of c-Jun N-terminal kinase in HeLa cells. *Infection and Immunity*, *67*(2), 496–503.

Leto, T. L., & Geiszt, M. (2006). Role of Nox family NADPH oxidases in host defense. *Antioxidants & Redox Signaling*, *8*(9–10), 1549–1561.

Leu, S. B., Shulman, S. C., Steelman, C. K., Lamps, L. W., Bulut, O. P., Abramowsky, C. R., … Shehata, B. M. (2013). Pathogenic *Yersinia* DNA in intestinal specimens of pediatric patients with Crohn's disease. *Fetal and Pediatric Pathology*, *32*(5), 367–70.

Levine, M. M., Black, R. E., & Lanata, C. (1982). Precise estimation of the numbers of chronic carriers of *Salmonella* Typhi in Santiago, Chile, an endemic area. *Journal of Infectious Diseases*, *146*(6), 724–726.

Lewis, N. D., Asim, M., Barry, D. P., de Sablet, T., Singh, K., Piazuelo, M. B., … Wilson, K. T. (2011). Immune evasion by *Helicobacter pylori* is mediated by induction of macrophage arginase II. *The Journal of Immunology*, *186*(6), 3632–3641.

Ley, R. E., Backhed, F., Turnbaugh, P., Lozupone, C. A., Knight, R. D., & Gordon, J. I. (2005). Obesity alters gut microbial ecology. *Proc Natl Acad Sci U S A*, *102*(31), 11070–11075.

Ley, R. E., Peterson, D. A., & Gordon, J. I. (2006). Ecological and evolutionary forces shaping microbial diversity in the human intestine. *Cell*. http://doi.org/10.1016/j.cell.2006.02.017

Li, P., Allen, H., Banerjee, S., Franklin, S., Herzog, L., Johnston, C., … et al. (1995). Mice deficient in IL-1 beta-converting enzyme are defective in production of mature IL-1 beta and resistant to endotoxic shock. *Cell*, *80*(3), 401–411.

Li, D. Y., Brooke, B., Davis, E. C., Mecham, R. P., Sorensen, L. K., Boak, B. B., … Keating, M. T. (1998). Elastin is an essential determinant of arterial morphogenesis. *Nature*, *393*(May), 276–280.

Li, C. K. F., Pender, S. L. F., Pickard, K. M., Chance, V., Holloway, J. A., Huett, A., … MacDonald, T. T. (2004). Impaired immunity to intestinal bacterial infection in stromelysin-1 (matrix metalloproteinase-3)-deficient mice. *The Journal of Immunology*, *173*(8), 5171–5179.

Li, J. Y., Paragas, N., Ned, R. M., Qiu, A., Viltard, M., Leete, T., … Barasch, J. (2009). Scara5 is a ferritin receptor mediating non-transferrin iron delivery. *Developmental Cell*, *16*(1), 35–46. http://doi.org/10.1016/j.devcel.2008.12.002

Lian, C. J., Hwang, W. S., Kelly, J. K., & Pai, C. H. (1987). Invasiveness of *Yersinia enterocolitica* lacking the virulence plasmid: an in-vivo study. *Journal of Medical Microbiology*, *24*(3), 219–226.

Lin, E. A., & Liu, C. J. (2010, January). The role of ADAMTSs in arthritis. *Protein and Cell*. Springer. http://doi.org/10.1007/s13238-010-0002-5

Liu, W.-T., Karavolos, M. H., Bulmer, D. M., Allaoui, A., Hormaeche, R. D. C. E., Lee, J. J., & Anjam Khan, C. M. (2007). Role of the universal stress protein UspA of *Salmonella* in growth arrest, stress and virulence. *Microbial Pathogenesis*, *42*(1), 2–10.

Liu, H., Wang, H., Qiu, J., Wang, X., Guo, Z., Qiu, Y., … Yang, R. (2009). Transcriptional profiling of a mice plague model: Insights into interaction between *Yersinia pestis* and its host. *Journal of Basic Microbiology*, *49*(1), 92–99.

Liu, M. H., Tang, Z. H., Li, G. H., Qu, S. L., Zhang, Y., Ren, Z., … Jiang, Z. S. (2013a). Janus-like role of fibroblast growth factor 2 in arteriosclerotic coronary artery disease: Atherogenesis and angiogenesis. *Atherosclerosis*. http://doi.org/10.1016/j.atherosclerosis.2013.03.013

Liu, Y., Li, S., Zhang, G., Nie, G., Meng, Z., Mao, D., … Zeng, G. (2013b). Genetic variants in IL1A and IL1B contribute to the susceptibility to 2009 pandemic H1N1 influenza A virus. *BMC Immunology*, *14*(1), 37.

Lo, J. C., Chin, R. K., Lee, Y., Kang, H.-S., Wang, Y., Weinstock, J. V., … Fu, Y.-X. (2003). Differential regulation of CCL21 in lymphoid/nonlymphoid tissues for effectively attracting T cells to peripheral tissues. *Journal of Clinical Investigation*, *112*(10), 1495–1505.

Locati, M., Mantovani, A., & Sica, A. (2013). Macrophage activation and polarization as an adaptive component of innate immunity. *Advances in Immunology*, *120*, 163–184.

Lockman, H. A., Gillespie, R. A., Baker, B. D., & Shakhnovich, E. (2002). *Yersinia pseudotuberculosis* produces a cytotoxic necrotizing factor. *Infection and Immunity*, *70*(5), 2708–2714.

Longenberger, A. H., Gronostaj, M. P., Yee, G. Y., Johnson, L. M., Lando, J. F., Voorhees, R. E., … Ostroff, S. M. (2014). *Yersinia enterocolitica* infections associated with improperly pasteurized milk products: southwest Pennsylvania, March-August, 2011. *Epidemiology and Infection*, *142*(8), 1640–50

Loof, T. G., Mörgelin, M., Johansson, L., Oehmcke, S., Olin, A. I., Dickneite, G., … Herwald, H. (2011). Coagulation, an ancestral serine protease cascade, exerts a novel function in early immune defense. *Blood*, *118*(9), 2589–98.

Loughman, J. A., & Hunstad, D. A. (2012). Induction of indoleamine 2,3-dioxygenase by uropathogenic bacteria attenuates innate responses to epithelial infection. *Journal of Infectious Diseases*, *205*(12), 1830–1839.

Love, M. I., Huber, W., & Anders, S. (2014). Moderated estimation of fold change and dispersion for RNA-seq data with DESeq2. *Genome Biology*, *15*(12), 550.

Lu, R., Wu, S., Liu, X., Xia, Y., Zhang, Y., & Sun, J. (2010). Chronic effects of a *Salmonella* Type III secretion effector protein AvrA *in vivo*. *PLoS ONE*, *5*(5), e10505.

Luan, H. H., & Medzhitov, R. (2016). Food Fight: Role of itaconate and other metabolites in antimicrobial defense. *Cell Metabolism*, *24*(3), 379–387.

Lupp, C., Robertson, M. L., Wickham, M. E., Sekirov, I., Champion, O. L., Gaynor, E. C., & Finlay, B. B. (2007). Host-mediated inflammation disrupts the intestinal microbiota and promotes the overgrowth of *Enterobacteriaceae*. *Cell Host and Microbe*, *2*(2), 119–129.

MacMicking, J. D. (2012). Interferon-inducible effector mechanisms in cell-autonomous immunity. *Nature Reviews. Immunology*, *12*(5), 367–82.

Maddugoda, M. P., Stefani, C., Gonzalez-Rodriguez, D., Saarikangas, J., Torrino, S., Janel, S., … Lemichez, E. (2011). CAMP signaling by Anthrax edema toxin induces transendothelial cell tunnels, which Are resealed by MIM via Arp2/3-Driven actin polymerization. *Cell Host and Microbe*, *10*(5), 464–474.

Madouri, F., Guillou, N., Fauconnier, L., Marchiol, T., Rouxel, N., Chenuet, P., … Togbe, D. (2015). Caspase-1 activation by NLRP3 inflammasome dampens IL-33-dependent house dust mite-induced allergic lung inflammation. *Journal of Molecular Cell Biology*, *7*(4), 351–65.

Mahdavi, J., Sondén, B., Hurtig, M., Olfat, F. O., Forsberg, L., Roche, N., … Borén, T. (2002). *Helicobacter pylori* SabA adhesin in persistent infection and chronic inflammation. *Science (New York, N.Y.)*, *297*(5581), 573–8.

Mair, N. S., Fox, E., & Thal, E. (1979). Biochemical, pathogenicity and toxicity studies of type III strains of *Yersinia pseudotuberculosis* isolated from the cecal contents of pigs. *Contrib. Microbiol. Immunol.*, *5*, 359–365.

Majdalawieh, A., Zhang, L., & Ro, H.-S. (2007). Adipocyte Enhancer-binding Protein-1 Promotes Macrophage Inflammatory Responsiveness by Up-Regulating NF- B via I B Negative Regulation. *Molecular Biology of the Cell*, *18*(3), 930–942.

Malorni, W., Quaranta, M. G., Straface, E., Falzano, L., Fabbri, A., Viora, M., & Fiorentini, C. (2003). The Rac-activating toxin cytotoxic necrotizing factor 1 oversees NK cell-mediated activity by regulating the actin/microtubule interplay. *J Immunol*, *171*(8), 4195–4202.

Man, S. M., Karki, R., Malireddi, R. K. S., Neale, G., Vogel, P., Yamamoto, M., … Kanneganti, T.-D. (2015). The transcription factor IRF1 and guanylate-binding proteins target activation of the AIM2 inflammasome by *Francisella* infection. *Nature Immunology*, *16*(5), 467–75.

Man, S. M., & Kanneganti, T.-D. (2016). Converging roles of caspases in inflammasome activation, cell death and innate immunity TL - 16. *Nature Reviews Immunology*, *16 VN-r*(1), 7–21.

Manni, M. L., Robinson, K. M., & Alcorn, J. F. (2014). A tale of two cytokines: IL-17 and IL-22 in asthma and infection. *Expert Review of Respiratory Medicine*, *8*(1), 25–42.

Mantovani, A., Cassatella, M. A., Costantini, C., & Jaillon, S. (2011). Neutrophils in the activation and regulation of innate and adaptive immunity. *Nature Reviews. Immunology*, *11*(8), 519–531.

Marineli, F., Tsoucalas, G., Karamanou, M., & Androutsos, G. (2013). Mary Mallon (1869-1938) and the history of typhoid fever. *Annals of Gastroenterology*, *26*(2), 132–134.

Marra, A., & Isberg, R. R. (1997). Invasin-dependent and invasin-independent pathways for translocation of *Yersinia pseudotuberculosis* across the Peyer's patch intestinal epithelium. *Infect. Immun.*, *65*(8), 3412–3421.

Martin, N. T., & Martin, M. U. (2016). Interleukin 33 is a guardian of barriers and a local alarmin. *Nature Immunology*, *17*(2), 122–131.

Martinez, J. J., Mulvey, M. A., Schilling, J. D., Pinkner, J. S., & Hultgren, S. J. (2000). Type 1 pilus-mediated bacterial invasion of bladder epithelial cells. *The EMBO Journal*, *19*(12), 2803–12.

Martinez, J. J., & Hultgren, S. J. (2002). Requirement of Rho-family GTPases in the invasion of type 1-piliated uropathogenic *Escherichia coli*. *Cellular Microbiology*, *4*(1), 19–28.

Martinez, A. N., Mehra, S., & Kaushal, D. (2013). Role of interleukin 6 in innate immunity to *Mycobacterium tuberculosis* infection. *The Journal of Infectious Diseases*, *207*(8), 1253–61.

Mascarenhas, D. P. A., & Zamboni, D. S. (2016). Inflammasome biology taught by *Legionella pneumophila*. *Journal of Leukocyte Biology*. http://doi.org/10.1189/jlb.3MR0916-380R

Masli, S., Sheibani, N., Cursiefen, C., & Zieske, J. (2014). Matricellular protein thrombospondins: influence on ocular angiogenesis, wound healing and immuneregulation. *Current Eye Research*, *39*(8), 759–74.

Mastroeni, P., & Ménager, N. (2003). Development of acquired immunity to *Salmonella*. *Journal of Medical Microbiology*. http://doi.org/10.1099/jmm.0.05173-0

Mattila, P. K., & Lappalainen, P. (2008). Filopodia: molecular architecture and cellular functions. *Nature Reviews Molecular Cell Biology*, *9*(6), 446–454.

Maytin, E. V. (2014). Hyaluronan synthase 2 protects skin fibroblasts against apoptosis induced by environmental stress. *The Journal of Biological Chemistry*, *289*(46), 32253–32265.

McCormick, B. A., Nusrat, A., Parkos, C. A., D'Andrea, L., Hofman, P. M., Carnes, D., … Madara, J. L. (1997). Unmasking of intestinal epithelial lateral membrane beta1 integrin consequent to transepithelial neutrophil migration *in vitro* facilitates inv-mediated invasion by *Yersinia pseudotuberculosis*. *Infection and Immunity*, *65*(4), 1414–21.

McKenney, P. T., & Pamer, E. G. (2015). From hype to hope: The gut microbiota in enteric infectious disease. *Cell*. http://doi.org/10.1016/j.cell.2015.11.032

McLachlan, J. B., Catron, D. M., Moon, J. J., & Jenkins, M. K. (2009). Dendritic cell antigen presentation drives simultaneous cytokine production by effector and regulatory T cells in inflamed skin. *Immunity*, *30*(2), 277–288.

McLaughlin, L. M., Govoni, G. R., Gerke, C., Gopinath, S., Peng, K., Laidlaw, G., … Monack, D. (2009). The *Salmonella* SPI2 effector SseI mediates long-term systemic infection by modulating host cell migration. *PLoS Pathogens*, *5*(11).

McPhee, J. B., Mena, P., & Bliska, J. B. (2010). Delineation of regions of the *Yersinia* YopM protein required for interaction with the RSK1 and PRK2 host kinases and their requirement for interleukin-10 production and virulence. *Infection and Immunity*, *78*(8), 3529–3539.

McPhee, J. B., Mena, P., Zhang, Y., & Bliska, J. B. (2012). Interleukin-10 induction is an important virulence function of the *Yersinia pseudotuberculosis* Type III Effector YopM. *Infection and Immunity*, *80*(7), 2519–2527.

Medzhitov, R. (2010). Inflammation 2010: New Adventures of an Old Flame. *Cell*. http://doi.org/10.1016/j.cell.2010.03.006

Mehnert-Kay, S. A. (2005). Diagnosis and management of uncomplicated urinary tract infections. *American Family Physician*, *72*(3), 451–456.

Meinzer, U., Barreau, F., Esmiol-Welterlin, S., Jung, C., Villard, C., Léger, T., … Hugot, J.-P. (2012). *Yersinia pseudotuberculosis* effector YopJ subverts the Nod2/RICK/TAK1 pathway and activates caspase-1 to induce intestinal barrier dysfunction. *Cell Host & Microbe*, *11*(4), 337–351.

Mellor, A. L., & Munn, D. H. (2004). IDO expression by dendritic cells: tolerance and tryptophan catabolism. *Nature Reviews Immunology*, *4*(10), 762–774.

Mellor, A. L., & Munn, D. H. (2008). Creating immune privilege: active local suppression that benefits friends, but protects foes. *Nat Rev Immunol*, *8*(1), 74–80.

Menu, P., & Vince, J. E. (2011). The NLRP3 inflammasome in health and disease: the good, the bad and the ugly. *Clinical & Experimental Immunology*, *166*(1), 1–15.

Merad, M., Sathe, P., Helft, J., Miller, J., & Mortha, A. (2013). The dendritic cell lineage: ontogeny and function of dendritic cells and their subsets in the steady state and the inflamed setting. *Annual Review of Immunology*, *31*, 563–604.

Merhej, V., Adékambi, T., Pagnier, I., Raoult, D., & Drancourt, M. (2008). *Yersinia massiliensis* sp. nov., isolated from fresh water. *International Journal of Systematic and Evolutionary Microbiology*, *58*(4), 779–784.

Mertz, A. K. H., Ugrinovic, S., Lauster, R., Wu, P., Grolms, M., Böttcher, U., … Sieper, J. (1998). Characterization of the synovial T cell response to various recombinant *Yersinia* antigens in *Yersinia enterocolitica*-triggered reactive arthritis: Heat-shock protein 60 drives a major immune response. *Arthritis and Rheumatism*, *41*(2), 315–326.

Mertz, A. K. H., Wu, P., Sturniolo, T., Stoll, D., Rudwaleit, M., Lauster, R., … Sieper, J. (2000). Multispecific CD4+ T cell response to a single 12-mer epitope of the immunodominant heat-shock protein 60 of *Yersinia enterocolitica* in *Yersinia*-triggered reactive arthritis: Overlap with the B27-restricted CD8 epitope, functional properties, and epitope. *The Journal of Immunology*, *164*(3), 1529–1537.

Mesali, H., Ajami, A., Hussein-Nattaj, H., Rafiei, A., Rajabian, Z., Asgarian-Omran, H., … Tehrani, M. (2016). Regulatory T Cells and myeloid-derived suppressor cells in patients with peptic ulcer and gastric cancer. *Iranian Journal of Immunology : IJI*, *13*(3), 167–77.

Meunier, E., Dick, M. S., Dreier, R. F., Schürmann, N., Kenzelmann Broz, D., Warming, S., … Broz, P. (2014). Caspase-11 activation requires lysis of pathogen-containing vacuoles by IFN-induced GTPases. *Nature*, *509*(7500), 366–70.

Meunier, E., Wallet, P., Dreier, R. F., Costanzo, S., Anton, L., Rühl, S., … Broz, P. (2015). Guanylate-binding proteins promote activation of the AIM2 inflammasome during infection with *Francisella novicida*. *Nature Immunology*, *16*(5), 476–84.

Meunier, E., & Broz, P. (2016). Interferon-inducible GTPases in cell autonomous and innate immunity. *Cellular Microbiology*. http://doi.org/10.1111/cmi.12546

Miao, E. A., Leaf, I. A., Treuting, P. M., Mao, D. P., Dors, M., Sarkar, A., … Aderem, A. (2010). Caspase-1-induced pyroptosis is an innate immune effector mechanism against intracellular bacteria. *Nature Immunology*, *11*(12), 1136–1142.

Michel, G., Ferrua, B., Munro, P., Boyer, L., Mathal, N., Gillet, D., … Lemichez, E. (2016). Immunoadjuvant properties of the Rho activating factor CNF1 in prophylactic and curative vaccination against *Leishmania infantum*. *PLOS ONE*, *11*(6), e0156363.

Mihai, M. M., Holban, A. M., Giurcaneanu, C., Popa, L. G., Oanea, R. M., Lazar, V., … Popa, M. I. (2015). Microbial biofilms: impact on the pathogenesis of periodontitis, cystic fibrosis, chronic wounds and medical device-related infections. *Current Topics in Medicinal Chemistry*, *15*(16), 1552–76.

Miki, Y., Yamamoto, K., Taketomi, Y., Sato, H., Shimo, K., Kobayashi, T., … Murakami, M. (2013). Lymphoid tissue phospholipase A2 group IID resolves contact hypersensitivity by driving antiinflammatory lipid mediators. *The Journal of Experimental Medicine*, *210*(6), 1217–1234.

Miklossy, J., & McGeer, P. L. (2016). Common mechanisms involved in Alzheimer's disease and type 2 diabetes: a key role of chronic bacterial infection and inflammation. *Aging*, *8*(3), 1–14.

Miller, H., Zhang, J., KuoLee, R., Patel, G. B., & Chen, W. (2007, March 14). Intestinal M cells: The fallible sentinels? *World Journal of Gastroenterology*, *13*(10), 1477–1486.

Mills, C. D., Kincaid, K., Alt, J. M., Heilman, M. J., & Hill, A. M. (2000a). M-1/M-2 macrophages and the Th1/Th2 paradigm. *Journal of Immunology (Baltimore, Md. : 1950)*, *164*(12), 6166–73.

Mills, M., Meysick, K. C., & O'Brien, A. D. (2000b). Cytotoxic necrotizing factor type 1 of uropathogenic *Escherichia coli* kills cultured human uroepithelial 5637 cells by an apoptotic mechanism. *Infection and Immunity*, *68*(10), 5869–5880.

Miyara, M., & Sakaguchi, S. (2007). Natural regulatory T cells: mechanisms of suppression. *Trends in Molecular Medicine*. http://doi.org/10.1016/j.molmed.2007.01.003

Mizoguchi, A. (2012). Healing of intestinal inflammation by IL-22. *Inflammatory Bowel Diseases*, *18*(9), 1777–84.

Mobley, H. L., & Hausinger, R. P. (1989). Microbial ureases: significance, regulation, and molecular characterization. *Microbiological Reviews*, *53*(1), 85–108.

Mohammadi, S., & Isberg, R. R. (2009). *Yersinia pseudotuberculosis* virulence determinants invasin, YopE, and YopT modulate RhoG activity and localization. *Infection and Immunity*, *77*(11), 4771–4782.

Molinari, M., Salio, M., Galli, C., Norais, N., Rappuoli, R., Lanzavecchia, A., & Montecucco, C. (1998). Selective inhibition of Ii-dependent antigen presentation by *Helicobacter pylori* toxin VacA. *The Journal of Experimental Medicine*, *187*(1), 135–40.

Molofsky, A. B., Savage, A. K., & Locksley, R. M. (2015). Interleukin-33 in tissue homeostasis, injury, and inflammation. *Immunity*. http://doi.org/10.1016/j.immuni.2015.06.006

Monack, D. M., Mecsas, J., Ghori, N., & Falkow, S. (1997). *Yersinia* signals macrophages to undergo apoptosis and YopJ is necessary for this cell death. *Proceedings of the National Academy of Sciences of the United States of America*, *94*(19), 10385–90.

Monack, D. M., Mecsas, J., Bouley, D., & Falkow, S. (1998). *Yersinia*-induced apoptosis *in vivo* aids in the establishment of a systemic infection of mice. *The Journal of Experimental Medicine*, *188*(11), 2127–37.

Monack, D. M., Bouley, D. M., & Falkow, S. (2004a). *Salmonella* Typhimurium persists within macrophages in the mesenteric lymph nodes of chronically infected Nramp1+/+ mice and can be reactivated by IFNγ neutralization. *The Journal of Experimental Medicine*, *199*(2), 231–241.

Monack, D. M., Mueller, A., & Falkow, S. (2004b). Persistent bacterial infections: the interface of the pathogen and the host immune system. *Nature Reviews. Microbiology*, *2*(9), 747–765.

Monack, D. M. (2013). *Helicobacter* and *Salmonella* persistent infection strategies. *Cold Spring Harbor Perspectives in Medicine*, *3*(12).

Monteiro, A. C., Schmitz, V., Svensjo, E., Gazzinelli, R. T., Almeida, I. C., Todorov, A., … Scharfstein, J. (2006). Cooperative activation of TLR2 and bradykinin B2 receptor is required for induction of type 1 immunity in a mouse model of subcutaneous infection by *Trypanosoma cruzi*. *Journal of Immunology (Baltimore, Md. : 1950)*, *177*(9), 6325–35.

Moran, A. P., Lindner, B., & Walsh, E. J. (1997). Structural characterization of the lipid A component of *Helicobacter pylori* rough- and smooth-form lipopolysaccharides. *Journal of Bacteriology*, *179*(20), 6453–6463.

Moran, A. P. (2007). Lipopolysaccharide in bacterial chronic infection: Insights from *Helicobacter pylori* lipopolysaccharide and lipid A. *International Journal of Medical Microbiology*. http://doi.org/10.1016/j.ijmm.2007.03.008

Moreau, K., Lacas-Gervais, S., Fujita, N., Sebbane, F., Yoshimori, T., Simonet, M., & Lafont, F. (2010). Autophagosomes can support *Yersinia pseudotuberculosis* replication in macrophages. *Cellular Microbiology*, *12*(8), 1108–1123.

Mostowy, S., & Shenoy, A. R. (2015). The cytoskeleton in cell-autonomous immunity: structural determinants of host defense. *Nature Reviews Immunology*, *15*(9), 559–573.

Mou, S., Cote, C. K., & Worsham, P. L. (2012). Cytotoxic necrotizing factor is an effective immunogen in a *Yersinia pseudotuberculosis* aerosol mouse model. In *Advances in experimental medicine and biology* (Vol. 954, pp. 179–181).

Moussion, C., Ortega, N., & Girard, J.-P. (2008). The IL-1-like cytokine IL-33 is constitutively expressed in the nucleus of endothelial cells and epithelial cells in vivo: a novel "alarmin"? PLoS ONE, 3(10), e3331.

Mullen, A. C., Hutchins, A. S., High, F. A., Lee, H. W., Sykes, K. J., Chodosh, L. A., & Reiner, S. L. (2002). Hlx is induced by and genetically interacts with T-bet to promote heritable TH1 gene induction. *Nature Immunology*, *3*(7), 652.

Muallem, G., & Hunter, C. A. (2014). ParadYm shift: Ym1 and Ym2 as innate immunological regulators of IL-17. *Nature Immunology*, *15*(12), 1099–100.

Mühldorfer, K., Wibbelt, G., Haensel, J., Riehm, J., & Speck, S. (2010). *Yersinia* species isolated from Bats, Germany. *Emerging Infectious Diseases*, *16*(3), 578–580.

Mukherjee, S., Vaishnava, S., & Hooper, L. V. (2008). Multi-layered regulation of intestinal antimicrobial defense. *Cellular and Molecular Life Sciences*. SP Birkhäuser Verlag Basel. http://doi.org/10.1007/s00018-008-8182-3

Mukherjee, S., Zheng, H., Derebe, M. G., Callenberg, K. M., Partch, C. L., Rollins, D., … Hooper, L. V. (2014). Antibacterial membrane attack by a pore-forming intestinal C-type lectin. *Nature*, *505*(7481), 103–7.

Müller, A. J., Hoffmann, C., & Hardt, W. D. (2010). Caspase-1 activation via Rho GTPases: A common theme in mucosal infections? *PLoS Pathogens*. http://doi.org/10.1371/journal. ppat.1000795

Mulvey, M. A., Schilling, J. D., & Hultgren, S. J. (2001). Establishment of a persistent *Escherichia coli* reservoir during the acute phase of a bladder infection. *Infection and Immunity*, *69*(7), 4572–4579.

Muñoz, N. M., Meliton, A. Y., Meliton, L. N., Dudek, S. M., & Leff, A. R. (2009). Secretory group V phospholipase A2 regulates acute lung injury and neutrophilic inflammation caused by LPS in mice. *American Journal of Physiology. Lung Cellular and Molecular Physiology*, *296*(6), L879–L887.

Munro, S. A., Lewin, S. A., Smith, H. J., Engel, M. E., Fretheim, A., & Volmink, J. (2007). Patient adherence to tuberculosis treatment: a systematic review of qualitative research. *PloS Medicine*, *4*(7), 1230–1245.

Murakami, Y., Hoshi, M., Imamura, Y., Arioka, Y., Yamamoto, Y., & Saito, K. (2013). Remarkable role of indoleamine 2,3-dioxygenase and tryptophan metabolites in infectious diseases: potential role in macrophage-mediated inflammatory diseases. *Mediators Inflamm*, *2013*, 391984.

Murali, A., & Rajalingam, K. (2014). Small Rho GTPases in the control of cell shape and mobility. *Cellular and Molecular Life Sciences*. http://doi.org/10.1007/s00018-013-1519-6

Murphy, E. A., Sathiyaseelan, J., Parent, M. A., Zou, B., & Baldwin, C. L. (2001). Interferon-gamma is crucial for surviving a *Brucella abortus* infection in both resistant C57BL/6 and susceptible BALB/c mice. *Immunology*, *103*(4), 511–8.

Murphy, K. M., Travers, P., Walport, M. Janeway's Immunobiology 8th edition. New York: Garland Science, 2011. Print. ISBN: 0-8153-4243-8.

Murros-Kontiainen, A., Fredriksson-Ahomaa, M., Korkeala, H., Johansson, P., Rahkila, R., & Björkroth, J. (2011a). *Yersinia nurmii* sp. nov. *International Journal of Systematic and Evolutionary Microbiology*, *61*(10), 2368–2372.

Murros-Kontiainen, A., Johansson, P., Niskanen, T., Fredriksson-Ahomaa, M., Korkeala, H., & Björkroth, J. (2011b). *Yersinia pekkanenii* sp. nov. *International Journal of Systematic and Evolutionary Microbiology*, *61*(10), 2363–2367.

Nagasaki, T., Hara, M., Nakanishi, H., Takahashi, H., Sato, M., & Takeyama, H. (2014). Interleukin-6 released by colon cancer-associated fibroblasts is critical for tumor angiogenesis: anti-interleukin-6 receptor antibody suppressed angiogenesis and inhibited tumor–stroma interaction. *British Journal of Cancer*, *110*(2), 469–478.

Napolioni, V., & MacMurray, J. (2016). Infectious diseases, IL6 −174G>C polymorphism, and human development. *Brain, Behavior, and Immunity*, *51*, 196–203.

Nathan, C. (2015). From transient infection to chronic disease. *Science*, *350*(6257), 161–161.

Netea, M. G., van der Leij, F., Drenth, J. P. H., Joosten, L. A. B., te Morsche, R., Verweij, P., … van der Meer, J. W. M. (2010). Chronic yersiniosis due to defects in the TLR5 and NOD2 recognition pathways. *The Netherlands Journal of Medicine*, *68*(10), 310–5.

Neutra, M. R., & Kraehenbuhl, J. P. (1992). Transepithelial transport and mucosal defense I: the role of M cells. *Trends in Cell Biology*, *2*(5), 134–8.

Nobes, C. D., & Hall, A. (1995). Rho, Rac, and Cdc42 GTPases regulate the assembly of multimolecular focal complexes associated with actin stress fibers, lamellipodia, and filopodia. *Cell*, *81*(1), 53–62.

Nordahl, E. A., Rydengård, V., Mörgelin, M., & Schmidtchen, A. (2005). Domain 5 of high molecular weight kininogen is antibacterial. *Journal of Biological Chemistry*, *280*(41), 34832–34839.

Nordenfelt, P., & Tapper, H. (2011). Phagosome dynamics during phagocytosis by neutrophils. *J Leukoc Biol*, *90*(2), 271–284.

Nuorti, J. P., Niskanen, T., Hallanvuo, S., Mikkola, J., Kela, E., Hatakka, M., … Ruutu, P. (2004). A widespread outbreak of *Yersinia pseudotuberculosis* O:3 infection from iceberg lettuce. *The Journal of Infectious Diseases*, *189*(5), 766–774.

Nusrat, A., Von Eichel-Streiber, C., Turner, J. R., Verkade, P., Madara, J. L., & Parkos, C. A. (2001). *Clostridium difficile* toxins disrupt epithelial barrier function by altering membrane microdomain localization of tight junction proteins. *Infection and Immunity*, *69*(3), 1329–1336.

Nuss, A. M., Heroven, A. K., Waldmann, B., Reinkensmeier, J., Jarek, M., Beckstette, M., & Dersch, P. (2015). Transcriptomic profiling of *Yersinia pseudotuberculosis* reveals reprogramming of the Crp regulon by temperature and uncovers Crp as a master regulator of small RNAs. *PLoS Genetics*, *11*(3), e1005087.

Nuss, A. M., Beckstette, M., Pimenova, M., Schmühl, C., Opitz, W., Pisano, F., … Dersch, P. (2017). Tissue dual RNA-seq allows fast discovery of infection-specific functions and riboregulators shaping host-pathogen transcriptomes. *Proceedings of the National Academy of Sciences of the United States of America*, 201613405.

Nyren-Erickson, E. K., Jones, J. M., Srivastava, D. K., & Mallik, S. (2013, October). A disintegrin and metalloproteinase-12 (ADAM12): Function, roles in disease progression, and clinical implications. *Biochimica et Biophysica Acta - General Subjects*. NIH Public Access. http://doi.org/10.1016/j.bbagen.2013.05.011

O'Hara, A. M., Shanahan, F., Abreu, M., Vora, P., Faure, E., Thomas, L., … DeVos, W. (2006). The gut flora as a forgotten organ. *EMBO Reports*, *7*(7), 688–93.

O'Neil, K. M., Ochs, H. D., Heller, S. R., Cork, L. C., Morris, J. M., & Winkelstein, J. A. (1988). Role of C3 in humoral immunity. Defective antibody production in C3-deficient dogs. *Journal of Immunology (Baltimore, Md. : 1950)*, *140*(6), 1939–45.

O'Sullivan, Clayton, Breslin, Harman, Bountra, Mclaren, & O'Morain. (2000). Increased mast cells in the irritable bowel syndrome. *Neurogastroenterology and Motility*, *12*(5), 449–457.

Oberst, A. (2015). Death in the fast lane: What's next for necroptosis? *FEBS Journal*, *283*(14), 1–10.

Ochman, H. (2001). Evolution of bacterial pathogens. In *Principles of Bacterial Pathogenesis* (p. 41). ACADEMIC PRESS. http://doi.org/10.1016/B978-012304220-0/50002-9

Oertli, M., Sundquist, M., Hitzler, I., Engler, D. B., Arnold, I. C., Reuter, S., … Müller, A. (2012). DC-derived IL-18 drives Treg differentiation, murine *Helicobacter pylori*-specific immune tolerance, and asthma protection. *The Journal of Clinical Investigation*, *122*(3), 1082–1096.

Oertli, M., Noben, M., Engler, D. B., Semper, R. P., Reuter, S., Maxeiner, J., … Müller, A. (2013). *Helicobacter pylori* γ-glutamyl transpeptidase and vacuolating cytotoxin promote gastric persistence and immune tolerance. *Proceedings of the National Academy of Sciences of the United States of America*, *110*(8), 3047–52.

Oh, J. D., Kling-Bäckhed, H., Giannakis, M., Xu, J., Fulton, R. S., Fulton, L. a, … Gordon, J. I. (2006). The complete genome sequence of a chronic atrophic gastritis *Helicobacter pylori* strain: evolution during disease progression. *Proceedings of the National Academy of Sciences of the United States of America*, *103*(26), 9999–10004.

Ohlson, M. B., Huang, Z., Alto, N. M., Blanc, M. P., Dixon, J. E., Chai, J., & Miller, S. I. (2008). Structure and function of *Salmonella* SifA indicate that its interactions with SKIP, SseJ, and RhoA family GTPases induce endosomal tubulation. *Cell Host and Microbe*, *4*(5), 434–446.

Ohta, S., Imamura, M., Xing, W., Boyce, J. A., & Balestrieri, B. (2013). Group V secretory phospholipase A2 is involved in macrophage activation and is sufficient for macrophage effector functions in allergic pulmonary inflammation. *Journal of Immunology (Baltimore, Md. : 1950)*, *190*(12), 5927–38.

Ohya, K., Handa, Y., Ogawa, M., Suzuki, M., & Sasakawa, C. (2005). IpgB1 is a novel *Shigella* effector protein involved in bacterial invasion of host cells: Its activity to promote membrane ruffling via Rac1 and Cdc42 activation. *Journal of Biological Chemistry*, *280*(25), 24022–24034.

Ojha, A. K., Baughn, A. D., Sambandan, D., Hsu, T., Trivelli, X., Guerardel, Y., … Hatfull, G. F. (2008). Growth of *Mycobacterium tuberculosis* biofilms containing free mycolic acids and harbouring drug-tolerant bacteria. *Molecular Microbiology*, *69*(1), 164–174.

Om Alblazi, K. M., & Siar, C. H. (2015). Cellular protrusions - Lamellipodia, filopodia, invadopodia and podosomes - and their roles in progression of orofacial tumours: Current understanding. *Asian Pacific Journal of Cancer Prevention*. http://doi.org/10.7314/APJCP.2015.16.6.2187

Opipari, A., & Franchi, L. (2015). Role of inflammasomes in intestinal inflammation and Crohn's disease. *Inflammatory Bowel Diseases*, *21*(1), 173–181.

Orden, J. A., Dominguez-Bernal, G., Martinez-Pulgarin, S., Blanco, M., Blanco, J. E., Mora, A., … De La Fuente, R. (2007). Necrotoxigenic *Escherichia coli* from sheep and goats produce a new type of cytotoxic necrotizing factor (CNF3) associated with the *eae* and *ehxA* genes. *International Microbiology*, *10*(1), 47–55.

Orth, J. H. C., Preuss, I., Fester, I., Schlosser, A., Wilson, B. A., & Aktories, K. (2009). *Pasteurella multocida* toxin activation of heterotrimeric G proteins by deamidation. *Proceedings of the National Academy of Sciences of the United States of America*, *106*(17), 7179–84.

Oswald, E., De Rycke, J., Guillot, J. F., & Boivin, R. (1989). Cytotoxic effect of multinucleation in HeLa cell cultures associated with the presence of Vir plasmid in *Escherichia coli* strains. *FEMS Microbiol Lett*, *49*(1), 95–99.

Ottemann, K. M., & Lowenthal, A. C. (2002). *Helicobacter pylori* uses motility for initial colonization and to attain robust infection. *Infection and Immunity*, *70*(4), 1984–1990.

Ouyang, W., Kolls, J. K., & Zheng, Y. (2008). The biological functions of T helper 17 cell effector cytokines in inflammation. *Immunity*. http://doi.org/10.1016/j.immuni.2008.03.004

Pabst, O., Bernhardt, G., & Förster, R. (2007). The impact of cell-bound antigen transport on mucosal tolerance induction. *Journal of Leukocyte Biology*, *82*(4), 795–800.

Palenski, T. L., Gurel, Z., Sorenson, C. M., Hankenson, K. D., & Sheibani, N. (2013). Cyp1B1 expression promotes angiogenesis by suppressing NF-κB activity. *American Journal of Physiology. Cell Physiology*, *305*(8), C1170-84.

Pantaloni, D., Hill, T. L., Carlier, M. F., & Korn, E. D. (1985). A model for actin polymerization and the kinetic effects of ATP hydrolysis. *Proceedings of the National Academy of Sciences*, *82*(21), 7207–7211.

Pantoja, L. G., Miller, R. D., Ramirez, J. A., Molestina, R. E., & Summersgill, J. T. (2001). Characterization of *Chlamydia pneumoniae* persistence in HEp-2 cells treated with gamma interferon. *Infection and Immunity*, *69*(12), 7927–32.

Papamichail, M., Gutierrez, C., Embling, P., Johnson, P., Holborow, E. J., & Pepys, M. B. (1975). Complement dependence of localization of aggregated IgG in germinal centers. *Scandinavian Journal of Immunology*, *4*(4), 343–47.

Papareddy, P., Kalle, M., Kasetty, G., Mörgelin, M., Rydengård, V., Albiger, B., … Schmidtchen, A. (2010). C-terminal peptides of tissue factor pathway inhibitor are novel host defense molecules. *Journal of Biological Chemistry*, *285*(36), 28387–28398.

Parks, O. B., Pociask, D. A., Hodzic, Z., Kolls, J. K., & Good, M. (2015). Interleukin-22 signaling in the regulation of intestinal health and disease. *Frontiers in Cell and Developmental Biology*, *3*(January), 85.

Pärn, T., Hallanvuo, S., Salmenlinna, S., Pihlajasaari, A., Heikkinen, S., Telkki-Nykänen, H., … Rimhanen-Finne, R. (2015). Outbreak of *Yersinia pseudotuberculosis* O:1 infection associated with raw milk consumption, Finland, spring 2014. *Eurosurveillance*, *20*(40), 30033.

Parry, C. M., Hien, T. T., Dougan, G., White, N. J., & Farrar, J. J. (2002). Typhoid Fever. *New England Journal of Medicine*, *347*(22), 1770–1782.

Patel, H., Fellowes, R., Coade, S., & Woo, P. (1998). Human serum amyloid A has cytokine-like properties. *Scandinavian Journal of Immunology*, *48*(4), 410–418.

Patel, J. C., & Galán, J. E. (2005). Manipulation of the host actin cytoskeleton by *Salmonella*--all in the name of entry. *Current Opinion in Microbiology*, *8*(1), 10–5.

Pearson, J. S., Giogha, C., Ong, S. Y., Kennedy, C. L., Kelly, M., Robinson, K. S., … Hartland, E. L. (2013). A type III effector antagonizes death receptor signaling during bacterial gut infection. *Nature*, *501*(7466), 247–51.

Peek Jr., R. M., Blaser, M. J., Peek, R. M., & Blaser, M. J. (2002). *Helicobacter pylori* and gastrointestinal tract adenocarcinomas. *Nat Rev Cancer*, *2*(1), 28–37.

Pei, S., Doye, A., & Boquet, P. (2001). Mutation of specific acidic residues of the CNF1 T domain into lysine alters cell membrane translocation of the toxin. *Molecular Microbiology*, *41*(6), 1237–1247.

Pellegrin, S., & Mellor, H. (2007). Actin stress fibers. *Journal of Cell Science*, *120*(20).

Pennock, N. D., White, J. T., Cross, E. W., Cheney, E. E., Tamburini, B. A., & Kedl, R. M. (2013). T cell responses: naive to memory and everything in between. *Advances in Physiology Education*, *37*(4), 273–283.

Pepe, J. C., Badger, J. L., & Miller, V. L. (1994). Growth phase and low pH affect the thermal regulation of the *Yersinia enterocolitica* inv gene. *Molecular Microbiology*, *11*(1), 123–135.

Percival, S. L., & Suleman, L. (2014). Biofilms and *Helicobacter pylori*: Dissemination and persistence within the environment and host. *World Journal of Gastrointestinal Pathophysiology*, *5*(3), 122–32.

Perez, C. J., Dumas, A., Vallières, L., Guénet, J. L., & Benavides, F. (2013). Several classical mouse inbred strains, including DBA/2, NOD/Lt, FVB/N, and SJL/J, carry a putative loss-of-function Allele of Gpr84. *Journal of Heredity*, *104*(4), 565–571.

Perry, R. D., & Fetherston, J. D. (1997). *Yersinia pestis* - Etiologic agent of plague. *MIcrobiology Reviews*, *10(1)*(1), 35–66.

Pfaffl, M. W. (2001). A new mathematical model for relative quantification in real-time RT-PCR. *Nucleic Acids Research*, *29*(9), e45.

Pfeiffer, A. (ed.): Über die bacilläre Pseudotuberkulose bei Nagethieren. Verlag von George Thieme, Leipzig, 1889, pp. 1-42.

Pha, K., & Navarro, L. (2016). *Yersinia* type III effectors perturb host innate immune responses. *World Journal of Biological Chemistry*, *7*(1), 1–13.

Philip, N. H., & Brodsky, I. E. (2012). Cell death programs in *Yersinia* immunity and pathogenesis. *Frontiers in Cellular and Infection Microbiology*, *2*, 149.

Philip, N. H., Dillon, C. P., Snyder, A. G., Fitzgerald, P., Wynosky-Dolfi, M. A., Zwack, E. E., … Brodsky, I. E. (2014). Caspase-8 mediates caspase-1 processing and innate immune defense in response to bacterial blockade of NF- B and MAPK signaling. *Proceedings of the National Academy of Sciences*, *111*(20), 7385–7390.

Piccotti, J. R., Chan, S. Y., Li, K., Eichwald, E. J., & Bishop, D. K. (1997). Differential effects of IL-12 receptor blockade with IL-12 p40 homodimer on the induction of CD4+ and CD8+ IFN-gamma-producing cells. *Journal of Immunology (Baltimore, Md. : 1950)*, *158*(2), 643–8.

Pichery, M., Mirey, E., Mercier, P., Lefrancais, E., Dujardin, A., Ortega, N., & Girard, J.-P. (2012). Endogenous IL-33 is highly expressed in mouse epithelial barrier tissues, lymphoid organs, brain, embryos, and inflamed tissues: *in situ* analysis using a novel IL-33-*lacZ* gene trap reporter strain. The Journal of Immunology, 188(7), 3488–3495.

Pierson, D. E., & Falkow, S. (1993). The *ail* gene of *Yersinia enterocolitica* has a role in the ability of the organism to survive serum killing. *Infection and Immunity*, *61*(5), 1846–1852.

Pilla, D. M., Hagar, J. A., Haldar, A. K., Mason, A. K., Degrandi, D., Pfeffer, K., … Coers, J. (2014). Guanylate binding proteins promote caspase-11-dependent pyroptosis in response to cytoplasmic LPS. *Proceedings of the National Academy of Sciences of the United States of America*, *111*(16), 6046–51.

Pisano, F., Heine, W., Rosenheinrich, M., Schweer, J., Nuss, A. M., Dersch, P., … Lowry, C. (2014). Influence of PhoP and intra-species variations on virulence of *Yersinia pseudotuberculosis* during the natural oral infection route. *PLoS ONE*, *9*(7), e103541.

Piteau, M., Papatheodorou, P., Schwan, C., Schlosser, A., Aktories, K., & Schmidt, G. (2014). Lu/BCAM adhesion glycoprotein is a receptor for *Escherichia coli* cytotoxic necrotizing factor 1 (CNF1). *PLoS Pathogens*, *10*(1).

Pollard, T. D., & Weeds, A. G. (1984). The rate constant for ATP hydrolysis by polymerized actin. *FEBS Letters*, *170*(1), 94–98.

Popoff, M. R., Chaves-Olarte, E., Lemichez, E., Von Eichel-Streiber, C., Thelestam, M., Chardin, P., … Boquet, P. (1996). Ras, Rap, and Rac small GTP-binding proteins are targets for *Clostridium sordellii* lethal toxin glucosylation. *Journal of Biological Chemistry*, *271*(17), 10217–10224.

Popoff, M. R. (2014). Bacterial factors exploit eukaryotic Rho GTPase signaling cascades to promote invasion and proliferation within their host. *Small GTPases*, *5*(February), e28209.

Popov, A., Abdullah, Z., Wickenhauser, C., Saric, T., Driesen, J., Hanisch, F.-G., … Schultze, J. L. (2006). Indoleamine 2,3-dioxygenase-expressing dendritic cells form suppurative granulomas following *Listeria monocytogenes* infection. *The Journal of Clinical Investigation*, *116*(12), 3160–70.

Popov, A., Driesen, J., Abdullah, Z., Wickenhauser, C., Beyer, M., Debey-Pascher, S., … Schultze, J. L. (2008). Infection of myeloid dendritic cells with *Listeria monocytogenes* leads to the suppression of T cell function by multiple inhibitory mechanisms. *Journal of Immunology (Baltimore, Md. : 1950)*, *181*(7), 4976–88.

Popovic, P. J., Zeh, H. J., & Ochoa, J. B. (2007). Arginine and immunity. *The Journal of Nutrition*, *137*(6 Suppl 2), 1681S–1686S.

Portnoy, D. A., & Falkow, S. (1981). Virulence-associated plasmids from *Yersinia enterocolitica* and *Yersinia pestis*. *Journal of Bacteriology*, *148*(3), 877–883.

Pothoulakis, C. (2000). Effects of *Clostridium difficile* toxins on epithelial cell barrier. *Ann N Y Acad Sci*, *915*(1), 347–356.

Price, M. N., Dehal, P. S., & Arkin, A. P. (2010). FastTree 2 - Approximately maximum-likelihood trees for large alignments. *PLoS ONE*, *5*(3), e9490.

Price, C. T. D., & Abu Kwaik, Y. (2014). The transcriptome of *Legionella pneumophila*-infected human monocyte-derived macrophages. *PLoS ONE*, *9*(12), e114914.

Proietto, A. I., van Dommelen, S., Zhou, P., Rizzitelli, A., D'Amico, A., Steptoe, R. J., … Wu, L. (2008). Dendritic cells in the thymus contribute to T-regulatory cell induction. *Proceedings of the National Academy of Sciences of the United States of America*, *105*(50), 19869–74.

Pujol, C., & Bliska, J. B. (2003). The ability to replicate in macrophages is conserved between *Yersinia pestis* and *Yersinia pseudotuberculosis*. *Infection and Immunity*, *71*(10), 5892–9.

Radovanovic, I., Mullick, A., Gros, P., Mathews, H.-J., Spellberg, B., Filler, S., … Churchill, G. (2011). Genetic control of susceptibility to infection with *Candida albicans* in mice. *PLoS ONE*, *6*(4), e18957.

Rahman, A., Bonny, T. S., Stonsaovapak, S., & Ananchaipattana, C. (2011). *Yersinia enterocolitica* : Epidemiological studies and outbreaks. *Journal of Pathogens*, *2011*, 1–11.

Raisch, J., Buc, E., Bonnet, M., Sauvanet, P., Vazeille, E., de Vallée, A., … Darfeuille-Michaud, A. (2014). Colon cancer-associated B2 *Escherichia coli* colonize gut mucosa and promote cell proliferation. *World Journal of Gastroenterology*, *20*(21), 6560–6572.

Ramamurthi, K. S., & Schneewind, O. (2002). Type III protein secretion in *Yersinia* species. *Annual Review of Cell and Developmental Biology*, *18*, 107–33.

Ramanan, D., & Cadwell, K. (2016). Intrinsic defense mechanisms of the intestinal epithelium. *Cell Host and Microbe*, *19*(4), 1–8.

Randow, F., MacMicking, J. D., & James, L. C. (2013). Cellular self-defense: how cell-autonomous immunity protects against pathogens. *Science (New York, N.Y.)*, *340*(6133), 701–6.

Rao, A., Luo, C., & Hogan, P. G. (1997). Transcription factors of the NFAT family: Regulation and function. *Annual Review of Immunology*, *15*(1), 707–747.

Raphael, I., Nalawade, S., Eagar, T. N., & Forsthuber, T. G. (2014). T cell subsets and their signature cytokines in autoimmune and inflammatory diseases. *Cytokine*, *74*(1), 1043–4666.

Rasmussen, S., Allentoft, M. E., Nielsen, K., Nielsen, R., Kristiansen, K., Correspondence, E. W., … Willerslev, E. (2015). Early divergent strains of *Yersinia pestis* in Eurasia 5,000 years ago. *Cell*, *163*, 571–582.

Ratner, D., Orning, M. P. A., Starheim, K. K., Marty-Roix, R., Proulx, M. K., Goguen, J. D., & Lien, E. (2016). Manipulation of interleukin-1 β and interleukin-18 production by *Yersinia pestis* effectors YopJ and YopM and redundant impact on virulence. *The Journal of Biological Chemistry*, *291*(19), 9894–905.

Reaves, T. A., Chin, A. C., & Parkos, C. A. (2005). Neutrophil transepithelial migration: role of toll-like receptors in mucosal inflammation. *Memórias Do Instituto Oswaldo Cruz*, *100*, 191–198.

Reipschläger, S., Kubatzky, K., Taromi, S., Burger, M., Orth, J., Aktories, K., & Schmidt, G. (2012). Toxin-induced RhoA activity mediates CCL1-triggered signal transducers and activators of transcription protein signaling. *Journal of Biological Chemistry*, *287*(14), 11183–11194.

Reuter, S., Connor, T. R., Barquist, L., Walker, D., Feltwell, T., Harris, S. R., … Thomson, N. R. (2014). Parallel independent evolution of pathogenicity within the genus *Yersinia*. *Proceedings of the National Academy of Sciences*, *111*(18), 6768–6773.

Rhen, M., Eriksson, S., Clements, M., Bergström, S., & Normark, S. J. (2003). The basis of persistent bacterial infections. *Trends in Microbiology*. http://doi.org/10.1016/S0966-842X(02)00038-0

Ribet, D., & Cossart, P. (2015). How bacterial pathogens colonize their hosts and invade deeper tissues. *Microbes and Infection*, *17*(3), 173–183.

Rider, P., Carmi, Y., Voronov, E., & Apte, R. N. (2013). Interleukin-1α. *Seminars in Immunology*. http://doi.org/10.1016/j.smim.2013.10.005

Rippere-Lampe, K. E., Lang, M., Ceri, H., Olson, M., Lockman, H. A., & O'Brien, A. D. (2001a). Cytotoxic necrotizing factor type 1-positive *Escherichia coli* causes increased inflammation and tissue damage to the prostate in a rat prostatitis model. *Infection and Immunity*, *69*(10), 6515–6519.

Rippere-Lampe, K. E., O'Brien, A. D., Conran, R., & Lockman, H. A. (2001b). Mutation of the gene encoding cytotoxic necrotizing factor type 1 (*cnf1*) attenuates the virulence of uropathogenic *Escherichia coli*. *Infection and Immunity*, *69*(6), 3954–3964.

Robins-Browne, R. M., Tzipori, S., Gonis, G., Hayes, J., Withers, M., & Prpic, J. K. (1985). The pathogenesis of *Yersinia enterocolitica* infection in gnotobiotic piglets. *Journal of Medical Microbiology*, *19*(3), 297–308.

Robinson, N., McComb, S., Mulligan, R., Dudani, R., Krishnan, L., & Sad, S. (2012). Type I interferon induces necroptosis in macrophages during infection with *Salmonella enterica* serovar Typhimurium. *Nature Immunology*, *13*(10), 954–62.

Rodriguez-Rojas, A., Mena, A., Martin, S., Borrell, N., Oliver, A., & Blazquez, J. (2009). Inactivation of the *hmgA* gene of *Pseudomonas aeruginosa* leads to pyomelanin hyperproduction, stress resistance and increased persistence in chronic lung infection. *Microbiology*, *155*(4), 1050–1057.

Romani, L., Bistoni, F., Perruccio, K., Montagnoli, C., Gaziano, R., Bozza, S., … Puccetti, P. (2006). Thymosin 1 activates dendritic cell tryptophan catabolism and establishes a regulatory environment for balance of inflammation and tolerance. *Blood*, *108*(7), 2265–2274.

Ronald, A. (2003). The etiology of urinary tract infection: Traditional and emerging pathogens. *Disease-a-Month*. http://doi.org/10.1016/S0011-5029(03)90001-0

Ronald, P. C., & Beutler, B. (2010). Plant and animal sensors of conserved microbial signatures. *Science (New York, N.Y.)*, *330*(6007), 1061–1064.

Rosqvist, R., Bölin, I., & Wolf-Watz, H. (1988). Inhibition of phagocytosis in *Yersinia pseudotuberculosis*: a virulence plasmid-encoded ability involving the Yop2b protein. *Infection and Immunity*, *56*(8), 2139–43.

Rubin, E. J., Gill, D. M., Boquet, P., & Popoff, M. R. (1988). Functional modification of a 21-kilodalton G protein when ADP-ribosylated by exoenzyme C3 of *Clostridium botulinum*. *Molecular and Cellular Biology*, *8*(1), 418–426.

Ruckdeschel, K., Roggenkamp, A., Schubert, S., & Heesemann, J. (1996). Differential contribution of *Yersinia enterocolitica* virulence factors to evasion of microbicidal action of neutrophils. *Infection and Immunity*, *64*(3), 724–33.

Russell, H. I., York, I. A., Rock, K. L., & Monaco, J. J. (1999). Class II antigen processing defects in two H2d mouse cell lines are caused by point mutations in the H2-DMa gene. *European Journal of Immunology*, *29*(3), 905–11.

Sabbah, M., Prunier, C., Ferrand, N., Megalophonos, V., Lambein, K., De Wever, O., … Redeuilh, G. (2011). CCN5, a novel transcriptional repressor of the transforming growth factor β signaling pathway. *Molecular and Cellular Biology*, *31*(7), 1459–69.

Salama, N. R., Hartung, M. L., & Müller, A. (2013). Life in the human stomach: persistence strategies of the bacterial pathogen *Helicobacter pylori*. *Nature Reviews. Microbiology*, *11*(6), 385–99.

Sanchez, A. M., & Yang, Y. (2011). The role of natural regulatory T cells in infection. *Immunologic Research*. http://doi.org/10.1007/s12026-010-8176-8

Sansonetti, P. (2002). Host-pathogen interactions: the seduction of molecular cross talk. *Gut*, *50 Suppl 3*, III2-8.

Sansonetti, P. J. (2004). War and peace at mucosal surfaces. *Nature Reviews Immunology*, *4*(12), 953–964.

Sasindran, S. J., & Torrelles, J. B. (2011). *Mycobacterium tuberculosis* infection and inflammation: What is beneficial for the host and for the bacterium? *Frontiers in Microbiology*, *2*(JAN).

Sato, T., Kudo, T., Ikehara, Y., Ogawa, H., Hirano, T., Kiyohara, K., … Narimatsu, H. (2011). Chondroitin sulfate N-acetylgalactosaminyltransferase 1 is necessary for normal endochondral ossification and aggrecan metabolism. *Journal of Biological Chemistry*, *286*(7), 5803–5812.

Savin, C., Martin, L., Bouchier, C., Filali, S., Chenau, J. Ô., Zhou, Z., … Carniel, E. (2014). The *Yersinia pseudotuberculosis* complex: Characterization and delineation of a new species, *Yersinia wautersii*. *International Journal of Medical Microbiology*, *304*(3–4), 452–463.

Sayi, A., Kohler, E., Hitzler, I., Arnold, I., Schwendener, R., Rehrauer, H., & Müller, A. (2009). The CD4+ T cell-mediated IFN-gamma response to *Helicobacter* infection is essential for clearance and determines gastric cancer risk. *Journal of Immunology (Baltimore, Md.: 1950)*, *182*(11), 7085–101.

Scheller, J., Chalaris, A., Schmidt-Arras, D., & Rose-John, S. (2011). The pro- and anti-inflammatory properties of the cytokine interleukin-6. *Biochimica et Biophysica Acta - Molecular Cell Research*. http://doi.org/10.1016/j.bbamcr.2011.01.034

Schlag, G., Redl, H., & Hallström, S. (1991). The cell in shock: the origin of multiple organ failure. *Resuscitation*, *21*(2–3), 137–180.

Schlegel, N., Meir, M., Spindler, V., Germer, C. T., & Waschke, J. (2011). Differential role of Rho GTPases in intestinal epithelial barrier regulation *in vitro*. *Journal of Cellular Physiology*, *226*(5), 1196–1203.

Schmees, C., Prinz, C., Treptau, T., Rad, R., Hengst, L., Voland, P., … Gerhard, M. (2007). Inhibition of T-cell proliferation by *Helicobacter pylori* gamma-glutamyl transpeptidase. *Gastroenterology*, *132*(5), 1820–1833.

Schmid, A., Kopp, A., Hanses, F., Karrasch, T., & Schäffler, A. (2014). C1q/TNF-related protein-3 (CTRP-3) attenuates lipopolysaccharide (LPS)-induced systemic inflammation and adipose tissue Erk-1/-2 phosphorylation in mice *in vivo*. *Biochemical and Biophysical Research Communications*, *452*(1), 8–13.

Schmidt, G., Sehr, P., Wilm, M., Selzer, J., Mann, M., & Aktories, K. (1997). Gln63 of Rho is deamidated by *Escherichia coli* cytotoxic necrotizing factor-1. *Nature*, *387*(6634), 725–729.

Schoberle, T. J., Chung, L. K., McPhee, J. B., Bogin, B., & Bliska, J. B. (2016). Uncovering an important role for YopJ in the Inhibition of caspase-1 in activated macrophages and promoting *Yersinia pseudotuberculosis* virulence. *Infection and Immunity*, *84*(4), 1062–1072.

Schoebel, S., Oesterlin, L. K., Blankenfeldt, W., Goody, R. S., & Itzen, A. (2009). RabGDI displacement by DrrA from *Legionella* is a consequence of its guanine nucleotide exchange activity. *Molecular Cell*, *36*(6), 1060–1072.

Schoep, T. D., Fulurija, A., Good, F., Lu, W., Himbeck, R. P., Schwan, C., … Marshall, B. J. (2010). Surface properties of *Helicobacter pylori* urease complex are essential for persistence. *PLoS ONE*, *5*(11).

Schoppet, M., Bubert, A., & Huppertz, H. I. (2000). Dendritic cell function is perturbed by *Yersinia enterocolitica* infection *in vitro*. *Clin.Exp.Immunol.*, *122*(3), 316–323.

Schotte, P., Denecker, G., Van Den Broeke, A., Vandenabeele, P., Cornelis, G. R., & Beyaert, R. (2004). Targeting Rac1 by the *Yersinia* effector protein YopE inhibits caspase-1-mediated maturation and release of interleukin-1β. *The Journal of Biological Chemistry*, *279*(24), 25134–42.

Schulte, R., Autenrieth, I. B., & Pettenkofer-institut, M. Von. (1998). *Yersinia enterocolitica* -Induced Interleukin-8 Secretion by Human Intestinal Epithelial Cells Depends on Cell Differentiation. *Infection and Immunity*, *66*(3), 1216–1224.

Schulte, R., Grassl, G. a, Preger, S., Fessele, S., Jacobi, C. a, Schaller, M., … Autenrieth, I. B. (2000a). *Yersinia enterocolitica* invasin protein triggers IL-8 production in epithelial cells via activation of Rel p65-p65 homodimers. *The FASEB Journal : Official Publication of the Federation of American Societies for Experimental Biology*, *14*(11), 1471–1484.

Schulte, R., Kerneis, S., Klinke, S., Bartels, H., Preger, S., Kraehenbuhl, J. P., … Autenrieth, I. B. (2000b). Translocation of *Yersinia enterocolitica* across reconstituted intestinal epithelial monolayers is triggered by *Yersinia* invasin binding to β1 integrins apically expressed on M-like cells. *Cellular Microbiology*, *2*(2), 173–185.

Schuster, F. (2015). Underlying principles of bistability in the expression of the pivotal virulence regulator RovA of *Yersinia pseudotuberculosis* and its role for virulence.

Schweer, J., Kulkarni, D., Kochut, A., Pezoldt, J., Pisano, F., Pils, M. C., … Dersch, P. (2013). The cytotoxic necrotizing factor of *Yersinia pseudotuberculosis* (CNFY) enhances inflammation and Yop delivery during infection by activation of Rho GTPases. *PLoS Pathogens*, *9*(11).

Schweer, J. N. G. (2014). Molecular function of the cytotoxic necrotizing factor CNFY and its impact on the virulence of *Yersinia pseudotuberculosis*.

Scott, V. C. S., Haake, D. A., Churchill, B. M., Justice, S. S., & Kim, J. H. (2015). Intracellular Bacterial Communities: A Potential Etiology for Chronic Lower Urinary Tract Symptoms. *Urology*. http://doi.org/10.1016/j.urology.2015.04.002

Segura, E., & Villadangos, J. A. (2009). Antigen presentation by dendritic cells *in vivo*. *Current Opinion in Immunology*. http://doi.org/10.1016/j.coi.2009.03.011

Seroussi, E., Klompus, S., Silanikove, M., Krifucks, O., Shapiro, F., Gertler, A., & Leitner, G. (2013). Nonbactericidal secreted phospholipase A2s are potential anti-inflammatory factors in the mammary gland. *Immunogenetics*, *65*(12), 861–871.

Shah, C., Hari-Dass, R., & Raynes, J. G. (2006). Serum amyloid A is an innate immune opsonin for Gram-negative bacteria. *Blood*, *108*(5), 1751–7.

Shah, M., & Reed, C. (2014). Complications of tuberculosis. *Current Opinion in Infectious Diseases*, *27*(5), 403–410.

Shan, J., Oshima, T., Muto, T., Yasuda, K., Fukui, H., Watari, J., … Miwa, H. (2015). Epithelial-derived nuclear IL-33 aggravates inflammation in the pathogenesis of reflux esophagitis. *Journal of Gastroenterology*, *50*(4), 414–423.

Sharma, A., Steichen, A. L., Jondle, C. N., Mishra, B. B., & Sharma, J. (2014). Protective role of mincle in bacterial pneumonia by regulation of neutrophil mediated phagocytosis and extracellular trap formation. *Journal of Infectious Diseases*, *209*(11), 1837–1846.

Shen, H., Gonzalez-Juarbe, N., Blanchette, K., Crimmins, G., Bergman, M. A., Isberg, R. R., … Dube, P. H. (2016). CD8+ T cells specific to a single *Yersinia pseudotuberculosis* epitope restrict bacterial replication in the liver but fail to provide sterilizing immunity. *Infection, Genetics and Evolution*, *43*, 289–296.

Shi, J., Zhao, Y., Wang, Y., Gao, W., Ding, J., Li, P., … Shao, F. (2014). Inflammatory caspases are innate immune receptors for intracellular LPS. *Nature*, *514*(7521), 187.

Shin, S., & Brodsky, I. E. (2015). The inflammasome: Learning from bacterial evasion strategies. *Seminars in Immunology*. http://doi.org/10.1016/j.smim.2015.03.006

Shrivastava, S., McVey, J. H., & Dorling, A. (2007, March). The interface between coagulation and immunity. *American Journal of Transplantation*. http://doi.org/10.1111/j.1600-6143.2006.01653.x

Shukla, V. K., Singh, H., Pandey, M., Upadhyay, S. K., & Nath, G. (2000). Carcinoma of the gallbladder--is it a sequel of typhoid? *Digestive Diseases and Sciences*, *45*(5), 900–903.

Shukla, S. K., Rose, W., & Schrodi, S. J. (2015). Complex host genetic susceptibility to *Staphylococcus aureus* infections. *Trends in Microbiology*, *23*(9), 529–536.

Shurin, G. V, Tourkova, I. L., Chatta, G. S., Schmidt, G., Wei, S., Djeu, J. Y., & Shurin, M. R. (2005). Small Rho GTPases regulate antigen presentation in dendritic cells. *Journal of Immunology (Baltimore, Md. : 1950)*, *174*(6), 3394–3400.

Sieper, J. (2004). Disease mechanisms in reactive arthritis. *Current Rheumatology Reports*, *6*(2), 110–6.

Simon, R., Priefer, U., & Pühler, A. (1983). A broad host range mobilization system for *in vivo* genetic engineering: transposon mutagenesis in gram negative bacteria. *Bio/Technology*, *1*(9), 784–791.

Simon, A. K., Seipelt, E., & Sieper, J. (1994). Divergent T-cell cytokine patterns in inflammatory arthritis. *Proceedings of the National Academy of Sciences of the United States of America*, *91*(18), 8562–8566.

Simonet, M., Richard, S., & Berche, P. (1990). Electron microscopic evidence for *in vivo* extracellular localization of *Yersinia pseudotuberculosis* harboring the pYV plasmid. *Infection and Immunity*, *58*(3), 841–845.

Singh, P. K., Schaefer, a L., Parsek, M. R., Moninger, T. O., Welsh, M. J., & Greenberg, E. P. (2000). Quorum-sensing signals indicate that cystic fibrosis lungs are infected with bacterial biofilms. *Nature*, *407*(6805), 762–764.

Sinnott, C. R., & Teall, A. J. (1987). Persistent gallbladder carriage of *Salmonella* Typhi. *The Lancet*, *329*(8539), 976.

Skurnik, M., Bolin, I., Heikkinen, H., Piha, S., & Wolf-watz, H. (1984). Virulence plasmid-associated autoagglutination in *Yersinia* spp . *Journal of Bacteriology*, *158*(3), 1033–1036.

Skurnik, M., & Poikonen, K. (1986). Experimental intestinal infection of rats by *Yersinia enterocolitica* O:3. A follow-up study with specific antibodies to the virulence plasmid specified antigens. *Scandinavian Journal of Infectious Diseases*, *18*(4), 355–364.

Smeets, T. J., Dolhain, R. J., Breedveld, F. C., & Tak, P. P. (1998). Analysis of the cellular infiltrates and expression of cytokines in synovial tissue from patients with rheumatoid arthritis and reactive arthritis. *J Pathol*, *186*(1), 75–81.

Smego, R. A., Frean, J., & Koornhof, H. J. (1999). Yersiniosis I: Microbiological and clinicoepidemiological aspects of plague and non-plague *Yersinia* infections. *European Journal of Clinical Microbiology and Infectious Diseases* (Vol. 18). http://doi.org/10.1007/s1009 60050219

Smith, J. E. & Thal, E.: A taxonomic study of the genus *Pasteurella* using a numeral technique. *Acta Pathologica et Bacteriologica Scandinavica*, 1965, **64**, 213-223

Smith, M. A., Weingarten, R. A., Russo, L. M., Ventura, C. L., & O'Brien, A. D. (2015). Antibodies against hemolysin and cytotoxic necrotizing factor type 1 (CNF1) reduce bladder inflammation in a mouse model of urinary tract infection with toxigenic uropathogenic *Escherichia coli*. *Infection and Immunity*, *83*(4), 1661–1673.

Sneller, M. C., & Strober, W. (1986). M cells and host defense. *The Journal of Infectious Diseases*, *154*(5), 737–41.

Soehnlein, O. (2009, December). Direct and alternative antimicrobial mechanisms of neutrophil-derived granule proteins. *Journal of Molecular Medicine*. http://doi.org/10.1007/s00109-009-0508-6

Song, J., Bishop, B. L., Li, G., Duncan, M. J., & Abraham, S. N. (2007). TLR4-initiated and cAMP-mediated abrogation of bacterial invasion of the bladder. *Cell Host and Microbe*, *1*(4), 287–298.

Song, J., Bishop, B. L., Li, G., Grady, R., Stapleton, A., & Abraham, S. N. (2009). TLR4-mediated expulsion of bacteria from infected bladder epithelial cells. *Proceedings of the National Academy of Sciences of the United States of America*, *106*(35), 14966–14971.

Song, X., He, X., Li, X., & Qian, Y. (2016). The roles and functional mechanisms of interleukin-17 family cytokines in mucosal immunity. *Cellular & Molecular Immunology*, *13*, 418–431.

Sonnenberg, G. F., Monticelli, L. A., Elloso, M. M., Fouser, L. A., & Artis, D. (2011). CD4+ Lymphoid Tissue-Inducer Cells Promote Innate Immunity in the Gut. *Immunity*, *34*(1), 122–134.

Sonnenberg, G. F., Monticelli, L. a., Alenghat, T., Fung, T. C., Hutnick, N. A., Kunisawa, J., … Artis, D. (2012). Innate lymphoid cells promote anatomical containment of lymphoid-resident commensal bacteria. *Science*, *336*(6086), 1321–1325.

Souza, R. A., Falcão, D. P., & Falcão, J. P. (2011). Emended description of *Yersinia massiliensis*. *International Journal of Systematic and Evolutionary Microbiology*, *61*(5), 1094–1097.

Spinner, J. L., Cundiff, J. A., & Kobayashi, S. D. (2008). *Yersinia pestis* type III secretion system-dependent inhibition of human polymorphonuclear leukocyte function. *Infection and Immunity*, *76*(8), 3754–3760.

Sprague, L. D., & Neubauer, H. (2005). *Yersinia aleksiciae* sp. nov. *International Journal of Systematic and Evolutionary Microbiology*, *55*(2), 831–835.

Sprague, L. D., Scholz, H. C., Amann, S., Busse, H. J., & Neubauer, H. (2008). *Yersinia similis* sp. nov. *International Journal of Systematic and Evolutionary Microbiology*, *58*(4), 952–958.

Srinivasan, R., & Bogdanov, V. Y. (2012). Splice variants of Tissue Factor and integrin-mediated signaling. *Thrombosis Research*. http://doi.org/10.1016/j.thromres.2012.02.027

Stavropoulos, P. G., Soura, E., Kanelleas, A., Katsambas, A., & Antoniou, C. (2015). Reactive arthritis. *Journal of the European Academy of Dermatology and Venereology*, *29*(3), 415–424.

Stecher, B., Barthel, M., Schlumberger, M. C., Haberli, L., Rabsch, W., Kremer, M., & Hardt, W. D. (2008). Motility allows S. Typhimurium to benefit from the mucosal defense. *Cellular Microbiology*, *10*(5), 1166–1180.

Stetsko, D., & Sauder, D. N. (2008). IL-12 and IL-23 in health and disease. Expert Review of Clinical Immunology, 4(3), 301–3.

Stevens, M. G., Olsen, S. C., Pugh, G. W., & Palmer, M. V. (1994). Immune and pathologic responses in mice infected with *Brucella abortus* 19, RB51, or 2308. *Infection and Immunity*, *62*(8), 3206–12.

Stewart, G. R., Robertson, B. D., & Young, D. B. (2003). Tuberculosis: a problem with persistence. *Nat.Rev.Microbiol.*, *1*(1740–1526 (Print)), 97–105.

Stewart, M. K., & Cookson, B. T. (2016). Evasion and interference: intracellular pathogens modulate caspase-dependent inflammatory responses. *Nature Reviews Microbiology*, *14*(6), 346–359.

Straley, S. C., Plano, G. V, Skrzypek, E., Haddix, P. L., & Fields, K. A. (1993). Regulation by Ca2+ in the *Yersinia* low-Ca2+ response. *Molecular Microbiology*. http://doi.org/10.1111/j.1365-2958.1993.tb01644.x

Striz, I., Brabcova, E., Kolesar, L., & Sekerkova, A. (2014). Cytokine networking of innate immunity cells: a potential target of therapy. *Clinical Science*, *126*(9), 593–612.

Suh, H.-Y., Lee, D.-W., Lee, K.-H., Ku, B., Choi, S.-J., Woo, J.-S., … Oh, B.-H. (2010). Structural insights into the dual nucleotide exchange and GDI displacement activity of SidM/DrrA. *The EMBO Journal*, *29*(2), 496–504.

Sukupolvi, S., Edelstein, A., Rhen, M., Normark, S. J., & Pfeifer, J. D. (1997). Development of a murine model of chronic *Salmonella* infection. *Infection and Immunity*, *65*(2), 838–42.

Sulakvelidze, A., Dalakishvili, K., Barry, E., Wauters, G., Robins-Browne, R., Imnadze, P., & Morris, J. G. (1996). Analysis of clinical and environmental *Yersinia* isolates in the republic of Georgia. *Journal of Clinical Microbiology*, *34*(9), 2325–2327.

Sun, Y.-C., Koumoutsi, A., & Darby, C. (2009). The response regulator PhoP negatively regulates *Yersinia pseudotuberculosis* and *Yersinia pestis* biofilms. *FEMS Microbiology Letters*, *290*(1), 85–90.

Sun, L., Zhou, H., Zhu, Z., Yan, Q., Wang, L., Liang, Q., & Ye, R. D. (2015). Ex vivo and *in vitro* effect of serum amyloid a in the induction of macrophage M2 markers and efferocytosis of apoptotic neutrophils. *Journal of Immunology (Baltimore, Md. : 1950)*, *194*(10), 4891–900.

Sundrud, M. S., Torres, V. J., Unutmaz, D., & Cover, T. L. (2004). Inhibition of primary human T cell proliferation by *Helicobacter pylori* vacuolating toxin (VacA) is independent of VacA effects on IL-2 secretion. *Proceedings of the National Academy of Sciences of the United States of America*, *101*(20), 7727–32.

Swain, S. L., Weinberg, A. D., English, M., & Huston, G. (1990). IL-4 directs the development of Th2-like helper effectors. *Journal of Immunology (Baltimore, Md. : 1950)*, *145*(11), 3796–806.

Sydenham, M., Douce, G., Bowe, F., Ahmed, S., Chatfield, S., & Dougan, G. (2000). *Salmonella enterica* serovar Typhimurium *surA* mutants are attenuated and effective live oral vaccines. *Infection and Immunity*, *68*(3), 1109–1115.

Szerszynski, B. (2002). Ecological Rites. *Theory, Culture & Society*, *19*(3), 51.

Taheri, N., Fahlgren, A., & Fällman, M. (2016). *Yersinia pseudotuberculosis* blocks neutrophil degranulation. *Infection and Immunity*, *84*(12), 3369–3378.

Taleb, K., Auffray, C., Villefroy, P., Pereira, A., Hosmalin, A., Gaudry, M., & Le Bon, A. (2017). Chronic type I IFN is sufficient to promote immunosuppression through accumulation of myeloid-derived suppressor cells. *The Journal of Immunology*, *198*(3), 1156–1163.

Tan, S., Tompkins, L. S., & Amieva, M. R. (2009). *Helicobacter pylori* usurps cell polarity to turn the cell surface into a replicative niche. *PLoS Pathogens*, *5*(5).

Tan, S., Noto, J. M., Romero-Gallo, J., Peek, R. M., & Amieva, M. R. (2011). *Helicobacter pylori* perturbs iron trafficking in the epithelium to grow on the cell surface. *PLoS Pathogens*, *7*(5).

Tarchouna, M., Ferjani, A., Ben-Selma, W., & Boukadida, J. (2013). Distribution of uropathogenic virulence genes in *Escherichia coli* isolated from patients with urinary tract infection. *International Journal of Infectious Diseases*, *17*(6), e450–e453.

Taylor, G. A., Collazo, C. M., Yap, G. S., Nguyen, K., Gregorio, T. A., Taylor, L. S., … Vande Woude, G. F. (2000). Pathogen-specific loss of host resistance in mice lacking the IFN-gamma-inducible gene IGTP. *Proceedings of the National Academy of Sciences of the United States of America*, *97*(2), 751–5.

Tcherkezian, J., & Lamarche-vane, N. (2007). Current knowledge of the large RhoGAP family of proteins. *Biology of the Cell*, *99*(2), 67–86.

Teixeira, L. K., Fonseca, B. P., Barboza, B. A., & Viola, J. P. (2005). The role of interferon-γ on immune and allergic responses. *Mem.Inst.Oswaldo Cruz*. http://doi.org/10.1590/S0074-02762005000900024

Ternhag, A., Törner, A., Svensson, A., Ekdahl, K., & Giesecke, J. (2008). Short- and long-term effects of bacterial gastrointestinal infections. *Emerging Infectious Diseases*, *14*(1), 143–8.

Tertti, R., Granfors, K., Lehtonen, O. P., Mertsola, J., Mäkelä, A. L., Välimäki, I., … Toivanen, A. (1984). An outbreak of *Yersinia pseudotuberculosis* infection. *The Journal of Infectious Diseases*, *149*(2), 245–50.

Tertti, R., Skurnik, M., Vartio, T., & Kuusela, P. (1992). Adhesion protein YadA of *Yersinia* species mediates binding of bacteria to fibronectin. *Infection and Immunity*, *60*(7), 3021–3024.

Thänert, R., Goldmann, O., Beineke, A., & Medina, E. (2017). Host-inherent variability influences the transcriptional response of *Staphylococcus aureus* during *in vivo* infection. *Nature Communications*, *8*(14268).

Thinwa, J., Segovia, J. A., Bose, S., & Dube, P. H. (2014). Integrin-mediated first signal for inflammasome activation in intestinal epithelial cells. *Journal of Immunology (Baltimore, Md. : 1950)*, *193*(3), 1373–1382.

Thomas, W. E., Trintchina, E., Forero, M., Vogel, V., & Sokurenko, E. V. (2002). Bacterial adhesion to target cells enhanced by shear force. *Cell*, *109*(7), 913–923.

Thompson, L. J., Dunstan, S. J., Dolecek, C., Perkins, T., House, D., Dougan, G., … Falkow, S. (2009). Transcriptional response in the peripheral blood of patients infected with *Salmonella enterica* serovar Typhi. *Proceedings of the National Academy of Sciences of the United States of America*, *106*(52), 22433–22438.

Tietzel, I., El-Haibi, C., & Carabeo, R. A. (2009). Human guanylate binding proteins potentiate the anti-*Chlamydia* effects of interferon-gamma. *PloS One*, *4*(8), e6499.

Tomita, T., Jackson, a M., Hida, N., Hayat, M., Dixon, M. F., Shimoyama, T., … Crabtree, J. E. (2001). Expression of Interleukin-18, a Th1 cytokine, in human gastric mucosa is increased in *Helicobacter pylori* infection. *The Journal of Infectious Diseases*, *183*(4), 620–7.

Traven, A., Naderer, T., Miao, E., Leaf, I., Treuting, P., Mao, D., … Kerjaschki, D. (2014). Microbial egress: A hitchhiker's guide to freedom. *PLoS Pathogens*, *10*(7), e1004201.

Tsiotou, A. G., Sakorafas, G. H., Anagnostopoulos, G., & Bramis, J. (2005). Septic shock; current pathogenetic concepts from a clinical perspective. *Medical Science Monitor : International Medical Journal of Experimental and Clinical Research*, *11*(3), RA76-85.

Tu, S., Bhagat, G., Cui, G., Takaishi, S., Kurt-Jones, E. A., Rickman, B., … Wang, T. C. (2008). Overexpression of interleukin-1 β induces gastric inflammation and cancer and mobilizes myeloid-derived suppressor cells in mice. *Cancer Cell*, *14*(5), 408–419.

Tumitan, A. R. P., Monnazzi, L. G. S., Ghiraldi, F. R., Cilli, E. M., & Machado de Medeiros, B. M. (2007). Pattern of macrophage activation in *Yersinia*-resistant and *Yersinia*-susceptible strains of mice. *Microbiology and Immunology*, *51*(10), 1021–8.

Turner, J. R. (2009). Intestinal mucosal barrier function in health and disease. *Nature Reviews. Immunology*, *9*(11), 799–809.

Ugrinovic, S., Mertz, A., Wu, P., Braun, J., & Sieper, J. (1997). A single nonamer from the *Yersinia* 60-kDa heat shock protein is the target of HLA-B27-restricted CTL response in *Yersinia*-induced reactive arthritis. *J Immunol.*, *159*(11), 5715–23.

Uliczka, F., Pisano, F., Kochut, A., Opitz, W., Herbst, K., Stolz, T., & Dersch, P. (2011). Monitoring of gene expression in bacteria during infections using an adaptable set of bioluminescent, fluorescent and colorigenic fusion vectors. *PLoS ONE*, *6*(6), 1–12.

Urieli-Shoval, S., Linke, R. P., & Matzner, Y. (2000). Expression and function of serum amyloid A, a major acute-phase protein, in normal and disease states. *Current Opinion in Hematology*, *7*(1), 64–9.

Ursing, J., Herv, J. B., Fanning, O. R., Steigerwalt, I. A. G., & Mollaretw, H. H. (1980). *Yersinia frederiksenii :* A new species of enterobacteriaceae composed of rhamnose-positive strains (formerly called atypical *Yersinia enterocolitica* or *Yersinia enterocolitica*-like). *Current Microbiology*, *4*, 213–217.

Vagima, Y., Zauberman, A., Levy, Y., Gur, D., Tidhar, A., Aftalion, M., … Mamroud, E. (2015). Circumventing *Y. pestis* virulence by early recruitment of neutrophils to the lungs during pneumonic plague. *PLOS Pathogens*, *11*(5), e1004893.

Vaishnava, S., Yamamoto, M., Severson, K. M., Ruhn, K. A., Yu, X., Koren, O., … Hooper, L. V. (2011). The antibacterial lectin RegIIIγ promotes the spatial segregation of microbiota and host in the intestine. *Science*, *334*(6053), 255–258.

van Ampting, M. T. J., Loonen, L. M. P., Schonewille, A. J., Konings, I., Vink, C., Iovanna, J., … Bovee-Oudenhoven, I. M. J. (2012). Intestinally secreted c-type lectin Reg3β attenuates salmonellosis but not listeriosis in mice. *Infection and Immunity*, *80*(3), 1115–1120.

van de Veerdonk, F. L., Netea, M. G., Dinarello, C. A., & Joosten, L. A. B. (2011). Inflammasome activation and IL-1β and IL-18 processing during infection. *Trends in Immunology*, *32*(3), 110–116. http://doi.org/10.1016/j.it.2011.01.003

van der Poll, T., & Herwald, H. (2014). The coagulation system and its function in early immune defense. *Thrombosis and Haemostasis*, *112*(4), 640–648.

van Erp, K., Dach, K., Koch, I., Heesemann, J., & Hoffmann, R. (2006). Role of strain differences on host resistance and the transcriptional response of macrophages to infection with *Yersinia enterocolitica*. *Physiological Genomics*, *25*(1), 75–84.

van Loghem, J. J. (1944). The classification of the plague-bacillus. *Antonie van Leeuwenhoek*, *10*(1), 15–16.

Vanden Berghe, T., Hassannia, B., & Vandenabeele, P. (2016). An outline of necrosome triggers. *Cellular and Molecular Life Sciences : CMLS*, *73*(11–12), 2137–52.

Vandesompele, J., De Preter, K., Pattyn, F., Poppe, B., Van Roy, N., De Paepe, A., & Speleman, F. (2002). Accurate normalization of real-time quantitative RT-PCR data by geometric averaging of multiple internal control genes. *Genome Biology*, *3*(7), RESEARCH0034.

Vasala, M., Hallanvuo, S., Ruuska, P., Suokas, R., Siitonen, A., & Hakala, M. (2014). High frequency of reactive arthritis in adults after *Yersinia pseudotuberculosis* O:1 outbreak caused by contaminated grated carrots. *Annals of the Rheumatic Diseases*, *73*(10), 1793–6.

Vazquez-Torres, a, Jones-Carson, J., Bäumler, a J., Falkow, S., Valdivia, R., Brown, W., … Fang, F. C. (1999). Extraintestinal dissemination of *Salmonella* by CD18-expressing phagocytes. *Nature*, *401*(6755), 804–808.

Velin, D., Favre, L., Bernasconi, E., Bachmann, D., Pythoud, C., Saiji, E., … Michetti, P. (2009). Interleukin-17 Is a critical mediator of vaccine-induced reduction of *Helicobacter* infection in the mouse model. *Gastroenterology*, *136*(7).

Versteeg, H. H., Heemskerk, J. W. M., Levi, M., & Reitsma, P. H. (2013). New fundamentals in hemostasis. *Physiological Reviews*, *93*(1), 327–58.

Verstrepen, L., Carpentier, I., Verhelst, K., & Beyaert, R. (2009). ABINs: A20 binding inhibitors of NF-κB and apoptosis signaling. *Biochemical Pharmacology*, *78*(2), 105–114.

Viboud, G. I., & Bliska, J. B. (2005). *Yersinia* outer proteins: role in modulation of host cell signaling responses and pathogenesis. *Annual Review of Microbiology*, *59*, 69–89.

Viganò, E., & Mortellaro, A. (2013). Caspase-11: The driving factor for noncanonical inflammasomes. *European Journal of Immunology*, *43*(9), 2240–2245.

Vignali, D. A., & Kuchroo, V. K. (2012). IL-12 family cytokines: immunological playmakers. *Nature Immunology*, *13*(8), 722–728.

Villadangos, J. A., & Schnorrer, P. (2007). Intrinsic and cooperative antigen-presenting functions of dendritic-cell subsets *in vivo*. *Nature Reviews. Immunology*, *7*(7), 543–555.

Visser, L. G., Annema, A., & Van Furth, R. (1995). Role of Yops in inhibition of phagocytosis and killing of opsonized *Yersinia enterocolitica* by human granulocytes. *Infection and Immunity*, *63*(7), 2570–2575.

Vitali, C., Mingozzi, F., Broggi, A., Barresi, S., Zolezzi, F., Bayry, J., … Granucci, F. (2012). Migratory, and not lymphoid-resident, dendritic cells maintain peripheral self-tolerance and prevent autoimmunity via induction of iTreg cells. *Blood*, *120*(6), 1237–1245.

Vitetta, E. S., Ohara, J., Myers, C. D., Layton, J. E., Krammer, P. H., & Paul, W. E. (1985). Serological, biochemical, and functional identity of B cell-stimulatory factor 1 and B cell differentiation factor for IgG1. *The Journal of Experimental Medicine*, *162*(5), 1726–31.

Vogelsang, T. M., & Bøe, J. (1948). Temporary and chronic carriers of *Salmonella* Typhi and *Salmonella* Paratyphi B. *The Journal of Hygiene*, *46*(3), 252–61.

von Altrock, A., Seinige, D., & Kehrenberg, C. (2015). *Yersinia enterocolitica* isolates from wild boars hunted in Lower Saxony, Germany. *Applied and Environmental Microbiology*, *81*(14), 4835–4840.

von Boehmer, H. (2005). Mechanisms of suppression by suppressor T cells. *Nature Immunology*, *6*(4), 338–344.

Von Pawel-Rammingen, U., Telepnev, M. V., Schmidt, G., Aktories, K., Wolf-Watz, H., & Rosqvist, R. (2000). GAP activity of the *Yersinia* YopE cytotoxin specifically targets the Rho pathway: A mechanism for disruption of actin microfilament structure. *Molecular Microbiology*, *36*(3), 737–748.

Wain, J., Bay, P. V. B., Vinh, H., Duong, N. M., Diep, T. S., Walsh, A. L., … Day, N. P. J. (2001). Quantitation of bacteria in bone marrow from patients with typhoid fever: Relationship between counts and clinical features. *Journal of Clinical Microbiology*, *39*(4), 1571–1576.

Wang, S., Miura, M., Jung, Y. K., Zhu, H., Li, E., & Yuan, J. (1998). Murine caspase-11, an ICE-interacting protease, is essential for the activation of ICE. *Cell*, *92*(4), 501–9.

Wang, Q., Garrity, G. M., Tiedje, J. M., & Cole, J. R. (2007). Naïve Bayesian classifier for rapid assignment of rRNA sequences into the new bacterial taxonomy. *Applied and Environmental Microbiology*, *73*(16), 5261–5267.

Wang, M. H., & Kim, K. S. (2013). Cytotoxic necrotizing factor 1 contributes to *Escherichia coli* meningitis. *Toxins*. http://doi.org/10.3390/toxins5112270

Wang, H., Avican, K., Fahlgren, A., Erttmann, S. F., Nuss, A. M., Dersch, P., … Wolf-Watz, H. (2016a). Increased plasmid copy number is essential for *Yersinia* T3SS function and virulence. *Science (New York, N.Y.)*, *353*(6298), 492–5.

Wang, K.-C., Huang, C.-H., Huang, C.-J., & Fang, S.-B. (2016b). Impacts of *Salmonella enterica* serovar Typhimurium and its *speg* gene on the transcriptomes of *in vitro* M cells and Caco-2 cells. *PLOS ONE*, *11*(4), e0153444.

Watson, G. T., Huaman, M. A., Semler, M. W., Manners, J., Woron, A. M., Carpenter, L. R., & Christman, B. W. (2013). When nature meets nurture: Persistent Y*ersinia* infection. *American Journal of Medicine*, *126*(7), 578–580.

Wauters, G., Janssens, M., Steigerwalt, A. G., & Brenner, D. J. (1988). *Yersinia mollaretii* sp. nov. and *Yersinia bercovieri* sp. nov., formerly called *Yersinia enterocolitica* biogroups 3A and 3B. *International Journal of Systematic Bacteriology*, *38*(4), 424–429.

Weeks, D. L., Eskandari, S., Scott, D. R., & Sachs, G. (2000). A H+-gated urea channel: the link between *Helicobacter pylori* urease and gastric colonization. *Science (New York, N.Y.)*, *287*(5452), 482–485.

Weiss, G., Forster, S., Irving, A., Tate, M., Ferrero, R. L., Hertzog, P., … Kaparakis-Liaskos, M. (2013). *Helicobacter pylori* VacA suppresses *Lactobacillus acidophilus*-induced interferon beta signaling in macrophages via alterations in the endocytic pathway. *mBio*, *4*(3), e00609-12.

Weldon, S., & Taggart, C. C. (2007). Innate host defense functions of secretory leucoprotease inhibitor. *Experimental Lung Research*, *33*(10), 485–491.

Weng, D., Marty-Roix, R., Ganesan, S., Proulx, M. K., Vladimer, G. I., Kaiser, W. J., … Lien, E. (2014). Caspase-8 and RIP kinases regulate bacteria-induced innate immune responses and cell death. *Proceedings of the National Academy of Sciences*, *111 VN*-(20), 7391–7396.

Wennerberg, K., & Der, C. J. (2004). Rho-family GTPases: it's not only Rac and Rho (and I like it). *Journal of Cell Science*, *117*(Pt 8), 1301–1312.

Wennerberg, K., Rossman, K. L., & Der, C. J. (2005). The Ras superfamily at a glance. *Journal of Cell Science*, *118*(Pt 5), 843–846.

Wershil, B. K., & Furuta, G. T. (2008). 4. Gastrointestinal mucosal immunity. *Journal of Allergy and Clinical Immunology*, *121*(2 SUPPL. 2), S380–S383.

Westermark, L., Fahlgren, A., & Fällman, M. (2014). *Yersinia pseudotuberculosis* efficiently escapes polymorphonuclear neutrophils during early infection. *Infection and Immunity*, *82*(3), 1181–1191.

Weston, A. P., Biddle, W. L., Bhatia, P. S., & Miner, P. B. (1993). Terminal ileal mucosal mast cells in irritable bowel syndrome. *Digestive Diseases and Sciences*, *38*(9), 1590–1595.

WHO. (2013). Diarrhoeal disease. Retrieved February 3, 2017, from http://www.who.int/mediacentre/factsheets/fs330/en/

WHO. (2017). WHO | Estimates for 2000–2015. *WHO*.

Wikenheiser, D. J., & Stumhofer, J. S. (2016). ICOS co-stimulation: Friend or foe? *Frontiers in Immunology*, *7*(August), 1–16.

Wilson, G. J., Marakalala, M. J., Hoving, J. C., Van Laarhoven, A., Drummond, R. A., Kerscher, B., … Brown, G. D. (2015). The C-type lectin receptor CLECSF8/CLEC4D is a key component of anti-mycobacterial immunity. *Cell Host and Microbe*, *17*(2), 252–259.

Winter, S. E., Thiennimitr, P., Winter, M. G., Butler, B. P., Huseby, D. L., Crawford, R. W., … Bäumler, A. J. (2010). Gut inflammation provides a respiratory electron acceptor for *Salmonella*. *Nature*, *467*(7314), 426–9.

Witko-Sarsat, V., Rieu, P., Descamps-Latscha, B., Lesavre, P., & Halbwachs-Mecarelli, L. (2000). Neutrophils: molecules, functions and pathophysiological aspects. *Laboratory Investigation; a Journal of Technical Methods and Pathology*, *80*(5), 617–53.

Wolters, M., Boyle, E. C., Lardong, K., Trülzsch, K., Steffen, A., Rottner, K., … Aepfelbacher, M. (2013). Cytotoxic necrotizing factor-Y boosts *Yersinia* effector translocation by activating Rac protein. *Journal of Biological Chemistry*, *288*(32), 23543–23553.

Wu, H., Li, X.-M., Wang, J.-R., Gan, W.-J., Jiang, F.-Q., Liu, Y., … Li, J.-M. (2016). NUR77 exerts a protective effect against inflammatory bowel disease by negatively regulating the TRAF6/TLR-IL-1R signalling axis. *The Journal of Pathology*, *238*(3), 457–469.

Wu, U.-I., & Holland, S. M. (2016). A genetic perspective on granulomatous diseases with an emphasis on mycobacterial infections. *Seminars in Immunopathology*, *38*(2), 199–212.

Wucherpfennig, K. W. (2001). Mechanisms for the induction of autoimmunity by infectious agents. *Journal of Clinical Investigation*. http://doi.org/10.1172/JCI200114235

Yamamoto, T., Sashinami, H., Takaya, A., Tomoyasu, T., Matsui, H., Kikuchi, Y., … Nakane, A. (2001). Disruption of the genes for ClpXP protease in *Salmonella enterica* serovar Typhimurium results in persistent infection in mice, and development of persistence requires endogenous gamma interferon and tumor necrosis factor alpha. *Infection and Immunity*, *69*(5), 3164–74.

Yamashita, S., Lukacik, P., Barnard, T. J., Noinaj, N., Felek, S., Tsang, T. M., … Buchanan, S. K. (2011). Structural insights into Ail-mediated adhesion in *Yersinia pestis*. *Structure*, *19*(11), 1672–1682.

Yan, Y., Su, S., Meng, X., Ji, X., Qu, Y., Liu, Z., … Han, Y. (2013). Determination of sRNA expressions by RNA-seq in *Yersinia pestis* grown *in vitro* and during infection. *PloS One*, *8*(9), e74495.

Yang, Y., Merriam, J. J., Mueller, J. P., & Isberg, R. R. (1996). The *psa* locus is responsible for thermoinducible binding of *Yersinia pseudotuberculosis* to cultured cells. *Infection and Immunity*, *64*(7), 2483–2489.

Yarbrough, M. L., Li, Y., Kinch, L. N., Grishin, N. V, Ball, H. L., & Orth, K. (2009). AMPylation of Rho GTPases by *Vibrio* VopS disrupts effector binding and downstream signaling. *Science*, *323*(5911), 269–272.

Yazdi, A. S., & Drexler, S. K. (2013). Regulation of interleukin 1α secretion by inflammasomes. *Annals of the Rheumatic Diseases*, *72 Suppl 2*(suppl 2), ii96-9.

Yen, E. F., & Pardi, D. S. (2011). Review article: microscopic colitis - lymphocytic, collagenous and "mast cell" colitis. *Alimentary Pharmacology & Therapeutics*, *34*(1), 21–32.

Yin, Z. H., Braun, J., Neure, L., Wu, P. H., Liu, L. Z., Eggens, U., & Sieper, J. (1997). crucial role of interleukin-10/interleukin-12 balance in the regulation of the type 2 T helper cytokine response in reactive arthritis. *Arthritis Rheum.*, *40*(10), 1788–1797.

Younesy, H., Möller, T., Lorincz, M. C., Karimi, M. M., & Jones, S. J. (2015). VisRseq: R-based visual framework for analysis of sequencing data. *BMC Bioinformatics*, *16*(Suppl 11), S2.

Young, D., Stark, J., & Kirschner, D. (2008). Systems biology of persistent infection: tuberculosis as a case study. *Nature Reviews. Microbiology*, *6*(7), 520–528.

Yu, H., & Kim, K. S. (2010). Ferredoxin is involved in secretion of cytotoxic necrotizing factor 1 across the cytoplasmic membrane in *Escherichia coli* K1. *Infection and Immunity*, *78*(2), 838–844.

Yu, H., & Kim, K. S. (2012). YgfZ contributes to secretion of cytotoxic necrotizing factor 1 into outer-membrane vesicles in *Escherichia coli*. *Microbiology*, *158*(3), 612–621.

Yu, S., & Gao, N. (2015). Compartmentalizing intestinal epithelial cell toll-like receptors for immune surveillance. *Cellular and Molecular Life Sciences*. Springer Basel.

Zabaleta, J., McGee, D. J., Zea, A. H., Hernández, C. P., Rodriguez, P. C., Sierra, R. A., … Ochoa, A. C. (2004). *Helicobacter pylori* arginase inhibits T cell proliferation and reduces the expression of the TCR zeta-chain (CD3zeta). *Journal of Immunology (Baltimore, Md. : 1950)*, *173*(1), 586–93.

Zabieglo, K., Majewski, P., Majchrzak-Gorecka, M., Wlodarczyk, A., Grygier, B., Zegar, A., … Cichy, J. (2015). The inhibitory effect of secretory leukocyte protease inhibitor (SLPI) on formation of neutrophil extracellular traps. *Journal of Leukocyte Biology*, *98*(1), 99–106.

Zahrt, T. C. (2003). Molecular mechanisms regulating persistent *Mycobacterium tuberculosis* infection. *Microbes and Infection*, *5*(2), 159–167.

Zav'yalov, V. P., Abramov, V. M., Cherepanov, P. G., Spirina, G. V, Chernovskaya, T. V, Vasiliev, A. M., & Zav'yalova, G. A. (1996). pH6 antigen (PsaA protein) of *Yersinia pestis*, a novel bacterial Fc-receptor. *FEMS Immunology and Medical Microbiology*, *14*(1), 53–7.

Zdziarski, J., Svanborg, C., Wullt, B., Hacker, J., & Dobrindt, U. (2008). Molecular basis of commensalism in the urinary tract: Low virulence or virulence attenuation? *Infection and Immunity*, *76*(2), 695–703.

Zegers, M. M., & Friedl, P. (2014). Rho GTPases in collective cell migration. *Small GTPases*, *5*, e28997.

Zelante, T., Fallarino, F., Bistoni, F., Puccetti, P., & Romani, L. (2009). Indoleamine 2,3-dioxygenase in infection: the paradox of an evasive strategy that benefits the host. *Microbes and Infection*, *11*(1), 133–141.

Zeng, L., Sullivan, L. C., Vivian, J. P., Walpole, N. G., Harpur, C. M., Rossjohn, J., … Brooks, A. G. (2012). A structural basis for antigen presentation by the MHC class Ib molecule, Qa-1b. *Journal of Immunology (Baltimore, Md. : 1950)*, *188*(1), 302–10.

Zeng, M. Y., Inohara, N., & Nuñez, G. (2016). Mechanisms of inflammation-driven bacterial dysbiosis in the gut. *Mucosal Immunology*, (August), 1–9.

Zhang, M., Liu, M., Luther, J., & Kao, J. Y. (2010). *Helicobacter pylori* directs tolerogenic programming of dendritic cells. *Gut Microbes*, *1*(5).

Zhang, Y., Romanov, G., & Bliska, J. B. (2011). Type III secretion system-dependent translocation of ectopically expressed yop effectors into macrophages by intracellular *Yersinia pseudotuberculosis*. *Infection and Immunity*, *79*(11), 4322–4331.

Zhang, Y., Tam, J. W., Mena, P., van der Velden, A. W. M., & Bliska, J. B. (2015). CCR2+ inflammatory dendritic cells and translocation of antigen by type III secretion are required for the exceptionally large CD8+ T cell response to the protective YopE69-77 epitope during *Yersinia* infection. *PLoS Pathogens*, *11*(10), 1–24.

Zhang, L., Mei, M., Yu, C., Shen, W., Ma, L., He, J., & Yi, L. (2016a). The functions of effector proteins in *Yersinia* virulence. *Polish Journal of Microbiology*, *65*(1), 5–12.

Zhang, Y., Garcia-Ibanez, L., & Toellner, K. M. (2016b). Regulation of germinal center B-cell differentiation. *Immunological Reviews*. http://doi.org/10.1111/imr.12396

Zheng, Y., Valdez, P. A., Danilenko, D. M., Hu, Y., Sa, S. M., Gong, Q., … Ouyang, W. (2008). Interleukin-22 mediates early host defense against attaching and effacing bacterial pathogens. *Nature Medicine*, *14*(3), 282–9.

Zheng, Y., Lilo, S., Brodsky, I. E., Zhang, Y., Medzhitov, R., Marcu, K. B., & Bliska, J. B. (2011). A *Yersinia* effector with enhanced inhibitory activity on the NF-κB pathway activates the NLRP3/ASC/caspase-1 inflammasome in macrophages. *PLoS Pathogens*, *7*(4), e1002026.

Zhou, D., & Yang, R. (2009). Molecular Darwinian evolution of virulence in *Yersinia pestis*. *Infection and Immunity*, *77*(6), 2242–2250.

Zhu, Y., Thangamani, S., Ho, B., Ding, J. L., Armstrong, P., Melchior, R., … Lambris, J. (2005). The ancient origin of the complement system. *The EMBO Journal*, *24*(2), 382–394.

Zink, D., Feeley, J., Wells, J., Vanderzant, C., Vickery, J., Roof, W., & O'Donovan, G. (1980). Plasmid-mediated tissue invasiveness in *Yersinia enterocolitica*. *Nature*, *283*(5743), 224–226.

Zwack, E. E., Snyder, A. G., Wynosky-Dolfi, M. A., Ruthel, G., Philip, N. H., Marketon, M. M., … Brodsky, I. E. (2015). Inflammasome activation in response to the *Yersinia* type III secretion system requires hyperinjection of translocon proteins YopB and YopD. *mBio*, *6*(1), e02095-14.

Supplementary information

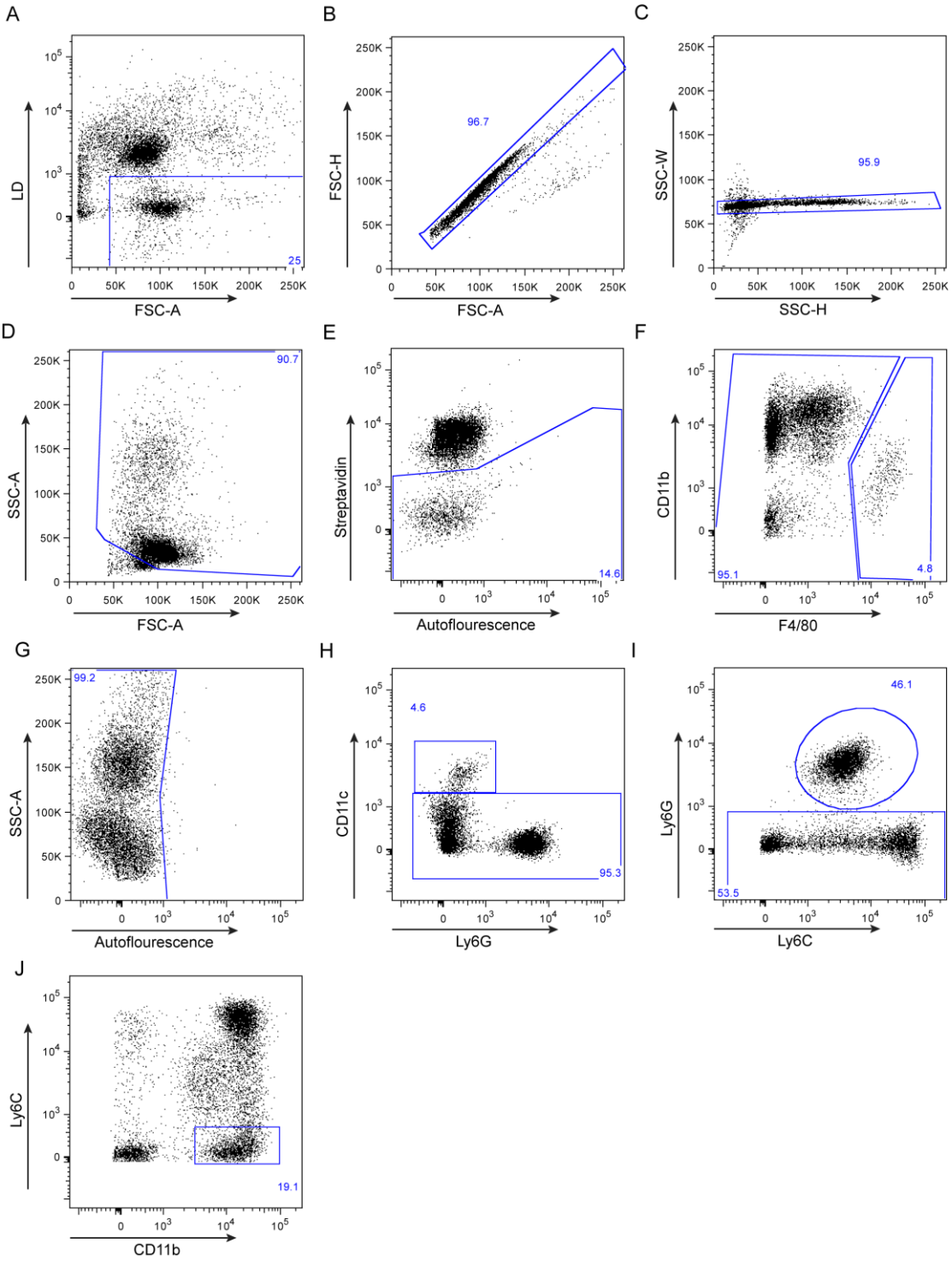

Figure S1 Gating strategy of the "innate" panel.

(A) Gating of living cells. (B-C) Gating of single cells. (D) Exclusion of small particles and cell debris. (E) Gating for "lineage negative" cells; exclusion of NK cells and lymphocytes. (F) Gating for macrophages ($F4/80^{hi}$). (G) Exclusion of autofluorescent cells. (H) Remaining cells were gated for dendritic cells ($CD11c^{+}$ $Ly6G^{-}$). (I) The remaining cells were gated for $Ly6G^{+}$PMNs. (J) The rest of the cells was gated for $CD11b^{+}$ $Ly6C^{-}$ cells, denoted as monocytes.

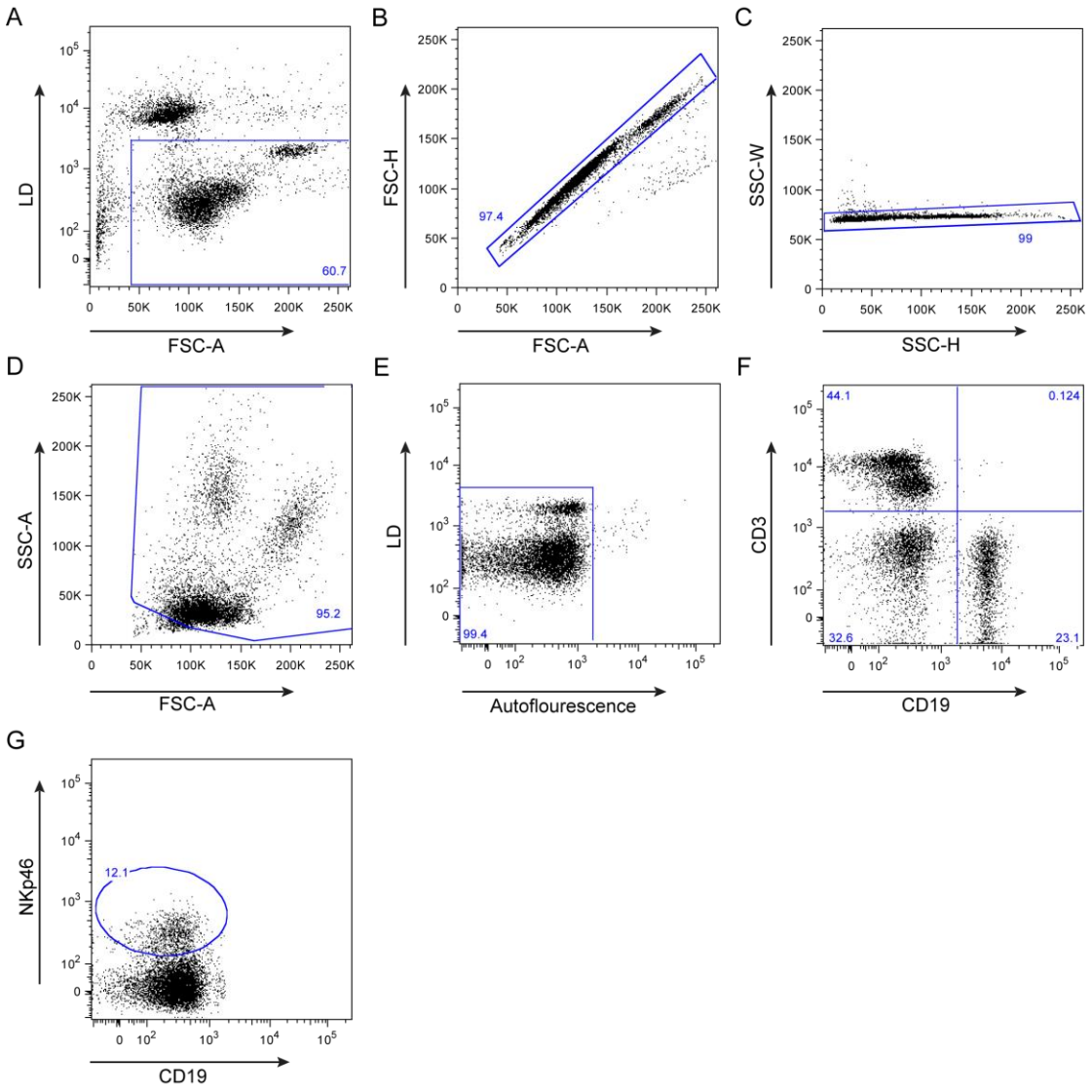

Figure S2 Gating strategy for the "adaptive" panel.

(A) Gating of living cells. (B-C) Gating of single cells. (D) Exclusion of small particles and cell debris. (E) Exclusion of autofluorescent cells. (F) Gating for $CD3^-$ $CD19^+$ B cells and $CD3^+$ $CD19^-$ T cells. (G) $CD3^-$ $CD19^-$ cells were gated for $NKp46^+$ NK cells.

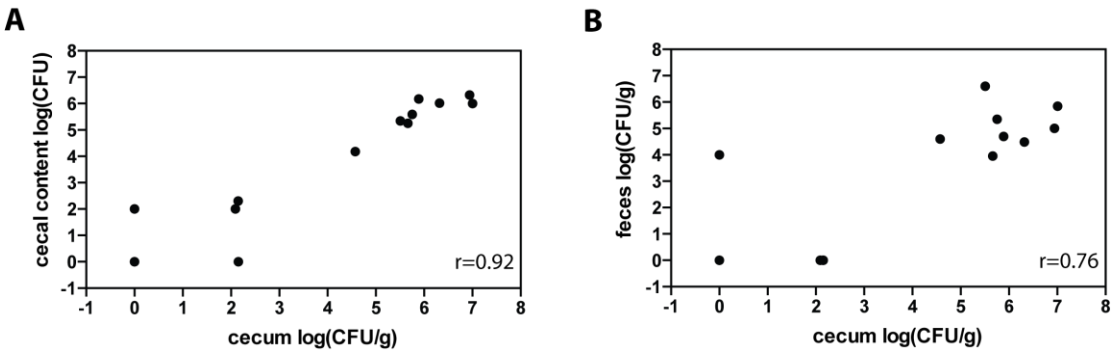

Figure S3 Correlation of *Yersinia* loads in the cecum to luminal contents and feces.

BALB/c mice were intra-gastrically infected with 1x10^6 CFU of *Y. pseudotuberculosis* YPIII Δ*cnfY*. At 40 dpi, egesta were assayed for *Yersinia* loads and bacterial burdens in the cecum or its luminal content at 42 days of infection. *Yersinia* burdens in the cecum of individual mice were plotted against the associated burdens in (A) the luminal content of the cecum and (B) the feces. Linear relationships were analyzed using Spearman's correlation. The r-value specifies the correlation coefficient.

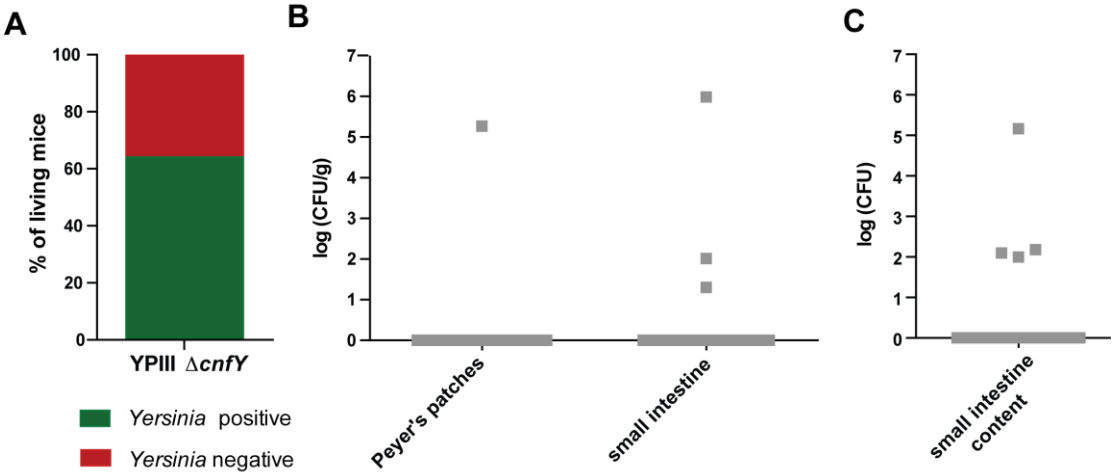

Figure S4 Deletion of *cnfY* does not lead to increased persistent colonization of the small intestine.

BALB/c mice were intra-gastrically infected with 1x10^6 CFU of *Y. pseudotuberculosis* YPIII Δ*cnfY*. The presented data were combined from two independent experiments: n=25. (A) *Yersinia* colonization in the feces at 40 dpi of mice analyzed for persisting *Yersinia* infection in the small intestine. (B) *Yersinia* loads in the PPs and the small intestine. Detection limits were: PPs ca. 227 CFU/g, small intestine ca. 25 CFU/g. (C) *Yersinia* burden in the luminal content of the small intestine (detection limit: 50 CFU).

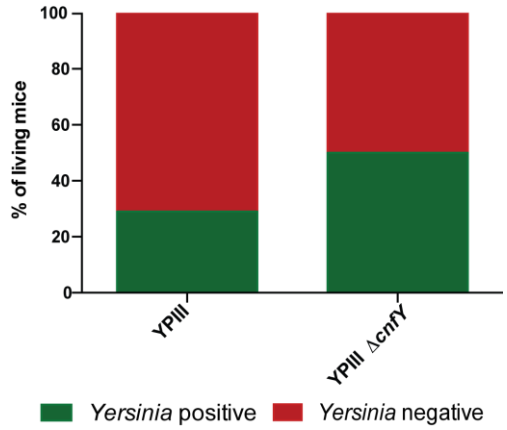

Figure S5 Increased persistency rates due to *cnfY* absence are transferable to FVB/N mouse model.

FVB/N mice were intra-gastrically infected with $1x10^6$ CFU of *Y. pseudotuberculosis* YPIII or YPIII Δ*cnfY*. At 42 dpi, *Yersinia* colonization rates were determined by bacterial burden assessment in the cecum. Colonization rates of the cecum were calculated using data from YPIII: n=7 and YPIII Δ*cnfY*: n=10 infected mice.

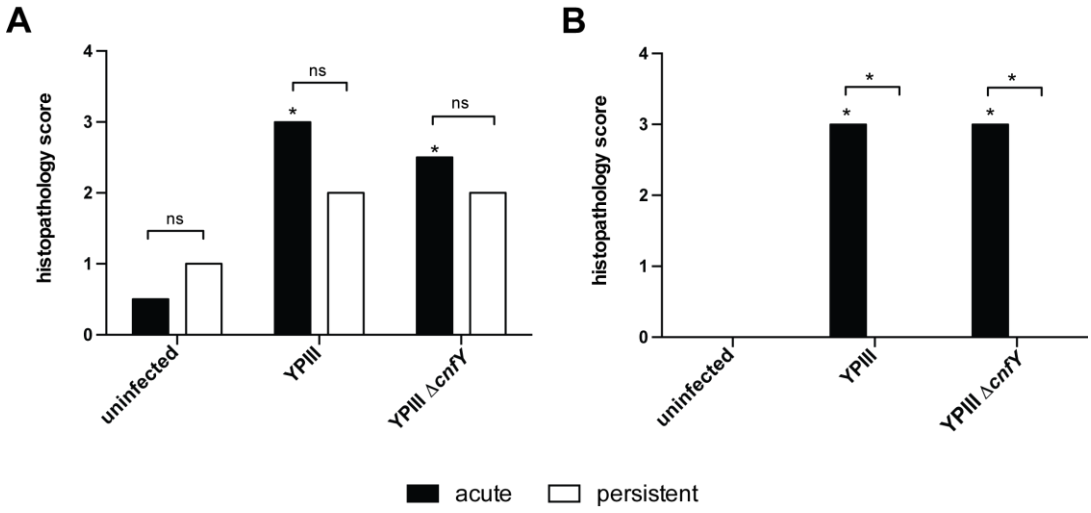

Figure S6 The grade of inflammation in the cecum is independent of *cnfY* and differs between the infection phases.

BALB/c mice were intra-gastrically infected with either $2x10^8$ CFU (acute infection) or $1x10^6$ CFU (persistent infection) of *Y. pseudotuberculosis* YPIII or YPIII Δ*cnfY*, respectively. After 3 dpi (acute infection) or 42 dpi (persistent infection) the inflammation grades were scored on the basis of H&E stained sections of the cecum. The data show the median scores of groups of 4 to 5 mice and was statistically analyzed with multiple t-tests employing Holm-Šídák's correction: * $p<0.01$, ns: not significant. (A) Histopathology score of the lamina propria. (B) Histopathology score of the cecal lymphoid tissue.

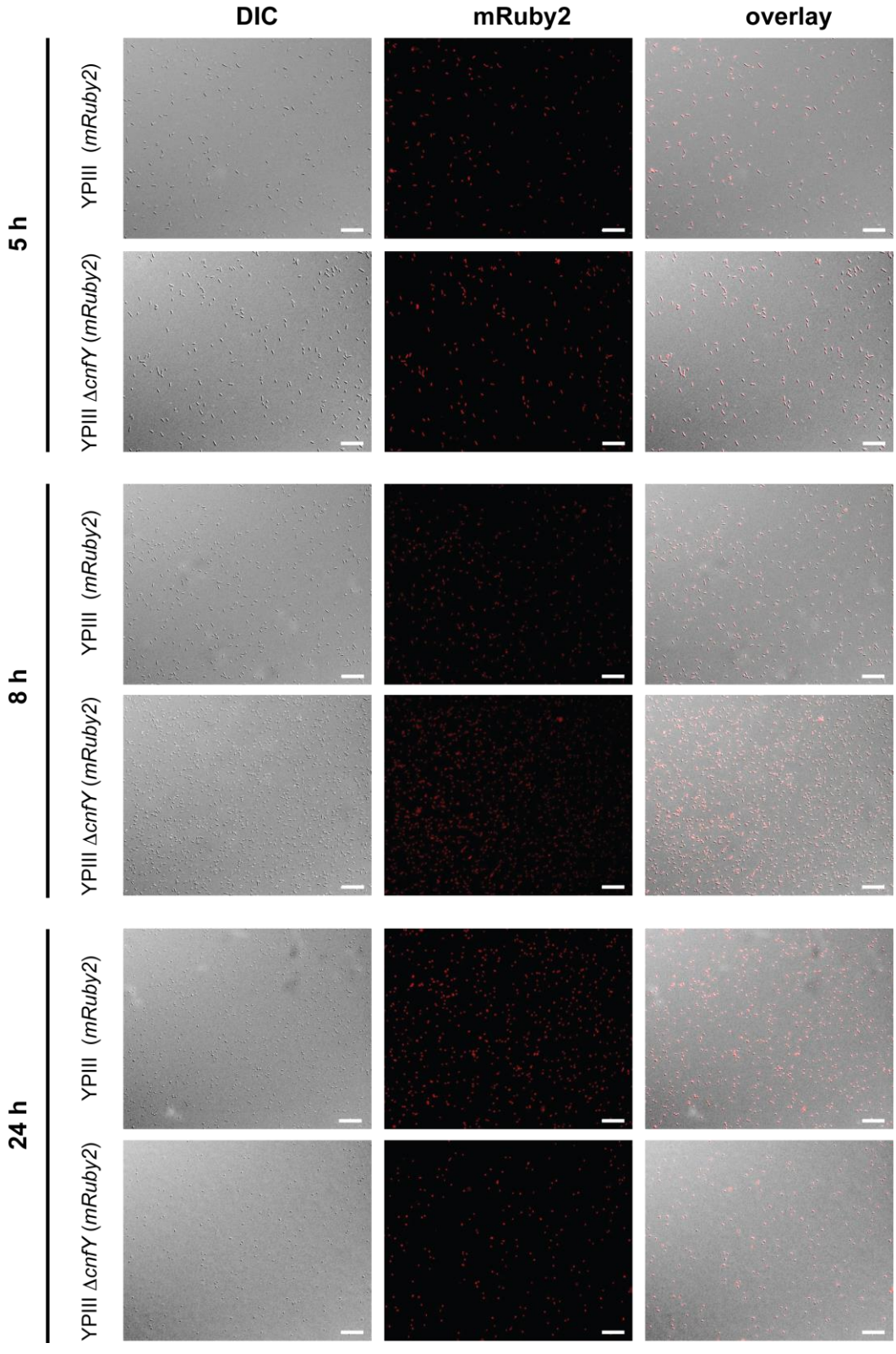

Figure S7 Expression of chromosomally integrated $P_{LtetO-1}$*::mRuby2* is detectable during different growth phases at 25 °C.

Stable mRuby2 labeled *Y. pseudotuberculosis* YPIII or YPIII Δ*cnfY* were grown to exponential (5 h, upper panel), early stationary (8 h, middle panel) or late stationary growth phase (24 h, lower panel) at 25 °C. Fixated bacteria were analyzed with the fluorescence microscope using the DIC and the mRuby2 channel. The microscopic pictures are representatives of 9 microscopic fields and were adjusted in brightness and exposure (mRuby2 channel) or in contrast (DIC channel). The bar indicates 20 µm.

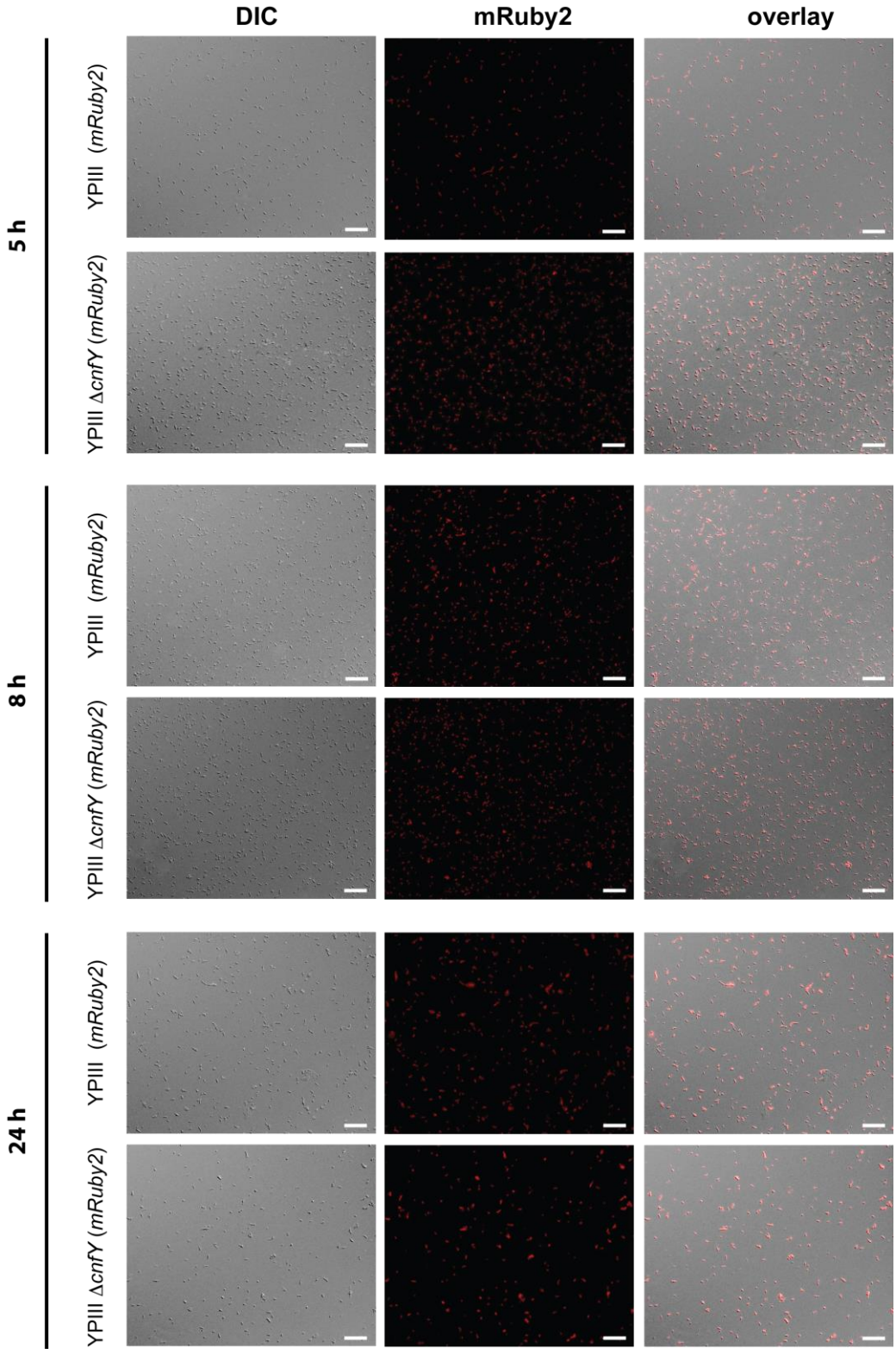

Figure S8 Expression of chromosomally integrated $P_{LtetO-1}$*::mRuby2* is detectable during different growth phases at 37 °C.

Stable mRuby2 labeled *Y. pseudotuberculosis* YPIII or YPIII Δ*cnfY* were grown to exponential (5 h, upper panel), early stationary (8 h, middle panel) or late stationary growth phase (24 h, lower panel) at 37 °C. The fixated bacteria were analyzed with the fluorescence microscope using the differential interference contrast (DIC) and the mRuby2 channel. The microscopic pictures are representatives of 9 microscopic fields and were adjusted in brightness and exposure (mRuby2 channel) or in contrast (DIC channel). The bar indicates 20 µm.

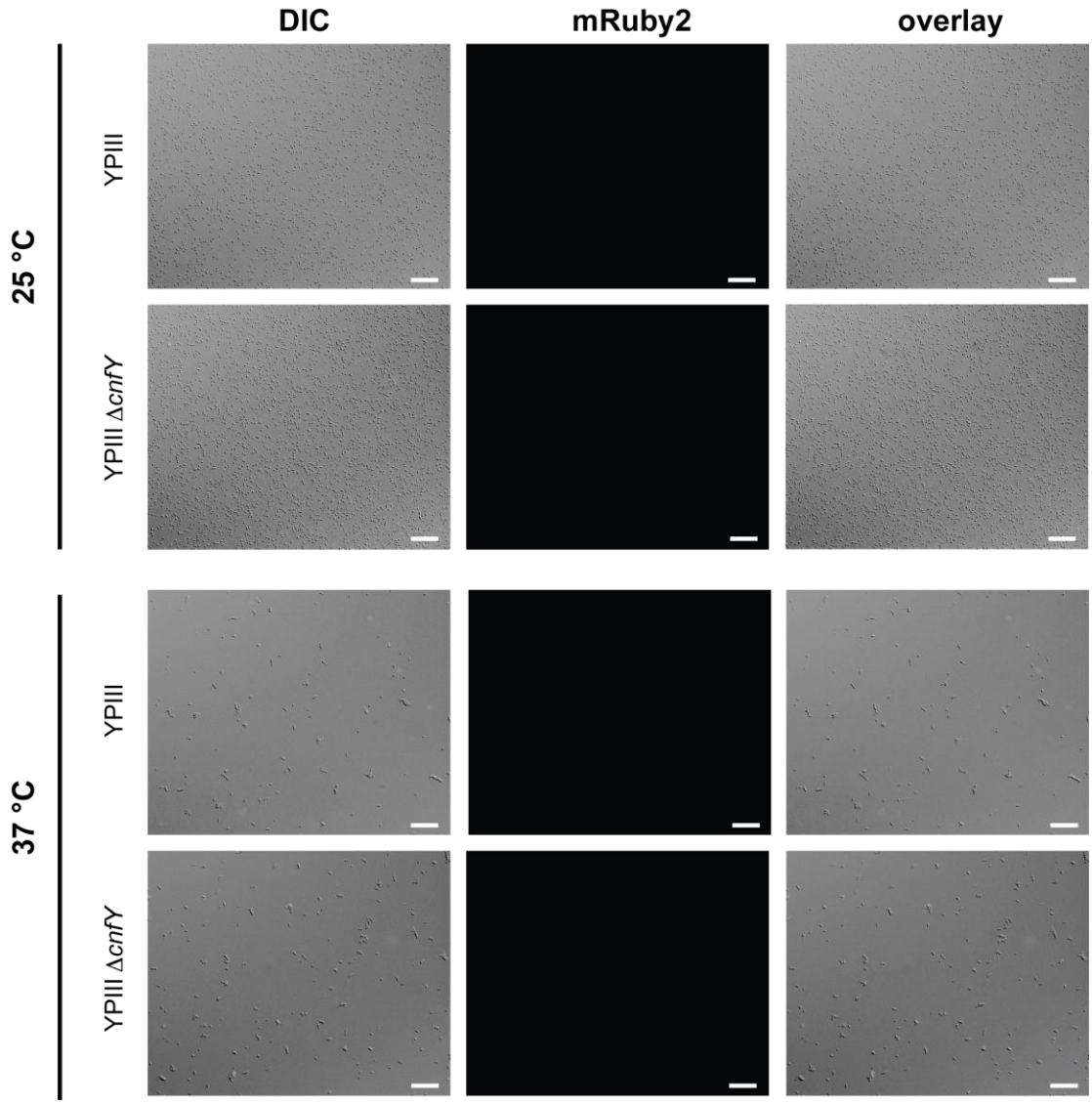

Figure S9 Red fluorescence is specific for mRuby2 labeled *Y. pseudotuberculosis* strains.

The unlabeled *Y. pseudotuberculosis* strains, YPIII and YPIII Δ*cnfY*, were grown to late stationary growth phase (24 h) at 25 °C or 37 °C, respectively. Fixated bacteria were analyzed with the fluorescence microscope using the DIC and the mRuby2 channel. The microscopic pictures are representatives of 9 microscopic fields and were adjusted in brightness and exposure (mRuby2 channel) or in contrast (DIC channel). The bar indicates 20 µm.

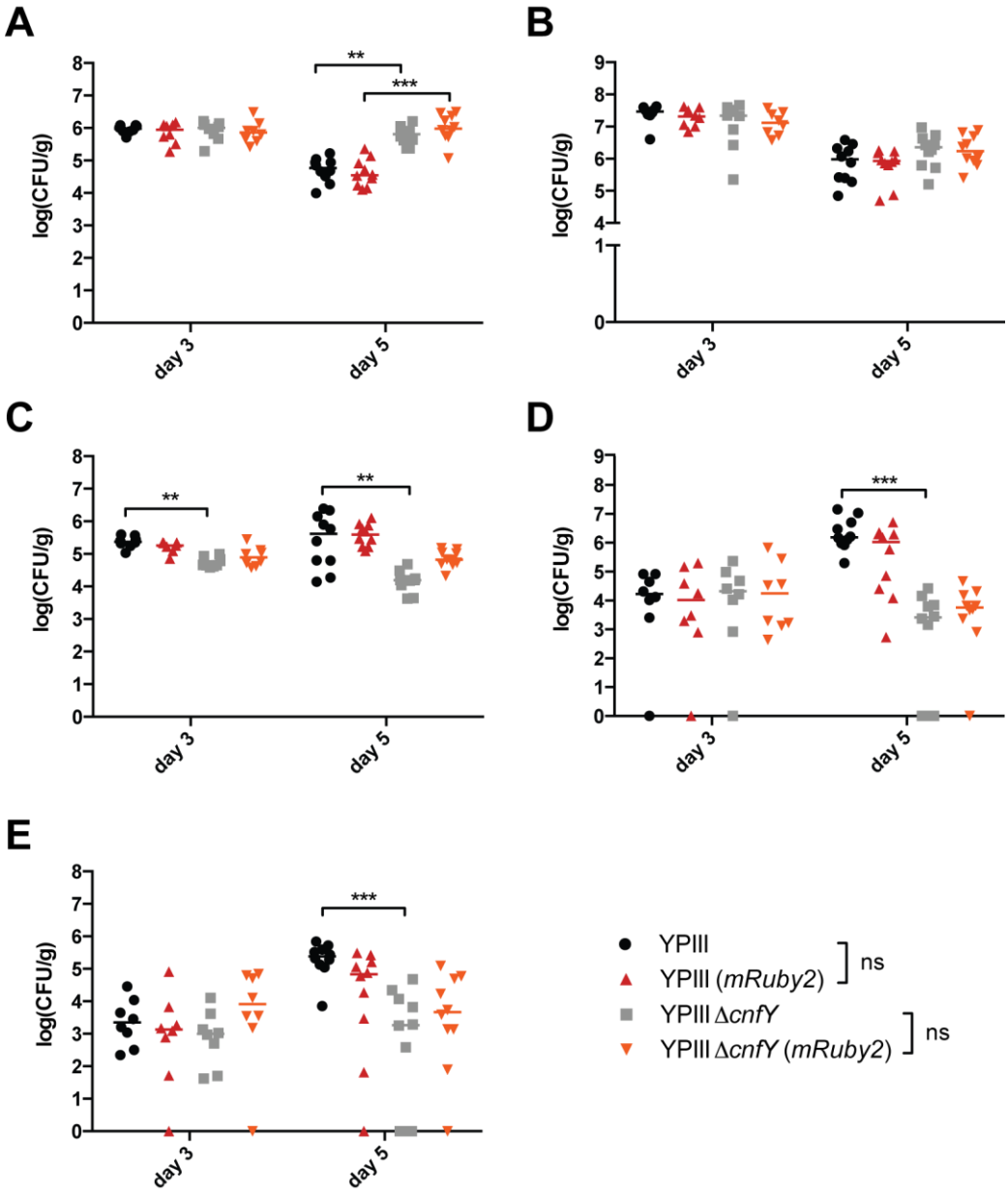

Figure S10 The integration of $P_{LtetO-1}$*::mRuby2* into the *Y. pseudotuberculosis* chromosome does not influence organ colonization traits.

Groups of eight to ten BALB/c mice were intra-gastrically infected with $2x10^8$ CFU of *Y. pseudotuberculosis* YPIII, YPIII Δ*cnfY* or the isogenic mRuby2 labeled strains. At the indicated time points (A) small intestine, (B) PPs, (C) mesenteric lymph nodes, (D) spleen and (E) liver were isolated and bacterial loads were determined. Detection limits were at ca. 330 CFU/g in the spleen and ca. 50 CFU/g in the liver. The data were combined from two independent experiments. Statistical analysis was performed using the Kruskal-Wallis test and Dunn's correction: ns: not significant; ** $p<0.01$, *** $p<0.001$.

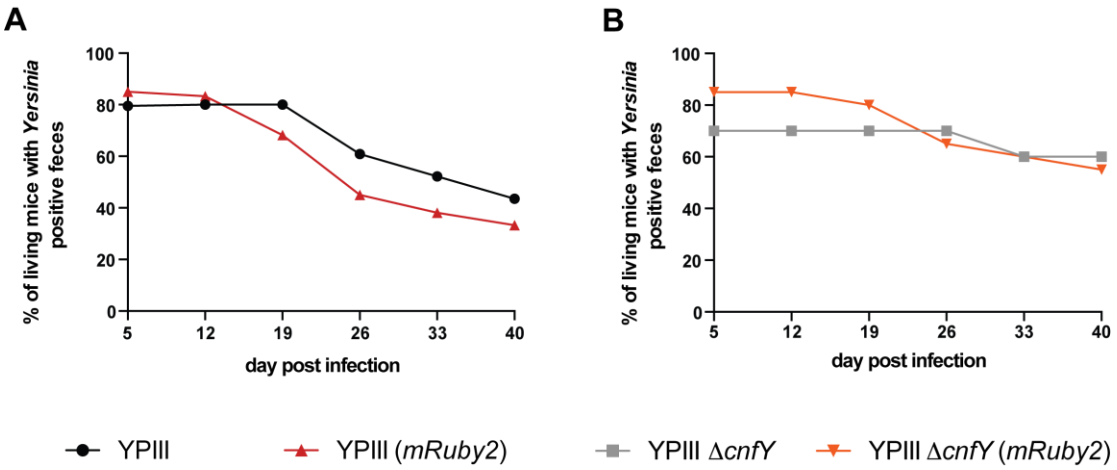

Figure S11 Chromosomal integration of $P_{LtetO-1}$*::mRuby2* does not affect *Y. pseudotuberculosis* persistence rates in the feces.

Mice were intra-gastrically challenged with $1x10^6$ CFU of *Y. pseudotuberculosis* YPIII, YPIII Δ*cnfY* or their respective mRuby2 labeled strains. The rate of mice positively tested for *Yersinia* colonization was determined after cold enrichment of the egesta at the indicated time points. The frequencies were calculated using data of (A) YPIII n=40 mice, YPIII (*mRuby2*) n=40 mice, and (B) YPIII Δ*cnfY* n=10 mice, YPIII Δ*cnfY* (*mRuby2*) n=20 mice.

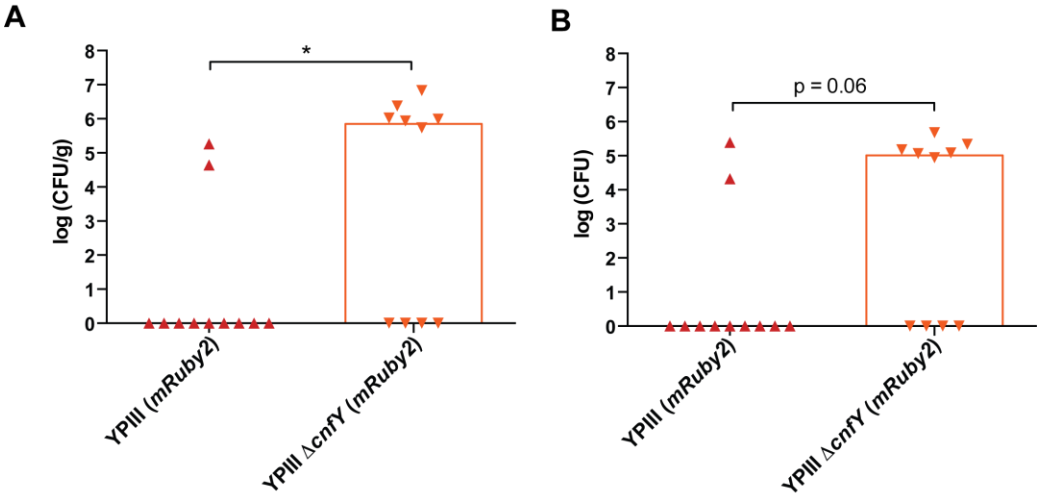

Figure S12 The integration of $P_{LtetO-1}$*::mRuby2* into the *Yersinia* chromosome does not impact the colonization characteristics in the cecum during persistency.

BALB/c mice were intra-gastrically infected with $1x10^6$ CFU of *Y. pseudotuberculosis* YPIII (*mRuby2*) or YPIII Δ*cnfY* (*mRuby2*). (A-B) At 42 dpi, bacterial colonization rates and burden in the cecal compartment were assessed: YPIII (*mRuby2*) n= 11, YPIII Δ*cnfY* (*mRuby2*) n=10. The bar represents the median. The data were statistically analyzed with the Mann-Whitney U test: * $p<0.05$. (A) *Yersinia* loads in the cecum. The detection limit was at ca. 125 CFU/g. (B) *Yersinia* burden in the luminal content of the cecum. The detection limit was at 50 CFU.

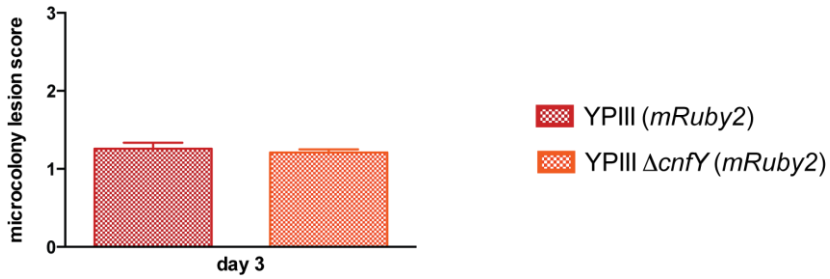

Figure S13 Microcolony caused lesion severity in the cecal lymphoid tissue is independent of *cnfY*.
BALB/c mice were intra-gastrically infected with $2x10^8$ CFU of *Y. pseudotuberculosis* YPIII (*mRuby2*) or YPIII Δ*cnfY* (*mRuby2*). At 3 dpi (acute), sections of highly colonized ceca were prepared, fixated, stained and scored. The sections were scored for bacterial microcolony caused lesions in the cecal lymphoid tissue by the analyses of multiple sections of multiple fields (n): YPIII n=85, YPIII Δ*cnfY* n=165. The data show the mean scores ±SEM combined from 3 mice per group. Statistical analyses were performed using the student's t-test; ns, not significant.

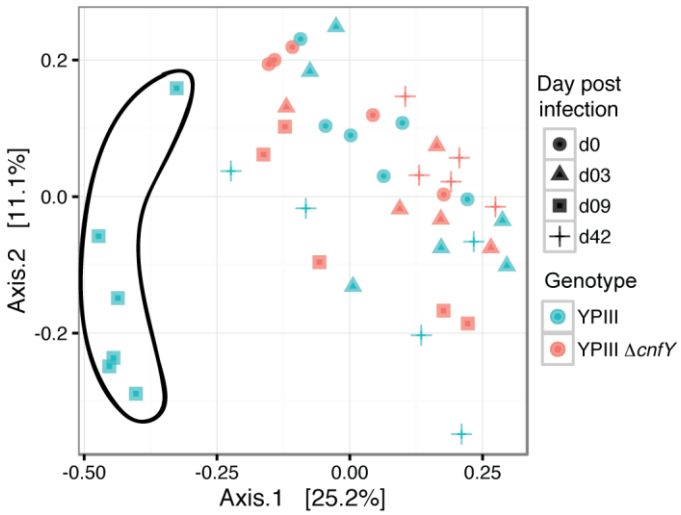

Figure S14 Principal coordinates analysis of the 16S rDNA sequencing from egesta of *Y. pseudotuberculosis* infected mice.
Mice were intra-gastrically challenged with $1x10^6$ CFU of *Y. pseudotuberculosis* YPIII or YPIII Δ*cnfY*. At indicated time points post infection, fresh feces was sampled. Colonized samples were further analyzed for the relative abundance of commensal bacteria by 16S rDNA sequencing. The Plot shows the principal coordinates analysis of the sequenced samples.

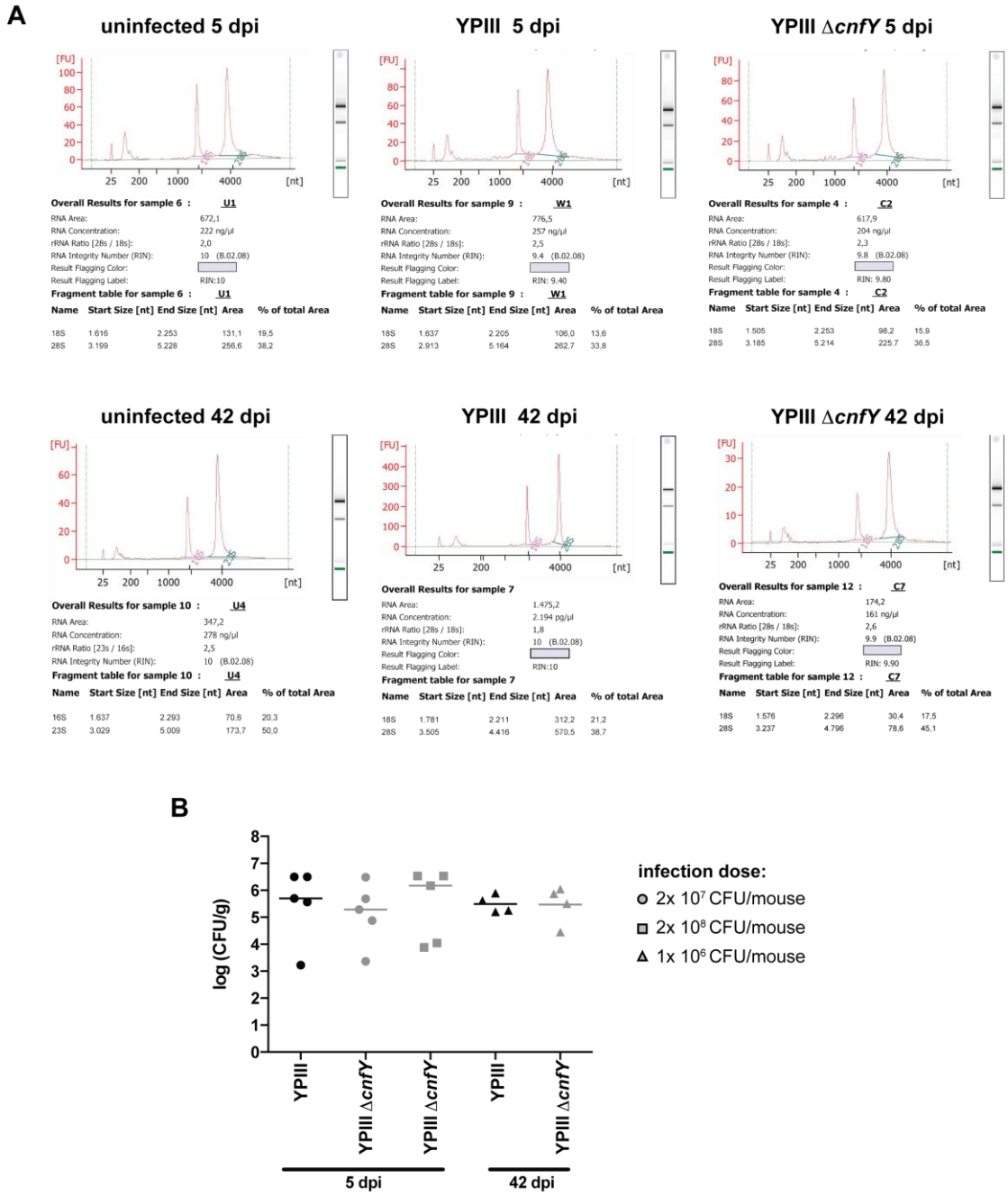

Figure S15 The *Yersinia* colonization levels in the cecum are independent of the infection dose and infection stage.

(A) RNA electropherograms of exemplary RNA pools from cecal tissue total RNA extracts. The RIN indicates the quality of the total RNA pools. (B) BALB/c mice were intra-gastrically challenged with the indicated infection doses of *Y. pseudotuberculosis* YPIII or YPIII Δ*cnfY*. At 5 dpi and 42 dpi highly colonized mice were sacrificed and the cecum was assayed for the *Yersinia* burdens. The individual data points represent single mice and the line the median. Statistical analysis was performed with One-way ANOVA employing Holm-Šídák's correction. No significant differences were found.

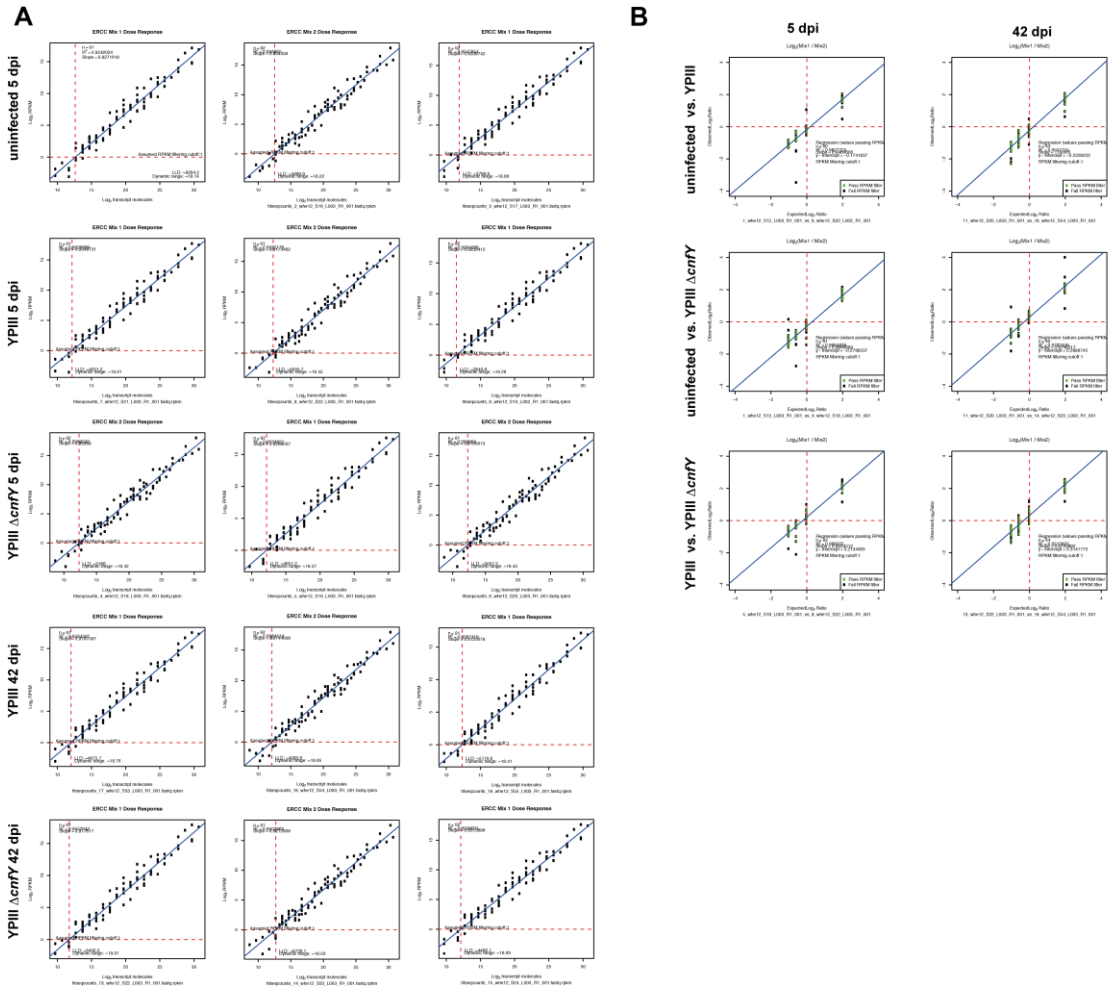

Figure S16 Sequencing platform performance.

Exemplary ERCC RNA Spike-In Control mixes analysis to determine the platform performance. (A) Dose response to determine the lower detection limit (LLD) and dynamic range. (B) Fold-change response to determine platform accuracy.

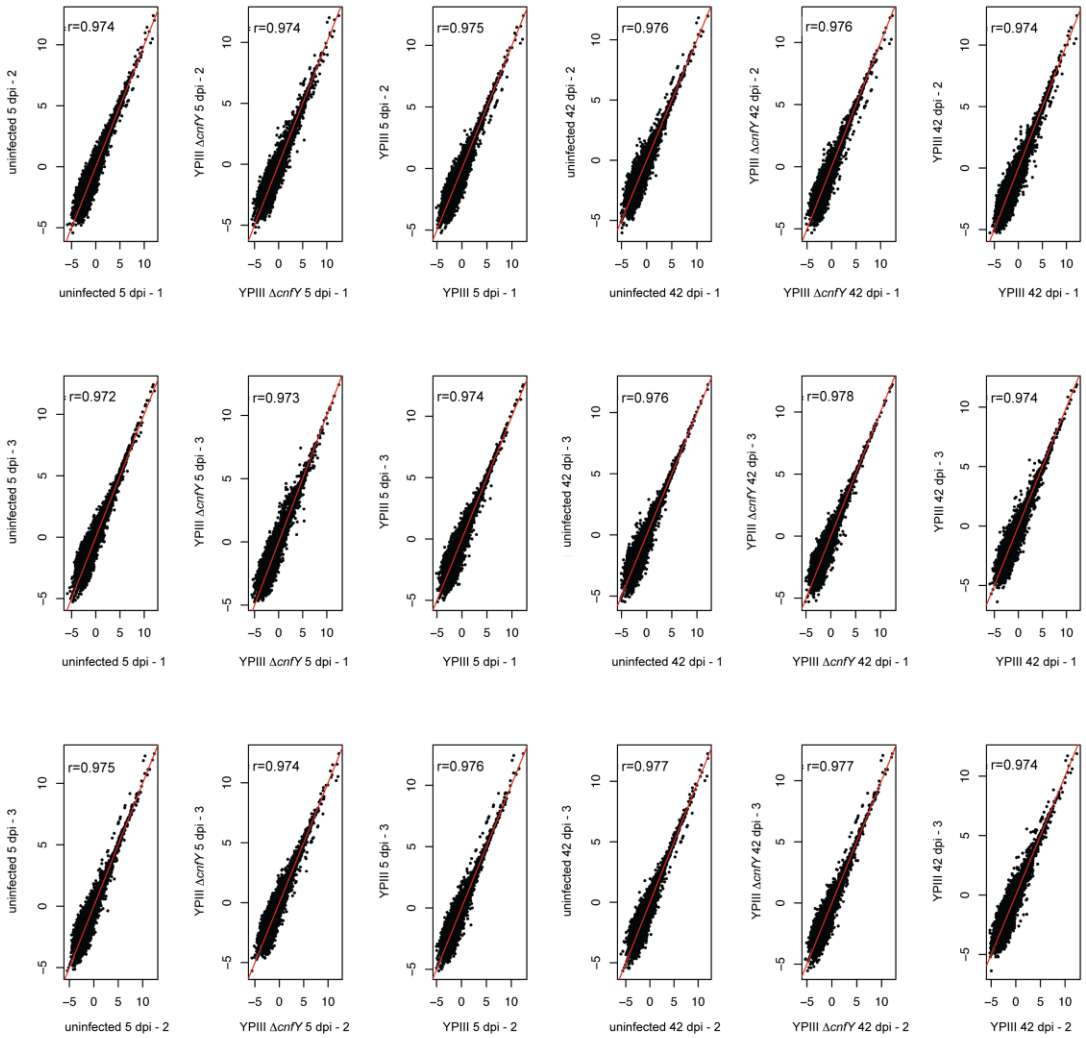

Figure S17 Replicate correlation of RNA-Sequencing data.

RPKM normalized read counts for all detected genes are plotted for 3 biological replicates. The Pearson-coefficient (r) is given for each replicate.

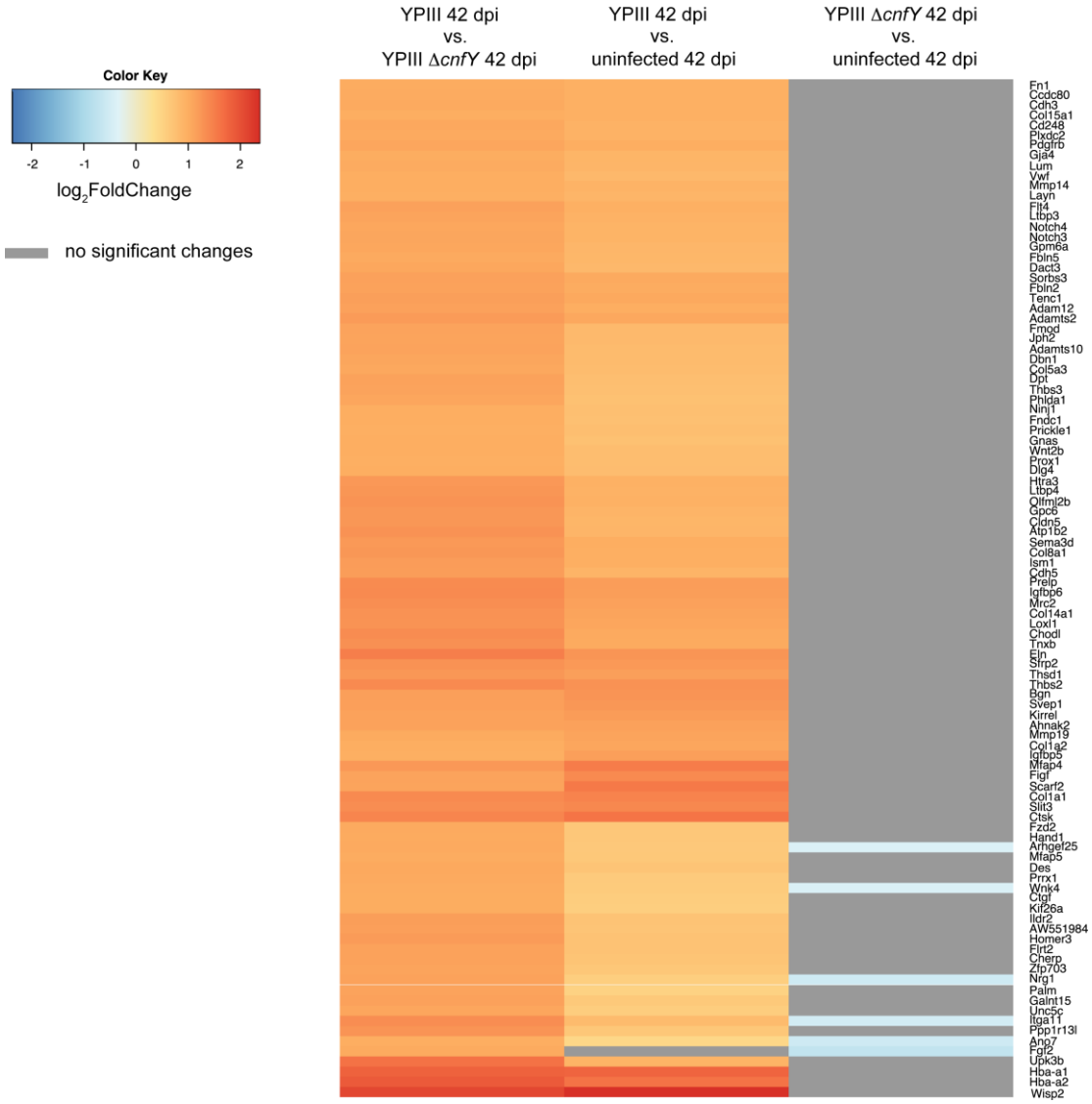

Figure S18 Tissue repair genes are transcribed during persistent *Y. pseudotuberculosis* YPIII infection.

Heat map of a selection of more abundant transcripts associated with tissue repair ($(-1 < \log_2 FC > 1; p<0.05)$ at 42 dpi comparing YPIII to YPIII Δ*cnfY* infection (left column). The respective $\log_2$ FC of each gene compared to uninfected mice are displayed: YPIII infected mice 5 dpi compared to uninfected (middle column) and YPIII Δ*cnfY* infected mice 5 dpi compared to uninfected (right column). Grey fields indicate no significant changes ($p \geq 0.05$) compared to uninfected mice.

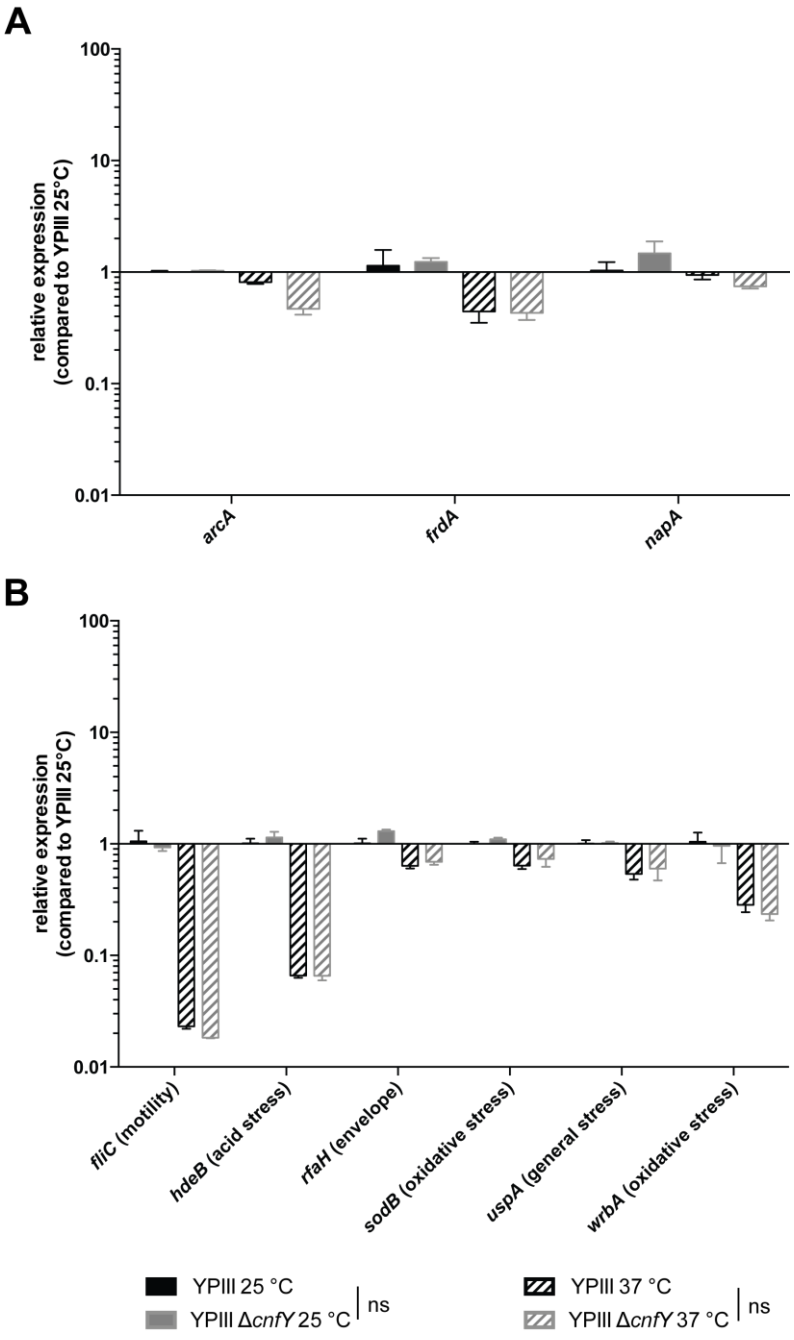

Figure S19 *In vitro* characterization of anaerobiosis and stress gene expression in *Y. pseudotuberculosis* YPIII and YPIII Δ*cnfY*.

Bacterial liquid cultures were grown to stationary phase (16 h) at 25 °C and 37 °C, respectively. Total RNA extracts were analyzed for the indicated relative transcript expression using qRT-PCR. The relative expression levels were normalized to *sopB* and *if-3* expression levels and calculated relative to YPIII at 25 °C. (A) Anaerobiosis genes. (B) Stress genes reacting to environmental cues. The data show the mean ±SEM and was statistically analyzed with multiple t-tests employing Holm-Šídák's correction: no significant differences between YPIII and YPIII Δ*cnfY* were found. ns: not significant.

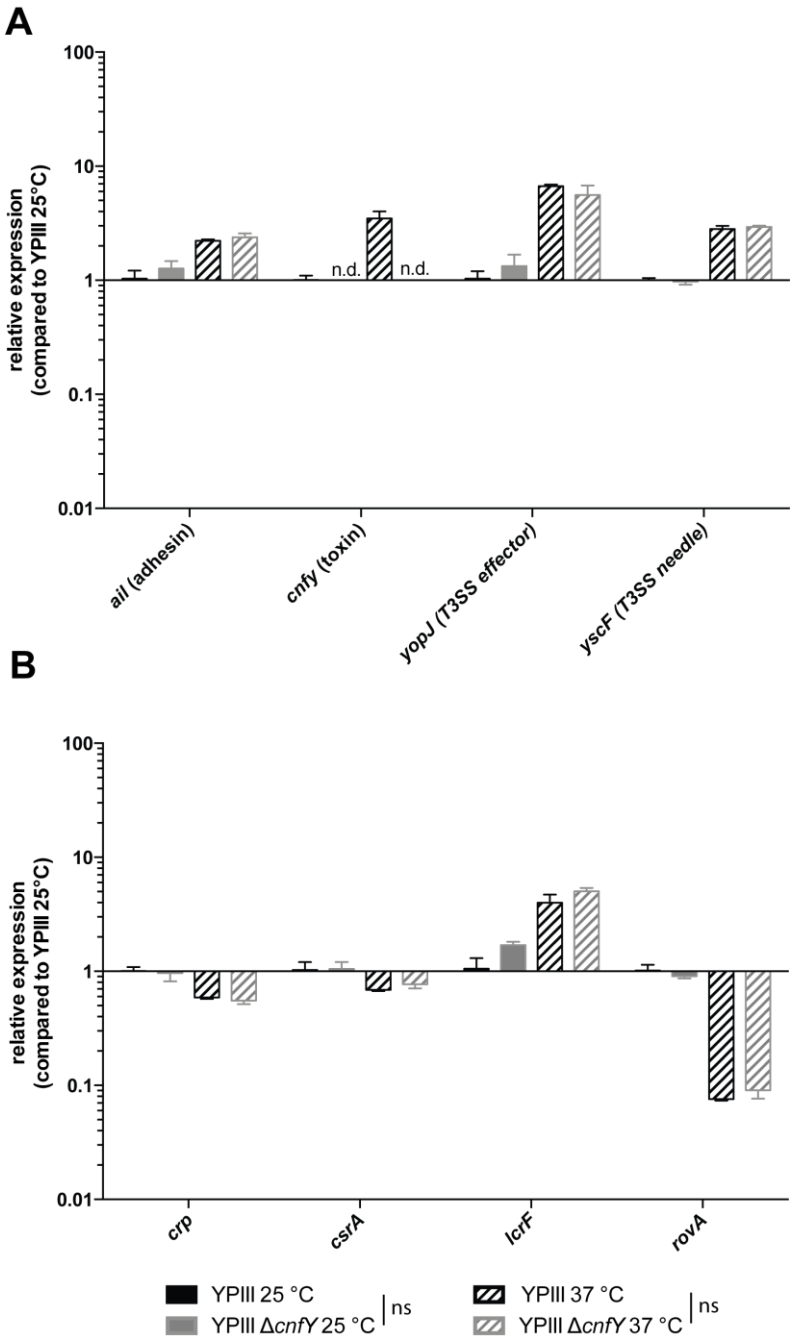

Figure S20 *In vitro* characterization of virulence and regulator gene expression in *Y. pseudotuberculosis* YPIII and YPIII Δ*cnfY*.

Bacterial liquid cultures were grown to stationary phase (16 h) at 25 °C and 37 °C, respectively. Total RNA extracts were analyzed for the indicated relative transcript expression using qRT-PCR. The relative expression levels were normalized to *sopB* and *if-3* expression levels and calculated relative to YPIII at 25 °C. (A) Virulence genes. (B) Metabolic and virulence regulator genes. The data show the mean ±SEM and was statistically analyzed with multiple t-tests employing Holm-Šídák's correction: no significant differences between YPIII and YPIII Δ*cnfY* were found. ns: not significant.

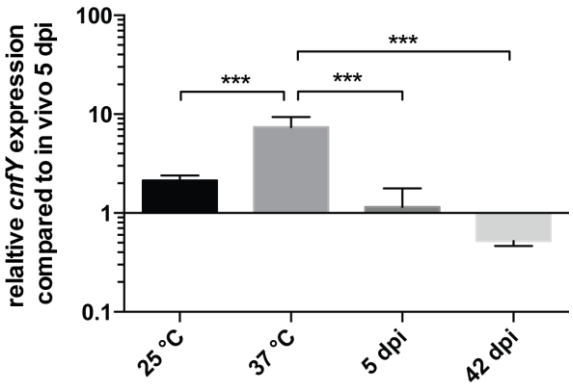

Figure S21 *cnfY* expression is down-regulated during acute and persistent *Y. pseudotuberculosis* YPIII infection compared to *in vitro* cultures.

The *cnfY* expression levels of *Y. pseudotuberculosis* YPIII liquid cultures from stationary phase (16 h) at 25 °C and 37 °C were compared to the total RNA extracts from YPIII infected ceca at 5 and 42 dpi employing qRT-PCR. The relative expression levels were normalized to *sopB* and *if-3* expression levels and calculated relative to YPIII infection in the cecum 5 dpi. The data show the mean ±SEM and was statistically analyzed with one-way ANOVA using Holm-Šídák's correction: *** $p<0.001$.

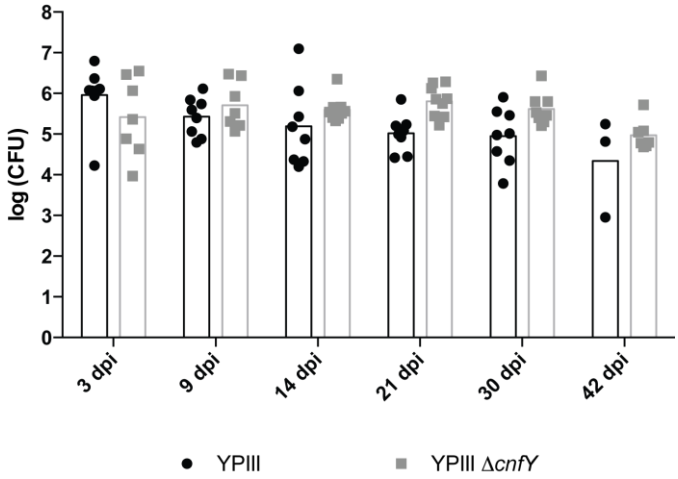

Figure S22 *Yersinia* colonization levels in the cecal content of mice analyzed for the cytokine profiles in serum and cecum.

BALB/c mice were intra-gastrically challenged with $1x10^6$ CFU of *Y. pseudotuberculosis* YPIII or YPIII Δ*cnfY*. At indicated time points post infection ceca were excised and the cecal content was screened for *Yersinia* colonization levels. The presented data show the bacterial loads in the cecal content of the most highly colonized mice. The cytokine levels in the serum and the cecum of these mice were further characterized. The bars indicate the median CFU in the cecal content. The detection limit was at 25 CFU. The data were analyzed with multiple t-tests employing Holm-Šídák's correction: no significant differences were found between YPIII and YPIII Δ*cnfY*.

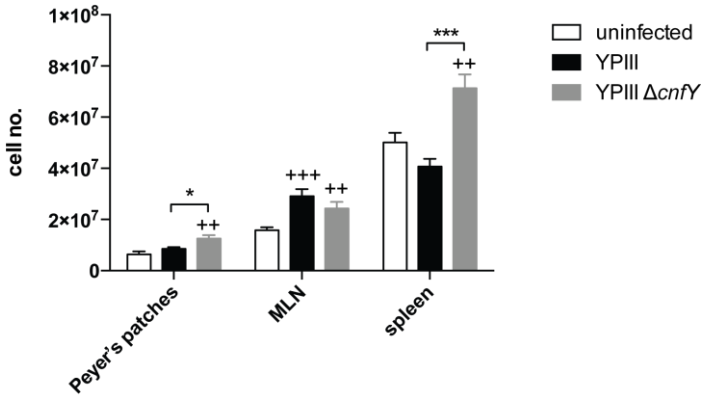

Figure S23 Total cell numbers isolated from PPs, mesenteric lymph nodes and spleen at 3 dpi.

C57BL/6N mice were intra-gastrically infected with $2x10^8$ CFU of *Y. pseudotuberculosis* YPIII or YPIII Δ*cnfY*. At 3 dpi, PP, MLNs and spleen were isolated, single cell suspensions were generated, and counted. The bar chart shows the absolute cell numbers obtained from the different organs. The bar represents the mean ±SEM. The data were combined from two independent experiments: YPIII n=10, YPIII Δ*cnfY* n=10. Statistical analysis was performed with multiple t-tests employing Holm-Šídák's correction: +, comparison of infected to uninfected group; ++, $p<0.01$; +++, $p<0.001$. *, comparison of the YPIII to the YPIII Δ*cnfY* infected group; *, $p<0.05$; ***, $p<0.001$.

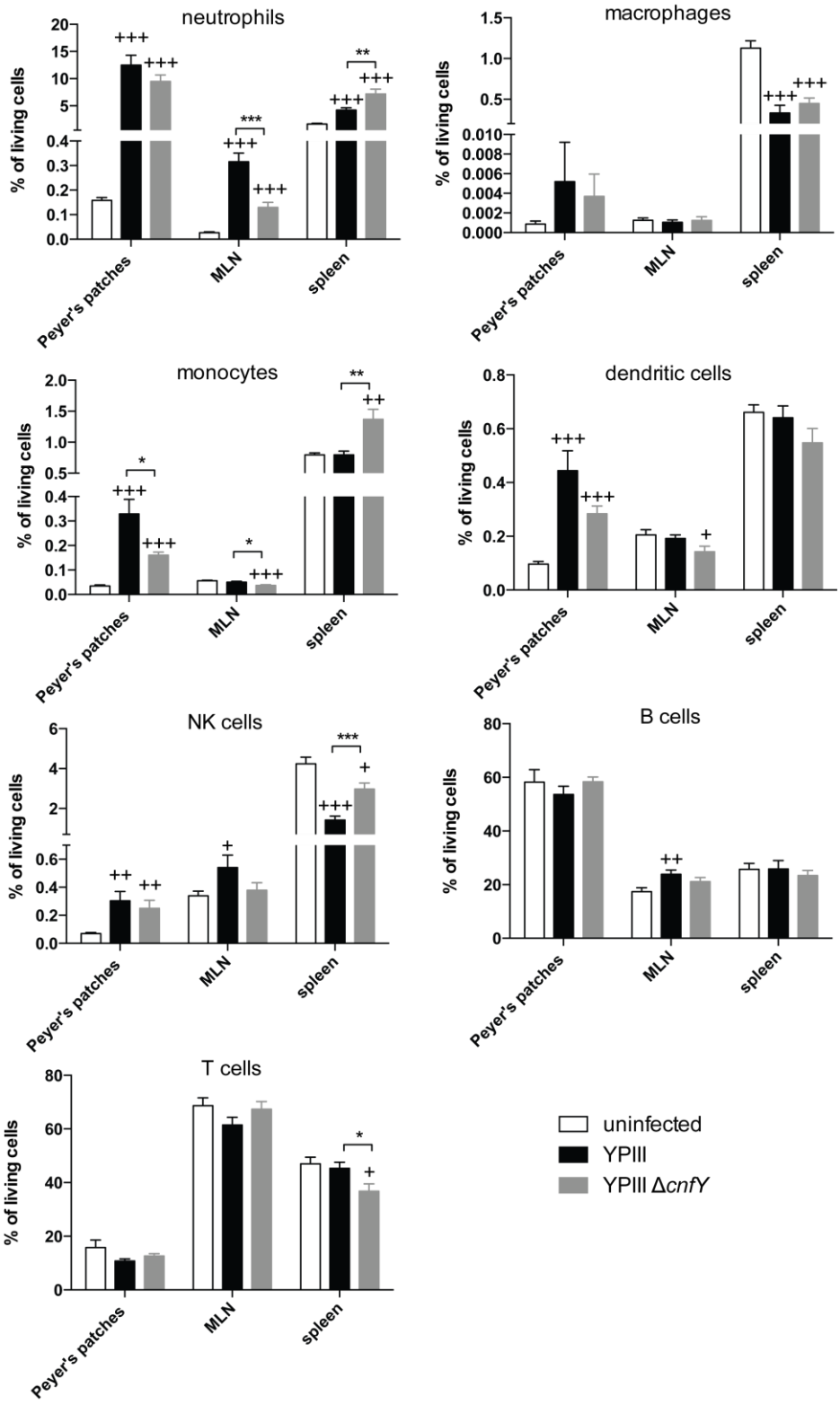

Figure S24 CNF_Y of *Y. pseudotuberculosis* modulates relative immune cell composition

C57BL/6N mice were intra-gastrically challenged with $2x10^8$ CFU of *Y. pseudotuberculosis* YPIII or YPIII Δ*cnfY*. At 3 dpi, PPs, MLNs and spleen were analyzed for their relative immune cell composition of neutrophils, macrophages, monocytes, DCs, NK cells, B cells, and T cells. The data were combined from two independent experiments, YPIII n=10; YPIII Δ*cnfY* n=10. Bars indicate mean ±SEM. Statistical analysis was performed with multiple t-tests employing Holm-Šídák's correction; + comparison between infected and uninfected mice, + $p<0.05$; ++, $p<0.01$; +++, $p<0.001$. * comparison between YPIII and YPIII Δ*cnfY* infected mice: * $p<0.05$, ** $p<0.01$, *** $p<0.001$.

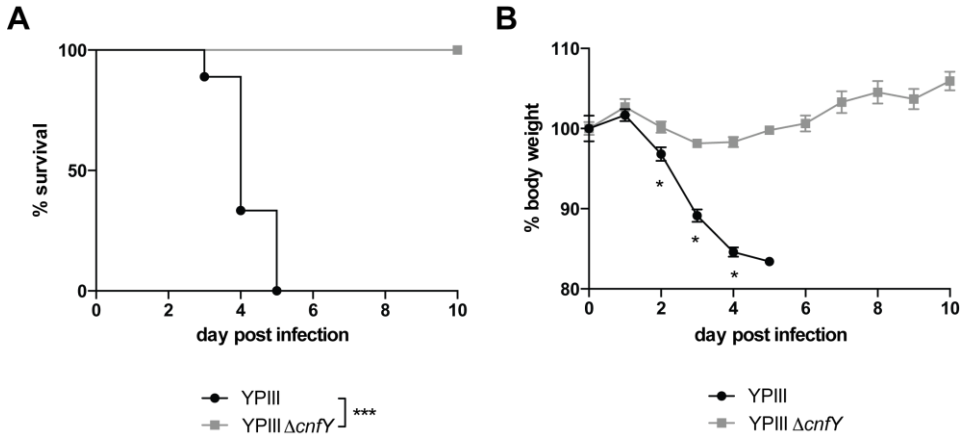

Figure S25 *Y. pseudotuberculosis* YPIII Δ*cnfY* is severely attenuated during intravenous challenge.
C57BL/6N mice were intravenously infected with 5000 CFU of *Y. pseudotuberculosis* YPIII or YPIII Δ*cnfY*. The health status of the mice was monitored over a period of 10 days. The data were combined from two independent experiments: YPIII n=9; YPIII Δ*cnfY* n=9. (A) Survival of C57BL/6N mice. Statistical analysis was performed with the log-rank test (Mantel-Cox): *** $p<0.001$. (B) Body weight loss curves. The data shows the mean ±SEM and statistical analysis was performed with multiple t-tests using Holm-Šídák's correction: * $p<0.05$.

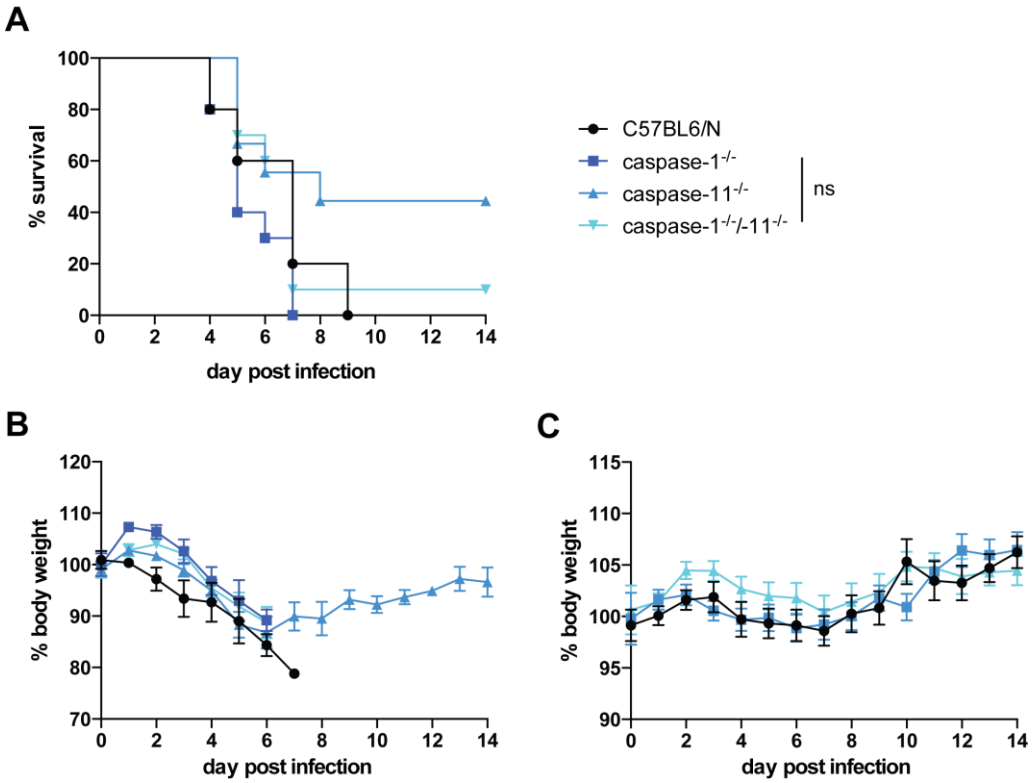

Figure S26 The inflammasome has no impact on C57BL/6N susceptibility.
C57BL/6N mice and the respective caspase-1/-11 mutants were challenged with $2x10^8$ CFU of *Y. pseudotuberculosis* YPIII (A & B) or YPIII Δ*cnfY* (C). The health status of the infected mice was monitored over a time period of 14 days. The data were combined from two independent experiments: C57BL/6N, YPIII/ YPIII Δ*cnfY* n=8; caspase-$1^{-/-}$, YPIII n=10; caspase-$11^{-/-}$, YPIII n=9, YPIII Δ*cnfY* n=8; caspase-$1^{-/-}$/-$11^{-/-}$, YPIII/ YPIII Δ*cnfY* n=10 (A) Survival of C57BL/6N mice in comparison to caspase-$1^{-/-}$, caspase-$11^{-/-}$ and caspase-$1^{-/-}$/-$11^{-/-}$ mice after YPIII challenge. Statistical analysis was performed with the log-rank test (Mantel-Cox): no significant differences of the caspase knock out mice compared to wild type mice were observed. (B) Body weight loss curves upon YPIII infection. (C) Body weight loss curves upon YPIII Δ*cnfY* infection. (B & C) The data shows the mean ±SEM and was statistically analyzed with multiple t-tests employing Holm- Šídák's correction. No significant differences were observed. ns: not significant.

Table S1 Mapping statistics.

Sample	Replicate	Read length	Total reads	Total mapped including ERCC	Total mapped to genome	Total mapped to genes
Uninfected 5 dpi	1	51	22,047,027	20,430,012	14,669,574	11,138,040
Uninfected 5 dpi	2	51	21,873,833	20,052,447	14,223,693	10,367,252
Uninfected 5 dpi	3	51	22,107,361	20,344,484	12,210,972	8,657,003
YPIII 5 dpi	1	51	18,014,829	16,589,782	10,540,510	7,211,779
YPIII 5 dpi	2	51	23,817,131	21,771,321	15,347,411	10,181,473
YPIII 5 dpi	3	51	26,875,039	24,533,224	13,632,231	8,654,807
YPIII Δ*cnfY* 5 dpi	1	51	26,009,339	23,785,082	16,411,709	11,073,180
YPIII Δ*cnfY* 5 dpi	2	51	19,350,404	17,666,055	11,466,580	8,342,268
YPIII Δ*cnfY* 5 dpi	3	51	19,536,186	17,715,178	12,440,019	8,207,709
Uninfected 42 dpi	1	51	24,908,621	22,820,056	17,182,363	12,736,288
Uninfected 42 dpi	2	51	27,407,426	25,187,148	17,482,471	12,846,119
Uninfected 42 dpi	3	51	27,665624	25,073,102	18,191,840	12,969,359
YPIII 42 dpi	1	51	39,795,513	36,477,547	23,818,604	14,934,833
YPIII 42 dpi	2	51	38,071,123	35,199,382	24,552,069	16,591,558
YPIII 42 dpi	3	51	38,140,082	34,745,298	24,762,343	16,507,236
YPIII Δ*cnfY* 42 dpi	1	51	25,239,634	22,980,418	13,956,701	10,008,228
YPIII Δ*cnfY* 42 dpi	2	51	24,297,789	22,003,730	16,606,374	11,899,990
YPIII Δ*cnfY* 42 dpi	3	51	27,823,321	25,326,423	16,275,006	11,698,916

Table S2 Differentially expressed genes of BALB/c (YPIII infected 5 dpi vs. uninfected 5 dpi)

Ensembl ID	Gene Symbol	Gene name	log_2 fold change	p-value
ENSMUSG00000058427	Cxcl2	chemokine (C-X-C motif) ligand 2	4.37	9.51E-37
ENSMUSG00000031722	Hp	haptoglobin	3.97	4.15E-32
ENSMUSG00000027398	Il1b	interleukin 1 beta	3.68	1.85E-30
ENSMUSG00000040809	Chil3	chitinase-like 3	3.64	2.70E-22
ENSMUSG00000022126	Irg1	immunoresponsive gene 1	3.60	4.69E-31
ENSMUSG00000026822	Lcn2	lipocalin 2	3.60	4.56E-28
ENSMUSG00000005800	Mmp8	matrix metallopeptidase 8	3.51	6.58E-22
ENSMUSG00000024087	Cyp1b1	cytochrome P450, family 1, subfamily b, polypeptide 1	3.46	2.46E-27
ENSMUSG00000001131	Timp1	tissue inhibitor of metalloproteinase 1	3.44	1.09E-25
ENSMUSG00000028859	Csf3r	colony stimulating factor 3 receptor (granulocyte)	3.43	1.32E-31
ENSMUSG00000064246	Chil1	chitinase-like 1	3.36	1.13E-25
ENSMUSG00000006403	Adamts4	a disintegrin-like and metallopeptidase (reprolysin type) with thrombospondin type 1 motif, 4	3.24	4.71E-25
ENSMUSG00000021091	Serpina3n	serine (or cysteine) peptidase inhibitor, clade A, member 3N	3.14	2.27E-44
ENSMUSG00000029371	Cxcl5	chemokine (C-X-C motif) ligand 5	3.11	6.64E-16
ENSMUSG00000042265	Trem1	triggering receptor expressed on myeloid cells 1	3.11	2.69E-17
ENSMUSG00000043613	Mmp3	matrix metallopeptidase 3	3.07	1.21E-19
ENSMUSG00000029380	Cxcl1	chemokine (C-X-C motif) ligand 1	3.04	2.16E-18
ENSMUSG00000025746	Il6	interleukin 6	2.96	4.29E-16
ENSMUSG00000030144	Clec4d	C-type lectin domain family 4, member d	2.95	5.34E-16
ENSMUSG00000056071	S100a9	S100 calcium binding protein A9 (calgranulin B)	2.92	6.33E-14
ENSMUSG00000000204	Slfn4	schlafen 4	2.91	1.05E-28
ENSMUSG00000027832	Ptx3	pentraxin related gene	2.90	1.06E-14
ENSMUSG00000052270	Fpr2	formyl peptide receptor 2	2.89	2.24E-19
ENSMUSG00000019987	Arg1	arginase, liver	2.85	1.12E-18
ENSMUSG00000032691	Nlrp3	NLR family, pyrin domain containing 3	2.80	1.56E-19
ENSMUSG00000079012	Serpina3m	serine (or cysteine) peptidase inhibitor, clade A, member 3M	2.80	1.24E-18
ENSMUSG00000030142	Clec4e	C-type lectin domain family 4, member e	2.78	1.07E-13
ENSMUSG00000048636			2.78	8.16E-14
ENSMUSG00000024529	Lox	lysyl oxidase	2.70	1.92E-17
ENSMUSG00000044103	Il1f9	interleukin 1 family, member 9	2.69	1.11E-15
ENSMUSG00000089672	Gp49a	glycoprotein 49 A	2.67	4.34E-20
ENSMUSG00000027399	Il1a	interleukin 1 alpha	2.62	3.28E-16
ENSMUSG00000031444	F10	coagulation factor X	2.58	3.74E-14
ENSMUSG00000073530	Pappa2	pappalysin 2	2.56	7.54E-17
ENSMUSG00000022651	Retnlg	resistin like gamma	2.53	2.05E-15
ENSMUSG00000027656	Wisp2	WNT1 inducible signaling pathway protein 2	2.50	2.87E-11
ENSMUSG00000024697	Gna14	guanine nucleotide binding protein, alpha 14	2.46	1.11E-20
ENSMUSG00000026180	Cxcr2	chemokine (C-X-C motif) receptor 2	2.46	1.86E-16
ENSMUSG00000036040	Adamtsl2	ADAMTS-like 2	2.45	3.70E-19
ENSMUSG00000047798	Cd300lf	CD300 antigen like family member F	2.45	1.80E-15
ENSMUSG00000047562	Mmp10	matrix metallopeptidase 10	2.43	2.50E-10
ENSMUSG00000034855	Cxcl10	chemokine (C-X-C motif) ligand 10	2.41	1.32E-13
ENSMUSG00000052749	Trim30b	tripartite motif-containing 30B	2.39	1.44E-10
ENSMUSG00000029379	Cxcl3	chemokine (C-X-C motif) ligand 3	2.39	4.03E-10

ENSMUSG00000056054	S100a8	S100 calcium binding protein A8 (calgranulin A)	2.38	6.97E-10
ENSMUSG00000000182	Fgf23	fibroblast growth factor 23	2.36	5.62E-10
ENSMUSG00000030732	Chrdl2	chordin-like 2	2.36	6.70E-11
ENSMUSG00000026580	Selp	selectin, platelet	2.35	4.72E-16
ENSMUSG00000032068	Plet1	placenta expressed transcript 1	2.32	3.37E-14
ENSMUSG00000021950	Anxa8	annexin A8	2.32	3.54E-11
ENSMUSG00000027360	Hdc	histidine decarboxylase	2.30	3.58E-10
ENSMUSG00000044162	Tnip3	TNFAIP3 interacting protein 3	2.30	1.38E-19
ENSMUSG00000035385	Ccl2	chemokine (C-C motif) ligand 2	2.29	3.02E-11
ENSMUSG00000032796	Lama1	laminin, alpha 1	2.28	3.19E-18
ENSMUSG00000041449			2.28	2.64E-14
ENSMUSG00000000982	Ccl3	chemokine (C-C motif) ligand 3	2.26	2.21E-09
ENSMUSG00000022548	Apod	apolipoprotein D	2.25	1.79E-14
ENSMUSG00000022181	C6	complement component 6	2.24	2.40E-16
ENSMUSG00000028766	Alpl	alkaline phosphatase, liver/bone/kidney	2.24	1.20E-21
ENSMUSG00000030187	Klra2	killer cell lectin-like receptor, subfamily A, member 2	2.19	1.41E-12
ENSMUSG00000074934	Grem1	gremlin 1	2.18	7.63E-21
ENSMUSG00000000318	Clec10a	C-type lectin domain family 10, member A	2.17	1.65E-14
ENSMUSG00000059657	Stfa2l1	stefin A2 like 1	2.15	9.04E-09
ENSMUSG00000027068	Dhrs9	dehydrogenase/reductase (SDR family) member 9	2.14	2.12E-19
ENSMUSG00000062593	Lilrb4	leukocyte immunoglobulin-like receptor, subfamily B, member 4	2.12	2.83E-12
ENSMUSG00000081665			2.12	8.31E-10
ENSMUSG00000068196	Col8a1	collagen, type VIII, alpha 1	2.11	5.96E-17
ENSMUSG00000040026	Saa3	serum amyloid A 3	2.09	7.53E-11
ENSMUSG00000086320			2.09	6.06E-18
ENSMUSG00000032690	Oas2	2'-5' oligoadenylate synthetase 2	2.06	9.91E-12
ENSMUSG00000012428	Steap4	STEAP family member 4	2.04	3.90E-17
ENSMUSG00000089942	Pira2	paired-Ig-like receptor A2	2.03	4.03E-10
ENSMUSG00000053113	Socs3	suppressor of cytokine signaling 3	2.03	1.27E-10
ENSMUSG00000078763	Slfn1	schlafen 1	2.02	6.00E-13
ENSMUSG00000095788	Sirpb1a	signal-regulatory protein beta 1A	2.02	8.19E-08
ENSMUSG00000037095	Lrg1	leucine-rich alpha-2-glycoprotein 1	1.99	1.84E-10
ENSMUSG00000026073	Il1r2	interleukin 1 receptor, type II	1.98	3.10E-09
ENSMUSG00000060183	Cxcl11	chemokine (C-X-C motif) ligand 11	1.97	4.56E-08
ENSMUSG00000056749	Nfil3	nuclear factor, interleukin 3, regulated	1.95	7.88E-14
ENSMUSG00000025877	Hk3	hexokinase 3	1.95	2.88E-09
ENSMUSG00000040264	Gbp2b	guanylate binding protein 2b	1.94	3.61E-10
ENSMUSG00000052353	Cemip	cell migration inducing protein, hyaluronan binding	1.94	1.41E-07
ENSMUSG00000059089	Fcgr4	Fc receptor, IgG, low affinity IV	1.94	1.42E-12
ENSMUSG00000093916			1.93	3.84E-07
ENSMUSG00000016024	Lbp	lipopolysaccharide binding protein	1.93	3.48E-17
ENSMUSG00000067780	Pi15	peptidase inhibitor 15	1.93	1.46E-16
ENSMUSG00000066363	Serpina3f	serine (or cysteine) peptidase inhibitor, clade A, member 3F	1.92	1.30E-10
ENSMUSG00000049103	Ccr2	chemokine (C-C motif) receptor 2	1.92	7.86E-16
ENSMUSG00000029675	Eln	elastin	1.91	1.91E-12
ENSMUSG00000037411	Serpine1	serine (or cysteine) peptidase inhibitor, clade E, member 1	1.90	8.62E-15

ENSMUSG00000064147	Rab44	RAB44, member RAS oncogene family	1.90	2.78E-07
ENSMUSG00000054072	Iigp1	interferon inducible GTPase 1	1.90	1.99E-08
ENSMUSG00000075602	Ly6a	lymphocyte antigen 6 complex, locus A	1.89	2.26E-14
ENSMUSG00000015947	Fcgr1	Fc receptor, IgG, high affinity I	1.86	5.39E-12
ENSMUSG00000013974	Mcemp1	mast cell expressed membrane protein 1	1.86	4.81E-07
ENSMUSG00000020826	Nos2	nitric oxide synthase 2, inducible	1.85	2.45E-09
ENSMUSG00000002289	Angptl4	angiopoietin-like 4	1.85	1.78E-10
ENSMUSG00000026981	Il1rn	interleukin 1 receptor antagonist	1.83	4.31E-12
ENSMUSG00000079227	Ccr5	chemokine (C-C motif) receptor 5	1.82	1.58E-15
ENSMUSG00000000031			1.79	3.69E-06
ENSMUSG00000024679	Ms4a6d	membrane-spanning 4-domains, subfamily A, member 6D	1.79	7.08E-13
ENSMUSG00000028111	Ctsk	cathepsin K	1.79	1.01E-11
ENSMUSG00000028655	Mfsd2a	major facilitator superfamily domain containing 2A	1.78	1.52E-06
ENSMUSG00000026249	Serpine2	serine (or cysteine) peptidase inhibitor, clade E, member 2	1.78	5.50E-13
ENSMUSG00000069792	Wfdc17	WAP four-disulfide core domain 17	1.78	5.43E-07
ENSMUSG00000074677	LOC100038947	signal-regulatory protein beta 1-like	1.77	4.17E-06
ENSMUSG00000024810	Il33	interleukin 33	1.77	4.48E-15
ENSMUSG00000090307	1700071M16Rik	RIKEN cDNA 1700071M16 gene	1.77	2.70E-08
ENSMUSG00000054555	Adam12	a disintegrin and metallopeptidase domain 12 (meltrin alpha)	1.76	4.00E-09
ENSMUSG00000024053	Emilin2	elastin microfibril interfacer 2	1.76	1.80E-14
ENSMUSG00000016194	Hsd11b1	hydroxysteroid 11-beta dehydrogenase 1	1.75	8.08E-11
ENSMUSG00000043832	Clec4a3	C-type lectin domain family 4, member a3	1.75	7.13E-12
ENSMUSG00000025161	Slc16a3	solute carrier family 16 (monocarboxylic acid transporters), member 3	1.74	4.02E-09
ENSMUSG00000030474	Siglece	sialic acid binding Ig-like lectin E	1.74	2.70E-06
ENSMUSG00000007682	Dio2	deiodinase, iodothyronine, type II	1.74	1.07E-06
ENSMUSG00000073555	Gm4951	predicted gene 4951	1.74	2.20E-10
ENSMUSG00000029553	Tfec	transcription factor EC	1.72	1.58E-06
ENSMUSG00000030022	Adamts9	a disintegrin-like and metallopeptidase (reprolysin type) with thrombospondin type 1 motif, 9	1.72	2.14E-13
ENSMUSG00000022534	Mefv	Mediterranean fever	1.71	9.04E-09
ENSMUSG00000008845	Cd163	CD163 antigen	1.71	5.47E-14
ENSMUSG00000096528	G430049J08Rik	RIKEN cDNA G430049J08 gene	1.71	7.11E-12
ENSMUSG00000040152	Thbs1	thrombospondin 1	1.70	3.24E-20
ENSMUSG00000074151	Nlrc5	NLR family, CARD domain containing 5	1.70	1.09E-10
ENSMUSG00000050578	Mmp13	matrix metallopeptidase 13	1.69	4.84E-06
ENSMUSG00000051748	Wfdc21	WAP four-disulfide core domain 21	1.68	1.29E-05
ENSMUSG00000037035	Inhbb	inhibin beta-B	1.68	2.75E-07
ENSMUSG00000090942	F830016B08Rik	RIKEN cDNA F830016B08 gene	1.68	1.60E-08
ENSMUSG00000022860	Chodl	chondrolectin	1.68	4.33E-08
ENSMUSG00000041193	Pla2g5	phospholipase A2, group V	1.67	1.99E-10
ENSMUSG00000085977			1.66	3.61E-06
ENSMUSG00000029484	Anxa3	annexin A3	1.66	2.34E-14
ENSMUSG00000009185	Ccl8	chemokine (C-C motif) ligand 8	1.65	2.63E-09
ENSMUSG00000047330	Kcne4	potassium voltage-gated channel, Isk-related subfamily, gene 4	1.65	7.36E-11
ENSMUSG00000038156	Spon1	spondin 1, (f-spondin) extracellular matrix protein	1.65	9.11E-16
ENSMUSG00000028583	Pdpn	podoplanin	1.64	7.24E-15
ENSMUSG00000074415	2610203C20Rik	RIKEN cDNA 2610203C20 gene	1.64	1.17E-11

ENSMUSG00000030786	Itgam	integrin alpha M	1.64	3.03E-15
ENSMUSG00000058818	Pirb	paired Ig-like receptor B	1.63	1.21E-10
ENSMUSG00000046402	Rbp1	retinol binding protein 1, cellular	1.63	4.24E-09
ENSMUSG00000079419	Ms4a6c	membrane-spanning 4-domains, subfamily A, member 6C	1.63	8.95E-13
ENSMUSG00000041481			1.62	5.25E-11
ENSMUSG00000035373	Ccl7	chemokine (C-C motif) ligand 7	1.62	1.27E-05
ENSMUSG00000021614	Vcan	versican	1.62	1.16E-15
ENSMUSG00000018930	Ccl4	chemokine (C-C motif) ligand 4	1.61	2.89E-05
ENSMUSG00000029417	Cxcl9	chemokine (C-X-C motif) ligand 9	1.59	2.23E-06
ENSMUSG00000046688	Tifa	TRAF-interacting protein with forkhead-associated domain	1.58	2.16E-10
ENSMUSG00000085786			1.58	4.73E-09
ENSMUSG00000022582	Ly6g	lymphocyte antigen 6 complex, locus G	1.57	2.97E-07
ENSMUSG00000055978	Fut2	fucosyltransferase 2	1.57	1.15E-10
ENSMUSG00000081448			1.57	5.37E-07
ENSMUSG00000079014	Serpina3i	serine (or cysteine) peptidase inhibitor, clade A, member 3I	1.57	5.26E-06
ENSMUSG00000096768	Erdr1	erythroid differentiation regulator 1	1.57	2.07E-06
ENSMUSG00000025044	Msr1	macrophage scavenger receptor 1	1.56	1.64E-08
ENSMUSG00000051439	Cd14	CD14 antigen	1.56	4.09E-09
ENSMUSG00000021281	Tnfaip2	tumor necrosis factor, alpha-induced protein 2	1.56	1.31E-10
ENSMUSG00000074417	Pira11	paired-Ig-like receptor A11	1.56	4.95E-07
ENSMUSG00000058755	Osm	oncostatin M	1.54	6.31E-05
ENSMUSG00000042759	Apobr	apolipoprotein B receptor	1.54	6.57E-08
ENSMUSG00000075270	Pde11a	phosphodiesterase 11A	1.53	7.44E-06
ENSMUSG00000079363	Gbp4	guanylate binding protein 4	1.53	9.25E-07
ENSMUSG00000019997	Ctgf	connective tissue growth factor	1.53	6.31E-10
ENSMUSG00000026185	Igfbp5	insulin-like growth factor binding protein 5	1.53	5.66E-13
ENSMUSG00000078921	Tgtp2	T cell specific GTPase 2	1.53	1.98E-07
ENSMUSG00000031972	Acta1	actin, alpha 1, skeletal muscle	1.52	5.73E-06
ENSMUSG00000053101	Gpr141	G protein-coupled receptor 141	1.52	1.84E-07
ENSMUSG00000041695	Kcnj2	potassium inwardly-rectifying channel, subfamily J, member 2	1.51	3.22E-06
ENSMUSG00000044254	Pcsk9	proprotein convertase subtilisin/kexin type 9	1.51	3.67E-10
ENSMUSG00000018339	Gpx3	glutathione peroxidase 3	1.51	7.40E-11
ENSMUSG00000079362	Gbp6	guanylate binding protein 6	1.51	3.14E-07
ENSMUSG00000025330	Padi4	peptidyl arginine deiminase, type IV	1.50	6.33E-05
ENSMUSG00000003665	Has1	hyaluronan synthase1	1.50	1.09E-04
ENSMUSG00000060063	Alox5ap	arachidonate 5-lipoxygenase activating protein	1.49	1.14E-09
ENSMUSG00000054588			1.49	4.76E-05
ENSMUSG00000068452	Duox2	dual oxidase 2	1.49	2.95E-09
ENSMUSG00000041347	Bdkrb1	bradykinin receptor, beta 1	1.49	1.09E-04
ENSMUSG00000031963	Bmper	BMP-binding endothelial regulator	1.48	6.83E-08
ENSMUSG00000040133	Gpr176	G protein-coupled receptor 176	1.48	5.96E-05
ENSMUSG00000025804	Ccr1	chemokine (C-C motif) receptor 1	1.47	3.96E-10
ENSMUSG00000022367	Has2	hyaluronan synthase 2	1.47	5.35E-06
ENSMUSG00000001435	Col18a1	collagen, type XVIII, alpha 1	1.47	4.71E-12
ENSMUSG00000073489	Ifi204	interferon activated gene 204	1.47	3.18E-09
ENSMUSG00000024481	Lvrn	laeverin	1.47	1.65E-05

ENSMUSG00000028370	Pappa	pregnancy-associated plasma protein A	1.46	5.75E-13
ENSMUSG00000024411	Aqp4	aquaporin 4	1.46	2.46E-06
ENSMUSG00000050747	Trim15	tripartite motif-containing 15	1.46	1.08E-04
ENSMUSG00000022146	Osmr	oncostatin M receptor	1.46	1.14E-11
ENSMUSG00000029082	Bst1	bone marrow stromal cell antigen 1	1.45	3.10E-07
ENSMUSG00000056025	Clca3a1	chloride channel calcium activated 3A1	1.45	5.55E-08
ENSMUSG00000027460	Angpt4	angiopoietin 4	1.45	1.56E-04
ENSMUSG00000027737	Slc7a11	solute carrier family 7 (cationic amino acid transporter, y+ system), member 11	1.44	3.08E-10
ENSMUSG00000028874	Fgr	Gardner-Rasheed feline sarcoma viral (Fgr) oncogene homolog	1.44	1.28E-08
ENSMUSG00000071714	Csf2rb2	colony stimulating factor 2 receptor, beta 2, low-affinity (granulocyte-macrophage)	1.44	2.39E-08
ENSMUSG00000046223	Plaur	plasminogen activator, urokinase receptor	1.44	4.39E-06
ENSMUSG00000063388			1.44	1.76E-04
ENSMUSG00000029915	Clec5a	C-type lectin domain family 5, member a	1.43	1.28E-05
ENSMUSG00000035004	Igsf6	immunoglobulin superfamily, member 6	1.42	6.71E-09
ENSMUSG00000028633	Ctps	cytidine 5'-triphosphate synthase	1.42	6.14E-11
ENSMUSG00000062345	Serpinb2	serine (or cysteine) peptidase inhibitor, clade B, member 2	1.41	2.56E-04
ENSMUSG00000079445	B3gnt7	UDP-GlcNAc:betaGal beta-1,3-N-acetylglucosaminyltransferase 7	1.41	7.34E-06
ENSMUSG00000024640	Psat1	phosphoserine aminotransferase 1	1.40	1.56E-06
ENSMUSG00000030353	Tead4	TEA domain family member 4	1.40	1.17E-04
ENSMUSG00000041324	Inhba	inhibin beta-A	1.39	4.22E-05
ENSMUSG00000042808	Gpx2	glutathione peroxidase 2	1.39	7.62E-09
ENSMUSG00000030077	Chl1	cell adhesion molecule with homology to L1CAM	1.39	5.05E-09
ENSMUSG00000027323	Rad51	RAD51 homolog	1.39	9.17E-07
ENSMUSG00000033508	Asprv1	aspartic peptidase, retroviral-like 1	1.39	1.40E-04
ENSMUSG00000045551	Fpr1	formyl peptide receptor 1	1.38	3.39E-04
ENSMUSG00000029084	Cd38	CD38 antigen	1.38	1.13E-06
ENSMUSG00000047230	Cldn2	claudin 2	1.38	7.59E-06
ENSMUSG00000097815			1.38	3.05E-11
ENSMUSG00000025473	Adam8	a disintegrin and metallopeptidase domain 8	1.37	3.44E-07
ENSMUSG00000022440	C1qtnf6	C1q and tumor necrosis factor related protein 6	1.37	1.78E-04
ENSMUSG00000037613	Tnfrsf23	tumor necrosis factor receptor superfamily, member 23	1.36	2.96E-05
ENSMUSG00000034438	Gbp8	guanylate-binding protein 8	1.35	1.37E-06
ENSMUSG00000036356	Csgalnact1	chondroitin sulfate N-acetylgalactosaminyltransferase 1	1.35	7.94E-07
ENSMUSG00000039252	Lgi2	leucine-rich repeat LGI family, member 2	1.35	5.91E-06
ENSMUSG00000086653	9130015L21Rik	RIKEN cDNA 9130015L21 gene	1.34	4.54E-04
ENSMUSG00000024235	Map3k8	mitogen-activated protein kinase kinase kinase 8	1.34	1.86E-08
ENSMUSG00000020256	Aldh1l2	aldehyde dehydrogenase 1 family, member L2	1.34	7.46E-06
ENSMUSG00000021647	Cartpt	CART prepropeptide	1.34	3.33E-05
ENSMUSG00000029659	Medag	mesenteric estrogen dependent adipogenesis	1.34	2.00E-07
ENSMUSG00000071713	Csf2rb	colony stimulating factor 2 receptor, beta, low-affinity (granulocyte-macrophage)	1.33	5.06E-09
ENSMUSG00000004371	Il11	interleukin 11	1.33	5.18E-04
ENSMUSG00000076694			1.33	5.98E-04
ENSMUSG00000005824	Tnfsf14	tumor necrosis factor (ligand) superfamily, member 14	1.33	5.08E-04
ENSMUSG00000078922	Tgtp1	T cell specific GTPase 1	1.32	1.11E-04
ENSMUSG00000058794	Nfe2	nuclear factor, erythroid derived 2	1.32	6.00E-04
ENSMUSG00000035448	Ccr3	chemokine (C-C motif) receptor 3	1.32	6.27E-04

ENSMUSG00000028262	Clca3a2	chloride channel calcium activated 3A2	1.32	4.09E-05
ENSMUSG00000092274			1.32	7.38E-09
ENSMUSG00000037440	Vnn1	vanin 1	1.31	1.76E-05
ENSMUSG00000060445	Sycp2	synaptonemal complex protein 2	1.31	7.05E-04
ENSMUSG00000024349	Tmem173	transmembrane protein 173	1.31	1.74E-07
ENSMUSG00000082292			1.31	4.52E-05
ENSMUSG00000056501	Cebpb	CCAAT/enhancer binding protein (C/EBP), beta	1.31	5.29E-06
ENSMUSG00000028613	Lrp8	low density lipoprotein receptor-related protein 8, apolipoprotein e receptor	1.30	1.40E-06
ENSMUSG00000004668	Abca13	ATP-binding cassette, sub-family A (ABC1), member 13	1.30	2.25E-04
ENSMUSG00000057596	Trim30d	tripartite motif-containing 30D	1.30	3.37E-05
ENSMUSG00000053675	Tgm5	transglutaminase 5	1.30	7.49E-04
ENSMUSG00000048852	Gm12185	predicted gene 12185	1.30	6.48E-05
ENSMUSG00000052125	F730043M19 Rik	RIKEN cDNA F730043M19 gene	1.30	5.90E-05
ENSMUSG00000060131	Atp8b4	ATPase, class I, type 8B, member 4	1.29	7.29E-06
ENSMUSG00000073492			1.29	5.29E-04
ENSMUSG00000056427	Slit3	slit homolog 3 (Drosophila)	1.29	1.71E-09
ENSMUSG00000042943			1.29	3.89E-04
ENSMUSG00000003617	Cp	ceruloplasmin	1.28	8.31E-11
ENSMUSG00000023886	Smoc2	SPARC related modular calcium binding 2	1.28	3.83E-10
ENSMUSG00000085363			1.28	8.02E-04
ENSMUSG00000034206	Polq	polymerase (DNA directed), theta	1.28	5.25E-08
ENSMUSG00000084956			1.28	8.27E-04
ENSMUSG00000078606	Gm4070	predicted gene 4070	1.28	5.00E-06
ENSMUSG00000030043	Tacr1	tachykinin receptor 1	1.28	6.08E-07
ENSMUSG00000020363	Gfpt2	glutamine fructose-6-phosphate transaminase 2	1.28	1.18E-06
ENSMUSG00000026787	Gad2	glutamic acid decarboxylase 2	1.28	3.25E-04
ENSMUSG00000074892	B3galt5	UDP-Gal:betaGlcNAc beta 1,3-galactosyltransferase, polypeptide 5	1.28	1.66E-07
ENSMUSG00000080917			1.27	3.99E-04
ENSMUSG00000017493	Igfbp4	insulin-like growth factor binding protein 4	1.27	2.26E-10
ENSMUSG00000026536	Mnda	myeloid cell nuclear differentiation antigen	1.27	7.71E-06
ENSMUSG00000059108	Ifitm6	interferon induced transmembrane protein 6	1.27	1.08E-03
ENSMUSG00000028527	Ak4	adenylate kinase 4	1.27	3.52E-05
ENSMUSG00000029299	Abcg3	ATP-binding cassette, sub-family G (WHITE), member 3	1.26	1.72E-06
ENSMUSG00000000628	Hk2	hexokinase 2	1.26	1.22E-07
ENSMUSG00000036596	Cpz	carboxypeptidase Z	1.26	1.15E-03
ENSMUSG00000038751	Ptk6	PTK6 protein tyrosine kinase 6	1.26	1.73E-07
ENSMUSG00000049436	Upk1b	uroplakin 1B	1.26	9.03E-04
ENSMUSG00000063286			1.25	6.56E-09
ENSMUSG00000058715	Fcer1g	Fc receptor, IgE, high affinity I, gamma polypeptide	1.25	1.10E-05
ENSMUSG00000087070	Gm12505	predicted gene 12505	1.25	6.14E-06
ENSMUSG00000074813			1.25	2.94E-04
ENSMUSG00000022220	Adcy4	adenylate cyclase 4	1.25	2.11E-05
ENSMUSG00000068606	Gm4841	predicted gene 4841	1.25	9.80E-05
ENSMUSG00000018924	Alox15	arachidonate 15-lipoxygenase	1.24	8.63E-04
ENSMUSG00000028864	Hgf	hepatocyte growth factor	1.24	3.25E-06
ENSMUSG00000053338	Tarm1	T cell-interacting, activating receptor on myeloid cells 1	1.24	1.32E-03

ENSMUSG00000058099	Nfam1	Nfat activating molecule with ITAM motif 1	1.24	3.14E-06
ENSMUSG00000044041	Krt13	keratin 13	1.24	9.68E-04
ENSMUSG00000002847	Pla1a	phospholipase A1 member A	1.24	9.54E-04
ENSMUSG00000097423			1.23	7.39E-05
ENSMUSG00000046295	Ankle1	ankyrin repeat and LEM domain containing 1	1.23	3.06E-04
ENSMUSG00000022894	Adamts5	a disintegrin-like and metallopeptidase (reprolysin type) with thrombospondin type 1 motif, 5 (aggrecanase-2)	1.23	2.39E-09
ENSMUSG00000020676	Ccl11	chemokine (C-C motif) ligand 11	1.23	3.50E-09
ENSMUSG00000017737	Mmp9	matrix metallopeptidase 9	1.22	1.39E-05
ENSMUSG00000024066	Xdh	xanthine dehydrogenase	1.22	1.12E-08
ENSMUSG00000090665			1.22	1.57E-03
ENSMUSG00000049130	C5ar1	complement component 5a receptor 1	1.22	1.33E-04
ENSMUSG00000038011	Dnah10	dynein, axonemal, heavy chain 10	1.22	1.32E-03
ENSMUSG00000001670	Tat	tyrosine aminotransferase	1.21	2.88E-07
ENSMUSG00000057191	AB124611	cDNA sequence AB124611	1.21	1.44E-05
ENSMUSG00000025491	Ifitm1	interferon induced transmembrane protein 1	1.21	7.72E-07
ENSMUSG00000061540	Orm2	orosomucoid 2	1.21	1.50E-03
ENSMUSG00000020932	Gfap	glial fibrillary acidic protein	1.20	7.77E-06
ENSMUSG00000041293	Gpr110	G protein-coupled receptor 110	1.20	1.65E-03
ENSMUSG00000055541	Lair1	leukocyte-associated Ig-like receptor 1	1.20	3.90E-07
ENSMUSG00000039109	F13a1	coagulation factor XIII, A1 subunit	1.20	4.64E-08
ENSMUSG00000081723			1.20	1.16E-03
ENSMUSG00000000957	Mmp14	matrix metallopeptidase 14 (membrane-inserted)	1.20	2.50E-11
ENSMUSG00000020649	Rrm2	ribonucleotide reductase M2	1.20	8.69E-09
ENSMUSG00000073902			1.19	8.84E-06
ENSMUSG00000046718	Bst2	bone marrow stromal cell antigen 2	1.19	8.92E-05
ENSMUSG00000041734	Kirrel	kin of IRRE like (Drosophila)	1.19	2.32E-07
ENSMUSG00000024401	Tnf	tumor necrosis factor	1.19	3.09E-05
ENSMUSG00000003355	Fkbp11	FK506 binding protein 11	1.19	2.74E-06
ENSMUSG00000078122	F630028O10Rik	RIKEN cDNA F630028O10 gene	1.19	2.11E-06
ENSMUSG00000079553	Kifc1	kinesin family member C1	1.19	4.51E-04
ENSMUSG00000057604	Lmcd1	LIM and cysteine-rich domains 1	1.19	1.36E-05
ENSMUSG00000033777	Tlr13	toll-like receptor 13	1.18	1.39E-07
ENSMUSG00000056018	1700008F21Rik	RIKEN cDNA 1700008F21 gene	1.18	1.56E-04
ENSMUSG00000032586	Traip	TRAF-interacting protein	1.18	5.67E-05
ENSMUSG00000005124	Wisp1	WNT1 inducible signaling pathway protein 1	1.18	4.86E-06
ENSMUSG00000045502	Hcar2	hydroxycarboxylic acid receptor 2	1.18	4.70E-04
ENSMUSG00000070315	4930581F22Rik	RIKEN cDNA 4930581F22 gene	1.17	9.47E-04
ENSMUSG00000040522	Tlr8	toll-like receptor 8	1.17	8.41E-06
ENSMUSG00000078780	Gm5150	predicted gene 5150	1.17	1.86E-03
ENSMUSG00000091956	C2cd4b	C2 calcium-dependent domain containing 4B	1.17	1.90E-03
ENSMUSG00000097344			1.17	5.94E-04
ENSMUSG00000022237	Ankrd33b	ankyrin repeat domain 33B	1.16	5.36E-04
ENSMUSG00000085913			1.16	1.36E-03
ENSMUSG00000059498	Fcgr3	Fc receptor, IgG, low affinity III	1.16	1.85E-07
ENSMUSG00000075611			1.16	6.88E-06
ENSMUSG00000028195	Cyr61	cysteine rich protein 61	1.16	3.52E-05

ENSMUSG00000093846			1.16	2.36E-03
ENSMUSG00000043740	B430306N03Rik	RIKEN cDNA B430306N03 gene	1.15	3.11E-05
ENSMUSG00000029641	Rasl11a	RAS-like, family 11, member A	1.15	1.26E-03
ENSMUSG00000049281	Scn3b	sodium channel, voltage-gated, type III, beta	1.15	2.03E-04
ENSMUSG00000051279	Gdf6	growth differentiation factor 6	1.15	2.69E-03
ENSMUSG00000061878	Sphk1	sphingosine kinase 1	1.15	2.06E-04
ENSMUSG00000022032	Scara5	scavenger receptor class A, member 5 (putative)	1.15	1.83E-07
ENSMUSG00000047728	BC025446	cDNA sequence BC025446	1.14	1.05E-03
ENSMUSG00000078853	Igtp	interferon gamma induced GTPase	1.14	4.46E-04
ENSMUSG00000030428	Ttyh1	tweety homolog 1 (Drosophila)	1.14	1.08E-06
ENSMUSG00000011171	Vipr2	vasoactive intestinal peptide receptor 2	1.14	4.59E-05
ENSMUSG00000029377	Ereg	epiregulin	1.14	2.22E-06
ENSMUSG00000031502	Col4a1	collagen, type IV, alpha 1	1.13	1.16E-09
ENSMUSG00000032915	Emr4	EGF-like module containing, mucin-like, hormone receptor-like sequence 4	1.13	8.11E-04
ENSMUSG00000031825	Crispld2	cysteine-rich secretory protein LCCL domain containing 2	1.13	8.30E-09
ENSMUSG00000044017	Gpr133	G protein-coupled receptor 133	1.13	3.01E-07
ENSMUSG00000028037	Ifi44	interferon-induced protein 44	1.13	1.40E-05
ENSMUSG00000048699	4732456N10Rik	RIKEN cDNA 4732456N10 gene	1.13	3.07E-03
ENSMUSG00000026605	Cenpf	centromere protein F	1.13	3.08E-06
ENSMUSG00000039146	Ifi44l	interferon-induced protein 44 like	1.12	9.33E-04
ENSMUSG00000003484	Cyp4f18	cytochrome P450, family 4, subfamily f, polypeptide 18	1.12	3.55E-03
ENSMUSG00000032204	Aqp9	aquaporin 9	1.12	3.95E-03
ENSMUSG00000025492	Ifitm3	interferon induced transmembrane protein 3	1.12	4.01E-08
ENSMUSG00000078817	Nlrp12	NLR family, pyrin domain containing 12	1.12	3.22E-03
ENSMUSG00000066755	Tnfsf18	tumor necrosis factor (ligand) superfamily, member 18	1.11	3.96E-03
ENSMUSG00000022221	Ripk3	receptor-interacting serine-threonine kinase 3	1.11	3.42E-06
ENSMUSG00000030748	Il4ra	interleukin 4 receptor, alpha	1.11	1.99E-08
ENSMUSG00000026535	Ifi202b	interferon activated gene 202B	1.11	1.49E-05
ENSMUSG00000027224	Duoxa1	dual oxidase maturation factor 1	1.11	9.71E-04
ENSMUSG00000028539	Artn	artemin	1.11	3.91E-03
ENSMUSG00000016496	Cd274	CD274 antigen	1.11	5.47E-06
ENSMUSG00000044574			1.10	3.86E-03
ENSMUSG00000040253	Gbp7	guanylate binding protein 7	1.10	1.84E-04
ENSMUSG00000037243	Zfp692	zinc finger protein 692	1.10	1.65E-04
ENSMUSG00000040711	Sh3pxd2b	SH3 and PX domains 2B	1.09	2.55E-07
ENSMUSG00000001506	Col1a1	collagen, type I, alpha 1	1.09	2.72E-07
ENSMUSG00000028871	Rspo1	R-spondin homolog (Xenopus laevis)	1.09	3.46E-03
ENSMUSG00000023913	Pla2g7	phospholipase A2, group VII (platelet-activating factor acetylhydrolase, plasma)	1.09	2.58E-07
ENSMUSG00000026177	Slc11a1	solute carrier family 11 (proton-coupled divalent metal ion transporters), member 1	1.09	2.96E-05
ENSMUSG00000070390	Nlrp1b	NLR family, pyrin domain containing 1B	1.09	9.60E-04
ENSMUSG00000032487	Ptgs2	prostaglandin-endoperoxide synthase 2	1.08	7.09E-04
ENSMUSG00000041707	1810011H11Rik	RIKEN cDNA 1810011H11 gene	1.08	4.29E-03
ENSMUSG00000073565	Prr16	proline rich 16	1.08	2.82E-03
ENSMUSG00000058624	Gda	guanine deaminase	1.08	2.70E-04
ENSMUSG00000086311			1.08	1.75E-03
ENSMUSG00000025986	Slc39a10	solute carrier family 39 (zinc transporter), member 10	1.08	1.11E-06

ENSMUSG00000078161	Erich3	glutamate rich 3	1.08	3.34E-03
ENSMUSG00000063193	Cd300lb	CD300 antigen like family member B	1.08	3.79E-03
ENSMUSG00000084213			1.08	3.23E-03
ENSMUSG00000024989	Cep55	centrosomal protein 55	1.08	5.40E-07
ENSMUSG00000003283	Hck	hemopoietic cell kinase	1.08	5.07E-06
ENSMUSG00000073490	AI607873	expressed sequence AI607873	1.08	2.86E-05
ENSMUSG00000093800			1.08	5.28E-03
ENSMUSG00000055491	Pprc1	peroxisome proliferative activated receptor, gamma, coactivator-related 1	1.07	5.56E-06
ENSMUSG00000027907	S100a11	S100 calcium binding protein A11 (calgizzarin)	1.07	3.14E-06
ENSMUSG00000001517	Foxm1	forkhead box M1	1.07	1.50E-05
ENSMUSG00000040658	Dnph1	2'-deoxynucleoside 5'-phosphate N-hydrolase 1	1.07	2.54E-03
ENSMUSG00000044258	Ctla2a	cytotoxic T lymphocyte-associated protein 2 alpha	1.07	2.46E-06
ENSMUSG00000036777	Anln	anillin, actin binding protein	1.07	2.94E-07
ENSMUSG00000032254	Kif23	kinesin family member 23	1.06	1.29E-07
ENSMUSG00000024798	Htr7	5-hydroxytryptamine (serotonin) receptor 7	1.06	2.71E-03
ENSMUSG00000033453	Adamts15	a disintegrin-like and metallopeptidase (reprolysin type) with thrombospondin type 1 motif, 15	1.06	8.35E-06
ENSMUSG00000025665	Rps6ka6	ribosomal protein S6 kinase polypeptide 6	1.06	1.47E-04
ENSMUSG00000006522	Itih3	inter-alpha trypsin inhibitor, heavy chain 3	1.06	7.96E-04
ENSMUSG00000089950			1.06	2.21E-03
ENSMUSG00000027514	Zbp1	Z-DNA binding protein 1	1.06	3.65E-05
ENSMUSG00000020916	Krt36	keratin 36	1.06	6.01E-03
ENSMUSG00000084390			1.06	6.31E-03
ENSMUSG00000017861	Mybl2	myeloblastosis oncogene-like 2	1.06	2.38E-05
ENSMUSG00000086479			1.06	3.77E-03
ENSMUSG00000031380	Figf	c-fos induced growth factor	1.05	1.87E-04
ENSMUSG00000046841	Ckap4	cytoskeleton-associated protein 4	1.05	5.32E-07
ENSMUSG00000071547	Nt5dc2	5'-nucleotidase domain containing 2	1.05	3.30E-04
ENSMUSG00000097814			1.05	6.45E-03
ENSMUSG00000073821			1.05	6.33E-03
ENSMUSG00000027322	Siglec1	sialic acid binding Ig-like lectin 1, sialoadhesin	1.05	4.46E-06
ENSMUSG00000026068	Il18rap	interleukin 18 receptor accessory protein	1.05	1.53E-04
ENSMUSG00000022893	Adamts1	a disintegrin-like and metallopeptidase (reprolysin type) with thrombospondin type 1 motif, 1	1.05	2.78E-06
ENSMUSG00000035105	Egln3	egl-9 family hypoxia-inducible factor 3	1.05	3.03E-05
ENSMUSG00000029752	Asns	asparagine synthetase	1.05	7.62E-06
ENSMUSG00000022372	Sla	src-like adaptor	1.05	6.43E-08
ENSMUSG00000006958	Chrd	chordin	1.05	3.98E-03
ENSMUSG00000026646	Suv39h2	suppressor of variegation 3-9 homolog 2 (Drosophila)	1.05	2.59E-04
ENSMUSG00000049939	Lrrc4	leucine rich repeat containing 4	1.04	8.32E-04
ENSMUSG00000026786	Apbb1ip	amyloid beta (A4) precursor protein-binding, family B, member 1 interacting protein	1.04	3.40E-06
ENSMUSG00000031821	Gins2	GINS complex subunit 2 (Psf2 homolog)	1.04	7.20E-05
ENSMUSG00000046006	Gapt	Grb2-binding adaptor, transmembrane	1.04	5.87E-03
ENSMUSG00000031450	Grk1	G protein-coupled receptor kinase 1	1.04	8.32E-04
ENSMUSG00000036036	Zfp57	zinc finger protein 57	1.04	1.73E-03
ENSMUSG00000046245	Pilra	paired immunoglobin-like type 2 receptor alpha	1.04	2.18E-04
ENSMUSG00000040165	Cd209c	CD209c antigen	1.04	3.90E-05
ENSMUSG00000086451			1.04	6.45E-03

ENSMUSG00000034652	Cd300a	CD300A antigen	1.03	2.87E-05
ENSMUSG00000021260	Hhipl1	hedgehog interacting protein-like 1	1.03	3.91E-03
ENSMUSG00000037185	Krt80	keratin 80	1.03	5.17E-03
ENSMUSG00000027004	Frzb	frizzled-related protein	1.03	4.17E-04
ENSMUSG00000090293			1.03	5.88E-03
ENSMUSG00000022021	Diap3	diaphanous homolog 3 (Drosophila)	1.03	5.22E-06
ENSMUSG00000073274			1.03	1.02E-03
ENSMUSG00000092500			1.03	3.92E-04
ENSMUSG00000021728	Emb	embigin	1.03	2.32E-05
ENSMUSG00000079339	Gm14446	predicted gene 14446	1.03	4.07E-04
ENSMUSG00000041498	Kif14	kinesin family member 14	1.03	6.30E-08
ENSMUSG00000022148	Fyb	FYN binding protein	1.02	3.71E-07
ENSMUSG00000081305			1.02	3.91E-03
ENSMUSG00000046179	E2f8	E2F transcription factor 8	1.02	6.57E-06
ENSMUSG00000029414	Kntc1	kinetochore associated 1	1.02	3.23E-06
ENSMUSG00000027248	Pdia3	protein disulfide isomerase associated 3	1.02	8.08E-07
ENSMUSG00000030560	Ctsc	cathepsin C	1.02	2.42E-06
ENSMUSG00000029321	Slc10a6	solute carrier family 10 (sodium/bile acid cotransporter family), member 6	1.01	5.18E-03
ENSMUSG00000032115	Hyou1	hypoxia up-regulated 1	1.01	6.27E-06
ENSMUSG00000026566	Mpzl1	myelin protein zero-like 1	1.01	2.24E-06
ENSMUSG00000034311	Kif4	kinesin family member 4	1.01	2.27E-08
ENSMUSG00000023903	Mmp25	matrix metallopeptidase 25	1.01	2.71E-03
ENSMUSG00000021187	Tc2n	tandem C2 domains, nuclear	1.01	8.37E-06
ENSMUSG00000043939	A530064D06 Rik	RIKEN cDNA A530064D06 gene	1.01	9.19E-03
ENSMUSG00000031596	Slc7a2	solute carrier family 7 (cationic amino acid transporter, y+ system), member 2	1.00	3.76E-04
ENSMUSG00000000386	Mx1	MX dynamin-like GTPase 1	1.00	8.62E-04
ENSMUSG00000022797	Tfrc	transferrin receptor	1.00	5.13E-06
ENSMUSG00000028010	Gar1	GAR1 ribonucleoprotein homolog (yeast)	1.00	3.50E-03
ENSMUSG00000034394	Lif	leukemia inhibitory factor	1.00	3.06E-03
ENSMUSG00000027670	Ocstamp	osteoclast stimulatory transmembrane protein	1.00	3.00E-03
ENSMUSG00000069540			1.00	7.84E-03
ENSMUSG00000024300	Myo1f	myosin IF	1.00	1.16E-05
ENSMUSG00000026950	Neb	nebulin	1.00	2.61E-04
ENSMUSG00000027225	Duoxa2	dual oxidase maturation factor 2	1.00	3.18E-03
ENSMUSG00000035673	Sbno2	strawberry notch homolog 2 (Drosophila)	1.00	2.75E-06
ENSMUSG00000041754	Trem3	triggering receptor expressed on myeloid cells 3	1.00	9.20E-03
ENSMUSG00000022836	Mylk	myosin, light polypeptide kinase	-1.00	1.40E-09
ENSMUSG00000068299	1700019G17R ik	RIKEN cDNA 1700019G17 gene	-1.00	1.59E-03
ENSMUSG00000040420	Cdh18	cadherin 18	-1.00	9.53E-03
ENSMUSG00000061531	Tmem236	transmembrane protein 236	-1.00	8.02E-05
ENSMUSG00000028307	Aldob	aldolase B, fructose-bisphosphate	-1.00	3.49E-06
ENSMUSG00000085942			-1.00	9.04E-03
ENSMUSG00000031376	Atp2b3	ATPase, Ca++ transporting, plasma membrane 3	-1.00	6.71E-03
ENSMUSG00000021376	Tpmt	thiopurine methyltransferase	-1.00	3.15E-06
ENSMUSG00000020183	Cpm	carboxypeptidase M	-1.00	5.15E-06
ENSMUSG00000021336	Slc17a4	solute carrier family 17 (sodium phosphate), member 4	-1.00	2.59E-05

ENSMUSG00000032727	Mier3	mesoderm induction early response 1, family member 3	-1.00	1.07E-05
ENSMUSG00000035473	Galm	galactose mutarotase	-1.01	9.42E-07
ENSMUSG00000031613	Hpgd	hydroxyprostaglandin dehydrogenase 15 (NAD)	-1.01	1.95E-05
ENSMUSG00000085121			-1.01	8.99E-03
ENSMUSG00000096410			-1.01	9.35E-03
ENSMUSG00000058806	Col13a1	collagen, type XIII, alpha 1	-1.01	1.68E-03
ENSMUSG00000002032	Tmem25	transmembrane protein 25	-1.01	4.09E-03
ENSMUSG00000090124	Ugt1a7c	UDP glucuronosyltransferase 1 family, polypeptide A7C	-1.01	4.73E-08
ENSMUSG00000041986	Elmod1	ELMO/CED-12 domain containing 1	-1.01	6.81E-03
ENSMUSG00000034918	Cdhr2	cadherin-related family member 2	-1.01	2.95E-08
ENSMUSG00000025467	Prap1	proline-rich acidic protein 1	-1.01	2.42E-04
ENSMUSG00000019775	Rgs17	regulator of G-protein signaling 17	-1.01	3.16E-04
ENSMUSG00000023122	Sult1c2	sulfotransferase family, cytosolic, 1C, member 2	-1.01	5.66E-06
ENSMUSG00000074261	Erich4	glutamate rich 4	-1.01	6.17E-03
ENSMUSG00000051243	Islr2	immunoglobulin superfamily containing leucine-rich repeat 2	-1.01	7.65E-03
ENSMUSG00000042834	Nrep	neuronal regeneration related protein	-1.01	5.14E-04
ENSMUSG00000048337	Npy4r	neuropeptide Y receptor Y4	-1.01	1.03E-03
ENSMUSG00000003273	Car11	carbonic anhydrase 11	-1.01	8.75E-03
ENSMUSG00000049536	Tceal1	transcription elongation factor A (SII)-like 1	-1.01	4.51E-04
ENSMUSG00000027861	Casq2	calsequestrin 2	-1.01	9.14E-04
ENSMUSG00000022758	P2rx6	purinergic receptor P2X, ligand-gated ion channel, 6	-1.01	6.44E-03
ENSMUSG00000045871	Slitrk6	SLIT and NTRK-like family, member 6	-1.02	1.73E-04
ENSMUSG00000021684	Pde8b	phosphodiesterase 8B	-1.02	1.18E-06
ENSMUSG00000022474	Pmm1	phosphomannomutase 1	-1.02	7.43E-06
ENSMUSG00000039364	Sectm1b	secreted and transmembrane 1B	-1.02	6.29E-06
ENSMUSG00000020620	Abca8b	ATP-binding cassette, sub-family A (ABC1), member 8b	-1.02	4.22E-05
ENSMUSG00000071711	Mpst	mercaptopyruvate sulfurtransferase	-1.02	1.71E-07
ENSMUSG00000048388	Fam171b	family with sequence similarity 171, member B	-1.02	2.26E-04
ENSMUSG00000042498	D330045A20Rik	RIKEN cDNA D330045A20 gene	-1.02	1.23E-03
ENSMUSG00000043088	Il17re	interleukin 17 receptor E	-1.02	5.77E-04
ENSMUSG00000031647	Mfap3l	microfibrillar-associated protein 3-like	-1.02	7.32E-05
ENSMUSG00000021943	Gdf10	growth differentiation factor 10	-1.02	7.84E-03
ENSMUSG00000097184	4632428C04Rik	RIKEN cDNA 4632428C04 gene	-1.02	7.05E-03
ENSMUSG00000018796	Acsl1	acyl-CoA synthetase long-chain family member 1	-1.02	3.32E-06
ENSMUSG00000030321	Efcab12	EF-hand calcium binding domain 12	-1.03	8.19E-03
ENSMUSG00000044550	Tceal3	transcription elongation factor A (SII)-like 3	-1.03	6.38E-03
ENSMUSG00000055675	Kbtbd11	kelch repeat and BTB (POZ) domain containing 11	-1.03	1.59E-06
ENSMUSG00000032548	Slco2a1	solute carrier organic anion transporter family, member 2a1	-1.03	8.22E-06
ENSMUSG00000036390	Gadd45a	growth arrest and DNA-damage-inducible 45 alpha	-1.03	1.18E-04
ENSMUSG00000046589	Lrrc8e	leucine rich repeat containing 8 family, member E	-1.03	2.66E-05
ENSMUSG00000023046	Igfbp6	insulin-like growth factor binding protein 6	-1.03	6.56E-05
ENSMUSG00000021719	Rgs7bp	regulator of G-protein signalling 7 binding protein	-1.03	3.21E-05
ENSMUSG00000020774	Aspa	aspartoacylase	-1.03	3.30E-04
ENSMUSG00000070000	Fcho1	FCH domain only 1	-1.03	1.51E-04
ENSMUSG00000018861	Fdxr	ferredoxin reductase	-1.03	1.16E-05
ENSMUSG00000090626	Tex9	testis expressed gene 9	-1.03	6.61E-06

ENSMUSG00000030605	Mfge8	milk fat globule-EGF factor 8 protein	-1.04	6.21E-09
ENSMUSG00000048031	Fcrl5	Fc receptor-like 5	-1.04	5.78E-03
ENSMUSG00000037493	Cib2	calcium and integrin binding family member 2	-1.04	2.93E-03
ENSMUSG00000034308	Sdr42e1	short chain dehydrogenase/reductase family 42E, member 1	-1.04	3.00E-06
ENSMUSG00000019359	Gdpd2	glycerophosphodiester phosphodiesterase domain containing 2	-1.04	7.71E-04
ENSMUSG00000073557	Ppp1r12b	protein phosphatase 1, regulatory (inhibitor) subunit 12B	-1.04	1.00E-09
ENSMUSG00000016495	Plgrkt	plasminogen receptor, C-terminal lysine transmembrane protein	-1.04	2.26E-07
ENSMUSG00000019943	Atp2b1	ATPase, Ca++ transporting, plasma membrane 1	-1.04	3.30E-06
ENSMUSG00000083282	Ctsf	cathepsin F	-1.04	8.41E-06
ENSMUSG00000054477	Kcnn2	potassium intermediate/small conductance calcium-activated channel, subfamily N, member 2	-1.04	6.71E-03
ENSMUSG00000022445	Cyp2d26	cytochrome P450, family 2, subfamily d, polypeptide 26	-1.04	1.36E-05
ENSMUSG00000039329	Tex19.1	testis expressed gene 19.1	-1.05	7.09E-03
ENSMUSG00000076522			-1.05	3.48E-03
ENSMUSG00000026840	Lamc3	laminin gamma 3	-1.05	1.14E-03
ENSMUSG00000049086	Bmyc	brain expressed myelocytomatosis oncogene	-1.05	6.68E-03
ENSMUSG00000055546	Timd4	T cell immunoglobulin and mucin domain containing 4	-1.05	4.06E-05
ENSMUSG00000053963	6330403A02Rik	RIKEN cDNA 6330403A02 gene	-1.05	2.05E-06
ENSMUSG00000023829	Slc22a1	solute carrier family 22 (organic cation transporter), member 1	-1.05	7.71E-07
ENSMUSG00000037126	Psd	pleckstrin and Sec7 domain containing	-1.05	1.23E-06
ENSMUSG00000076670			-1.05	6.72E-03
ENSMUSG00000048096	Lmod1	leiomodin 1 (smooth muscle)	-1.06	6.01E-08
ENSMUSG00000017639	Rab11fip4	RAB11 family interacting protein 4 (class II)	-1.06	1.09E-06
ENSMUSG00000063529	Stmnd1	stathmin domain containing 1	-1.06	5.89E-03
ENSMUSG00000079507	H2-Q1	histocompatibility 2, Q region locus 1	-1.06	3.88E-05
ENSMUSG00000062496			-1.06	4.17E-03
ENSMUSG00000027359	Slc27a2	solute carrier family 27 (fatty acid transporter), member 2	-1.06	9.02E-06
ENSMUSG00000064351	COX1	cytochrome c oxidase subunit I	-1.06	8.88E-06
ENSMUSG00000020963	Tshr	thyroid stimulating hormone receptor	-1.06	5.25E-03
ENSMUSG00000032006	Pdgfd	platelet-derived growth factor, D polypeptide	-1.06	3.67E-05
ENSMUSG00000087528			-1.06	3.26E-03
ENSMUSG00000037855	Zfp365	zinc finger protein 365	-1.06	4.44E-03
ENSMUSG00000029821	Dfna5	deafness, autosomal dominant 5 (human)	-1.06	6.94E-06
ENSMUSG00000030724	Cd19	CD19 antigen	-1.06	1.58E-05
ENSMUSG00000078157	4931440F15Rik	RIKEN cDNA 4931440F15 gene	-1.07	5.99E-04
ENSMUSG00000036334	Igsf10	immunoglobulin superfamily, member 10	-1.07	3.48E-08
ENSMUSG00000004035	Gstm7	glutathione S-transferase, mu 7	-1.07	8.46E-05
ENSMUSG00000026012	Cd28	CD28 antigen	-1.07	1.40E-05
ENSMUSG00000061080	Lsamp	limbic system-associated membrane protein	-1.07	8.51E-04
ENSMUSG00000021379	Id4	inhibitor of DNA binding 4	-1.07	1.20E-05
ENSMUSG00000020607	Fam84a	family with sequence similarity 84, member A	-1.07	2.14E-03
ENSMUSG00000022389	Tef	thyrotroph embryonic factor	-1.07	2.62E-05
ENSMUSG00000022309	Angpt1	angiopoietin 1	-1.07	1.22E-04
ENSMUSG00000039956	Mrap	melanocortin 2 receptor accessory protein	-1.08	5.62E-03
ENSMUSG00000003477	Inmt	indolethylamine N-methyltransferase	-1.08	5.44E-03
ENSMUSG00000064778			-1.08	5.16E-03
ENSMUSG00000027792	Bche	butyrylcholinesterase	-1.08	6.09E-06

ENSMUSG00000001943	Vsig2	V-set and immunoglobulin domain containing 2	-1.08	6.59E-07
ENSMUSG00000028138	Adh5	alcohol dehydrogenase 5 (class III), chi polypeptide	-1.08	2.68E-07
ENSMUSG00000053519	Kcnip1	Kv channel-interacting protein 1	-1.08	8.35E-04
ENSMUSG00000015396	Cd83	CD83 antigen	-1.08	2.55E-07
ENSMUSG00000024600	Slc27a6	solute carrier family 27 (fatty acid transporter), member 6	-1.08	4.65E-03
ENSMUSG00000052957	Gas1	growth arrest specific 1	-1.08	1.87E-05
ENSMUSG00000024892	Pcx	pyruvate carboxylase	-1.08	7.96E-07
ENSMUSG00000020019	Ntn4	netrin 4	-1.09	5.76E-07
ENSMUSG00000030351	Tspan11	tetraspanin 11	-1.09	4.67E-03
ENSMUSG00000074004	B3gnt6	UDP-GlcNAc:betaGal beta-1,3-N-acetylglucosaminyltransferase 6 (core 3 synthase)	-1.09	2.26E-04
ENSMUSG00000053199	Arhgap20	Rho GTPase activating protein 20	-1.09	4.47E-07
ENSMUSG00000029333	Rasgef1b	RasGEF domain family, member 1B	-1.09	3.44E-06
ENSMUSG00000027282	Mtch2	mitochondrial carrier homolog 2 (C. elegans)	-1.09	8.71E-09
ENSMUSG00000086596	Susd5	sushi domain containing 5	-1.09	4.76E-03
ENSMUSG00000016283	H2-M2	histocompatibility 2, M region locus 2	-1.10	2.31E-03
ENSMUSG00000029630	Cyp3a25	cytochrome P450, family 3, subfamily a, polypeptide 25	-1.10	4.08E-03
ENSMUSG00000025498	Irf7	interferon regulatory factor 7	-1.10	8.03E-10
ENSMUSG00000074736	Syndig1	synapse differentiation inducing 1	-1.10	1.67E-04
ENSMUSG00000035811	Ugt2b35	UDP glucuronosyltransferase 2 family, polypeptide B35	-1.10	3.33E-07
ENSMUSG00000028919	Arhgef19	Rho guanine nucleotide exchange factor (GEF) 19	-1.10	6.90E-05
ENSMUSG00000089960	Ugt1a1	UDP glucuronosyltransferase 1 family, polypeptide A1	-1.10	4.79E-05
ENSMUSG00000022265	Ank	progressive ankylosis	-1.11	1.11E-08
ENSMUSG00000028039	Efna3	ephrin A3	-1.11	1.21E-03
ENSMUSG00000002308	Cd320	CD320 antigen	-1.11	4.44E-07
ENSMUSG00000017868	Sgk2	serum/glucocorticoid regulated kinase 2	-1.11	2.57E-04
ENSMUSG00000061356	Nuggc	nuclear GTPase, germinal center associated	-1.11	1.43E-04
ENSMUSG00000022853	Ehhadh	enoyl-Coenzyme A, hydratase/3-hydroxyacyl Coenzyme A dehydrogenase	-1.11	3.46E-09
ENSMUSG00000054545	Ugt1a6a	UDP glucuronosyltransferase 1 family, polypeptide A6A	-1.11	5.10E-06
ENSMUSG00000043631	Ecm2	extracellular matrix protein 2, female organ and adipocyte specific	-1.11	1.27E-06
ENSMUSG00000031886	Ces2e	carboxylesterase 2E	-1.11	2.94E-07
ENSMUSG00000027858	Tspan2	tetraspanin 2	-1.11	3.44E-06
ENSMUSG00000049336	Tenm2	teneurin transmembrane protein 2	-1.11	3.47E-04
ENSMUSG00000033152	Podxl2	podocalyxin-like 2	-1.11	1.20E-03
ENSMUSG00000023914	Mep1a	meprin 1 alpha	-1.11	3.19E-07
ENSMUSG00000023243	Kcnk5	potassium channel, subfamily K, member 5	-1.12	1.36E-06
ENSMUSG00000031712	Il15	interleukin 15	-1.12	1.50E-06
ENSMUSG00000028545	Bend5	BEN domain containing 5	-1.12	8.07E-05
ENSMUSG00000040289	Hey1	hairy/enhancer-of-split related with YRPW motif 1	-1.12	1.18E-03
ENSMUSG00000099215			-1.12	3.40E-03
ENSMUSG00000000903	Vpreb3	pre-B lymphocyte gene 3	-1.12	1.09E-03
ENSMUSG00000042155	Klhl23	kelch-like 23	-1.12	4.98E-08
ENSMUSG00000032064	Dixdc1	DIX domain containing 1	-1.12	1.34E-06
ENSMUSG00000058070	Eml1	echinoderm microtubule associated protein like 1	-1.12	2.15E-10
ENSMUSG00000078794	Dact3	dapper homolog 3, antagonist of beta-catenin (xenopus)	-1.12	5.21E-05
ENSMUSG00000046027	Stard5	StAR-related lipid transfer (START) domain containing 5	-1.13	4.96E-09
ENSMUSG00000029644	Pdx1	pancreatic and duodenal homeobox 1	-1.13	3.72E-03

ENSMUSG00000023094	Msrb2	methionine sulfoxide reductase B2	-1.13	5.63E-04
ENSMUSG00000055632	Hmcn2	hemicentin 2	-1.13	3.12E-09
ENSMUSG00000034528	Hsd17b13	hydroxysteroid (17-beta) dehydrogenase 13	-1.13	4.66E-05
ENSMUSG00000028033	Kcnq5	potassium voltage-gated channel, subfamily Q, member 5	-1.13	3.90E-04
ENSMUSG00000029811	Aoc1	amine oxidase, copper-containing 1	-1.13	1.68E-09
ENSMUSG00000055022	Cntn1	contactin 1	-1.13	1.28E-05
ENSMUSG00000030278	Cidec	cell death-inducing DFFA-like effector c	-1.13	5.32E-06
ENSMUSG00000024670	Cd6	CD6 antigen	-1.13	1.11E-03
ENSMUSG00000026574	Dpt	dermatopontin	-1.13	1.51E-08
ENSMUSG00000046329	Slc25a23	solute carrier family 25 (mitochondrial carrier; phosphate carrier), member 23	-1.13	4.96E-08
ENSMUSG00000068614	Actc1	actin, alpha, cardiac muscle 1	-1.14	6.05E-07
ENSMUSG00000001827	Folr1	folate receptor 1 (adult)	-1.14	3.44E-03
ENSMUSG00000045316	Fahd1	fumarylacetoacetate hydrolase domain containing 1	-1.14	2.77E-06
ENSMUSG00000034449	Dhrs11	dehydrogenase/reductase (SDR family) member 11	-1.14	1.31E-10
ENSMUSG00000030643	Rab30	RAB30, member RAS oncogene family	-1.14	1.01E-04
ENSMUSG00000060181	Slc35e3	solute carrier family 35, member E3	-1.14	7.77E-07
ENSMUSG00000033308	Dpyd	dihydropyrimidine dehydrogenase	-1.14	4.87E-07
ENSMUSG00000020439	Smtn	smoothelin	-1.14	1.26E-09
ENSMUSG00000024924	Vldlr	very low density lipoprotein receptor	-1.14	3.65E-06
ENSMUSG00000079470	Utp14b	UTP14, U3 small nucleolar ribonucleoprotein, homolog B (yeast)	-1.14	9.30E-07
ENSMUSG00000027863	Cd2	CD2 antigen	-1.14	3.52E-07
ENSMUSG00000028020	Glrb	glycine receptor, beta subunit	-1.14	2.47E-03
ENSMUSG00000029130	Rnf32	ring finger protein 32	-1.14	8.19E-05
ENSMUSG00000020672	Sntg2	syntrophin, gamma 2	-1.15	8.83E-07
ENSMUSG00000036278	Macrod1	MACRO domain containing 1	-1.15	5.00E-06
ENSMUSG00000021390	Ogn	osteoglycin	-1.15	1.81E-06
ENSMUSG00000014846	Tppp3	tubulin polymerization-promoting protein family member 3	-1.15	6.34E-07
ENSMUSG00000040896	Kcnd3	potassium voltage-gated channel, Shal-related family, member 3	-1.15	2.10E-08
ENSMUSG00000053783	1700016K19Rik	RIKEN cDNA 1700016K19 gene	-1.15	2.11E-03
ENSMUSG00000041378	Cldn5	claudin 5	-1.15	2.59E-04
ENSMUSG00000044986	Tst	thiosulfate sulfurtransferase, mitochondrial	-1.15	8.20E-10
ENSMUSG00000045441	Gprin3	GPRIN family member 3	-1.15	1.33E-05
ENSMUSG00000026415	Fcamr	Fc receptor, IgA, IgM, high affinity	-1.16	4.73E-05
ENSMUSG00000033342	Lppr5	lipid phosphate phosphatase-related protein type 5	-1.16	2.57E-03
ENSMUSG00000026062	Slc9a2	solute carrier family 9 (sodium/hydrogen exchanger), member 2	-1.16	2.03E-08
ENSMUSG00000025347	Mettl7b	methyltransferase like 7B	-1.16	1.04E-08
ENSMUSG00000032324	Tspan3	tetraspanin 3	-1.16	3.43E-07
ENSMUSG00000069814	E130309D14Rik	RIKEN cDNA E130309D14 gene	-1.16	1.55E-03
ENSMUSG00000025504	Eps8l2	EPS8-like 2	-1.16	1.83E-10
ENSMUSG00000046743	Fat4	FAT tumor suppressor homolog 4 (Drosophila)	-1.16	2.04E-11
ENSMUSG00000029499	Pxmp2	peroxisomal membrane protein 2	-1.16	2.67E-04
ENSMUSG00000001604	Tcea3	transcription elongation factor A (SII), 3	-1.16	1.86E-07
ENSMUSG00000063430	Wscd2	WSC domain containing 2	-1.16	4.11E-07
ENSMUSG00000059201	Lep	leptin	-1.17	1.84E-03
ENSMUSG00000057378	Ryr3	ryanodine receptor 3	-1.17	6.89E-07
ENSMUSG00000044749	Abca6	ATP-binding cassette, sub-family A (ABC1), member 6	-1.17	8.39E-05

ENSMUSG00000086706			-1.17	6.55E-04
ENSMUSG00000061728			-1.17	4.81E-05
ENSMUSG00000087291	Gm11946	predicted gene 11946	-1.18	1.01E-04
ENSMUSG00000019989	Enpp3	ectonucleotide pyrophosphatase/phosphodiesterase 3	-1.18	1.31E-06
ENSMUSG00000063873	Slc24a3	solute carrier family 24 (sodium/potassium/calcium exchanger), member 3	-1.18	1.35E-11
ENSMUSG00000095120			-1.18	1.92E-03
ENSMUSG00000033715	Akr1c14	aldo-keto reductase family 1, member C14	-1.18	6.22E-05
ENSMUSG00000005763	Cd247	CD247 antigen	-1.18	8.18E-05
ENSMUSG00000040703	Cyp2s1	cytochrome P450, family 2, subfamily s, polypeptide 1	-1.18	2.45E-09
ENSMUSG00000062257	Opcml	opioid binding protein/cell adhesion molecule-like	-1.19	3.96E-06
ENSMUSG00000019326	Aoc3	amine oxidase, copper containing 3	-1.19	6.00E-11
ENSMUSG00000038393	Txnip	thioredoxin interacting protein	-1.19	6.66E-11
ENSMUSG00000007038	Neu1	neuraminidase 1	-1.19	9.08E-09
ENSMUSG00000017453	Pipox	pipecolic acid oxidase	-1.19	2.20E-03
ENSMUSG00000020889	Nr1d1	nuclear receptor subfamily 1, group D, member 1	-1.19	8.23E-05
ENSMUSG00000004360	9330159F19Rik	RIKEN cDNA 9330159F19 gene	-1.19	3.52E-05
ENSMUSG00000023960	Enpp5	ectonucleotide pyrophosphatase/phosphodiesterase 5	-1.19	4.04E-10
ENSMUSG00000036218	Pdzrn4	PDZ domain containing RING finger 4	-1.19	7.67E-04
ENSMUSG00000042476	Abcb4	ATP-binding cassette, sub-family B (MDR/TAP), member 4	-1.19	1.98E-03
ENSMUSG00000050751	Pgbd5	piggyBac transposable element derived 5	-1.20	1.56E-04
ENSMUSG00000020811	Wscd1	WSC domain containing 1	-1.20	1.71E-03
ENSMUSG00000008193	Spib	Spi-B transcription factor (Spi-1/PU.1 related)	-1.20	6.64E-08
ENSMUSG00000004105	Angptl2	angiopoietin-like 2	-1.20	4.06E-08
ENSMUSG00000020431	Adcy1	adenylate cyclase 1	-1.20	2.44E-04
ENSMUSG00000079037	Prnp	prion protein	-1.20	4.97E-10
ENSMUSG00000020251	Glt8d2	glycosyltransferase 8 domain containing 2	-1.21	4.00E-04
ENSMUSG00000079355	Ackr4	atypical chemokine receptor 4	-1.21	5.98E-07
ENSMUSG00000074971	Fibin	fin bud initiation factor homolog (zebrafish)	-1.21	1.32E-05
ENSMUSG00000022479	Vdr	vitamin D receptor	-1.21	1.76E-09
ENSMUSG00000030409	Dmpk	dystrophia myotonica-protein kinase	-1.21	1.49E-11
ENSMUSG00000041660	Bbox1	butyrobetaine (gamma), 2-oxoglutarate dioxygenase 1 (gamma-butyrobetaine hydroxylase)	-1.21	1.78E-03
ENSMUSG00000028461	Ccdc107	coiled-coil domain containing 107	-1.21	2.94E-08
ENSMUSG00000027875	Hmgcs2	3-hydroxy-3-methylglutaryl-Coenzyme A synthase 2	-1.21	9.72E-10
ENSMUSG00000057123	Gja5	gap junction protein, alpha 5	-1.21	4.50E-05
ENSMUSG00000030092	Cntn6	contactin 6	-1.22	1.21E-03
ENSMUSG00000051079	Rgs13	regulator of G-protein signaling 13	-1.22	6.26E-04
ENSMUSG00000032134	Muc16	mucin 16	-1.22	4.20E-04
ENSMUSG00000002475	Abhd3	abhydrolase domain containing 3	-1.22	4.27E-05
ENSMUSG00000031938	4931406C07Rik	RIKEN cDNA 4931406C07 gene	-1.22	1.65E-08
ENSMUSG00000023959	Clic5	chloride intracellular channel 5	-1.22	1.61E-07
ENSMUSG00000073802	Cdkn2b	cyclin-dependent kinase inhibitor 2B (p15, inhibits CDK4)	-1.22	4.06E-08
ENSMUSG00000075318	Scn2a1	sodium channel, voltage-gated, type II, alpha 1	-1.23	5.24E-05
ENSMUSG00000032648	Pygm	muscle glycogen phosphorylase	-1.23	1.65E-07
ENSMUSG00000027894	Slc6a17	solute carrier family 6 (neurotransmitter transporter), member 17	-1.23	1.07E-05
ENSMUSG00000032883	Acsl3	acyl-CoA synthetase long-chain family member 3	-1.23	4.71E-08
ENSMUSG00000038967	Pdk2	pyruvate dehydrogenase kinase, isoenzyme 2	-1.23	1.46E-07

ENSMUSG00000005951	Shpk	sedoheptulokinase	-1.23	9.19E-07
ENSMUSG00000047462	A530099J19Rik	RIKEN cDNA A530099J19 gene	-1.23	3.50E-05
ENSMUSG00000032482	Cspg5	chondroitin sulfate proteoglycan 5	-1.23	1.15E-03
ENSMUSG00000027698	Nceh1	neutral cholesterol ester hydrolase 1	-1.23	5.88E-09
ENSMUSG00000024049	Myom1	myomesin 1	-1.23	2.63E-09
ENSMUSG00000003271	Sult2b1	sulfotransferase family, cytosolic, 2B, member 1	-1.24	6.82E-08
ENSMUSG00000027562	Car2	carbonic anhydrase 2	-1.24	8.35E-09
ENSMUSG00000022018	Rgcc	regulator of cell cycle	-1.24	3.03E-07
ENSMUSG00000076435	Acsf2	acyl-CoA synthetase family member 2	-1.24	8.04E-12
ENSMUSG00000018566	Slc2a4	solute carrier family 2 (facilitated glucose transporter), member 4	-1.24	4.67E-08
ENSMUSG00000071540	3425401B19Rik	RIKEN cDNA 3425401B19 gene	-1.24	1.40E-03
ENSMUSG00000084092			-1.24	1.26E-03
ENSMUSG00000063296	Tmem117	transmembrane protein 117	-1.24	7.35E-08
ENSMUSG00000021200	Asb2	ankyrin repeat and SOCS box-containing 2	-1.24	3.94E-09
ENSMUSG00000071604	Fam189a2	family with sequence similarity 189, member A2	-1.24	1.54E-11
ENSMUSG00000029134	Plb1	phospholipase B1	-1.24	3.93E-04
ENSMUSG00000056091	St3gal5	ST3 beta-galactoside alpha-2,3-sialyltransferase 5	-1.24	7.09E-07
ENSMUSG00000050103	Agmo	alkylglycerol monooxygenase	-1.25	1.61E-06
ENSMUSG00000032607	Amt	aminomethyltransferase	-1.25	2.73E-07
ENSMUSG00000037904	Ankrd9	ankyrin repeat domain 9	-1.25	3.99E-06
ENSMUSG00000038555	Reep2	receptor accessory protein 2	-1.25	1.54E-04
ENSMUSG00000027358	Bmp2	bone morphogenetic protein 2	-1.25	1.29E-08
ENSMUSG00000031636	Pdlim3	PDZ and LIM domain 3	-1.25	5.78E-11
ENSMUSG00000049811	Fam161a	family with sequence similarity 161, member A	-1.25	1.37E-05
ENSMUSG00000030577	Cd22	CD22 antigen	-1.25	1.74E-09
ENSMUSG00000031844	Hsd17b2	hydroxysteroid (17-beta) dehydrogenase 2	-1.25	5.22E-11
ENSMUSG00000060843	Ctnna3	catenin (cadherin associated protein), alpha 3	-1.25	2.70E-07
ENSMUSG00000061959	Ces1e	carboxylesterase 1E	-1.25	3.59E-07
ENSMUSG00000016552	Foxred2	FAD-dependent oxidoreductase domain containing 2	-1.26	3.97E-05
ENSMUSG00000031933	Izumo1r	IZUMO1 receptor, JUNO	-1.26	4.82E-04
ENSMUSG00000031173	Otc	ornithine transcarbamylase	-1.26	1.04E-06
ENSMUSG00000055653	Gpc3	glypican 3	-1.26	1.75E-08
ENSMUSG00000030865	Chp2	calcineurin-like EF hand protein 2	-1.27	3.37E-09
ENSMUSG00000038756	Ttll6	tubulin tyrosine ligase-like family, member 6	-1.27	7.98E-04
ENSMUSG00000024747	Aldh1a7	aldehyde dehydrogenase family 1, subfamily A7	-1.27	3.28E-07
ENSMUSG00000021792	Fam213a	family with sequence similarity 213, member A	-1.27	2.13E-09
ENSMUSG00000035184	Fam124a	family with sequence similarity 124, member A	-1.27	5.75E-06
ENSMUSG00000029838	Ptn	pleiotrophin	-1.27	1.34E-07
ENSMUSG00000041845	Rhod	ras homolog gene family, member D	-1.27	8.52E-06
ENSMUSG00000007097	Atp1a2	ATPase, Na+/K+ transporting, alpha 2 polypeptide	-1.27	4.04E-09
ENSMUSG00000029162	Khk	ketohexokinase	-1.28	3.28E-07
ENSMUSG00000061013	Mkx	mohawk homeobox	-1.28	6.54E-07
ENSMUSG00000097960	A330074K22Rik	RIKEN cDNA A330074K22 gene	-1.28	7.06E-04
ENSMUSG00000069601	Ank3	ankyrin 3, epithelial	-1.28	5.62E-09
ENSMUSG00000044860	Gm1123	predicted gene 1123	-1.28	8.33E-09
ENSMUSG00000092008	Cyp2c69	cytochrome P450, family 2, subfamily c, polypeptide 69	-1.28	9.04E-04

ENSMUSG00000058135	Gstm1	glutathione S-transferase, mu 1	-1.29	2.59E-10
ENSMUSG00000020182	Ddc	dopa decarboxylase	-1.29	2.24E-09
ENSMUSG00000052485	Tmem171	transmembrane protein 171	-1.29	1.62E-09
ENSMUSG00000004110	Cacna1e	calcium channel, voltage-dependent, R type, alpha 1E subunit	-1.29	1.82E-07
ENSMUSG00000055333	Fat2	FAT tumor suppressor homolog 2 (Drosophila)	-1.29	1.35E-04
ENSMUSG00000038526	Car14	carbonic anhydrase 14	-1.29	5.57E-04
ENSMUSG00000040147	Maob	monoamine oxidase B	-1.29	1.14E-09
ENSMUSG00000048498	Cd300e	CD300e antigen	-1.29	6.37E-04
ENSMUSG00000032085	Tagln	transgelin	-1.30	2.20E-14
ENSMUSG00000023336	Wfdc1	WAP four-disulfide core domain 1	-1.30	7.72E-08
ENSMUSG00000023073	Slc10a2	solute carrier family 10, member 2	-1.30	2.21E-04
ENSMUSG00000028255	Clca1	chloride channel calcium activated 1	-1.30	2.70E-13
ENSMUSG00000022383			-1.30	3.65E-10
ENSMUSG00000003849	Nqo1	NAD(P)H dehydrogenase, quinone 1	-1.30	1.52E-10
ENSMUSG00000042751	Nmnat2	nicotinamide nucleotide adenylyltransferase 2	-1.30	7.72E-07
ENSMUSG00000025037	Maoa	monoamine oxidase A	-1.30	4.03E-10
ENSMUSG00000023800	Tiam2	T cell lymphoma invasion and metastasis 2	-1.30	2.02E-09
ENSMUSG00000025780	Itih5	inter-alpha (globulin) inhibitor H5	-1.30	1.96E-11
ENSMUSG00000041828	Abca8a	ATP-binding cassette, sub-family A (ABC1), member 8a	-1.30	1.79E-09
ENSMUSG00000048304	Slitrk3	SLIT and NTRK-like family, member 3	-1.31	1.89E-04
ENSMUSG00000069919	Hba-a1	hemoglobin alpha, adult chain 1	-1.31	2.24E-06
ENSMUSG00000029273	Sult1d1	sulfotransferase family 1D, member 1	-1.31	1.67E-05
ENSMUSG00000039063	Echdc3	enoyl Coenzyme A hydratase domain containing 3	-1.31	3.74E-06
ENSMUSG00000029260	Ugt2b34	UDP glucuronosyltransferase 2 family, polypeptide B34	-1.31	1.17E-08
ENSMUSG00000064202	4430402I18Rik	RIKEN cDNA 4430402I18 gene	-1.31	5.11E-04
ENSMUSG00000038421	Fcrla	Fc receptor-like A	-1.31	6.55E-08
ENSMUSG00000020081	Tacr2	tachykinin receptor 2	-1.31	2.36E-09
ENSMUSG00000025731	0610011F06Rik	RIKEN cDNA 0610011F06 gene	-1.32	1.08E-10
ENSMUSG00000059994	Fcrl1	Fc receptor-like 1	-1.32	5.22E-08
ENSMUSG00000020839	Tmigd1	transmembrane and immunoglobulin domain containing 1	-1.32	3.97E-05
ENSMUSG00000032902	Slc16a1	solute carrier family 16 (monocarboxylic acid transporters), member 1	-1.32	7.89E-12
ENSMUSG00000029727	Cyp3a13	cytochrome P450, family 3, subfamily a, polypeptide 13	-1.32	1.13E-09
ENSMUSG00000055730	Ces2a	carboxylesterase 2A	-1.32	3.87E-04
ENSMUSG00000027820	Mme	membrane metallo endopeptidase	-1.32	4.90E-05
ENSMUSG00000046959	Slc26a1	solute carrier family 26 (sulfate transporter), member 1	-1.32	1.15E-09
ENSMUSG00000018659	Pnpo	pyridoxine 5'-phosphate oxidase	-1.33	8.86E-11
ENSMUSG00000040543	Pitpnm3	PITPNM family member 3	-1.33	1.45E-08
ENSMUSG00000006345	Ggt1	gamma-glutamyltransferase 1	-1.33	3.47E-07
ENSMUSG00000020732	Rab37	RAB37, member RAS oncogene family	-1.33	3.38E-06
ENSMUSG00000050505	Pcdh20	protocadherin 20	-1.33	4.95E-04
ENSMUSG00000026452	Syt2	synaptotagmin II	-1.33	1.18E-04
ENSMUSG00000034842	Art3	ADP-ribosyltransferase 3	-1.33	6.48E-08
ENSMUSG00000031700	Gpt2	glutamic pyruvate transaminase (alanine aminotransferase) 2	-1.33	3.76E-10
ENSMUSG00000061100	Retnla	resistin like alpha	-1.34	4.25E-04
ENSMUSG00000061808	Ttr	transthyretin	-1.34	7.98E-08
ENSMUSG00000026463	Atp2b4	ATPase, Ca++ transporting, plasma membrane 4	-1.34	1.91E-15

ENSMUSG00000039323	Igfbp2	insulin-like growth factor binding protein 2	-1.34	1.87E-05
ENSMUSG00000064267	Hvcn1	hydrogen voltage-gated channel 1	-1.34	6.02E-10
ENSMUSG00000040413	Timd2	T cell immunoglobulin and mucin domain containing 2	-1.34	5.05E-04
ENSMUSG00000014030	Pax5	paired box 5	-1.35	1.05E-07
ENSMUSG00000039691	Tspan10	tetraspanin 10	-1.35	4.83E-04
ENSMUSG00000001334	Fndc5	fibronectin type III domain containing 5	-1.35	3.80E-06
ENSMUSG00000018570	2810408A11Rik	RIKEN cDNA 2810408A11 gene	-1.35	4.64E-06
ENSMUSG00000042474	Faim3	Fas apoptotic inhibitory molecule 3	-1.36	2.73E-09
ENSMUSG00000026208	Des	desmin	-1.36	1.96E-16
ENSMUSG00000074210			-1.36	1.74E-04
ENSMUSG00000020080	Hkdc1	hexokinase domain containing 1	-1.36	2.19E-08
ENSMUSG00000038209	Itln1	intelectin 1 (galactofuranose binding)	-1.36	6.99E-11
ENSMUSG00000004038	Gstm3	glutathione S-transferase, mu 3	-1.37	3.59E-05
ENSMUSG00000003949	Hlf	hepatic leukemia factor	-1.37	6.61E-08
ENSMUSG00000034687	Fras1	Fraser syndrome 1 homolog (human)	-1.37	2.15E-06
ENSMUSG00000068762	Gstm6	glutathione S-transferase, mu 6	-1.37	4.33E-07
ENSMUSG00000024978	Gpam	glycerol-3-phosphate acyltransferase, mitochondrial	-1.37	4.09E-12
ENSMUSG00000024076	Vit	vitrin	-1.37	4.81E-05
ENSMUSG00000062410	Hsd3b3	hydroxy-delta-5-steroid dehydrogenase, 3 beta- and steroid delta-isomerase 3	-1.37	4.07E-11
ENSMUSG00000028976	Slc2a5	solute carrier family 2 (facilitated glucose transporter), member 5	-1.38	2.15E-05
ENSMUSG00000070498	Tmem132b	transmembrane protein 132B	-1.38	2.77E-04
ENSMUSG00000079440	Alpi	alkaline phosphatase, intestinal	-1.38	8.51E-09
ENSMUSG00000028737	Aldh4a1	aldehyde dehydrogenase 4 family, member A1	-1.38	2.06E-06
ENSMUSG00000026616	Cr2	complement receptor 2	-1.38	1.73E-10
ENSMUSG00000024292	Cyp4f14	cytochrome P450, family 4, subfamily f, polypeptide 14	-1.38	4.97E-09
ENSMUSG00000034324	Tmem132c	transmembrane protein 132C	-1.38	2.98E-05
ENSMUSG00000038591	Colec10	collectin sub-family member 10	-1.38	1.11E-07
ENSMUSG00000040812	Agbl2	ATP/GTP binding protein-like 2	-1.39	7.53E-07
ENSMUSG00000038167	Plekhg6	pleckstrin homology domain containing, family G (with RhoGef domain) member 6	-1.39	5.54E-09
ENSMUSG00000032010	Usp2	ubiquitin specific peptidase 2	-1.39	3.09E-07
ENSMUSG00000038370	Pcp4l1	Purkinje cell protein 4-like 1	-1.39	9.46E-12
ENSMUSG00000042254	Cilp	cartilage intermediate layer protein, nucleotide pyrophosphohydrolase	-1.40	1.75E-10
ENSMUSG00000094091	Gm21885	predicted gene, 21885	-1.40	2.12E-07
ENSMUSG00000068877	Selenbp2	selenium binding protein 2	-1.41	3.89E-10
ENSMUSG00000094924			-1.41	2.46E-05
ENSMUSG00000020068			-1.41	8.10E-07
ENSMUSG00000029095	Ablim2	actin-binding LIM protein 2	-1.41	3.67E-06
ENSMUSG00000050315	Synpo2	synaptopodin 2	-1.41	3.16E-18
ENSMUSG00000034936	Arl4d	ADP-ribosylation factor-like 4D	-1.41	3.26E-07
ENSMUSG00000026676	Ccdc3	coiled-coil domain containing 3	-1.42	2.51E-08
ENSMUSG00000029772	Ahcyl2	S-adenosylhomocysteine hydrolase-like 2	-1.42	6.34E-13
ENSMUSG00000047880	Cxcr5	chemokine (C-X-C motif) receptor 5	-1.42	4.43E-09
ENSMUSG00000040666	Sh3bgr	SH3-binding domain glutamic acid-rich protein	-1.42	5.46E-08
ENSMUSG00000028088	Fmo5	flavin containing monooxygenase 5	-1.42	1.69E-09
ENSMUSG00000057346	Apol9a	apolipoprotein L 9a	-1.43	1.56E-04
ENSMUSG00000087582			-1.43	1.20E-04

ENSMUSG00000034157	Cipc	CLOCK interacting protein, circadian	-1.43	9.09E-10
ENSMUSG00000038173	Enpp6	ectonucleotide pyrophosphatase/phosphodiesterase 6	-1.43	4.64E-05
ENSMUSG00000026489	Adck3	aarF domain containing kinase 3	-1.43	2.15E-09
ENSMUSG00000090223	Pcp4	Purkinje cell protein 4	-1.43	4.69E-05
ENSMUSG00000028179	Cth	cystathionase (cystathionine gamma-lyase)	-1.44	8.14E-12
ENSMUSG00000015354	Pcolce2	procollagen C-endopeptidase enhancer 2	-1.45	3.13E-07
ENSMUSG00000047496	Rnf152	ring finger protein 152	-1.45	1.32E-10
ENSMUSG00000001663	Gstt1	glutathione S-transferase, theta 1	-1.45	1.80E-09
ENSMUSG00000047146	Tet1	tet methylcytosine dioxygenase 1	-1.46	1.07E-08
ENSMUSG00000005540	Fcer2a	Fc receptor, IgE, low affinity II, alpha polypeptide	-1.46	3.78E-09
ENSMUSG00000025528	2010106E10Rik	RIKEN cDNA 2010106E10 gene	-1.46	8.13E-05
ENSMUSG00000019945	1700040L02Rik	RIKEN cDNA 1700040L02 gene	-1.46	1.25E-06
ENSMUSG00000029201	Ugdh	UDP-glucose dehydrogenase	-1.46	1.54E-12
ENSMUSG00000029603	Dtx1	deltex 1 homolog (Drosophila)	-1.46	1.97E-09
ENSMUSG00000074207	Adh1	alcohol dehydrogenase 1 (class I)	-1.46	1.86E-11
ENSMUSG00000047394	Odf3b	outer dense fiber of sperm tails 3B	-1.47	1.44E-04
ENSMUSG00000029309	Sparcl1	SPARC-like 1	-1.47	5.69E-17
ENSMUSG00000025545	Clybl	citrate lyase beta like	-1.47	2.26E-10
ENSMUSG00000013415	Igf2bp1	insulin-like growth factor 2 mRNA binding protein 1	-1.48	7.64E-07
ENSMUSG00000001225	Slc26a3	solute carrier family 26, member 3	-1.48	9.42E-10
ENSMUSG00000041073	Nacad	NAC alpha domain containing	-1.48	1.47E-09
ENSMUSG00000028464	Tpm2	tropomyosin 2, beta	-1.48	1.58E-17
ENSMUSG00000057880	Abat	4-aminobutyrate aminotransferase	-1.48	1.14E-12
ENSMUSG00000025213	Kazald1	Kazal-type serine peptidase inhibitor domain 1	-1.48	6.26E-05
ENSMUSG00000050860	Phospho1	phosphatase, orphan 1	-1.49	8.39E-05
ENSMUSG00000021319	Sfrp4	secreted frizzled-related protein 4	-1.50	8.68E-07
ENSMUSG00000022425	Enpp2	ectonucleotide pyrophosphatase/phosphodiesterase 2	-1.50	4.55E-16
ENSMUSG00000024899	Papss2	3'-phosphoadenosine 5'-phosphosulfate synthase 2	-1.50	8.21E-11
ENSMUSG00000094651	Gal3st2	galactose-3-O-sulfotransferase 2	-1.50	3.95E-10
ENSMUSG00000068748	Ptprz1	protein tyrosine phosphatase, receptor type Z, polypeptide 1	-1.50	1.11E-06
ENSMUSG00000045725	Prr15	proline rich 15	-1.50	1.31E-11
ENSMUSG00000054630	Ugt2b5	UDP glucuronosyltransferase 2 family, polypeptide B5	-1.51	2.26E-10
ENSMUSG00000006360	Crip1	cysteine-rich protein 1 (intestinal)	-1.51	6.69E-13
ENSMUSG00000025176	Hoga1	4-hydroxy-2-oxoglutarate aldolase 1	-1.51	2.79E-07
ENSMUSG00000067818	Myl9	myosin, light polypeptide 9, regulatory	-1.51	6.31E-20
ENSMUSG00000041559	Fmod	fibromodulin	-1.52	3.67E-06
ENSMUSG00000059430	Actg2	actin, gamma 2, smooth muscle, enteric	-1.53	5.60E-14
ENSMUSG00000026614	Slc30a10	solute carrier family 30, member 10	-1.53	1.13E-05
ENSMUSG00000022040	Ephx2	epoxide hydrolase 2, cytoplasmic	-1.53	3.39E-11
ENSMUSG00000040627	Aicda	activation-induced cytidine deaminase	-1.53	7.67E-06
ENSMUSG00000023057	Fabp2	fatty acid binding protein 2, intestinal	-1.53	6.13E-06
ENSMUSG00000070704	Ugt2b36	UDP glucuronosyltransferase 2 family, polypeptide B36	-1.54	1.60E-05
ENSMUSG00000026418	Tnni1	troponin I, skeletal, slow 1	-1.54	9.60E-06
ENSMUSG00000038776	Ephx1	epoxide hydrolase 1, microsomal	-1.54	2.43E-14
ENSMUSG00000049971	Glt1d1	glycosyltransferase 1 domain containing 1	-1.54	4.49E-08
ENSMUSG00000025196	Cpn1	carboxypeptidase N, polypeptide 1	-1.54	8.33E-10

ENSMUSG00000074218	Cox7a1	cytochrome c oxidase subunit VIIa 1	-1.55	7.85E-13
ENSMUSG00000035557	Krt17	keratin 17	-1.56	2.65E-08
ENSMUSG00000018830	Myh11	myosin, heavy polypeptide 11, smooth muscle	-1.56	3.93E-20
ENSMUSG00000059898	Dsc3	desmocollin 3	-1.57	5.72E-07
ENSMUSG00000044309	Apol7c	apolipoprotein L 7c	-1.57	1.44E-07
ENSMUSG00000040592	Cd79b	CD79B antigen	-1.58	8.44E-13
ENSMUSG00000009075	Cabp7	calcium binding protein 7	-1.59	3.00E-05
ENSMUSG00000032854	Ugt8a	UDP galactosyltransferase 8A	-1.60	1.56E-05
ENSMUSG00000045348	Nyap1	neuronal tyrosine-phosphorylated phosphoinositide 3-kinase adaptor 1	-1.60	1.30E-08
ENSMUSG00000051228	Nyx	nyctalopin	-1.61	6.80E-06
ENSMUSG00000021573	Tppp	tubulin polymerization promoting protein	-1.61	9.59E-13
ENSMUSG00000028713	Cyp4b1	cytochrome P450, family 4, subfamily b, polypeptide 1	-1.61	2.61E-07
ENSMUSG00000030554	Synm	synemin, intermediate filament protein	-1.62	2.14E-20
ENSMUSG00000027513	Pck1	phosphoenolpyruvate carboxykinase 1, cytosolic	-1.62	2.70E-14
ENSMUSG00000036123	Slc9a3	solute carrier family 9 (sodium/hydrogen exchanger), member 3	-1.62	6.72E-07
ENSMUSG00000019278	Dpep1	dipeptidase 1 (renal)	-1.62	5.17E-16
ENSMUSG00000026166	Ccl20	chemokine (C-C motif) ligand 20	-1.64	9.44E-07
ENSMUSG00000038550	Ciart	circadian associated repressor of transcription	-1.64	6.38E-08
ENSMUSG00000053399	Adamts18	a disintegrin-like and metallopeptidase (reprolysin type) with thrombospondin type 1 motif, 18	-1.64	1.50E-05
ENSMUSG00000003379	Cd79a	CD79A antigen (immunoglobulin-associated alpha)	-1.64	7.90E-13
ENSMUSG00000081169			-1.66	1.14E-06
ENSMUSG00000074882	Cyp2c68	cytochrome P450, family 2, subfamily c, polypeptide 68	-1.67	6.22E-07
ENSMUSG00000002565	Scin	scinderin	-1.67	2.99E-14
ENSMUSG00000027761	Aadac	arylacetamide deacetylase (esterase)	-1.67	6.40E-09
ENSMUSG00000030546	Plin1	perilipin 1	-1.67	9.42E-08
ENSMUSG00000030256	Bhlhe41	basic helix-loop-helix family, member e41	-1.67	4.21E-10
ENSMUSG00000025479	Cyp2e1	cytochrome P450, family 2, subfamily e, polypeptide 1	-1.67	1.15E-07
ENSMUSG00000025658	Cnksr2	connector enhancer of kinase suppressor of Ras 2	-1.67	4.31E-08
ENSMUSG00000061780	Cfd	complement factor D (adipsin)	-1.68	5.85E-10
ENSMUSG00000068105	Tnfrsf13c	tumor necrosis factor receptor superfamily, member 13c	-1.69	3.80E-13
ENSMUSG00000041012	Cmtm8	CKLF-like MARVEL transmembrane domain containing 8	-1.69	6.17E-10
ENSMUSG00000021236	Entpd5	ectonucleoside triphosphate diphosphohydrolase 5	-1.70	7.66E-16
ENSMUSG00000028755	Cda	cytidine deaminase	-1.70	4.46E-12
ENSMUSG00000034579	Pla2g3	phospholipase A2, group III	-1.70	1.00E-11
ENSMUSG00000098132	Rassf10	Ras association (RalGDS/AF-6) domain family (N-terminal) member 10	-1.71	1.23E-07
ENSMUSG00000019890	Nts	neurotensin	-1.71	1.27E-14
ENSMUSG00000019970	Sgk1	serum/glucocorticoid regulated kinase 1	-1.72	2.71E-09
ENSMUSG00000034785	Dio1	deiodinase, iodothyronine, type I	-1.72	2.31E-13
ENSMUSG00000052131	Akr1b7	aldo-keto reductase family 1, member B7	-1.72	2.39E-06
ENSMUSG00000068874	Selenbp1	selenium binding protein 1	-1.72	4.90E-14
ENSMUSG00000060548	Tnfrsf19	tumor necrosis factor receptor superfamily, member 19	-1.73	1.13E-08
ENSMUSG00000051726	Kcnf1	potassium voltage-gated channel, subfamily F, member 1	-1.74	2.36E-09
ENSMUSG00000041202	Pla2g2d	phospholipase A2, group IID	-1.74	1.56E-14
ENSMUSG00000029369	Afm	afamin	-1.74	3.77E-13
ENSMUSG00000040584	Abcb1a	ATP-binding cassette, sub-family B (MDR/TAP), member 1A	-1.75	1.48E-07
ENSMUSG00000033207	Mamdc2	MAM domain containing 2	-1.75	1.02E-13

ENSMUSG00000051295	9630028B13Rik	RIKEN cDNA 9630028B13 gene	-1.75	1.95E-11
ENSMUSG00000024673	Ms4a1	membrane-spanning 4-domains, subfamily A, member 1	-1.77	1.11E-15
ENSMUSG00000060780	Lrrtm1	leucine rich repeat transmembrane neuronal 1	-1.77	2.90E-06
ENSMUSG00000027559	Car3	carbonic anhydrase 3	-1.78	2.38E-09
ENSMUSG00000017607	Tns4	tensin 4	-1.78	3.68E-14
ENSMUSG00000022878	Adipoq	adiponectin, C1Q and collagen domain containing	-1.79	6.04E-12
ENSMUSG00000073608	Gm6086	predicted gene 6086	-1.79	1.82E-08
ENSMUSG00000095385	D630033O11Rik	RIKEN cDNA D630033O11 gene	-1.81	1.82E-06
ENSMUSG00000027556	Car1	carbonic anhydrase 1	-1.81	7.67E-17
ENSMUSG00000053279	Aldh1a1	aldehyde dehydrogenase family 1, subfamily A1	-1.81	8.60E-16
ENSMUSG00000001349	Cnn1	calponin 1	-1.81	7.98E-26
ENSMUSG00000069917	Hba-a2	hemoglobin alpha, adult chain 2	-1.81	5.54E-10
ENSMUSG00000022546	Gpt	glutamic pyruvic transaminase, soluble	-1.82	7.99E-13
ENSMUSG00000027401	Tgm3	transglutaminase 3, E polypeptide	-1.84	1.86E-06
ENSMUSG00000039760	Il22ra2	interleukin 22 receptor, alpha 2	-1.84	8.30E-13
ENSMUSG00000073424	Cyp4f15	cytochrome P450, family 4, subfamily f, polypeptide 15	-1.84	6.43E-07
ENSMUSG00000019762	Iyd	iodotyrosine deiodinase	-1.84	3.35E-08
ENSMUSG00000061825	Ces2c	carboxylesterase 2C	-1.86	1.36E-14
ENSMUSG00000027870	Hao2	hydroxyacid oxidase 2	-1.87	1.64E-15
ENSMUSG00000024727	Trpm6	transient receptor potential cation channel, subfamily M, member 6	-1.88	9.73E-09
ENSMUSG00000054619	Mettl7a1	methyltransferase like 7A1	-1.88	2.83E-18
ENSMUSG00000025002	Cyp2c55	cytochrome P450, family 2, subfamily c, polypeptide 55	-1.88	9.75E-07
ENSMUSG00000060600	Eno3	enolase 3, beta muscle	-1.90	2.16E-14
ENSMUSG00000062760	1810041L15Rik	RIKEN cDNA 1810041L15 gene	-1.90	2.20E-10
ENSMUSG00000030762	Aqp8	aquaporin 8	-1.91	3.29E-08
ENSMUSG00000026701	Prdx6	peroxiredoxin 6	-1.95	6.57E-17
ENSMUSG00000040405	Havcr1	hepatitis A virus cellular receptor 1	-1.97	1.68E-07
ENSMUSG00000031937	Vstm5	V-set and transmembrane domain containing 5	-1.98	1.46E-09
ENSMUSG00000060615	Ang4	angiogenin, ribonuclease A family, member 4	-1.99	6.99E-10
ENSMUSG00000043439	E130012A19Rik	RIKEN cDNA E130012A19 gene	-2.00	2.29E-15
ENSMUSG00000020334	Slc22a4	solute carrier family 22 (organic cation transporter), member 4	-2.00	1.57E-10
ENSMUSG00000084174	Sycn	syncollin	-2.04	4.10E-15
ENSMUSG00000031725	Ces1f	carboxylesterase 1F	-2.04	8.44E-21
ENSMUSG00000056973	Ces1d	carboxylesterase 1D	-2.06	3.08E-20
ENSMUSG00000099065			-2.07	3.71E-16
ENSMUSG00000030711	Sult1a1	sulfotransferase family 1A, phenol-preferring, member 1	-2.08	8.95E-13
ENSMUSG00000027397	Slc20a1	solute carrier family 20, member 1	-2.09	3.90E-18
ENSMUSG00000090136	Gm10177	predicted gene 10177	-2.14	3.04E-09
ENSMUSG00000049580	Tsku	tsukushi	-2.16	1.11E-17
ENSMUSG00000081488			-2.18	3.17E-14
ENSMUSG00000000805	Car4	carbonic anhydrase 4	-2.18	3.96E-24
ENSMUSG00000020793	Galr2	galanin receptor 2	-2.23	1.24E-11
ENSMUSG00000059824	Dbp	D site albumin promoter binding protein	-2.25	2.95E-14
ENSMUSG00000037762	Slc16a9	solute carrier family 16 (monocarboxylic acid transporters), member 9	-2.25	1.05E-24
ENSMUSG00000092586	Ly6g6c	lymphocyte antigen 6 complex, locus G6C	-2.26	2.27E-09
ENSMUSG00000024575	Pde6a	phosphodiesterase 6A, cGMP-specific, rod, alpha	-2.28	1.37E-13

ENSMUSG00000037071	Scd1	stearoyl-Coenzyme A desaturase 1	-2.31	1.06E-12
ENSMUSG00000035686	Thrsp	thyroid hormone responsive	-2.31	4.06E-11
ENSMUSG00000085375			-2.31	1.72E-12
ENSMUSG00000030399	Ckm	creatine kinase, muscle	-2.32	1.73E-25
ENSMUSG00000012705	Retn	resistin	-2.35	1.07E-12
ENSMUSG00000010311	Optc	opticin	-2.76	1.20E-26
ENSMUSG00000032122	Slc37a2	solute carrier family 37 (glycerol-3-phosphate transporter), member 2	-3.00	3.32E-24
ENSMUSG00000057074	Ces1g	carboxylesterase 1G	-3.01	7.47E-21
ENSMUSG00000022491	Glycam1	glycosylation dependent cell adhesion molecule 1	-3.17	3.85E-44

Table S3 Differentially expressed genes of BALB/c (YPIII Δ*cnfy* infected 5 dpi vs. uninfected 5 dpi)

Ensembl ID	Gene-symbol	Gene name	lo_2 fold change	p-value
ENSMUSG00000032068	Plet1	placenta expressed transcript 1	4.17	1.64E-42
ENSMUSG00000027398	Il1b	interleukin 1 beta	3.99	1.53E-35
ENSMUSG00000022126	Irg1	immunoresponsive gene 1	3.82	9.40E-35
ENSMUSG00000026822	Lcn2	lipocalin 2	3.77	1.09E-30
ENSMUSG00000020826	Nos2	nitric oxide synthase 2, inducible	3.69	7.60E-33
ENSMUSG00000029417	Cxcl9	chemokine (C-X-C motif) ligand 9	3.57	2.06E-26
ENSMUSG00000043613	Mmp3	matrix metallopeptidase 3	3.40	1.22E-23
ENSMUSG00000028859	Csf3r	colony stimulating factor 3 receptor (granulocyte)	3.38	1.04E-30
ENSMUSG00000064246	Chil1	chitinase-like 1	3.31	7.68E-25
ENSMUSG00000044162	Tnip3	TNFAIP3 interacting protein 3	3.30	1.53E-39
ENSMUSG00000052270	Fpr2	formyl peptide receptor 2	3.28	1.50E-24
ENSMUSG00000034855	Cxcl10	chemokine (C-X-C motif) ligand 10	3.27	4.14E-24
ENSMUSG00000075602	Ly6a	lymphocyte antigen 6 complex, locus A	3.26	6.72E-40
ENSMUSG00000058427	Cxcl2	chemokine (C-X-C motif) ligand 2	3.21	5.75E-20
ENSMUSG00000030142	Clec4e	C-type lectin domain family 4, member e	3.21	8.54E-18
ENSMUSG00000029371	Cxcl5	chemokine (C-X-C motif) ligand 5	3.16	2.34E-16
ENSMUSG00000031444	F10	coagulation factor X	3.09	7.57E-20
ENSMUSG00000054072	Iigp1	interferon inducible GTPase 1	3.09	7.99E-20
ENSMUSG00000040264	Gbp2b	guanylate binding protein 2b	3.02	1.50E-22
ENSMUSG00000031551	Ido1	indoleamine 2,3-dioxygenase 1	2.97	2.82E-29
ENSMUSG00000024697	Gna14	guanine nucleotide binding protein, alpha 14	2.97	1.79E-29
ENSMUSG00000041481			2.96	3.86E-34
ENSMUSG00000027399	Il1a	interleukin 1 alpha	2.95	4.38E-20
ENSMUSG00000029380	Cxcl1	chemokine (C-X-C motif) ligand 1	2.86	2.27E-16
ENSMUSG00000001131	Timp1	tissue inhibitor of metalloproteinase 1	2.86	7.76E-18
ENSMUSG00000079363	Gbp4	guanylate binding protein 4	2.85	7.24E-20
ENSMUSG00000000204	Slfn4	schlafen 4	2.84	2.68E-27
ENSMUSG00000042265	Trem1	triggering receptor expressed on myeloid cells 1	2.84	1.64E-14
ENSMUSG00000030144	Clec4d	C-type lectin domain family 4, member d	2.81	1.42E-14
ENSMUSG00000041193	Pla2g5	phospholipase A2, group V	2.81	2.18E-27
ENSMUSG00000031722	Hp	haptoglobin	2.81	1.02E-16
ENSMUSG00000074195	Clca4b	chloride channel calcium activated 4B	2.81	1.86E-15
ENSMUSG00000028527	Ak4	adenylate kinase 4	2.80	3.55E-20

ENSMUSG00000040026	Saa3	serum amyloid A 3	2.79	3.41E-18
ENSMUSG00000073555	Gm4951	predicted gene 4951	2.78	9.94E-25
ENSMUSG00000090942	F830016B08Rik	RIKEN cDNA F830016B08 gene	2.77	4.47E-21
ENSMUSG00000066363	Serpina3f	serine (or cysteine) peptidase inhibitor, clade A, member 3F	2.77	9.55E-21
ENSMUSG00000082976	Gm15056	predicted gene 15056	2.77	1.11E-13
ENSMUSG00000078922	Tgtp1	T cell specific GTPase 1	2.75	1.39E-16
ENSMUSG00000024411	Aqp4	aquaporin 4	2.74	7.94E-19
ENSMUSG00000079362	Gbp6	guanylate binding protein 6	2.74	6.97E-21
ENSMUSG00000060183	Cxcl11	chemokine (C-X-C motif) ligand 11	2.72	3.27E-14
ENSMUSG00000047562	Mmp10	matrix metallopeptidase 10	2.72	1.56E-12
ENSMUSG00000025877	Hk3	hexokinase 3	2.70	1.14E-16
ENSMUSG00000012428	Steap4	STEAP family member 4	2.67	2.02E-28
ENSMUSG00000056071	S100a9	S100 calcium binding protein A9 (calgranulin B)	2.67	6.72E-12
ENSMUSG00000054588			2.67	2.64E-13
ENSMUSG00000032691	Nlrp3	NLR family, pyrin domain containing 3	2.65	1.97E-17
ENSMUSG00000022582	Ly6g	lymphocyte antigen 6 complex, locus G	2.64	1.97E-18
ENSMUSG00000030187	Klra2	killer cell lectin-like receptor, subfamily A, member 2	2.63	1.42E-17
ENSMUSG00000047728	BC025446	cDNA sequence BC025446	2.63	7.89E-15
ENSMUSG00000049281	Scn3b	sodium channel, voltage-gated, type III, beta	2.59	1.70E-17
ENSMUSG00000034438	Gbp8	guanylate-binding protein 8	2.55	1.73E-20
ENSMUSG00000085977			2.55	6.24E-13
ENSMUSG00000005800	Mmp8	matrix metallopeptidase 8	2.55	5.66E-12
ENSMUSG00000028655	Mfsd2a	major facilitator superfamily domain containing 2A	2.54	6.39E-12
ENSMUSG00000078921	Tgtp2	T cell specific GTPase 2	2.53	2.69E-18
ENSMUSG00000055978	Fut2	fucosyltransferase 2	2.50	8.08E-25
ENSMUSG00000027068	Dhrs9	dehydrogenase/reductase (SDR family) member 9	2.50	7.15E-26
ENSMUSG00000059089	Fcgr4	Fc receptor, IgG, low affinity IV	2.49	4.22E-20
ENSMUSG00000068452	Duox2	dual oxidase 2	2.49	3.32E-23
ENSMUSG00000048852	Gm12185	predicted gene 12185	2.41	4.40E-14
ENSMUSG00000053113	Socs3	suppressor of cytokine signaling 3	2.41	2.17E-14
ENSMUSG00000068606	Gm4841	predicted gene 4841	2.41	2.48E-14
ENSMUSG00000009185	Ccl8	chemokine (C-C motif) ligand 8	2.36	1.07E-17
ENSMUSG00000021091	Serpina3n	serine (or cysteine) peptidase inhibitor, clade A, member 3N	2.35	2.28E-25
ENSMUSG00000089672	Gp49a	glycoprotein 49 A	2.33	1.53E-15
ENSMUSG00000042943			2.32	6.13E-11
ENSMUSG00000047798	Cd300lf	CD300 antigen like family member F	2.32	6.01E-14
ENSMUSG00000041293	Gpr110	G protein-coupled receptor 110	2.32	1.38E-09
ENSMUSG00000074151	Nlrc5	NLR family, CARD domain containing 5	2.32	8.82E-19
ENSMUSG00000057465	Saa2	serum amyloid A 2	2.31	6.06E-18
ENSMUSG00000082292			2.31	5.72E-13
ENSMUSG00000078853	Igtp	interferon gamma induced GTPase	2.29	1.49E-12
ENSMUSG00000087070	Gm12505	predicted gene 12505	2.28	9.64E-17
ENSMUSG00000095788	Sirpb1a	signal-regulatory protein beta 1A	2.26	1.76E-09
ENSMUSG00000029084	Cd38	CD38 antigen	2.26	1.85E-15
ENSMUSG00000038751	Ptk6	PTK6 protein tyrosine kinase 6	2.25	3.98E-21
ENSMUSG00000029915	Clec5a	C-type lectin domain family 5, member a	2.24	4.88E-12

ENSMUSG00000053101	Gpr141	G protein-coupled receptor 141	2.24	8.20E-15
ENSMUSG00000027360	Hdc	histidine decarboxylase	2.20	1.98E-09
ENSMUSG00000026180	Cxcr2	chemokine (C-X-C motif) receptor 2	2.20	2.73E-13
ENSMUSG00000019987	Arg1	arginase, liver	2.20	2.17E-11
ENSMUSG00000079227	Ccr5	chemokine (C-C motif) receptor 5	2.19	5.28E-22
ENSMUSG00000056054	S100a8	S100 calcium binding protein A8 (calgranulin A)	2.19	1.51E-08
ENSMUSG00000037095	Lrg1	leucine-rich alpha-2-glycoprotein 1	2.18	2.96E-12
ENSMUSG00000027225	Duoxa2	dual oxidase maturation factor 2	2.17	1.42E-10
ENSMUSG00000035385	Ccl2	chemokine (C-C motif) ligand 2	2.17	3.67E-10
ENSMUSG00000046688	Tifa	TRAF-interacting protein with forkhead-associated domain	2.17	2.69E-18
ENSMUSG00000096528	G430049J08Rik	RIKEN cDNA G430049J08 gene	2.14	4.77E-18
ENSMUSG00000022534	Mefv	Mediterranean fever	2.14	5.99E-13
ENSMUSG00000071356	Reg3b	regenerating islet-derived 3 beta	2.13	9.08E-10
ENSMUSG00000052749	Trim30b	tripartite motif-containing 30B	2.12	1.47E-08
ENSMUSG00000021214	Akr1c18	aldo-keto reductase family 1, member C18	2.12	6.59E-09
ENSMUSG00000021281	Tnfaip2	tumor necrosis factor, alpha-induced protein 2	2.12	2.26E-18
ENSMUSG00000085786			2.12	2.67E-15
ENSMUSG00000024087	Cyp1b1	cytochrome P450, family 1, subfamily b, polypeptide 1	2.11	1.24E-10
ENSMUSG00000013974	Mcemp1	mast cell expressed membrane protein 1	2.11	1.03E-08
ENSMUSG00000079014	Serpina3i	serine (or cysteine) peptidase inhibitor, clade A, member 3I	2.11	6.59E-10
ENSMUSG00000025161	Slc16a3	solute carrier family 16 (monocarboxylic acid transporters), member 3	2.11	1.01E-12
ENSMUSG00000025746	Il6	interleukin 6	2.11	1.28E-08
ENSMUSG00000079012	Serpina3m	serine (or cysteine) peptidase inhibitor, clade A, member 3M	2.11	7.10E-11
ENSMUSG00000052353	Cemip	cell migration inducing protein, hyaluronan binding	2.10	1.13E-08
ENSMUSG00000050747	Trim15	tripartite motif-containing 15	2.10	2.21E-08
ENSMUSG00000028269			2.09	7.89E-11
ENSMUSG00000078763	Slfn1	schlafen 1	2.08	1.31E-13
ENSMUSG00000078161	Erich3	glutamate rich 3	2.08	9.62E-09
ENSMUSG00000044254	Pcsk9	proprotein convertase subtilisin/kexin type 9	2.07	7.41E-18
ENSMUSG00000074892	B3galt5	UDP-Gal:betaGlcNAc beta 1,3-galactosyltransferase, polypeptide 5	2.07	2.27E-17
ENSMUSG00000016496	Cd274	CD274 antigen	2.06	1.07E-17
ENSMUSG00000029082	Bst1	bone marrow stromal cell antigen 1	2.06	1.98E-13
ENSMUSG00000044103	Il1f9	interleukin 1 family, member 9	2.05	1.67E-09
ENSMUSG00000029553	Tfec	transcription factor EC	2.05	9.54E-09
ENSMUSG00000027514	Zbp1	Z-DNA binding protein 1	2.04	1.24E-15
ENSMUSG00000000628	Hk2	hexokinase 2	2.04	1.30E-17
ENSMUSG00000028270	Gbp2	guanylate binding protein 2	2.03	3.21E-16
ENSMUSG00000029379	Cxcl3	chemokine (C-X-C motif) ligand 3	2.03	1.14E-07
ENSMUSG00000021950	Anxa8	annexin A8	2.02	7.87E-09
ENSMUSG00000056749	Nfil3	nuclear factor, interleukin 3, regulated	2.02	1.19E-14
ENSMUSG00000035004	Igsf6	immunoglobulin superfamily, member 6	2.01	1.36E-16
ENSMUSG00000024401	Tnf	tumor necrosis factor	1.99	1.52E-12
ENSMUSG00000040253	Gbp7	guanylate binding protein 7	1.99	1.52E-11
ENSMUSG00000049103	Ccr2	chemokine (C-C motif) receptor 2	1.98	1.09E-16
ENSMUSG00000043832	Clec4a3	C-type lectin domain family 4, member a3	1.97	1.42E-14
ENSMUSG00000030017	Reg3g	regenerating islet-derived 3 gamma	1.97	3.12E-08

ENSMUSG00000027224	Duoxa1	dual oxidase maturation factor 1	1.96	2.97E-09
ENSMUSG00000022181	C6	complement component 6	1.96	1.31E-12
ENSMUSG00000064346			1.94	4.49E-08
ENSMUSG00000006403	Adamts4	a disintegrin-like and metallopeptidase (reprolysin type) with thrombospondin type 1 motif, 4	1.93	1.95E-09
ENSMUSG00000078606	Gm4070	predicted gene 4070	1.93	3.71E-12
ENSMUSG00000089942	Pira2	paired-Ig-like receptor A2	1.92	4.06E-09
ENSMUSG00000079445	B3gnt7	UDP-GlcNAc:betaGal beta-1,3-N-acetylglucosaminyltransferase 7	1.92	7.23E-10
ENSMUSG00000026580	Selp	selectin, platelet	1.92	5.35E-11
ENSMUSG00000024679	Ms4a6d	membrane-spanning 4-domains, subfamily A, member 6D	1.92	1.52E-14
ENSMUSG00000097423			1.91	4.83E-10
ENSMUSG00000062593	Lilrb4	leukocyte immunoglobulin-like receptor, subfamily B, member 4	1.91	3.91E-10
ENSMUSG00000004668	Abca13	ATP-binding cassette, sub-family A (ABC1), member 13	1.91	5.03E-08
ENSMUSG00000046031	Fam26f	family with sequence similarity 26, member F	1.90	3.12E-08
ENSMUSG00000026981	Il1rn	interleukin 1 receptor antagonist	1.89	9.17E-13
ENSMUSG00000079293	Clec7a	C-type lectin domain family 7, member a	1.89	5.09E-15
ENSMUSG00000027737	Slc7a11	solute carrier family 7 (cationic amino acid transporter, y+ system), member 11	1.88	1.64E-16
ENSMUSG00000000982	Ccl3	chemokine (C-C motif) ligand 3	1.87	8.98E-07
ENSMUSG00000026073	Il1r2	interleukin 1 receptor, type II	1.87	2.54E-08
ENSMUSG00000026880	Stom	stomatin	1.85	1.20E-19
ENSMUSG00000032690	Oas2	2'-5' oligoadenylate synthetase 2	1.85	1.33E-09
ENSMUSG00000079339	Gm14446	predicted gene 14446	1.84	2.27E-10
ENSMUSG00000075270	Pde11a	phosphodiesterase 11A	1.84	6.98E-08
ENSMUSG00000074115	Saa1	serum amyloid A 1	1.84	2.28E-08
ENSMUSG00000073489	Ifi204	interferon activated gene 204	1.81	2.44E-13
ENSMUSG00000037321	Tap1	transporter 1, ATP-binding cassette, sub-family B (MDR/TAP)	1.81	2.54E-17
ENSMUSG00000048699	4732456N10Rik	RIKEN cDNA 4732456N10 gene	1.80	1.83E-06
ENSMUSG00000073902			1.78	2.50E-11
ENSMUSG00000063286			1.78	2.02E-16
ENSMUSG00000007989	Fzd3	frizzled homolog 3 (Drosophila)	1.77	1.16E-10
ENSMUSG00000031596	Slc7a2	solute carrier family 7 (cationic amino acid transporter, y+ system), member 2	1.76	2.15E-10
ENSMUSG00000001670	Tat	tyrosine aminotransferase	1.76	7.85E-14
ENSMUSG00000058715	Fcer1g	Fc receptor, IgE, high affinity I, gamma polypeptide	1.75	6.24E-10
ENSMUSG00000042102	Dmgdh	dimethylglycine dehydrogenase precursor	1.75	4.58E-06
ENSMUSG00000046245	Pilra	paired immunoglobin-like type 2 receptor alpha	1.74	2.69E-10
ENSMUSG00000026104	Stat1	signal transducer and activator of transcription 1	1.74	2.73E-14
ENSMUSG00000075010	AW112010	expressed sequence AW112010	1.74	1.91E-14
ENSMUSG00000035105	Egln3	egl-9 family hypoxia-inducible factor 3	1.73	5.85E-12
ENSMUSG00000079516	Reg3a	regenerating islet-derived 3 alpha	1.72	3.96E-06
ENSMUSG00000069874	Irgm2	immunity-related GTPase family M member 2	1.72	4.11E-09
ENSMUSG00000032796	Lama1	laminin, alpha 1	1.72	9.02E-11
ENSMUSG00000024640	Psat1	phosphoserine aminotransferase 1	1.71	3.84E-09
ENSMUSG00000053398	Phgdh	3-phosphoglycerate dehydrogenase	1.71	9.91E-13
ENSMUSG00000040809	Chil3	chitinase-like 3	1.71	8.36E-06
ENSMUSG00000029484	Anxa3	annexin A3	1.70	7.23E-15
ENSMUSG00000039304	Tnfsf10	tumor necrosis factor (ligand) superfamily, member 10	1.69	2.34E-11
ENSMUSG00000024529	Lox	lysyl oxidase	1.69	1.13E-07

ENSMUSG00000022221	Ripk3	receptor-interacting serine-threonine kinase 3	1.69	1.53E-12
ENSMUSG00000081665			1.69	1.46E-06
ENSMUSG00000041449			1.68	3.90E-08
ENSMUSG00000030111	A2m	alpha-2-macroglobulin	1.68	1.05E-05
ENSMUSG00000036040	Adamtsl2	ADAMTS-like 2	1.67	2.34E-09
ENSMUSG00000061947	Serpina10	serine (or cysteine) peptidase inhibitor, clade A (alpha-1 antiproteinase, antitrypsin), member 10	1.67	5.63E-06
ENSMUSG00000028544	Slc5a9	solute carrier family 5 (sodium/glucose cotransporter), member 9	1.67	9.92E-09
ENSMUSG00000015947	Fcgr1	Fc receptor, IgG, high affinity I	1.66	9.75E-10
ENSMUSG00000046879	Irgm1	immunity-related GTPase family M member 1	1.66	6.66E-09
ENSMUSG00000028268	Gbp3	guanylate binding protein 3	1.66	2.65E-07
ENSMUSG00000073530	Pappa2	pappalysin 2	1.66	1.19E-07
ENSMUSG00000024675	Ms4a4c	membrane-spanning 4-domains, subfamily A, member 4C	1.65	1.79E-09
ENSMUSG00000029752	Asns	asparagine synthetase	1.65	1.73E-12
ENSMUSG00000051439	Cd14	CD14 antigen	1.65	5.97E-10
ENSMUSG00000026536	Mnda	myeloid cell nuclear differentiation antigen	1.63	7.73E-09
ENSMUSG00000022797	Tfrc	transferrin receptor	1.63	1.49E-13
ENSMUSG00000081467			1.62	2.74E-07
ENSMUSG00000079298	Klrb1b	killer cell lectin-like receptor subfamily B member 1B	1.62	2.33E-05
ENSMUSG00000060550	H2-Q7	histocompatibility 2, Q region locus 7	1.61	1.04E-11
ENSMUSG00000058908	Pla2g2a	phospholipase A2, group IIA (platelets, synovial fluid)	1.61	6.67E-07
ENSMUSG00000078920	Ifi47	interferon gamma inducible protein 47	1.61	2.21E-10
ENSMUSG00000024066	Xdh	xanthine dehydrogenase	1.59	1.12E-13
ENSMUSG00000029298	Gbp9	guanylate-binding protein 9	1.58	4.73E-11
ENSMUSG00000060131	Atp8b4	ATPase, class I, type 8B, member 4	1.58	3.11E-08
ENSMUSG00000024349	Tmem173	transmembrane protein 173	1.58	2.47E-10
ENSMUSG00000046718	Bst2	bone marrow stromal cell antigen 2	1.57	2.00E-07
ENSMUSG00000057596	Trim30d	tripartite motif-containing 30D	1.57	5.30E-07
ENSMUSG00000037820	Tgm2	transglutaminase 2, C polypeptide	1.57	9.56E-15
ENSMUSG00000028037	Ifi44	interferon-induced protein 44	1.57	1.44E-09
ENSMUSG00000024798	Htr7	5-hydroxytryptamine (serotonin) receptor 7	1.56	9.66E-06
ENSMUSG00000057191	AB124611	cDNA sequence AB124611	1.55	2.17E-08
ENSMUSG00000016024	Lbp	lipopolysaccharide binding protein	1.55	1.89E-11
ENSMUSG00000050578	Mmp13	matrix metallopeptidase 13	1.55	2.70E-05
ENSMUSG00000079018	Ly6c1	lymphocyte antigen 6 complex, locus C1	1.55	1.30E-09
ENSMUSG00000052212	Cd177	CD177 antigen	1.54	3.57E-14
ENSMUSG00000071713	Csf2rb	colony stimulating factor 2 receptor, beta, low-affinity (granulocyte-macrophage)	1.54	1.41E-11
ENSMUSG00000034206	Polq	polymerase (DNA directed), theta	1.53	7.56E-11
ENSMUSG00000038037	Socs1	suppressor of cytokine signaling 1	1.53	7.01E-06
ENSMUSG00000038301	Snx10	sorting nexin 10	1.53	1.26E-11
ENSMUSG00000027639	Samhd1	SAM domain and HD domain, 1	1.53	3.90E-13
ENSMUSG00000073399	Trim40	tripartite motif-containing 40	1.53	2.89E-11
ENSMUSG00000033508	Asprv1	aspartic peptidase, retroviral-like 1	1.52	3.11E-05
ENSMUSG00000028613	Lrp8	low density lipoprotein receptor-related protein 8, apolipoprotein e receptor	1.52	2.00E-08
ENSMUSG00000045932	Ifit2	interferon-induced protein with tetratricopeptide repeats 2	1.51	9.10E-10
ENSMUSG00000045502	Hcar2	hydroxycarboxylic acid receptor 2	1.51	6.48E-06
ENSMUSG00000020649	Rrm2	ribonucleotide reductase M2	1.51	3.55E-13

ENSMUSG00000027323	Rad51	RAD51 homolog	1.50	1.19E-07
ENSMUSG00000058624	Gda	guanine deaminase	1.50	4.62E-07
ENSMUSG00000065629			1.50	9.55E-05
ENSMUSG00000064400			1.49	1.05E-04
ENSMUSG00000035186	Ubd	ubiquitin D	1.49	2.46E-10
ENSMUSG00000087700			1.49	1.03E-05
ENSMUSG00000024810	Il33	interleukin 33	1.48	7.07E-11
ENSMUSG00000024053	Emilin2	elastin microfibril interfacer 2	1.48	1.49E-10
ENSMUSG00000090293			1.48	7.25E-05
ENSMUSG00000079419	Ms4a6c	membrane-spanning 4-domains, subfamily A, member 6C	1.48	1.10E-10
ENSMUSG00000030732	Chrdl2	chordin-like 2	1.47	6.35E-05
ENSMUSG00000004371	Il11	interleukin 11	1.47	1.27E-04
ENSMUSG00000024164	C3	complement component 3	1.47	8.55E-15
ENSMUSG00000096727	Psmb9	proteasome (prosome, macropain) subunit, beta type 9 (large multifunctional peptidase 2)	1.46	8.70E-10
ENSMUSG00000035373	Ccl7	chemokine (C-C motif) ligand 7	1.46	8.45E-05
ENSMUSG00000039699	Batf2	basic leucine zipper transcription factor, ATF-like 2	1.46	6.86E-10
ENSMUSG00000025491	Ifitm1	interferon induced transmembrane protein 1	1.46	2.27E-09
ENSMUSG00000017861	Mybl2	myeloblastosis oncogene-like 2	1.45	5.22E-09
ENSMUSG00000023272	Creld2	cysteine-rich with EGF-like domains 2	1.45	1.05E-08
ENSMUSG00000001095	Slc13a2	solute carrier family 13 (sodium-dependent dicarboxylate transporter), member 2	1.45	4.15E-11
ENSMUSG00000071714	Csf2rb2	colony stimulating factor 2 receptor, beta 2, low-affinity (granulocyte-macrophage)	1.44	2.37E-08
ENSMUSG00000042808	Gpx2	glutathione peroxidase 2	1.44	2.21E-09
ENSMUSG00000030353	Tead4	TEA domain family member 4	1.44	7.95E-05
ENSMUSG00000058818	Pirb	paired Ig-like receptor B	1.43	1.91E-08
ENSMUSG00000030560	Ctsc	cathepsin C	1.43	2.99E-11
ENSMUSG00000025044	Msr1	macrophage scavenger receptor 1	1.43	2.61E-07
ENSMUSG00000024737	Slc15a3	solute carrier family 15, member 3	1.42	3.67E-07
ENSMUSG00000024397	Aif1	allograft inflammatory factor 1	1.42	6.62E-10
ENSMUSG00000056148	Rdh9	retinol dehydrogenase 9	1.41	1.68E-05
ENSMUSG00000074934	Grem1	gremlin 1	1.41	1.36E-09
ENSMUSG00000026535	Ifi202b	interferon activated gene 202B	1.40	4.24E-08
ENSMUSG00000022686	B3gnt5	UDP-GlcNAc:betaGal beta-1,3-N-acetylglucosaminyltransferase 5	1.40	1.77E-08
ENSMUSG00000037679	Inf2	inverted formin, FH2 and WH2 domain containing	1.40	2.91E-09
ENSMUSG00000046402	Rbp1	retinol binding protein 1, cellular	1.40	6.18E-07
ENSMUSG00000026605	Cenpf	centromere protein F	1.39	7.46E-09
ENSMUSG00000074417	Pira11	paired-Ig-like receptor A11	1.39	8.30E-06
ENSMUSG00000032496	Ltf	lactotransferrin	1.39	3.12E-04
ENSMUSG00000056025	Clca3a1	chloride channel calcium activated 3A1	1.38	2.59E-07
ENSMUSG00000076534			1.38	5.42E-06
ENSMUSG00000028874	Fgr	Gardner-Rasheed feline sarcoma viral (Fgr) oncogene homolog	1.38	6.25E-08
ENSMUSG00000021266	Wars	tryptophanyl-tRNA synthetase	1.37	3.39E-10
ENSMUSG00000049939	Lrrc4	leucine rich repeat containing 4	1.37	1.05E-05
ENSMUSG00000059498	Fcgr3	Fc receptor, IgG, low affinity III	1.37	6.60E-10
ENSMUSG00000058163	Gm5431	predicted gene 5431	1.36	6.58E-09
ENSMUSG00000070427	Il18bp	interleukin 18 binding protein	1.36	1.59E-07
ENSMUSG00000097194	9330175E14Rik	RIKEN cDNA 9330175E14 gene	1.36	9.01E-05

ENSMUSG00000075611			1.36	1.29E-07
ENSMUSG00000030786	Itgam	integrin alpha M	1.35	9.34E-11
ENSMUSG00000032487	Ptgs2	prostaglandin-endoperoxide synthase 2	1.34	2.71E-05
ENSMUSG00000046179	E2f8	E2F transcription factor 8	1.34	2.91E-09
ENSMUSG00000043263	Pyhin1	pyrin and HIN domain family, member 1	1.34	2.39E-06
ENSMUSG00000041324	Inhba	inhibin beta-A	1.34	8.82E-05
ENSMUSG00000028599	Tnfrsf1b	tumor necrosis factor receptor superfamily, member 1b	1.34	5.11E-11
ENSMUSG00000035208	Slfn8	schlafen 8	1.33	2.01E-09
ENSMUSG00000021322	Aoah	acyloxyacyl hydrolase	1.33	4.66E-05
ENSMUSG00000032109	Nlrx1	NLR family member X1	1.33	4.20E-08
ENSMUSG00000050014	Apol10b	apolipoprotein L 10B	1.32	4.86E-07
ENSMUSG00000042129	Rassf4	Ras association (RalGDS/AF-6) domain family member 4	1.32	1.03E-09
ENSMUSG00000057610			1.31	6.22E-04
ENSMUSG00000025804	Ccr1	chemokine (C-C motif) receptor 1	1.31	2.91E-08
ENSMUSG00000092500			1.31	5.64E-06
ENSMUSG00000067653	Ankrd23	ankyrin repeat domain 23	1.31	3.86E-04
ENSMUSG00000032586	Traip	TRAF-interacting protein	1.31	8.16E-06
ENSMUSG00000016194	Hsd11b1	hydroxysteroid 11-beta dehydrogenase 1	1.29	2.08E-06
ENSMUSG00000039146	Ifi44l	interferon-induced protein 44 like	1.29	1.44E-04
ENSMUSG00000015340	Cybb	cytochrome b-245, beta polypeptide	1.29	5.88E-11
ENSMUSG00000003283	Hck	hemopoietic cell kinase	1.29	4.79E-08
ENSMUSG00000094094			1.29	4.52E-04
ENSMUSG00000076598			1.29	8.48E-04
ENSMUSG00000022769	Sdf2l1	stromal cell-derived factor 2-like 1	1.29	3.53E-09
ENSMUSG00000039934	Gsap	gamma-secretase activating protein	1.29	1.55E-08
ENSMUSG00000030149	Klrk1	killer cell lectin-like receptor subfamily K, member 1	1.28	3.15E-06
ENSMUSG00000056501	Cebpb	CCAAT/enhancer binding protein (C/EBP), beta	1.28	8.63E-06
ENSMUSG00000028312	Smc2	structural maintenance of chromosomes 2	1.28	7.13E-09
ENSMUSG00000021702	Thbs4	thrombospondin 4	1.28	1.42E-06
ENSMUSG00000030790	Adm	adrenomedullin	1.28	3.52E-05
ENSMUSG00000038156	Spon1	spondin 1, (f-spondin) extracellular matrix protein	1.28	5.66E-10
ENSMUSG00000025492	Ifitm3	interferon induced transmembrane protein 3	1.28	3.57E-10
ENSMUSG00000054203	Ifi205	interferon activated gene 205	1.27	6.15E-07
ENSMUSG00000026185	Igfbp5	insulin-like growth factor binding protein 5	1.27	2.00E-09
ENSMUSG00000020469	Myl7	myosin, light polypeptide 7, regulatory	1.27	1.13E-04
ENSMUSG00000024338	Psmb8	proteasome (prosome, macropain) subunit, beta type 8 (large multifunctional peptidase 7)	1.27	5.88E-09
ENSMUSG00000070777	Ceacam20	carcinoembryonic antigen-related cell adhesion molecule 20	1.27	2.86E-08
ENSMUSG00000023913	Pla2g7	phospholipase A2, group VII (platelet-activating factor acetylhydrolase, plasma)	1.27	2.09E-09
ENSMUSG00000046841	Ckap4	cytoskeleton-associated protein 4	1.26	1.74E-09
ENSMUSG00000069793	Slfn9	schlafen 9	1.26	2.12E-05
ENSMUSG00000061577	Gpr114	G protein-coupled receptor 114	1.26	7.66E-05
ENSMUSG00000046223	Plaur	plasminogen activator, urokinase receptor	1.26	6.46E-05
ENSMUSG00000032561	Acpp	acid phosphatase, prostate	1.26	2.98E-10
ENSMUSG00000060508	Nlrp9b	NLR family, pyrin domain containing 9B	1.26	2.98E-04
ENSMUSG00000055541	Lair1	leukocyte-associated Ig-like receptor 1	1.26	1.08E-07
ENSMUSG00000001517	Foxm1	forkhead box M1	1.26	3.40E-07

ENSMUSG00000047810	Ccdc88b	coiled-coil domain containing 88B	1.26	1.67E-08
ENSMUSG00000064147	Rab44	RAB44, member RAS oncogene family	1.26	8.07E-04
ENSMUSG00000086320			1.25	4.35E-07
ENSMUSG00000022651	Retnlg	resistin like gamma	1.25	1.44E-04
ENSMUSG00000020120	Plek	pleckstrin	1.25	1.47E-09
ENSMUSG00000026177	Slc11a1	solute carrier family 11 (proton-coupled divalent metal ion transporters), member 1	1.25	1.63E-06
ENSMUSG00000035692	Isg15	ISG15 ubiquitin-like modifier	1.25	9.87E-07
ENSMUSG00000037405	Icam1	intercellular adhesion molecule 1	1.25	5.74E-10
ENSMUSG00000031490	Eif4ebp1	eukaryotic translation initiation factor 4E binding protein 1	1.24	2.82E-08
ENSMUSG00000093916			1.24	1.26E-03
ENSMUSG00000034361	Cpne2	copine II	1.24	1.98E-10
ENSMUSG00000020256	Aldh1l2	aldehyde dehydrogenase 1 family, member L2	1.24	3.91E-05
ENSMUSG00000022548	Apod	apolipoprotein D	1.24	3.59E-05
ENSMUSG00000021187	Tc2n	tandem C2 domains, nuclear	1.24	4.30E-08
ENSMUSG00000031821	Gins2	GINS complex subunit 2 (Psf2 homolog)	1.24	2.53E-06
ENSMUSG00000003355	Fkbp11	FK506 binding protein 11	1.23	1.31E-06
ENSMUSG00000080917			1.23	6.40E-04
ENSMUSG00000099296			1.23	1.51E-03
ENSMUSG00000039748	Exo1	exonuclease 1	1.23	5.55E-06
ENSMUSG00000017737	Mmp9	matrix metallopeptidase 9	1.23	1.43E-05
ENSMUSG00000028885	Smpdl3b	sphingomyelin phosphodiesterase, acid-like 3B	1.22	1.58E-06
ENSMUSG00000022650	Retnlb	resistin like beta	1.22	1.92E-11
ENSMUSG00000026039	Sgol2a	shugoshin-like 2a (S. pombe)	1.22	2.19E-05
ENSMUSG00000027333	Smox	spermine oxidase	1.22	2.29E-07
ENSMUSG00000037731	Themis2	thymocyte selection associated family member 2	1.21	3.21E-07
ENSMUSG00000049134	Nrap	nebulin-related anchoring protein	1.21	2.86E-06
ENSMUSG00000091956	C2cd4b	C2 calcium-dependent domain containing 4B	1.21	1.36E-03
ENSMUSG00000029299	Abcg3	ATP-binding cassette, sub-family G (WHITE), member 3	1.21	5.46E-06
ENSMUSG00000017146	Brca1	breast cancer 1	1.21	5.98E-08
ENSMUSG00000007682	Dio2	deiodinase, iodothyronine, type II	1.21	8.34E-04
ENSMUSG00000033538	Casp4	caspase 4, apoptosis-related cysteine peptidase	1.21	3.12E-08
ENSMUSG00000029798	Herc6	hect domain and RLD 6	1.20	1.65E-07
ENSMUSG00000096768	Erdr1	erythroid differentiation regulator 1	1.20	3.25E-04
ENSMUSG00000037411	Serpine1	serine (or cysteine) peptidase inhibitor, clade E, member 1	1.20	1.54E-06
ENSMUSG00000067780	Pi15	peptidase inhibitor 15	1.20	3.94E-07
ENSMUSG00000052125	F730043M19Rik	RIKEN cDNA F730043M19 gene	1.20	2.20E-04
ENSMUSG00000032575	Manf	mesencephalic astrocyte-derived neurotrophic factor	1.20	6.95E-08
ENSMUSG00000025665	Rps6ka6	ribosomal protein S6 kinase polypeptide 6	1.20	1.89E-05
ENSMUSG00000024300	Myo1f	myosin IF	1.20	1.54E-07
ENSMUSG00000092730	Snora24	small nucleolar RNA, H/ACA box 24	1.20	3.83E-04
ENSMUSG00000036944	Tmem71	transmembrane protein 71	1.20	1.71E-04
ENSMUSG00000022696	Sidt1	SID1 transmembrane family, member 1	1.20	1.37E-06
ENSMUSG00000033268	Duox1	dual oxidase 1	1.20	5.51E-04
ENSMUSG00000037313	Tacc3	transforming, acidic coiled-coil containing protein 3	1.19	3.01E-09
ENSMUSG00000073598	1700066B19Rik	RIKEN cDNA 1700066B19 gene	1.19	7.78E-07
ENSMUSG00000035673	Sbno2	strawberry notch homolog 2 (Drosophila)	1.19	2.67E-08

ENSMUSG00000018920	Cxcl16	chemokine (C-X-C motif) ligand 16	1.19	2.31E-08
ENSMUSG00000022146	Osmr	oncostatin M receptor	1.18	3.72E-08
ENSMUSG00000058099	Nfam1	Nfat activating molecule with ITAM motif 1	1.18	9.34E-06
ENSMUSG00000047230	Cldn2	claudin 2	1.18	1.24E-04
ENSMUSG00000085873			1.18	7.43E-04
ENSMUSG00000024730	Ms4a8a	membrane-spanning 4-domains, subfamily A, member 8A	1.18	2.00E-08
ENSMUSG00000040522	Tlr8	toll-like receptor 8	1.18	8.56E-06
ENSMUSG00000013483	Card14	caspase recruitment domain family, member 14	1.18	3.26E-06
ENSMUSG00000040033	Stat2	signal transducer and activator of transcription 2	1.18	2.09E-07
ENSMUSG00000028633	Ctps	cytidine 5'-triphosphate synthase	1.18	6.01E-08
ENSMUSG00000021196	Pfkp	phosphofructokinase, platelet	1.18	3.06E-09
ENSMUSG00000028028	Alpk1	alpha-kinase 1	1.17	4.61E-08
ENSMUSG00000004296			1.17	1.05E-03
ENSMUSG00000090307	1700071M16Rik	RIKEN cDNA 1700071M16 gene	1.17	3.04E-04
ENSMUSG00000027379	Bub1	budding uninhibited by benzimidazoles 1 homolog (S. cerevisiae)	1.17	1.05E-06
ENSMUSG00000026068	Il18rap	interleukin 18 receptor accessory protein	1.17	2.48E-05
ENSMUSG00000036875	Dna2	DNA replication helicase 2 homolog (yeast)	1.17	2.31E-06
ENSMUSG00000028194	Ddah1	dimethylarginine dimethylaminohydrolase 1	1.17	1.73E-08
ENSMUSG00000017715	Pgs1	phosphatidylglycerophosphate synthase 1	1.17	3.00E-06
ENSMUSG00000038058	Nod1	nucleotide-binding oligomerization domain containing 1	1.17	1.62E-06
ENSMUSG00000053541			1.17	1.03E-06
ENSMUSG00000054404	Slfn5	schlafen 5	1.16	5.48E-09
ENSMUSG00000020057	Dram1	DNA-damage regulated autophagy modulator 1	1.16	7.02E-08
ENSMUSG00000073409	H2-Q8	histocompatibility 2, Q region locus 8	1.16	3.92E-08
ENSMUSG00000028718	Stil	Scl/Tal1 interrupting locus	1.16	1.88E-06
ENSMUSG00000020572	Nampt	nicotinamide phosphoribosyltransferase	1.16	1.29E-07
ENSMUSG00000046971	Pla2g4f	phospholipase A2, group IVF	1.16	1.44E-03
ENSMUSG00000051220	Ercc6l	excision repair cross-complementing rodent repair deficiency complementation group 6 like	1.16	9.97E-08
ENSMUSG00000048636			1.16	2.45E-03
ENSMUSG00000043953	Ccrl2	chemokine (C-C motif) receptor-like 2	1.16	9.18E-05
ENSMUSG00000093809			1.15	2.73E-03
ENSMUSG00000000028	Cdc45	cell division cycle 45	1.15	3.62E-07
ENSMUSG00000068086	Cyp2d9	cytochrome P450, family 2, subfamily d, polypeptide 9	1.15	1.13E-03
ENSMUSG00000034394	Lif	leukemia inhibitory factor	1.15	6.82E-04
ENSMUSG00000042306	S100a14	S100 calcium binding protein A14	1.15	3.82E-08
ENSMUSG00000030022	Adamts9	a disintegrin-like and metallopeptidase (reprolysin type) with thrombospondin type 1 motif, 9	1.15	1.17E-06
ENSMUSG00000020914	Top2a	topoisomerase (DNA) II alpha	1.15	6.61E-09
ENSMUSG00000069456	Rdh16	retinol dehydrogenase 16	1.15	2.03E-06
ENSMUSG00000022964	Tmem50b	transmembrane protein 50B	1.15	1.04E-06
ENSMUSG00000072621	Slfn10-ps	schlafen 10, pseudogene	1.15	1.18E-03
ENSMUSG00000086479			1.14	1.73E-03
ENSMUSG00000027408	Cpxm1	carboxypeptidase X 1 (M14 family)	1.14	4.39E-05
ENSMUSG00000027199	Gatm	glycine amidinotransferase (L-arginine:glycine amidinotransferase)	1.14	2.82E-07
ENSMUSG00000024795	Kif20b	kinesin family member 20B	1.14	2.93E-04
ENSMUSG00000020303	Stc2	stanniocalcin 2	1.14	4.60E-06
ENSMUSG00000015451			1.14	1.16E-04

ENSMUSG00000017716	Birc5	baculoviral IAP repeat-containing 5	1.14	3.44E-08
ENSMUSG00000032254	Kif23	kinesin family member 23	1.14	1.74E-08
ENSMUSG00000069792	Wfdc17	WAP four-disulfide core domain 17	1.14	1.64E-03
ENSMUSG00000024989	Cep55	centrosomal protein 55	1.14	1.43E-07
ENSMUSG00000027994	Ccdc109b	coiled-coil domain containing 109B	1.14	3.81E-06
ENSMUSG00000032115	Hyou1	hypoxia up-regulated 1	1.13	3.88E-07
ENSMUSG00000030474	Siglece	sialic acid binding Ig-like lectin E	1.13	2.55E-03
ENSMUSG00000022218	Tgm1	transglutaminase 1, K polypeptide	1.13	7.39E-04
ENSMUSG00000030921	Trim30a	tripartite motif-containing 30A	1.13	6.29E-09
ENSMUSG00000022847	Thpo	thrombopoietin	1.13	3.25E-03
ENSMUSG00000065870			1.12	5.40E-04
ENSMUSG00000003617	Cp	ceruloplasmin	1.12	1.55E-08
ENSMUSG00000026581	Sell	selectin, lymphocyte	1.12	4.73E-07
ENSMUSG00000024481	Lvrn	laeverin	1.12	1.24E-03
ENSMUSG00000022824	Muc13	mucin 13, epithelial transmembrane	1.12	8.79E-08
ENSMUSG00000028766	Alpl	alkaline phosphatase, liver/bone/kidney	1.12	3.19E-06
ENSMUSG00000068227	Il2rb	interleukin 2 receptor, beta chain	1.12	4.31E-05
ENSMUSG00000040010	Slc7a5	solute carrier family 7 (cationic amino acid transporter, y+ system), member 5	1.12	1.40E-05
ENSMUSG00000041695	Kcnj2	potassium inwardly-rectifying channel, subfamily J, member 2	1.12	7.05E-04
ENSMUSG00000030413	Pglyrp1	peptidoglycan recognition protein 1	1.11	1.32E-08
ENSMUSG00000033777	Tlr13	toll-like receptor 13	1.11	8.33E-07
ENSMUSG00000016498	Pdcd1lg2	programmed cell death 1 ligand 2	1.11	2.92E-03
ENSMUSG00000056529	Ptafr	platelet-activating factor receptor	1.11	2.50E-06
ENSMUSG00000029414	Kntc1	kinetochore associated 1	1.11	4.48E-07
ENSMUSG00000022148	Fyb	FYN binding protein	1.11	3.92E-08
ENSMUSG00000029561	Oasl2	2'-5' oligoadenylate synthetase-like 2	1.11	1.20E-05
ENSMUSG00000053063	Clec12a	C-type lectin domain family 12, member a	1.11	5.15E-05
ENSMUSG00000052271	Bhlha15	basic helix-loop-helix family, member a15	1.10	5.20E-04
ENSMUSG00000028965	Tnfrsf9	tumor necrosis factor receptor superfamily, member 9	1.10	7.97E-04
ENSMUSG00000046295	Ankle1	ankyrin repeat and LEM domain containing 1	1.10	1.40E-03
ENSMUSG00000027907	S100a11	S100 calcium binding protein A11 (calgizzarin)	1.10	1.92E-06
ENSMUSG00000097467			1.09	4.26E-03
ENSMUSG00000083161			1.09	4.30E-03
ENSMUSG00000088252	Snord13	small nucleolar RNA, C/D box 13	1.09	1.35E-03
ENSMUSG00000096954			1.09	3.65E-05
ENSMUSG00000010601	Apol7a	apolipoprotein L 7a	1.08	2.49E-05
ENSMUSG00000021553	Slc28a3	solute carrier family 28 (sodium-coupled nucleoside transporter), member 3	1.08	1.06E-03
ENSMUSG00000039005	Tlr4	toll-like receptor 4	1.08	7.29E-06
ENSMUSG00000000386	Mx1	MX dynamin-like GTPase 1	1.08	3.65E-04
ENSMUSG00000026464			1.08	4.88E-04
ENSMUSG00000029657	Hsph1	heat shock 105kDa/110kDa protein 1	1.08	1.64E-03
ENSMUSG00000021109	Hif1a	hypoxia inducible factor 1, alpha subunit	1.08	1.73E-06
ENSMUSG00000056018	1700008F21Rik	RIKEN cDNA 1700008F21 gene	1.07	6.67E-04
ENSMUSG00000042759	Apobr	apolipoprotein B receptor	1.07	2.19E-04
ENSMUSG00000035929	H2-Q4	histocompatibility 2, Q region locus 4	1.07	1.11E-06
ENSMUSG00000047330	Kcne4	potassium voltage-gated channel, Isk-related subfamily, gene 4	1.07	3.25E-05

ENSMUSG00000079553	Kifc1	kinesin family member C1	1.07	1.72E-03
ENSMUSG00000005413	Hmox1	heme oxygenase (decycling) 1	1.07	2.70E-04
ENSMUSG00000055447	Cd47	CD47 antigen (Rh-related antigen, integrin-associated signal transducer)	1.07	2.52E-07
ENSMUSG00000070315	4930581F22Rik	RIKEN cDNA 4930581F22 gene	1.07	2.84E-03
ENSMUSG00000045328	Cenpe	centromere protein E	1.07	2.47E-04
ENSMUSG00000071637			1.07	2.14E-07
ENSMUSG00000089844	A530032D15Rik	RIKEN cDNA A530032D15Rik gene	1.07	4.34E-04
ENSMUSG00000060063	Alox5ap	arachidonate 5-lipoxygenase activating protein	1.07	2.00E-05
ENSMUSG00000017002	Slpi	secretory leukocyte peptidase inhibitor	1.07	5.84E-03
ENSMUSG00000038379	Ttk	Ttk protein kinase	1.06	7.62E-07
ENSMUSG00000079343	C1s2	complement component 1, s subcomponent 2	1.06	1.31E-05
ENSMUSG00000084384			1.06	2.14E-03
ENSMUSG00000034311	Kif4	kinesin family member 4	1.06	4.03E-09
ENSMUSG00000074300	BC030870	cDNA sequence BC030870	1.06	5.38E-06
ENSMUSG00000070390	Nlrp1b	NLR family, pyrin domain containing 1B	1.06	1.38E-03
ENSMUSG00000067367	Lyar	Ly1 antibody reactive clone	1.06	2.05E-07
ENSMUSG00000061540	Orm2	orosomucoid 2	1.06	5.66E-03
ENSMUSG00000000031			1.06	6.47E-03
ENSMUSG00000037601	Nme1	NME/NM23 nucleoside diphosphate kinase 1	1.06	6.31E-06
ENSMUSG00000005667	Mthfd2	methylenetetrahydrofolate dehydrogenase (NAD+ dependent), methenyltetrahydrofolate cyclohydrolase	1.06	3.28E-05
ENSMUSG00000027496	Aurka	aurora kinase A	1.06	2.63E-07
ENSMUSG00000041135	Ripk2	receptor (TNFRSF)-interacting serine-threonine kinase 2	1.06	2.47E-06
ENSMUSG00000026656	Fcgr2b	Fc receptor, IgG, low affinity IIb	1.06	2.89E-07
ENSMUSG00000028555	Ttc39a	tetratricopeptide repeat domain 39A	1.05	1.64E-07
ENSMUSG00000049037	Clec4a1	C-type lectin domain family 4, member a1	1.05	2.87E-04
ENSMUSG00000049988	Lrrc25	leucine rich repeat containing 25	1.05	2.29E-03
ENSMUSG00000032908	Sgpp2	sphingosine-1-phosphate phosphotase 2	1.05	4.34E-08
ENSMUSG00000022860	Chodl	chondrolectin	1.05	8.04E-04
ENSMUSG00000058290	Espl1	extra spindle pole bodies 1 (S. cerevisiae)	1.05	1.46E-05
ENSMUSG00000020869	Lrrc59	leucine rich repeat containing 59	1.05	6.98E-08
ENSMUSG00000078780	Gm5150	predicted gene 5150	1.05	5.84E-03
ENSMUSG00000030043	Tacr1	tachykinin receptor 1	1.04	5.56E-05
ENSMUSG00000074345	Tnfaip8l3	tumor necrosis factor, alpha-induced protein 8-like 3	1.04	2.75E-03
ENSMUSG00000051682	Treml4	triggering receptor expressed on myeloid cells-like 4	1.04	1.66E-03
ENSMUSG00000096672			1.04	6.47E-03
ENSMUSG00000025473	Adam8	a disintegrin and metallopeptidase domain 8	1.04	1.39E-04
ENSMUSG00000033107	Rnf125	ring finger protein 125	1.04	3.95E-05
ENSMUSG00000032815	Fanca	Fanconi anemia, complementation group A	1.04	4.77E-05
ENSMUSG00000023832	Acat2	acetyl-Coenzyme A acetyltransferase 2	1.04	1.74E-05
ENSMUSG00000053318	Slamf8	SLAM family member 8	1.04	9.56E-04
ENSMUSG00000091747			1.04	3.92E-09
ENSMUSG00000039682	Lap3	leucine aminopeptidase 3	1.04	1.18E-06
ENSMUSG00000030659	Nucb2	nucleobindin 2	1.04	1.45E-05
ENSMUSG00000029605	Oas1b	2'-5' oligoadenylate synthetase 1B	1.03	5.95E-03
ENSMUSG00000025059	Gyk	glycerol kinase	1.03	7.95E-04
ENSMUSG00000002835	Chaf1a	chromatin assembly factor 1, subunit A (p150)	1.03	2.78E-06

ENSMUSG00000027326	Casc5	cancer susceptibility candidate 5	1.03	7.67E-06
ENSMUSG00000020185	E2f7	E2F transcription factor 7	1.03	3.54E-04
ENSMUSG00000027962	Vcam1	vascular cell adhesion molecule 1	1.03	1.37E-06
ENSMUSG00000026107	Nabp1	nucleic acid binding protein 1	1.03	1.62E-05
ENSMUSG00000051235	Gen1	Gen homolog 1, endonuclease (Drosophila)	1.03	1.80E-04
ENSMUSG00000033031	C330027C09Rik	RIKEN cDNA C330027C09 gene	1.03	6.16E-05
ENSMUSG00000085550			1.03	7.74E-03
ENSMUSG00000006442	Srm	spermidine synthase	1.03	1.47E-04
ENSMUSG00000044201	Cdc25c	cell division cycle 25C	1.03	3.47E-04
ENSMUSG00000043629	1700019D03Rik	RIKEN cDNA 1700019D03 gene	1.03	1.10E-06
ENSMUSG00000069300	Hist1h2bj	histone cluster 1, H2bj	1.02	2.41E-04
ENSMUSG00000032584	Mst1r	macrophage stimulating 1 receptor (c-met-related tyrosine kinase)	1.02	7.65E-06
ENSMUSG00000024677	Ms4a6b	membrane-spanning 4-domains, subfamily A, member 6B	1.02	6.01E-06
ENSMUSG00000037868	Egr2	early growth response 2	1.02	2.69E-03
ENSMUSG00000021831	Ero1l	ERO1-like (S. cerevisiae)	1.02	7.19E-06
ENSMUSG00000027248	Pdia3	protein disulfide isomerase associated 3	1.02	7.31E-07
ENSMUSG00000072620	Slfn2	schlafen 2	1.02	8.83E-07
ENSMUSG00000030748	Il4ra	interleukin 4 receptor, alpha	1.02	2.88E-07
ENSMUSG00000006517	Mvd	mevalonate (diphospho) decarboxylase	1.02	7.06E-06
ENSMUSG00000025986	Slc39a10	solute carrier family 39 (zinc transporter), member 10	1.02	4.67E-06
ENSMUSG00000016028	Celsr1	cadherin, EGF LAG seven-pass G-type receptor 1 (flamingo homolog, Drosophila)	1.02	1.34E-06
ENSMUSG00000021728	Emb	embigin	1.02	2.91E-05
ENSMUSG00000032400	Zwilch	zwilch kinetochore protein	1.02	1.30E-05
ENSMUSG00000074519	Etohi1	ethanol induced 1	1.02	6.43E-04
ENSMUSG00000061207	Stk19	serine/threonine kinase 19	1.02	2.81E-05
ENSMUSG00000027171	Prrg4	proline rich Gla (G-carboxyglutamic acid) 4 (transmembrane)	1.01	1.64E-03
ENSMUSG00000078616			1.01	4.72E-03
ENSMUSG00000032344	Mb21d1	Mab-21 domain containing 1	1.01	3.24E-04
ENSMUSG00000074656	Eif2s2	eukaryotic translation initiation factor 2, subunit 2 (beta)	1.01	4.59E-04
ENSMUSG00000079620	Muc4	mucin 4	1.01	3.65E-06
ENSMUSG00000046591	Ticrr	TOPBP1-interacting checkpoint and replication regulator	1.01	7.09E-05
ENSMUSG00000022587	Ly6e	lymphocyte antigen 6 complex, locus E	1.01	1.67E-07
ENSMUSG00000027896	Slc16a4	solute carrier family 16 (monocarboxylic acid transporters), member 4	1.01	5.03E-04
ENSMUSG00000081723			1.01	6.58E-03
ENSMUSG00000026480	Ncf2	neutrophil cytosolic factor 2	1.01	3.44E-06
ENSMUSG00000036777	Anln	anillin, actin binding protein	1.01	1.38E-06
ENSMUSG00000026864	Hspa5	heat shock protein 5	1.00	3.17E-04
ENSMUSG00000092392			1.00	2.82E-04
ENSMUSG00000045106	Ccdc73	coiled-coil domain containing 73	1.00	5.54E-03
ENSMUSG00000028864	Hgf	hepatocyte growth factor	1.00	1.91E-04
ENSMUSG00000028873	Cdca8	cell division cycle associated 8	1.00	6.67E-06
ENSMUSG00000026009	Icos	inducible T cell co-stimulator	1.00	1.16E-03
ENSMUSG00000024924	Vldlr	very low density lipoprotein receptor	-1.00	4.83E-05
ENSMUSG00000032372	Plscr2	phospholipid scramblase 2	-1.00	3.87E-05
ENSMUSG00000022836	Mylk	myosin, light polypeptide kinase	-1.00	1.25E-09
ENSMUSG00000033768	Nrxn2	neurexin II	-1.00	5.87E-03

ENSMUSG00000033174	Mgll	monoglyceride lipase	-1.01	5.61E-07
ENSMUSG00000038984	Tspyl5	testis-specific protein, Y-encoded-like 5	-1.01	7.38E-03
ENSMUSG00000025213	Kazald1	Kazal-type serine peptidase inhibitor domain 1	-1.01	6.09E-03
ENSMUSG00000033618	Map3k13	mitogen-activated protein kinase kinase kinase 13	-1.01	1.15E-05
ENSMUSG00000050368	Hoxd10	homeobox D10	-1.01	6.40E-05
ENSMUSG00000036334	Igsf10	immunoglobulin superfamily, member 10	-1.01	1.84E-07
ENSMUSG00000059201	Lep	leptin	-1.01	6.92E-03
ENSMUSG00000045613	Chrm2	cholinergic receptor, muscarinic 2, cardiac	-1.01	5.19E-07
ENSMUSG00000002944	Cd36	CD36 antigen	-1.02	1.26E-06
ENSMUSG00000047604	Frat2	frequently rearranged in advanced T cell lymphomas 2	-1.02	5.08E-05
ENSMUSG00000004360	9330159F19Rik	RIKEN cDNA 9330159F19 gene	-1.02	4.00E-04
ENSMUSG00000038298	Pdzk1	PDZ domain containing 1	-1.02	8.45E-03
ENSMUSG00000061013	Mkx	mohawk homeobox	-1.02	6.46E-05
ENSMUSG00000020620	Abca8b	ATP-binding cassette, sub-family A (ABC1), member 8b	-1.02	4.78E-05
ENSMUSG00000030278	Cidec	cell death-inducing DFFA-like effector c	-1.02	4.08E-05
ENSMUSG00000058070	Eml1	echinoderm microtubule associated protein like 1	-1.02	7.72E-09
ENSMUSG00000056666	Retsat	retinol saturase (all trans retinol 13,14 reductase)	-1.03	1.26E-08
ENSMUSG00000034579	Pla2g3	phospholipase A2, group III	-1.03	2.73E-05
ENSMUSG00000069805	Fbp1	fructose bisphosphatase 1	-1.03	3.12E-03
ENSMUSG00000022010	Tsc22d1	TSC22 domain family, member 1	-1.03	7.31E-09
ENSMUSG00000046618	Olfml2a	olfactomedin-like 2A	-1.03	1.00E-04
ENSMUSG00000050520	Cldn8	claudin 8	-1.03	8.14E-04
ENSMUSG00000019775	Rgs17	regulator of G-protein signaling 17	-1.04	2.54E-04
ENSMUSG00000021373	Cap2	CAP, adenylate cyclase-associated protein, 2 (yeast)	-1.04	3.27E-06
ENSMUSG00000021763	BC067074	cDNA sequence BC067074	-1.04	3.33E-03
ENSMUSG00000021838	Samd4	sterile alpha motif domain containing 4	-1.04	1.35E-05
ENSMUSG00000021573	Tppp	tubulin polymerization promoting protein	-1.04	3.00E-06
ENSMUSG00000040957	Cables1	CDK5 and Abl enzyme substrate 1	-1.04	1.03E-07
ENSMUSG00000010066	Cacna2d2	calcium channel, voltage-dependent, alpha 2/delta subunit 2	-1.04	4.17E-05
ENSMUSG00000003657	Calb2	calbindin 2	-1.05	1.78E-05
ENSMUSG00000031712	Il15	interleukin 15	-1.05	7.27E-06
ENSMUSG00000027858	Tspan2	tetraspanin 2	-1.05	1.36E-05
ENSMUSG00000040896	Kcnd3	potassium voltage-gated channel, Shal-related family, member 3	-1.05	3.69E-07
ENSMUSG00000032064	Dixdc1	DIX domain containing 1	-1.05	7.17E-06
ENSMUSG00000020672	Sntg2	syntrophin, gamma 2	-1.05	7.52E-06
ENSMUSG00000018861	Fdxr	ferredoxin reductase	-1.05	9.81E-06
ENSMUSG00000029369	Afm	afamin	-1.05	9.73E-06
ENSMUSG00000061780	Cfd	complement factor D (adipsin)	-1.05	8.42E-05
ENSMUSG00000060843	Ctnna3	catenin (cadherin associated protein), alpha 3	-1.05	1.50E-05
ENSMUSG00000028461	Ccdc107	coiled-coil domain containing 107	-1.05	1.43E-06
ENSMUSG00000041828	Abca8a	ATP-binding cassette, sub-family A (ABC1), member 8a	-1.06	1.08E-06
ENSMUSG00000029333	Rasgef1b	RasGEF domain family, member 1B	-1.06	7.69E-06
ENSMUSG00000032324	Tspan3	tetraspanin 3	-1.06	3.29E-06
ENSMUSG00000079037	Prnp	prion protein	-1.06	4.44E-08
ENSMUSG00000090136	Gm10177	predicted gene 10177	-1.06	2.18E-03
ENSMUSG00000056481	Cd248	CD248 antigen, endosialin	-1.06	9.91E-06

ENSMUSG00000030092	Cntn6	contactin 6	-1.06	4.64E-03
ENSMUSG00000069919	Hba-a1	hemoglobin alpha, adult chain 1	-1.06	1.14E-04
ENSMUSG00000027359	Slc27a2	solute carrier family 27 (fatty acid transporter), member 2	-1.07	8.62E-06
ENSMUSG00000034157	Cipc	CLOCK interacting protein, circadian	-1.07	4.70E-06
ENSMUSG00000019326	Aoc3	amine oxidase, copper containing 3	-1.07	3.91E-09
ENSMUSG00000022383			-1.07	2.21E-07
ENSMUSG00000019359	Gdpd2	glycerophosphodiester phosphodiesterase domain containing 2	-1.07	6.06E-04
ENSMUSG00000029130	Rnf32	ring finger protein 32	-1.07	2.45E-04
ENSMUSG00000044550	Tceal3	transcription elongation factor A (SII)-like 3	-1.07	4.59E-03
ENSMUSG00000020889	Nr1d1	nuclear receptor subfamily 1, group D, member 1	-1.07	3.87E-04
ENSMUSG00000044749	Abca6	ATP-binding cassette, sub-family A (ABC1), member 6	-1.07	3.40E-04
ENSMUSG00000025716	Myo3a	myosin IIIA	-1.07	2.66E-05
ENSMUSG00000027015	Cybrd1	cytochrome b reductase 1	-1.07	3.07E-05
ENSMUSG00000068699	Flnc	filamin C, gamma	-1.07	2.25E-09
ENSMUSG00000037362	Nov	nephroblastoma overexpressed gene	-1.08	4.50E-04
ENSMUSG00000034472	Rasd2	RASD family, member 2	-1.08	3.72E-05
ENSMUSG00000042476	Abcb4	ATP-binding cassette, sub-family B (MDR/TAP), member 4	-1.08	5.06E-03
ENSMUSG00000021294	Kif26a	kinesin family member 26A	-1.08	1.13E-03
ENSMUSG00000040543	Pitpnm3	PITPNM family member 3	-1.08	3.34E-06
ENSMUSG00000059824	Dbp	D site albumin promoter binding protein	-1.08	1.73E-04
ENSMUSG00000029838	Ptn	pleiotrophin	-1.09	6.57E-06
ENSMUSG00000044921	Rassf9	Ras association (RalGDS/AF-6) domain family (N-terminal) member 9	-1.09	9.58E-05
ENSMUSG00000040147	Maob	monoamine oxidase B	-1.09	2.60E-07
ENSMUSG00000079440	Alpi	alkaline phosphatase, intestinal	-1.09	4.94E-06
ENSMUSG00000007655	Cav1	caveolin 1, caveolae protein	-1.09	1.09E-08
ENSMUSG00000039405	Prss23	protease, serine 23	-1.09	1.64E-07
ENSMUSG00000038756	Ttll6	tubulin tyrosine ligase-like family, member 6	-1.09	3.89E-03
ENSMUSG00000022878	Adipoq	adiponectin, C1Q and collagen domain containing	-1.09	1.87E-05
ENSMUSG00000098220			-1.09	2.87E-03
ENSMUSG00000032278	Paqr5	progestin and adipoQ receptor family member V	-1.09	2.68E-09
ENSMUSG00000035783	Acta2	actin, alpha 2, smooth muscle, aorta	-1.10	5.06E-11
ENSMUSG00000025272	Tro	trophinin	-1.10	3.69E-04
ENSMUSG00000041559	Fmod	fibromodulin	-1.10	6.74E-04
ENSMUSG00000038555	Reep2	receptor accessory protein 2	-1.10	8.59E-04
ENSMUSG00000038393	Txnip	thioredoxin interacting protein	-1.10	1.41E-09
ENSMUSG00000038370	Pcp4l1	Purkinje cell protein 4-like 1	-1.10	5.80E-08
ENSMUSG00000047146	Tet1	tet methylcytosine dioxygenase 1	-1.10	1.12E-05
ENSMUSG00000076435	Acsf2	acyl-CoA synthetase family member 2	-1.11	1.00E-09
ENSMUSG00000064343			-1.11	1.91E-03
ENSMUSG00000067889	Sptbn2	spectrin beta, non-erythrocytic 2	-1.11	5.28E-07
ENSMUSG00000046329	Slc25a23	solute carrier family 25 (mitochondrial carrier; phosphate carrier), member 23	-1.11	1.15E-07
ENSMUSG00000028255	Clca1	chloride channel calcium activated 1	-1.11	3.73E-10
ENSMUSG00000055653	Gpc3	glypican 3	-1.11	7.52E-07
ENSMUSG00000040505	Abcg5	ATP-binding cassette, sub-family G (WHITE), member 5	-1.11	1.55E-03
ENSMUSG00000032192	Gnb5	guanine nucleotide binding protein (G protein), beta 5	-1.12	7.81E-05
ENSMUSG00000029201	Ugdh	UDP-glucose dehydrogenase	-1.12	5.86E-08

ENSMUSG00000032514	Ttc21a	tetratricopeptide repeat domain 21A	-1.12	3.13E-03
ENSMUSG00000057123	Gja5	gap junction protein, alpha 5	-1.12	1.71E-04
ENSMUSG00000028003	Lrat	lecithin-retinol acyltransferase (phosphatidylcholine-retinol-O-acyltransferase)	-1.12	1.51E-04
ENSMUSG00000023829	Slc22a1	solute carrier family 22 (organic cation transporter), member 1	-1.13	1.49E-07
ENSMUSG00000060181	Slc35e3	solute carrier family 35, member E3	-1.13	1.22E-06
ENSMUSG00000049176	Frmpd4	FERM and PDZ domain containing 4	-1.13	3.19E-03
ENSMUSG00000057880	Abat	4-aminobutyrate aminotransferase	-1.13	5.66E-08
ENSMUSG00000000253	Gmpr	guanosine monophosphate reductase	-1.13	8.75E-05
ENSMUSG00000071656	Lrrn4cl	LRRN4 C-terminal like	-1.13	4.31E-05
ENSMUSG00000046460	Sh2d7	SH2 domain containing 7	-1.13	1.24E-03
ENSMUSG00000038776	Ephx1	epoxide hydrolase 1, microsomal	-1.13	1.25E-08
ENSMUSG00000074971	Fibin	fin bud initiation factor homolog (zebrafish)	-1.14	4.71E-05
ENSMUSG00000053963	6330403A02Rik	RIKEN cDNA 6330403A02 gene	-1.14	4.19E-07
ENSMUSG00000032609	Klhdc8b	kelch domain containing 8B	-1.14	1.11E-04
ENSMUSG00000027698	Nceh1	neutral cholesterol ester hydrolase 1	-1.14	7.49E-08
ENSMUSG00000019278	Dpep1	dipeptidase 1 (renal)	-1.14	9.69E-09
ENSMUSG00000074826	Gm10767	predicted gene 10767	-1.14	2.42E-03
ENSMUSG00000043439	E130012A19Rik	RIKEN cDNA E130012A19 gene	-1.15	3.06E-06
ENSMUSG00000050097	Ces2b	carboxyesterase 2B	-1.15	5.89E-06
ENSMUSG00000035686	Thrsp	thyroid hormone responsive	-1.15	8.18E-04
ENSMUSG00000089960	Ugt1a1	UDP glucuronosyltransferase 1 family, polypeptide A1	-1.15	2.70E-05
ENSMUSG00000042254	Cilp	cartilage intermediate layer protein, nucleotide pyrophosphohydrolase	-1.15	1.18E-07
ENSMUSG00000062542	Syt9	synaptotagmin IX	-1.15	2.83E-03
ENSMUSG00000038167	Plekhg6	pleckstrin homology domain containing, family G (with RhoGef domain) member 6	-1.15	1.27E-06
ENSMUSG00000029864	Gstk1	glutathione S-transferase kappa 1	-1.15	1.50E-09
ENSMUSG00000049409	Prokr1	prokineticin receptor 1	-1.16	8.42E-04
ENSMUSG00000029868	Trpv6	transient receptor potential cation channel, subfamily V, member 6	-1.16	2.62E-03
ENSMUSG00000033717	Adra2a	adrenergic receptor, alpha 2a	-1.16	2.57E-08
ENSMUSG00000027894	Slc6a17	solute carrier family 6 (neurotransmitter transporter), member 17	-1.16	3.67E-05
ENSMUSG00000087535			-1.16	2.31E-03
ENSMUSG00000087582			-1.16	1.75E-03
ENSMUSG00000021567	Nkd2	naked cuticle 2 homolog (Drosophila)	-1.16	1.09E-06
ENSMUSG00000018659	Pnpo	pyridoxine 5'-phosphate oxidase	-1.17	9.84E-09
ENSMUSG00000060548	Tnfrsf19	tumor necrosis factor receptor superfamily, member 19	-1.17	6.45E-05
ENSMUSG00000018570	2810408A11Rik	RIKEN cDNA 2810408A11 gene	-1.17	7.30E-05
ENSMUSG00000036585	Fgf1	fibroblast growth factor 1	-1.17	7.30E-08
ENSMUSG00000069917	Hba-a2	hemoglobin alpha, adult chain 2	-1.18	3.66E-05
ENSMUSG00000027318	Adam33	a disintegrin and metallopeptidase domain 33	-1.18	1.17E-03
ENSMUSG00000024049	Myom1	myomesin 1	-1.18	1.30E-08
ENSMUSG00000033419	Snap91	synaptosomal-associated protein 91	-1.19	8.95E-04
ENSMUSG00000063430	Wscd2	WSC domain containing 2	-1.19	3.33E-07
ENSMUSG00000026463	Atp2b4	ATPase, Ca++ transporting, plasma membrane 4	-1.19	1.25E-12
ENSMUSG00000020431	Adcy1	adenylate cyclase 1	-1.19	3.18E-04
ENSMUSG00000020439	Smtn	smoothelin	-1.19	2.45E-10
ENSMUSG00000025194	Abcc2	ATP-binding cassette, sub-family C (CFTR/MRP), member 2	-1.19	1.95E-03
ENSMUSG00000074207	Adh1	alcohol dehydrogenase 1 (class I)	-1.19	4.02E-08

ENSMUSG00000062410	Hsd3b3	hydroxy-delta-5-steroid dehydrogenase, 3 beta- and steroid delta-isomerase 3	-1.20	8.79E-09
ENSMUSG00000031636	Pdlim3	PDZ and LIM domain 3	-1.20	4.13E-10
ENSMUSG00000087347			-1.21	1.75E-03
ENSMUSG00000055493	Epm2a	epilepsy, progressive myoclonic epilepsy, type 2 gene alpha	-1.21	1.69E-04
ENSMUSG00000020405	Fabp6	fatty acid binding protein 6, ileal (gastrotropin)	-1.21	1.72E-03
ENSMUSG00000023094	Msrb2	methionine sulfoxide reductase B2	-1.21	2.61E-04
ENSMUSG00000049971	Glt1d1	glycosyltransferase 1 domain containing 1	-1.21	1.29E-05
ENSMUSG00000027556	Car1	carbonic anhydrase 1	-1.22	1.99E-08
ENSMUSG00000094651	Gal3st2	galactose-3-O-sulfotransferase 2	-1.22	3.37E-07
ENSMUSG00000012705	Retn	resistin	-1.22	1.17E-04
ENSMUSG00000032648	Pygm	muscle glycogen phosphorylase	-1.22	2.55E-07
ENSMUSG00000013415	Igf2bp1	insulin-like growth factor 2 mRNA binding protein 1	-1.22	3.78E-05
ENSMUSG00000001663	Gstt1	glutathione S-transferase, theta 1	-1.23	3.56E-07
ENSMUSG00000050751	Pgbd5	piggyBac transposable element derived 5	-1.23	1.42E-04
ENSMUSG00000021792	Fam213a	family with sequence similarity 213, member A	-1.23	8.45E-09
ENSMUSG00000049811	Fam161a	family with sequence similarity 161, member A	-1.23	2.52E-05
ENSMUSG00000032649	Colgalt2	collagen beta(1-O)galactosyltransferase 2	-1.23	6.59E-04
ENSMUSG00000069601	Ank3	ankyrin 3, epithelial	-1.23	2.29E-08
ENSMUSG00000021943	Gdf10	growth differentiation factor 10	-1.23	1.42E-03
ENSMUSG00000031700	Gpt2	glutamic pyruvate transaminase (alanine aminotransferase) 2	-1.23	8.55E-09
ENSMUSG00000018217	Pmp22	peripheral myelin protein 22	-1.23	2.26E-11
ENSMUSG00000062257	Opcml	opioid binding protein/cell adhesion molecule-like	-1.23	2.28E-06
ENSMUSG00000022490	Ppp1r1a	protein phosphatase 1, regulatory (inhibitor) subunit 1A	-1.24	1.41E-04
ENSMUSG00000087528			-1.24	6.85E-04
ENSMUSG00000018566	Slc2a4	solute carrier family 2 (facilitated glucose transporter), member 4	-1.25	4.98E-08
ENSMUSG00000052957	Gas1	growth arrest specific 1	-1.25	1.42E-06
ENSMUSG00000044860	Gm1123	predicted gene 1123	-1.26	1.84E-08
ENSMUSG00000048498	Cd300e	CD300e antigen	-1.26	9.20E-04
ENSMUSG00000061100	Retnla	resistin like alpha	-1.26	8.86E-04
ENSMUSG00000020653	Klf11	Kruppel-like factor 11	-1.26	1.81E-06
ENSMUSG00000028976	Slc2a5	solute carrier family 2 (facilitated glucose transporter), member 5	-1.26	1.04E-04
ENSMUSG00000062760	1810041L15Rik	RIKEN cDNA 1810041L15 gene	-1.26	1.37E-05
ENSMUSG00000029309	Sparcl1	SPARC-like 1	-1.27	6.23E-13
ENSMUSG00000030865	Chp2	calcineurin-like EF hand protein 2	-1.27	4.03E-09
ENSMUSG00000050505	Pcdh20	protocadherin 20	-1.27	9.18E-04
ENSMUSG00000036814	Slc6a20a	solute carrier family 6 (neurotransmitter transporter), member 20A	-1.27	4.17E-04
ENSMUSG00000031790	Mmp15	matrix metallopeptidase 15	-1.27	2.98E-11
ENSMUSG00000030711	Sult1a1	sulfotransferase family 1A, phenol-preferring, member 1	-1.27	1.18E-05
ENSMUSG00000038967	Pdk2	pyruvate dehydrogenase kinase, isoenzyme 2	-1.28	5.51E-08
ENSMUSG00000004038	Gstm3	glutathione S-transferase, mu 3	-1.28	1.14E-04
ENSMUSG00000074218	Cox7a1	cytochrome c oxidase subunit VIIa 1	-1.29	1.96E-09
ENSMUSG00000032122	Slc37a2	solute carrier family 37 (glycerol-3-phosphate transporter), member 2	-1.29	1.23E-05
ENSMUSG00000072720	Myo18b	myosin XVIIIb	-1.30	3.68E-06
ENSMUSG00000031173	Otc	ornithine transcarbamylase	-1.30	6.40E-07
ENSMUSG00000025545	Clybl	citrate lyase beta like	-1.30	2.22E-08
ENSMUSG00000068748	Ptprz1	protein tyrosine phosphatase, receptor type Z, polypeptide 1	-1.30	2.47E-05

ENSMUSG00000015354	Pcolce2	procollagen C-endopeptidase enhancer 2	-1.30	4.79E-06
ENSMUSG00000020334	Slc22a4	solute carrier family 22 (organic cation transporter), member 4	-1.30	1.63E-05
ENSMUSG00000098132	Rassf10	Ras association (RalGDS/AF-6) domain family (N-terminal) member 10	-1.30	4.31E-05
ENSMUSG00000046275	Tusc5	tumor suppressor candidate 5	-1.31	5.38E-06
ENSMUSG00000031938	4931406C07Rik	RIKEN cDNA 4931406C07 gene	-1.31	1.60E-09
ENSMUSG00000032607	Amt	aminomethyltransferase	-1.31	1.19E-07
ENSMUSG00000024978	Gpam	glycerol-3-phosphate acyltransferase, mitochondrial	-1.31	4.14E-11
ENSMUSG00000010122	Slc47a1	solute carrier family 47, member 1	-1.31	2.00E-04
ENSMUSG00000050315	Synpo2	synaptopodin 2	-1.31	5.31E-16
ENSMUSG00000070704	Ugt2b36	UDP glucuronosyltransferase 2 family, polypeptide B36	-1.32	2.08E-04
ENSMUSG00000072723			-1.32	2.59E-05
ENSMUSG00000074736	Syndig1	synapse differentiation inducing 1	-1.32	1.11E-05
ENSMUSG00000023046	Igfbp6	insulin-like growth factor binding protein 6	-1.33	6.05E-07
ENSMUSG00000030409	Dmpk	dystrophia myotonica-protein kinase	-1.33	2.36E-13
ENSMUSG00000027397	Slc20a1	solute carrier family 20, member 1	-1.33	3.04E-08
ENSMUSG00000020080	Hkdc1	hexokinase domain containing 1	-1.33	4.66E-08
ENSMUSG00000040703	Cyp2s1	cytochrome P450, family 2, subfamily s, polypeptide 1	-1.33	3.29E-11
ENSMUSG00000058135	Gstm1	glutathione S-transferase, mu 1	-1.34	5.70E-11
ENSMUSG00000026489	Adck3	aarF domain containing kinase 3	-1.34	2.66E-08
ENSMUSG00000055748	Gsdmc4	gasdermin C4	-1.34	1.65E-05
ENSMUSG00000064036	Mro	maestro	-1.34	8.67E-05
ENSMUSG00000027761	Aadac	arylacetamide deacetylase (esterase)	-1.34	2.66E-06
ENSMUSG00000023057	Fabp2	fatty acid binding protein 2, intestinal	-1.34	7.70E-05
ENSMUSG00000005540	Fcer2a	Fc receptor, IgE, low affinity II, alpha polypeptide	-1.34	6.42E-08
ENSMUSG00000087291	Gm11946	predicted gene 11946	-1.34	1.35E-05
ENSMUSG00000032387	Rbpms2	RNA binding protein with multiple splicing 2	-1.35	1.01E-07
ENSMUSG00000023800	Tiam2	T cell lymphoma invasion and metastasis 2	-1.35	8.03E-10
ENSMUSG00000061825	Ces2c	carboxylesterase 2C	-1.35	2.35E-08
ENSMUSG00000063011	Msln	mesothelin	-1.35	2.66E-04
ENSMUSG00000045348	Nyap1	neuronal tyrosine-phosphorylated phosphoinositide 3-kinase adaptor 1	-1.35	1.36E-06
ENSMUSG00000041073	Nacad	NAC alpha domain containing	-1.36	3.42E-08
ENSMUSG00000031877	Ces2g	carboxylesterase 2G	-1.36	1.77E-06
ENSMUSG00000047496	Rnf152	ring finger protein 152	-1.36	1.80E-09
ENSMUSG00000036832	Lpar3	lysophosphatidic acid receptor 3	-1.37	2.69E-04
ENSMUSG00000006360	Crip1	cysteine-rich protein 1 (intestinal)	-1.37	8.34E-11
ENSMUSG00000020019	Ntn4	netrin 4	-1.38	7.93E-10
ENSMUSG00000034785	Dio1	deiodinase, iodothyronine, type I	-1.38	3.84E-09
ENSMUSG00000019970	Sgk1	serum/glucocorticoid regulated kinase 1	-1.38	1.70E-06
ENSMUSG00000028356	Ambp	alpha 1 microglobulin/bikunin	-1.38	1.78E-04
ENSMUSG00000025196	Cpn1	carboxypeptidase N, polypeptide 1	-1.38	3.50E-08
ENSMUSG00000050103	Agmo	alkylglycerol monooxygenase	-1.39	1.43E-07
ENSMUSG00000021236	Entpd5	ectonucleoside triphosphate diphosphohydrolase 5	-1.39	4.76E-11
ENSMUSG00000043430	Psapl1	prosaposin-like 1	-1.39	2.99E-04
ENSMUSG00000022546	Gpt	glutamic pyruvic transaminase, soluble	-1.39	3.75E-08
ENSMUSG00000026726	Cubn	cubilin (intrinsic factor-cobalamin receptor)	-1.39	1.31E-04
ENSMUSG00000067818	Myl9	myosin, light polypeptide 9, regulatory	-1.40	3.84E-17

ENSMUSG00000038725	Pkhd1l1	polycystic kidney and hepatic disease 1-like 1	-1.40	3.70E-07
ENSMUSG00000074882	Cyp2c68	cytochrome P450, family 2, subfamily c, polypeptide 68	-1.41	2.43E-05
ENSMUSG00000018830	Myh11	myosin, heavy polypeptide 11, smooth muscle	-1.41	8.75E-17
ENSMUSG00000073608	Gm6086	predicted gene 6086	-1.41	9.00E-06
ENSMUSG00000060600	Eno3	enolase 3, beta muscle	-1.41	9.62E-09
ENSMUSG00000074004	B3gnt6	UDP-GlcNAc:betaGal beta-1,3-N-acetylglucosaminyltransferase 6 (core 3 synthase)	-1.42	3.35E-06
ENSMUSG00000019577	Pdk4	pyruvate dehydrogenase kinase, isoenzyme 4	-1.43	6.04E-05
ENSMUSG00000063296	Tmem117	transmembrane protein 117	-1.43	1.01E-09
ENSMUSG00000017607	Tns4	tensin 4	-1.43	1.12E-09
ENSMUSG00000034687	Fras1	Fraser syndrome 1 homolog (human)	-1.43	1.22E-06
ENSMUSG00000049336	Tenm2	teneurin transmembrane protein 2	-1.44	7.51E-06
ENSMUSG00000027559	Car3	carbonic anhydrase 3	-1.44	1.38E-06
ENSMUSG00000022040	Ephx2	epoxide hydrolase 2, cytoplasmic	-1.44	5.81E-10
ENSMUSG00000019945	1700040L02Rik	RIKEN cDNA 1700040L02 gene	-1.44	2.23E-06
ENSMUSG00000028464	Tpm2	tropomyosin 2, beta	-1.44	9.14E-17
ENSMUSG00000033207	Mamdc2	MAM domain containing 2	-1.45	6.06E-10
ENSMUSG00000023336	Wfdc1	WAP four-disulfide core domain 1	-1.45	4.36E-09
ENSMUSG00000046589	Lrrc8e	leucine rich repeat containing 8 family, member E	-1.46	6.73E-09
ENSMUSG00000032085	Tagln	transgelin	-1.47	6.02E-18
ENSMUSG00000019989	Enpp3	ectonucleotide pyrophosphatase/phosphodiesterase 3	-1.48	5.04E-09
ENSMUSG00000025658	Cnksr2	connector enhancer of kinase suppressor of Ras 2	-1.48	1.26E-06
ENSMUSG00000035184	Fam124a	family with sequence similarity 124, member A	-1.49	2.45E-07
ENSMUSG00000028039	Efna3	ephrin A3	-1.49	2.37E-05
ENSMUSG00000052485	Tmem171	transmembrane protein 171	-1.49	3.99E-12
ENSMUSG00000029772	Ahcyl2	S-adenosylhomocysteine hydrolase-like 2	-1.50	2.51E-14
ENSMUSG00000031937	Vstm5	V-set and transmembrane domain containing 5	-1.51	2.70E-06
ENSMUSG00000051726	Kcnf1	potassium voltage-gated channel, subfamily F, member 1	-1.53	1.42E-07
ENSMUSG00000040812	Agbl2	ATP/GTP binding protein-like 2	-1.54	1.05E-07
ENSMUSG00000038591	Colec10	collectin sub-family member 10	-1.54	5.73E-09
ENSMUSG00000037071	Scd1	stearoyl-Coenzyme A desaturase 1	-1.54	1.95E-06
ENSMUSG00000042751	Nmnat2	nicotinamide nucleotide adenylyltransferase 2	-1.55	1.29E-08
ENSMUSG00000028755	Cda	cytidine deaminase	-1.56	2.40E-10
ENSMUSG00000031725	Ces1f	carboxylesterase 1F	-1.56	6.11E-13
ENSMUSG00000026418	Tnni1	troponin I, skeletal, slow 1	-1.57	7.24E-06
ENSMUSG00000032883	Acsl3	acyl-CoA synthetase long-chain family member 3	-1.58	2.00E-12
ENSMUSG00000095385	D630033O11Rik	RIKEN cDNA D630033O11 gene	-1.59	2.76E-05
ENSMUSG00000020068			-1.59	5.69E-08
ENSMUSG00000002565	Scin	scinderin	-1.59	3.73E-13
ENSMUSG00000060780	Lrrtm1	leucine rich repeat transmembrane neuronal 1	-1.60	2.46E-05
ENSMUSG00000054619	Mettl7a1	methyltransferase like 7A1	-1.60	1.19E-13
ENSMUSG00000032854	Ugt8a	UDP galactosyltransferase 8A	-1.61	1.42E-05
ENSMUSG00000085375			-1.61	3.54E-07
ENSMUSG00000055730	Ces2a	carboxylesterase 2A	-1.61	1.48E-05
ENSMUSG00000039323	Igfbp2	insulin-like growth factor binding protein 2	-1.62	4.78E-07
ENSMUSG00000021367	Edn1	endothelin 1	-1.63	4.70E-12
ENSMUSG00000081169			-1.63	2.11E-06

ENSMUSG00000020182	Ddc	dopa decarboxylase	-1.66	5.19E-14
ENSMUSG00000030554	Synm	synemin, intermediate filament protein	-1.67	1.36E-21
ENSMUSG00000028088	Fmo5	flavin containing monooxygenase 5	-1.67	2.08E-12
ENSMUSG00000027870	Hao2	hydroxyacid oxidase 2	-1.68	7.60E-13
ENSMUSG00000047501	Cldn4	claudin 4	-1.69	1.19E-12
ENSMUSG00000052131	Akr1b7	aldo-keto reductase family 1, member B7	-1.70	3.64E-06
ENSMUSG00000026614	Slc30a10	solute carrier family 30, member 10	-1.70	9.71E-07
ENSMUSG00000027875	Hmgcs2	3-hydroxy-3-methylglutaryl-Coenzyme A synthase 2	-1.72	4.54E-18
ENSMUSG00000040584	Abcb1a	ATP-binding cassette, sub-family B (MDR/TAP), member 1A	-1.73	1.85E-07
ENSMUSG00000026208	Des	desmin	-1.74	9.86E-26
ENSMUSG00000061808	Ttr	transthyretin	-1.74	8.04E-12
ENSMUSG00000056973	Ces1d	carboxylesterase 1D	-1.75	3.67E-15
ENSMUSG00000041012	Cmtm8	CKLF-like MARVEL transmembrane domain containing 8	-1.76	2.27E-10
ENSMUSG00000020793	Galr2	galanin receptor 2	-1.77	4.66E-08
ENSMUSG00000053399	Adamts18	a disintegrin-like and metallopeptidase (reprolysin type) with thrombospondin type 1 motif, 18	-1.77	3.52E-06
ENSMUSG00000029811	Aoc1	amine oxidase, copper-containing 1	-1.77	7.50E-21
ENSMUSG00000027401	Tgm3	transglutaminase 3, E polypeptide	-1.78	4.10E-06
ENSMUSG00000027513	Pck1	phosphoenolpyruvate carboxykinase 1, cytosolic	-1.80	3.61E-17
ENSMUSG00000024727	Trpm6	transient receptor potential cation channel, subfamily M, member 6	-1.82	3.04E-08
ENSMUSG00000079355	Ackr4	atypical chemokine receptor 4	-1.84	4.09E-13
ENSMUSG00000025002	Cyp2c55	cytochrome P450, family 2, subfamily c, polypeptide 55	-1.87	1.14E-06
ENSMUSG00000059430	Actg2	actin, gamma 2, smooth muscle, enteric	-1.88	2.18E-20
ENSMUSG00000001349	Cnn1	calponin 1	-1.89	5.36E-28
ENSMUSG00000051295	9630028B13Rik	RIKEN cDNA 9630028B13 gene	-1.90	1.02E-12
ENSMUSG00000019762	Iyd	iodotyrosine deiodinase	-1.95	8.93E-09
ENSMUSG00000024575	Pde6a	phosphodiesterase 6A, cGMP-specific, rod, alpha	-1.97	1.09E-10
ENSMUSG00000026166	Ccl20	chemokine (C-C motif) ligand 20	-1.98	8.73E-09
ENSMUSG00000073424	Cyp4f15	cytochrome P450, family 4, subfamily f, polypeptide 15	-2.00	7.78E-08
ENSMUSG00000029630	Cyp3a25	cytochrome P450, family 3, subfamily a, polypeptide 25	-2.01	1.89E-07
ENSMUSG00000030399	Ckm	creatine kinase, muscle	-2.07	7.98E-21
ENSMUSG00000060615	Ang4	angiogenin, ribonuclease A family, member 4	-2.07	2.41E-10
ENSMUSG00000092586	Ly6g6c	lymphocyte antigen 6 complex, locus G6C	-2.08	3.99E-08
ENSMUSG00000026701	Prdx6	peroxiredoxin 6	-2.10	1.92E-19
ENSMUSG00000010311	Optc	opticin	-2.13	1.92E-17
ENSMUSG00000081488			-2.15	1.24E-13
ENSMUSG00000028713	Cyp4b1	cytochrome P450, family 4, subfamily b, polypeptide 1	-2.19	4.72E-12
ENSMUSG00000037762	Slc16a9	solute carrier family 16 (monocarboxylic acid transporters), member 9	-2.20	2.41E-23
ENSMUSG00000084174	Sycn	syncollin	-2.23	2.52E-17
ENSMUSG00000035557	Krt17	keratin 17	-2.29	2.14E-14
ENSMUSG00000039760	Il22ra2	interleukin 22 receptor, alpha 2	-2.33	1.79E-17
ENSMUSG00000057074	Ces1g	carboxylesterase 1G	-2.37	1.29E-13
ENSMUSG00000049580	Tsku	tsukushi	-2.42	4.47E-21
ENSMUSG00000022491	Glycam1	glycosylation dependent cell adhesion molecule 1	-2.83	2.54E-36

Table S4 Differentially expressed genes of BALB/c (YPIII Δ*cnfy* infected 5 dpi vs. YPIII infected 5 dpi)

Ensembl ID	Gene symbol	Gene name	log_2 fold change	p-value
ENSMUSG00000031551	Ido1	indoleamine 2,3-dioxygenase 1	2.74	4.41E-26
ENSMUSG00000068086	Cyp2d9	cytochrome P450, family 2, subfamily d, polypeptide 9	2.08	9.23E-09
ENSMUSG00000029417	Cxcl9	chemokine (C-X-C motif) ligand 9	1.98	2.92E-09
ENSMUSG00000074195	Clca4b	chloride channel calcium activated 4B	1.98	2.15E-08
ENSMUSG00000036123	Slc9a3	solute carrier family 9 (sodium/hydrogen exchanger), member 3	1.95	2.05E-09
ENSMUSG00000032068	Plet1	placenta expressed transcript 1	1.86	9.10E-10
ENSMUSG00000020826	Nos2	nitric oxide synthase 2, inducible	1.84	1.39E-09
ENSMUSG00000032122	Slc37a2	solute carrier family 37 (glycerol-3-phosphate transporter), member 2	1.71	7.43E-09
ENSMUSG00000074115	Saa1	serum amyloid A 1	1.60	1.13E-06
ENSMUSG00000000805	Car4	carbonic anhydrase 4	1.58	2.44E-13
ENSMUSG00000028527	Ak4	adenylate kinase 4	1.54	3.32E-07
ENSMUSG00000053862	Slc51b	solute carrier family 51, beta subunit	1.54	4.55E-10
ENSMUSG00000057465	Saa2	serum amyloid A 2	1.51	6.13E-09
ENSMUSG00000099065			1.50	5.45E-09
ENSMUSG00000047728	BC025446	cDNA sequence BC025446	1.49	2.61E-06
ENSMUSG00000021214	Akr1c18	aldo-keto reductase family 1, member C18	1.47	5.10E-05
ENSMUSG00000049281	Scn3b	sodium channel, voltage-gated, type III, beta	1.44	7.29E-07
ENSMUSG00000078922	Tgtp1	T cell specific GTPase 1	1.43	3.42E-06
ENSMUSG00000065629			1.43	2.03E-04
ENSMUSG00000010601	Apol7a	apolipoprotein L 7a	1.41	4.84E-08
ENSMUSG00000075602	Ly6a	lymphocyte antigen 6 complex, locus A	1.37	1.30E-08
ENSMUSG00000026880	Stom	stomatin	1.36	1.51E-11
ENSMUSG00000035186	Ubd	ubiquitin D	1.36	5.37E-09
ENSMUSG00000064400			1.36	4.06E-04
ENSMUSG00000041481			1.34	3.88E-09
ENSMUSG00000079363	Gbp4	guanylate binding protein 4	1.31	2.29E-05
ENSMUSG00000050982	Apol10a	apolipoprotein L 10A	1.30	6.15E-05
ENSMUSG00000027375	Mal	myelin and lymphocyte protein, T cell differentiation protein	1.29	4.04E-08
ENSMUSG00000024411	Aqp4	aquaporin 4	1.28	3.17E-05
ENSMUSG00000076526			1.28	2.03E-04
ENSMUSG00000045725	Prr15	proline rich 15	1.27	1.23E-08
ENSMUSG00000041202	Pla2g2d	phospholipase A2, group IID	1.27	4.22E-08
ENSMUSG00000032010	Usp2	ubiquitin specific peptidase 2	1.25	4.17E-06
ENSMUSG00000056148	Rdh9	retinol dehydrogenase 9	1.25	1.08E-04
ENSMUSG00000028269			1.25	9.80E-05
ENSMUSG00000053279	Aldh1a1	aldehyde dehydrogenase family 1, subfamily A1	1.24	3.33E-08
ENSMUSG00000025557	Slc15a1	solute carrier family 15 (oligopeptide transporter), member 1	1.24	9.06E-05
ENSMUSG00000045932	Ifit2	interferon-induced protein with tetratricopeptide repeats 2	1.23	4.68E-07
ENSMUSG00000071356	Reg3b	regenerating islet-derived 3 beta	1.23	4.09E-04
ENSMUSG00000079362	Gbp6	guanylate binding protein 6	1.23	1.11E-05
ENSMUSG00000027820	Mme	membrane metallo endopeptidase	1.23	1.66E-04
ENSMUSG00000030762	Aqp8	aquaporin 8	1.22	4.19E-04
ENSMUSG00000030017	Reg3g	regenerating islet-derived 3 gamma	1.22	6.17E-04
ENSMUSG00000030742	Lat	linker for activation of T cells	1.21	1.83E-04
ENSMUSG00000061531	Tmem236	transmembrane protein 236	1.21	1.98E-06
ENSMUSG00000024731	Ms4a10	membrane-spanning 4-domains, subfamily A, member 10	1.20	9.56E-05
ENSMUSG00000034438	Gbp8	guanylate-binding protein 8	1.20	2.97E-06
ENSMUSG00000095866			1.20	6.16E-05
ENSMUSG00000037649	H2-DMa	histocompatibility 2, class II, locus DMa	1.19	3.87E-08
ENSMUSG00000054072	Iigp1	interferon inducible GTPase 1	1.18	4.52E-04
ENSMUSG00000054588			1.17	9.75E-04
ENSMUSG00000076598			1.17	2.38E-03
ENSMUSG00000026009	Icos	inducible T cell co-stimulator	1.17	1.39E-04
ENSMUSG00000028270	Gbp2	guanylate binding protein 2	1.17	2.39E-06

ENSMUSG00000059824	Dbp	D site albumin promoter binding protein	1.17	1.01E-04
ENSMUSG00000027225	Duoxa2	dual oxidase maturation factor 2	1.17	4.85E-04
ENSMUSG00000024673	Ms4a1	membrane-spanning 4-domains, subfamily A, member 1	1.17	1.67E-07
ENSMUSG00000025150	Cbr2	carbonyl reductase 2	1.16	1.86E-07
ENSMUSG00000035686	Thrsp	thyroid hormone responsive	1.16	1.03E-03
ENSMUSG00000079507	H2-Q1	histocompatibility 2, Q region locus 1	1.16	6.19E-06
ENSMUSG00000096638			1.16	8.33E-05
ENSMUSG00000068606	Gm4841	predicted gene 4841	1.16	1.11E-04
ENSMUSG00000078853	Igtp	interferon gamma induced GTPase	1.15	3.48E-04
ENSMUSG00000033715	Akr1c14	aldo-keto reductase family 1, member C14	1.15	9.96E-05
ENSMUSG00000059898	Dsc3	desmocollin 3	1.14	3.53E-04
ENSMUSG00000041193	Pla2g5	phospholipase A2, group V	1.14	1.97E-06
ENSMUSG00000012705	Retn	resistin	1.13	8.55E-04
ENSMUSG00000074261	Erich4	glutamate rich 4	1.13	2.18E-03
ENSMUSG00000058908	Pla2g2a	phospholipase A2, group IIA (platelets, synovial fluid)	1.13	4.77E-04
ENSMUSG00000096498			1.12	3.76E-03
ENSMUSG00000023959	Clic5	chloride intracellular channel 5	1.12	1.70E-06
ENSMUSG00000048852	Gm12185	predicted gene 12185	1.12	2.16E-04
ENSMUSG00000068227	Il2rb	interleukin 2 receptor, beta chain	1.11	3.45E-05
ENSMUSG00000093861			1.11	6.05E-04
ENSMUSG00000005763	Cd247	CD247 antigen	1.11	2.34E-04
ENSMUSG00000015437	Gzmb	granzyme B	1.10	1.74E-03
ENSMUSG00000064346			1.10	1.30E-03
ENSMUSG00000094559	Cyp2d34	cytochrome P450, family 2, subfamily d, polypeptide 34	1.10	3.22E-06
ENSMUSG00000068105	Tnfrsf13c	tumor necrosis factor receptor superfamily, member 13c	1.10	3.70E-06
ENSMUSG00000090942	F830016B08 Rik	RIKEN cDNA F830016B08 gene	1.10	9.07E-05
ENSMUSG00000055069	Rab39	RAB39, member RAS oncogene family	1.09	1.22E-03
ENSMUSG00000020407	Upp1	uridine phosphorylase 1	1.09	1.40E-03
ENSMUSG00000028544	Slc5a9	solute carrier family 5 (sodium/glucose cotransporter), member 9	1.08	9.47E-05
ENSMUSG00000040264	Gbp2b	guanylate binding protein 2b	1.08	4.07E-04
ENSMUSG00000086706			1.08	1.76E-03
ENSMUSG00000090136	Gm10177	predicted gene 10177	1.08	3.90E-03
ENSMUSG00000025203	Scd2	stearoyl-Coenzyme A desaturase 2	1.07	3.62E-04
ENSMUSG00000095193	Gm20939	predicted gene, 20939	1.07	3.16E-03
ENSMUSG00000022582	Ly6g	lymphocyte antigen 6 complex, locus G	1.07	1.08E-04
ENSMUSG00000025479	Cyp2e1	cytochrome P450, family 2, subfamily e, polypeptide 1	1.06	9.18E-04
ENSMUSG00000075010	AW112010	expressed sequence AW112010	1.05	2.80E-06
ENSMUSG00000079103	Tgm7	transglutaminase 7	1.05	1.24E-03
ENSMUSG00000024670	Cd6	CD6 antigen	1.05	2.57E-03
ENSMUSG00000024338	Psmb8	proteasome (prosome, macropain) subunit, beta type 8 (large multifunctional peptidase 7)	1.05	1.37E-06
ENSMUSG00000084806	Gm15232	predicted gene 15232	1.05	1.77E-03
ENSMUSG00000073555	Gm4951	predicted gene 4951	1.05	4.23E-05
ENSMUSG00000042943			1.04	1.84E-03
ENSMUSG00000038037	Socs1	suppressor of cytokine signaling 1	1.04	1.71E-03
ENSMUSG00000037321	Tap1	transporter 1, ATP-binding cassette, sub-family B (MDR/TAP)	1.04	8.26E-07
ENSMUSG00000064364			1.03	3.28E-03
ENSMUSG00000030149	Klrk1	killer cell lectin-like receptor subfamily K, member 1	1.03	1.14E-04
ENSMUSG00000087070	Gm12505	predicted gene 12505	1.03	1.03E-04
ENSMUSG00000043931	Gimap7	GTPase, IMAP family member 7	1.03	4.30E-05
ENSMUSG00000068299	1700019G17 Rik	RIKEN cDNA 1700019G17 gene	1.02	1.19E-03
ENSMUSG00000039304	Tnfsf10	tumor necrosis factor (ligand) superfamily, member 10	1.02	4.76E-05
ENSMUSG00000054435	Gimap4	GTPase, IMAP family member 4	1.02	3.57E-07
ENSMUSG00000070777	Ceacam20	carcinoembryonic antigen-related cell adhesion molecule 20	1.01	8.22E-06
ENSMUSG00000023073	Slc10a2	solute carrier family 10, member 2	1.01	3.95E-03
ENSMUSG00000046031	Fam26f	family with sequence similarity 26, member F	1.01	2.05E-03
ENSMUSG00000078921	Tgtp2	T cell specific GTPase 2	1.00	2.24E-04
ENSMUSG00000091649	Phf11b	PHD finger protein 11B	1.00	7.66E-04

ENSMUSG00000044162	Tnip3	TNFAIP3 interacting protein 3	1.00	4.77E-06
ENSMUSG00000050232	Cxcr3	chemokine (C-X-C motif) receptor 3	1.00	3.87E-03
ENSMUSG00000024529	Lox	lysyl oxidase	-1.01	1.22E-03
ENSMUSG00000022548	Apod	apolipoprotein D	-1.01	2.83E-04
ENSMUSG00000039109	F13a1	coagulation factor XIII, A1 subunit	-1.02	3.37E-06
ENSMUSG00000036356	Csgalnact1	chondroitin sulfate N-acetylgalactosaminyltransferase 1	-1.02	1.38E-04
ENSMUSG00000019772	Vip	vasoactive intestinal polypeptide	-1.03	1.29E-05
ENSMUSG00000007440	Pcdha11	protocadherin alpha 11	-1.03	1.22E-03
ENSMUSG00000072949	Acot1	acyl-CoA thioesterase 1	-1.04	4.67E-04
ENSMUSG00000044017	Gpr133	G protein-coupled receptor 133	-1.05	1.67E-06
ENSMUSG00000097451			-1.06	1.87E-06
ENSMUSG00000029675	Eln	elastin	-1.09	2.74E-05
ENSMUSG00000022032	Scara5	scavenger receptor class A, member 5 (putative)	-1.09	5.72E-07
ENSMUSG00000081448			-1.11	2.75E-04
ENSMUSG00000026938	Fcna	ficolin A	-1.11	7.91E-04
ENSMUSG00000028766	Alpl	alkaline phosphatase, liver/bone/kidney	-1.12	4.67E-07
ENSMUSG00000040152	Thbs1	thrombospondin 1	-1.13	7.51E-10
ENSMUSG00000054555	Adam12	a disintegrin and metallopeptidase domain 12 (meltrin alpha)	-1.13	9.50E-05
ENSMUSG00000025716	Myo3a	myosin IIIA	-1.14	7.10E-06
ENSMUSG00000022894	Adamts5	a disintegrin-like and metallopeptidase (reprolysin type) with thrombospondin type 1 motif, 5 (aggrecanase-2)	-1.15	1.93E-08
ENSMUSG00000031722	Hp	haptoglobin	-1.16	2.86E-04
ENSMUSG00000058427	Cxcl2	chemokine (C-X-C motif) ligand 2	-1.16	6.16E-05
ENSMUSG00000023034	Nr4a1	nuclear receptor subfamily 4, group A, member 1	-1.17	1.42E-04
ENSMUSG00000037225	Fgf2	fibroblast growth factor 2	-1.17	4.59E-04
ENSMUSG00000020363	Gfpt2	glutamine fructose-6-phosphate transaminase 2	-1.19	5.50E-06
ENSMUSG00000022367	Has2	hyaluronan synthase 2	-1.20	1.62E-04
ENSMUSG00000022651	Retnlg	resistin like gamma	-1.28	1.68E-05
ENSMUSG00000061048	Cdh3	cadherin 3	-1.28	6.62E-05
ENSMUSG00000063011	Msln	mesothelin	-1.28	5.07E-04
ENSMUSG00000006403	Adamts4	a disintegrin-like and metallopeptidase (reprolysin type) with thrombospondin type 1 motif, 4	-1.31	3.26E-06
ENSMUSG00000000318	Clec10a	C-type lectin domain family 10, member A	-1.32	6.14E-07
ENSMUSG00000024087	Cyp1b1	cytochrome P450, family 1, subfamily b, polypeptide 1	-1.35	1.53E-06
ENSMUSG00000028111	Ctsk	cathepsin K	-1.46	1.76E-08
ENSMUSG00000027656	Wisp2	WNT1 inducible signaling pathway protein 2	-1.59	1.69E-05
ENSMUSG00000048636			-1.62	7.05E-06
ENSMUSG00000040809	Chil3	chitinase-like 3	-1.93	1.06E-07
ENSMUSG00000002289	Angptl4	angiopoietin-like 4	-2.03	3.57E-12
ENSMUSG00000068196	Col8a1	collagen, type VIII, alpha 1	-2.34	3.55E-20

Table S5 Differentially expressed genes of BALB/c (uninfected 42 dpi vs. uninfected 5 dpi)

Ensembl ID	Gene symbol	Gene name	log_2 fold change	p-value
ENSMUSG00000006403	Adamts4	a disintegrin-like and metallopeptidase (reprolysin type) with thrombospondin type 1 motif, 4	1.99	5.05E-10
ENSMUSG00000055116	Arntl	aryl hydrocarbon receptor nuclear translocator-like	1.87	1.66E-16
ENSMUSG00000084671			1.60	3.18E-08
ENSMUSG00000022389	Tef	thyrotroph embryonic factor	-1.83	1.24E-12
ENSMUSG00000059824	Dbp	D site albumin promoter binding protein	-2.39	1.25E-15
ENSMUSG00000038550	Ciart	circadian associated repressor of transcription	-2.54	2.77E-15

Table S6 Differentially expressed genes of BALB/c (YPIII infected 42 dpi vs. YPIII infected 5 dpi)

Ensembl ID	Gene symbol	Gene name	log$_2$ fold change	p-value
ENSMUSG00000057074	Ces1g	carboxylesterase 1G	3.38	6.70E-26
ENSMUSG00000041559	Fmod	fibromodulin	3.07	6.57E-23
ENSMUSG00000010311	Optc	opticin	3.03	1.82E-32
ENSMUSG00000022491	Glycam1	glycosylation dependent cell adhesion molecule 1	3.02	8.56E-41
ENSMUSG00000030399	Ckm	creatine kinase, muscle	3.00	1.33E-43
ENSMUSG00000092586	Ly6g6c	lymphocyte antigen 6 complex, locus G6C	2.95	6.15E-15
ENSMUSG00000012705	Retn	resistin	2.90	4.02E-19
ENSMUSG00000069917	Hba-a2	hemoglobin alpha, adult chain 2	2.89	4.03E-24
ENSMUSG00000032122	Slc37a2	solute carrier family 37 (glycerol-3-phosphate transporter), member 2	2.83	9.53E-22
ENSMUSG00000069919	Hba-a1	hemoglobin alpha, adult chain 1	2.67	1.93E-23
ENSMUSG00000000805	Car4	carbonic anhydrase 4	2.58	2.25E-33
ENSMUSG00000025479	Cyp2e1	cytochrome P450, family 2, subfamily e, polypeptide 1	2.54	1.98E-16
ENSMUSG00000057123	Gja5	gap junction protein, alpha 5	2.51	1.21E-18
ENSMUSG00000022227	Mcpt1	mast cell protease 1	2.50	1.31E-11
ENSMUSG00000037071	Scd1	stearoyl-Coenzyme A desaturase 1	2.45	3.99E-14
ENSMUSG00000056973	Ces1d	carboxylesterase 1D	2.42	9.57E-28
ENSMUSG00000020793	Galr2	galanin receptor 2	2.40	8.94E-14
ENSMUSG00000035686	Thrsp	thyroid hormone responsive	2.36	1.22E-11
ENSMUSG00000018830	Myh11	myosin, heavy polypeptide 11, smooth muscle	2.35	1.46E-43
ENSMUSG00000032925	Itgbl1	integrin, beta-like 1	2.33	1.25E-09
ENSMUSG00000051295	9630028B13Rik	RIKEN cDNA 9630028B13 gene	2.31	1.75E-19
ENSMUSG00000047976	Kcna1	potassium voltage-gated channel, shaker-related subfamily, member 1	2.30	1.80E-16
ENSMUSG00000042254	Cilp	cartilage intermediate layer protein, nucleotide pyrophosphohydrolase	2.28	3.08E-27
ENSMUSG00000001349	Cnn1	calponin 1	2.28	3.31E-40
ENSMUSG00000041378	Cldn5	claudin 5	2.24	3.51E-14
ENSMUSG00000071361	Mcpt9	mast cell protease 9	2.23	5.63E-09
ENSMUSG00000030546	Plin1	perilipin 1	2.23	2.36E-13
ENSMUSG00000060548	Tnfrsf19	tumor necrosis factor receptor superfamily, member 19	2.22	2.02E-14
ENSMUSG00000061780	Cfd	complement factor D (adipsin)	2.21	1.65E-16
ENSMUSG00000097960	A330074K22Rik	RIKEN cDNA A330074K22 gene	2.21	9.83E-10
ENSMUSG00000034579	Pla2g3	phospholipase A2, group III	2.20	3.67E-19
ENSMUSG00000060615	Ang4	angiogenin, ribonuclease A family, member 4	2.19	7.17E-12
ENSMUSG00000044309	Apol7c	apolipoprotein L 7c	2.18	3.37E-14
ENSMUSG00000023885	Thbs2	thrombospondin 2	2.18	1.14E-28
ENSMUSG00000064999			2.17	5.26E-28
ENSMUSG00000041202	Pla2g2d	phospholipase A2, group IID	2.17	3.03E-23
ENSMUSG00000023046	Igfbp6	insulin-like growth factor binding protein 6	2.17	1.65E-18
ENSMUSG00000062760	1810041L15Rik	RIKEN cDNA 1810041L15 gene	2.17	1.02E-13
ENSMUSG00000095130			2.16	1.93E-09
ENSMUSG00000040488	Ltbp4	latent transforming growth factor beta binding protein 4	2.16	1.85E-30
ENSMUSG00000030554	Synm	synemin, intermediate filament protein	2.16	2.01E-35
ENSMUSG00000062329	Cytl1	cytokine-like 1	2.15	6.61E-10
ENSMUSG00000073424	Cyp4f15	cytochrome P450, family 4, subfamily f, polypeptide 15	2.15	3.18E-09
ENSMUSG00000015354	Pcolce2	procollagen C-endopeptidase enhancer 2	2.14	9.73E-15

ENSMUSG00000058914	C1qtnf3	C1q and tumor necrosis factor related protein 3	2.12	5.81E-10
ENSMUSG00000024727	Trpm6	transient receptor potential cation channel, subfamily M, member 6	2.12	1.09E-10
ENSMUSG00000026208	Des	desmin	2.11	1.33E-37
ENSMUSG00000076614			2.11	5.91E-08
ENSMUSG00000024575	Pde6a	phosphodiesterase 6A, cGMP-specific, rod, alpha	2.11	4.14E-12
ENSMUSG00000022878	Adipoq	adiponectin, C1Q and collagen domain containing	2.10	3.14E-16
ENSMUSG00000029309	Sparcl1	SPARC-like 1	2.09	1.02E-32
ENSMUSG00000022226	Mcpt2	mast cell protease 2	2.09	5.21E-08
ENSMUSG00000059430	Actg2	actin, gamma 2, smooth muscle, enteric	2.08	1.20E-24
ENSMUSG00000084671			2.07	4.18E-13
ENSMUSG00000045348	Nyap1	neuronal tyrosine-phosphorylated phosphoinositide 3-kinase adaptor 1	2.05	5.30E-14
ENSMUSG00000020963	Tshr	thyroid stimulating hormone receptor	2.04	2.54E-08
ENSMUSG00000051726	Kcnf1	potassium voltage-gated channel, subfamily F, member 1	2.04	4.65E-13
ENSMUSG00000035557	Krt17	keratin 17	2.03	7.85E-14
ENSMUSG00000031725	Ces1f	carboxylesterase 1F	2.03	1.01E-20
ENSMUSG00000030711	Sult1a1	sulfotransferase family 1A, phenol-preferring, member 1	2.01	4.47E-12
ENSMUSG00000028713	Cyp4b1	cytochrome P450, family 4, subfamily b, polypeptide 1	2.01	1.09E-10
ENSMUSG00000026574	Dpt	dermatopontin	2.00	8.48E-24
ENSMUSG00000026676	Ccdc3	coiled-coil domain containing 3	2.00	2.47E-16
ENSMUSG00000048096	Lmod1	leiomodin 1 (smooth muscle)	2.00	4.15E-25
ENSMUSG00000034936	Arl4d	ADP-ribosylation factor-like 4D	1.99	5.93E-14
ENSMUSG00000024076	Vit	vitrin	1.99	7.05E-10
ENSMUSG00000029369	Afm	afamin	1.99	8.32E-17
ENSMUSG00000055632	Hmcn2	hemicentin 2	1.98	1.23E-25
ENSMUSG00000026489	Adck3	aarF domain containing kinase 3	1.98	1.33E-17
ENSMUSG00000029603	Dtx1	deltex 1 homolog (Drosophila)	1.97	3.02E-17
ENSMUSG00000037762	Slc16a9	solute carrier family 16 (monocarboxylic acid transporters), member 9	1.97	1.48E-19
ENSMUSG00000033207	Mamdc2	MAM domain containing 2	1.97	1.61E-17
ENSMUSG00000058135	Gstm1	glutathione S-transferase, mu 1	1.96	3.71E-22
ENSMUSG00000061825	Ces2c	carboxylesterase 2C	1.96	4.82E-16
ENSMUSG00000026418	Tnni1	troponin I, skeletal, slow 1	1.95	6.76E-09
ENSMUSG00000019970	Sgk1	serum/glucocorticoid regulated kinase 1	1.95	1.33E-11
ENSMUSG00000033327	Tnxb	tenascin XB	1.94	3.15E-23
ENSMUSG00000076612			1.94	8.93E-08
ENSMUSG00000034324	Tmem132c	transmembrane protein 132C	1.94	8.33E-10
ENSMUSG00000063430	Wscd2	WSC domain containing 2	1.92	3.15E-18
ENSMUSG00000041073	Nacad	NAC alpha domain containing	1.92	3.40E-16
ENSMUSG00000067818	Myl9	myosin, light polypeptide 9, regulatory	1.91	9.21E-31
ENSMUSG00000038725	Pkhd1l1	polycystic kidney and hepatic disease 1-like 1	1.90	4.13E-14
ENSMUSG00000039329	Tex19.1	testis expressed gene 19.1	1.90	6.17E-07
ENSMUSG00000030762	Aqp8	aquaporin 8	1.90	3.75E-08
ENSMUSG00000025658	Cnksr2	connector enhancer of kinase suppressor of Ras 2	1.90	1.27E-10
ENSMUSG00000060600	Eno3	enolase 3, beta muscle	1.90	1.39E-14
ENSMUSG00000026463	Atp2b4	ATPase, Ca++ transporting, plasma membrane 4	1.90	9.07E-30
ENSMUSG00000032648	Pygm	muscle glycogen phosphorylase	1.89	5.18E-17
ENSMUSG00000028464	Tpm2	tropomyosin 2, beta	1.89	1.27E-27

ENSMUSG00000030409	Dmpk	dystrophia myotonica-protein kinase	1.88	1.21E-26
ENSMUSG00000032085	Tagln	transgelin	1.88	1.30E-28
ENSMUSG00000076540			1.87	9.86E-07
ENSMUSG00000025784	Clec3b	C-type lectin domain family 3, member b	1.87	2.52E-19
ENSMUSG00000027397	Slc20a1	solute carrier family 20, member 1	1.87	7.59E-15
ENSMUSG00000026879	Gsn	gelsolin	1.87	2.04E-25
ENSMUSG00000027559	Car3	carbonic anhydrase 3	1.86	3.99E-10
ENSMUSG00000099065			1.86	1.51E-13
ENSMUSG00000022546	Gpt	glutamic pyruvic transaminase, soluble	1.86	1.95E-13
ENSMUSG00000050860	Phospho1	phosphatase, orphan 1	1.85	5.58E-07
ENSMUSG00000025213	Kazald1	Kazal-type serine peptidase inhibitor domain 1	1.85	3.22E-07
ENSMUSG00000037624	Kcnk2	potassium channel, subfamily K, member 2	1.84	2.47E-12
ENSMUSG00000046329	Slc25a23	solute carrier family 25 (mitochondrial carrier; phosphate carrier), member 23	1.84	2.02E-19
ENSMUSG00000049580	Tsku	tsukushi	1.83	2.87E-13
ENSMUSG00000004110	Cacna1e	calcium channel, voltage-dependent, R type, alpha 1E subunit	1.83	1.68E-14
ENSMUSG00000076569			1.83	1.10E-07
ENSMUSG00000021200	Asb2	ankyrin repeat and SOCS box-containing 2	1.83	3.28E-19
ENSMUSG00000003379	Cd79a	CD79A antigen (immunoglobulin-associated alpha)	1.83	4.73E-16
ENSMUSG00000085375			1.82	2.08E-08
ENSMUSG00000042474	Faim3	Fas apoptotic inhibitory molecule 3	1.80	3.88E-16
ENSMUSG00000084174	Sycn	syncollin	1.80	3.55E-12
ENSMUSG00000074207	Adh1	alcohol dehydrogenase 1 (class I)	1.79	1.41E-16
ENSMUSG00000047394	Odf3b	outer dense fiber of sperm tails 3B	1.79	3.04E-06
ENSMUSG00000061068	Mcpt4	mast cell protease 4	1.79	3.76E-06
ENSMUSG00000022371	Col14a1	collagen, type XIV, alpha 1	1.79	2.26E-20
ENSMUSG00000024670	Cd6	CD6 antigen	1.79	8.19E-08
ENSMUSG00000014846	Tppp3	tubulin polymerization-promoting protein family member 3	1.79	1.49E-15
ENSMUSG00000068263	Efcc1	EF hand and coiled-coil domain containing 1	1.78	4.70E-12
ENSMUSG00000034059	Ypel4	yippee-like 4 (Drosophila)	1.78	1.98E-07
ENSMUSG00000020439	Smtn	smoothelin	1.78	1.22E-21
ENSMUSG00000005540	Fcer2a	Fc receptor, IgE, low affinity II, alpha polypeptide	1.78	1.67E-13
ENSMUSG00000050315	Synpo2	synaptopodin 2	1.77	4.90E-28
ENSMUSG00000017817	Jph2	junctophilin 2	1.77	1.00E-18
ENSMUSG00000041012	Cmtm8	CKLF-like MARVEL transmembrane domain containing 8	1.77	5.52E-11
ENSMUSG00000076538			1.76	5.89E-06
ENSMUSG00000068289	Cma2	chymase 2, mast cell	1.76	5.02E-06
ENSMUSG00000026614	Slc30a10	solute carrier family 30, member 10	1.76	4.27E-07
ENSMUSG00000041828	Abca8a	ATP-binding cassette, sub-family A (ABC1), member 8a	1.76	2.69E-16
ENSMUSG00000076596			1.75	5.98E-06
ENSMUSG00000040666	Sh3bgr	SH3-binding domain glutamic acid-rich protein	1.75	5.89E-12
ENSMUSG00000090223	Pcp4	Purkinje cell protein 4	1.75	2.81E-07
ENSMUSG00000071984	Fndc1	fibronectin type III domain containing 1	1.75	5.96E-18
ENSMUSG00000033152	Podxl2	podocalyxin-like 2	1.74	1.20E-07
ENSMUSG00000028755	Cda	cytidine deaminase	1.74	5.60E-13
ENSMUSG00000021573	Tppp	tubulin polymerization promoting protein	1.74	7.46E-15
ENSMUSG00000032243	Itga11	integrin alpha 11	1.74	1.56E-13

ENSMUSG00000078794	Dact3	dapper homolog 3, antagonist of beta-catenin (xenopus)	1.74	6.18E-11
ENSMUSG00000001943	Vsig2	V-set and immunoglobulin domain containing 2	1.74	2.73E-16
ENSMUSG00000068874	Selenbp1	selenium binding protein 1	1.74	3.10E-14
ENSMUSG00000055653	Gpc3	glypican 3	1.73	1.29E-15
ENSMUSG00000054619	Mettl7a1	methyltransferase like 7A1	1.73	9.92E-16
ENSMUSG00000005338	Cadm3	cell adhesion molecule 3	1.73	3.18E-14
ENSMUSG00000026077	Npas2	neuronal PAS domain protein 2	1.73	1.93E-11
ENSMUSG00000038967	Pdk2	pyruvate dehydrogenase kinase, isoenzyme 2	1.72	6.62E-14
ENSMUSG00000043122	A530016L24Rik	RIKEN cDNA A530016L24 gene	1.72	7.61E-06
ENSMUSG00000043439	E130012A19Rik	RIKEN cDNA E130012A19 gene	1.72	6.37E-12
ENSMUSG00000020081	Tacr2	tachykinin receptor 2	1.72	6.02E-16
ENSMUSG00000063564	Col23a1	collagen, type XXIII, alpha 1	1.72	1.51E-13
ENSMUSG00000034785	Dio1	deiodinase, iodothyronine, type I	1.72	1.72E-13
ENSMUSG00000065645			1.72	5.31E-10
ENSMUSG00000061808	Ttr	transthyretin	1.71	2.87E-12
ENSMUSG00000020427	Igfbp3	insulin-like growth factor binding protein 3	1.71	4.58E-18
ENSMUSG00000095285			1.71	3.26E-07
ENSMUSG00000058571	Gpc6	glypican 6	1.71	1.94E-12
ENSMUSG00000046532	Ar	androgen receptor	1.71	1.66E-12
ENSMUSG00000076580			1.71	6.51E-06
ENSMUSG00000031636	Pdlim3	PDZ and LIM domain 3	1.70	2.71E-19
ENSMUSG00000022425	Enpp2	ectonucleotide pyrophosphatase/phosphodiesterase 2	1.70	1.27E-20
ENSMUSG00000001663	Gstt1	glutathione S-transferase, theta 1	1.70	3.54E-13
ENSMUSG00000046743	Fat4	FAT tumor suppressor homolog 4 (Drosophila)	1.70	4.47E-23
ENSMUSG00000020251	Glt8d2	glycosyltransferase 8 domain containing 2	1.69	2.25E-07
ENSMUSG00000040289	Hey1	hairy/enhancer-of-split related with YRPW motif 1	1.69	3.42E-07
ENSMUSG00000055116	Arntl	aryl hydrocarbon receptor nuclear translocator-like	1.69	5.77E-14
ENSMUSG00000076928			1.69	2.78E-06
ENSMUSG00000035783	Acta2	actin, alpha 2, smooth muscle, aorta	1.69	5.05E-24
ENSMUSG00000058070	Eml1	echinoderm microtubule associated protein like 1	1.69	2.91E-22
ENSMUSG00000038776	Ephx1	epoxide hydrolase 1, microsomal	1.68	1.69E-17
ENSMUSG00000081488			1.68	3.44E-09
ENSMUSG00000029096	Htra3	HtrA serine peptidase 3	1.68	4.30E-13
ENSMUSG00000036123	Slc9a3	solute carrier family 9 (sodium/hydrogen exchanger), member 3	1.68	2.36E-07
ENSMUSG00000035258	Abi3bp	ABI gene family, member 3 (NESH) binding protein	1.68	3.04E-18
ENSMUSG00000001270	Ckb	creatine kinase, brain	1.67	1.07E-21
ENSMUSG00000027894	Slc6a17	solute carrier family 6 (neurotransmitter transporter), member 17	1.67	4.95E-10
ENSMUSG00000068748	Ptprz1	protein tyrosine phosphatase, receptor type Z, polypeptide 1	1.67	2.69E-08
ENSMUSG00000051228	Nyx	nyctalopin	1.66	1.70E-06
ENSMUSG00000009075	Cabp7	calcium binding protein 7	1.66	1.06E-05
ENSMUSG00000020099	Unc5b	unc-5 homolog B (C. elegans)	1.66	4.96E-16
ENSMUSG00000019278	Dpep1	dipeptidase 1 (renal)	1.66	8.13E-17
ENSMUSG00000025780	Itih5	inter-alpha (globulin) inhibitor H5	1.66	1.04E-17
ENSMUSG00000036395	Glb1l2	galactosidase, beta 1-like 2	1.66	2.64E-06
ENSMUSG00000000125	Wnt3	wingless-type MMTV integration site family, member 3	1.66	1.36E-05
ENSMUSG00000036854	Hspb6	heat shock protein, alpha-crystallin-related, B6	1.65	4.28E-10

ENSMUSG00000004038	Gstm3	glutathione S-transferase, mu 3	1.65	2.54E-07
ENSMUSG00000030092	Cntn6	contactin 6	1.65	6.47E-06
ENSMUSG00000047842	Diras2	DIRAS family, GTP-binding RAS-like 2	1.65	1.76E-07
ENSMUSG00000002565	Scin	scinderin	1.65	4.57E-14
ENSMUSG00000053199	Arhgap20	Rho GTPase activating protein 20	1.65	4.97E-15
ENSMUSG00000018566	Slc2a4	solute carrier family 2 (facilitated glucose transporter), member 4	1.65	1.40E-13
ENSMUSG00000056481	Cd248	CD248 antigen, endosialin	1.65	1.48E-12
ENSMUSG00000073608	Gm6086	predicted gene 6086	1.64	2.50E-07
ENSMUSG00000060780	Lrrtm1	leucine rich repeat transmembrane neuronal 1	1.64	1.15E-05
ENSMUSG00000059146	Ntrk3	neurotrophic tyrosine kinase, receptor, type 3	1.64	3.26E-06
ENSMUSG00000022309	Angpt1	angiopoietin 1	1.63	9.69E-10
ENSMUSG00000020672	Sntg2	syntrophin, gamma 2	1.63	5.66E-13
ENSMUSG00000040543	Pitpnm3	PITPNM family member 3	1.63	9.60E-13
ENSMUSG00000020811	Wscd1	WSC domain containing 1	1.63	1.41E-05
ENSMUSG00000079440	Alpi	alkaline phosphatase, intestinal	1.63	8.09E-12
ENSMUSG00000021319	Sfrp4	secreted frizzled-related protein 4	1.63	5.20E-08
ENSMUSG00000063873	Slc24a3	solute carrier family 24 (sodium/potassium/calcium exchanger), member 3	1.62	6.94E-22
ENSMUSG00000070000	Fcho1	FCH domain only 1	1.62	3.64E-10
ENSMUSG00000020334	Slc22a4	solute carrier family 22 (organic cation transporter), member 4	1.62	1.53E-07
ENSMUSG00000028255	Clca1	chloride channel calcium activated 1	1.62	6.43E-20
ENSMUSG00000079037	Prnp	prion protein	1.62	4.52E-17
ENSMUSG00000038173	Enpp6	ectonucleotide pyrophosphatase/phosphodiesterase 6	1.62	1.85E-06
ENSMUSG00000019326	Aoc3	amine oxidase, copper containing 3	1.61	8.88E-20
ENSMUSG00000043631	Ecm2	extracellular matrix protein 2, female organ and adipocyte specific	1.61	4.25E-13
ENSMUSG00000018740	Slc25a35	solute carrier family 25, member 35	1.61	1.92E-15
ENSMUSG00000038555	Reep2	receptor accessory protein 2	1.61	4.22E-07
ENSMUSG00000027217	Tspan18	tetraspanin 18	1.61	2.89E-16
ENSMUSG00000048498	Cd300e	CD300e antigen	1.61	1.48E-05
ENSMUSG00000034156	Bzrap1	benzodiazepine receptor associated protein 1	1.61	1.04E-05
ENSMUSG00000046658	Zfp316	zinc finger protein 316	1.61	1.36E-13
ENSMUSG00000095612			1.60	2.37E-06
ENSMUSG00000060843	Ctnna3	catenin (cadherin associated protein), alpha 3	1.60	8.94E-12
ENSMUSG00000038218			1.60	1.53E-06
ENSMUSG00000005339	Fcer1a	Fc receptor, IgE, high affinity I, alpha polypeptide	1.60	3.04E-05
ENSMUSG00000024049	Myom1	myomesin 1	1.60	4.19E-15
ENSMUSG00000021575	Ahrr	aryl-hydrocarbon receptor repressor	1.60	5.17E-11
ENSMUSG00000086596	Susd5	sushi domain containing 5	1.60	2.82E-05
ENSMUSG00000061356	Nuggc	nuclear GTPase, germinal center associated	1.60	1.27E-08
ENSMUSG00000035504	Reep6	receptor accessory protein 6	1.60	2.88E-13
ENSMUSG00000028047	Thbs3	thrombospondin 3	1.60	1.78E-12
ENSMUSG00000049971	Glt1d1	glycosyltransferase 1 domain containing 1	1.60	5.72E-09
ENSMUSG00000064267	Hvcn1	hydrogen voltage-gated channel 1	1.59	3.99E-14
ENSMUSG00000001604	Tcea3	transcription elongation factor A (SII), 3	1.59	5.03E-13
ENSMUSG00000055322	Tns1	tensin 1	1.59	1.95E-22
ENSMUSG00000032607	Amt	aminomethyltransferase	1.59	1.34E-11
ENSMUSG00000028020	Glrb	glycine receptor, beta subunit	1.58	1.55E-05

ENSMUSG00000059401	Mamld1	mastermind-like domain containing 1	1.58	2.34E-07
ENSMUSG00000023336	Wfdc1	WAP four-disulfide core domain 1	1.58	1.21E-11
ENSMUSG00000028179	Cth	cystathionase (cystathionine gamma-lyase)	1.58	3.63E-14
ENSMUSG00000001334	Fndc5	fibronectin type III domain containing 5	1.58	2.68E-08
ENSMUSG00000029134	Plb1	phospholipase B1	1.58	3.77E-06
ENSMUSG00000021792	Fam213a	family with sequence similarity 213, member A	1.58	4.36E-14
ENSMUSG00000052957	Gas1	growth arrest specific 1	1.57	1.19E-10
ENSMUSG00000060586	H2-Eb1	histocompatibility 2, class II antigen E beta	1.57	1.26E-17
ENSMUSG00000034687	Fras1	Fraser syndrome 1 homolog (human)	1.57	1.74E-08
ENSMUSG00000094124			1.57	7.99E-07
ENSMUSG00000095416			1.57	1.60E-06
ENSMUSG00000052305	Hbb-b1	hemoglobin, beta adult major chain	1.57	2.87E-06
ENSMUSG00000020159	Gabrp	gamma-aminobutyric acid (GABA) A receptor, pi	1.56	2.65E-08
ENSMUSG00000076613			1.56	1.25E-05
ENSMUSG00000094651	Gal3st2	galactose-3-O-sulfotransferase 2	1.56	4.12E-11
ENSMUSG00000025002	Cyp2c55	cytochrome P450, family 2, subfamily c, polypeptide 55	1.56	4.70E-05
ENSMUSG00000026840	Lamc3	laminin gamma 3	1.56	4.41E-07
ENSMUSG00000037206	Islr	immunoglobulin superfamily containing leucine-rich repeat	1.56	2.56E-13
ENSMUSG00000022265	Ank	progressive ankylosis	1.56	3.57E-16
ENSMUSG00000098132	Rassf10	Ras association (RalGDS/AF-6) domain family (N-terminal) member 10	1.56	7.54E-07
ENSMUSG00000061080	Lsamp	limbic system-associated membrane protein	1.56	4.52E-07
ENSMUSG00000026117	Zap70	zeta-chain (TCR) associated protein kinase	1.56	4.53E-07
ENSMUSG00000070867	Trabd2b	TraB domain containing 2B	1.56	4.95E-08
ENSMUSG00000001865	Cpa3	carboxypeptidase A3, mast cell	1.56	1.15E-05
ENSMUSG00000020388	Pdlim4	PDZ and LIM domain 4	1.55	6.37E-09
ENSMUSG00000074818	Pdzd7	PDZ domain containing 7	1.55	1.50E-09
ENSMUSG00000019989	Enpp3	ectonucleotide pyrophosphatase/phosphodiesterase 3	1.55	3.48E-11
ENSMUSG00000076563			1.55	8.26E-06
ENSMUSG00000016552	Foxred2	FAD-dependent oxidoreductase domain containing 2	1.55	1.32E-07
ENSMUSG00000044749	Abca6	ATP-binding cassette, sub-family A (ABC1), member 6	1.55	6.22E-08
ENSMUSG00000004105	Angptl2	angiopoietin-like 2	1.55	8.68E-13
ENSMUSG00000074882	Cyp2c68	cytochrome P450, family 2, subfamily c, polypeptide 68	1.55	2.69E-06
ENSMUSG00000066513	Klk1b4	kallikrein 1-related pepidase b4	1.54	4.12E-05
ENSMUSG00000076435	Acsf2	acyl-CoA synthetase family member 2	1.54	1.21E-17
ENSMUSG00000061740	Cyp2d22	cytochrome P450, family 2, subfamily d, polypeptide 22	1.54	2.47E-09
ENSMUSG00000027513	Pck1	phosphoenolpyruvate carboxykinase 1, cytosolic	1.54	3.16E-13
ENSMUSG00000027401	Tgm3	transglutaminase 3, E polypeptide	1.54	6.20E-05
ENSMUSG00000020395	Itk	IL2 inducible T cell kinase	1.54	7.34E-12
ENSMUSG00000027870	Hao2	hydroxyacid oxidase 2	1.54	5.80E-11
ENSMUSG00000053279	Aldh1a1	aldehyde dehydrogenase family 1, subfamily A1	1.54	8.22E-12
ENSMUSG00000049241	Hcar1	hydrocarboxylic acid receptor 1	1.54	2.59E-07
ENSMUSG00000028545	Bend5	BEN domain containing 5	1.53	1.84E-08
ENSMUSG00000039760	Il22ra2	interleukin 22 receptor, alpha 2	1.53	1.35E-09
ENSMUSG00000037379	Spon2	spondin 2, extracellular matrix protein	1.53	1.27E-12
ENSMUSG00000007097	Atp1a2	ATPase, Na+/K+ transporting, alpha 2 polypeptide	1.53	7.11E-13
ENSMUSG00000048644	Ctxn1	cortexin 1	1.53	1.71E-05

ENSMUSG00000067276	Capn6	calpain 6	1.53	8.18E-06
ENSMUSG00000040420	Cdh18	cadherin 18	1.53	5.70E-05
ENSMUSG00000022836	Mylk	myosin, light polypeptide kinase	1.53	2.09E-20
ENSMUSG00000096635			1.52	2.36E-12
ENSMUSG00000029095	Ablim2	actin-binding LIM protein 2	1.52	2.89E-07
ENSMUSG00000030630	Fah	fumarylacetoacetate hydrolase	1.52	4.14E-13
ENSMUSG00000073557	Ppp1r12b	protein phosphatase 1, regulatory (inhibitor) subunit 12B	1.52	2.40E-19
ENSMUSG00000083282	Ctsf	cathepsin F	1.52	1.20E-11
ENSMUSG00000022199	Slc22a17	solute carrier family 22 (organic cation transporter), member 17	1.52	5.28E-05
ENSMUSG00000030577	Cd22	CD22 antigen	1.52	8.51E-14
ENSMUSG00000040841	Six5	sine oculis-related homeobox 5	1.52	2.63E-07
ENSMUSG00000032482	Cspg5	chondroitin sulfate proteoglycan 5	1.52	4.51E-05
ENSMUSG00000027985	Lef1	lymphoid enhancer binding factor 1	1.52	4.04E-10
ENSMUSG00000038167	Plekhg6	pleckstrin homology domain containing, family G (with RhoGef domain) member 6	1.52	1.08E-10
ENSMUSG00000024395	Lims2	LIM and senescent cell antigen like domains 2	1.51	2.81E-11
ENSMUSG00000053963	6330403A02Rik	RIKEN cDNA 6330403A02 gene	1.51	1.64E-12
ENSMUSG00000029811	Aoc1	amine oxidase, copper-containing 1	1.51	6.32E-16
ENSMUSG00000027761	Aadac	arylacetamide deacetylase (esterase)	1.51	1.04E-07
ENSMUSG00000095351			1.51	1.78E-05
ENSMUSG00000022040	Ephx2	epoxide hydrolase 2, cytoplasmic	1.51	3.37E-11
ENSMUSG00000037813	D630003M21Rik	RIKEN cDNA D630003M21 gene	1.51	8.06E-07
ENSMUSG00000061603	Akap6	A kinase (PRKA) anchor protein 6	1.51	1.09E-12
ENSMUSG00000040584	Abcb1a	ATP-binding cassette, sub-family B (MDR/TAP), member 1A	1.51	6.01E-06
ENSMUSG00000027863	Cd2	CD2 antigen	1.51	3.87E-12
ENSMUSG00000038209	Itln1	intelectin 1 (galactofuranose binding)	1.50	3.89E-13
ENSMUSG00000042751	Nmnat2	nicotinamide nucleotide adenylyltransferase 2	1.50	3.61E-09
ENSMUSG00000004098	Col5a3	collagen, type V, alpha 3	1.50	2.61E-10
ENSMUSG00000096341			-1.51	1.79E-09
ENSMUSG00000022582	Ly6g	lymphocyte antigen 6 complex, locus G	-1.52	1.98E-07
ENSMUSG00000076370			-1.52	2.89E-07
ENSMUSG00000064472			-1.53	8.57E-05
ENSMUSG00000004371	Il11	interleukin 11	-1.53	5.78E-05
ENSMUSG00000095857			-1.54	6.98E-06
ENSMUSG00000051748	Wfdc21	WAP four-disulfide core domain 21	-1.55	6.93E-05
ENSMUSG00000064742			-1.56	2.12E-05
ENSMUSG00000057359			-1.57	3.87E-06
ENSMUSG00000064346			-1.57	1.19E-05
ENSMUSG00000093999			-1.58	9.32E-06
ENSMUSG00000024697	Gna14	guanine nucleotide binding protein, alpha 14	-1.58	2.49E-10
ENSMUSG00000095624			-1.58	3.47E-05
ENSMUSG00000042265	Trem1	triggering receptor expressed on myeloid cells 1	-1.59	2.80E-06
ENSMUSG00000077565			-1.60	2.18E-11
ENSMUSG00000094199			-1.61	2.37E-06
ENSMUSG00000094400			-1.61	2.25E-05
ENSMUSG00000094471			-1.62	1.23E-05
ENSMUSG00000095396			-1.65	1.36E-05

ENSMUSG00000065373			-1.68	1.82E-07
ENSMUSG00000093983			-1.69	3.03E-06
ENSMUSG00000030144	Clec4d	C-type lectin domain family 4, member d	-1.69	6.64E-07
ENSMUSG00000029371	Cxcl5	chemokine (C-X-C motif) ligand 5	-1.70	8.74E-06
ENSMUSG00000000182	Fgf23	fibroblast growth factor 23	-1.71	1.12E-05
ENSMUSG00000044103	Il1f9	interleukin 1 family, member 9	-1.71	3.16E-08
ENSMUSG00000026822	Lcn2	lipocalin 2	-1.74	6.01E-10
ENSMUSG00000093916			-1.74	3.28E-06
ENSMUSG00000021091	Serpina3n	serine (or cysteine) peptidase inhibitor, clade A, member 3N	-1.80	1.15E-16
ENSMUSG00000040026	Saa3	serum amyloid A 3	-1.82	1.17E-08
ENSMUSG00000096434			-1.85	1.77E-06
ENSMUSG00000000982	Ccl3	chemokine (C-C motif) ligand 3	-1.85	5.63E-07
ENSMUSG00000047728	BC025446	cDNA sequence BC025446	-1.87	7.06E-08
ENSMUSG00000001131	Timp1	tissue inhibitor of metalloproteinase 1	-1.87	8.67E-11
ENSMUSG00000065104			-1.88	1.32E-07
ENSMUSG00000027399	Il1a	interleukin 1 alpha	-1.92	1.50E-10
ENSMUSG00000031722	Hp	haptoglobin	-1.92	1.82E-09
ENSMUSG00000064689			-1.97	1.02E-08
ENSMUSG00000096222			-2.10	3.25E-10
ENSMUSG00000027832	Ptx3	pentraxin related gene	-2.11	5.49E-09
ENSMUSG00000030142	Clec4e	C-type lectin domain family 4, member e	-2.11	9.08E-09
ENSMUSG00000069792	Wfdc17	WAP four-disulfide core domain 17	-2.12	1.21E-09
ENSMUSG00000073530	Pappa2	pappalysin 2	-2.16	6.07E-14
ENSMUSG00000048636			-2.16	1.53E-09
ENSMUSG00000022651	Retnlg	resistin like gamma	-2.16	3.73E-13
ENSMUSG00000094655			-2.17	9.84E-18
ENSMUSG00000059657	Stfa2l1	stefin A2 like 1	-2.37	6.41E-10
ENSMUSG00000005800	Mmp8	matrix metallopeptidase 8	-2.39	3.46E-12
ENSMUSG00000029380	Cxcl1	chemokine (C-X-C motif) ligand 1	-2.41	7.94E-14
ENSMUSG00000064246	Chil1	chitinase-like 1	-2.47	4.18E-18
ENSMUSG00000022126	Irg1	immunoresponsive gene 1	-2.64	1.69E-20
ENSMUSG00000040809	Chil3	chitinase-like 3	-2.69	1.21E-13
ENSMUSG00000025746	Il6	interleukin 6	-2.84	6.21E-16
ENSMUSG00000058427	Cxcl2	chemokine (C-X-C motif) ligand 2	-3.03	1.86E-23

Table S7 Differentially expressed genes of BALB/c (YPIII Δ*cnfy* infected 42 dpi vs. YPIII Δ*cnfy* infected 5 dpi)

Ensembl ID	Gene symbol	Gene name	log_2 fold change	p-value
ENSMUSG00000022491	Glycam1	glycosylation dependent cell adhesion molecule 1	2.89	5.20E-38
ENSMUSG00000057074	Ces1g	carboxylesterase 1G	2.68	6.06E-17
ENSMUSG00000084671			2.34	5.57E-15
ENSMUSG00000028713	Cyp4b1	cytochrome P450, family 4, subfamily b, polypeptide 1	2.31	2.82E-13
ENSMUSG00000039760	Il22ra2	interleukin 22 receptor, alpha 2	2.27	7.46E-17
ENSMUSG00000056973	Ces1d	carboxylesterase 1D	2.20	2.28E-23
ENSMUSG00000084174	Sycn	syncollin	2.17	1.52E-16

ENSMUSG00000060615	Ang4	angiogenin, ribonuclease A family, member 4	2.06	2.66E-10
ENSMUSG00000030399	Ckm	creatine kinase, muscle	2.03	2.31E-20
ENSMUSG00000073424	Cyp4f15	cytochrome P450, family 4, subfamily f, polypeptide 15	1.96	1.36E-07
ENSMUSG00000092586	Ly6g6c	lymphocyte antigen 6 complex, locus G6C	1.95	2.64E-07
ENSMUSG00000081488			1.92	3.66E-11
ENSMUSG00000037762	Slc16a9	solute carrier family 16 (monocarboxylic acid transporters), member 9	1.88	2.00E-17
ENSMUSG00000026166	Ccl20	chemokine (C-C motif) ligand 20	1.87	4.20E-08
ENSMUSG00000049580	Tsku	tsukushi	1.81	2.55E-12
ENSMUSG00000039329	Tex19.1	testis expressed gene 19.1	1.80	2.63E-06
ENSMUSG00000024575	Pde6a	phosphodiesterase 6A, cGMP-specific, rod, alpha	1.80	3.39E-09
ENSMUSG00000024727	Trpm6	transient receptor potential cation channel, subfamily M, member 6	1.78	5.26E-08
ENSMUSG00000035557	Krt17	keratin 17	1.77	5.01E-09
ENSMUSG00000087291	Gm11946	predicted gene 11946	1.77	5.61E-09
ENSMUSG00000064999			1.76	2.63E-18
ENSMUSG00000030554	Synm	synemin, intermediate filament protein	1.71	1.48E-22
ENSMUSG00000057123	Gja5	gap junction protein, alpha 5	1.69	7.24E-09
ENSMUSG00000020793	Galr2	galanin receptor 2	1.69	1.45E-07
ENSMUSG00000020182	Ddc	dopa decarboxylase	1.69	1.26E-14
ENSMUSG00000019970	Sgk1	serum/glucocorticoid regulated kinase 1	1.67	6.69E-09
ENSMUSG00000028039	Efna3	ephrin A3	1.66	1.82E-06
ENSMUSG00000040812	Agbl2	ATP/GTP binding protein-like 2	1.65	6.23E-09
ENSMUSG00000029811	Aoc1	amine oxidase, copper-containing 1	1.65	2.07E-18
ENSMUSG00000022227	Mcpt1	mast cell protease 1	1.65	8.19E-06
ENSMUSG00000059430	Actg2	actin, gamma 2, smooth muscle, enteric	1.64	7.41E-16
ENSMUSG00000025002	Cyp2c55	cytochrome P450, family 2, subfamily c, polypeptide 55	1.64	2.03E-05
ENSMUSG00000026614	Slc30a10	solute carrier family 30, member 10	1.63	2.91E-06
ENSMUSG00000026701	Prdx6	peroxiredoxin 6	1.62	3.45E-12
ENSMUSG00000061808	Ttr	transthyretin	1.61	2.65E-10
ENSMUSG00000045348	Nyap1	neuronal tyrosine-phosphorylated phosphoinositide 3-kinase adaptor 1	1.60	5.97E-09
ENSMUSG00000027875	Hmgcs2	3-hydroxy-3-methylglutaryl-Coenzyme A synthase 2	1.60	7.33E-16
ENSMUSG00000026077	Npas2	neuronal PAS domain protein 2	1.58	2.29E-09
ENSMUSG00000027318	Adam33	a disintegrin and metallopeptidase domain 33	1.56	1.26E-05
ENSMUSG00000028356	Ambp	alpha 1 microglobulin/bikunin	1.56	1.90E-05
ENSMUSG00000019762	Iyd	iodotyrosine deiodinase	1.56	4.68E-06
ENSMUSG00000051295	9630028B13Rik	RIKEN cDNA 9630028B13 gene	1.55	6.32E-09
ENSMUSG00000093999			1.54	1.14E-05
ENSMUSG00000055116	Arntl	aryl hydrocarbon receptor nuclear translocator-like	1.53	1.51E-11
ENSMUSG00000041559	Fmod	fibromodulin	1.52	1.50E-06
ENSMUSG00000027870	Hao2	hydroxyacid oxidase 2	1.52	9.79E-11
ENSMUSG00000010311	Optc	opticin	1.52	1.84E-09
ENSMUSG00000053399	Adamts18	a disintegrin-like and metallopeptidase (reprolysin type) with thrombospondin type 1 motif, 18	1.52	6.88E-05
ENSMUSG00000001349	Cnn1	calponin 1	1.51	1.75E-18
ENSMUSG00000038591	Colec10	collectin sub-family member 10	1.51	8.84E-09
ENSMUSG00000031877	Ces2g	carboxylesterase 2G	1.51	7.58E-08
ENSMUSG00000078921	Tgtp2	T cell specific GTPase 2	-1.50	4.39E-08
ENSMUSG00000042265	Trem1	triggering receptor expressed on myeloid cells 1	-1.50	1.91E-05

ENSMUSG00000001095	Slc13a2	solute carrier family 13 (sodium-dependent dicarboxylate transporter), member 2	-1.51	4.49E-12
ENSMUSG00000029484	Anxa3	annexin A3	-1.51	1.99E-12
ENSMUSG00000064400			-1.51	8.15E-05
ENSMUSG00000021281	Tnfaip2	tumor necrosis factor, alpha-induced protein 2	-1.51	1.59E-10
ENSMUSG00000075010	AW112010	expressed sequence AW112010	-1.52	1.73E-11
ENSMUSG00000064346			-1.52	1.15E-05
ENSMUSG00000074417	Pira11	paired-Ig-like receptor A11	-1.52	8.95E-07
ENSMUSG00000029553	Tfec	transcription factor EC	-1.53	9.97E-06
ENSMUSG00000024679	Ms4a6d	membrane-spanning 4-domains, subfamily A, member 6D	-1.53	3.27E-10
ENSMUSG00000037095	Lrg1	leucine-rich alpha-2-glycoprotein 1	-1.53	1.74E-07
ENSMUSG00000040253	Gbp7	guanylate binding protein 7	-1.53	1.73E-07
ENSMUSG00000058427	Cxcl2	chemokine (C-X-C motif) ligand 2	-1.55	9.98E-07
ENSMUSG00000022651	Retnlg	resistin like gamma	-1.56	2.36E-06
ENSMUSG00000001670	Tat	tyrosine aminotransferase	-1.56	1.27E-11
ENSMUSG00000029082	Bst1	bone marrow stromal cell antigen 1	-1.57	5.86E-09
ENSMUSG00000026580	Selp	selectin, platelet	-1.57	2.82E-08
ENSMUSG00000016496	Cd274	CD274 antigen	-1.57	2.97E-11
ENSMUSG00000078161	Erich3	glutamate rich 3	-1.57	8.86E-06
ENSMUSG00000026073	Il1r2	interleukin 1 receptor, type II	-1.57	1.45E-06
ENSMUSG00000065629			-1.58	3.86E-05
ENSMUSG00000096528	G430049J08Rik	RIKEN cDNA G430049J08 gene	-1.59	1.14E-11
ENSMUSG00000026880	Stom	stomatin	-1.61	1.88E-15
ENSMUSG00000027360	Hdc	histidine decarboxylase	-1.61	8.64E-06
ENSMUSG00000095788	Sirpb1a	signal-regulatory protein beta 1A	-1.62	1.10E-05
ENSMUSG00000037411	Serpine1	serine (or cysteine) peptidase inhibitor, clade E, member 1	-1.63	1.11E-10
ENSMUSG00000012428	Steap4	STEAP family member 4	-1.63	2.13E-12
ENSMUSG00000025161	Slc16a3	solute carrier family 16 (monocarboxylic acid transporters), member 3	-1.63	1.32E-08
ENSMUSG00000074892	B3galt5	UDP-Gal:betaGlcNAc beta 1,3-galactosyltransferase, polypeptide 5	-1.65	1.29E-11
ENSMUSG00000013974	Mcemp1	mast cell expressed membrane protein 1	-1.65	5.17E-06
ENSMUSG00000030144	Clec4d	C-type lectin domain family 4, member d	-1.65	2.17E-06
ENSMUSG00000025877	Hk3	hexokinase 3	-1.66	6.91E-08
ENSMUSG00000000982	Ccl3	chemokine (C-C motif) ligand 3	-1.66	1.11E-05
ENSMUSG00000027514	Zbp1	Z-DNA binding protein 1	-1.67	4.38E-11
ENSMUSG00000038550	Ciart	circadian associated repressor of transcription	-1.68	2.31E-07
ENSMUSG00000046031	Fam26f	family with sequence similarity 26, member F	-1.68	5.46E-07
ENSMUSG00000029084	Cd38	CD38 antigen	-1.70	1.86E-09
ENSMUSG00000079014	Serpina3i	serine (or cysteine) peptidase inhibitor, clade A, member 3I	-1.71	2.52E-07
ENSMUSG00000068452	Duox2	dual oxidase 2	-1.71	6.41E-12
ENSMUSG00000079516	Reg3a	regenerating islet-derived 3 alpha	-1.72	3.49E-06
ENSMUSG00000030187	Klra2	killer cell lectin-like receptor, subfamily A, member 2	-1.73	1.48E-09
ENSMUSG00000056054	S100a8	S100 calcium binding protein A8 (calgranulin A)	-1.74	7.38E-06
ENSMUSG00000074115	Saa1	serum amyloid A 1	-1.74	1.20E-07
ENSMUSG00000078853	Igtp	interferon gamma induced GTPase	-1.75	5.74E-08
ENSMUSG00000068606	Gm4841	predicted gene 4841	-1.75	8.70E-09
ENSMUSG00000028270	Gbp2	guanylate binding protein 2	-1.76	1.55E-12
ENSMUSG00000048852	Gm12185	predicted gene 12185	-1.76	1.06E-08

ENSMUSG00000078763	Slfn1	schlafen 1	-1.77	1.10E-10
ENSMUSG00000097423			-1.77	3.70E-09
ENSMUSG00000031444	F10	coagulation factor X	-1.77	6.94E-09
ENSMUSG00000075270	Pde11a	phosphodiesterase 11A	-1.78	1.17E-07
ENSMUSG00000044254	Pcsk9	proprotein convertase subtilisin/kexin type 9	-1.78	5.25E-14
ENSMUSG00000021091	Serpina3n	serine (or cysteine) peptidase inhibitor, clade A, member 3N	-1.78	7.76E-16
ENSMUSG00000085977			-1.78	1.69E-07
ENSMUSG00000041293	Gpr110	G protein-coupled receptor 110	-1.79	3.50E-06
ENSMUSG00000038751	Ptk6	PTK6 protein tyrosine kinase 6	-1.79	2.41E-14
ENSMUSG00000046688	Tifa	TRAF-interacting protein with forkhead-associated domain	-1.80	2.18E-13
ENSMUSG00000028859	Csf3r	colony stimulating factor 3 receptor (granulocyte)	-1.80	7.17E-12
ENSMUSG00000047562	Mmp10	matrix metallopeptidase 10	-1.80	2.41E-06
ENSMUSG00000040809	Chil3	chitinase-like 3	-1.81	2.47E-06
ENSMUSG00000079362	Gbp6	guanylate binding protein 6	-1.81	1.29E-10
ENSMUSG00000021950	Anxa8	annexin A8	-1.82	1.67E-07
ENSMUSG00000079012	Serpina3m	serine (or cysteine) peptidase inhibitor, clade A, member 3M	-1.83	5.16E-09
ENSMUSG00000043613	Mmp3	matrix metallopeptidase 3	-1.83	3.75E-08
ENSMUSG00000060183	Cxcl11	chemokine (C-X-C motif) ligand 11	-1.83	2.00E-07
ENSMUSG00000078922	Tgtp1	T cell specific GTPase 1	-1.83	4.68E-09
ENSMUSG00000034438	Gbp8	guanylate-binding protein 8	-1.83	2.50E-12
ENSMUSG00000047798	Cd300lf	CD300 antigen like family member F	-1.83	6.35E-10
ENSMUSG00000053101	Gpr141	G protein-coupled receptor 141	-1.83	4.15E-11
ENSMUSG00000028269			-1.85	8.33E-09
ENSMUSG00000053113	Socs3	suppressor of cytokine signaling 3	-1.87	2.53E-09
ENSMUSG00000082976	Gm15056	predicted gene 15056	-1.90	1.57E-07
ENSMUSG00000000204	Slfn4	schlafen 4	-1.90	4.73E-14
ENSMUSG00000035105	Egln3	egl-9 family hypoxia-inducible factor 3	-1.91	2.81E-14
ENSMUSG00000050747	Trim15	tripartite motif-containing 15	-1.91	3.71E-07
ENSMUSG00000024401	Tnf	tumor necrosis factor	-1.92	3.27E-12
ENSMUSG00000054588			-1.95	5.54E-08
ENSMUSG00000056071	S100a9	S100 calcium binding protein A9 (calgranulin B)	-1.97	4.28E-07
ENSMUSG00000066363	Serpina3f	serine (or cysteine) peptidase inhibitor, clade A, member 3F	-1.97	1.41E-12
ENSMUSG00000082292			-1.97	6.06E-10
ENSMUSG00000029380	Cxcl1	chemokine (C-X-C motif) ligand 1	-1.98	1.87E-09
ENSMUSG00000087070	Gm12505	predicted gene 12505	-1.99	1.78E-13
ENSMUSG00000073530	Pappa2	pappalysin 2	-2.01	1.81E-10
ENSMUSG00000055978	Fut2	fucosyltransferase 2	-2.02	7.60E-17
ENSMUSG00000027068	Dhrs9	dehydrogenase/reductase (SDR family) member 9	-2.03	8.28E-18
ENSMUSG00000027398	Il1b	interleukin 1 beta	-2.05	5.96E-11
ENSMUSG00000029371	Cxcl5	chemokine (C-X-C motif) ligand 5	-2.05	7.81E-08
ENSMUSG00000027399	Il1a	interleukin 1 alpha	-2.10	5.26E-12
ENSMUSG00000041481			-2.11	1.05E-19
ENSMUSG00000021214	Akr1c18	aldo-keto reductase family 1, member C18	-2.12	6.66E-09
ENSMUSG00000041193	Pla2g5	phospholipase A2, group V	-2.13	5.92E-18
ENSMUSG00000049281	Scn3b	sodium channel, voltage-gated, type III, beta	-2.14	4.49E-13
ENSMUSG00000024697	Gna14	guanine nucleotide binding protein, alpha 14	-2.17	9.32E-18

ENSMUSG00000090942	F830016B08Rik	RIKEN cDNA F830016B08 gene	-2.18	2.43E-14
ENSMUSG00000024411	Aqp4	aquaporin 4	-2.19	1.31E-12
ENSMUSG00000028655	Mfsd2a	major facilitator superfamily domain containing 2A	-2.19	2.45E-09
ENSMUSG00000079363	Gbp4	guanylate binding protein 4	-2.21	1.13E-12
ENSMUSG00000031722	Hp	haptoglobin	-2.22	1.69E-11
ENSMUSG00000034855	Cxcl10	chemokine (C-X-C motif) ligand 10	-2.23	3.03E-13
ENSMUSG00000025746	Il6	interleukin 6	-2.23	1.49E-09
ENSMUSG00000042102	Dmgdh	dimethylglycine dehydrogenase precursor	-2.25	4.05E-09
ENSMUSG00000030017	Reg3g	regenerating islet-derived 3 gamma	-2.25	2.27E-10
ENSMUSG00000057465	Saa2	serum amyloid A 2	-2.26	1.25E-17
ENSMUSG00000032068	Plet1	placenta expressed transcript 1	-2.27	6.89E-14
ENSMUSG00000059089	Fcgr4	Fc receptor, IgG, low affinity IV	-2.31	2.15E-18
ENSMUSG00000030142	Clec4e	C-type lectin domain family 4, member e	-2.32	2.78E-10
ENSMUSG00000005800	Mmp8	matrix metallopeptidase 8	-2.35	1.21E-10
ENSMUSG00000040026	Saa3	serum amyloid A 3	-2.37	1.17E-13
ENSMUSG00000044162	Tnip3	TNFAIP3 interacting protein 3	-2.37	6.74E-25
ENSMUSG00000022582	Ly6g	lymphocyte antigen 6 complex, locus G	-2.38	3.26E-16
ENSMUSG00000054072	Iigp1	interferon inducible GTPase 1	-2.40	1.34E-12
ENSMUSG00000071356	Reg3b	regenerating islet-derived 3 beta	-2.43	2.82E-12
ENSMUSG00000047728	BC025446	cDNA sequence BC025446	-2.45	1.16E-13
ENSMUSG00000073555	Gm4951	predicted gene 4951	-2.46	1.45E-20
ENSMUSG00000028527	Ak4	adenylate kinase 4	-2.46	4.48E-16
ENSMUSG00000040264	Gbp2b	guanylate binding protein 2b	-2.48	7.14E-16
ENSMUSG00000031551	Ido1	indoleamine 2,3-dioxygenase 1	-2.48	3.77E-22
ENSMUSG00000075602	Ly6a	lymphocyte antigen 6 complex, locus A	-2.49	1.21E-24
ENSMUSG00000052270	Fpr2	formyl peptide receptor 2	-2.57	5.56E-18
ENSMUSG00000029417	Cxcl9	chemokine (C-X-C motif) ligand 9	-2.63	3.25E-15
ENSMUSG00000074195	Clca4b	chloride channel calcium activated 4B	-2.66	5.24E-14
ENSMUSG00000022126	Irg1	immunoresponsive gene 1	-2.68	1.84E-20
ENSMUSG00000064246	Chil1	chitinase-like 1	-2.69	5.36E-19
ENSMUSG00000020826	Nos2	nitric oxide synthase 2, inducible	-2.81	3.76E-20
ENSMUSG00000026822	Lcn2	lipocalin 2	-2.89	1.81E-21

Table S8 Differentially expressed genes of BALB/c (YPIII infected 42 dpi vs. uninfected 42 dpi)

Ensembl ID	Gene symbol	Gene name	log_2 fold change	p-value
ENSMUSG00000031722	Hp	haptoglobin	2.68	6.17E-15
ENSMUSG00000027656	Wisp2	WNT1 inducible signaling pathway protein 2	2.37	1.93E-10
ENSMUSG00000032496	Ltf	lactotransferrin	2.22	8.68E-09
ENSMUSG00000076614			2.15	3.06E-08
ENSMUSG00000022227	Mcpt1	mast cell protease 1	2.10	1.24E-08
ENSMUSG00000022226	Mcpt2	mast cell protease 2	1.98	2.41E-07
ENSMUSG00000069919	Hba-a1	hemoglobin alpha, adult chain 1	1.79	4.03E-12
ENSMUSG00000027398	Il1b	interleukin 1 beta	1.76	3.56E-08
ENSMUSG00000079105	C7	complement component 7	1.73	5.79E-08
ENSMUSG00000076540			1.73	5.98E-06

ENSMUSG00000020473	Aebp1	AE binding protein 1	1.71	4.50E-18
ENSMUSG00000000204	Slfn4	schlafen 4	1.68	1.31E-10
ENSMUSG00000030474	Siglece	sialic acid binding Ig-like lectin E	1.67	5.99E-06
ENSMUSG00000032484	Ngp	neutrophilic granule protein	1.66	1.35E-06
ENSMUSG00000095130			1.64	4.80E-06
ENSMUSG00000024011	Pi16	peptidase inhibitor 16	1.64	7.85E-11
ENSMUSG00000019987	Arg1	arginase, liver	1.63	2.95E-07
ENSMUSG00000076596			1.63	2.64E-05
ENSMUSG00000069917	Hba-a2	hemoglobin alpha, adult chain 2	1.62	1.92E-09
ENSMUSG00000076538			1.62	3.22E-05
ENSMUSG00000028111	Ctsk	cathepsin K	1.62	9.32E-10
ENSMUSG00000095682			1.62	7.71E-06
ENSMUSG00000016024	Lbp	lipopolysaccharide binding protein	1.60	1.78E-12
ENSMUSG00000026822	Lcn2	lipocalin 2	1.59	9.67E-07
ENSMUSG00000028859	Csf3r	colony stimulating factor 3 receptor (granulocyte)	1.58	7.91E-09
ENSMUSG00000096461			1.58	3.45E-05
ENSMUSG00000012017	Scarf2	scavenger receptor class F, member 2	1.57	4.62E-07
ENSMUSG00000043613	Mmp3	matrix metallopeptidase 3	1.55	4.45E-06
ENSMUSG00000040133	Gpr176	G protein-coupled receptor 176	1.54	2.09E-05
ENSMUSG00000042436	Mfap4	microfibrillar-associated protein 4	1.53	4.42E-09
ENSMUSG00000024529	Lox	lysyl oxidase	1.50	2.32E-06
ENSMUSG00000095351			1.49	2.33E-05
ENSMUSG00000042265	Trem1	triggering receptor expressed on myeloid cells 1	1.49	6.14E-05
ENSMUSG00000039252	Lgi2	leucine-rich repeat LGI family, member 2	1.48	7.16E-07
ENSMUSG00000032068	Plet1	placenta expressed transcript 1	1.48	1.18E-06
ENSMUSG00000017002	Slpi	secretory leukocyte peptidase inhibitor	1.48	1.24E-04
ENSMUSG00000079012	Serpina3m	serine (or cysteine) peptidase inhibitor, clade A, member 3M	1.47	3.75E-06
ENSMUSG00000021260	Hhipl1	hedgehog interacting protein-like 1	1.46	3.95E-05
ENSMUSG00000089672	Gp49a	glycoprotein 49 A	1.46	4.33E-07
ENSMUSG00000001506	Col1a1	collagen, type I, alpha 1	1.45	6.71E-12
ENSMUSG00000066363	Serpina3f	serine (or cysteine) peptidase inhibitor, clade A, member 3F	1.45	1.02E-06
ENSMUSG00000032691	Nlrp3	NLR family, pyrin domain containing 3	1.44	1.33E-06
ENSMUSG00000056071	S100a9	S100 calcium binding protein A9 (calgranulin B)	1.43	2.39E-04
ENSMUSG00000047562	Mmp10	matrix metallopeptidase 10	1.43	1.96E-04
ENSMUSG00000030732	Chrdl2	chordin-like 2	1.42	1.21E-04
ENSMUSG00000058427	Cxcl2	chemokine (C-X-C motif) ligand 2	1.41	8.26E-05
ENSMUSG00000056427	Slit3	slit homolog 3 (Drosophila)	1.41	2.25E-11
ENSMUSG00000024164	C3	complement component 3	1.39	1.76E-13
ENSMUSG00000036412	Arsi	arylsulfatase i	1.39	4.37E-05
ENSMUSG00000027360	Hdc	histidine decarboxylase	1.39	1.52E-04
ENSMUSG00000031380	Figf	c-fos induced growth factor	1.39	1.07E-06
ENSMUSG00000064147	Rab44	RAB44, member RAS oncogene family	1.38	1.70E-04
ENSMUSG00000076612			1.37	1.63E-04
ENSMUSG00000021091	Serpina3n	serine (or cysteine) peptidase inhibitor, clade A, member 3N	1.37	1.38E-09
ENSMUSG00000047798	Cd300lf	CD300 antigen like family member F	1.36	1.06E-05
ENSMUSG00000027408	Cpxm1	carboxypeptidase X 1 (M14 family)	1.35	9.41E-07

ENSMUSG00000031239	Itm2a	integral membrane protein 2A	1.35	9.46E-06
ENSMUSG00000052749	Trim30b	tripartite motif-containing 30B	1.33	3.16E-04
ENSMUSG00000076580			1.32	4.70E-04
ENSMUSG00000038725	Pkhd1l1	polycystic kidney and hepatic disease 1-like 1	1.31	1.12E-07
ENSMUSG00000074151	Nlrc5	NLR family, CARD domain containing 5	1.30	4.19E-07
ENSMUSG00000023885	Thbs2	thrombospondin 2	1.30	1.79E-11
ENSMUSG00000032796	Lama1	laminin, alpha 1	1.30	5.87E-07
ENSMUSG00000021702	Thbs4	thrombospondin 4	1.30	5.56E-07
ENSMUSG00000026442	Nfasc	neurofascin	1.29	2.49E-06
ENSMUSG00000031596	Slc7a2	solute carrier family 7 (cationic amino acid transporter, y+ system), member 2	1.29	1.38E-06
ENSMUSG00000031375	Bgn	biglycan	1.28	1.02E-10
ENSMUSG00000073418	C4b	complement component 4B (Chido blood group)	1.28	3.35E-11
ENSMUSG00000029675	Eln	elastin	1.27	7.93E-07
ENSMUSG00000020264	Slc36a2	solute carrier family 36 (proton/amino acid symporter), member 2	1.27	1.81E-04
ENSMUSG00000029371	Cxcl5	chemokine (C-X-C motif) ligand 5	1.27	9.92E-04
ENSMUSG00000005800	Mmp8	matrix metallopeptidase 8	1.26	7.05E-04
ENSMUSG00000000031			1.26	1.14E-03
ENSMUSG00000095416			1.26	9.74E-05
ENSMUSG00000032690	Oas2	2'-5' oligoadenylate synthetase 2	1.25	2.78E-05
ENSMUSG00000021950	Anxa8	annexin A8	1.25	3.79E-04
ENSMUSG00000028369	Svep1	sushi, von Willebrand factor type A, EGF and pentraxin domain containing 1	1.25	5.08E-10
ENSMUSG00000024481	Lvrn	laeverin	1.24	5.33E-05
ENSMUSG00000058914	C1qtnf3	C1q and tumor necrosis factor related protein 3	1.24	2.51E-04
ENSMUSG00000072941	Sod3	superoxide dismutase 3, extracellular	1.24	3.92E-09
ENSMUSG00000022032	Scara5	scavenger receptor class A, member 5 (putative)	1.23	1.32E-08
ENSMUSG00000027996	Sfrp2	secreted frizzled-related protein 2	1.22	1.71E-04
ENSMUSG00000024087	Cyp1b1	cytochrome P450, family 1, subfamily b, polypeptide 1	1.22	6.43E-05
ENSMUSG00000067203			1.22	1.06E-06
ENSMUSG00000004296			1.22	4.54E-04
ENSMUSG00000076587			1.20	1.71E-03
ENSMUSG00000041734	Kirrel	kin of IRRE like (Drosophila)	1.20	1.13E-07
ENSMUSG00000073555	Gm4951	predicted gene 4951	1.20	9.08E-06
ENSMUSG00000030144	Clec4d	C-type lectin domain family 4, member d	1.19	1.23E-03
ENSMUSG00000041577	Prelp	proline arginine-rich end leucine-rich repeat	1.19	2.03E-13
ENSMUSG00000001865	Cpa3	carboxypeptidase A3, mast cell	1.18	7.75E-04
ENSMUSG00000045322	Tlr9	toll-like receptor 9	1.18	4.69E-04
ENSMUSG00000023046	Igfbp6	insulin-like growth factor binding protein 6	1.17	6.37E-07
ENSMUSG00000041695	Kcnj2	potassium inwardly-rectifying channel, subfamily J, member 2	1.17	3.08E-04
ENSMUSG00000074417	Pira11	paired-Ig-like receptor A11	1.17	2.24E-04
ENSMUSG00000015947	Fcgr1	Fc receptor, IgG, high affinity I	1.17	1.10E-05
ENSMUSG00000031480	Thsd1	thrombospondin, type I, domain 1	1.17	6.64E-04
ENSMUSG00000026185	Igfbp5	insulin-like growth factor binding protein 5	1.17	3.55E-08
ENSMUSG00000030427	Lilra6	leukocyte immunoglobulin-like receptor, subfamily A (with TM domain), member 6	1.16	2.51E-04
ENSMUSG00000052353	Cemip	cell migration inducing protein, hyaluronan binding	1.16	1.65E-03
ENSMUSG00000027225	Duoxa2	dual oxidase maturation factor 2	1.15	6.10E-04
ENSMUSG00000020695	Mrc2	mannose receptor, C type 2	1.15	4.34E-08

ENSMUSG00000046245	Pilra	paired immunoglobin-like type 2 receptor alpha	1.15	2.91E-05
ENSMUSG00000096638			1.14	9.95E-05
ENSMUSG00000072812	Ahnak2	AHNAK nucleoprotein 2	1.14	1.25E-07
ENSMUSG00000038456	Dennd2a	DENN/MADD domain containing 2A	1.14	2.90E-06
ENSMUSG00000000901	Mmp11	matrix metallopeptidase 11	1.14	2.52E-04
ENSMUSG00000036437	Npy1r	neuropeptide Y receptor Y1	1.14	7.74E-06
ENSMUSG00000025877	Hk3	hexokinase 3	1.13	4.17E-04
ENSMUSG00000060063	Alox5ap	arachidonate 5-lipoxygenase activating protein	1.13	4.32E-06
ENSMUSG00000038156	Spon1	spondin 1, (f-spondin) extracellular matrix protein	1.13	2.84E-08
ENSMUSG00000031762	Mt2	metallothionein 2	1.13	5.15E-04
ENSMUSG00000025355	Mmp19	matrix metallopeptidase 19	1.12	3.58E-06
ENSMUSG00000022371	Col14a1	collagen, type XIV, alpha 1	1.12	6.63E-09
ENSMUSG00000041449			1.12	2.61E-04
ENSMUSG00000049103	Ccr2	chemokine (C-C motif) receptor 2	1.12	2.20E-06
ENSMUSG00000048965	Mrgpre	MAS-related GPR, member E	1.11	1.19E-04
ENSMUSG00000062593	Lilrb4	leukocyte immunoglobulin-like receptor, subfamily B, member 4	1.11	2.03E-04
ENSMUSG00000053113	Socs3	suppressor of cytokine signaling 3	1.11	4.51E-04
ENSMUSG00000095285			1.11	7.53E-04
ENSMUSG00000026773	Pfkfb3	6-phosphofructo-2-kinase/fructose-2,6-biphosphatase 3	1.10	6.20E-07
ENSMUSG00000094134			1.10	4.88E-03
ENSMUSG00000025701	Alox5	arachidonate 5-lipoxygenase	1.09	1.76E-05
ENSMUSG00000040809	Chil3	chitinase-like 3	1.09	4.34E-03
ENSMUSG00000032334	Loxl1	lysyl oxidase-like 1	1.09	3.30E-07
ENSMUSG00000029661	Col1a2	collagen, type I, alpha 2	1.09	4.47E-08
ENSMUSG00000076653			1.09	8.57E-06
ENSMUSG00000053889			1.08	4.19E-04
ENSMUSG00000052212	Cd177	CD177 antigen	1.08	8.35E-08
ENSMUSG00000052270	Fpr2	formyl peptide receptor 2	1.08	6.36E-04
ENSMUSG00000001435	Col18a1	collagen, type XVIII, alpha 1	1.08	3.48E-07
ENSMUSG00000036545	Adamts2	a disintegrin-like and metallopeptidase (reprolysin type) with thrombospondin type 1 motif, 2	1.08	3.46E-07
ENSMUSG00000041673	Lrrc18	leucine rich repeat containing 18	1.08	2.14E-04
ENSMUSG00000098470	C1rb	complement component 1, r subcomponent B	1.07	1.65E-04
ENSMUSG00000064246	Chil1	chitinase-like 1	1.07	1.38E-03
ENSMUSG00000000552	Zfp385a	zinc finger protein 385A	1.07	3.57E-04
ENSMUSG00000005465	Il27ra	interleukin 27 receptor, alpha	1.07	3.71E-04
ENSMUSG00000079227	Ccr5	chemokine (C-C motif) receptor 5	1.07	1.31E-06
ENSMUSG00000029070	Mxra8	matrix-remodelling associated 8	1.07	1.56E-07
ENSMUSG00000016763	Scube1	signal peptide, CUB domain, EGF-like 1	1.07	1.42E-06
ENSMUSG00000025784	Clec3b	C-type lectin domain family 3, member b	1.06	1.27E-07
ENSMUSG00000076613			1.06	2.98E-03
ENSMUSG00000070691	Runx3	runt related transcription factor 3	1.06	1.27E-05
ENSMUSG00000037003	Tenc1	tensin like C1 domain-containing phosphatase	1.06	3.90E-08
ENSMUSG00000015053	Gata2	GATA binding protein 2	1.06	2.17E-03
ENSMUSG00000044456	Rin3	Ras and Rab interactor 3	1.06	3.55E-06
ENSMUSG00000040345	Arhgap9	Rho GTPase activating protein 9	1.06	1.36E-04
ENSMUSG00000078763	Slfn1	schlafen 1	1.06	1.35E-04

ENSMUSG00000050989	Sepn1	selenoprotein N, 1	1.06	2.13E-06
ENSMUSG00000022623	Shank3	SH3/ankyrin domain gene 3	1.05	2.02E-04
ENSMUSG00000022091	Sorbs3	sorbin and SH3 domain containing 3	1.05	2.34E-07
ENSMUSG00000022860	Chodl	chondrolectin	1.05	3.64E-04
ENSMUSG00000034059	Ypel4	yippee-like 4 (Drosophila)	1.05	1.59E-03
ENSMUSG00000095612			1.04	1.74E-03
ENSMUSG00000033327	Tnxb	tenascin XB	1.04	8.67E-08
ENSMUSG00000041193	Pla2g5	phospholipase A2, group V	1.04	7.86E-05
ENSMUSG00000020901	Pik3r5	phosphoinositide-3-kinase, regulatory subunit 5, p101	1.04	1.24E-05
ENSMUSG00000006344	Ggt5	gamma-glutamyltransferase 5	1.04	1.15E-06
ENSMUSG00000046207	Pik3r6	phosphoinositide-3-kinase, regulatory subunit 6	1.04	9.48E-04
ENSMUSG00000028874	Fgr	Gardner-Rasheed feline sarcoma viral (Fgr) oncogene homolog	1.03	3.99E-05
ENSMUSG00000002847	Pla1a	phospholipase A1 member A	1.03	5.82E-03
ENSMUSG00000064080	Fbln2	fibulin 2	1.03	2.49E-07
ENSMUSG00000020889	Nr1d1	nuclear receptor subfamily 1, group D, member 1	1.03	6.26E-04
ENSMUSG00000022102	Dok2	docking protein 2	1.03	2.78E-03
ENSMUSG00000084159			1.03	2.14E-04
ENSMUSG00000079014	Serpina3i	serine (or cysteine) peptidase inhibitor, clade A, member 3I	1.02	2.80E-03
ENSMUSG00000054555	Adam12	a disintegrin and metallopeptidase domain 12 (meltrin alpha)	1.01	6.93E-04
ENSMUSG00000043531	Sorcs1	VPS10 domain receptor protein SORCS 1	1.01	1.09E-03
ENSMUSG00000076508			1.01	4.82E-03
ENSMUSG00000040254	Sema3d	sema domain, immunoglobulin domain (Ig), short basic domain, secreted, (semaphorin) 3D	1.01	2.99E-06
ENSMUSG00000024620	Pdgfrb	platelet derived growth factor receptor, beta polypeptide	1.01	4.20E-07
ENSMUSG00000042286	Stab1	stabilin 1	1.01	1.99E-07
ENSMUSG00000076695			1.01	5.45E-03
ENSMUSG00000031765	Mt1	metallothionein 1	1.01	6.80E-05
ENSMUSG00000024053	Emilin2	elastin microfibril interfacer 2	1.01	7.62E-06
ENSMUSG00000068196	Col8a1	collagen, type VIII, alpha 1	1.00	7.70E-05
ENSMUSG00000018339	Gpx3	glutathione peroxidase 3	1.00	1.42E-05
ENSMUSG00000025479	Cyp2e1	cytochrome P450, family 2, subfamily e, polypeptide 1	1.00	6.75E-04
ENSMUSG00000033715	Akr1c14	aldo-keto reductase family 1, member C14	-1.01	6.01E-04
ENSMUSG00000029664	Tfpi2	tissue factor pathway inhibitor 2	-1.01	1.95E-05
ENSMUSG00000051235	Gen1	Gen homolog 1, endonuclease (Drosophila)	-1.02	7.80E-05
ENSMUSG00000064343			-1.02	3.49E-03
ENSMUSG00000077711			-1.02	8.03E-04
ENSMUSG00000078784	1810022K09Rik	RIKEN cDNA 1810022K09 gene	-1.02	2.96E-04
ENSMUSG00000063383	Zfp947	zinc finger protein 947	-1.02	1.48E-03
ENSMUSG00000029334	Prkg2	protein kinase, cGMP-dependent, type II	-1.02	4.69E-04
ENSMUSG00000049799	Lrrc19	leucine rich repeat containing 19	-1.02	2.82E-03
ENSMUSG00000056383	AI987944	expressed sequence AI987944	-1.02	2.99E-04
ENSMUSG00000039221	Rpl22l1	ribosomal protein L22 like 1	-1.03	3.53E-04
ENSMUSG00000075983			-1.03	7.87E-03
ENSMUSG00000026049	Tex30	testis expressed 30	-1.04	2.47E-04
ENSMUSG00000078193			-1.04	1.75E-04
ENSMUSG00000065145			-1.04	3.71E-08
ENSMUSG00000092203	1110038B12Rik	RIKEN cDNA 1110038B12 gene	-1.05	7.13E-08

ENSMUSG00000094245			-1.05	2.38E-03
ENSMUSG00000032372	Plscr2	phospholipid scramblase 2	-1.05	8.75E-06
ENSMUSG00000098274	Rpl24	ribosomal protein L24	-1.06	5.11E-06
ENSMUSG00000064356	ATP8	ATP synthase F0 subunit 8	-1.07	7.33E-04
ENSMUSG00000064339			-1.07	1.07E-04
ENSMUSG00000064840			-1.07	3.05E-03
ENSMUSG00000065258			-1.07	1.85E-05
ENSMUSG00000054630	Ugt2b5	UDP glucuronosyltransferase 2 family, polypeptide B5	-1.07	1.70E-06
ENSMUSG00000088273			-1.08	4.53E-03
ENSMUSG00000059898	Dsc3	desmocollin 3	-1.08	5.82E-05
ENSMUSG00000064647			-1.08	8.18E-04
ENSMUSG00000094199			-1.08	1.68E-03
ENSMUSG00000071748			-1.08	2.66E-05
ENSMUSG00000064945	Rny3	RNA, Y3 small cytoplasmic (associated with Ro protein)	-1.08	7.30E-07
ENSMUSG00000072762			-1.09	2.39E-04
ENSMUSG00000039114	Nrn1	neuritin 1	-1.10	4.64E-03
ENSMUSG00000088604			-1.10	1.79E-06
ENSMUSG00000009628	Tex15	testis expressed gene 15	-1.10	4.94E-04
ENSMUSG00000047534	Mis18bp1	MIS18 binding protein 1	-1.11	1.56E-05
ENSMUSG00000070704	Ugt2b36	UDP glucuronosyltransferase 2 family, polypeptide B36	-1.11	8.23E-04
ENSMUSG00000078435	AU041133	expressed sequence AU041133	-1.11	5.23E-04
ENSMUSG00000094026			-1.12	3.25E-03
ENSMUSG00000032854	Ugt8a	UDP galactosyltransferase 8A	-1.13	1.95E-03
ENSMUSG00000074800			-1.13	7.09E-06
ENSMUSG00000054091	1810037I17Rik	RIKEN cDNA 1810037I17 gene	-1.13	1.57E-07
ENSMUSG00000058748	Zfp958	zinc finger protein 958	-1.14	1.62E-04
ENSMUSG00000064901			-1.14	2.81E-07
ENSMUSG00000056531	Ccdc18	coiled-coil domain containing 18	-1.14	1.42E-04
ENSMUSG00000081094			-1.15	2.60E-06
ENSMUSG00000035133	Arhgap5	Rho GTPase activating protein 5	-1.15	3.11E-04
ENSMUSG00000025528	2010106E10Rik	RIKEN cDNA 2010106E10 gene	-1.15	1.32E-03
ENSMUSG00000093864			-1.17	7.48E-04
ENSMUSG00000076501			-1.17	1.62E-08
ENSMUSG00000088516			-1.17	2.76E-08
ENSMUSG00000026166	Ccl20	chemokine (C-C motif) ligand 20	-1.17	1.32E-04
ENSMUSG00000064653			-1.18	4.10E-04
ENSMUSG00000064472			-1.18	2.39E-03
ENSMUSG00000089308			-1.18	8.59E-04
ENSMUSG00000096341			-1.18	3.18E-06
ENSMUSG00000005802	Slc30a4	solute carrier family 30 (zinc transporter), member 4	-1.19	2.80E-07
ENSMUSG00000060419			-1.20	8.96E-05
ENSMUSG00000080921			-1.20	4.13E-06
ENSMUSG00000060149	BC002059	cDNA sequence BC002059	-1.21	3.61E-04
ENSMUSG00000078546	2210404O09Rik	RIKEN cDNA 2210404O09 gene	-1.22	3.85E-04
ENSMUSG00000029273	Sult1d1	sulfotransferase family 1D, member 1	-1.22	5.84E-05
ENSMUSG00000022034	Esco2	establishment of cohesion 1 homolog 2 (S. cerevisiae)	-1.23	3.91E-07

ENSMUSG00000065876			-1.23	1.49E-04
ENSMUSG00000095857			-1.23	3.63E-04
ENSMUSG00000090136	Gm10177	predicted gene 10177	-1.25	1.79E-04
ENSMUSG00000056032			-1.25	4.62E-06
ENSMUSG00000021714	Cenpk	centromere protein K	-1.27	3.54E-05
ENSMUSG00000080365			-1.27	2.90E-05
ENSMUSG00000019888	Mgat4c	MGAT4 family, member C	-1.29	5.65E-05
ENSMUSG00000047344	Lancl3	LanC lantibiotic synthetase component C-like 3 (bacterial)	-1.30	8.08E-05
ENSMUSG00000089855			-1.31	1.69E-04
ENSMUSG00000095624			-1.31	5.86E-04
ENSMUSG00000023073	Slc10a2	solute carrier family 10, member 2	-1.33	1.50E-04
ENSMUSG00000064352			-1.35	3.24E-05
ENSMUSG00000094400			-1.35	3.94E-04
ENSMUSG00000076332			-1.37	4.24E-08
ENSMUSG00000064346			-1.39	1.25E-04
ENSMUSG00000025912	Mybl1	myeloblastosis oncogene-like 1	-1.41	1.95E-08
ENSMUSG00000093413			-1.42	4.10E-06
ENSMUSG00000028175	Depdc1a	DEP domain containing 1a	-1.44	1.03E-07
ENSMUSG00000098178			-1.46	1.72E-09
ENSMUSG00000095396			-1.46	1.18E-04
ENSMUSG00000081043			-1.46	1.33E-05
ENSMUSG00000095738			-1.46	6.50E-05
ENSMUSG00000029821	Dfna5	deafness, autosomal dominant 5 (human)	-1.47	5.32E-10
ENSMUSG00000057359			-1.48	1.40E-05
ENSMUSG00000062083			-1.48	4.49E-09
ENSMUSG00000064358	COX3	cytochrome c oxidase subunit III	-1.49	3.53E-07
ENSMUSG00000064360	ND3	NADH dehydrogenase subunit 3	-1.50	1.85E-09
ENSMUSG00000065104			-1.50	2.85E-05
ENSMUSG00000076320			-1.53	5.18E-10
ENSMUSG00000067870			-1.54	9.19E-08
ENSMUSG00000091509			-1.56	1.27E-07
ENSMUSG00000056412			-1.56	4.85E-06
ENSMUSG00000076355			-1.57	2.07E-08
ENSMUSG00000095422			-1.58	1.27E-05
ENSMUSG00000064355			-1.61	2.99E-08
ENSMUSG00000076370			-1.61	4.87E-08
ENSMUSG00000064823			-1.65	1.25E-08
ENSMUSG00000093983			-1.67	3.64E-06
ENSMUSG00000077345			-1.71	2.02E-08
ENSMUSG00000096801			-1.80	2.98E-07
ENSMUSG00000087412			-1.80	4.43E-07
ENSMUSG00000092661			-1.82	1.41E-15
ENSMUSG00000077565			-1.87	3.58E-15
ENSMUSG00000064689			-1.89	4.72E-08
ENSMUSG00000077082			-1.89	1.78E-13
ENSMUSG00000064742			-1.91	1.80E-07

ENSMUSG00000083705	Gm8624	predicted gene 8624	-2.04	5.79E-13
ENSMUSG00000096222			-2.14	1.63E-10
ENSMUSG00000065373			-2.17	1.26E-11
ENSMUSG00000093999			-2.51	5.82E-13

Table S9 Differentially expressed genes of BALB/c (YPIII Δ*cnfy* infected 42 dpi vs. uninfected 42 dpi)

Ensembl ID	Gene symbol	Gene name	log2 fold change	p-value
ENSMUSG00000076614			1.94	6.22E-07
ENSMUSG00000017002	Slpi	secretory leukocyte peptidase inhibitor	1.80	3.21E-06
ENSMUSG00000058427	Cxcl2	chemokine (C-X-C motif) ligand 2	1.74	1.62E-06
ENSMUSG00000022227	Mcpt1	mast cell protease 1	1.72	3.19E-06
ENSMUSG00000022226	Mcpt2	mast cell protease 2	1.72	7.66E-06
ENSMUSG00000019987	Arg1	arginase, liver	1.64	3.85E-07
ENSMUSG00000032068	Plet1	placenta expressed transcript 1	1.57	2.50E-07
ENSMUSG00000027398	Il1b	interleukin 1 beta	1.51	2.23E-06
ENSMUSG00000071361	Mcpt9	mast cell protease 9	1.46	1.64E-04
ENSMUSG00000076633			1.40	2.91E-04
ENSMUSG00000043613	Mmp3	matrix metallopeptidase 3	1.38	4.71E-05
ENSMUSG00000076612			1.31	3.19E-04
ENSMUSG00000042265	Trem1	triggering receptor expressed on myeloid cells 1	1.30	5.69E-04
ENSMUSG00000068289	Cma2	chymase 2, mast cell	1.27	9.80E-04
ENSMUSG00000031722	Hp	haptoglobin	1.22	5.28E-04
ENSMUSG00000094769			1.19	1.11E-03
ENSMUSG00000030144	Clec4d	C-type lectin domain family 4, member d	1.09	3.65E-03
ENSMUSG00000029380	Cxcl1	chemokine (C-X-C motif) ligand 1	1.08	3.11E-03
ENSMUSG00000096326			1.08	5.11E-03
ENSMUSG00000025893	Kbtbd3	kelch repeat and BTB (POZ) domain containing 3	-1.00	1.81E-03
ENSMUSG00000086269			-1.02	8.83E-03
ENSMUSG00000020607	Fam84a	family with sequence similarity 84, member A	-1.03	2.32E-03
ENSMUSG00000029644	Pdx1	pancreatic and duodenal homeobox 1	-1.04	7.27E-03
ENSMUSG00000038094	Atp13a4	ATPase type 13A4	-1.06	1.70E-03
ENSMUSG00000050520	Cldn8	claudin 8	-1.06	6.73E-05
ENSMUSG00000054932	Afp	alpha fetoprotein	-1.07	5.76E-03
ENSMUSG00000039114	Nrn1	neuritin 1	-1.07	5.69E-03
ENSMUSG00000024558	Mapk4	mitogen-activated protein kinase 4	-1.08	1.12E-03
ENSMUSG00000076589			-1.12	3.47E-03
ENSMUSG00000042734	Ttc9	tetratricopeptide repeat domain 9	-1.13	1.23E-03
ENSMUSG00000030725	Lipt2	lipoyl(octanoyl) transferase 2 (putative)	-1.15	6.76E-04
ENSMUSG00000024912	Fosl1	fos-like antigen 1	-1.16	1.46E-03
ENSMUSG00000091844	Ccdc168	coiled-coil domain containing 168	-1.18	1.42E-03
ENSMUSG00000009628	Tex15	testis expressed gene 15	-1.18	1.99E-04
ENSMUSG00000027801	Tm4sf4	transmembrane 4 superfamily member 4	-1.23	1.02E-03
ENSMUSG00000024827	Gldc	glycine decarboxylase	-1.28	7.67E-04
ENSMUSG00000048455	Sprr1b	small proline-rich protein 1B	-1.57	6.66E-07
ENSMUSG00000071665	Foxr2	forkhead box R2	-1.58	8.25E-07

Table S10 Differentially expressed genes of BALB/c (YPIII infected 42 dpi vs. YPIII Δ*cnfy* infected 42 dpi)

Ensembl ID	Gene symbol	Gene name	log2 fold change	pvalue
ENSMUSG00000027656	Wisp2	WNT1 inducible signaling pathway protein 2	2.11	1.23E-08
ENSMUSG00000069917	Hba-a2	hemoglobin alpha, adult chain 2	1.89	3.06E-12
ENSMUSG00000069919	Hba-a1	hemoglobin alpha, adult chain 1	1.81	1.54E-12
ENSMUSG00000024011	Pi16	peptidase inhibitor 16	1.78	1.78E-12
ENSMUSG00000032496	Ltf	lactotransferrin	1.77	4.74E-06
ENSMUSG00000021260	Hhipl1	hedgehog interacting protein-like 1	1.75	1.02E-06
ENSMUSG00000020473	Aebp1	AE binding protein 1	1.69	7.98E-18
ENSMUSG00000032484	Ngp	neutrophilic granule protein	1.69	8.68E-07
ENSMUSG00000042985	Upk3b	uroplakin 3B	1.64	2.45E-05
ENSMUSG00000079105	C7	complement component 7	1.58	6.07E-07
ENSMUSG00000024481	Lvrn	laeverin	1.52	1.01E-06
ENSMUSG00000029675	Eln	elastin	1.51	5.51E-09
ENSMUSG00000031722	Hp	haptoglobin	1.46	9.50E-06
ENSMUSG00000038725	Pkhd1l1	polycystic kidney and hepatic disease 1-like 1	1.45	4.43E-09
ENSMUSG00000028111	Ctsk	cathepsin K	1.44	3.39E-08
ENSMUSG00000016024	Lbp	lipopolysaccharide binding protein	1.43	1.50E-10
ENSMUSG00000058914	C1qtnf3	C1q and tumor necrosis factor related protein 3	1.42	2.83E-05
ENSMUSG00000023034	Nr4a1	nuclear receptor subfamily 4, group A, member 1	1.41	1.06E-06
ENSMUSG00000076580			1.40	2.14E-04
ENSMUSG00000033170	Card10	caspase recruitment domain family, member 10	1.39	2.29E-07
ENSMUSG00000023046	Igfbp6	insulin-like growth factor binding protein 6	1.39	4.27E-09
ENSMUSG00000023885	Thbs2	thrombospondin 2	1.39	7.05E-13
ENSMUSG00000001506	Col1a1	collagen, type I, alpha 1	1.38	6.51E-11
ENSMUSG00000022032	Scara5	scavenger receptor class A, member 5 (putative)	1.38	1.60E-10
ENSMUSG00000041577	Prelp	proline arginine-rich end leucine-rich repeat	1.38	1.58E-17
ENSMUSG00000071656	Lrrn4cl	LRRN4 C-terminal like	1.37	1.90E-07
ENSMUSG00000020889	Nr1d1	nuclear receptor subfamily 1, group D, member 1	1.37	5.57E-06
ENSMUSG00000022860	Chodl	chondrolectin	1.37	4.60E-06
ENSMUSG00000036036	Zfp57	zinc finger protein 57	1.36	1.90E-05
ENSMUSG00000032243	Itga11	integrin alpha 11	1.35	3.80E-09
ENSMUSG00000056427	Slit3	slit homolog 3 (Drosophila)	1.35	1.26E-10
ENSMUSG00000084159			1.35	1.61E-06
ENSMUSG00000036437	Npy1r	neuropeptide Y receptor Y1	1.35	1.44E-07
ENSMUSG00000020695	Mrc2	mannose receptor, C type 2	1.34	1.84E-10
ENSMUSG00000059146	Ntrk3	neurotrophic tyrosine kinase, receptor, type 3	1.33	1.26E-04
ENSMUSG00000033327	Tnxb	tenascin XB	1.33	1.11E-11
ENSMUSG00000076596			1.31	7.37E-04
ENSMUSG00000025784	Clec3b	C-type lectin domain family 3, member b	1.30	1.21E-10
ENSMUSG00000027996	Sfrp2	secreted frizzled-related protein 2	1.30	6.30E-05
ENSMUSG00000022371	Col14a1	collagen, type XIV, alpha 1	1.30	1.80E-11
ENSMUSG00000041329	Atp1b2	ATPase, Na+/K+ transporting, beta 2 polypeptide	1.30	3.00E-06
ENSMUSG00000095682			1.30	3.39E-04

ENSMUSG00000095130			1.29	2.85E-04
ENSMUSG00000038463	Olfml2b	olfactomedin-like 2B	1.29	5.73E-11
ENSMUSG00000031762	Mt2	metallothionein 2	1.29	7.56E-05
ENSMUSG00000032334	Loxl1	lysyl oxidase-like 1	1.28	2.26E-09
ENSMUSG00000040734	Ppp1r13l	protein phosphatase 1, regulatory (inhibitor) subunit 13 like	1.28	9.25E-05
ENSMUSG00000079012	Serpina3m	serine (or cysteine) peptidase inhibitor, clade A, member 3M	1.27	4.27E-05
ENSMUSG00000029070	Mxra8	matrix-remodelling associated 8	1.27	4.40E-10
ENSMUSG00000040488	Ltbp4	latent transforming growth factor beta binding protein 4	1.26	9.54E-12
ENSMUSG00000037624	Kcnk2	potassium channel, subfamily K, member 2	1.25	7.58E-07
ENSMUSG00000031480	Thsd1	thrombospondin, type I, domain 1	1.25	2.52E-04
ENSMUSG00000058571	Gpc6	glypican 6	1.25	1.53E-07
ENSMUSG00000068196	Col8a1	collagen, type VIII, alpha 1	1.25	9.72E-07
ENSMUSG00000041378	Cldn5	claudin 5	1.25	4.53E-06
ENSMUSG00000042436	Mfap4	microfibrillar-associated protein 4	1.24	1.30E-06
ENSMUSG00000029096	Htra3	HtrA serine peptidase 3	1.24	5.12E-08
ENSMUSG00000039004	Bmp6	bone morphogenetic protein 6	1.24	2.24E-05
ENSMUSG00000027931	Npr1	natriuretic peptide receptor 1	1.23	8.86E-07
ENSMUSG00000040254	Sema3d	sema domain, immunoglobulin domain (Ig), short basic domain, secreted, (semaphorin) 3D	1.23	1.46E-08
ENSMUSG00000041482	Piezo2	piezo-type mechanosensitive ion channel component 2	1.22	2.57E-08
ENSMUSG00000036545	Adamts2	a disintegrin-like and metallopeptidase (reprolysin type) with thrombospondin type 1 motif, 2	1.22	8.67E-09
ENSMUSG00000038456	Dennd2a	DENN/MADD domain containing 2A	1.21	5.94E-07
ENSMUSG00000072941	Sod3	superoxide dismutase 3, extracellular	1.21	7.89E-09
ENSMUSG00000003573	Homer3	homer homolog 3 (Drosophila)	1.20	3.50E-05
ENSMUSG00000074766	Ism1	isthmin 1 homolog (zebrafish)	1.20	7.96E-05
ENSMUSG00000031765	Mt1	metallothionein 1	1.19	2.72E-06
ENSMUSG00000031871	Cdh5	cadherin 5	1.18	3.91E-11
ENSMUSG00000023411	Nfatc4	nuclear factor of activated T cells, cytoplasmic, calcineurin dependent 4	1.18	3.08E-06
ENSMUSG00000040612	Ildr2	immunoglobulin-like domain containing receptor 2	1.18	7.91E-06
ENSMUSG00000094124			1.17	1.74E-04
ENSMUSG00000059401	Mamld1	mastermind-like domain containing 1	1.17	8.46E-05
ENSMUSG00000037003	Tenc1	tensin like C1 domain-containing phosphatase	1.17	1.32E-09
ENSMUSG00000031375	Bgn	biglycan	1.17	3.58E-09
ENSMUSG00000028369	Svep1	sushi, von Willebrand factor type A, EGF and pentraxin domain containing 1	1.16	6.87E-09
ENSMUSG00000038112	AW551984	expressed sequence AW551984	1.16	1.23E-04
ENSMUSG00000067203			1.16	2.96E-06
ENSMUSG00000024663	Rab3il1	RAB3A interacting protein (rabin3)-like 1	1.15	1.21E-06
ENSMUSG00000057706	Mex3b	mex3 homolog B (C. elegans)	1.15	5.20E-04
ENSMUSG00000030546	Plin1	perilipin 1	1.15	6.10E-05
ENSMUSG00000054555	Adam12	a disintegrin and metallopeptidase domain 12 (meltrin alpha)	1.15	1.23E-04
ENSMUSG00000045333	Zfp423	zinc finger protein 423	1.15	2.55E-05
ENSMUSG00000021903	Galnt15	UDP-N-acetyl-alpha-D-galactosamine:polypeptide N-acetylgalactosaminyltransferase 15	1.15	5.09E-06
ENSMUSG00000034659	Tmem109	transmembrane protein 109	1.15	2.07E-09
ENSMUSG00000048387	Osr1	odd-skipped related 1 (Drosophila)	1.14	1.35E-06
ENSMUSG00000022091	Sorbs3	sorbin and SH3 domain containing 3	1.14	1.85E-08
ENSMUSG00000028341	Nr4a3	nuclear receptor subfamily 4, group A, member 3	1.14	1.16E-06
ENSMUSG00000020357	Flt4	FMS-like tyrosine kinase 4	1.14	5.76E-09

ENSMUSG00000047414	Flrt2	fibronectin leucine rich transmembrane protein 2	1.14	8.05E-07
ENSMUSG00000041734	Kirrel	kin of IRRE like (Drosophila)	1.14	4.48E-07
ENSMUSG00000059201	Lep	leptin	1.14	2.25E-03
ENSMUSG00000064080	Fbln2	fibulin 2	1.14	1.31E-08
ENSMUSG00000026574	Dpt	dermatopontin	1.14	9.33E-09
ENSMUSG00000072812	Ahnak2	AHNAK nucleoprotein 2	1.14	1.39E-07
ENSMUSG00000062991	Nrg1	neuregulin 1	1.13	4.37E-05
ENSMUSG00000025479	Cyp2e1	cytochrome P450, family 2, subfamily e, polypeptide 1	1.13	1.18E-04
ENSMUSG00000065645			1.13	2.11E-05
ENSMUSG00000052488	Cherp	calcium homeostasis endoplasmic reticulum protein	1.13	5.53E-08
ENSMUSG00000002799	Jag2	jagged 2	1.13	4.74E-04
ENSMUSG00000041559	Fmod	fibromodulin	1.13	4.30E-05
ENSMUSG00000043388	Tmem130	transmembrane protein 130	1.13	1.09E-03
ENSMUSG00000035863	Palm	paralemmin	1.12	2.43E-07
ENSMUSG00000024299	Adamts10	a disintegrin-like and metallopeptidase (reprolysin type) with thrombospondin type 1 motif, 10	1.12	1.03E-06
ENSMUSG00000031380	Figf	c-fos induced growth factor	1.12	5.75E-05
ENSMUSG00000028047	Thbs3	thrombospondin 3	1.12	3.32E-07
ENSMUSG00000076540			1.12	3.30E-03
ENSMUSG00000069893	9930111J21Rik1	RIKEN cDNA 9930111J21 gene 1	1.12	2.10E-04
ENSMUSG00000024940	Ltbp3	latent transforming growth factor beta binding protein 3	1.12	1.50E-09
ENSMUSG00000017817	Jph2	junctophilin 2	1.12	7.76E-09
ENSMUSG00000040133	Gpr176	G protein-coupled receptor 176	1.12	1.62E-03
ENSMUSG00000085795	Zfp703	zinc finger protein 703	1.11	4.36E-06
ENSMUSG00000012017	Scarf2	scavenger receptor class F, member 2	1.11	2.26E-04
ENSMUSG00000027230	Creb3l1	cAMP responsive element binding protein 3-like 1	1.11	4.50E-07
ENSMUSG00000051811	Cox6b2	cytochrome c oxidase subunit VIb polypeptide 2	1.11	5.05E-04
ENSMUSG00000020614	Fam20a	family with sequence similarity 20, member A	1.10	7.51E-05
ENSMUSG00000032997	Chpf	chondroitin polymerizing factor	1.10	2.31E-05
ENSMUSG00000061535	C1qtnf7	C1q and tumor necrosis factor related protein 7	1.10	3.89E-05
ENSMUSG00000034675	Dbn1	drebrin 1	1.10	9.91E-08
ENSMUSG00000000794	Kcnn3	potassium intermediate/small conductance calcium-activated channel, subfamily N, member 3	1.10	1.81E-05
ENSMUSG00000045799			1.10	4.91E-06
ENSMUSG00000038146	Notch3	notch 3	1.10	1.65E-05
ENSMUSG00000013921	Clip3	CAP-GLY domain containing linker protein 3	1.09	2.38E-06
ENSMUSG00000059921	Unc5c	unc-5 homolog C (C. elegans)	1.09	2.66E-04
ENSMUSG00000024620	Pdgfrb	platelet derived growth factor receptor, beta polypeptide	1.09	4.77E-08
ENSMUSG00000033200	Tpsg1	tryptase gamma 1	1.09	2.28E-05
ENSMUSG00000070802	Pnmal2	PNMA-like 2	1.09	8.43E-06
ENSMUSG00000020205	Phlda1	pleckstrin homology-like domain, family A, member 1	1.09	3.31E-06
ENSMUSG00000078794	Dact3	dapper homolog 3, antagonist of beta-catenin (xenopus)	1.09	1.71E-05
ENSMUSG00000031517	Gpm6a	glycoprotein m6a	1.09	2.86E-05
ENSMUSG00000015468	Notch4	notch 4	1.08	6.44E-05
ENSMUSG00000026249	Serpine2	serine (or cysteine) peptidase inhibitor, clade E, member 2	1.08	8.35E-06
ENSMUSG00000074743	Thbd	thrombomodulin	1.08	5.09E-08
ENSMUSG00000030222	Rerg	RAS-like, estrogen-regulated, growth-inhibitor	1.08	1.77E-04
ENSMUSG00000037379	Spon2	spondin 2, extracellular matrix protein	1.08	4.06E-07

ENSMUSG00000039252	Lgi2	leucine-rich repeat LGI family, member 2	1.08	2.13E-04
ENSMUSG00000037326	Capn15	calpain 15	1.08	6.27E-05
ENSMUSG00000062329	Cytl1	cytokine-like 1	1.08	1.09E-03
ENSMUSG00000026399	Cd55	CD55 antigen	1.07	1.42E-08
ENSMUSG00000029420	Rimbp2	RIMS binding protein 2	1.07	1.97E-04
ENSMUSG00000009614	Sardh	sarcosine dehydrogenase	1.07	4.33E-04
ENSMUSG00000056481	Cd248	CD248 antigen, endosialin	1.07	2.62E-06
ENSMUSG00000027257	Pacsin3	protein kinase C and casein kinase substrate in neurons 3	1.07	3.82E-05
ENSMUSG00000004098	Col5a3	collagen, type V, alpha 3	1.07	4.65E-06
ENSMUSG00000053293	Pom121	nuclear pore membrane protein 121	1.07	1.15E-06
ENSMUSG00000026208	Des	desmin	1.06	9.71E-11
ENSMUSG00000024164	C3	complement component 3	1.06	2.11E-08
ENSMUSG00000061048	Cdh3	cadherin 3	1.06	3.31E-04
ENSMUSG00000032735	Ablim3	actin binding LIM protein family, member 3	1.06	1.14E-04
ENSMUSG00000022099	Dmtn	dematin actin binding protein	1.06	5.84E-05
ENSMUSG00000050288	Fzd2	frizzled homolog 2 (Drosophila)	1.06	8.29E-05
ENSMUSG00000057280	Musk	muscle, skeletal, receptor tyrosine kinase	1.06	7.42E-05
ENSMUSG00000026586	Prrx1	paired related homeobox 1	1.05	2.15E-04
ENSMUSG00000021186	Fbln5	fibulin 5	1.05	1.08E-06
ENSMUSG00000040809	Chil3	chitinase-like 3	1.05	6.24E-03
ENSMUSG00000019467	Arhgef25	Rho guanine nucleotide exchange factor (GEF) 25	1.05	1.93E-08
ENSMUSG00000039477	Tnrc18	trinucleotide repeat containing 18	1.05	1.09E-07
ENSMUSG00000026748	Plxdc2	plexin domain containing 2	1.05	5.64E-06
ENSMUSG00000021130	Galnt16	UDP-N-acetyl-alpha-D-galactosamine:polypeptide N-acetylgalactosaminyltransferase 16	1.05	8.24E-04
ENSMUSG00000063382	Bcl9l	B cell CLL/lymphoma 9-like	1.05	2.40E-06
ENSMUSG00000001911	Nfix	nuclear factor I/X	1.05	8.18E-09
ENSMUSG00000026204	Ptprn	protein tyrosine phosphatase, receptor type, N	1.05	1.29E-04
ENSMUSG00000021070	Bdkrb2	bradykinin receptor, beta 2	1.05	4.03E-05
ENSMUSG00000037225	Fgf2	fibroblast growth factor 2	1.04	1.77E-03
ENSMUSG00000043155	Hpdl	4-hydroxyphenylpyruvate dioxygenase-like	1.04	4.01E-04
ENSMUSG00000037335	Hand1	heart and neural crest derivatives expressed transcript 1	1.04	2.37E-04
ENSMUSG00000022475	Hdac7	histone deacetylase 7	1.04	2.30E-05
ENSMUSG00000025355	Mmp19	matrix metallopeptidase 19	1.04	1.37E-05
ENSMUSG00000044017	Gpr133	G protein-coupled receptor 133	1.04	1.05E-06
ENSMUSG00000008734	Gprc5b	G protein-coupled receptor, family C, group 5, member B	1.04	1.17E-05
ENSMUSG00000037411	Serpine1	serine (or cysteine) peptidase inhibitor, clade E, member 1	1.04	3.70E-05
ENSMUSG00000022665	Ccdc80	coiled-coil domain containing 80	1.04	1.42E-07
ENSMUSG00000070509	Rgma	repulsive guidance molecule family member A	1.04	1.82E-05
ENSMUSG00000098470	C1rb	complement component 1, r subcomponent B	1.04	2.39E-04
ENSMUSG00000036446	Lum	lumican	1.03	8.29E-07
ENSMUSG00000090399			1.03	2.92E-04
ENSMUSG00000025409	Mbd6	methyl-CpG binding domain protein 6	1.03	9.57E-06
ENSMUSG00000026211	Obsl1	obscurin-like 1	1.03	1.02E-04
ENSMUSG00000030787	Lyve1	lymphatic vessel endothelial hyaluronan receptor 1	1.03	6.53E-08
ENSMUSG00000030116	Mfap5	microfibrillar associated protein 5	1.03	2.77E-04
ENSMUSG00000035112	Wnk4	WNK lysine deficient protein kinase 4	1.03	4.65E-07

ENSMUSG00000094686	Ccl21a	chemokine (C-C motif) ligand 21A (serine)	1.03	5.07E-07
ENSMUSG00000022484	Hoxc10	homeobox C10	1.03	1.38E-03
ENSMUSG00000025402	Nab2	Ngfi-A binding protein 2	1.03	2.30E-04
ENSMUSG00000026193	Fn1	fibronectin 1	1.03	2.80E-08
ENSMUSG00000045322	Tlr9	toll-like receptor 9	1.03	2.15E-03
ENSMUSG00000050234	Gja4	gap junction protein, alpha 4	1.02	1.99E-03
ENSMUSG00000031875	Cmtm3	CKLF-like MARVEL transmembrane domain containing 3	1.02	2.35E-04
ENSMUSG00000097353			1.02	2.29E-03
ENSMUSG00000073418	C4b	complement component 4B (Chido blood group)	1.02	1.11E-07
ENSMUSG00000021294	Kif26a	kinesin family member 26A	1.02	5.48E-04
ENSMUSG00000019997	Ctgf	connective tissue growth factor	1.02	2.42E-05
ENSMUSG00000020627	Klhl29	kelch-like 29	1.02	4.56E-04
ENSMUSG00000027221	Chst1	carbohydrate (keratan sulfate Gal-6) sulfotransferase 1	1.02	1.93E-05
ENSMUSG00000039377	Hlx	H2.0-like homeobox	1.01	1.85E-05
ENSMUSG00000000957	Mmp14	matrix metallopeptidase 14 (membrane-inserted)	1.01	8.74E-09
ENSMUSG00000020810	Cygb	cytoglobin	1.01	2.64E-05
ENSMUSG00000037966	Ninj1	ninjurin 1	1.01	1.14E-05
ENSMUSG00000029661	Col1a2	collagen, type I, alpha 2	1.01	4.11E-07
ENSMUSG00000036412	Arsi	arylsulfatase i	1.01	2.51E-03
ENSMUSG00000019539	Rcn3	reticulocalbin 3, EF-hand calcium binding domain	1.01	1.50E-07
ENSMUSG00000001930	Vwf	Von Willebrand factor homolog	1.01	8.43E-08
ENSMUSG00000027840	Wnt2b	wingless-type MMTV integration site family, member 2B	1.01	2.87E-07
ENSMUSG00000071984	Fndc1	fibronectin type III domain containing 1	1.01	4.33E-07
ENSMUSG00000020886	Dlg4	discs, large homolog 4 (Drosophila)	1.01	2.15E-05
ENSMUSG00000071516	Hist1h2ai	histone cluster 1, H2ai	1.01	8.84E-06
ENSMUSG00000018672	Copz2	coatomer protein complex, subunit zeta 2	1.01	8.43E-05
ENSMUSG00000020042	Btbd11	BTB (POZ) domain containing 11	1.01	4.78E-04
ENSMUSG00000026797	Stxbp1	syntaxin binding protein 1	1.01	7.16E-06
ENSMUSG00000044456	Rin3	Ras and Rab interactor 3	1.01	9.66E-06
ENSMUSG00000034107	Ano7	anoctamin 7	1.01	2.02E-06
ENSMUSG00000027523	Gnas	GNAS (guanine nucleotide binding protein, alpha stimulating) complex locus	1.00	8.72E-05
ENSMUSG00000033960	9430020K01Rik	RIKEN cDNA 9430020K01 gene	1.00	3.08E-07
ENSMUSG00000062825	Actg1	actin, gamma, cytoplasmic 1	1.00	5.54E-08
ENSMUSG00000028339	Col15a1	collagen, type XV, alpha 1	1.00	2.50E-07
ENSMUSG00000025223	Ldb1	LIM domain binding 1	1.00	1.82E-07
ENSMUSG00000010175	Prox1	prospero homeobox 1	1.00	3.76E-07
ENSMUSG00000026185	Igfbp5	insulin-like growth factor binding protein 5	1.00	2.16E-06
ENSMUSG00000036158	Prickle1	prickle homolog 1 (Drosophila)	1.00	2.72E-06
ENSMUSG00000060594	Layn	layilin	1.00	1.30E-04
ENSMUSG00000030218	Mgp	matrix Gla protein	1.00	6.82E-05
ENSMUSG00000089308			-1.02	4.22E-03
ENSMUSG00000081094			-1.04	1.94E-05
ENSMUSG00000083992			-1.05	3.77E-04
ENSMUSG00000076940	2010309G21Rik	RIKEN cDNA 2010309G21 gene	-1.05	5.86E-03
ENSMUSG00000083337			-1.06	1.44E-03
ENSMUSG00000084416			-1.06	8.34E-05

ENSMUSG00000080440			-1.06	1.39E-03
ENSMUSG00000094026			-1.07	4.89E-03
ENSMUSG00000064358	COX3	cytochrome c oxidase subunit III	-1.08	2.30E-04
ENSMUSG00000064945	Rny3	RNA, Y3 small cytoplasmic (associated with Ro protein)	-1.10	4.82E-07
ENSMUSG00000056412			-1.11	1.33E-03
ENSMUSG00000094655			-1.12	1.12E-05
ENSMUSG00000095584			-1.13	2.65E-03
ENSMUSG00000087819			-1.13	4.70E-04
ENSMUSG00000076332			-1.15	4.62E-06
ENSMUSG00000064346			-1.16	1.45E-03
ENSMUSG00000080921			-1.17	7.03E-06
ENSMUSG00000064352			-1.18	2.62E-04
ENSMUSG00000074800			-1.18	2.23E-06
ENSMUSG00000056032			-1.19	1.32E-05
ENSMUSG00000064653			-1.20	2.91E-04
ENSMUSG00000078193			-1.21	1.15E-05
ENSMUSG00000064360	ND3	NADH dehydrogenase subunit 3	-1.21	1.19E-06
ENSMUSG00000064472			-1.22	1.75E-03
ENSMUSG00000077711			-1.23	4.78E-05
ENSMUSG00000095422			-1.24	6.54E-04
ENSMUSG00000065104			-1.27	3.67E-04
ENSMUSG00000095396			-1.28	7.57E-04
ENSMUSG00000095624			-1.30	7.03E-04
ENSMUSG00000096801			-1.31	2.08E-04
ENSMUSG00000064355			-1.33	4.75E-06
ENSMUSG00000090136	Gm10177	predicted gene 10177	-1.35	4.16E-05
ENSMUSG00000057359			-1.36	6.79E-05
ENSMUSG00000076355			-1.37	1.05E-06
ENSMUSG00000076320			-1.39	1.96E-08
ENSMUSG00000094400			-1.40	2.45E-04
ENSMUSG00000095738			-1.41	1.21E-04
ENSMUSG00000080365			-1.43	2.38E-06
ENSMUSG00000077345			-1.49	1.15E-06
ENSMUSG00000093413			-1.53	5.43E-07
ENSMUSG00000093983			-1.54	1.97E-05
ENSMUSG00000067870			-1.55	6.84E-08
ENSMUSG00000062083			-1.56	5.06E-10
ENSMUSG00000092661			-1.62	1.38E-12
ENSMUSG00000077082			-1.63	2.55E-10
ENSMUSG00000064823			-1.64	1.65E-08
ENSMUSG00000064689			-1.67	1.43E-06
ENSMUSG00000076370			-1.67	1.21E-08
ENSMUSG00000064742			-1.77	1.35E-06
ENSMUSG00000087412			-1.80	4.16E-07
ENSMUSG00000096222			-1.82	6.23E-08
ENSMUSG00000077565			-1.93	4.36E-16

ENSMUSG00000083705	Gm8624	predicted gene 8624	-1.99	1.66E-12
ENSMUSG00000065373			-2.07	9.30E-11
ENSMUSG00000093999			-2.27	8.28E-11

Danksagung

Als erstes möchte ich meiner Mentorin Prof. Dr. Petra Dersch für die gute Betreuung meiner Arbeit danken. Danke, für die motivierenden Worte, deine Begeisterung für meine Arbeit, dein Vertrauen und dein Engagement.

Des Weiteren danke ich Prof. Dr. Michael Steinert für die Übernahme des Koreferats und Prof. Dr. André Fleißner für die Teilnahme an der Prüfungskommission.

Ein weiterer Dank geht an Dr. Marc Erhardt und Dr. Oliver Goldmann für die Teilnahme und Diskussionen bei meinen „Thesis Committees".

Der Helmholtz „International Graduate School for Infection Research" danke ich für die Vergabe des Stipendiums sowie für die Finanzierung von Konferenzen und Weiterbildungen. Weiterhin möchte ich mich bei der Graduierten Schule „Grad^{TUBS}" für die Ermöglichung und Finanzierung von Weiterbildungen bedanken.

Zudem möchte ich unseren Kooperationspartnern Ulrike Heise, Marina Pils, Till Strowig und Sophie Thiemann aus der Mauspathologie und Mikrobiellen Immunregulation am Helmholtz-Zentrum für Infektionsforschung für die gute Zusammenarbeit und den Austausch von Gedanken danken.

Dr. Fabio Pisano danke ich für die Betreuung in den ersten zwei Jahren meiner Doktorarbeit. Du warst immer hilfsbereit und standst mit deinem guten Rat zur Seite. Ein besonderer Dank gilt Dr. Sabrina Mühlen, die meine Arbeit in kürzester Zeit Korrektur gelesen hat. Des Weiteren danke ich Tanja Krause, Karin Paduch, Sandra Stengel und Jennifer Wolf für die Unterstützung meiner Tierversuche. Ein besonders großes Dankeschön geht dabei an Karin, die mir unermüdlich bei der Vorbereitung und Durchführung meiner Experimente geholfen hat. Außerdem möchte ich Dr. Jörn Pezoldt für die Unterstützung und den Rat bei den Zytokinmessungen danken.

Ein weiterer Dank geht an Claudia, die bei jedem Problem unterstützenden Rat wusste. Außerdem danke ich der gesamten Arbeitsgruppe, insbesondere Paweena, Lisa, Vanessa, Carina und Maria für die gute Arbeitsatmosphäre.

Zudem danke ich meinem „altem" Büro, Franzi, Jörn und Maik, für die schöne Zeit und die produktiven, unterhaltsamen, lustigen wie traurigen Gespräche. Insbesondere danke ich Maik für die leckeren Kekse sowie Franzi und Jörn für ihr offenes Ohr für Probleme jeglicher Art und ihre aufbauenden Worte.

Ich danke Aleksandra und Marek für ihr fortwährendes Interesse. Ein ganz besonderes Dankeschön geht an Alex, der mich immer unterstützt, meine Probleme zu verstehen versucht und für mich da ist. Ich danke auch Klaus und Edith für die Unterstützung als es mir nicht gut ging. Zudem möchte ich mich bei meiner Oma Ilse für ihre Unterstützung bedanken. Außerdem danke ich meiner Mutter aus tiefsten Herzen für ihre zeitlebens erbrachte Unterstützung und Anteilnahme.